ISSN 0031 - 9465

PHYTOPATHOLOGIA MEDITERRANEA

Plant health and food safety

Volume 64 • No. 3 • December 2025

The international journal of the
Mediterranean Phytopathological Union

FIRENZE UNIVERSITY PRESS

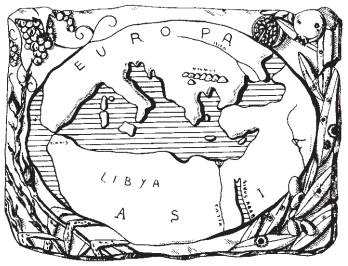

PHYTOPATHOLOGIA MEDITERRANEA

Plant health and food safety

The international journal edited by the Mediterranean Phytopathological Union
founded by A. Ciccarone and G. Goidànich

Phytopathologia Mediterranea is an international journal edited by the Mediterranean Phytopathological Union. The journal's mission is the promotion of plant health for Mediterranean climate and regions, safe food production, and the transfer of knowledge on diseases and their sustainable management.
The journal deals with all areas of plant pathology, including epidemiology, disease control, biochemical and physiological aspects, and utilization of molecular technologies. All types of plant pathogens are covered, including fungi, nematodes, protozoa, bacteria, phytoplasmas, viruses, and viroids. Papers on mycotoxins, biological and integrated management of plant diseases, and the use of natural substances in disease and weed control are also strongly encouraged. The journal focuses on phytopathology and closely related fields in the Mediterranean agro-ecological regions. The journal includes three issues each year, publishing Reviews, Original research papers, Research notes, New or unusual disease reports, News and opinion, Current topics, Commentaries, and Letters to the Editor.

PHYTOPATHOLOGIA MEDITERRANEA

The international journal of the Mediterranean Phytopathological Union

Volume 64, December, 2025

Firenze University Press

Phytopathologia Mediterranea. The international journal of the Mediterranean Phytopathological Union
https://www.fupress.com/pm
ISSN 0031-9465 (print) | ISSN 1593-2095 (online)
Published three times a year

Published by Firenze University Press

Firenze University Press
Università degli Studi di Firenze
via Cittadella, 7, 50144 Firenze, Italy
www.fupress.com

Phytopathologia Mediterranea
The international journal of the
Mediterranean Phytopathological Union

Firenze University Press
www.fupress.com/pm

Dr Alan J.L. Phillips, BSc, PhD, 1952-2025

Past President of the Mediterranean Phytopathological Union

It is with sadness and regret that we acknowledge the death of Dr Alan Phillips, on 29 August 2025.

Alan Phillips was born in Victoria, Hong Kong, on 19 March 1952. He attended Wolverhampton Polytechnic, England, graduating in Applied Biology in 1973, was accepted Member of the Institute of Biology in 1975, and obtained his PhD degree in 1980. His thesis was on the colonisers and antagonists of *Sclerotinia sclerotiorum* sclerotia. He was a lecturer at Wolverhampton Polytechnic and Harper Adams Agricultural College from 1981 to 1983, and an agricultural researcher at the Plant Protection Institute, Pretoria, South Africa from 1983 to 1995. In 1996, he moved to Portugal, where he worked in several institutions, becoming a national authority in mycology. He recently retired from the Faculty of Sciences at the University of Lisbon.

Dr Phillips has had long association with the Mediterranean Phytopathological Union (MPU) and the journal *Phytopathologia Mediterranea*. This began when he became a member of the Union, and expanded as he took responsibilities as a Section Editor for the journal, with oversight for manuscripts on grapevine trunk diseases. He had expanded contributions, with Prof Giuseppe Surico, as Consulting Editor of the journal, where he gave positive and constructive inputs on publication strategies and growth. He was elected President of the MPU from 2011 to 2017, and continued to support the MPU and the journal until his death.

Dr Phillips made enduring contributions to fungal taxonomy and phylogeny, and plant pathology, with particular focus on pathogens associated with woody hosts. His most influential research was on the systematics of *Botryosphaeriaceae*, combining culture-based studies with multi-locus DNA sequencing to clarify genus and species boundaries. His landmark monograph *"The Botryosphaeriaceae: genera and species known from culture"* (2013) provided authoritative phylogenies, diagnostic keys, and taxonomic treatments that standardised identifications across 17 genera and more than 100 species. He championed integrated phylogenetic and morphological approaches, emphasizing that morphology alone was often inadequate for defining species. This perspective guided his extensive revisions of *Botryosphaeriaceae* and *Diaporthe,* refining species concepts that remain fundamental to modern mycology. Much of his research addressed grapevine trunk diseases, but also pathogens of other woody hosts, describing new taxa and host associations, and advancing understanding of disease management. He also contributed to higher-level fungal classification and diversity, redefining families within *Botryosphaeriales*, participating in compendia including the series Outline of Fungi and Fungus-like Taxa. His research has provided phylogenetic and nomenclatural foundation for modern research on these ecologically and economically significant fungi He became particu-

ISSN 0031-9465 (print) | ISSN 1593-2095 (online) | DOI: 10.36253/phyto-16849

larly recognised as a Highly Cited Researcher (Plant and Animal Science) for the years 2018 to 2024, reflecting enduring influence and global relevance of his research contributions and leadership.

Dr Phillips will also be remembered for his mentorship and generosity. He guided numerous early-career mycologists and plant pathologists, offering technical expertise, and also patient encouragement and thoughtful advice. He maintained a strong and enduring association with the Center of Excellence in Fungal Research (CEFR), Mae Fah Luang University, Thailand, where he served as a mentor and visiting Professor for many years. His commitment to training and inspiring young mycologists and plant pathologists has left a lasting legacy within the Center, where his guidance has shaped the careers of many young researchers. He was heavily involved in academic activities at CEFR, serving on thesis committees and attending defences, where his meticulous reviewing strengthened student output. His engagement extended beyond formal obligations, as a patient teacher, rigorous researcher, and source of encouragement to all who sought his advice. He continued this mentorship after his retirement, and his last service as an External Committee member for a PhD defence was in May 2025.

Alan Phillips was a gifted photographer, as he expressed his appreciation for nature and people using the lens of his camera. He captured landscapes and everyday life with sensitivity and an artistic eye. Photography was his creative outlet and a pursuit he practised with great dedication; his outputs were sold on professionally, and he often reinvested the proceeds to acquire new equipment to improve his craft. His images, as with his research, reflected patience, precision, and an enduring curiosity.

Dr Alan Phillips always listened discreetly, and made colleagues feel understood and respected. He evoked gratitude and affection, and is remembered for his personable, courteous, and respectful interactions, and a legacy of major contributions to fungal taxonomy, phytopathology, and grapevine disease research. This also included constructive mentorship, and enduring collegial spirit with his colleagues and friends.

The legacy of Dr Alan Phillips includes his contributions in collegial mentorship, his personal achievements in knowledge development, and his leadership in plant pathology.

Artur Alves,
Ishara Sandeepani Manawasinghe,
Laura Mugnai

Phytopathologia Mediterranea
The international journal of the
Mediterranean Phytopathological Union

Firenze University Press
www.fupress.com/pm

Abstracts

Abstracts of oral and poster papers presented at the 13th International Workshop on Grapevine Trunk Diseases, held in Ensenada, Baja California, Mexico (20–24 July 2025)

The 13th International Workshop on Grapevine Trunk Diseases (IWGTD) was chaired by Dr Rufina Hernández-Martínez, and was organized by the Center for Scientific Research and Higher Education of Ensenada (CICESE). The Workshop was supported by the Ministry of Science, Humanities, Technology and Innovation of Mexico (SECIHTI), and the International Organization of Vine and Wine (OIV). The ICGTD Council meeting took place on July 20, prior to the Workshop welcome reception.

The Workshop scientific programme was opened by Dr Philippe Rolshausen (University of California, Riverside, USA), who outlined recent advances in pathogen genomics that have deepened understanding of grapevine trunk diseases, enabling improvements in vineyard practices, nursery standards, and development of biocontrol strategies. The other Keynote speakers were Dr Catarina da Cunha Maia Leal (Instituto de Ciencias de la Vid y el Vino, Spain), who discussed how grapevine-associated microbial communities shape disease, host defense, and biocontrol, highlighting sequencing-based tools for sustainable vineyard management, and Dr Akif Eskalen (University of California, Davis, USA), who outlined integrated nursery and vineyard disease management strategies, combining prevention, sanitation, and biocontrol, to reduce grapevine trunk diseases and extend vineyard longevity.

The Workshop was attended by 105 participants from 14 countries. A total of 35 oral and 29 poster papers were presented, across the ten Workshop sessions. The papers covered pathogen characterization, detection and disease epidemiology, host plant interactions, and disease management.

During the Workshop field trip to the Guadalupe Valley, delegates visited vineyards affected by GTD pathogens, where local growers shared their perspectives and key challenges in managing vineyards under semiarid conditions, as well as the strategies they have adopted. The field trip concluded with a wine tasting at Mexico's largest vineyard, L.A. Cetto.

Student competitions for best oral and poster paper presentations included contributions from 16 students. The best student poster paper award was presented to MSc student Grecia Paniagua Pérez (CICESE, Mexico) for her paper "Comparative cellular morphology and stress tolerance of *Botryosphaeriaceae* fungi affecting grapevines in Mexico. Second place went to PhD student Angelos Floudas (Aristotle University of Thessaloniki, Greece) for paper "Evaluation of selected fungal biological control agents for the protection of grapevine pruning wounds against *Diplodia seriata*". Third place was awarded to MSc student Yessica Osorio Sánchez (CICESE, Baja California, Mexico) for her paper "Evaluation and characterization of the biological activity of secondary metabolites from actinobacteria of the genus *Streptomyces*".

In the oral student competition, first place went to PhD student Isidora Silva Valderrama (University of British Columbia, Vancouver, Canada) for her presentation "Host phylogenetic diversity and virulence in *Botryosphaeriaceae*". Second place was awarded to PhD student Karen Andrea Corrales Adame (Institut des Sciences Analytiques et de Physico-Chimie pour l'Environnement et les Matériaux, France) for her paper, "Limited influence of pruning practice on the fungal community of asymptomatic Esca-infected grapevines", and third place went to PhD student Martín Puebla (University of California, Riverside, USA) for his paper "Evaluation of commercial bioinoculant products on the health of potted nursery vines".

The 14th IWGTD will be held in Greece in 2026.

Phytopathologia Mediterranea 64(3): 459-492, 2025
ISSN 0031-9465 (print) | ISSN 1593-2095 (online) | DOI: 10.36253/phyto-16743

Delegates attending the 13th International Workshop on Grapevine Trunk Diseases, in Ensenada, Baja California, Mexico.

Publication disclaimer

This Supplement to *Phytopathologia Mediterranea* publishes abstracts of the papers presented at the 13th International Workshop on Grapevine Trunk Diseases. The abstracts are here presented as submitted by the respective authors. The texts have been checked for consistency of presentation, but have not been through the peer review processes used for research papers published in *Phytopathologia Mediterranea*.

ORAL PAPERS

Closing the Gaps on Grapevine Trunk Diseases' Research. P. ROLSHAUSEN. *University of California, Riverside. Department of Botany and Plant Sciences, USA. E-mail:* philrols@ucr.edu

Knowledge on grapevine trunk diseases etiology has improved significantly with the emergence of omics technologies. The increasing availability of reference genomes of trunk disease pathogens has enabled studies spanning from gene function to evolutionary relationships within and across species. Our scientific community has gained clarity on the GTD disease complex and the dynamics of microbial communities including the interaction of those community members with each other, but also with the plant host and its environment, and how it affects disease outcome. That knowledge has enabled the improvement of plant quality standards in nursery and the adoption of best cultural practices in vineyards. This work has also facilitated understanding of the beneficial organisms associated with grapevine and how these could be developed and marketed into biological control agents or plant biostimulants to better manage infection with trunk pathogens. My talk will highlight the progress that has been made in the past decade and where our research efforts should be invested in the future to improve vineyard health, longevity and productivity.

Microbial balance in grapevine: from pathogen pressure to biocontrol protection. C. LEAL[1]. [1]*Instituto de Ciencias de la Vid y del Vino (ICVV), Consejo Superior de Investigaciones Científicas - Universidad de la Rioja - Gobierno de La Rioja, Ctra. LO-20 Salida 13, Finca La Grajera, 26071 Logroño, Spain. E-mail:* catarina.leal@icvv.es

Grapevines exist within a highly dynamic microbial ecosystem where plant health is determined by the complex interplay between pathogenic and beneficial microorganisms. The microbial communities inhabiting the rhizos-

phere and xylem play pivotal roles in both the expression of grapevine trunk diseases and the activation of plant defense mechanisms. This presentation scanned recent advances in microbial ecology applied to viticulture, highlighting the functional roles of key fungal pathogens and the potential of bacterial and fungal biological control agents. By integrating data from transcriptomic analyses and high throughput metabarcoding, this talk will explore how these microbes shape the grapevine's immune landscape and how their establishment and efficacy are influenced by environmental factors, including soil conditions and drought stress. Studies of both disease development and biocontrol implementation reveal a context-dependent response of the plant and its microbiome, underscoring the need for ecologically tailored management strategies. Emphasis will be placed on the potential of sequencing-based approaches to serve as predictive tools in sustainable viticulture, aiding in the design of biologically informed, site-specific disease control programs.

From propagation to production: integrated strategies for Grapevine Trunk Disease Management in nurseries and vineyards. A. ESKALEN. *Department of Plant Pathology, University of California, Davis, CA 95616, U.S.A. E-mail:* aeskalen@ucdavis.edu

Grapevine trunk diseases (GTDs) are among the most economically damaging challenges in viticulture, often establishing early during propagation and progressing silently until vine productivity declines. This presentation will provide an overview of integrated disease management strategies that bridge the nursery and vineyard systems. Emphasis will be placed on preventative practices, including sanitation, grafting hygiene, pruning wound protection, and the strategic use of biocontrol agents. Drawing from multi-year research trials across diverse California regions, I will highlight how combining biological and cultural tools can reduce GTD incidence and severity in both young and mature vines. The lecture will also address the practical challenges of implementation in commercial settings and offer regionally adaptable, sustainable solutions for growers and nurseries. Attendees will gain a comprehensive understanding of how early intervention and coordinated management can improve vine health and vineyard longevity.

Elucidating the distribution and pathogenicity of *Cryptovalsa ampelina* in Australian **vineyards.** M. ANDRES-SODUPE[1,2], M.R. SOSNOWSKI[3,4], J. HRYCAN[2], C.C. STEEL[1,2], S. SAVOCCHIA[1,2]. *[1] Faculty of Science and Health, School of Agricultural, Environmental and Veterinary Sciences, Charles Sturt University, Wagga Wagga, New South Wales, 2678, Australia.[2] Gulbali Institute, Charles Sturt University, Wagga Wagga, New South Wales, 2678, Australia. [3]South Australian Research and Development Institute, Adelaide, SA, 5001, Australia.[4] School of Agriculture, Food and Wine, Waite Research Institute, The University of Adelaide, Adelaide, SA 5005, Australia. E-mail:* mandressodupe@csu.edu.au

Cryptovalsa ampelina is a fungal species associated with the Eutypa dieback (ED) complex. Limited information is available regarding its biology and pathogenicity, despite its presence worldwide. Previous studies have reported low to moderate levels of virulence, with some suggesting pathogenicity comparable to *Eutypa lata*, the primary cause of ED. To investigate the distribution of *C. ampelina* in Australian vineyards, dead grapevine wood tissues were collected from 43 vineyards across 12 wine regions in South Australia, New South Wales, Western Australia and Tasmania. Two methods were used to detect the pathogen: internal wood tissues were cultured on potato dextrose agar amended with chloramphenicol (PDA-C), and perithecia on the wood surface were dissected and asci inspected under a microscope. When asci were observed with 32 spores, characteristic of *C. ampelina*, they were cultured on PDA-C. Cultures were identified morphologically and confirmed using Loop-mediated isothermal amplification (LAMP) with species-specific primers and DNA sequencing of the internal transcribed spacer (ITS) region. A total of 36 *C. ampelina* isolates were identified. Pathogen prevalence varied between regions, providing insight into the distribution of this pathogen in Australian vineyards. To assess pathogenicity, a detached cane assay was performed using 26 isolates of *C. ampelina* and six of *E. lata* for comparison. After 3 months, the bark was removed, and the lesion length was measured. Koch's postulates were confirmed by re-isolating the pathogens from necrotic tissue plated on PDA-C. Additionally, the extent of colonisation was assessed by sampling tissue at 5 mm intervals above and below the lesion margins. *C. ampelina* was found to colonise wood up to 25 mm beyond the visible lesion boundaries. *E. lata* showed longer lesions and colonisation than *C. ampelina*. These results suggest the ability of these fungi to spread extensively within grapevine tissues and far beyond the staining lesion.

This research was financially supported by Wine Australia, with levies from Australia's grape growers and winemakers and matching funds from the Australian Government.

Phytosanitary analysis of Misión grapevines from Baja California, Mexico, focusing on grapevine trunk disease fungi. C.S. DELGADO-RAMÍREZ, E. SEPÚLVEDA[1], E.A. RANGEL-MONTOYA[1,3], C. VALENZUELA-SOLANO[2], R. HERNANDEZ-MARTINEZ[1]. *[1]CICESE. Departamento de Microbiología. Ensenada, Baja California. [2]INIFAP Sitio experimental costa de Ensenada. [3]Facultad de Ciencias Quimicas, UABC, Tijuana. E-mail:* cdelgado@cicese.edu.mx

In Baja California, Misión grapevines were introduced in 1869 and are currently cultivated under rainfed conditions with minimal agricultural management. There is growing interest in using this variety for wine production, which requires the evaluation of its phytosanitary status to support large-scale propagation. Like other varieties, Misión grapevines show symptoms associated with grapevine trunk diseases, although the responsible pathogens have yet to be identified. In this study, endophytic fungi were isolated from Misión grapevines. Tissue samples from eight vineyards were analyzed, from which 78 fungal strains were obtained. Thirteen fungi were morphologically and molecularly identified as grapevine trunk pathogens, specifically *Diaporthe ampelina* and *Diplodia seriata*. For these isolates, optimal growth temperatures and pathogenicity on three grapevine varieties were determined. All evaluated strains showed optimal growth temperatures between 25 and 28°C. In the pathogenicity assay, all thirteen strains induced necrotic lesions in the wood of the Tempranillo, Malvasía Blanca, and Misión cultivars, confirming their infective capacity. A histological analysis was performed to observe changes in starch, cellulose, and lignin content in tissue from two grapevine varieties inoculated with *Lasiodiplodia brasiliensis* MXBCL28 and *D. seriata* HP12BCMX. Plants inoculated with *L. brasiliensis* MXBCL28 showed lower levels of the analyzed components compared to those inoculated with *D. seriata*, which might be related to its higher virulence. In conclusion, Misión grapevines serve as a reservoir for grapevine trunk fungi with intermediate virulence. This finding is crucial for supporting future decisions regarding the propagation and management of these grapevines in the region.

This research was financially supported by the Secretaría de Ciencia, Humanidades, Tecnología e Innovación (SECIHTI), Mexico.

Environmental variables associated with *Botryosphaeriaceae* spore release in Oregon vineyards. A.N. KC[1,2], M. HERNANDEZ[2]. *[1]Southern Oregon Research and Extension Center, 569 Hanley Rd, Central Point, OR 97502. [2]Department of Botany and Plant Pathology, Oregon State University, 2082 Cordley Hall, Corvallis, OR 97331. E-mail:* achala.kc@oregonstate.edu

Botryosphaeria dieback is one of the most common Grapevine Trunk Disease (GTD) in Oregon vineyards. Due to winter rain and possible availability of spores, the pruning wounds become most susceptible to infection during these months (November to March). To understand the temporal dispersal pattern of *Botryosphaeriaceae* spores and the effect of environmental variables on their availability, four Burkard seven-day recording volumetric spore traps were placed in vineyard blocks in northern and southern Oregon. The traps were installed from December 2019 to March 2021 to collect 477 days of samples from each spore trap. Total DNA was extracted from the spore tapes and qPCR was performed to quantify the number of spores. Weather data including daily average and hourly temperature, relative humidity (RH), wind speed, total daily precipitation, and total hours of precipitation per day, were obtained from nearby weather stations. In addition to individual weather variables, ten days cumulative precipitation, hours of rain, and growing degree days (GDD) were calculated. Pearson Correlation analysis was performed between these variables and the total number of spores detected at both locations. In northern Oregon, the detection occurred between December and February; and the first spore detection occurred when cumulative growing degree day (GDD) totaled to 4357 and 4351units during the first and second seasons respectively. Similarly, in southern Oregon, the detection occurred between November and January; and the first spore detection occurred when cumulative GDD was 4405 units during the second season. Hours of continuous RH >86% was significantly associated with numbers of spores released ($P = 0.026$; $r = 0.42$). During the spore detected dates, the RH was >86% for at least 19 consecutive hours. This study suggests environmental variables such as GDD and RH are the critical components of *Botryosphaeriaceae* spores availability during the main pruning season in Oregon.

This research was financially supported by the Oregon Wine Board.

Monitoring trunk disease pathogen spore deposits on grapevine pruning wounds. T. FURLAN[1,2], J. HRYCAN[3], M. LIU[3], S. SAVOCCHIA[3], M.R. SOSNOWSKI[1,2]. *[1]South Australian Research and Development Institute, Adelaide SA 5001, Australia. [2]School of Agriculture, Food and Wine, Waite Research Institute, The University of Adelaide, SA 5005, Australia. [3]Gulbali Institute, School*

of Agricultural, Environmental and Veterinary Sciences, Charles Sturt University, NSW, Australia. E-mail: mark.sosnowski@sa.gov.au

Eutypa (ED) and Botryosphaeria dieback (BD) are caused by fungal species of the Diatrypaceae and *Botryosphaeriaceae*, respectively. Perithecia on infected wood release spores during rain events, which are dispersed by wind and rain splash to land on fresh pruning wounds and infect the exposed vascular tissue to cause dieback and eventually vine death. Research conducted in the 1960's on apricots reported that as little as 10 *Eutypa lata* spores could land on a wound in an orchard. Since then, researchers have used a large range of artificial inoculum spore concentrations for experiments, but there are no reports quantifying natural spore deposits on pruning wounds in grapevines. This research aims to determine the likelihood and quantity of ED and BD pathogen spores naturally landing on pruning wounds in vineyards. Glass microscope slides containing Melinex tape covered with Vaseline, to simulate small (1 cm^2), medium (2 cm^2) and large (4 cm^2) wounds, were placed in Shiraz blocks during winter in 2023 and 2024. Different scenarios regarding vine age, timing, rainfall and location were tested. DNA was extracted from spores on the tapes and analysed using qPCR to quantify the number of ED and BD pathogen spores deposited. Both incidence of tapes with spores and spore numbers varied greatly between years, most likely due to rainfall differences. Although ED pathogen spores were deposited in greater numbers than those of BD, the incidence of tapes detected with spores was greater for BD pathogens, possibly due to different spore dispersion dynamics. This is the first known report quantifying spore numbers deposited on grapevine pruning wounds naturally in a vineyard. Monitoring of spore deposits will continue in 2025, and results will provide valuable insights on the epidemiology of ED and BD to provide better guidance for managing infections in the vineyard.

This research was supported by Wine Australia, with levies from Australia's grape growers and winemakers and matching funds from the Australian Government.

Status of young vine decline fungi in source blocks, commercial nursery grapevines, and young vineyards in Australia. J. HRYCAN[1], M. LIU[1], M.R. SOSNOWSKI[2,3], R. BILLONES-BAAIJENS[1,4], T. FURLAN[2,3], S. SAVOCCHIA[1]. *[1]Gulbali Institute, School of Agricultural, Environmental and Veterinary Sciences, Charles Sturt University, NSW. [2]South Australian Research and Development Institute, Adelaide SA 5001, Australia, [3]School of Agriculture, Food and Wine, Waite Research Institute, The University of Adelaide, SA 5005, [4]Affinity Labs, Australian Wine Research Institute, PO Box 46, Glenside, SA 5064, Australia. E-mail:* jhrycan@csu.edu.au

Young vine decline (YVD) is caused by several fungal species that colonize the grapevine xylem, causing internal necrosis and leading to grapevine decline and death within the first few years after planting. Nursery studies worldwide have identified *Botryosphaeriaceae* spp., *Cadophora luteo-olivacea, Dactylonectria* spp., *Ilyonectria* spp., *Phaeoacremonium minimum,* and *Phaeomoniella chlamydospora* as the most prevalent YVD fungi, but the status in Australia is not known. Dormant canes from nursery source blocks in Australia were collected in the winters of 2023 and 2024. Canes were screened for mechanical damage and internal necrosis and DNA was extracted from wood of composite samples of five canes per block. Presence and abundance of the most prevalent YVD pathogens was analysed with qPCR. Pathogen presence and abundance varied widely between source blocks in 2023 and 2024, and YVD incidence in composite samples ranged from 0 to 100% infection. *Botryosphaeriaceae* spp. were the most prevalent fungi. In 2024, commercial nursery grapevines propagated from 2023 source block material were also analysed with qPCR, and 100% of composite samples were positive for YVD fungi, with *C. luteo-olivaceae, Dactylonectria* spp. and *P. minimum* the most prevalent. To understand the potential impact infected nursery material has on young grapevine health, vineyard surveys were conducted on 0 to 5-year-old grapevines in New South Wales (NSW), South Australia (SA), and Victoria (VIC). Symptoms of YVD included reduced vigour, stunted growth, leaf chlorosis or reddening, wilting and grapevine death. Symptomatic grapevines were screened for internal necrosis and fungal isolation onto artificial media. Young vine decline symptoms were recorded in 3.1%, 0% and 0.3% of young grapevines in NSW, SA, and VIC, respectively. The incidence of symptomatic grapevines in individual vineyard assessments varied between 0% to 40.7%. These results provide insight into the health status of source blocks and young vineyards regarding YVD in Australia.

This research was supported by Wine Australia, with levies from Australia's grape growers and winemakers and matching funds from the Australian Government.

Epidemiology, aggressiveness and fungicide sensitivity of *Aspergillus* species causing vine canker and sour rot in California vineyards. M.I. BUSTAMANTE, A. ADASKAVEG, J. CHAN, K. ELFAR, A. ESKALEN.

Department of Plant Pathology, University of California, Davis, CA 95616, U.S.A. E-mail: aeskalen@ucdavis.edu

Black aspergilli, primarily *Aspergillus tubingensis*, followed by *A. niger* and *A. carbonarius*, are the main causal agents of Aspergillus vine canker and summer bunch rot (sour rot) of table grapes in California vineyards. Current management relies largely on cultural practices. However, despite routine fungicide applications targeting *Erysiphe necator* (powdery mildew) and *Botrytis cinerea* (Botrytis bunch rot), high incidences of *Aspergillus* spp. are still frequently observed at harvest, leading to significant economic losses. In this study, we analyzed populations of black aspergilli obtained from vine canker and bunch rot samples, focusing on temperature response, pathogenicity, and sensitivity to six fungicides commonly used in California vineyards. *Aspergillus tubingensis* and *A. niger* exhibited similar mycelial growth rates between 15°C and 40°C, with optimal growth observed between 30°C and 35°C. *Aspergillus carbonarius* isolates showed significantly higher growth rates between 25°C and 35°C, with an optimum at 35°C. Pathogenicity assays on one-year-old grape canes revealed that *A. tubingensis* and *A. niger* isolates induced more aggressive cankers—larger in length, width and vascular discoloration—than *A. carbonarius*. However, on inoculated berries, *A. carbonarius* caused significantly larger lesions compared to the other two species. Fungicide sensitivity assays revealed that all isolates were sensitive to fludioxonil and iprodione. Low levels of resistance were observed for tebuconazole and cyprodinil, while high levels of resistance were detected for boscalid and pyraclostrobin. These findings provide critical insights into the epidemiology and aggressiveness of black aspergilli in both wood and fruit tissues and highlight the need for targeted fungicide programs to effectively manage *Aspergillus*-related diseases in California table grape vineyards.

Exploring the role of soil in Esca Complex: a first integrated assessment of physical, chemical, and biological properties in a Tuscan vineyard. F. BIGAZZI[1], G. CARELLA[1], S. DEL DUCA[2], S. MOCALI[2], S. PRIORI[3], F. VITALI[2], L. MUGNAI[1] *[1]Department of Agricultural, Food, Environmental and Forestry Science and Technology (DAGRI), Plant pathology and Entomology section,* P.le *delle Cascine 28, 50142 Firenze, Italy. [2]Council for Agricultural Research and Economics - Research Centre for Agriculture and Environment (CREA-AA), Via di Lanciola 12/A, 50125 Firenze, Italy. [3] University of Tuscia, Department of Agriculture and Forest Sciences (DAFNE), via San Camillo de Lellis, 01100 Viterbo, Italy. E-mail:* francesco.bigazzi1@unifi.it

Although multiple fungal pathogens and heavy May–June rainfall are recognized drivers of the Esca complex, the role of soil properties in symptom expression remains largely unexplored. In this study, we present the first integrated analysis of soil physicochemical and microbiological characteristics in relation to Esca incidence. We focused on a 1.5-ha Cabernet Sauvignon vineyard in Tuscany (Italy), where five years of monitoring data allowed us to delineate zones of high and low disease prevalence. To assess soil spatial heterogeneity, we employed an electromagnetic induction (EMI) sensor to map apparent soil electrical conductivity (ECa). By overlaying disease incidence maps with ECa data, we identified four locations for detailed pedological profiling and sampling. From each soil horizon within these profiles, three rhizosphere samples were collected and analyzed to characterize microbial community composition and functional traits using Biolog EcoPlate assays. Low-disease-incidence soils were characterized by a clay-loam texture, high lime content, alkaline pH (8.3–8.5), and low levels of bioavailable manganese (6.8–12.3 mg/kg). In contrast, high-incidence soils exhibited deeper profiles with a sandy clay-loam texture, minimal lime (<3%), sub-alkaline pH (7.8–8.1), higher nitrogen content, and increased organic matter. Bioavailable manganese was also higher (13–18 mg/kg). Preliminary microbiome analyses will be presented. Biolog EcoPlate assays showed a non-significant trend toward higher AWCD (Average Well Color Development) values in low-incidence zones, suggesting increased microbial metabolic activity in soils where vines were consistently less affected by the disease. Together, these findings indicate that soil texture, pH, and organic matter buffering capacity can substantially influence micronutrient dynamics—particularly manganese availability—potentially enhancing the wood-degrading enzymatic activity of *Fomitiporia mediterranea*. This, in turn, may lead to greater production of toxic byproducts that contribute to foliar symptom development. This study highlights the critical role of soil properties in Esca disease dynamics.

Epidemiology and impact of Grapevine Trunk Diseases on Chilean patrimonial vineyards. D. GRINBERGS[1], J. CHILIAN[1], R. ORREGO[2], M. ISLA[1], C. FERNÁNDEZ[1]. *[1]Instituto de Investigaciones Agropecuarias INIA-Quilamapu. Av. Vicente Méndez 515, Chillán. Chile. [1]Fruit Pathology Lab, [2]Climate change risk unit. E-mail:* dgrinbergs@inia.cl

Grapevine Trunk Diseases (GTDs) are a major threat to Chilean patrimonial vineyards, primarily composed of País, Moscatel, Cinsault, and Carignan cultivars. While GTDs have been extensively studied in commercial cultivars such as Cabernet Sauvignon, Sauvignon Blanc, Merlot, and Chardonnay, information on their impact in patrimonial vineyards remains scarce. Previous studies identified *Neofusicoccum* spp., *Diplodia* spp., *Seimatosporium vitifusiforme*, and *Arambarria destruens* as the most prevalent and virulent pathogens. This study aimed to evaluate the effects of GTDs on vine physiology, fruit yield, and the quality of both grapes and wine. Symptomatic and apparently healthy País vines (n = 30) were selected. Measurements included water potential, chlorophyll fluorescence, chlorophyll content, and gas exchange. Grapes were analyzed and subjected to microvinification. Results showed that the most affected parameters in symptomatic vines were water potential and fluorescence. Fruits from symptomatic plants were smaller and had lower soluble solids content. In addition, wines exhibited higher acidity and lower color intensity compared to those from healthy vines. A second objective was to investigate the epidemiology of *Neofusicoccum* spp. and *Diplodia* spp., identifying periods of infection risk in the Ñuble region of Chile. A País vineyard was monitored weekly for 24 months using glass spore traps to collect airborne inoculum. DNA was extracted, and standard qPCR curves were developed for each pathogen, relating Ct values to log DNA concentrations. Inoculum data were correlated with climate variables from nearby meteorological stations, after removing the seasonal component. Precipitation and humidity were the most influential factors, with a stronger correlation for *Diplodia* spp. (87%) compared to *Neofusicoccum* spp. (45%). Temperature also played a role, showing a stronger correlation with *Neofusicoccum* spp.

This research was financially supported by the Project Fondef ID23I10398, Agencia Nacional de Investigación y Desarrollo, ANID.

Influence of rootstock-scion interaction on vine decline in different grapevine cultivars in Hungary. A. KUN[1], A. CSIKÁSZ-KRISZICS[1], B. SZABÓ[1], P. TESZLÁK[1]. *[1]University of Pécs, Research Institute for Viticulture and Oenology, Hungary. E-mail:* kun.agnes@pte.hu

The productivity of the vineyards declines with the appearance of vine decline symptoms, which in turn reduces both competitivity and sustainability, key aspects in modern viticulture. While the susceptibility of cultivated grapevine varieties to vine decline has been studied, the influence of rootstock-scion interactions remains less understood. This study aimed to evaluate the effect of rootstock-scion combinations on vine decline expression in a long-term field experiment involving 'Cabernet Sauvignon', 'Chardonnay', and 'Merlot' grafted onto six different rootstocks: 'T5C', 'TK5BB', '125AA', (V. *berlandieri* x V. *riparia*), '110R', '140Ru' (V. *berlandieri* x V. *rupestris*), and 'Fercal' (V. *vinifera* x V. *berlandieri*). The trial is located on non-irrigated, south-facing steep slopes in the Mecsek Hills, Hungary (46°07' N, 18°17' E, 210-230 m a.s.l.). Twenty-four-year-old vines, cultivated under uniform agronomic conditions, were visually assessed for grapevine trunk disease (GTD)-related symptoms before ripening in 2023-2024. In addition to symptoms scoring, meteorological data, nutrient content of leaf samples, and yield-related parameters (pH, sugar content, and acidity) were evaluated. The results were compared with previous years' data to assess the evolution of vine health and trunk viability. Among the cultivars, 'Cabernet Sauvignon' exhibited the highest incidence of GTD symptoms, while 'Merlot' showed the lowest, based on the average across all rootstocks. Although cultivar susceptibility varied significantly, no consistent pattern of susceptibility emerged among rootstocks. Nevertheless, the rootstock-scion combination clearly influenced vine resilience, longevity, and overall vineyard productivity.

Anatomical characterization of table grape cultivars in relation to susceptibility to *Lasiodiplodia brasiliensis*. E.A. RANGEL-MONTOYA[1,2], I. CÓRDOVA-GUERRERO[1], R. HERNANDEZ-MARTINEZ[2]. *[1]Facultad de Ciencias Químicas e Ingeniería, UABC. [2]Centro de Investigación Científica y de Educación Superior de Ensenada. E-mail:* erangel@cicese.mx

In Mexico, the state of Sonora is the leading producer of table grapes. This crop is significantly affected by trunk diseases fungi, resulting in considerable economic losses. *Lasiodiplodia brasiliensis* is among the most virulent among the trunk pathogens recorded, causing xylem necrosis and vessel occlusion, which disrupt water transport and ultimately lead to plant death. This study aimed to evaluate the anatomical characteristics of eleven table grape cultivars and their potential relationship with susceptibility to *L. brasiliensis* strain MXBCL28. Detached shoots from 'Cotton Candy', 'Flame Seedless', 'Prime Seedless', 'Summer Royal', 'Sweet Celebration', 'Superior', 'Timpson', 'Candy Snaps', 'Sweet Bond', 'Candy Hearts', and 'Sweet Globe' were mechanically wounded, inoculated, and incubated for 15 days in a

growth chamber. Necrotic lesion length was measured to assess susceptibility. For anatomical analysis, non-inoculated shoots were fixed in FAA solution, and 70 µm transverse sections were obtained. Five samples per cultivar were analyzed using a light microscope (Zeiss AxioVert2000), and images captured using a Zeiss AxioCam HRc. Xylem vascular bundle areas were measured using IMAGE J, and the equivalent diameter (D) was calculated using the formula: $D = \sqrt{(4A/\pi)}$. Results showed that 'Cotton Candy' had the largest average vascular bundle diameter (127.1±26.1 µm), followed by 'Summer Royal' (108.5±29.7 µm) and 'Sweet Globe' (108.1±25.9 µm). The smallest diameters were observed in 'Candy Hearts' (53.9±9.8 µm) and 'Candy Snaps' (54.2±9.7 µm). Regarding susceptibility, Prime Seedless' was the most affected cultivar, followed by 'Summer Royal'. In contrast, Candy Hearts', 'Sweet Bond' and 'Flame Seedless' showed lower susceptibility. Further analysis of wood composition is ongoing to allow a better understanding of the relationship between xylem anatomy and susceptibility to *L. brasiliensis*, which may support the development of more resistant grapevine cultivars.

This research was financially supported by the Secretaría de Ciencia, Humanidades, Tecnología e Innovación (SECIHTI), Mexico and Molina group of Hermosillo, Sonora.

The broad host range in *Botryosphaeriaceae*: a result of anthropogenic movement of plant species. I. SILVA-VALDERRAMA[1,2], J.R. ÚRBEZ-TORRES[2], T.J. DAVIES[1,3]. [1]*Department of Botany, University of British Columbia, Vancouver, BC, Canada.* [2]*Agriculture and Agri-Food Canada, Summerland Research and Development Centre, Summerland, BC, Canada.* [3]*Department of Forest and Conservation Sciences, University of British Columbia, Vancouver, BC, Canada. E-mail:* ibsilva26@gmail.com

The *Botryosphaeriaceae* (*Ascomycota*, *Dothideomycetes*) is a diverse fungal family that includes many emerging pathogens of global concern. Some species are considered among the most aggressive pathogens in endophyte communities, causing diseases in a wide array of economically important plants, including Botryosphaeria dieback in grapevines. *Vitis vinifera* (grapevine) hosts the highest diversity of *Botryosphaeriaceae* species; however, little is known about their ecology, host breadth, and the factors that shape their association with plants. Over 27,000 DNA sequences from different loci were gathered to construct a comprehensive phylogenetic tree of the *Botryosphaeriaceae*, revealing a significant influence of both pathogen and plant-host evolutionary histories on fungal-plant associations. The majority of *Botryosphaeriaceae* species were found to be moderate generalists, with some notable exceptions of host hyper-generalists, including *Neofusicoccum parvum*, *Macrophomina phaseolina*, *Botryosphaeria dothidea* and *Diplodia seriata*, all commonly associated with *V. vinifera*. Contrary to the theory that suggests that pathogens should evolve towards host specialization, discrete states models of *Botryosphaeriaceae* indicate an increasing trend towards generalism. Analysis of the external factors influencing the host range of this family demonstrate the importance of anthropogenic movement of plant species, such as grapevines, and agricultural practices in determining the current distribution of *Botryosphaeriaceae* fungi across plant hosts. Understanding the factors that model pathogen-host associations can help predict the likelihood of emerging *Botryosphaeriaceae* fungi in new plant hosts and environments, helping inform efficient regulatory policies in plant and plant-derived products trade and influence the design of agricultural systems to reduce their host breadth expansion and the risk of epidemics.

This work was supported by NSERC Discovery Grant awarded to T. Jonathan Davies (2020).

Host phylogenetic diversity and virulence in *Botryosphaeriaceae*. I. SILVA-VALDERRAMA[1,2], J.R. ÚRBEZ-TORRES[2], T.J. DAVIES[1,3]. [1]*Department of Botany, University of British Columbia, Vancouver, BC, Canada.* [2]*Agriculture and Agri-Food Canada, Summerland Research and Development Centre, Summerland, BC, Canada.* [3]*Department of Forest and Conservation Sciences, University of British Columbia, Vancouver, BC, Canada. E-mail:* ibsilva26@gmail.com

Botryosphaeriaceae are one of the most devastating pathogens of grapevines (*Vitis vinifera*) and several other economically important plants. Globalization, international plant trade, and the lowering of geographical dispersal barriers have increased ecological opportunities for associations between *Botryosphaeriaceae* and novel plant hosts, increasing the risk of emergence and disease epidemics. However, the damage caused by new fungal-plant associations is challenging to predict, with few studies exploring the factors that determine pathogen virulence on a new host. A total of 4000 grapevine cv. Chardonnay dormant canes were collected between 2021 and 2023 and inoculated with 155 *Botryosphaeriaceae* isolates belonging to 32 species obtained from *V. vinifera*. After incubation under controlled conditions in a growing chamber for 10 weeks, canes were dissected, and the area of necrotic tissue was assessed as a measure of pathogen virulence. Canes inoculated with *Neoscyta-*

lidium and *Neofusicoccum* species produced the most extensive necrotic lesions, while *Dothiorella* appeared to be the least virulent genus. Most *Botryosphaeriaceae* isolates showed low virulence in grapevines, with an area of necrosis < 1 cm^2 in 90% of the cases. However, quantile regression models revealed a significant positive relationship between virulence and the phylogenetic diversity of host plants a fungal species was associated with. Accurate data on host breadth of fungal species could help predict the virulence posed in new plant hosts, preventing emerging pathogens becoming the cause of a new outbreak.

This work was supported by NSERC Discovery Grant awarded to T. Jonathan Davies (2020).

Susceptibility of spring shoot thinning wounds to *Eutypa lata* and *Diplodia seriata*. M.R. SOSNOWSKI[1,2], T. FURLAN[1,2], M.R. AYRES[1]. [1]*South Australian Research and Development Institute, Adelaide SA 5001, Australia.* [2]*School of Agriculture, Food and Wine, Waite Research Institute, The University of Adelaide, SA 5005, Australia. E-mail:* mark.sosnowski@sa.gov.au

The grapevine trunk diseases (GTDs) Eutypa (ED) and Botryosphaeria dieback (BD) are caused primarily by infection of winter pruning wounds with spores of the causal fungi, species of the *Diatrypaceae* and *Botryosphaeriaceae*, respectively. Shoot thinning is a canopy management strategy applied in vineyards during spring to alleviate excessive shading of bunches, improve air flow within the canopy and reduce the number of cuts needed during winter pruning. Spore trapping in Australian vineyards has detected GTD pathogens throughout spring and summer in association with rainfall. It is well documented that BD pathogens can infect green grapevine tissue but there is no evidence of green shoot infection by ED pathogen spores. Preliminary shadehouse experiments showed that wounds left following spring shoot removal, by either tearing off or cutting with secateurs, were highly susceptible to artificial inoculation with *Eutypa lata* (ED) and *Diplodia seriata* (BD) spores. A vineyard trial was established to determine whether shoot thinning wounds are susceptible to infection by GTDs in a natural setting. In late September 2023, during dry weather conditions, Shiraz vines in the Barossa Valley at growth stage EL 12 were shoot thinned by manually tearing or cutting the shoot with secateurs. The wounds were inoculated with *E. lata* and *D. seriata* or left uninoculated to monitor natural infection. Isolations onto potato dextrose agar revealed that pathogen recovery was significantly greater from the rough tear wounds (33 and 83%, respectively) than from the smooth cut wounds (13 and 43%, respectively), but there was negligible pathogen recovery from naturally infected wounds (0-11% for both pathogens). The vineyard trial was repeated in 2024, and in 2025 a new trial will compare shoot thinning in dry conditions with during rainfall, when natural spore infection is most likely.

This research was supported by Wine Australia, with levies from Australia's grape growers and winemakers and matching funds from the Australian Government.

Biocontrol comparison of the pathogens *Diplodia seriata* and *Neofusicoccum parvum* in the context of Botryosphaeria dieback on *Vitis vinifera*. X. BESOAIN[1,3], D. CASTILLO-NOVALES[1,2,3], P. VEGA-CELEDÓN[1,2] A. LARACH[1], M. SEEGER[2,3]. [1]*Escuela de Agronomía, Facultad de Ciencias Agronómicas y de los Alimentos, Pontificia Universidad Católica de Valparaíso, San Francisco s/n La Palma, Quillota 2260000, Chile.* [2]*Molecular Microbiology and Environmental Biotechnology Laboratory, Department of Chemistry, Center of Biotechnology Daniel Alkalay Lowitt, Universidad Técnica Federico Santa María, Avenida España 1680, Valparaíso 2390123, Chile.* [3]*Millennium Nucleus Bioproducts, Genomics and Environmental Microbiology (BioGEM), Avenida España1680, Valparaíso 2390123, Chile. E- mail:* Ximena.besoain@pucv.cl

Botryosphaeria dieback is one of the most significant trunk diseases affecting vineyards worldwide, and it is associated with various fungi of the *Botryosphaeriaceae* family. This presentation compares the pathogenic profiles of *Diplodia seriata* and *Neofusicoccum parvum* based on pathogenicity and biocontrol trials conducted under field conditions on shoots and branches of *Vitis vinifera*, using Cabernet Sauvignon and Sauvignon Blanc varieties. These trials were conducted at the La Palma Experimental Station, Quillota, Chile. The pathogens were inoculated with 50 µl of a spore concentration of $1*10^4$ conidia mL^{-1}, and the bacteria were inoculated (1 day before pathogen inoculation) by applying 50 µL of $1*10^8$ cfu mL^{-1} to each cut. The results showed apparent pathogenic differences between the two pathogens according to the type of affected tissue. *D. seriata* was more aggressive in wood older than 7 years, while *N. parvum* showed greater severity in young shoots. At the variety level, Sauvignon Blanc was consistently more susceptible than Cabernet Sauvignon to both pathogens on young shoots. Regarding average severity, *N. parvum* had higher values for lesion length on Cabernet Sauvignon and Sauvignon Blanc compared to *D. seriata* on shoots.

Diplodia seriata had higher values of lesion length on Cabernet Sauvignon and Sauvignon Blanc than *N. parvum* on the trunk (10-year-old tissue. On the other hand, there were interesting biocontrol effects at different temperatures of *N. parvum* and *D. seriata* and their confrontation with biocontrollers at low, medium, and high temperatures. These findings indicate a differentiation in the mechanisms of infection and damage according to the pathogen, tissue, and variety, which is key for designing integrated management strategies and targeted application of biocontrol agents.

This research was financially supported by the project Millennium Nucleus Bioproducts, Genomics and Environmental Microbiology (BioGEM) NCN_2023-054

The endophytic bacterium *Erwinia billingiae* may promotes the virulence *Phaeomoniella chlamydospora*. D. SZABÓ[1], Á. NOVÁK[1], N. MOLNÁR[1], A. GOMBA-TÓTH[1], X. PÁLFI[1], K.Z. VÁCZY[1], Z. KARÁCSONY[1]. [1]*Eszterházy Károly Catholic University, Food and Wine Research Institute, Leányka str. 8/G, Eger, H3300, Hungary, E-mail:* karacsony.zoltan@uni-eszterhazy.hu

Phaeomoniella chlamydospora (Pch) among the fungal causal agents of Esca is considered a "pioneer" pathogen. The pathogenesis of Esca has an exceptionally long latent period, suggesting that the pathogens grow as harmless endophytes in the host for a long period and their pathogenic behavior is triggered by rare events like excessive stress, or the establishment of microbial interactions. An increasing number of studies suggest that bacterial endophytes may contribute to the development of Esca. A total of 54 grapevine endophytic bacterial strains were screened in confrontation assays against a Pch isolate. Strain TKP9/2 – belonging to *Erwinia billingiae* species according to 16S rDNA sequence – showed increased growth on the Pch mycelial mat compared to the not pre-inoculated medium. The interaction of TKP9/2 with Pch was tested further using three additional Pch strains. Growth assays carried out on a solid medium showed that both fungi and the bacterium can establish mixed cultures, and their interaction depends on the available carbon source. On a sugar mixture mimicking the grapevine xylem sap, Pch and TKP9/2 mutually promoted each other's growth. The microbes did not affect the growth of the confrontation partner on cellulose and starch carbon sources, while TKP9/2 inhibited the growth of Pch strains on pectin. Further experiments on media with sucrose carbon source showed that TKP9/2 increases the production of melanin and pullulan by Pch and it also promoted the ability of the fungus to degrade phenolics. This latter process believed to take part in the virulence of Pch. In artificially infected shoots, the co-inoculation of TKP9/2 with the Pch strains led to a significant decrease in photosynthetic pigment content of leaves. The above results suggest that *E. billingiae* may play a role in the pathogenesis of Esca, by increasing the growth as well as the production of some virulence factors in Pch.

This research was financially supported by the National Research, Development and Innovation Office through project OTKA_K143453.

Transcriptional changes in grapevine patrimonial varieties following *Botryosphaeriaceae* infection. J. CHILIAN, D. GRINBERGS, M. ISLA, C. FERNÁNDEZ. *Instituto de Investigaciones Agropecuarias INIA-Quilamapu. Av. Vicente Méndez 515, Chillán. Chile. Fruit Pathology Laboratory. E-mail:* jchilian@inia.cl

Grapevine trunk diseases (GTDs) pose a significant threat to the productivity and longevity of vineyards in Chile. While these diseases have been extensively studied in commercial cultivars such as Cabernet Sauvignon, Sauvignon Blanc, Merlot, and Chardonnay, there is limited information available for patrimonial vineyards, which are primarily composed of cultivars like País, Moscatel, Cinsault, and Carignan. In southern Chile, the most prevalent and virulent GTD pathogens in these vineyards belong to the *Botryosphaeriaceae* family, particularly *Neofusicoccum parvum* and *Diplodia* spp. This study aimed to characterize and compare transcriptional changes in defense-related genes during colonization by *N. parvum* and *Diplodia* spp. in the Cinsault and País cultivars. Healthy plants were inoculated with mycelial discs from virulent strains of both pathogens. Three treatments were applied: (i) plants inoculated with the pathogen, (ii) plants inoculated with sterile agar discs (control), and (iii) uninoculated plants. Wood samples were collected at 0-, 3-, and 24-hours post-inoculation for RNA extraction. Gene expression was assessed using quantitative RT-PCR (qPCR), focusing on key genes associated with fungal defense responses. The results showed that genes involved in reactive oxygen species (ROS) detoxification were expressed at levels up to four times higher in inoculated plants. Additionally, PAL and NPR1, which are associated with downstream defense signaling pathways, were also upregulated. No significant differences in gene expression were observed between the two cultivars. Identifying these differentially expressed genes enhances our understanding of the molecular response to *Botryosphaeriaceae* infection and

may inform future grapevine breeding programs, including marker-assisted selection for GTD resistance.

This research was financially supported by the Project Fondef ID23I10398, Agencia Nacional de Investigación y Desarrollo, ANID.

Mycobiome analysis reveals *Truncatella* and *Seimatosporium* spp. as potential contributors of grapevine trunk disease complex in Oregon vineyards. A.N. KC[1,2], J. ZIMMERMAN[2]. [1]*Southern Oregon Research and Extension Center, 569 Hanley Rd, Central Point, OR 97502;* [2]*Department of Botany and Plant Pathology, Oregon State University, 2082 Cordley Hall, Corvallis, OR 97331. E-mail: achala.kc@oregonstate.edu*

Grapevine trunk diseases (GTDs) are caused by many fungal pathogens that colonize and block xylem vessels and eventually lead to stunted shoot growth and vine decline. To advance our understanding of the grapevine fungal microbiome and to explore how fungal communities vary along gradients of GTD disease incidence, and geography in Oregon, we conducted a metabarcoding study, amplifying the ITS1 region of fungal rDNA extracted from trunk tissues. The samples were collected from 29 vineyards in the Rogue and Willamette Valleys (N = 396). In terms of average relative abundance, it was dominated by *Ascomycota* (85.15%) and *Basidiomycota* (14.29%). Across all OTUs there were 576 genus level identifications, the most abundant of which were *Cladosporium* (30%), *Penicillium* (8%), *Seimatosporium* (7%), *Alternaria* (5%), and *Aureobasidium* (5%). Although many GTD genera had a low relative abundance, vineyard level detection was often high. *Truncatella* and *Seimatosporium* were detected in 100% of vineyards, *Phaeomoniella* and *Phaeoacremonium* in 93%, *Cadophora* and *Botryosphaeria* in 79%, and *Dothiorella* in 57% of the vineyards. On average, GTD associated genera were detected in a higher percentage in the Willamette Valley than in the Rogue Valley (Willamette mean = 12%, Rogue mean = 6%, $P < 0.001$). *Phaeoacremonium*, *Phaeomoniella*, *Botryosphaeria*, and *Neonectria* were detected notably more in the Willamette Valley. Within the two locations, *Seimatosporium* and *Truncatella* were detected in the highest percentage in both valleys. These results suggest that among the major players of GTD in Oregon vineyards, *Seimatosporium* and *Truncatella* spp. also contribute to the GTD complex, and their roles need to be further investigated.

This research was financially supported by the Oregon Wine Board and Northwest Center for Small Fruits Research.

Limited influence of pruning practice on the fungal community of asymptomatic Esca-infected grapevines. K. CORRALES-ADAME[1], E. ATTARD[1], C. GASSIE[1], E. BRUEZ[2], R. HAIDAR[1], A. YACOUB[1], R. TRAVADON[1,3], P. REY[1], R. GUYONEAUD[1]. [1]*Université de Pau et des Pays de l'Adour/E2S/CNRS, Institut des Sciences Analytiques et de Physico-Chimie pour L'Environnement et les Matériaux (IPREM), UMR 5254, 64000, Pau, France.* [2]*Université de Bordeaux INP, INRAE, UMR 1366, ISVV, 33140 Villenave d'Ornon, France.* [3]*Department of Plant Pathology, University of California, One Shields Avenue, Davis, CA, 95616, USA. E-mail:* kcorrales@univ-pau.fr

Esca complex, one of the main GTDs associated with wood-colonizing fungi, alters the vascular system, reducing water and nutrients transport through the plant. During pruning season, cutting wounds becomes a potential entry point for fungal pathogens. We hypothesized that pruning practices influence the vine microbiome as a proxy for disease progression. For a 2-year survey, we selected ten asymptomatic grapevines (*Vitis vinifera* cv. Ugni Blanc) per sampling time; five pruned with a virtuous method (leaving ~4 cm of the branch to preserve sap flow), and five pruned with a non-virtuous method. We evaluated the diversity of fungal communities (ITS2 region) across 7 different plant tissues: arms, healthy and necrotic trunk and graft union. Here we present the results from the first sampling (February 2024). We showed that *Phaeomoniella chlamydospora*, a key causal agent of Esca, was the most abundant taxa with a global representation of 28%. Alpha diversity of the fungal communities didn't reveal significant differences between the two pruning methods across most plant tissues. However, in graft union tissues, fungal diversity was higher for vines pruned with the non-virtuous method. For beta diversity, our results indicated the health status of the vine tissue (i.e., healthy vs. necrotic) was the main factor to differentiate the fungal communities (R^2 = 28%) followed by 9% for type of plant tissue and 0.3% for pruning method. Overall, our results suggest that pruning practices have limited influence on the fungal community in asymptomatic vines. However, the variations observed in the graft union communities may indicate that roots tend to respond more dynamically to environmental disturbances. These findings recommend that further research should be done about the presence of Esca-related pathogens in soil and how the roots are influenced by pruning practices, since it could facilitate their colonization through the aerial and underground parts of the vine.

This work was supported by the Industrial Chair "WinEsca" funded by the ANR (French National Research Agency, grant

number ANR-22CHIN-0002-01), as well as the JAs Hennessy & Co and GreenCell companies.

Characterization of the microbiome of spontaneous grapevines. Building a reference standard. G. DEL FRARI[1,2], F. MARRONI[1], M. GUAZZINI[1], F. MARCOLIN[3,4], S. PONTE[1], R. BOAVIDA FERREIRA[2], G. ZDUNIC[5], G. DI GASPERO[6], M. MORGANTE[1,6]. *[1]Department of Agricultural, Food, Environmental and Animal Sciences, University of Udine, Via delle Scienze 206, 33100 Udine, Italy. [2]LEAF—Linking Landscape, Environment, Agriculture and Food—Research Center, Instituto Superior de Agronomia, Associated Laboratory TERRA, Universidade de Lisboa, Tapada da Ajuda, 1349-017 Lisbon, Portugal. [3]Forest Research Centre, Associated Laboratory TERRA, Instituto Superior de Agronomia, Universidade de Lisboa, Tapada da Ajuda, 1349-017 Lisbon, Portugal. [4]CIBIO/InBIO, Centro de Investigação em Biodiversidade e Recursos Genéticos, Instituto Superior de Agronomia, Universidade de Lisboa, Tapada da Ajuda, 1349-017 Lisbon, Portugal. [5]Institute for Adriatic Crops and Karst Reclamation, Put Duilova 11, 21000 Split, Croatia, [6]Istituto di Genomica Applicata, via Jacopo Linussio 51, I-33100 Udine, Italy. E-mail:* giovanni.delfrari@uniud.it

The grapevine microbiome is crucial for plant health and may play roles in grapevine trunk diseases (GTD). Endophytes are believed to help grapevines cope with biotic stress, but defining a "healthy" endophytic microbiome is challenging. Over a century of agricultural practices, including pruning, grafting, and fungicide application, have significantly altered the microbiome, with changes likely passed through clonal propagation. To identify a native microbiome, undisturbed grapevine stocks in natural environments, presumably originating from seedlings, provide an ideal model. Spontaneous grapevine populations, likely representing individuals of the crop progenitor (*Vitis vinifera* subsp. *sylvestris*), may offer these conditions. In this study, we used DNA metabarcoding, targeting the ITS gene (ITS1F2-ITS2 primer set; AVITI® sequencing), to investigate the microbial diversity of wood, rhizoplane and soil of spontaneous grapevines found in Portugal, Croatia, and Italy. Our data reveal that grapevines host significantly different microbial communities across sampling sites and plant materials. In wood, taxa *Cladosporium* spp. and *Alternaria alternata* were frequently observed, even though among the most abundant -across sampling sites- we found *Trichoderma lixii* and *Sebacina* sp., both rarely reported in the wood of cultivated grapevines. Several wood pathogens were detected, with *Phaeomoniella chlamydospora*, *Phaeoacremonium* spp., *Diaporthe ampelina*, and *Neofusicoccum parvum* ranking among the 20 most abundant taxa. These fungi were highly abundant in 20–30% of sampled grapevines, where they dominated the microbial community. Wood from these individuals also exhibited GTD-related symptoms, such as brown wood streaking and necrotic lesions. When comparing symptomatic and asymptomatic wood, significant differences were observed for multiple alpha diversity indices (Simpson, Shannon, Pielou's; $P < 0.05$), suggesting microbial dysbiosis. Interestingly, white rot symptoms were never detected, and *Fomitiporia mediterranea*, a white rot agent associated with GTD-affected vineyards, was absent from spontaneous grapevines. This study provides valuable insights into the microbiome composition of wild grapevines, which may contribute to future efforts of microbiome manipulation in cultivated varieties.

This research was financially supported by the European Union under a Marie Skłodowska-Curie Postdoctoral Fellowship, project WildWoodMicrobes (GA101064232).

Impact of nursery-inherited microbiome and pathobiome on health and productivity of a young vineyard. C. TODD, P. ROLSHAUSEN. *University of California, Riverside. Department of Botany and Plant Sciences, Riverside CA, USA. E-mail:* philrols@ucr.edu

This work focuses on the grapevine microbiome dynamic of the rhizosphere, root and wood endosphere from the nursery to the vineyard. The research goals were to determine the extent to which microbial inheritance from nursery shapes the microbiome of young grapevine and its impact on vine vigor and yield. We hypothesize that the microbial communities inhabiting the grapevine endosphere are relatively stable and shaped by cultural practices in nurseries. In contrast the communities composing the rhizosphere and root endosphere are highly dynamic and largely influenced by the vineyard soil. We used two Cabernet Sauvignon and Chardonnay cultivars grafted on 1103P rootstock from two nurseries that were planted in a commercial vineyard in California. We collected samples from the trunk above the graft union (scion), below the graft union (rootstock) and at the crown (rootstock), as well as from the root and the rhizosphere. Samples were collected on nursery vines prior to planting and in the vineyard every year for three consecutive years after planting. The fungal and bacterial taxa were profiled using an amplicon-based metagenomic Illumina sequencing approach. In parallel, trunk diameter (year 1-3), pruning weight (year 2-3), and yield (year 3) were recorded. Results show a strong imprint of the nursery vines on microbial communities that faded over time,

although microbial turnover was much faster in the rhizosphere than in the trunk. Many grapevine trunk disease pathogens originated from the two nurseries and the incidence of some of them increased overtime, although it did not appear to significantly affect vine vigor or yield. Results also identified several beneficial organisms that that may correlate with yield. The outcome from this work underscores the importance of the nursery life stage on the core microbiome of grapevine and its implication on vineyard productivity outcome.

This research was supported by the California Department of Food and Agriculture.

Soil microbiota exerted plant opportunistic disease-suppressive function by integrating various beneficial strains counteracting different pathogens. Y.H. LI[1], X.F. WANG[1], J.W. WU[1,2], W. ZHANG[1], X.C. WANG[1], H. WANG[1], J.B. PENG[1], J.Y. YAN[1]. *[1]Beijing Key Laboratory of Environment Friendly Management on Fruit Diseases and Pests in North China, Institute of Plant Protection, Beijing Academy of Agriculture and Forestry Sciences, Beijing 100097, China. [2]College of Bioscience and Resources Environment, Beijing University of Agriculture, Beijing 100096, China. E-mail:* liyonghua@baafs.net.cn

Opportunistic infections caused by pathogenic microbes pose a serious threat to plant health and productivity. It is commonly recognized that soil microorganisms possess a strong potential to suppress the occurrence of plant diseases. However, it remains unclear whether the soil microbiome can exert disease-suppressive function in cases of complex opportunistic plant diseases caused by diverse pathogens. Grapevine trunk diseases (GTDs) represent a kind of typical opportunistic diseases caused by pathogenic fungi and are major threats to viticulture in most grapevine growing regions. Here, we elucidated the critical importance of microbiome homeostasis in grapevine roots for the development of GTDs through microbiome analysis, microbial isolation, and greenhouse inoculation experiments. Symptomatic vines exhibited reduced complexity in co-occurrence networks and were enriched in *Fusarium* spp. Inoculation experiments demonstrated that co-infection with *Fusarium* spp. and GTD pathogens led to increased abundance of the inoculated GTD pathogen and exacerbated disease symptom severity in grapevines. Asymptomatic samples were enriched with *Pseudomonas* spp. and *Bacillus* spp., and this supplementation could effectively suppress the activity of the pathogenic fungi and significantly reduce the pathogen abundance of grapevine roots and trunks. Syncoms constructed based on *Pseudomonas* spp. and *Bacillus* spp. exhibited higher capacity in pathogen inhibition than single bacterial strains. The symcoms composed of different strains displayed the highest inhibitory abilities counteracting *Fusarium* spp. and GTDs pathogens. Taking together, our findings highlight the role of soil microbes in fighting disease and supporting plant health, and indicate the potential of using microbial inocula to fight plant opportunistic diseases.

This research was financially supported by the National Natural Science Foundation of China (32302459), Innovation Ability Building Project of the Beijing Academy of Agriculture and Forestry Sciences (KJCX20251102) and China Agriculture Research System of MOF and MARA (CARS-29).

Seasonal succession of *Cytospora* fungal communities in grapevine pruning wounds. C. LEAL[1], M. ŠPETÍK[2], A. EICHMEIER[2], R. BUJANDA[1], D. GRAMAJE[1]. *[1]Instituto de Ciencias de la Vid y del Vino (ICVV), Consejo Superior de Investigaciones Científicas - Universidad de la Rioja - Gobierno de La Rioja, Ctra. LO-20 Salida 13, Finca La Grajera, 26071 Logroño, Spain; [2]Mendeleum—Institute of Genetics, Mendel University in Brno, Valticka 334, 691 44 Lednice, Czech Republic. E-mail:* catarina.leal@lcvv.es

Cytospora canker, a grapevine trunk disease (GTD) caused by various species within the genus *Cytospora*, is a significant threat to vineyard longevity and productivity. While it has been extensively studied in North America, its occurrence, species composition, and ecological dynamics remain poorly understood in European viticulture. This study aimed to investigate the ecology and temporal behavior of *Cytospora* spp. colonizing grapevine pruning wounds and to explore how interannual climatic variability influences their species composition and diversity. Over three consecutive growing seasons (2020–2023), pruning wounds were monitored in a commercial 'Tempranillo' vineyard planted in 2001 in Samaniego, Álava (Northern Spain). Each February, 1-year-old canes were spur-pruned, and after 12 months, symptomatic wood samples were collected and processed for fungal isolation. A total of 372 *Cytospora* isolates were obtained and identified through multilocus sequencing of the ITS, ACT, and TEF regions. Six species were detected, with *C. viticola* being the most prevalent (87% of isolates), followed by *C. ribis, C. ceratosperma*, and others. Alpha diversity (Shannon and Simpson indices) and species richness fluctuated across years, showing strong correlations with climatic conditions—particularly temperature and relative humidity—during the critical infection window (March–April). The 2022 sea-

son, characterized by warm temperatures and moderate rainfall, supported the most diverse and evenly distributed *Cytospora* community. In contrast, the colder and much drier 2023 season, despite high humidity, showed a marked decline in richness and community evenness, with a near-monodominant structure. These findings suggest that temperature and moisture availability play pivotal roles in mediating infection success and species interactions. Principal Component Analysis further revealed distinct annual shifts in community composition, reflecting ecological niche partitioning and adaptive responses to environmental variation. This study provides novel insights into the ecology and environmental responsiveness of *Cytospora* species in grapevine pruning wounds and highlights the importance of integrating climate factors into GTD management and pruning timing strategies.

Preliminary characterization of volatile compounds against *Neofusicoccum parvum* on *Vitis vinifera* under biocontrol conditions. D. CASTILLO-NOVALES[1,2,3], P. VEGA-CELEDÓN[1,2,3], A. LARACH[1,2], M. SEEGER[2,3], X. BESOAIN[1,3]. [1]*Escuela de Agronomía, Facultad de Ciencias Agronómicas y de los Alimentos, Pontificia Universidad Católica de Valparaíso, San Francisco s/n La Palma, Quillota 2260000, Chile.* [2]*Molecular Microbiology and Environmental Biotechnology Laboratory, Department of Chemistry, Center of Biotechnology Daniel Alkalay Lowitt, Universidad Técnica Federico Santa María, Avenida España 1680, Valparaíso 2390123, Chile.* [3]*Millennium Nucleus Bioproducts, Genomics and Environmental Microbiology (BioGEM), Avenida España1680, Valparaíso 2390123, Chile. E-mail:* diyaniracastillonovales@gmail.com

Using plant growth-promoting bacteria as biocontrol agents represents a sustainable strategy for managing grapevine stem diseases. In this study, the production of volatile organic compounds (VOCs) was characterized under confrontation between native bacterial strains and the pathogen *Neofusicoccum parvum*. These assays were conducted on solid media under controlled conditions, and VOCs were collected by solid-phase microextraction (SPME) and analyzed by gas chromatography- mass spectrometry (GC-MS). More than 40 compounds were identified, including monoterpenes such as α-pinene and β-pinene, alcohols such as phenylethyl alcohol, cyclic ketones such as isophorone, and sesquiterpenes such as γ-muurolene, δ-cadinene, and trans-calamenene. The chemical profiles varied significantly among treatments, with higher relative abundances of compounds such as 1-undecene, palustradiene A/B, and (+)-2-bornanone observed under the highest fungal growth inhibition conditions. The differential presence of these VOCs suggests an active role in the inhibition of *N. parvum* and lays the groundwork for their potential use as biomarkers.

This research was financially supported by the project Millennium Nucleus Bioproducts, Genomics and Environmental Microbiology (BioGEM) NCN_2023-054.

Grapevine Trunk Diseases in Greece: fungi involved in discrete geographical zones and wood microbiome analysis in symptomatic and asymptomatic vines. S.G. TESTEMPASIS[1], E.A. MARKAKIS[2,3], F. BEKRIS[4], S. VASILEIADIS[4], G.I. TAVLAKI[3], S. SOULTATOS[2,3], C. TSOUKAS[5], A. SAMARAS[1], D. GKIZI[5], A. TZIMA[5], E. PAPLOMATAS[5], D.G. KARPOUZAS[4], G.S. KARAOGLANIDIS[1].[1]*Aristotle University of Thessaloniki, Department of Agriculture, 54124 Thessaloniki, Greece.* [2]*School of Agricultural Sciences, Hellenic Mediterranean University, Stavromenos 71004, Heraklion, Crete, Greece.* [3]*Institute of Olive Tree, Subtropical Crops and Viticulture, Hellenic Agricultural Organization "DIMITRA", Kastorias 32A, 71307, Heraklion, Crete, Greece.* [4] *University of Thessaly, Department of Biochemistry and Biotechnology, 41500 Larissa, Greece,* [5]*Agricultural University of Athens, School of Plant Sciences, Department of Crop Science, Iera Odos 75, Votanikos, 11855 Athens, Greece. E-mail:* gkarao@agro.auth.gr

Grapevine trunk diseases (GTDs) are caused by wood-inhabiting pathogenic fungi from a wide range of genera. This study aimed to investigate the incidence and etiology of GTDs in three distinct geographic regions of Greece (Crete, Nemea, and Amyntaio), and to characterize the fungal and bacterial microbiomes in the wood of symptomatic and asymptomatic vines using amplicon sequencing. A total of 310 vineyards were surveyed, and 533 fungal strains were isolated from diseased vines. Morphological and molecular analyses revealed that the isolates belonged to 35 distinct fungal genera. The composition of GTD-associated fungal populations varied significantly between geographic zones. *Phaeomoniella chlamydospore* was most prevalent in Heraklion, while *Diplodia seriata* predominated in Nemea and Amyntaio. Multi-gene sequencing (rDNA-ITS, LSU, tef1-α, tub2, and act), combined with pathogenicity tests, revealed several fungal species—*Neosetophoma italica*, *Seimatosporium vitis*, *Didymosphaeria variabile*, and *Kalmusia variispora*—as potential GTD agents newly reported in Greece. Amplicon sequencing analysis showed that the combined factor of cultivar and biogeography was the strongest determinant of the wood fungal microbiome

($P < 0.001$, 22.7%), followed by GTD symptom status ($P < 0.001$, 3.5%). Several fungal Amplicon Sequence Variants (ASVs), including *K. variispora*, *Fomitiporia* spp., and *P. chlamydospora*, were positively associated with symptomatic vines. Random Forest analysis identified *P. chlamydospora*, *K. variispora*, *Alternaria alternata*, and *Cladosporium* sp. as highly accurate predictors of symptomatic vines (0% error rate). The bacterial wood microbiome exhibited similar patterns, with biogeography/cultivar being the primary driver of composition ($P < 0.001$, 25.5%), followed by GTD symptom status ($P < 0.001$, 5.2%). Differential abundance analysis revealed a consistent positive correlation ($P < 0.001$) between *Bacillus* and *Streptomyces* ASVs and asymptomatic vines. Network analysis identified a significant negative co-occurrence between these beneficial bacterial genera and the pathogens *Phaeomoniella*, *Phaeoacremonium*, and *Seimatosporium*. In conclusion, this study discusses the associations of GTD pathogens with vine age, cultivar, and prevailing climatic conditions across different Greek viticultural zones. It also highlights the potential protective role of *Bacillus* and *Streptomyces* against GTD pathogens in the grapevine wood microbiome.

This research was financially supported by Greek national funds through the Public Investments Program (PIP) of the General Secretariat for Research & Technology (GSRT), under the Emblematic Action "Routes of Vineyards", Grant No. 6070.03.

Exploring the table grape microbial community for the identification of new potential biocontrol agents to manage grapevine trunk diseases. A. AGNUSDEI[1], D. SALAMONE[1], P. TANCREDI[1], F. DALENA[1], D. GERIN[1], D. CORNACCHIA[1], G.L. BRUNO[1], F. MANNERUCCI[1], F. FARETRA[1], S. MAVICA[2], D. AIELLO[2], S. POLLASTRO[1]. *[1]Department of Soil, Plants and Food Sciences, University of Bari Aldo Moro, via Amendola 165/A, Bari, Italy. [2]Department of Agriculture, Food and Environment, University of Catania, via S. Sofia, 100, Catania Italy. E mail:* francesco.faretra@uniba.it*;* dalia.aiello@unict.it

The antagonistic activity of *Aphanocladium album, Clonostachys rosea*, *Trichoderma* spp., *Bacillus* spp., *Streptomyces* spp. and *Pseudomonas* spp., selected as representative of the microbial communities of table grapes varieties from southern Italy, was investigated against GTDs pathogens. In a dual culture assay, an inhibition of the growth of *Neofusicoccum parvum* (37-62%), *Eutypa lata* (34-63%), *Diplodia seriata* (50-64%), *Cylindrocarpon destructans* (22-79%), *Phaeomoniella chlamydospora* (37%) and *Diaporthe neoviticola* (47 71%) was determined by 16 different *Trichoderma* species. A deadlock at mycelial contact was observed during the interactions between *A. album* and *Fomitiporia mediterranea* or *Phaeoacremonium minimum*, while the growth of the pathogens was stopped by the contact with *C. rosea*. *Bacillus amyloliquefaciens* (D747) and *Bacillus subtilis* (QST 713) moderately limited the growth of *N. parvum* (34 and 33%, respectively) and *E. lata* (13% and 16%, respectively). The ability of the BCAs to produce toxicants was evaluated by growing them in liquid media under stress conditions. An inhibition in the growth of *D. seriata* (60%), *E. lata* (76%), *N. parvum* (50%), *C. destructans* (30%), *P. minimum* (15%) and *D. neoviticola* (71%) was observed when the culture filtrate of *C. rosea* was added to growth media. Furthermore, the antifungal effect of possible volatile organic compounds was evaluated. Using the sandwich system, an inhibition in the growth of *P. chlamydospora* (24-58%), *C. destructans* (2-49%) and *P. minimum* (4-46%) was determined by 16 *Trichoderma* spp. The growth of *C. destructans* and *P. chlamydospora* was affected by *A. album* (7 and 29%, respectively), *C. rosea* (36 and 26%, respectively), *B. amyloliquefaciens* (D747) (10 and 39%, respectively), B. subtilis (QST 713) (3 and 37%, respectively), while the growth of *P. minimum* was also affected by *B. amyloliquefaciens* (D747) (30%). These results highlight the potential of members of the table-grape microbial communities as a promising approach to control GTDs-associated fungal pathogens.

This research was financially supported by the Project "New Therapeutic Approaches to Reinforce the natural Grapevine microbiomE against Grapevine Trunk Diseases (TARGET_GTDs)", P2022ENPCL, PNRR Missione 4 "Istruzione e Ricerca" - Componente C2 Investimento 1.1, "Fondo per il Programma Nazionale di Ricerca e Progetti di Rilevante Interesse Nazionale (PRIN)".

Ten years of non-virtuous pruning on Ugni blanc: a decline acceleration? E. BRUEZ[1], C. CHOLET[*], T. MARTIGNON[2], M. GIUDICI[2], M. BOISSEAU[3], X. POITOU[3], P. COLL[3], P. REY[4], L. GENY[1]. *[1]UMR Oenologie, EA 4577, Université de Bordeaux, INRAE, BSA, Institut des Sciences de la Vigne et du Vin, 210 Chemin de Leysotte - CS 50008, 33882 Villenave d'Ornon, France.[2] Simonit&Sirch, Maîtres Tailleurs de Vigne, 1 Rue Porte des Benauges, 33410 Cadillac, France. [3] Hennessy Jas et Cie, 1 rue Richonne 16100 Cognac, France. [4] Université de Pau et des Pays de l'Adour, E2S UPPA, CNRS, Institut des Sciences Analytiques et de Physicochimie pour l'Environnement et les Matériaux - UMR 5254, IBEAS*

Avenue de l'Université 64013, Pau, France Pau et Bordeaux. E-mail: emilie.bruez@u-bordeaux.fr

Ever since the ban of sodium arsenite, researchers have been trying to find alternative solutions to deal with grapevine trunk diseases (GTDs). Amongst other methods, quality of pruning is currently being used in attempts to protect the vines against pathogen entry and thus prolong grapevine life. Utilising an Ugni blanc vineyard planted in 2006, conducted in double Guyot-Poussard, this research aimed to demonstrate the effects of different pruning methods commencing from 2016 on vine decline over 10 years. Virtuous pruning leaves a chicot and preserves the diaphragm, unlike non-virtuous pruning, which damages the diaphragm. The diaphragm is a natural internal partition within the node of a vine shoot that acts as a barrier, helping to isolate wounds, thus protecting the vine from pathogens entry. Our experiment, which focused on the zone of desiccation formation of the wood below the pruning wound. It examined the correlation between spur diameter and the depth of desiccation, and also measured the evolution of desiccation cones according to the pruning quality. To verify the impact of non-virtuous pruning on the sap flow, sensors were put on the cordons of non-esca-foliar symptomatic plants each year from 2021 to 2024 for measurements. During the summer, other physiological indicators, transpiration and gas exchanges, were monitored in the vines. No correlations were demonstrated between the diameter spur and the necrotic zone depth. The sap flow seemed to be lower for the non-virtuous pruning vines and particularly the warm season (in 2022). The results of the other physiological indicators did not show any differences between the two pruning methods. However, the grape yield was impacted with a lower production with the non-virtuous pruning. More vines expressed esca-foliar symptoms in the non-virtuous modality, after 5 years of pruning. In conclusion, the non-virtuous pruning promotes significant development of an internal desiccation cone which has a negative medium-term impact on sap flow. So, retaining the diaphragm helps to protect the sap flow and allows the sap flow path to function fully and longer, and avoid decline acceleration.

This research was financially supported by the Project Chaire Industrielle WinEsca

Exploring grapevine microbial-based inoculants for trunk disease management: comparing a custom endophytic-based microbial synthetic community with a commercial microbial inoculum. W. CHITARRA[1,2], C. PAGLIARANI[2], L. MOFFA[1], NERVA[1,2]. [1]*Council for Agricultural Research and Economics, Research Centre for Viticulture and Enology (CREA-VE), Via XXVIII Aprile 26, 31015 Conegliano (TV), Italy.* [2]*National Research Council of Italy - Institute for Sustainable Plant Protection (CNR-IPSP), Strada delle Cacce 73, 10135 Torino (TO), Italy. E-mail:* walter.chitarra@crea.gov.it

Microbial inoculants for grapevine protection and growth promotion are commercially available, but only a few rely on microbial strains originally isolated from grapevine tissues. In this study, we developed a synthetic microbial consortium (SynCom) composed of seven endophytic bacterial strains isolated from grapevine woody tissues and selected based on their *in vitro* antagonism activity against key fungal pathogens associated with grapevine trunk diseases (GTDs). We hypothesized that a grapevine-specific SynCom would offer greater protective efficacy. To test this, we compared its effects with a commercial inoculant containing a mixture of arbuscular mycorrhizal fungi and a rhizospheric *Bacillus coagulans* strain (AMF+B). Grapevine cuttings were inoculated either with the SynCom or with the AMF+B product, while other vines served as uninoculated controls (CTRL). Following field transplant, gas exchange parameters were monitored on inoculated and CTRL plants, and stilbenes analyses were performed on leaf and root samples collected at the end of the experiment. Additionally, RNAseq in SynCom plants and root microbiome dynamics along treatments in root tissues were also investigated. Under the tested conditions, the customized SynCom successfully activated the plant's defence machinery at molecular level, leading to a significant accumulation of stilbenes in both leaves and roots. This protective effect was accompanied by a reduction in photosynthesis, indicating an energy shift towards defense. Conversely, the AMF+B treatment promoted more balanced physiological performance while still enhancing defence compounds. Notably, the metabarcoding analysis showed a reduced abundance of GTD-related pathogens in SynCom-treated plants. These findings highlight the potential of tailored SynComs, composed of biocontrol agents, for managing GTDs, particularly in vineyards under high disease pressure. This work highlights the value of microbiome-based practices in viticulture and encourages further development of SynCom strategies, including cross-kingdom designs, to support sustainable management of grapevine trunk diseases.

This research was financially supported by the LegnoSano project by the Fondazione Cariverona (Project ID 53737 - 2023.0094) and CIRCOVINO project (founded by

the Italian Ministry of Environment and Energy Security, EC-DEC n. 86 of 07 September 2023). This study was also conducted within the Agritech National Research Center and received funding from the European Union Next-Generation EU (PIANO NAZIONALE DI RIPRESA E RESILIENZA (PNRR)—MISSIONE 4 COMPONENTE 2, INVESTIMENTO 1.4—D.D. 1032 17/06/2022, CN00000022) and Shield4Grape project in the frame of Horizon Europe program (Grant agreement 101135088). This manuscript reflects only the authors' views and opinions, neither the European Union nor the European Commission can be considered responsible for them.

Evaluation of the retroactive effect of Mamull® in the control of *Diplodia seriata* in grapevines in Chile. W. HETTICH[1], E. DONOSO[1], L. ROMERO[1], M. PACHECO[2], J. CABALLERO[2]. [1]*Bio insumos Nativa, parcela antilhue lote 4b2, Maule.* [2] *Fitonova SPA, parcela antilhue lote 4b2, Maule. E-mail:* edonoso@bionativa.cl

The implementation of biological control in the management of wood diseases raises critical questions about optimal application timing during pruning. Previous trials in Peru using *Lasiodiplodia theobromae* demonstrated a retroactive effect of Mamull (a formulation of *Trichoderma spp.* and *Bionectria ochroleuca*) up to 48 hours post-inoculation. This study aimed to assess the effectiveness of Mamull application timing under natural infection conditions. The trial was conducted in Talca, Chile, on 35-year-old Semillón grapevines, trained on Spanish trellises with a high *Diplodia seriata* pressure. A 2x5 factorial randomized design was employed: two treatments (Control and Mamull®) at 100 g hL^{-1} + Break at 10 cc hL^{-1}, and seven post pruning applications intervals (0, 24, 48, 72, 96, 120, and 144 hours). Treatments were applied using a turbo-fogger at 600 L ha^{-1}. Each replicate covered 0.5 hectares, with 100 marked pruning wounds. Ten months later, incidence (lesion cuts) and severity (lesion length) were assessed. Control vines showed no differences across timepoints (14.7% incidence; 3.9 cm severity). Mamull® significantly reduced both incidence ($P < 0.001$) and severity ($P < 0.05$) up to 48 hours post pruning. From 72 to 120 hours, a significant reduction in severity was observed compared to the control (0.5, 0.7, and 1.6 cm, respectively), though incidence was not affected. After 120 hours, no differences were observed between Mamull® and the control. These results confirm that Mamull® maintains preventive efficacy for up to 48 hours post-pruning. The findings align with Peruvian data and highlight a logistic advantage of Mamull® over traditional protectants require immediate application.

Effect of an organic amendment made of grapevine pruning wood and kitchen waste on the endophyte microbiome structure and the latent Lasiodiplodia brasiliensis infection in grapevine cuttings. L. GUERRERO-CABRERA[1], M. PAOLINELLI[2,3], C. VALENZUELA-SOLANO[4], R. HERNANDEZ-MARTINEZ[1]. [1]*Centro de Investigación Científica y de Educación Superior de Ensenada, Baja California, México.* [2]*Estación Experimental Agropecuaria de Mendoza, Instituto Nacional de Tecnología Agropecuaria, Argentina.* [3]*Consejo Nacional de Investigaciones Científicas y Técnicas, Argentina.* [4]*Instituto Nacional de Investigaciones Forestales, Agrícolas y Pecuarias (INIFAP). Campo Experimental Costa de Ensenada, Ensenada, Baja California, 22880, México.* E-mail: luisgc@cicese.edu.mx

Botryosphaeria dieback affects grapevine and other crops worldwide. One of the causal agents is *Lasiodiplodia brasiliensis*, which has been frequently found in grapevines from Baja California and Sonora in Mexico, mainly in plants exhibiting wood cankers. Several control strategies have been tested, including biological control agents such as bacteria and fungi; however, alternatives like organic amendments (OAs) have not been explored. Therefore, this study aimed to evaluate the effect of OA on the co-occurrence of latent *L. brasiliensis* infection and the endophytic community in grapevines through qPCR and metabarcoding analysis. Three concentrations of the extract of the OA sludge KWW (kitchen waste and grapevine wood) were applied to grapevine cuttings inoculated with *L. brasiliensis*. The KWW extract at 10% applied on both infected and non-infected cuttings, performed the highest values of plant growth parameters on the development of buds' number, bud length, flower number, flower length, root number, and a suppressive effect of 70%. The abundance of endophyte genera *Acinetobacter, Hymenobacter, Pseudomonas, Flavobacterium*, were enhanced by KWW and significantly associated with antagonist activity. Meanwhile, *Sphingomonas*, *Ochrobactrum*, *Azospirillum*, and *Rheinheimer* were possibly involved in plant-induced systemic resistance mechanisms. Additionally, the dominant genera *DMER64* and *Orbiblia* present in KWW were recruited to colonize tissues with possible growth-promoting activity and other physiological processes. Organic amendments can be an effective strategy for controlling grapevine trunk diseases. In particular, the KWW sludge demonstrated multiple suppressive actions, such as providing humic substances and biochemical compounds. This allowed the plant to recruit beneficial bacteria and fungi across the rhizosphere interface in response to the latent *L. brasiliensis* infection. Additionally, KWW

enhanced the relative abundance of endophyte species capable of stabilizing the interaction network of the endophytic microbiome around the pathogen.

This research was supported by a doctoral scholarship from the Secretaría de Ciencia, Humanidades, Tecnología e Innovación (SECIHTI), Mexico.

Integrative approaches to Petri and esca disease mitigation in grapevine: from molecular interference to field applications. L. NERVA[1,2], F. FAVARETTO[1], M. GUASCHINO[1], W. CHITARRA[1,2]. *[1]Council for Agricultural Research and Economics - Research Centre for Viticulture and Enology (CREA-VE). Via XXVIII Aprile, 26, 31015 Conegliano (TV), Italy.[2]National Research Council of Italy - Institute for Sustainable Plant Protection (IPSP-CNR). Strada delle Cacce, 73, 10135 Torino (TO), Italy. E-mail:* luca.nerva@crea.gov.it

Along with grapevine trunk diseases (GTDs), esca poses increasing threats to viticulture due to its complex aetiology and lack of curative treatments. This study integrated fundamental and applied research to investigate Petri and esca-associated plant-pathogen interactions and to develop sustainable management strategies. Exogenous application of double-stranded RNA (dsRNA) targeting vital genes of *Phaeomoniella chlamydospora* and *Phaeoacremonium minimum* was evaluated for grafted grapevine plants in nurseries. The dsRNA treatments significantly reduced lesion length and pathogen isolation frequency, although full suppression of fungal colonization was not achieved. Additionally, grafting combinations influenced disease development and treatment efficacy, with the scion genotype modulating defence responses and rootstock microbial community. Metabarcoding revealed that both pathogen inoculation and dsRNA applications significantly altered the fungal endophytic community composition, suggesting a broader impact on plant-associated microbiota. In parallel, a four-years field trial assessed the effectiveness of a foliar fertilizer formulation in reducing esca incidence and severity under vineyard conditions. Three different pedoclimatic regions and two cultivars (Glera and Cabernet Sauvignon) with at least 1 hectare per site were monitored. The treatment consistently reduced disease incidence by 26–40% and severity by 35–50% relative to conventional protocols. Treated symptomatic vines exhibited improved stomatal conductance and transpiration, indicating reduced esca-related water stress. Furthermore, transcriptomic analysis revealed treatment-induced expression of genes involved in plant immunity and oxidative stress regulation, particularly in symptomatic plants. These findings offer new insight into grapevine defence mechanisms and demonstrate the potential of combining RNA-based biotechnological tools with novel field level approaches. Integrating dsRNA interference, scion-rootstock dynamics, eco-physiological measurements and transcriptomic profiling can stimulate the development of more effective and sustainable esca disease management strategies.

Support was provided by the 'Grape for vine: recycling grape wastes to protect grapevine from fungal pathogens (Grape-4vine)' project financed by Fondazione Cariplo (Ref. 2022-0617), the LegnoSano project supported by the Fondazione Cariverona (Project ID 53737 - 2023.0094) and CIRCOVINO project (founded by the Italian Ministry of Environment and Energy Security, EC-DEC n. 86 of 07 September 2023). This study was also conducted within the Agritech National Research Center and received funding from the European Union Next-Generation EU (PIANO NAZIONALE DI RIPRESA E RESILIENZA (PNRR)—MISSIONE 4 COMPONENTE 2, INVESTIMENTO 1.4—D.D. 1032 17/06/2022, CN00000022) and Shield4Grape project in the frame of Horizon Europe program (Grant agreement 101135088). This manuscript reflects only the authors' views and opinions, neither the European Union nor the European Commission can be considered responsible for them.

Evaluation of commercial bioinoculant products on the health of potted nursery vines. M. PUEBLA, P. ROLSHAUSEN. *University of California, Riverside. Department of Botany and Plant Sciences, Riverside CA, USA. E-mail:* philrols@ucr.edu

Our study investigated the effect of commercial bioinoculants used by nurseries on vine health and wood endophytic microbial communities. We partnered with two California nurseries that applied bioinoculants at different stages of vine propagation. Chardonnay plants grafted onto SO4 rootstock were treated during the callusing stage at the first nursery, whereas at the second nursery Cabernet Sauvignon plants grafted onto 110R rootstock were treated post-planting. Green vines were collected from both nurseries and kept in a lath house at UC Riverside for an additional 10 weeks. We measured shoot mass, root mass, and trunk diameter to compare vine vigor between treatments. Our results showed that vines treated with bioinoculants during callusing displayed significantly higher shoot and root biomass. We also measured internal tissue necrosis using imaging software and found that the bioinoculants significantly reduced wood necrotic area. Finally, next generation sequencing of the fungal ITS and bacterial 16S regions yielded at least 50,000 quality reads. We recorded a high-

er relative abundance of specific beneficial endophytic bacteria (*Bacillus*, *Paenibacillus*, *Streptomyces*) and fungi (*Trichoderma*) listed on the bioinoculant commercial labels, along with a lower relative abundance of GTD fungi (*Phaeoacremonium*) when treated at the callusing stage. In contrast, we observed no differences in all these parameters when vines were treated post-planting. These data suggest that the timing of application of bioinoculant treatments during vine propagation is critical for maximum effects on plant growth and GTD management in nurseries.

This research was supported by the California Department of Food and Agriculture.

Implementing remedial surgery to extend the lifespan of vineyards infected with grapevine trunk diseases in Canada. J.R. ÚRBEZ-TORRES, J. BOULÉ. *Agriculture and Agri-Food Canada, Summerland Research and Development Centre, Summerland, BC, Canada. E-mail:* joseramon.urbeztorres@agr.gc.ca

Grapevine trunk diseases (GTD) are the main biotic factor reducing vineyard lifespan worldwide. No systemic product is available to stop the infection caused by GTD fungi when inside the grapevine vascular system. Remedial surgery is a cultural practice consisting of cutting and removing visibly infected parts of the vine and retraining from canes and/or suckers left below the cut. It is the only technique currently available to eliminate GTD pathogen infection. A recent survey in British Columbia showed 100% of sampled vines (n=1,590) from different ages from 159 vineyard blocks to be infected (canker observed) at the lower part of the trunk (10 cm above ground). Accordingly, the main objective of this study was to determine whether remedial surgery can be used to expand the lifespan of vineyards when no healthy tissue can be found below the last possible cut. A total of 30 vines (3 vines in each of 10 panels) in two vineyards ('Pinot Gris' and 'Pinot Noir') planted in 1996 were cut and retrained in the winter of 2017 and their survival and performance compared against 30 uncut vines during six growing seasons. At the end of the experiment, 100% survival rate of retrained vines was recorded. Both 'Pinot Gris' and 'Pinot Noir' retrained vines showed significantly higher yields than the uncut control vines after two growing seasons. After six years, total yield estimated in the retrained 'Pinot Gris' and 'Pinot Noir' increased by 60% and 160%, respectively. Fruit quality (brix, pH, TA) was not statistically different between retrained and uncut vines. This study shows remedial surgery as an effective technique to extend the lifespan of vineyards even when infection has reached beyond the last possible cut allowed for retraining. Extending vineyard lifespan can provide growers with needed cash flow while preparing for vineyard replant.

This work was supported by the British Columbia Wine Grape Council and Agriculture and Agri-Food Canada under the Canadian Agricultural Partnership funding initiative (Project #J-001935)

Early infection, lasting impact: trunk diseases reduce cane quality and spread via rootstock material. W.J. VAN JAARSVELD[1,2], L. MOSTERT[1], J.J. HUNTER[2], M. HAVENGA[2], M. VAN DER RIJST[2], F. HALLEEN[1,2]. *[1]Stellenbosch University, Department of Plant Pathology, Matieland, 7602, South Africa. [2]ARC Infruitec-Nietvoorbji, Stellenbosch, 7599, South Africa. E-mail:* wynand@vititec.com

Infection of rootstock mother vines with grapevine trunk disease pathogens leads to reduced yields and compromised phytosanitary quality of propagation material. This poses a serious threat to the sustainability of the South African grapevine industry. The age for replacing rootstock mother vines to minimize these risks are unknown. Therefore, this study aimed to investigate how the age of rootstock mother blocks influences the physiological, morphological and infection status of both the mother vines and one-year-old canes. Thirty-nine rootstock mother blocks of different ages of 10 varieties were surveyed over three seasons. Morphological dimensions including cane length, thickness and fresh mass were determined. Physiological analyses determined the water and starch content, macro- and micronutrients and total phenolic index. Fungal isolations were made from one-year-old canes and heads of mother vines, and *Diplodia seriata* and *Phaeomoniella chlamydospora* were quantified in one-year-old canes using qPCR. The effects of block age and season varied across different rootstock varieties, without conclusive association with block age. Interactions between certain minerals and cane morphology were both synergistic or antagonistic. *Botryosphaeriaceae* and *Celotheliaceae* (*P. chlamydospora*) were the most prevalent grapevine trunk disease pathogens found in one-year-old canes (incidences up to 28% and 2% and DNA concentrations reaching 3171 and 1055 ng μL^{-1}, respectively) and in the mother vine heads (incidences up to 84% and 90%, respectively), generally regardless of vine age. *Diplodia seriata* infections in the vine heads resulted in contamination in one-year-old canes. *Botryosphaeriaceae* in mother vine heads negatively affected cane morphology, while *Celotheliaceae*

and *Diaporthaceae* were associated with reduced starch levels in canes. Infections by *Botryosphaeriaceae* and *Hymenochaetaceae* resulted in an elevated total phenolic index. Rootstock mother blocks, the heads as well as one-year-old canes, were infected with GTD pathogens from as young as three years-old, highlighting the need for starting with clean mother vines and ensuring that infections do not occur.

The research was funded by South Africa Wine Project number P04000235 and the Agricultural Research Council (ARC), Infruitec-Nietvoorbij, Stellenbosch. Wynand van Jaarsveld was supported by National Research Foundation (NRF) Grant Number 118269 and 138744.

Field evaluation of biocontrol and integrated strategies for managing grapevine trunk diseases in California. M. I. BUSTAMANTE, K. ELFAR, A. ESKALEN. *Department of Plant Pathology, University of California, Davis, CA 95616, U.S.A. E-mail:* aeskalen@ucdavis.edu

Grapevine trunk diseases (GTDs) are among the most damaging and persistent threats to viticulture worldwide. Over three consecutive years, we evaluated three integrated strategies involving biocontrol agents and fungicides for GTD management in both nursery and vineyard settings. Treatments were applied as (i) pre-grafting soaking of propagation material in nurseries, (ii) pruning wound sprays, and (iii) soil drenches in a mature experimental vineyard of *Vitis vinifera* cv. Cabernet Franc in Davis, CA. In nursery trials, both fungal and bacterial biocontrol agents improved callus formation at the graft union and rootstock. Lesion lengths and infection levels caused by *Neofusicoccum parvum* were significantly reduced by both fungicide and biocontrol treatments, while only infection levels (not lesion length) of *Eutypa lata* were lowered. No significant control was observed for *Phaeoacremonium minimum*. In vineyard trials, pruning wound protectants, especially synthetic fungicides and selected biocontrol agents significantly reduced infections by *N. parvum*. Soil drench applications also reduced lesion lengths and infection levels caused by *N. parvum*, *E. lata* and *P. minimum*. These findings demonstrate that integrating biocontrol agents across multiple application points (propagation, pruning, and soil) can contribute significantly to GTD management under California field conditions. Further validation in commercial vineyards is required for broad adoption of these strategies into IPM programs.

This research was financially supported by the Unified Grant Management for Viticulture and Enology

The occurrence and control strategies of grapevine black foot disease in China. W. ZHANG, B.Y. WANG, Y.H. LI, N.N. WANG, L.N. WU, Y.Y ZHOU, X.H. LI, J.Y. YAN. *Beijing Key Laboratory of Environment Friendly Management on Fruit Diseases and Pests in North China, Institute of Plant Protection, Beijing Academy of Agriculture and Forestry Sciences, Beijing 100097, China. E-mail:* zhangwei@baafs.net.cn

Grapevine black foot disease (BFD) is one of the major grapevine trunk diseases (GTDs) threatening Chinese viticulture, with its incidence and severity increasing annually. First reported in China in 2017, initial surveys conducted between 2017 and 2019 across five provinces revealed incidence rates ranging from 0.1% to 1%. Systematic surveys carried out from 2020 to 2023 showed that BFD has now been detected in 11 provinces, with pathogen carrier rate exceeding 20% in seven of them. Consequently, BFD has become the second most important GTD in China, following Botryosphaeria dieback. In addition, BFD-associated fungi are frequently found co-infecting grapevine alongside other GTD pathogens. Currently, effective management strategies for BFD are lacking, underscoring the need for early and accurate diagnosis to support timely cultural and preventive interventions. This study aimed to (i) develop a triplex droplet digital PCR (ddPCR) assay for the early detection of major BFD-associated species in China, and (ii) evaluate the efficacy of bacterial biocontrol agents for BFD management. A total of 193 fungal isolates associated with BFD were obtained and identified based on morphological and molecular analyses. Of these, 66.3% were *Dactylonectria* spp., followed by *Ilyonectria* (23.3%), *Cylindrocladiella* (7.8%), and *Campylocarpon* (2.6%). A triplex ddPCR assay was developed, enabling the simultaneous detection of seven major BFD-associated species, with a detection limit of 1×10^6 ng μL^{-1}, providing a sensitive tool for early diagnosis. Six bacterial strains exhibited over 70% mycelial inhibition against BFD-associated isolates, with strain O-C9 (*Pseudomonas aeruginosa*) showing the highest efficacy. A fermentation broth of O-C9 at 8.19×10^9 CFU mL^{-1} significantly reduced pathogen colonization by 76% in roots, 78% in trunks, and 43% in new shoots of one-year-old potted grapevine seedlings. Notably, O-C9 also showed broad-spectrum mycelial growth inhibition (48%–76%) against other GTD pathogens, presenting a promising strategy for integrated control of BFD co-infected with other GTDs in the field. Field trials of O-C9 are currently underway. This study provides an updated overview of BFD in China, and advances both diagnostic and management tools, contributing a scien-

tific basis for the integrated control of this increasingly important disease.

This research was financially supported by the China Agriculture Research System of MOF and MARA (CARS-29) and the Outstanding Scientist Project of Beijing Academy of Agriculture and Forestry Sciences (JKTD2025002).

POSTER PAPERS

Production of *Cryptovalsa ampelina* spore suspension and optimal inoculum dose for wound infection. M. ANDRES-SODUPE[1,2], M.R. SOSNOWSKI[3,4], J. HRYCAN[2], C.C. STEEL[1,2], S. SAVOCCHIA[1,2]. *[1] Faculty of Science and Health, School of Agricultural, Environmental and Veterinary Sciences, Charles Sturt University, Wagga Wagga, New South Wales, 2678, Australia.[2] Gulbali Institute, Charles Sturt University, Wagga Wagga, New South Wales, 2678, Australia. [3]South Australian Research and Development Institute, Adelaide, SA, 5001, Australia.[4] School of Agriculture, Food and Wine, Waite Research Institute, The University of Adelaide, Adelaide, SA 5005, Australia. E-mail:* mandressodupe@csu.edu.au

Eutypa lata and *Cryptovalsa ampelina* are the primary diatrypaceous species implicated in Eutypa dieback (ED) in Australia. These ED pathogens propagate through sexual reproduction by developing perithecia containing eight to multiple-spored asci in dead stroma tissues. Asexual reproduction produces conidia, but they are unable to germinate and cause disease, limiting the ability to use them for experiments to infect pruning wounds for the evaluation of control strategies. Additionally, ascospores cannot be produced *in vitro*. To overcome these challenges, a spore suspension protocol originally developed for *E. lata* was validated for *C. ampelina*. Firstly, perithecia in dead wood were dissected and observed under the microscope. When 32-spored asci were found, spores were transferred to potato dextrose agar amended with chloramphenicol (PDA-C). Cultures were morphologically identified and confirmed by loop-mediated isothermal amplification (LAMP) with species-specific primers. Small pieces of dead grapevine wood containing perithecia were fixed to a container lid and submerged in sterile distilled water for 1 hour. After soaking, the lid was screwed onto a clean container and left overnight at room temperature. The next day, the wood was removed, and the walls of the container were rinsed with sterile distilled water to collect spores. The identity of *C. ampelina* was confirmed morphologically by plating the suspension onto PDA-C and by LAMP analysis 3 days after spore release, while spores were kept in cool storage at 4°C. To determine the optimal spore dose for wound inoculation, a detached cane assay was conducted by applying 10 to 500 spores to fresh pruning wounds. After one-month, successful colonisation by *C. ampelina* was assessed by pathogen recovery on PDA-C. This spore liberation protocol provides a sound, reproducible method for future pathogenicity and wound protection studies.

This research was financially supported by Wine Australia, with levies from Australia's grapegrowers and winemakers and matching funds from the Australian Government.

Comparing qPCR and isolation methods to assess *Eutypa lata* infection in grapevine wounds. T. FURLAN[1,2], N. CAPOTE[3], K. HILL[1,2], D. GIBLOT-DUCRAY[1,2], I. DUMITRESCU[1], H. HERDINA[1], M.R. SOSNOWSKI[1,2]. *[1]South Australian Research and Development Institute, Adelaide SA 5001, Australia. [2]School of Agriculture, Food and Wine, Waite Research Institute, The University of Adelaide, SA 5005, Australia. [3]Andalusian Institute of Agricultural and Fisheries Research and Training (IFAPA), Seville, Spain. E-mail:* mark.sosnowski@sa.gov.au

Eutypa lata infects grapevines through wounds and colonises vascular tissue, causing Eutypa dieback. The presence of *E. lata* is traditionally assessed by isolating from wood pieces on potato dextrose agar (PDA). A widely used technique, it is time consuming and can be hindered by contamination or misidentification. To develop a more sensitive and consistent technique, a TaqMan qPCR assay for the specific detection of *E. lata* was evaluated. The assay, targeting the ITS region of the genome, was previously shown to be sensitive and mostly specific, only cross reacting with *Diatrypella vulgaris*, a related pathogen. The qPCR assay was compared with isolation using an existing pruning wound protection trial where wounds were inoculated with approximately 200 spores of *E. lata*. The trial included various treatments and positive and negative controls. One year later, treated canes were collected and cut in half longitudinally after removing the bark and desiccated stub. Half of the canes were assessed by isolation on PDA and the other half via qPCR. Plant crude extracts were prepared by grating 100 mg of tissue below the margin of discoloured wood into an extraction buffer and beating in a tissue lyser. Dilutions (1:5) of plant crude extracts were directly analysed in triplicate using qPCR. Of 638 samples analysed, 59% corresponded for both methods, with the Cohen's kappa index indicating 'fair agreement' between the two methods. Thirty-nine percent of samples were positive for

qPCR only, and 2% positive for isolation only. qPCR was considerably more sensitive than isolation for detecting *E. lata* in canes, offering a more rapid and sensitive method. qPCR assessment was estimated to cost 1.5 times more than the isolation method. Further evaluation is planned to investigate reducing replication and confirming accuracy of the method for wound susceptibility experiments.

This research was supported by Wine Australia, with levies from Australia's grapegrowers and winemakers and matching funds from the Australian Government and is part of the project PR.AVA23.INV23.007, co-financed at 85% by the European Regional Development Fund within the Andalusia ERDF Operational Program 2021-2027

On the hunt for grapevine trunk diseases: A preliminary survey of vineyards in Ontario, Canada. W. MCFADDEN-SMITH[1], J. RAMÓN ÚRBEZ-TORRES[2], O. ELLOUZ[3]. *[1]CCOVI, Brock University, 1812 Sir Isaac Brock Way, St. Catharines, Ontario, L1S2B1, Canada. [2]Summerland Research and Development Centre, 4200 Highway #97 Summerland, BC V0H 1Z0, Canada. [3]Agriculture and Agri-Food Canada, London Research and Development Centre, 4902 Victoria Avenue North, Vineland Station, ON L0R 2E0, Canada. E-mail:* mcsmith58@gmail.com

Until recently, grapevine trunk diseases (GTDs) have not been considered a major issue in the cool climate growing region of Ontario, the largest grape production area in Canada. To determine the prevalence of GTDs and their causal agents, randomly selected vineyards cultivar Chardonnay and Cabernet franc were surveyed in early and late summer during the 2024 growing season. The age of vines ranged from 2 to 30 years. From each selected vineyard, trunks were collected from 5 symptomatic vines, including poor vigor, dieback, lack of spring growth, and/or characteristic Eutypa dieback symptoms. Young vine decline symptoms were not observed. Fungal pathogens were first identified based on morphological characteristics and subsequently by multi-gene DNA analyses. Species within the *Botryosphaeriaceae* family were the most prevalent, specifically *Diplodia seriata* and *Neofusicoccum* spp., followed in number by *Phaeoacremonium minimum, Phaeomoniella chlamydospora* and *Eutypa* spp. This study represents the first attempt to demystify the status of GTD in Ontario, a grape-growing region with unique climatic conditions. Identifying the main GTDs pathogens in Ontario will assist to better understand their epidemiology and develop proper management strategies.

This research was funded in part by the Government of Canada under the Sustainable Canadian Agricultural Partnership, with additional support from Ontario Grape and Wine Research Inc., the Ontario Ministry of Agriculture, Food and Agribusiness through the Marketing Vineyard Improvement Program (MVIP), and the Canadian Grapevine Certification Network.

Identification and characterization of *Cytospora* species isolated from grapevine cankers in British Columbia, Canada. J.R. ÚRBEZ-TORRES, A. ROBERTS, J. BOULÉ. *Agriculture and Agri-Food Canada, Summerland Research and Development Centre, Summerland, BC, Canada. E-mail:* joseramon.urbeztorres@agr.gc.ca

Grapevine trunk diseases (GTDs), one of the major threats to the industry's future economic sustainability, are caused by a wide range of taxonomically unrelated fungi. Recent studies have reported species in the genus *Cytospora* to be isolated from GTDs symptomatic vines in different parts of the world. Members of this genus are long known to cause cankers on a wide range of perennial woody hosts, primarily fruit trees. However, their role as pathogens in grapevines is still not fully understood. The objective of this study was to identify by means of morphological and molecular studies *Cytospora* isolates obtained from GTDs symptomatic vines in British Columbia (BC), Canada and complete pathogenicity studies to determine their role as GTDs causing fungi. Results from field surveys showed *Cytospora* isolated from 25% of surveyed vineyards (49 out of 194). A total of 107 *Cytospora* isolates were obtained primarily from cankers observed in spurs, cordons and/or trunks. Among these, 65 isolates were selected for DNA analyses of four genes (ITS1-5.8S-ITS2, β-tubulin, TEF-1α, ACTIN). DNA sequencing showed *Cytospora viticola* to be the most prevalent species isolated from grapevine cankers in BC. Other identified species were *C. chrysosperma*, *C. parasitica*, *C. populicola*, *C. pruniopsis*, and a *Cytospora* sp. Eight isolates were selected to complete pathogenicity studies in both Chardonnay and Merlot cultivars in a detached cane assay using mycelium plugs as inoculum. Results showed all *Cytospora* isolates from the different species to cause vascular necrosis significantly larger than the non-inoculated controls in both cultivars. Pycnidia from the inoculated isolates was observed in the inoculated canes. The small necrosis length recorded from the different species (average 6.25 mm) suggests *Cytospora* spp. identified in this study to be weak pathogens of grapevines. Further studies are in progress to better understand the role that *Cytospora* spp. may play on GTDs development.

This work was supported by the British Columbia Wine Grape Council and Agriculture and Agri-Food Canada under the Canadian Agricultural Partnership funding initiative (Project #J-001935)

Characterization of *Diaporthe* spp. associated with grapevine trunk diseases in the northwest of Mexico. C.S. DELGADO-RAMÍREZ[1], E.A. RANGEL-MONTOYA[1,3], E. SEPÚLVEDA[1], C. VALENZUELA-SOLANO[2], R. HERNANDEZ-MARTINEZ[1]. [1]*CICESE. Departamento de Microbiología. Ensenada, Baja California.* [2] *INIFAP Sitio experimental costa de Ensenada.* [3]*Facultad de ciencias químicas, UABC, Tijuana. E-mail:* cdelgado@cicese.edu.mx

Phomopsis dieback is a grapevine trunk disease caused by *Diaporthe* spp. Symptoms in plants include small clusters, fruit rot, and dieback and cankers. Grapevine cultivation has significant socioeconomic importance in Mexico. In the wine-producing regions of the country, there are reports of trunk disease fungi causing dieback and cankers, but none involve *Diaporthe* species. Therefore, the aim of this work was to characterize *Diaporthe* species associated with grapevines in vineyards of Sonora and Baja California, Mexico. Isolates with morphological characteristics like *Diaporthe* spp. were obtained from grapevine plants showing dieback and cankers. Ten isolates were identified through morphological characterization and molecular analysis using ITS and EF1-α markers. Phylogenetic analysis allowed the identification of strains belonging to the species *D. ampelina*, *D. eres*, and *D. foeniculina*. The optimal growth temperature ranged between 25 and 28°C, and they exhibited higher growth when inoculated in media supplemented with cellulose, pectin, and grapevine wood as carbon sources. Pathogenicity tests confirmed that all strains could produce necrotic lesions. These findings expand the current understanding of grapevine trunk disease etiology in Mexico and highlight the need for further studies on the epidemiology and management of *Diaporthe* species in local vineyards.

This research was financially supported by the Secretaría de Ciencia, Humanidades, Tecnología e Innovación (SECIHTI), Mexico and Molina group of Hermosillo, Sonora.

Morphophysiological and phylogenetic characterization of Chilean isolates of *Eutypa lata* obtained from vineyards in Central Chile. Y. RUIZ[1], M. VALENZUELA[2], C. PACHECO[1], P. GONZÁLEZ[1], F. NUÑEZ[1], C. MUÑOZ[1], G. DÍAZ[1], M. LOLAS[1]. [1]*Laboratorio de Patología Frutal, Facultad de Ciencias Agrarias, Universidad de Talca, Talca, Chile.* [2]*Facultad de Agronomía, Universidad de Concepción, Chillán, Chile. E-mail:* mlolas@utalca.cl

Grapevine trunk diseases (GTDs) have become one of the most critical phytosanitary problems affecting this crop globally over the past three decades. Among them, Eutypa dieback, caused by the fungus *Eutypa lata* (family Diatrypaceae), is highly aggressive and widely distributed, with reports from vineyards across Africa, Europe, Asia, Oceania, and America. In Chile, *E. lata* was recently identified in grapevines and cherry trees, representing the only documented evidence of its presence in the country to date. The objective of this study was to characterize, from cultural, morphophysiological, and phylogenetic perspectives, the first Chilean isolates of *E. lata* obtained from vineyards located in central Chile. Five isolates were evaluated for growth rate and optimal growth temperature on four culture media (PDA, V8, corn agar, and tomato agar), incubated at 0, 5, 10, 15, 20, 25, 30, and 35 °C for 0, 7, 14, 21, and 28 days. Mycelial growth curves and temperature response models were developed using R Studio. Phylogenetic analysis was performed using ribosomal DNA (ITS region) and β-tubulin gene sequences, comparing the Chilean isolates with *E. lata* accessions from GenBank representing diverse global regions. Sequence alignment, phylogenetic inference, and visualization were conducted using MEGA 11, IQ-TREE, and iTOL. Results showed that PDA and corn agar supported the highest mycelial growth, with optimal temperatures ranging from 19.97 to 21.62 °C. Growth curves were similar across all isolates. Phylogenetic analysis revealed significant global genetic diversity of *E. lata*, and the Chilean isolates clustered with strains from Europe, the Americas, and Oceania. To date, the sexual stage of *E. lata* has not been reported in Chilean vineyards, highlighting the need for further studies aimed at its detection to better understand the epidemiology and management of this pathogen in local viticulture.

This research was financially supported by the Project FONDECYT 1230662.

Portable vineyard fungal diagnostics: a low-cost system for in-field *Lasiodiplodia* species identification. A. CRESPO-MICHEL[1], M. A. ALONSO-ARÉVALO[1], R. HERNANDEZ-MARTINEZ[2]. [1]*Department of Electronics & Telecommunications, Center for Scientific Research and Higher Education of Ensenada (CICESE), Ensenada, B.C, Mexico.* [2]*Department of Microbiology, Center for Scientific*

Research and Higher Education of Ensenada (CICESE), Ensenada, B.C, Mexico. E-mail: cmalexis95@gmail.com

A diagnostic system for *Lasiodiplodia* species classification was developed to address the challenge of accurately identifying these fungal pathogens, which pose a significant threat to grapevine and crop health. The system is designed to operate on a compact, low resource computing platform, making it suitable for deployment in field conditions. The system combines a bright-field microscope with a camera to capture high-resolution images of fungal spores. These images are processed through two parallel analysis pipelines. The first pipeline uses a MobileNetV2-based convolutional neural network (CNN) to directly classify species from raw images, achieving an accuracy of 96.25%. The second pipeline employs a fine-tuned Mask R-CNN model for segmenting individual spores, which are then analyzed using a feature extraction module that computes morphological traits such as area, shape descriptors, and color metrics. These extracted features are classified using an XGBoost model, which achieves 76.81% accuracy. The system was trained and tested on a dataset of 2,400 images representing eight different species of *Lasiodiplodia*. t-SNE visualization of the CNN extracted features revealed distinct species-level clustering, supporting the biological relevance of the extracted characteristics. Despite the lower accuracy of the feature-based approach, it provides interpretable insights into the morphological variability between species, which can be valuable for understanding phenotypic differences. All processing was performed on a low-cost, integrated computing unit, demonstrating the feasibility of deploying advanced fungal diagnostic tools in resource-limited environments. This system represents a promising step toward developing scalable, portable solutions for fungal identification and plant disease management, combining deep learning and interpretable models for more accessible and efficient monitoring of agricultural pathogens.

This work was partially supported by the Ministry of Science, Humanities, Technology and Innovation (SECIHTI Mexico) through the Graduate Research Fellowship No. 905896.

Persimmon is a new host of the black foot disease pathogen *Ilyonectria liriodendri*. N. MOLNÁR[1], D. SZABÓ[1], A. GEIGER[1], J. GEML[1], Z. KARÁCSONY[1], K.Z. VÁCZY[1]. *Eszterházy Károly Catholic University, Food and Wine Research Institute, Leányka str. 8/G, Eger, H3300, Hungary. E-mail:* vaczy.kalman@uni-eszterhazy.hu

Several members of the fungal genus *Ilyonectria* infect plants through the roots and basal stem, causing 'black foot' diseases, predominantly in woody plants such as grapevine and walnut. In 2021, four *Ilyonectria liriodendri* isolates were cultured from the necrotized roots of *Diospyros virginiana* (persimmon) plants in Eger, Hungary. The isolates were identified by sequencing the ITS, β-tubulin, and partial histone H3 genes. The obtained sequences were used for phylogenetic analysis through multiple sequence alignment and the construction of a Maximum Likelihood tree, which revealed that all four isolates aligned with sequences of *Ilyonectria liriodendri*. The macro- and micromorphological deviations, such as conidial size and morphology, as well as coloration and relative growth differences between the isolates, suggested that they represent a somewhat diverse set of isolates within *I. liriodendri*. To prove their association with the symptoms observed in the host plants, the roots of one-year-old *D. virginiana* cuttings were artificially inoculated by dipping in 10^5 spore/ml conidial suspensions of the isolates for 30 minutes. Five replicates were set up for each isolate and the mock-inoculated control which were inoculated with water. After 90 days of incubation in a greenhouse, 3 to 5 plants out of the five replicates for each fungal isolate (total of 16 symptomatic plants out of 20 inoculated cutting) showed necrosis in the taproots, while the mock-inoculated cuttings remained symptomless. Necroses developed in the roots of the infected plants, and the inoculated fungi were reisolated, confirming their pathogenicity to *D. virginiana*. To the best of our knowledge, this is the first report of *Ilyonectria liriodendri* causing disease in persimmon.

This research was financially supported by the Project TKP2021-NKTA-16.

Evaluation of the susceptibility period of grapevine pruning wounds to natural infection by trunk disease fungi. K.A. ASHLEY, R. BUJANDA, D. GRAMAJE, C. LEAL**.** *Instituto de Ciencias de la Vid y del Vino (ICVV), Consejo Superior de Investigaciones Científicas (CSIC), Gobierno de La Rioja, Universidad de La Rioja, Ctra. LO-20 Salida 13, 26006 Logroño, Spain. E-mail:* catarina.leal@icvv.es

Grapevine trunk diseases (GTDs) primarily infect through pruning wounds, which previous studies suggest remain susceptible for up to two months. Pruning timing may also influence the development of GTDs. Three GTD pathogens of importance in Spain are *Diaporthe ampelina*, *Diplodia seriata*, and *Cytospora viticola* responsible for Phomopsis dieback (PD), Botryosphaeria dieback (BD), and Cytospora canker (CC), respectively. In a vineyard plot located in Logroño (northern Spain),

80 grapevines were pruned in November (early pruning) and another 80 in February (late pruning). From each pruning group, wood samples were collected weekly over eight weeks from ten different vines. A total of 2 wood fragments per plant were processed for fungal isolation, and pathogens were identified by sequencing the ITS rDNA region. The incidence and severity of PD, BD, CC, and other GTD pathogens were evaluated using Kruskal-Wallis tests and correlation matrices in relation to climatic and temporal variables. There were no significant differences in GTD incidences across all weekly early and late pruning samples, supporting the hypothesis that pruning wounds remain vulnerable to infection for up to two months. However, GTD severity was overall significantly higher in late-pruned grapevines compared to early-pruned. Across climactic variables, temperature and precipitation had the most significant relationships with GTD pathogens. Overall, GTD pathogens incidence was positively correlated with temperature, while severity was positively correlated with precipitation. Individual pathogens responded differently: PD incidence positively correlated with temperature in fall, whereas BD incidence showed a negative correlation with temperature in spring. CC was only detected in spring samples, and its severity was negatively associated with humidity. These results highlight the importance of environmental conditions in disease development and suggest that pruning timing and climate affect both infection likelihood and disease progression.

This research was financially supported by the project EFA 033/01 – VITRES, which has been 65% cofinanced by the European Regional Development Fund through the Interreg V-A Spain-France-Andorra Program (POCTEFA 2021-2027).

Dispersal of grapevine trunk disease spores from an infected vineyard. T. FURLAN[1,2], J. HRYCAN[3], M. LIU[3], S. SAVOCCHIA[3] and M.R. SOSNOWSKI[1,2]. *[1]South Australian Research and Development Institute, Adelaide SA 5001, Australia. [2]School of Agriculture, Food and Wine, Waite Research Institute, The University of Adelaide, SA 5005, Australia. [3]Gulbali Institute, School of Agricultural, Environmental and Veterinary Sciences, Charles Sturt University, NSW, Australia. E-mail: mark.sosnowski@sa.gov.au*

The grapevine trunk diseases Eutypa (ED) and Botryosphaeria dieback (BD) are caused by fungal species of the Diatrypaceae and *Botryosphaeriaceae*, respectively. Perithecia of *Eutypa lata* on infected wood release ascospores during rain events, which are reported to be carried up to 50 km in wind. Pycnidiospores of BD pathogens are primarily dispersed by rain splash, and have been reported to only travel up to 20 m. For both ED and BD, spores land on fresh pruning wounds and infect the exposed vascular tissue to cause dieback and eventually vine death. It is important to understand the distance and quantity of spores that can be dispersed from an infected vineyard to adjacent blocks and neighboring vineyards. In this study, isolated old Shiraz blocks with dieback symptoms in South Australia were selected as source blocks. During August 2023 in the Barossa Valley, six Rotorod spore traps were positioned from 0 to 400 m from the source block in line with prevailing winds. During August 2024 in the Eden Valley, the spore traps were positioned from 0 to 4 km from the source block. At both sites, spores were repeatedly collected for 24-hour periods following rain events. DNA was extracted from spores on the rods and analysed using multi-species qPCR to quantify the number of ED and BD pathogen spores deposited at each position. Spores were detected at least 400 m away from the source with no reduction in quantity. When the distance was increased, ED and BD spores were detected up to 4 km away from the source during strong winds and heavy rainfall. Further research is planned for 2025 to increase intensity of sampling and at greater distances from the source. These results highlight the potential of trunk disease spread between vineyards and across a region, reinforcing the importance of proactive disease management.

This research was supported by Wine Australia, with levies from Australia's grapegrowers and winemakers and matching funds from the Australian Government.

Dissecting plant-microbe interactions in grapevine trunk disease: a genotype-focused approach. A. NARDUZZO[1,2], F. FAVARETTO[1,2], F. VILLANO4, M. GUASCHINO[1], W. CHITARRA[1,3], L. NERVA[1,3]. *[1]Council for Agricultural Research and Economics - Research Centre for Viticulture and Enology (CREA-VE). Via XXVIII Aprile, 26, 31015 Conegliano (TV), Italy; [2]University of Padua, Department of Agronomy, Food, Natural Resources, Animals and Environment, Agripolis, Viale dell'Università 16 - 35020 Legnaro (PD), Italy; [3]National Research Council of Italy - Institute for Sustainable Plant Protection (IPSP-CNR). Strada delle Cacce, 73, 10135 Torino (TO), Italy; [4]University of Turku, 20014 Turku, Finland. E-mail:* anna.narduzzo@crea.gov.it

The delicate balance between plants and their microbial communities is vulnerable to environmental and biological disruptions, increasing plant susceptibility to disease. Within this context, Esca disease is a

particularly challenging trunk disease of grapevine, involving a consortium of fungi whose interaction with the host, under partly unknown conditions, results in variable impacts on plant health. Our investigation started with an assessment of the resident endophytic fungal communities across a panel of 12 grapevine genotypes. This initial phase aimed to determine the profile of microbial composition within a large, randomized sample set by isolating from grapevine propagation material. After the assessment of diversity, we initiated a systematic evaluation of genotype-specific susceptibility to the primary etiological agents implicated in Grapevine Trunk Diseases (GTDs): *Phaeomoniella chlamydospora*, *Phaeocremonium minimum*, and *Diplodia seriata*. This involved inoculating 16 grapevine genotypes, selected among the most commercially important and traditional varieties known for their susceptibility or resistance to Esca-related fungi. These preliminary findings pave the way for future research, aimed at elucidating the holobiont changes brought by GTDs presence across different grapevine genotypes, wither classified as resistant or widely adopted commercially. In vivo analysis of microbial community dynamics during pathogenesis, through imaging of tagged reporter microbes or through metagenomic analysis, can significantly enhance our understanding of fungal communities associated with disease resistance. Future studies should prioritize identifying and characterizing, in one model genotype, resistance genes that are crucial in the plant-fungal interaction. Complementary, metabolomic profiling of both grapevine tissues and fungal communities, in healthy and diseased states, will be critical for pinpointing metabolic pathways involved both in plant defense and fungal protection/virulence. Ultimately, integrating the results of these analyses can lead to novel disease management strategies, such as selecting resilient grapevine varieties or manipulating the vineyard microbiome to enhance natural tolerance to diseases.

Support was provided by the 'Grape for vine: recycling grape wastes to protect grapevine from fungal pathogens (Grape-4vine)' project financed by Fondazione Cariplo (Ref. 2022 -0c17), the LegnoSano project supported by the Fondazione Cariverona (Project ID 53737 - 2023.00S4) and CIRCOVINO project (founded by the Italian Ministry of Environment and Energy Security, EC -DEC n. 8c of 07 September 2023). This study was also conducted within the Agritech National Research Center and received funding from the European Union Next-Generation EU (PIANO NAZIONALE DI RIPRESA E RESILIENZA (PNRR)—MISSIONE 4 COMPONENTE 2, INVESTIMENTO 1.4—D.D. 1032 17/0c/2022, CN00000022) and Shield4Grape project in the frame of Horizon Europe program (Grant agreement 101135088). This manuscript reflects only the authors' views and opinions, neither the European Union nor the European Commission can be considered responsible for them.

Comparative cellular morphology and stress tolerance of *Botryosphaeriaceae* fungi affecting grapevines in Mexico. G. PANIAGUA-PEREZ[1], E.A. RANGEL-MONTOYA[1,2], R. HERNANDEZ-MARTINEZ[1]. *[1]Departamento de Microbiología, Centro de Investigación Científica y de Educación Superior de Ensenada, Baja California (CICESE), Ensenada 22860, Mexico. [2]Facultad de Ciencias Químicas, Universidad Autónoma de Baja California, Tijuana, Mexico. E-mail:* grecia@cicese.edu.mx

Fungi from the *Botryosphaeriaceae* are associated with a wide range of diseases in numerous woody crops, including grapevine (*Vitis vinifera*). These pathogens significantly impact vineyard productivity and longevity by causing vascular necrosis, cankers, dieback, and, in severe cases, plant death. In Mexico, species from the genera *Lasiodiplodia*, *Neofusicoccum*, *Diplodia*, and *Botryosphaeria* have been identified in Baja California, Sonora, and Coahuila, exhibiting varying levels of virulence. Given their impact and the limited understanding of their cellular biology, this study aimed to analyze the cellular structures and stress tolerance of *Botryosphaeriaceae* strains with different levels of virulence. The strains used were *L. brasiliensis* MXBCL28, *N. parvum* MX14P4, and *B. dothidea* MXRJM25, all isolated from Mexican vineyards. Cellular analysis was performed using confocal laser scanning microscopy. Samples were stained with Calcofluor White (0.02%) for cell walls, FM4-64 for membranes, vesicles, and the Spitzenkörper, and DAPI/Hoechst 33258 for nuclei. No significant differences in cell wall structure were observed among the three species. However, variations in nuclear quantity were noted with *L. brasiliensis* displaying a higher number of nuclei compared to the other species. FM4-64 staining confirmed the presence of the Spitzenkörper in all three species. Additionally, fungal growth was evaluated under stress conditions induced by phenolic compounds (salicylic acid and benzoic acid at 10 and 15 mM) and oxidative stress (hydrogen peroxide at 1 and 5 mM). *Lasiodiplodia brasiliensis* was able to utilize both phenolic compounds as carbon sources at all tested concentrations. *Neofusicoccum parvum* and *B. dothidea* grew in the presence of salicylic and benzoic acids up to 10 mM. Under oxidative stress, all species showed growth comparable to the control. These findings provide a cellular level comparison of *Botryosphaeriaceae* and contribute to a better understanding of mechanisms and stress tolerance.

Comparative colonization and tissue degradation of grapevine wood by *Lasiodiplodia brasiliensis*, *Neofusicoccum parvum*, and *Botryosphaeria dothidea*. E.A. RANGEL-MONTOYA[1,2], I. CÓRDOVA-GUERRERO[1], R. HERNANDEZ-MARTINEZ[2]. [1]*Facultad de Ciencias Químicas e Ingeniería, UABC.* [2]*Centro de Investigación Científica y de Educación Superior de Ensenada. E-mail: erangel@cicese.mx*

Botryosphaeria dieback is one of the most aggressive grapevine trunk diseases caused by fungi from the *Botryosphaeriaceae* family. These pathogens typically infect the plant through pruning wounds and colonize the xylem, leading to necrosis and vascular dysfunction. In Mexico, *Lasiodiplodia brasiliensis* has been identified as highly virulent, followed by *Neofusicoccum parvum*, whereas *Botryosphaeria dothidea* exhibits low virulence. This study aimed to compare the colonization behavior of *Botryosphaeriaceae* fungi with varying levels of virulence in grapevine. 'Cabernet Sauvignon' plants were mechanically wounded and inoculated with *L. brasiliensis* MXB-CL28, *N. parvum* 14P4MX, and *B. dothidea* RJM25MX, and maintained under greenhouse conditions for two months. Half of the samples were used for histological analysis to observe structural changes in the grapevine tissue. Plants inoculated with *L. brasiliensis* and *N. parvum* showed reduced levels of starch, cellulose, hemicellulose, and lignin compared to control plants, whereas those inoculated with *B. dothidea* exhibited profiles like the control. The other half of the samples were analyzed to quantify starch and total phenolic content. Results indicated that plants inoculated with *L. brasiliensis* had significantly lower starch levels and higher phenolic content than the control. Additionally, fungal growth was assessed on various carbon sources related to grapevine tissue components. *L. brasiliensis* showed the highest growth rate on pectin, *N. parvum* on glycogen, and *B. dothidea* on tannic acid. These findings improve our understanding of the colonization strategies employed by these fungi and may contribute to the development of more effective disease management strategies.

This research was supported by a doctoral scholarship from the Secretaría de Ciencia, Humanidades, Tecnología e Innovación (SECIHTI), Mexico.

Evaluation and characterization of the biological activity of secondary metabolites from actinobacteria of the genus *Streptomyces*. Y. OSORIO-SÁNCHEZ, C.S. DELGADO-RAMÍREZ, L. M. DURÁN- RIVEROLL, R. HERNANDEZ-MARTINEZ, E. SEPÚLVEDA. *Centro de Investigación Científica y de Educación Superior de Ensenada, Ensenada, Baja California, México. E-mail:* yessica.osorio@cicese.edu.mx

The increasing global demand for food, intensified by climate change, has led to a greater reliance on agrochemicals to manage phytopathogenic fungi, bacteria, and uncontrolled weed proliferation. However, such dependence poses significant environmental and health concerns. As a sustainable alternative, biocontrol agents, particularly actinobacteria, have demonstrated considerable potential due to their ability to synthesize diverse secondary metabolites with herbicidal, antifungal, and antibacterial activities. In this study, four actinobacterial isolates (rbES158, rbES173, rbES339, and rbES331) were evaluated for their in vitro antifungal activity against *Lasiodiplodia brasiliensis* strain L28BCMX, one of the causal agents of dieback of grapevines in Baja California, Mexico. Among them, isolate rbES331 exhibited the highest antifungal activity, reaching 35% fungal growth inhibition under optimized temperature conditions (40 °C). To enhance the biosynthesis of bioactive secondary metabolites, rbES331 was cultured in the presence of filtered supernatants from *F. oxysporum* (iFOL) and *L. brasiliensis* (iL28) as elicitors. Induction with iFOL significantly increased antifungal efficacy, resulting in 50% inhibition against *F. oxysporum* and up to 70% against *L. brasiliensis*, whereas iL28 reduced antifungal activity to below 10% for both pathogens. These results suggest that the production of secondary metabolites in rbES331 is strongly influenced by specific biotic stimuli, underscoring the relevance of elicitor-based strategies for modulating secondary metabolism in actinobacteria for biocontrol applications.

This work was financed through institutional funds from the Centro de Investigación Científica y de Educación Superior de Ensenada, Ensenada, Baja California

Antibacterial activity of *Phaeomoniella chlamydospora* is regulated by acetate-mediated quorum sensing. Á. NOVÁK[1], D. SZABÓ[1], N. MOLNÁR[1], A. GOMBA-TÓTH[1], X. PÁLFI[1], K.Z. VÁCZY[1], Z. KARÁCSONY[1]. [1]*Eszterházy Károly Catholic University, Food and Wine Research Institute, Leányka str. 8/G, Eger, H3300, Hungary, E-mail:* karacsony.zoltan@uni-eszterhazy.hu

Phaeomoniella chlamydospora is regarded as a "pioneer" pathogen among the fungal agents responsible for Esca disease, playing a key role in the initiation and progression of symptoms. The disease has an unusually long asymptomatic phase, suggesting that these pathogens

may persist as endophytes within the host for extended periods. Their transition to pathogenic behavior appears to be triggered by rarely occurring factors, such as severe host stress or the accumulation of a threshold level of fungal biomass. Our previous findings demonstrated that *P. chlamydospora* secretes acetate, which positively affects biofilm development through quorum sensing mechanism. In this study, we investigated how exogenously applied acetate influences the expression of antibacterial activity by *P. chlamydospora*. Four bacterial strains belonging to the genus *Pseudomonas*, isolated from the grapevine xylem, were used in the experiments. All three examined *P. chlamydospora* strains exhibited antibacterial activity against these isolates in a preliminary confrontation assay. To assess the effect of acetate on this phenomenon, liquid culture assays were conducted with the fungi using an increasing acetate supplement (6.25-100 mM; five-step, two-fold dilution series). Bacterial growth in the presence of fungal culture filtrates was assayed by spectrophotometry. Our results indicated that acetate inhibits the antibacterial capacity in all bacterium-fungus strain combinations, especially at high concentrations. These results suggest that acetate-mediated quorum sensing regulates antibacterial activity of *P. chlamydospora* by permitting this process at lower fungal cell densities, whilst inhibiting antibacterial activity at higher cell densities.

This research was financially supported by the by the National Research, Development and Innovation Office through project TKP2021-NKTA-16.

Wood microbiome analysis in GTDs-symptomatic and asymptomatic table grape vines across Greece. A. FLOUDAS[1], F. BEKRIS[2], N. KRASAGAKIS[3,4], S.K. SOULTATOS[3,4], S.G. TESTEMPASIS[1], E. MARKAKIS[3,4], G.S. KARAOGLANIDIS[1], D.G. KARPOUZAS[2]. [1]*Plant Pathology Laboratory, Faculty of Agriculture, Aristotle University of Thessaloniki, Thessaloniki, Greece.* [2]*University of Thessaly, Department of Biochemistry and Biotechnology, Larissa, Greece.* [3]*Department of Agriculture, School of Agricultural Sciences, Hellenic Mediterranean University, Stavromenos, Heraklion, Greece.* [4]*Laboratory of Mycology, Department of Viticulture, Vegetable Crops, Floriculture and Plant Protection, Institute of Olive Tree, Subtropical Crops and Viticulture, Hellenic Agricultural Organization DIMITRA, Heraklion, Greece. E-mail:* afloud@agro.auth.gr

Grapevine Trunk Diseases (GTDs) are among the most destructive diseases affecting grapevines worldwide. This study examined the structure and diversity of microbial communities inhabiting grapevine wood, with a particular focus on the table grape cultivar Sultanina, to explore their potential roles in GTDs. Sampling was conducted in three geographically distinct viticultural regions of Greece (north, central, and south). Amplicon sequencing targeting the V4 region of the 16S rRNA gene and the ITS2 region was performed to characterize bacterial and fungal communities, respectively. Non-metric multidimensional scaling (NMDS) and permutational multivariate analysis of variance (PERMANOVA) were used to evaluate differences in microbial community composition between symptomatic and asymptomatic vines, as well as among geographic regions. The analysis identified biogeography as the strongest determinant of the fungal microbiome ($P < 0.001$, 18.5%), followed by vine age ($P < 0.001$, 7.3%). GTD symptom status also had a statistically significant, albeit smaller, effect ($P < 0.001$, 1.3%). The bacterial microbiome exhibited similar but weaker patterns compared to the fungal communities. Co-occurrence network analysis between GTD-associated fungal pathogens and bacterial taxa revealed interactions that may guide the isolation and development of novel biocontrol agents against GTDs.

The present study was conducted within the framework of the project entitled: «Innovations in Plant Protection for sustainable and environmentally friendly pest control» (InnoPP, TAEDR-0535675) «Funded by the European Union- Next Generation EU, Greece 2.0 National Recovery and Resilience plan»

Unraveling the interplay of soil health, water quality, and fungal pathogens in a Mexican vineyard: A multi-year assessment. R. RODRÍGUEZ-CUÉLLAR[1], E. JIMÉNEZ-GARCIA[2]. [1]*Universidad de Guanajuato, sede Departamento de Minas, Geología y Metalurgia.* [2]*Secretaria del Campo, Guanajuato E-mail:* info@rodrigo.wine

Grapevine trunk diseases (GTDs) represent a major constraint to global viticulture, compromising vine longevity and productivity. This study aimed to identify environmental stressors that contribute to GTD development and to propose integrated vineyard management strategies to improve vine health and sustainability. A multi-year investigation (2014–2023) was conducted in a *Vitis vinifera* vineyard located in San Miguel de Allende, Mexico, examining the complex interactions between soil health, irrigation water quality, and the emergence of trunk-associated fungi. Physicochemical analyses consistently revealed alkaline pH in both soil and water, along with variable salinity and sodicity. Microbial plate

counts indicated reduced populations of aerobic bacteria, suggesting soil compaction and impaired nutrient cycling. These environmental stressors likely induced chronic vine stress, creating conditions favorable for GTD development. The presence of *Aspergillus* spp. and *Lasiodiplodia* spp. was documented, potentially acting as opportunistic pathogens in weakened vines. The findings underscore the urgent need for integrated vineyard management strategies that simultaneously improve soil health, ensure water quality, and enhance plant defense mechanisms to mitigate GTD incidence and support long-term vineyard sustainability.

This research was financed personally and with help from historical data from Armando Cisneros Almazan

Effects of virtuous and non-virtuous pruning types on Charente Ugni blanc grape and wine quality. E. BRUEZ[1], C. CHOLET[1], M. BOISSEAU[2], X. POITOU[2], P. COLL[2], S. LACAMPAGNE[1], L. GENY[1]. *[1]UMR Oenologie, EA 4577, Université de Bordeaux, INRAE, BSA, Institut des Sciences de la Vigne et du Vin, 210 Chemin de Leysotte - CS 50008, 33882 Villenave d'Ornon, France. [2] Hennessy Jas et Cie, 1 rue Richonne 16100 Cognac, France. E-mail:* emilie.bruez@u-bordeaux.fr

Since the use of sodium arsenite was banned in 2001, Grapevine Trunk Diseases (GTDs) have become more widespread. Different methods are used to control the disease. As a preventive method to avoid pathogen entry and reduce disease expression, the question of pruning quality has come to the fore. Our trial concerned two Ugni blanc parcels planted in 2006 and 2015, in vineyards managed in double Guyot-Poussard,by JAS HENNESSY & CO, at Juillac-le-Coq and Saint-Preuil in Charente. The parcels were established as double Guyot-Poussard. Two different types of quality pruning were applied in each of the two parcels. Non-virtuous pruning damaged the diaphragm, whereas virtuous pruning ensured a desiccation cone to maintain the diaphragm. The diaphragm is a natural internal partition within the node of a vine shoot that acts as a barrier, helping to isolate wounds, thus protecting the vine from pathogens entry. The desiccation cone generated by the pruning is deeper. The aim of our work was to measure over two vintages, 2023 and 2024, the different impacts of these two types of pruning quality on grape and wine quality on non-esca-foliar symptomatic vines, before the appearance typical foliar symptoms. Weight and quality of grapes were analysed at harvest. Microvinifications were then carried out without sulphur use. The wines were distilled using the Cognac process. On musts, wines and distillates, chemical analyses were performed: ester and higher alcohol aroma wine markers. Triangular wine tasting was carried out on six-month-old wines. Although the wine tasting analyses did detect differences (such as vegetal flavour more detected in young vines) between virtuous and non-virtuous pruning for the young parcel, it was more difficult to do so for the older one. The present study confirms the interest of applying virtuous pruning on a long-term basis. It can have an indirect effect on the plant's physiological functioning, keeping the vines alive longer and preserving the grape quality.

Utilizing native biocontrol agents from Pacific Northwest vineyards for grapevine trunk disease management. J.B. DESHIELDS[1,2], A. HOWARD[2], J. WOODHALL[3], A. N. KC[1,2]. *[1]Southern Oregon Research and Extension Center, 569 Hanley Rd, Central Point, OR 97502. [2]Department of Botany and Plant Pathology, Oregon State University, 2082 Cordley Hall, Corvallis, OR 97331. [3]Department of Entomology, Plant Pathology and Nematology, University of Idaho, Parma, ID 83660. E-mail:* achala.kc@oregonstate.edu

Grapevine trunk diseases (GTDs) pose a significant threat to vineyard productivity due to yield losses and increased management costs. Chemical fungicides are commonly used; however, few products are labeled for GTDs. Biological control agents (BCAs) offer a potential alternative, but their efficacy varies based on regional and environmental conditions. This study aims to identify native microbial populations in Oregon vineyards with potential biocontrol properties against GTDs, focusing on their *in vitro* antagonistic effects against GTDs fungi. Two hundred spur samples were collected from eight vineyards across Oregon's Willamette and Rogue Valleys, from which microorganisms were isolated to assess their potential as BCAs. Samples were plated on selective media targeting suspected BCA genera, and distinct cultures were isolated based on morphology. Each isolation originated from a single fungal spore or bacterial colony and was characterized via PCR and sequencing. Potential BCA genera identified include *Aureobasidium* (95%), *Bacillus* (62%), *Pseudomonas* (95%), *Rhodotorula* (62%), and *Trichoderma* (6%), along with 97 isolates of potential GTD pathogens. The Willamette Valley exhibited significantly higher recovery rates for *Bacillus* (P = 0.003) and *Rhodotorula* (P = 0.044), highlighting regional differences. In vitro inhibition assays are ongoing to evaluate the antagonistic effects of isolates on GTD pathogens. Assays are performed at controlled temperatures (10°C, 15°C, 20°C, and 25°C) to assess

the temperature-dependent efficacy of BCAs, addressing concerns about diminished performance in Oregon's cooler climate. Preliminary results suggest *Bacillus velezensis*, collected from Oregon vineyards, has a significant effect (-23.4%; $P = 0.0261$), at 25°C, on the reduction of *in vitro* growth of *Dothiorella iberica*, a causative agent of Botryosphaeria dieback. These findings highlight the potential for GTD management in PNW vineyards. Further research with temperature-specific trials will help refine application recommendations for optimal performance in cooler climates where BCA efficacy has historically been limited.

This research was financially supported by the Northwest Center for Small Fruits Research.

Biological control of *Diplodia* spp. inoculum in dormant *Vitis vinifera* using *Trichoderma* spp. E. DONOSO[1], W. HETTICH[1], L. ROMERO[1]. [1]*Bio insumos Nativa, parcela antilhue lote 4b2, Maule. E-mail:* edonoso@bionativa.cl

This study investigated the efficacy of *Trichoderma* spp. (Mamull®) formulations in controlling *Diplodia seriata* inoculum on dormant *Vitis vinifera* following pruning. A field trial conducted in Talca, Central Chile, used a randomized block design with 10 replicates per treatment. Pruning debris inoculated with *Diplodia seriata* pycnidia was placed under Semillon grapevine. Treatments included: T0 (inoculated control), T1 (non-inoculated control), T2 (chemical pruning paste: pyraclostrobin), T3 (foliar Mamull®), and T4 (Mamull® soil application). Pycnidia parasitism and viability were assessed 15 days post-pruning while wood damage incidence and severity were evaluated 180 days. T3 (foliar Mamull®) had the lowest incidence (1.5%), significantly different from T0 (15.8%), and comparable to T2 (3.5%). T4 soil Mamull® (8.4%), while T1 was 5.8%. Severity followed a similar trend ($P<0.05$): T0 (3.23 cm), T3 (0.4 cm), T2 (0.5 cm), T4 (1.4 cm), and T1 (0.9 cm). Pycnidia parasitism was highest in T4 (63.4%) with lowest viability (10.5%), significantly different from all other treatments. T3 had 10.4% parasitism and 24.5% viability. T2 and T0 showed no significant difference (4.5% parasitism, 45.4% viability). These results support the potential of foliar and soil applications of Mamull® as effective biological control tools for managing *D. seriata* inoculum in pruning debris.

Evaluation of fungicides and biocontrol agents against *Aspergillus* Vine Canker. E.A. RANGEL-MONTOYA[1,2], M. SÁNCHEZ-SÁNCHEZ[2], R. HERNANDEZ-MARTINEZ[2]. [1]*Facultad de Ciencias Químicas e Ingeniería, Tijuana UABC.* [2]*Centro de Investigación Científica y de Educación Superior de Ensenada, CICESE. E-mail:* erangel@cicese.mx

Aspergillus Vine Canker (AVC) is an emerging disease affecting grapevine shoots, particularly during the training phase. Symptomatic plants show reddish sap exuding from infection sites, discolored, spongy vascular tissue, and black cankers. Recent reports from Mexico have identified highly virulent isolates of *Aspergillus niger* and *Aspergillus tubingensis* in vineyards in Sonora and Baja California. Currently, no effective management measurements are available for AVC. This study evaluated the efficacy of various fungicides and biocontrol agents against *Aspergillus* spp. A total of 18 commercial fungicides were tested using poisoned PDA media at recommended concentrations. Additionally, dual culture assays were conducted with five *Bacillus* spp. and six *Trichoderma* spp. strains. All assays were performed in triplicate, and data were analyzed using one-way ANOVA followed by Fisher's LSD test ($\alpha < 0.05$). Results showed that fungicides containing benzimidazole, myclobutanil, and hymexazol achieved nearly 100% inhibition of fungal growth. Among the biocontrol agents, *Bacillus amyloliquefaciens* isolates BEPVP26BCMX and BEPVP31BCMX, along with *Trichoderma harzianum* T06BCMX and *Trichoderma asperellum* EF09BCMX, inhibited fungal growth by 40–60%. Further analysis assessed the effect of the most effective treatment on conidial germination. Myclobutanil and benzimidazole completely inhibited germination, while biocontrol agents disrupted the fungal cell wall, thereby impeding germination. Finally, the efficacy of these treatments was assessed in planta. Grapevines inoculated with *Aspergillus* and treated with benzimidazole and myclobutanil-based fungicides, as well as *B. amyloliquefaciens* and *T. asperellum*, showed no necrotic lesions, indicating their potential to suppress *Aspergillus* growth in grapevines. These findings support the development of integrated and effective control strategies for managing AVC in Mexican vineyards.

This research was supported by a doctoral scholarship from the Secretaría de Ciencia, Humanidades, Tecnología e Innovación (SECIHTI), Mexico.

Improving and extending the productive life of grapevines affected by trunk disease using remedial surgery. M.R. SOSNOWSKI[1,2], E. VAN ZIJLL DE JONG[3]. [1]*South Australian Research and Development Institute, Adelaide SA 5001, Australia.* [2]*School of Agriculture, Food and Wine,*

Waite Research Institute, The University of Adelaide, SA 5005, Australia. [3]*Linnaeus Limited, PO Box 1199, Gisborne 4040, New Zealand. E-mail:* mark.sosnowski@sa.gov.au

Grapevine trunk diseases such as Botryosphaeria and Eutypa dieback undermine the economic viability of vineyards. Causal pathogens typically enter vines through pruning wounds, causing wood decay, reduced productivity, and eventually vine death. Remedial surgery is the only curative option for managing GTDs and involves removing diseased cordons and trunks and training a new watershoot. The objective of this research was to evaluate the benefits of remedial surgery to vine health, productivity and longevity in grafted vines. Trials were established in three mature commercial vineyard blocks using approximately 4000 vines each of 'Sauvignon Blanc', 'Cabernet Sauvignon' and 'Merlot'. Remedial surgery was undertaken over 5 years in winter, and spring and severity of disease was recorded prior to surgery and their performance following treatment was compared to untreated controls. Significant changes were recorded in incidence and severity of disease in both the canopy and trunk. Internal trunk staining did not correspond with canopy symptom severity. Multiple species of *Botryosphaeriaceae* pathogens were frequently detected in the trunks >200 mm in advance of the staining, occasionally at shoot removal wound sites and often at the bottom of trunks. *Eutypa lata* was occasionally detected together with these pathogens. Vine recovery after remedial surgery varied between cultivars, declined over time and with increased disease severity, but did not differ between winter and spring surgery. Over the 5-year study, yields in control vines declined significantly. Remedial surgery improved vine productivity and the yields from reworked vines often surpassed target levels for the blocks. Remedial surgery appeared to slow the trunk disease progression, with no obvious dieback observed in the canopies of reworked vines, though occasional vine deaths occurred. This is the most comprehensive study on remedial surgery worldwide, and ongoing monitoring of these blocks will elucidate the impact of remedial surgery on vineyard longevity.

This research was financially supported by the New Zealand Ministry of Business, Innovation and Employment, New Zealand Winegrowers and Bragato Research Institute.

Efficacy of Tachigaren® (hymexazol 360 g/L) SL in plant recovery of grapevine associated with *Lasiodiplodia theobromae* in Peru. L.A. ALVAREZ[1], G. ESPINO[2]. [1]*Facultad de Ciencias Agrarias. Universidad Nacional de Cañete. Cañete, Lima.* [2] *Summit Agro South America SpA, Sucursal Perú, E-mail:* lalvarez@undc.edu.pe

Peru is currently the leading exporter of table grapes in the world. Grapevine trunk pathogen such as *Lasiodiplodia theobromae* (teleomorph: *Botryosphaeria rhodina*) causes severe losses in the main grapevine producing areas of the country. Field studies were conducted to determine the efficacy of hymexazol in the control of infections by *L. theobromae* and its role as root growth promoter. Five doses of hymexazol were evaluated: 0.0, 1.5, 2.0, 2.5, and 3.0 L ha-1, which were applied via irrigation systems at the berry setting stage. Healthy vines were distributed among five treatments in a randomized complete block design. Canes from these vines were inoculated by wound using a plug colonized by an isolate of *L. theobromae* five days before hymexazol application. For evaluation of hymexazol as root promoter, five galvanized steel boxes were placed randomly around vines in each experimental unit to evaluate root development. Sixty days after hymexazol application, the galvanized steel boxes were collected to evaluate the weight of new roots per treatment, and the inoculated canes were also collected to evaluate the lesion expansion. Lesions registered in vines treated with hymexazol were significantly lower than the nontreated control. The lesion length was reduced compared to nontreated control by 68%, 77%, and 81% for 2.0, 2.5, and 3.0 L ha^{-1}, respectively. The doses of 2.5 and 3.0 L ha^{-1} had 28 % and 36 %, respectively, more root development than the control treatment. The use of hymexazol in an integrated management program may represent an interesting tool to control *L. theobromae* in grapevine plants.

Compost as a source of beneficial *Trichoderma* for the biocontrol of Grapevine Trunk Diseases. J. ANGUIANO[1], C. DELGADO-RAMÍREZ[1], L. GUERRERO[1], C. VALENZUELA-SOLANO[2], R. HERNANDEZ-MARTINEZ[1]. [1]*CICESE. Departamento de Microbiología. Ensenada, Baja California.* [2]*Instituto Nacional de Investigaciones Forestales, Agrícolas y Pecuarias (INIFAP). Campo Experimental Costa de Ensenada, Ensenada, Baja California, 22880, Mexico. E-mail:* anguiano@cicese.edu.mx

In northwestern Mexico, the main grapevine trunk diseases are caused by *Lasiodiplodia* spp. and *Cylindrocarpon*-like fungi, representing an increasing problem due to the scarcity of effective control strategies. Grapevine wood compost may serve as a promising source of beneficial microorganisms for managing these diseases. This study aimed to isolate and identify *Trichoderma* strains

from grape compost with biocontrol activity against grapevine trunk disease fungi. A total of twenty-five *Trichoderma* strains (TL01-TL25) were obtained from a four-month-old compost pile. All strains produced chitinases, and twenty-three also produced siderophores. Most strains showed optimal growth between 25°C and 30°C, but TL15 exhibited the highest adaptability to higher temperatures, maintaining growth across a broader range from 25°C to 37°C. Although none of the strains grew at 45°C, all resumed growth when returned to room temperature. Dual culture assays were conducted to assess antagonistic activity against *Lasiodiplodia brasiliensis* isolate MXBCL28, *Nectria* sp. isolate RCCM9 and *Dactylonectria* sp. isolate MGN2. Four strains of *T. asperellum* (TL06, TL09, TL11 and TL16) were selected, based on their consistent performance, inhibiting the growth of *Nectria* and *Dactylonectria* by over 70%. These four strains were further evaluated for their production of volatile and non-volatile compounds, as well as their mycoparasitic activity using a pre-colonized plate method. None inhibited *L. brasiliensis* through production of volatile compounds, although they inhibited both *Nectria* sp. and *Dactylonectria* sp. by up to 40%. In contrast, non-volatile compounds inhibited the growth of all tested fungi by up to 73%, and in the mycoparasitism assays, pathogens were eliminated from 23% to 100% of the agar plugs from the precolonized plates. In conclusion, *Trichoderma asperellum* strains capable of suppressing grapevine trunk pathogens through multiple mechanisms of action were identified. Further *in planta* studies are needed to confirm their effectiveness under field conditions.

This research was supported by a doctoral scholarship from the Secretaría de Ciencia, Humanidades, Tecnología e Innovación (SECIHTI), Mexico.

Evaluating the biocontrol potential of *Fusarium* spp. against the grapevine trunk disease pathogen *Lasiodiplodia brasiliensis*. L.A. CÓRDOBA-CASTRO[1], P.A. ROCHA LÓPEZ[1], E.A. RANGEL-MONTOYA[1,2], C. VELASCO-SOSA[3], R. HERNANDEZ-MARTINEZ[1]. *[1]Departamento de Microbiología, Centro de Investigación Científica y de Educación Superior de Ensenada, Baja California (CICESE), Ensenada 22860, México. [2]Facultad de Ciencias Químicas, Universidad Autónoma de Baja California, Tijuana. [3]Facultad de Ciencias, Universidad Autónoma de Baja California, Ensenada. E-mail:* lcordoba@cicese.mx

Trunk diseases caused by fungal pathogens represent one of the most critical phytosanitary concerns in grapevine production worldwide. *Lasiodiplodia brasiliensis* is a highly virulent species responsible for necrotic lesions, cankers, dieback, and premature plant death, leading to substantial economic losses in the northwestern region of Mexico. Non-pathogenic strains of *Fusarium* have the potential to be effective biocontrol agents against plant diseases through various mechanisms, including competition, induced resistance, and the production of antifungal metabolites. Given the limitations of chemical control and the need for sustainable alternatives, this study aimed to characterize *Fusarium* strains and assess their potential as biological control agents against *L. brasiliensis*. *Fusarium* spp. isolates were obtained from citrus trees and tested to be non-pathogenic after one year of inoculation. Sixteen isolates of *Fusarium* were identified through molecular analysis using ITS and EF-1α markers as *F. equiseti* (4), *F. nanum* (1), *F. citri* (1), *F. incarnatum* (7), *F. brachygibbosum* (1), and *F. denticulatum* (1). Enzymatic activity assays showed that *F. equiseti* isolate SCT04-5 had the highest amylase production, while *F. brachygibbosum* isolate SCT33-3 demonstrated the most potent protease activity. Antagonism, evaluated through in vitro dual culture assays, found that *F. brachygibbosum* isolate SCT33-3 showed the most significant inhibition (38.7%), followed by *F. denticulatum* isolate SCT58-3 (33.6%). Inhibition halos were also observed for *F. equiseti* (isolates SCT04-5 and SCT51-5) and *F. incarnatum* isolate SCT16-3, indicating the possible secretion of antifungal metabolites. Although in planta assays are underway, these findings suggest the potential use of *Fusarium* isolates as biocontrol agents for grapevine trunk diseases.

This research was supported by a doctoral scholarship from the Secretaría de Ciencia, Humanidades, Tecnología e Innovación (SECIHTI), Mexico.

Nanoparticles and selected chemical compounds significantly inhibit grapevine trunk disease pathogens. K. ŠTŮSKOVÁ[1], T. KISS[1], Z. BYTEŠNÍKOVÁ[2], L. RICHTERA[2], D. GRAMAJE[3], A. EICHMEIER[1]. *[1]Mendeleum—Institute of Genetics, Faculty of Horticulture, Mendel University in Brno, Valtická 334, 691 44 Lednice na Moravě, Czech Republic;[2]Department of Chemistry and Biochemistry, Mendel University in Brno, Zemědělská 1, 613 00, Brno, Czech Republic; [3]Instituto de Ciencias de la Vid y del Vino (ICVV), Consejo Superior de Investigaciones Científicas – Gobierno de La Rioja – Universidad de La Rioja, Ctra. LO-20 Salida 13, 26007 Logroño, Spain. E-mail:* ales.eichmeier@mendelu.cz

Grapevine is among the most important cultivated crops globally, but is increasingly threatened by the grapevine

trunk disease (GTD) complex. Due to the lack of effective curative treatments and growing restrictions on chemical pesticide use, alternative control methods—such as nanoparticle applications—are gaining attention. We hypothesized that the selected chemical compounds and nanoparticles would exhibit antifungal activity against GTD pathogens. In a two-year *in planta* study, the inhibitory effects of four chemical agents (sodium arsenite, silver nitrate, silver thiosulfate complex and 8-HCH), and one nanoparticle formulation (AgSe at 100 % concentration, containing 2.59 g l^{-1} of Ag and 0.90 g l^{-1} of Se) were tested against three key GTD pathogens: *Diaporthe eres* Nitschke, *Diplodia seriata* De Not., and *Eutypa lata* (Pers.) Tul. & C. Tul. The pathogens were artificially inoculated using fungal discs (3 mm in diameter). The percentage of inhibition was calculated using the formula: $I = ((r_c - r_t)/r_c) \times 100$, where I is the inhibition percentage, r_c is the average percentage of necrosis in the control group, and r_t is the average percentage of necrosis in the treated group. All tested chemical agents (excluding nanoparticles) demonstrated inhibitory activity, ranging from 33.64% to 93.65%, significantly different from the untreated control. The silver-selenium nanoparticle formulation showed inhibitory effects specifically against *D. eres* and *E. lata*, with inhibition ranging from 55.01% to 86.85%. These findings highlight the potential of nanoparticle-based treatments as a promising alternative in integrated GTD management strategies.

This research was financially supported by project No. CZ.02.1 .01/0.0/0.0/16_017/0002334, funded by the Ministry of Education, Youth and Sports.

Evaluation of selected fungal biological control agents for the protection of grapevine pruning wounds against *Diplodia seriata*. A. FLOUDAS[1], S. TESTEMPASIS[1,2], A. FLARI[1], E. DIMOU[1], A. ELEFTHERIADOU[1], G. S. KARAOGLANIDIS[1]. *[1]Aristotle University of Thessaloniki, Faculty of Agriculture, Forestry and Natural Environment, Plant Pathology Laboratory, Thessaloniki, Greece. [2]Department of Agriculture, School of Agricultural Sciences, University of Western Macedonia, 53100 Florina, Greece. E-mail:* afloud@agro.auth.gr

Grapevine Trunk Diseases (GTDs) are among the most destructive grapevine diseases, causing significant economic losses due to vineyard decline and replanting costs. The lack of effective chemical measures highlights the urgent need for environmentally and consumer-friendly alternatives. Biological Control Agents (BCAs) offer a promising, sustainable approach, targeting multiple GTD-associated fungi. This field study was conducted in the viticultural region of Nemea to evaluate the efficacy of four BCAs - *Trichoderma atroviride*, *T. citrinoviride*, *T. ghanense*, *Talaromyces pinophilus*—and a mixture (*T. ghanense* + *T. pinophilus*) in controlling infections by *Diplodia seriata*, a key GTD pathogen in Greece. Two Greek grapevine cultivars with contrasting susceptibility - Roditis (susceptible) and Limnio (tolerant) were used. BCAs were applied as conidial suspensions on fresh pruning wounds, followed 24 hours later by artificial inoculation with *D. seriata*. After six months, samples were collected and analyzed using a culture-based method. Pathogen re-isolation was conducted on PDA medium, and all obtained fungal isolates were identified molecularly. The results revealed that *T. pinophilus* and its mixture with *T. ghanense* provided strong protection in the susceptible cultivar Roditis, substantially reducing pathogen recovery. Conversely, *T. atroviridae* was more effective in the tolerant cultivar Limnio, indicating a potential cultivar-specific interaction. All BCAs demonstrated the ability to colonize and persist on pruning wounds. These findings reinforce the potential of BCAs as effective, sustainable tools for GTD management and support their integration into future vineyard protection strategies.

This research was funded by the European project SHIELD4GRAPE (HORIZON-CL6-2023-BIODIV-01, NUMBER 101135088).

Ozonated Water: A novel strategy for controlling grapevine trunk pathogens during grapevine's propagation. N. CHRISTOU[1], S. TESTEMPASIS[1,2], A. FLOUDAS[1], S. KARATSALOU-LEGAKI[3], K. BAKASIETAS[3], G.S. KARAOGLANIDIS[1]. *[1]Laboratory of Plant Pathology, Faculty of Agriculture, Forestry and Natural Environment, Aristotle University of Thessaloniki, 54124 Thessaloniki, Greece; [2]Vine Nurseries Bakasietas, Nemea, Greece; [3]Department of Agriculture, School of Agricultural Sciences, University of Western Macedonia, 53100 Florina, Greece E-mail:* gkarao@agro.auth.gr

Grapevine Trunk Diseases (GTDs), caused by various fungal pathogens, represent a major threat to viticultural production worldwide. Effective management of GTDs depends on multiple factors, including the pathogen species, geographic location, climate, grapevine cultivar, and agricultural practices. Notably, the propagation phase in nursery production has been identified as a critical point for the dissemination of GTD pathogens. This study evaluates the efficacy of ozonated water (2.5 ppm) as an alternative to a conventional fungicide (Switch 25/37.5 WG, Syngenta, Greece) in the grapevine

propagation process. Scion and rootstock materials were artificially inoculated with a conidial suspension (2×10^4 conidia mL^{-1}) of *Phaeomoniella chlamydospora* (Pch) and *Dactylonectria torresensis* (DacT). The commercial propagation protocol of VNB Bakasietas (Nemea, Greece) was followed. During the rehydration steps, plant materials were treated with either ozonated water or the conventional fungicide. The resulting grafted plants were established in commercial vineyards and assessed six months later for plant growth parameters (dry matter, stem and root length) and disease severity, the latter via RT-qPCR-based quantification of pathogen DNA. Overall, plants treated with ozonated water showed enhanced growth performance, with significantly longer roots and stems compared to those treated with fungicide. In artificially inoculated material, significantly lower levels ($P < 0.05$) of Pch and DacT were detected in ozonated water treatments. Specifically, the mean concentrations of Pch and DacT in ozonated plants were 3.94 and 4.14 copies μL^{-1}, respectively, versus 10.73 and 6.23 copies μL^{-1} in fungicide-treated plants. These results demonstrate that ozonated water is a promising, eco-friendly alternative to chemical fungicides, offering both improved vine growth and reduced pathogen presence during the propagation phase.

This research is co-financed by Greece and the European Union (European Social Fund- ESF) through the Operational Programme «Human Resources Development, Education and Lifelong Learning 2014-2020» in the context of the project "Optimization of the production of propagating material of the vine using natural, biological and biotechnological methods" (T2EDK-05084).

Pruning cut position affects the susceptibility of grapevine pruning wounds to *Eutypa lata* and natural dieback. D. MARCH[1], S.P.B. PARKER[1], E.S. SCOTT[1], M.R. SOSNOWSKI[1,2]. *[1]School of Agriculture, Food and Wine, Waite Research Institute, The University of Adelaide, SA 5005, Australia. [2]South Australian Research and Development Institute, Adelaide SA 5001, Australia. E-mail:* mark.sosnowski@sa.gov.au

Eutypa dieback is caused by infection of pruning wounds by spores of Diatrypaceaeous fungi, primarily *Eutypa lata*. Recently popularised pruning techniques claim to influence grapevine pathology and physiology. More specifically, retaining long wood stubs above the node on canes may decrease pathogen colonisation into live tissue beyond the node and natural dieback or desiccation into permanent vascular tissue to disrupt sap flow. Similarly, crown cuts that retain basal buds to produce shoots and retain sap flow may limit colonisation and dieback into permanent wood, compared to flush cuts which remove basal buds. Furthermore, the diaphragm, a zone of hardened pith cells that divides the pith at the node, has been proposed to limit dieback. The objective was to investigate the effect of pruning cut position on *E. lata* colonisation and natural dieback. Trials were established on Shiraz vines in South Australia. In 2021, two trials on spur-pruned vines involved cutting canes to two nodes either directly above the distal node or just below the next node to leave long stubs. In a third trial in 2022 on cane-pruned vines, 1-year-old canes were removed from 2-year-old canes by either cutting flush so that basal buds were removed or making crown cuts that retained the buds and diaphragm. Wounds were inoculated with spores of *E. lata* or left uninoculated and the following winter spurs and canes were removed and assessed for extent of staining and recovery of *E. lata*. Retention of stubs or basal buds reduced the incidence of recovery of *E. lata* following pruning, which may be related to diaphragm integrity or basal bud influence on wound responses. Staining, or natural dieback, was also limited where stubs or basal buds were retained; causal mechanisms require further investigation. These findings support retention of wood stubs and basal buds when pruning.

This research was the outcome of two honors projects undertaken by Daniel March and Sam Parker through the University of Adelaide, with support from the South Australian Research and Development Institute.

Phytopathologia Mediterranea
The international journal of the
Mediterranean Phytopathological Union

Firenze University Press
www.fupress.com/pm

Research Papers

Occurrence and characterization of *Stemphylium* and *Alternaria* species associated with lettuce leaf spot in Algeria

Nabahat BESSADAT[1,2], Nelly BATAILLÉ-SIMONEAU[1], Justine COLOU[1], Bruno HAMON[1], Mabrouk KIHAL[2], Philippe SIMONEAU[1,*]

[1] *University of Angers, Institut Agro, INRAE, UMR IRHS, SFR QUASAV, 42 rue G. Morel, CS60057, 49071 Beaucouzé, France*
[2] *Laboratoire de Microbiologie Appliquée, University Oran1 Ahmed Ben Bella, BP1524 El M'naouer, Oran 31000, Algeria*
*Corresponding author. E-mail simoneau@univ-angers.fr

Summary. Lettuce leaves (*Lactuca sativa*) with leaf spot symptoms were collected from an organic farm and from farm markets in Oran Province, Oran, northwest Algeria, during the 2022 and 2023 growing seasons. A total of 119 isolates with morphological characteristics of *Stemphylium* and *Alternaria* were obtained from brown necrotic lesions on lettuce leaves. Based on morphological and multi-gene sequencing analyses, these isolates were identified as *Stemphylium lycopersici*, *S. vesicarium*, *S. eturmiunum*, *S. amaranthi*, and *S. gracilariae*, and *Alternaria* in sections *Alternaria* and *Eureka*. Pathogenicity tests with 24 representative isolates were conducted on young lettuce plants under greenhouse conditions, and lesions similar to those observed on the field and market collected plants developed on leaves of inoculated plants. *Stemphylium gracilariae* and *S. lycopersici* were the most aggressive fungi, causing extensive leaf necroses and defoliation, while other *Stemphylium* and *Alternaria* isolates develop small necrotic spots on mature leaves. A series of cross-inoculation experiments compared disease severity when plants were inoculated with one of four *Stemphylium* species alone or paired with one of five *Alternaria* isolates (20 combinations total). Differences in pathogenicity of mixed inoculations compared to single inoculation were detected, but synergistic increases in leaf spot severity were not detected for any mixed inoculations. These results demonstrate the potential of emerging fungal pathogens to cause lettuce leaf spot, and that *Stemphylium* and *Alternaria* species combinations can damage economically important lettuce crops.

Keywords. Foliar disease, *Lactuca sativa*, morphology, *Pleosporaceae*, phylogeny, pathogenicity.

OPEN ACCESS

Citation: Bessadat, N., Bataillé-Simoneau, N., Colou, J., Hamon, B., Kihal, M., & Simoneau, P. (2025). Occurrence and characterization of *Stemphylium* and *Alternaria* species associated with lettuce leaf spot in Algeria. *Phytopathologia Mediterranea* 64(3): 493-512. DOI: 10.36253/phyto-16548

Accepted: August 27, 2025

Published: November 3, 2025

Data Availability Statement: All relevant data are within the paper and its Supporting Information files.

Competing Interests: The Author(s) declare(s) no conflict of interest.

Editor: Thomas A. Evans, University of Delaware, Newark, DE, United States.

ORCID:
NB: 0000-0001-7795-2606
NB-S: 0000-0001-6200-4259
JC: 0000-0002-9623-4412
BH: 0000-0001-5868-0676
MK: 0000-0003-2901-373X
PS: 0000-0002-3890-9848

INTRODUCTION

Lettuce (*Lactuca sativa*) is an economically important and widely grown leafy vegetable crop (Shatilov *et al*., 2019), for fresh use in salads, sandwiches, and wraps, or cooked (Katz and Weaver, 2003; Fearnley-Whittingstall, 2013). Lettuce has antioxidant, anti-diabetic, anti-inflammatory, anti-cardiovascular

disease, anti-cancer, and health-promoting effects (Kim *et al*., 2016), and is a low-calorie, low-fat, and low-sodium salad vegetable, rich in fiber, folate, vitamin C, and essential minerals, (Kim *et al*., 2016). Lettuce tissues also contain essential nutritional bioactive compounds (Yang *et al*., 2022). Several lettuce types and cultivars are grown throughout each year in Algeria, in open fields or greenhouses (Institut Technique des Cultures Maraîchères et Industrielles, 2010; Lallouche *et al*., 2020).

Lettuce production can be exposed to several biotic stresses. Among these, leaf spot diseases caused by fungi can be damaging in certain cropping situations (Subbarao *et al*., 2017), but little research has been carried out to characterize these diseases in Algeria.

Lettuce leaf spot symptoms are brownish angular or circular lesions, which are slightly sunken and have brown necrotic centers that can become holes with time. Fungal pathogens of *Pleosporaceae* (*Pleosporales*, *Dothideomycetes*, *Ascomycetes*), including *Stemphylium* and *Alternaria*, are reported to cause the most common foliar diseases of lettuce in temperate zones (Nasehi *et al*., 2013; 2014; Koike *et al*., 2017; Liu *et al*., 2019). In fact, *Alternaria* spp. and *Stemphylium* spp. are prevalent in Northwest of Algeria and cause major crop major losses in this country (Bessadat *et al*., 2017; 2019; 2022). These pathogens infect lettuce foliage and other plant tissues. *Alternaria* and *Stemphylium* are also abundant in the atmosphere (Damialis *et al*., 2017) and are important human allergens and pathogens (Gutiérez-Rodriguez *et al*., 2011; Grewling *et al*., 2020; Sánchez *et al*., 2022).

Alternaria and *Stemphylium* are introduced into lettuce fields by windblown conidia from neighbouring plants (including weedy hosts) and crop debris, or as seed-borne inoculum (Blancard, 2021; Roberts and Punja, 2021). Development of both fungi is favoured by warm weather and high humidity (Singh *et al*., 2015; Blancard, 2021). Reduced photosynthetic area leads to varying crop losses and economic impacts (Das *et al.* 2019). In lettuce, fungal toxins can inhibit seedling growth (Das *et al*., 2019; Wang *et al*., 2022). Additionally, small plants and cosmetic damage, such as leaf spotting, can reduce yields and render affected lettuce unsalable.

Alternaria and *Stemphylium* induce small necrotic spots on lettuce leaves that can enlarge over time, often appearing dark brown due to pathogen conidium production. Optimum temperatures for infection are from 18 to 25°C which are typical of Mediterranean climates, and these temperatures extend during winter in Algeria (Algeria Climate Fact Sheet, 2023). In severe cases, lesions enlarge and coalesce to blight entire leaves. As leaves age, they increase in susceptibility. Both fungi can overwinter on infested plant residue and infected volunteer plants (Hay *et al*., 2021; Matić *et al*., 2020). In the next life cycle stage, secondary conidia and ascospores are released and dispersed from dead plant tissues of the previous season or from leaf lesions of nearby plants (Basallote-Ureba *et al*., 1999; Damialis *et al*., 2017). Leaf infections from conidia can occur by various mechanisms such as entry through stomata (Thomma, 2003; Tayviah, 2017), wounds caused by other diseases, insect pest feeding, movement of workers or farm equipment, or by the action of wind (Thomma, 2003; Nischwitz, 2016).

Identification of *Stemphylium* and *Alternaria* spp. has been based on morphological characteristics including conidium shape, size, septation, length to width ratio, and conidiophore dimensions (Simmons, 1969; 2001; 2007). However, many of these characteristics overlap among species due to varying environmental conditions, which complicates species identification, so different species can appear to be similar and may be misidentified when relying on morphological traits. Beyond morphological analyses, the relationships among these fungi have been unclear, prompting discussion and analysis using molecular markers (Pryor and Gilbertson, 2000; Camara *et al*., 2002; Inderbitzin *et al*., 2009). Molecular methods combined with phylogenetic analyses are considered more accurate for delineating species within several related fungi, re-defining and expanding the morphological group concept and other taxonomic hypotheses for both genera (Woudenberg *et al*., 2013, 2017; Li *et al*., 2023). This has separated *Alternaria* into 29 sections and seven monotypic lineages (Woudenberg *et al*., 2013; Al Ghafri *et al*., 2019; Marin-Felix *et al*., 2019; Gannibal *et al*., 2022), while *Stemphylium* is now classified into 33 species, distinct from *Alternaria* (Ariyawansa *et al*., 2015; Woudenberg *et al*., 2017; Brahmanage *et al*., 2019; Marin-Felix *et al*., 2019; Crous *et al*., 2020).

Alternaria alternata is considered the main causal agent of lettuce leaf spot, but other species such as *A. cichorii* (Pegg *et al*., 2014), *A. sonchi* (Subbarao *et al*., 2017), *A. solani, A. brassicae*, *A. brassicicola* (Moses *et al*., 2016; Guo *et al*., 2018), and *A. dauci* (Koike *et al*., 2017) have also been found on symptomatic leaves. Similarly, several species of *Stemphylium* are associated with the disease on cultivated lettuce, including *S. lycopersici*, *S. vesicarium* (Liu *et al*., 2019), *S. solani* (Nasehi *et al*., 2013), *S. gracilariae* (Woudenberg *et al*., 2017), and *S. lactucae* (Zhang and Zhang, 2002).

During 2022 and 2023, severe necroses were observed on lettuce plants at an organic farm and in commercialized head lettuce. Precise identification of the responsible pathogens was necessary to implement effective disease management. The objectives of the present study were to characterize the causal agents of emerging

leaf spot diseases on lettuce, using morphological analysis, multi-gene sequencing, and pathogenicity tests of representative isolates to assess fulfilment of Koch's postulates. To achieve these objectives, random samples of lettuce were obtained from fields and markets in Oran province, Algeria, and related studies were initiated.

MATERIALS AND METHODS

Sample collection and fungal isolation

In the autumn of 2022 and spring of 2023, symptomatic romaine lettuce plants were sampled from fields or markets in Oran Province, northwest Algeria. Symptoms on leaves were brown to dark brown, irregular to circular, ranging from 2 to 18 mm in diameter, across much of the leaf surface. Fungi were isolated by cutting one or two fragments (5–10 mm^2) from the margins of lesions. The samples were surface disinfected by immersing in 2% sodium hypochlorite solution for 2 min, rinsing three times in sterile distilled water, drying with sterilized paper towels, and then placing them on potato carrot agar (PCA) in Petri plates (Simmons, 2007). The plates were then incubated at room temperature (18–25°C) under natural daylight for 7 to 14 d. Conidia that developed were observed under a light microscope (Optika B-190 series, OPTIKA Srl) to identify species based on conidium morphology, and to estimate the frequencies of *Stemphylium* and *Alternaria* in the different plant samples. The frequencies of isolated fungi per lesion were calculated using the formula of Saleemi *et al.* (2012):

$$\text{Isolation Frequency (IF)} = \frac{\text{Number of samples with a species or genus} \times 100}{\text{Total number of samples}}.$$

Hyphae of prevalent fungi were picked from the peripheries of colonies and inoculated onto new PCA plates. Pure cultures were grown on Potato Dextrose Agar (PDA) slants for 7 to 14 d and then stored at 4°C and -80°C in 30% glycerol at the fungal culture collection COMIC (Collection of Microorganisms) of the SFR 4207 QUASAV (Angers, France) for future experiments.

Micro- and macro-morphological examination of isolates

Twenty-three representative isolates (five of *Alternaria* and eighteen of *Stemphylium*) were each inoculated into plastic plates (90 mm diam.) (n = 3) each containing 15 mL of PCA, and were grown under standardized conditions (Simmons, 2007). Micro-morphological characteristics of the isolates were observed after 7–14 d. Conidiophore lengths (n = 30), and conidium (n = 30) dimensions , shapes (L/W ratio), colours, and ornamentation, were determined at ×400 magnification from microscope slide preparations in lactic acid, using clear Scotch tape (Samson *et al*., 2010). The PCA plates were further incubated and checked for ascomata after 1 month of incubation at room temperature. Colony characteristics (colour, texture and diameter) were recorded on PDA plates (n = 3) after 7 d incubation at 25°C. Colour determinations were made using the colour charts of Kornerup and Wanscher (1978). The morphological characteristics of each isolate were registered and compared to strains previously identified on *Solanaceae* hosts including *S. gracilariae* (NB717, NB690), *S. lycopersici* (NB751), *S. eturmiunum* (NB709, NB735), or *S. vesicarium* (NB713, NB737) (Bessadat *et al*., 2022).

Pathogenicity assessments

Pathogenicity testing was carried out using two techniques. A primary set of inoculations experiments was conducted using six *Alternaria* and 18 *Stemphylium* representative isolates for individual inoculations. The isolates were grown on PCA under natural day light for 7–14 d at ambient temperature to promote conidium production. Conidia were then gently dislodged from cultures using a rubber spatula and suspended in sterilized distilled water supplemented with 0.01% Tween20 (Bessadat *et al*., 2017; 2022). Inoculations were carried out by spraying 10 mL of conidium suspension of each isolate (1×10^4 mL^{-1}) onto three 50-d-old lettuce plants cv. Romaine grown in sterilized commercial potting mix. The second set of inoculations involved cross-inoculation experiments to assess how *Alternaria* spp. affected the virulence of *Stemphylium* isolates. These were conducted using a completely randomized experimental design. Representative isolates of *Alternaria* (n = 5) or *Stemphylium* species (n = 4) were used in 50:50 mixtures ratios. Inoculated plants were then covered with polyethylene bags for 48 h to maintain high relative humidity (90%), and were then grown at 12–20°C, 55% relative humidity (night), and 24–33°C, 72% relative humidity (day). Plants inoculated with sterile water served as controls. Five to six replicate plants were inoculated with each isolate, and the experiment was repeated three times. Leaf spot progression was recorded at 7, 14 and 21 d post inoculation (dpi). Percent leaf necrotic area (l. n. a.) was calculated by dividing the area of the lesions on each leaf by the total leaf area, and multiplying by 100. The areas under disease progress curves (AUDPC) were calculated using the open source 'agricolae' package in R software (Campbell and Madden, 1990). Data analyses were carried out using Kruskal-Wallis and Dunn's post-hoc tests with R (R4.3.1) (Faraway,

2002). Conidia formed on diseased plant tissues were observed after 21 dpi.

Extraction, PCR amplification and sequencing of isolate DNA

Total genomic DNA was extracted from 14–21 d -old PDA cultures of isolates, using the NucleoSpin® Genomic DNA kit (MACHEREY-NAGEL), according to the manufacturer's protocol. For *Stemphylium* spp. identification, amplification of the internal transcribed spacer regions of ribosomal DNA (*ITS rDNA*), glyceraldehyde-3-phosphate dehydrogenase (*gpd*), and calmodulin (*cmdA*) gene regions, was conducted using, respectively, the primer pairs ITS1/4, gpd1/gpd2, and CALDF1/CALDR1 (White *et al*., 1990; Berbee *et al*., 1999; Lawrence *et al*., 2013). *Alternaria* spp. characterization at section level was based on glyceraldehyde-3-phosphate dehydrogenase (*gpd*) gene sequences, after amplifications using gpd1/gpd2 primer pairs. Polymerase chain reaction (PCR) amplification procedures were set as those of Woudenberg *et al.* (2017). Each PCR amplification was carried out in a total volume of 25 µL, containing 75mM Tris-HCl pH 9.0, 20 mM $(NH_4)_2SO_4$, 0.01% (w/v) Tween 20, 1.5 mM $MgCl_2$, 200 µM desoxyribonucleotide triphosphate, 1 unit of thermostable DNA polymerase (GoTaq®, Promega), and 400 nM of each relevant oligonucleotide primer. PCR amplification was carried out in a Bio-Rad T100™ Thermal Cycler (Bio-Rad Inc.). The products were analyzed by electrophoresis in 1.2% (w/v) agarose in 0.5× TAE buffer, were visualized by ethidium bromide staining and UV illumination, and were then sent to Eurofins Genomics (Germany) for sequencing. The generated DNA sequences were submitted to GenBank, and additional DNA sequences from type strains for species of *Alternaria* and *Stemphylium* genera were downloaded from GenBank (https://www.ncbi.nlm.nih.gov/genbank/).

Phylogenetic analyses

DNA sequences of isolates and reference species retrieved from GenBank were concatenated and aligned by the MUSCLE algorithm using MEGA 7 (Kumar *et al*., 2016). Phylogenetic analysis used the maximum likelihood (ML) approach within IQTree v.1.6. (Nguyen *et al*., 2015). The best-fit evolutionary models for each dataset were calculated by ModelFinder (Kalyaanamoorthy *et al*., 2017) within the Bayesian Information Criterion (BIC) selection procedure. The ML analysis was carried out with 1000 ultrafast bootstrap replicates and only values greater than 90% were considered significant. Phylogenetic tree construction was carried out using the online tool Interactive Tree of Life (ITOL) version 6 (Letunic and Bork, 2024).

RESULTS

Stemphylium lettuce leaf spot symptoms can be confused with early symptoms of *Alternaria* leaf spot. Both pathogens cause large, brown or dark brown (Figure 1, A and B), and round spots with a light brown to beige necrotic center (Figure 1 C). The necrotic centre of each lesion often abscises and falls out leaving a hole in the spot centre. Heavily infected leaves turn yellow to brown and dry, with tendency to crack and tear in the necrotic tissue (Figure 1, B and D). A total of 106 naturally infected lettuce leaf samples were collected from five markets and one organic farm in Oran, and were analyzed. Fungi isolated from these samples using PCA showed varying frequencies. *Stemphylium* spp. had the greatest frequency (48.2%) followed by small-spored *Alternaria* species (35.2%). Other genera, including *Cladosporium* sp., *Mucor* sp., *Fusarium* sp., and *Botrytis* sp. were isolated at the least frequency (16%). Most of the symptomatic lesions (80%) had mixed infections of *Alternaria* and *Stemphylium* spp. Twenty-seven isolates with morphological characteristics of *Stemphylium* and *Alternaria* were selected for further characterization (Table 1).

Alternaria *spp. isolates*

Most of the *Alternaria* isolates from lettuce were small-spored *Alternaria* species which were morphologically identified as members of section *Alternaria* (NB1149, NB1150, NB1151) or section *Eureka* (NB1088, NB1089, NB1090).

Phylogenetic analyses of *gpd* sequences from these isolates and corresponding sequences from strains representative of the 29 sections in *Alternaria* confirmed that they belonged to these two sections (Figure 2). Isolates from section *Alternaria* developed olivaceous and dull, velvety to cottony mycelium, with colonies having white regular margins (Figure 3, A and B). Conidiophores were short to long, simple or branched, septate, and with 1–2 (–3) apical conidiogenous loci. Conidia were obclavate, ellipsoid, with 1 (–3) transverse and 0–3 longitudinal septa, and mean dimensions of 18.8–35.2 × 7.5–12.6 µm. They were medium brown, punctate, small or moderate in size, septate, slightly constricted near some septa, in moderately long to long, and simple or branched chains. Conidia each had a tapered beak or secondary conidiophore, each with one or a few conidiogenous loci from

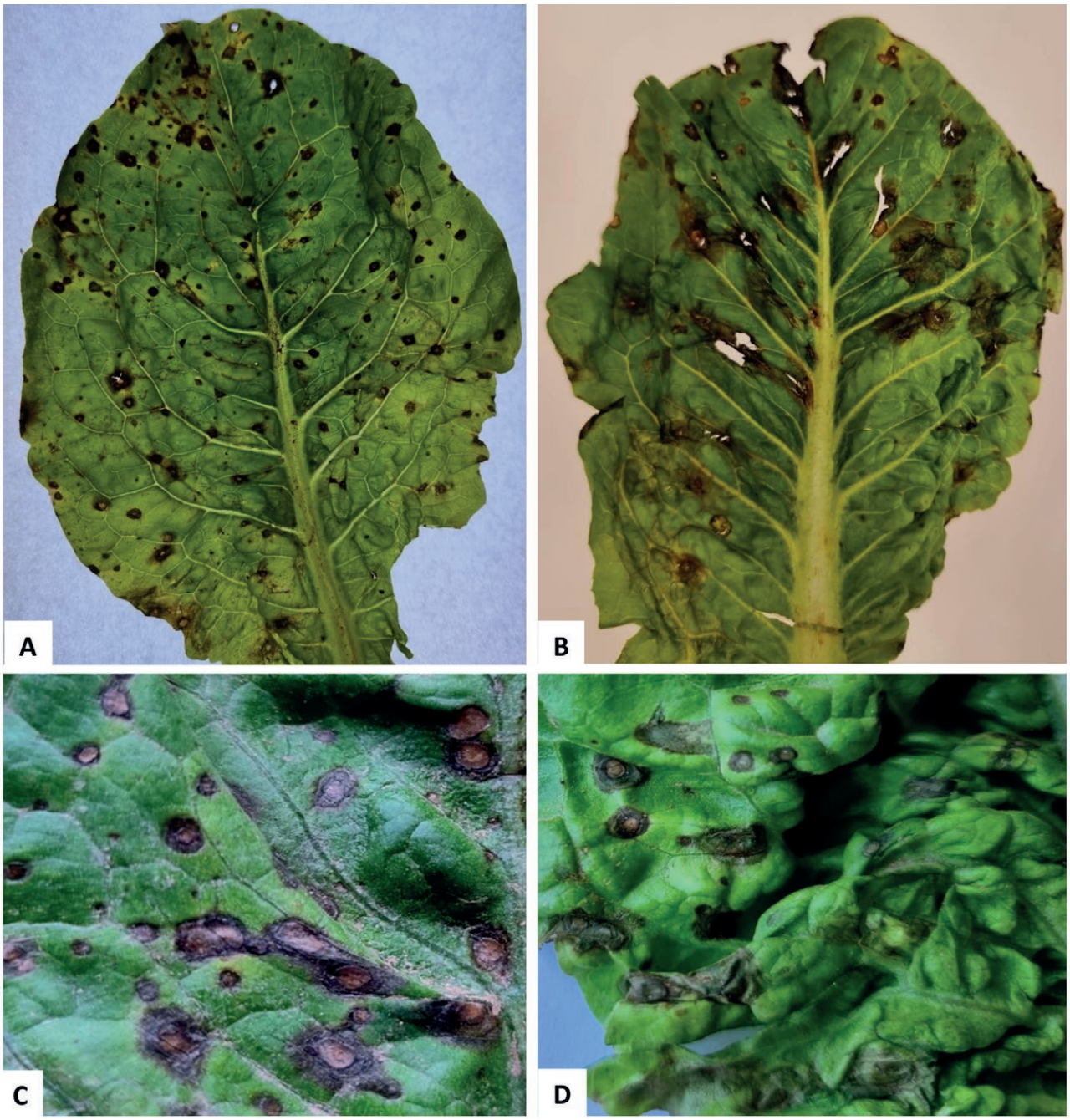

Figure 1. Foliar symptoms on leaves of field-grown lettuce: **(A)** circular to oval dark brown spots with chlorosis; **(B)** extended brown necrosis with numerous cracks and perforations; **(C)** brown necrosis with beige lesion centres caused by *Stemphylium* spp.; **(D)** brown and dark brown necroses caused by *Stemphylium* and *Alternaria* spp.

the apex or lateral cells, bearing one to three conidiogenous loci (Figure 4A).

The three isolates from section *Eureka* developed grayish brown to olive brown, cottony mycelium (Figure 3C). The conidiophores were simple or branched, straight or geniculate, medium brown, and were 17.6–113 × 4.5–6.3 µm, with 1–2 (–3) apical proliferations (Figure 4B). Conidia were ovoid, narrowly ellipsoid, with 1 (–3) transverse and 0–3 longitudinal septa per transverse segment, were 27.6– 42.7 × 13.8–25 µm, brown, constricted at the major transverse septa, and were solitary or in short chains of 2–3 conidia.

Table 1. Isolates characterized in this study and their GenBank accession numbers.

Isolate	Section/Species	Year of isolation	GenBank accession numbers		
			ITS	*gpd*	*cmd*
NB1088	*A.* section *Eureka*	2022	NA	PV007868	NA
NB1089	*A.* section *Eureka*	2022	NA	PV007869	NA
NB1090	*A.* section *Eureka*	2022	NA	PV007870	NA
NB1102	*S. lycopersici*	2022	PQ963026	PV007826	PV007847
NB1103	*S. lycopersici*	2022	PQ963027	PV007827	PV007848
NB1104	*S. lycopersici*	2022	PQ963028	PV007828	PV007849
NB1105	*S. lycopersici*	2022	PQ963029	PV007829	PV007850
NB1107	*S. gracilariae*	2022	PQ963030	PV007830	PV007851
NB1108	*S. gracilariae*	2022	PQ963031	PV007831	PV007852
NB1109	*S. lycopersici*	2022	PQ963032	PV007832	PV007853
NB1110	*S. gracilariae*	2022	PQ963033	PV007833	PV007854
NB1111	*S. eturmiunum*	2022	PQ963034	PV007834	PV007855
NB1116	*S. lycopersici*	2023	PQ963035	PV007835	PV007856
NB1117	*S. gracilariae*	2023	PQ963036	PV007836	PV007857
NB1118	*S. gracilariae*	2023	PQ963037	PV007837	PV007858
NB1120	*S. gracilariae*	2023	PQ963038	PV007838	PV007859
NB1122	*S. gracillariae*	2023	PQ963039	PV007839	PV007860
NB1123	*S. gracilariae*	2023	PQ963040	PV007840	PV007861
NB1124	*S. gracilariae*	2023	PQ963041	PV007841	PV007862
NB1149	*A.* section *Alternaria*	2023	NA	PV007871	NA
NB1150	*A.* section *Alternaria*	2023	NA	PV007872	NA
NB1151	*A.* section *Alternaria*	2023	NA	PV007873	NA
NB1153	*S. amaranthi*	2023	PQ963042	PV007842	PV007863
NB1154	*S. vesicarium*	2023	PQ963043	PV007843	PV007864
NB1155	*S. vesicarium*	2023	PQ963044	PV007844	PV007865
NB1156	*S. vesicarium*	2023	PQ963045	PV007845	PV007866
NB1157	*S. eturmiunum*	2023	PQ963046	PV007846	PV007867

Stemphylium *spp. isolates*

Morphological analysis showed that most of the isolates collected from symptomatic lettuce belonged to *Stemphylium*. To further characterize these isolates, sequences of the rDNA ITS region and portions of the *gpd* and *cmdA* genes from the *Stemphylium* isolates were obtained, and a multi-gene phylogeny approach was used to identify the isolates at species level. The combined dataset of the three gene sequences from 21 lettuce isolates, and from 68 representative strains of 31 recognized species of *Stemphylium* retrieved from GenBank was used to compare the lettuce isolates and GenBank strains. Sequences from *Alternaria alternata* strain GV14-634a1 were used as the outgroup. The dataset had a total length of 1102 bp, of which 154 bp were parsimony informative. The resulting phylogenetic tree (Figure 5) indicated that the 21 lettuce isolates grouped into five well-supported phylogenetic species: *S. amaranthi* (NB1153), *S. eturmiunum* (NB1111, NB1157), *S gracilariae* (NB1107, NB1108, NB1110, NB1117, NB1118, NB1120, NB1122, NB1124), *S. lycopersici* (NB1102, NB1103, NB1104, NB1105, NB1109, NB1116), and *S. vesicarium* (NB1154, NB1155, NB1156). Colony measurements of selected isolates were conducted on the isolates grown on PDA (Table 2). This macro-morphological analysis was not efficient for isolate grouping due to high morphological variability within species. Additional analysis of morphological characteristics was carried out to describe the isolates from lettuce, and is provided below.

Stemphylium amaranthi Y.F. Pei & X.G. Zhang

One isolate (NB1153) had brown to grayish beige velvety mycelium, with regular white to transparent colony margins (Figure 3 D). Colonies were 71.0 ± 0.8 mm diam. after 7 d incubation on PDA at 25 °C in the dark. Conidiophores were solitary, simple or branched, pale brown, smooth, cylindrical, 3–10-septate, and measured 27.8–108.0 × 5.0–6.5 µm. Conidiogenous cells were each swol-

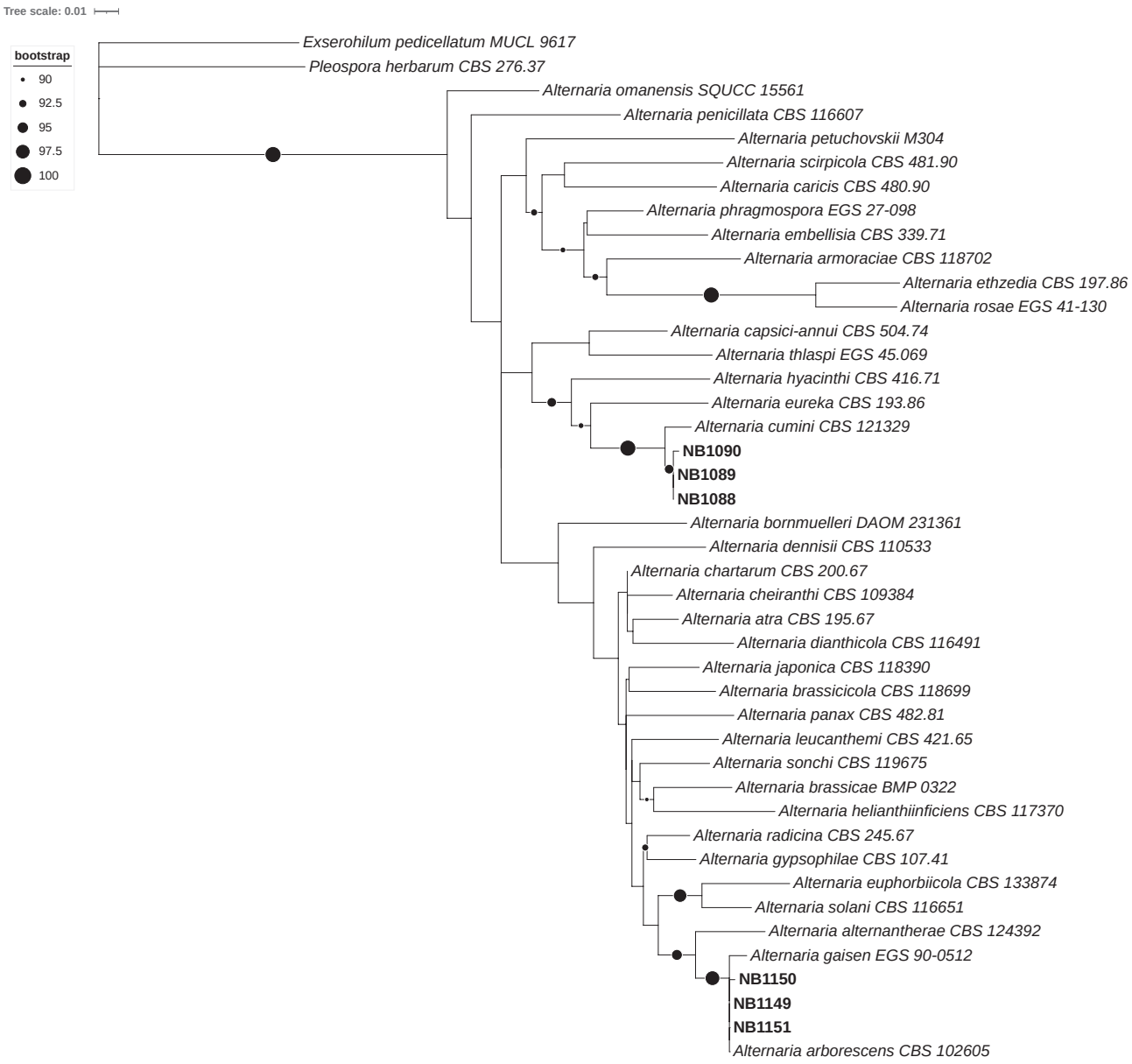

Figure 2. Phylogenetic tree reconstructed using the maximum likelihood method from the alignment of sequences of portions of the *gpd* gene from six small-spored *Alternaria* isolates and 35 *Alternaria* strains representative of 29 sections. Sequences of one isolate each of *Exserohilum pedicellatum* and *Pleospora herbarum* were included to root the tree. Sequences were retrieved from GenBank accessions reported in Woudenberg *et al.* (2013), Al Ghafri *et al.* (2019), Grum-Grzhimaylo *et al.* (2016). Bootstrap support values are indicated near nodes by black circles, whose sizes are proportional to the indicated support values. The tree scale bar indicates the expected number of substitutions per position.

len at the apex, medium brown, 5.0–7.5 µm wide, smooth, and occasionally had 1–5 apical proliferations. Conidia were, subspherical, oblong to oval, were each rounded at the base and spherical to conical at the apex. They had 1 (–4) transverse and 1–3 longitudinal/oblique septa, measured 21.4–38.4 × 9.0–18.8 µm, their L/W ratio was 1.4–4, they had one indistinctly constricted median septum, and were medium to dark brown (Figure 4 C). Conidia often generated short secondary conidiophores, which were 1–2-septate, 12.0–18.0 µm long, and were smooth. Sexual morphs were observed after 4 weeks in culture.

Stemphylium eturmiunum E.G. Simmons

Two isolates (NB1111, NB1157) had brownish orange to grayish brown cottony mycelium with regular

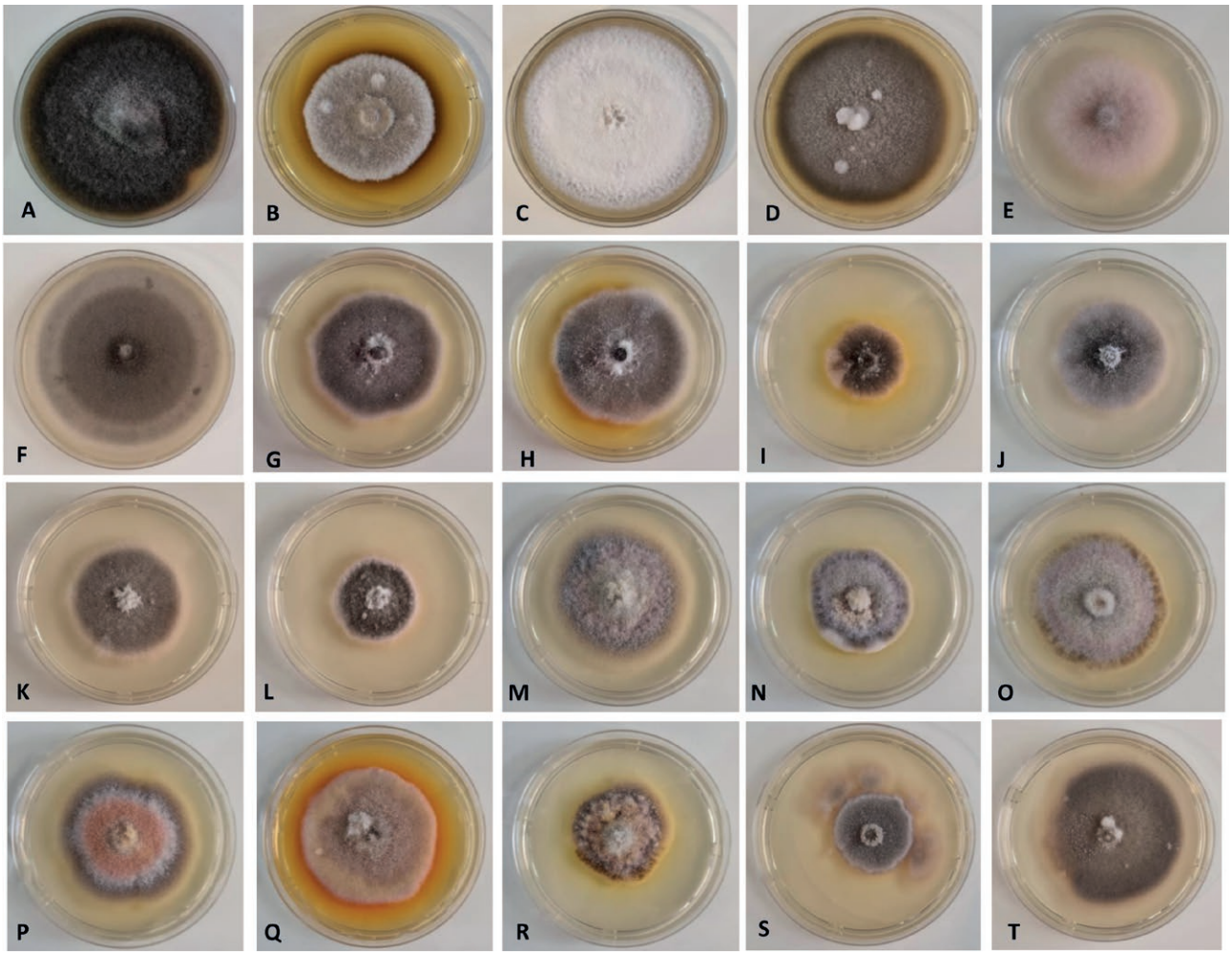

Figure 3. Morphology of selected *Alternaria* and *Stemphylium* isolates after 7 d growth on potato dextrose agar at 25°C. **(A)** *Alternaria* section *Alternaria*: NB1149; *A.* section *Eureka*: **(B)** NB1088, **(C)** NB1090; *S. amaranthi*: **(D)** NB1153, *S. eturmiunum*: **(E)** NB1111, **(F)** NB1157; *S. gracilariae*: **(G)** NB1107, **(H)** NB1110, **(I)** NB1117, **(J)** NB1118, **(K)** NB1120, **(L)** NB1122; *S. lycopersici*: **(M)** NB1102, **(N)** NB1103, **(O)** NB1104, **(P)** NB1105, **(Q)** NB1109, **(R)** NB1116; *S. vesicarium*: **(S)** NB1155, **(T)** NB1156.

colony margins, and sometimes produced yellow white pigmentation (Figure 3, E and F). Colonies were 62 to 77 mm in diameter after 7 d incubation, and occasionally produced yellowish white pigment on PDA at 25°C after 7d. Conidiophores were solitary, simple, brown, smooth, cylindrical, 3–10-septate, of short to moderate length of 21.4–70.0 × 5.0–12.6 µm. They were each swollen at the apex, medium brown, 5.0–7.5 µm wide, smooth, occasionally with 1–2 apical proliferations. Conidia were oblong to ovate, muriform, rectangular at the base and spherical at the apex, with 1–3 transverse and 1–3 longitudinal/oblique septa, measured 21.6– 34.0 (–41.0) × 10–20.1 µm, with L/W ratio of 1.3–2.5, one indistinctly constricted median septum, and were light to dark brown (Figure 4 D). Secondary conidiophores were rarely formed. Sexual morphs were observed after 4 weeks.

Stemphylium gracilariae E.G. Simmons

Eight isolates (NB1107, NB1108, NB1110, NB1117, NB1118, NB1120, NB1122, NB1124) developed olive brown, velvety to cottony mycelium, with white regular colony margins (Figure 3, G to L). The colonies were 37 to 60 mm diam. after 7 d incubation on PDA at 25°C in the dark. Conidiophores were solitary, simple or branched, pale brown, smooth, cylindrical, 1–5-septate, measuring 20–57 (–90) × 4.5–7.5 µm. Conidiogenous cells were swollen at the apex, medium brown, smooth, 5–7 µm wide, occasionally with 1–2 apical proliferations. Conidia were oblong to ovate, with 1(–3) transverse and 2–4 longitudinal septa, 17.6– 37.7 × 11.3–21.9 µm, with L/W

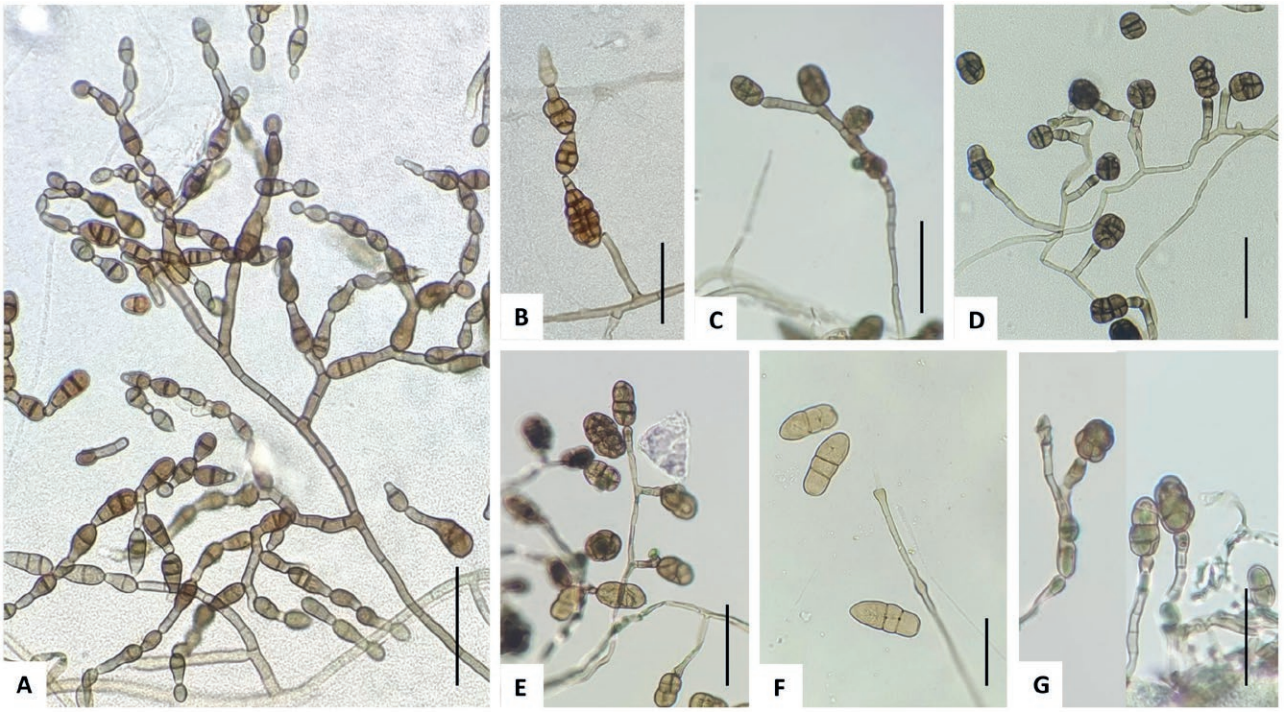

Figure 4. Conidiophores and conidia of *Alternaria* and *Stemphylium* spp. developed on potato carrot agar after 7 d incubation at room temperature. **(A)** *Alternaria* section *Alternaria* (NB1149), **(B)** *A.* section *Eureka* (NB1088), **(C)** *S. amaranthi* (NB1153), **(D)** *S. eturmiunum* (NB1111), **(E)** *S. gracilariae* (NB1122), **(F)** *S. lycopersici* (NB1104), **(G)** *S. vesicarium* (NB1156). Bars = 50 µm.

ratio of 1.2–2.5, one indistinctly constricted central transverse septum, medium brown, sometimes with punctuate ornamentation. Conidia often generated short secondary conidiophores, that were 1–2-septate, and 12–18 mm long. Secondary conidia formed in aged parts of colonies were ovoid or subcylindrical and smooth, with one or few transverse septa, and were 12.6–16.3 × 5–8 µm (Figure 4 E). Sexual morphs were observed after 3 to 4 weeks.

Stemphylium lycopersici (Enjoji) W. Yamam

Six isolates (NB1102, NB1103, NB1104, NB1105, NB1109, NB1116) developed cottony and raised colonies with irregular margins, with olive brown to grayish yellow mycelial pigmentation and a diffused yellow pigment into the culture medium (Figure 3, M to R). Colonies were 51 to 73 mm diam. after 7 d incubation on PDA at 25°C in the dark (Table 2). Conidiophores were simple, straight, 4–14-septate, measuring 98–376 × 6–10 µm, with swollen apical conidiogenous cells each bearing a single conidium. One to 5-septate secondary conidiophores emerged from conidia in aged parts of colonies, and these measured 12–90 × 4–6 µm. Conidia were dark brown, solitary, oblong with conical ends at the apices and bluntly rounded or rectangular at the bases, and measured 36–70 × 13–18.8 µm, with L/W ratios of 2.1–5.1, and 2–3 darkened constrictions, 3–7 transverse septa and 1–3 longitudinal septa per transverse segment (Figure 4 F). A sexual morph was not observed.

Stemphylium vesicarium (Wallr.) E.G. Simmons

Three isolates (NB1154, NB1155, NB1156) had cottony mycelium, with colonies 28–62 mm diam. and grayish brown to grayish orange after 7 d incubation on PDA at 25 °C in the dark (Figure 3, S and T). Conidiophores were straight or occasionally branched, pale to brown with dark edges, each with a swollen apex and 3–9 septa, and dimensions of 30–70.3 × 5–6.8 µm. Conidia were medium to olive-brown, ovoid to muriform, with 1–3 transverse segments and 1–3 longitudinal septa per transverse segment, and measured 22.6– 30.1 × 8.8–16.8 µm, with mean length/width ratio of 1.3 –2.3. The conidia were each constricted at 1–2 of the major transverse septa (Figure 4G). Sexual morphs were observed after 4 weeks.

Pathogenicity tests

Individual inoculations Pathogenicity tests showed that all the tested *Alternaria* and *Stemphylium* isolates caused symptoms on romaine lettuce (Figure 6). Numerous small spots appeared on plant basal leaves 3–4 d of

Table 2. Morphological variability among *Alternaria* and *Stemphylium* isolates grown on potato dextrose agar.

Section/Species	Isolate number	Colony aspect				Pigmentation	Colony diameter after 7 days (mm)
		Surface			Reverse		
		Type	Colour [a]	Margin			
A. sect. *Eureka*	NB1088	Cottony compact	Greyish beige (4C2) with white surface	Regular	Brown (6E7/6E6)	Olive brown (4E8)	52.9 ± 2.4
	NB1089	Velvety to cottony	Olive brown (4E3) with brownish grey (4D2) margins	Irregular	Yellowish brown (5F4) with a black center	Olive brown (4D8)	35.3 ± 3.1
	NB1090	Cottony	Greyish brown (4C2)	Regular	Yellowish brown (5F4)	None	79.0 ± 0.8
A. sect. *Alternaria*	NB1149	Velvety to cottony	Olive brown (4F7) with yellowish grey surface (3C2/3D2) and olive margins (3E3)	Regular	Olive brown (4F3)	None	79.5 ± 0.6
	NB1150	Cottony centre and velvety margins	Olive brown (4E4/ 4E5)	Irregular	Olive brown (4F7)	None	78.6 ± 1.8
S. amaranthi	NB1153	Velvety	Brown (5E4) with greyish beige (4C2) spots	Regular	Olive brown (4F4) with black center	Yellowish white (3A2)	71.0 ± 0.8
S. eturmiunum	NB1111	Cottony compact	Brownish orange (5C3) centre with a reddish white (7A2) surface and orange grey (5B2) margins	Regular	Light orange (5A4) with brownish orange (5C3) center	Yellowish white (3A2)	62.0 ± 2.4
	NB1157	Cottony	Greyish brown (5D3/5E3) to brownish grey (5D2)	Irregular	Greyish brown (5B4) to light brown (5D4)	None	76.8 ± 1.3
S. gracilariae	NB1107	Cottony centre and velvety margins	Olive brown (4D4) with brownish grey (4D2) margins	Irregular	Light brown (5D7) with pale orange (5A3) margins	Pale yellow (3A3)	59.9 ± 2.6
	NB1110	Velvety	Olive brown (4D3/ 4E3) with white borders	Irregular	Grayish brown (5D3) with light brown (5C6) margins	None	59.8 ± 1.9
	NB1117	Velvety	Olive brown (4E4) center and greyish yellow (4B3) to white margins	Irregular	Yellowish brown (5D5/ 5F5)	Yellow (3A7)	37.1 ± 1.4
	NB1118	Velvety	Olive brown (4D3) center and brownish grey (5C2) margins	Regular	Yellowish brown (5F4) with orange grey (5B2) margins	None	54.0 ± 1.8
	NB1120	Velvety to cottony	Olive brown (4D4/ 4D3) with white borders	Regular	Yellowish brown (5E4) to grayish orange (5B3)	None	55.4 ± 1.7
	NB1122	Cottony compact	Olive brown (4D4/ 4D3) with white borders	Irregular	Yellowish brown (5E4) to pale orange (5A3)	Light yellow (3A5)	47.1 ± 0.8

(Continued)

Table 2. (Continued).

Section/Species	Isolate number	Colony aspect				Pigmentation	Colony diameter after 7 days (mm)
		Surface			Reverse		
		Type	Colour [a]	Margin			
S. lycopersici	NB1102	Cottony centre and velvety margins	Dull red (9B3) with grayish brown (5E3) surface and orange grey (5B2) margins	Regular	Olive brown (4D6/ 4E5) with grayish yellow (4B3) margins	Pale yellow (3A3)	70.3 ± 2.2
	NB1103	Cottony centre and velvety margins	Grayish yellow (4C3) with a brownish grey (9D2) surface	Irregular	Olive brown (4E5) with grayish yellow (4C4) margins	Light yellow (3A4)	51.0 ± 4.2
	NB1104	Cottony centre and velvety margins	Dull red (9B3) with a grayish yellow (4C3) surface and olive brown (4D5) margins	Irregular	Grayish yellow (4C6) with light brown (5D7) center	Light yellow (3A4)	52.0 ± 10.3
	NB1105	Cottony centre and velvety margins	Brownish orange (5C3) center with pastel red (8A4) and brownish grey (8D2) margins	Irregular	Grayish yellow (4B3) with olive brown (4D7) center	Yellow (3A6)	59.5 ± 7.2
	NB1109	Cottony compact	Brownish orange (7C3) center with grayish yellow (4B3) surface and pale orange (5A3) margins	Irregular	Reddish brown (9D4) center with pastel red (9A4) margins	Reddish orange (7A8)	58.0 ± 3.2
	NB1116	Cottony centre and velvety margins	Grayish orange (5B5) center with grayish yellow (4B3) surface and olive brown (4D4) margins	Irregular	Olive brown (4E7) with grayish yellow (4B5) margins	Yellow (3A6)	56.8 ± 10.2
S. vesicarium	NB1154	Cottony	Greyish orange to brownish grey (5B3/5D2)	Irregular	Brown to pale orange (5A4/5A3)	None	28.0 ± 1.6
	NB1155	Cottony to floccose	Greyish brown (5D3) to greyish orange (5B3) with grey spots	Irregular	Brown (5E4) to brownish orange (5C4)	None	56.3 ± 3.5
	NB1156	Cottony to floccose	Greyish brown (5D3) to orange grey (5C2) spots	Irregular	Yellowish to light brown (5F4/5D4)	None	62.0 ± 1.2

[a] Colour designations were made using the colour charts of Kornerup and Wanscher (1978).

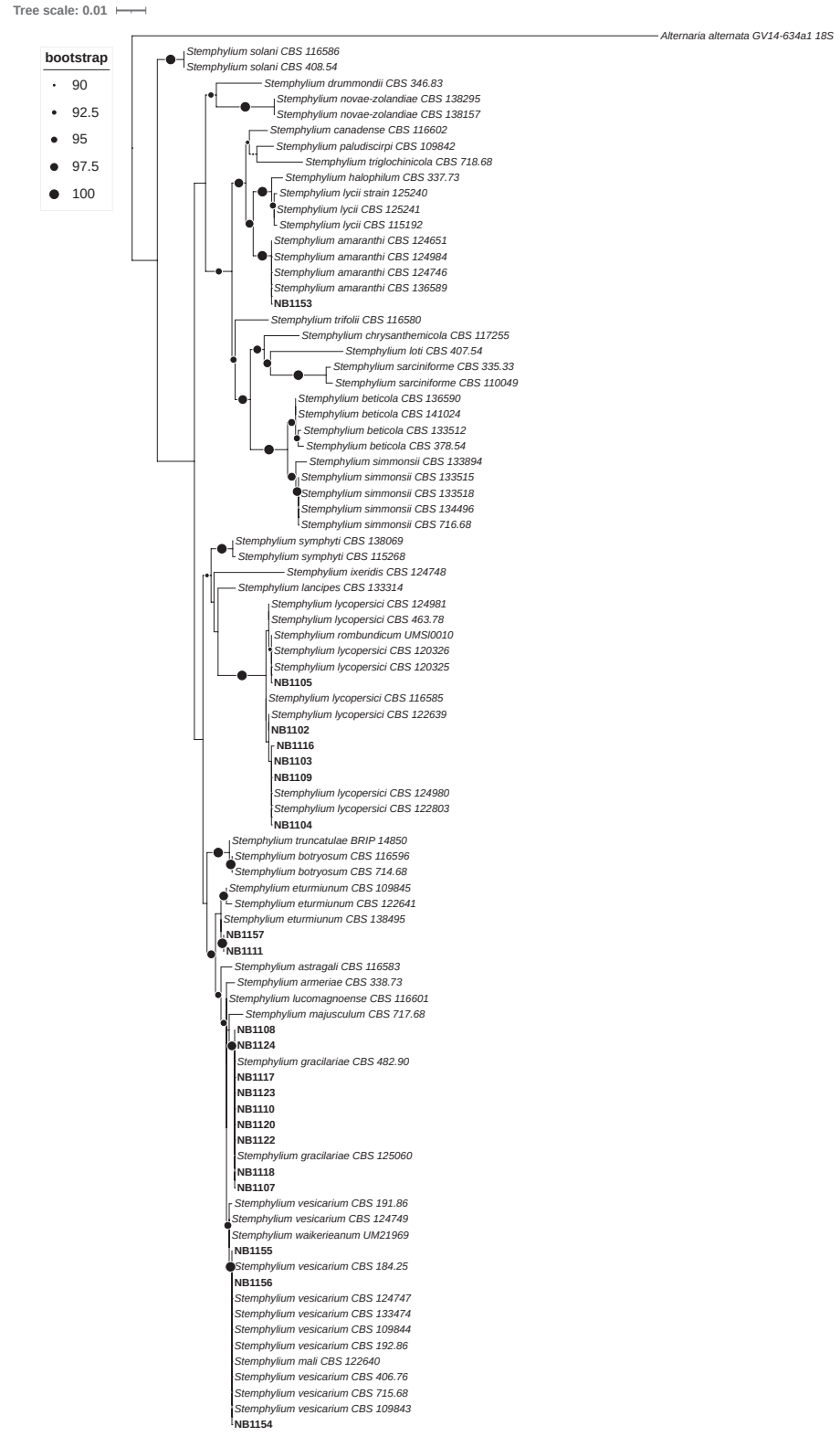

Figure 5. Phylogenetic tree reconstructed using the maximum likelihood method from the alignment of *ITS*, *gpd* and *cmdA* sequences of *Stemphylium* isolates. The tree was rooted with *Alternaria alternata* strain GV14-634a1. Sequences were retrieved from GenBank accessions reported in Woudenberg *et al.* (2017). Bootstrap support values are indicated near nodes by black circles whose size is proportional to the support values. The scale bar indicates the expected number of substitutions per position.

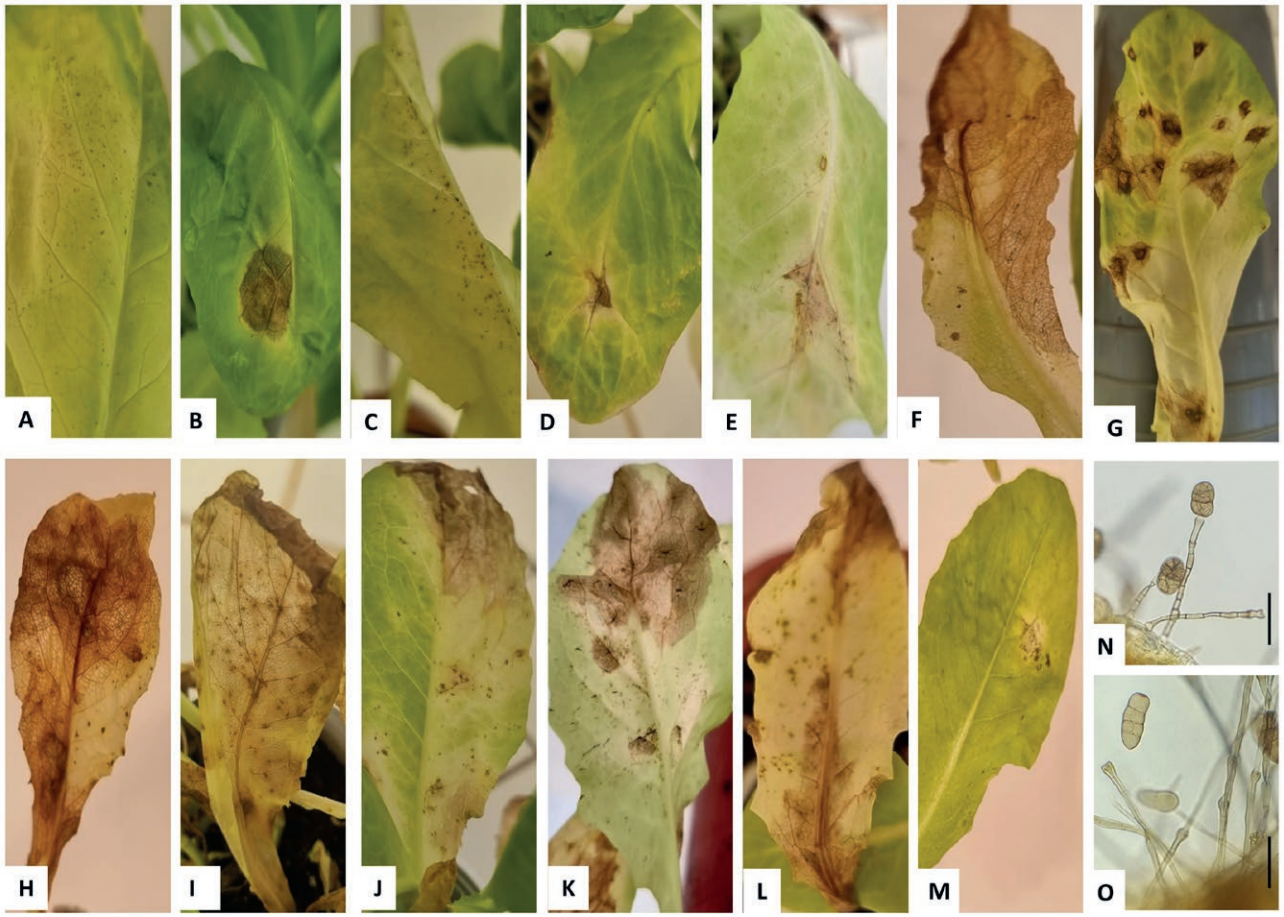

Figure 6. Foliar symptoms on inoculated romaine lettuce leaves after 21 dpi with different fungal isolates. **(A)** *Alternaria* section *Alternaria*: NB1149, **(B)** NB1150, **(C)** NB1151; *A.* section *Eureka*: **(D)** NB1089; *Stemphylium amaranthi*: **(E)** NB1153; *S. eturmiunum*: **(F)** NB1111; *S. gracillariae*: **(G)** NB1117, **(H)** NB1122, **(I)** NB1124; *S. lycopersici:* **(J)** NB1102, **(K)** NB1105, **(L)** NB1109; *S. vesicarium*: **(M)** NB1154. (**N**) Conidiophores and conidia of *S. gracilariae* (NB1120), and of **(O)** of *S. lycopersici* (NB1102); bars = 50μm.

inoculation. These spots expanded into long ellipsoid dark brown necrotic lesions. As these increase in size, entire leaves turned yellow, and the necrotic areas were easily ruptured. For isolates causing these symptoms, the lesions coalesced quickly into leaf blight. The symptoms were the same as observed on lettuce plants in the field and markets (Figure 6, A to M). Sporulation occurred in the necrotic lesions on basal leaves after inoculations with pathogenic isolates (Figure 6, N and O).

Seven of the nine assessed *S. gracilariae* isolates (NB1107, NB1108, NB1110, NB1117, NB1118, NB1122, NB1124) and one of the six assessed *S. lycopersici* isolates (NB1105) were more aggressive than the other tested isolates (Figure 7). The *S. eturmiunum* isolate was moderately aggressive (mean AUDPC = 425). Isolates of *S. vesicarium* and *S. amaranthi* and the small-spored *Alternaria* spp. were less aggressive (i.e. weakly pathogenic) with a mean AUDPCs between 110 and 240. These isolates produced small, brown necrotic lesions on leaves, which did not expand. Inoculation control plants remained healthy. To determine fulfilment of Koch's postulates, isolations of fungi from lesioned areas were carried out, and the recovered pathogens were found to be morphologically consistent with the fungi used in the inoculations.

Cross inoculations Four *Stemphylium* isolates were inoculated alone or in combinations with one of five *Alternaria* isolates in cross-inoculation tests. Symptom morphology from the double inoculations did not differ from that of *Stemphylium* isolate alone. The small-spored *Alternaria* isolates did not enhance disease development on lettuce plants when mixed with pathogenic *Stemphylium* strains (Figure 8). In most cases infection rates from mixed *Stemphylium* plus *Alternaria* inoculations were similar or less than for individual inoculations with *Stemphylium* alone. Cross inoculations with

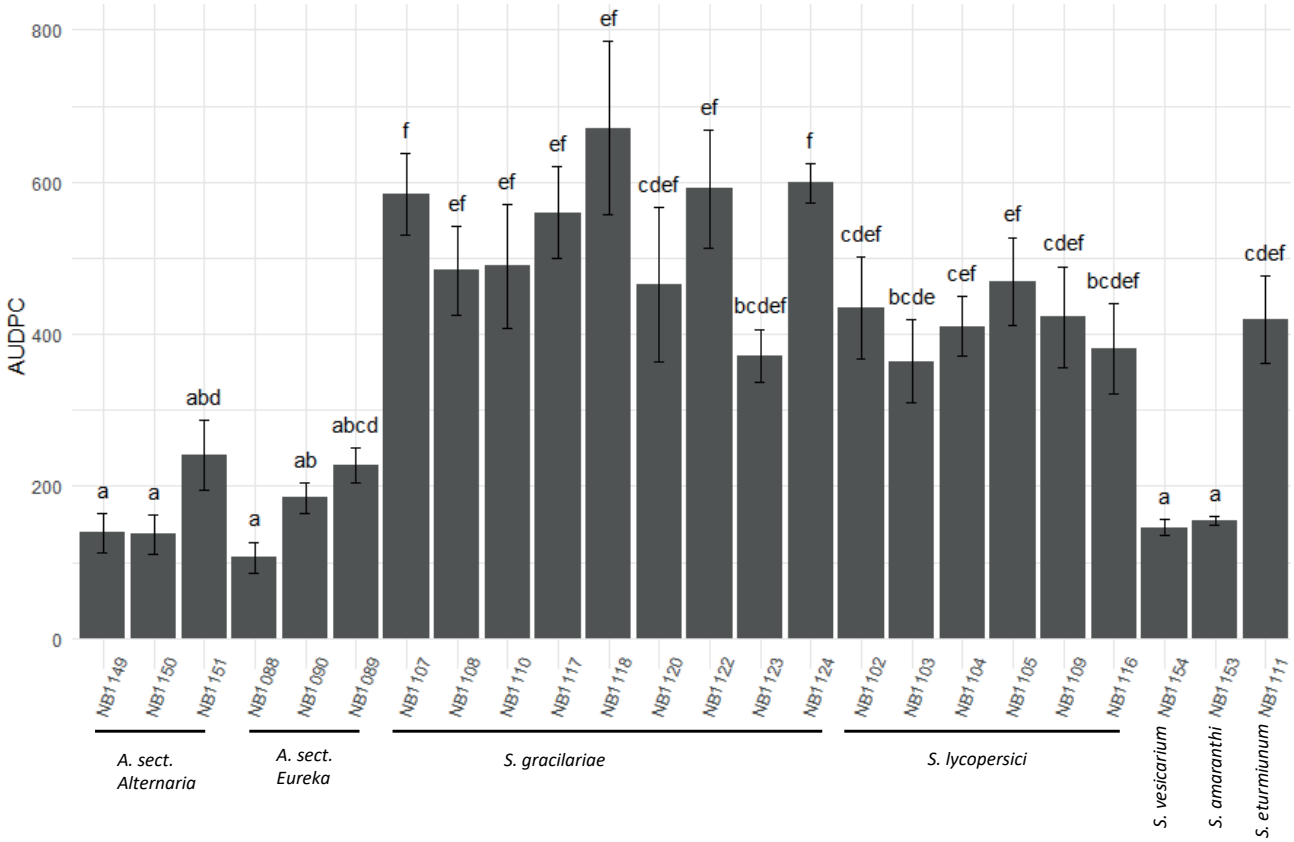

Figure 7. Mean areas under disease progress curves (AUDPCs) for romaine lettuce plants inoculated with the different *Alternaria* or *Stemphylium* spp. isolates after 7, 14 and 21 days. The letters above the standard deviation bars indicate significant differences ($P > 0.05$) between the means, as indicated by a Kruskal Wallis test and the Dunn *posthoc* test with Benjamini-Hochberg corrections.

S. lycopersici (NB1103, NB1104) and small-spored *Alternaria* isolates (respectively, NB1089, NB1090, NB1051, NB1089, NB1049) resulted in reduced AUDPCs. A similar trend was observed when *S. eturmiunum* (NB1111) was co-inoculated with isolates of section *Alternaria*. No differences were observed between the AUDPCs for plants inoculated by *S. gracilariae* alone or mixed with small-spored *Alternaria*, irrespective of the isolate.

DISCUSSION

In this study, the most commonly isolated fungi from lettuce plants with leaf spot symptoms were *Alternaria* spp. and *Stemphylium* spp. Different species were frequently isolated from the same leaf, or even from the same lesion. Morphologically, *Stemphylium* is distinguished from *Alternaria* by its percurrently or annellidically proliferating conidiophores that often each have a distinct swollen terminal apical cell or region (Simmons, 1967). However, based solely on morphological characteristics, reliable identification at species level is difficult, and sequence comparison at taxonomically informative loci is recommended (Woudenberg *et al*., 2017; Li *et al*., 2023).

Among the selected isolates, members of five *Stemphylium* spp. (*S. lycopersici*, *S. vesicarium*, *S. eturmiunum*, *S. amaranthi,* and *S. gracilariae*) and two *Alternaria* sections (sect. *Alternaria* and sect. *Eureka*), were identified using, respectively, multilocus *ITS-gpd-cmdA* and monolocus *gpd* analyses. Small-spored *Alternaria* spp. such as *A. alternata* have broad host ranges, and have been identified as causal agents of lettuce leaf spot (Guo *et al*., 2018; Naglaa and Safaa, 2020). Experimental inoculations of lettuce with Algerian isolates of sections *Alternaria* and *Eureka* showed that these fungi were weak pathogens. The weak pathogenicity of small-spored *Alternaria* spp. may be due to prolonged latency periods. These fungi may become active during host stress or increased age.

Some fungi (e.g. *Fusarium solani* and *F. proliferatum*) have the potential to exhibit both endophytic and pathogenic phases (Padhi *et al*., 2015). Similarly, *A. alternata* can be a pathogen and an endophyte in various

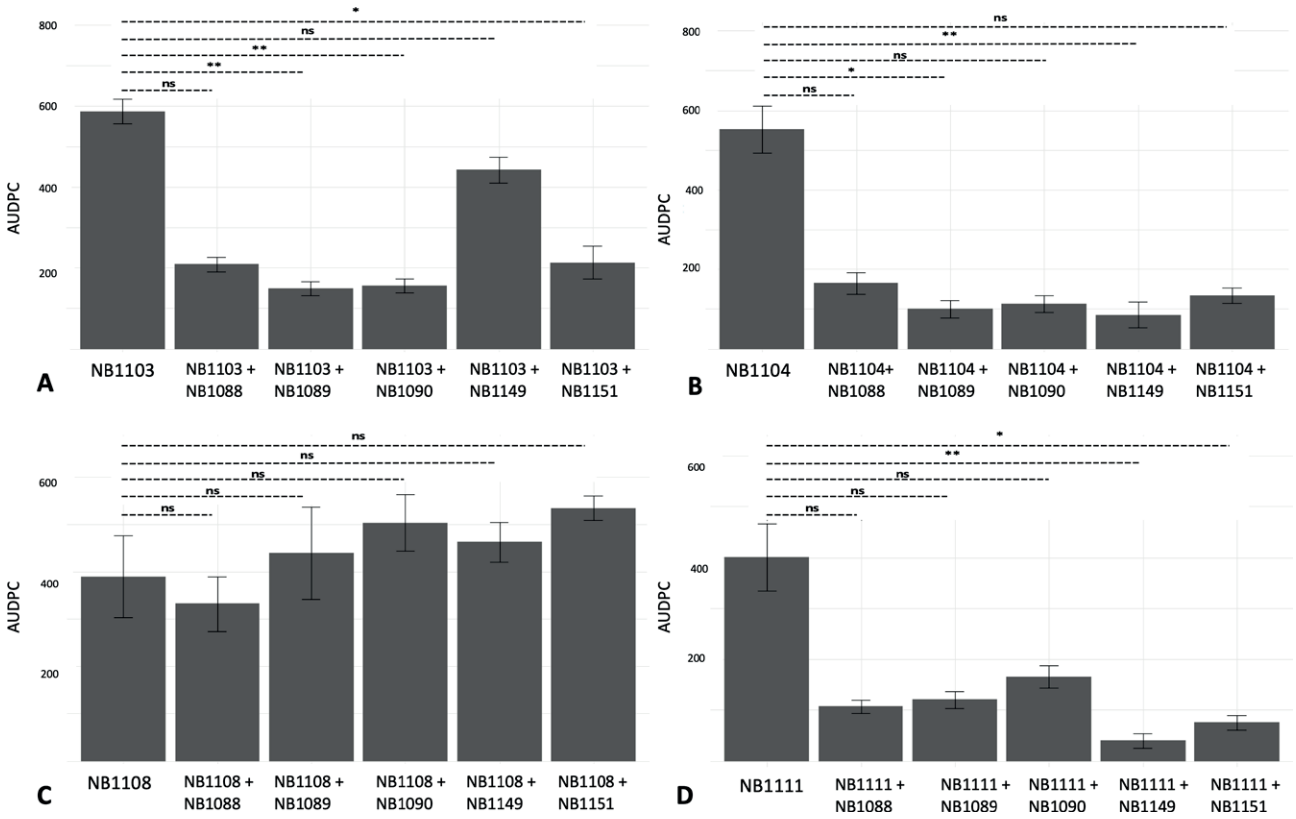

Figure 8. Mean areas under disease progress curves (AUDPCs) on romaine lettuce plants after individual (*Alternaria* **or** *Stemphylium* spp.) or cross (*Alternaria* **plus** *Stemphylium* spp.) inoculations. **(A and B)** *S. lycopersici*; **(C)** *S. gracilariae*; and **(D)** *S. eturmiunum* after 7, 14 and 21 d. Bars indicate standard errors of means. The stars indicate significant differences (*, $P < 0.05$; **, $P < 0.01$) between the individual and cross inoculations, as shown by Kruskal Wallis tests and Dunn posthoc tests with Bonferroni corrections.

plants (De Mers, 2022), and has been described in lettuce as endophytic (D'Amico *et al*., 2008) and pathogenic (Guo *et al*., 2018). In contrast, two *Stemphylium* isolates (*S. gracilariae* and *S. lycopersici*) were found to be highly pathogenic, one (*S. eturmiunum*) was moderately pathogenic to lettuce. While some *Stemphylium* species have been reported infecting single hosts, some can infect diverse hosts (Brahamanage *et al*., 2018). *Stemphylium lycopersici* has a broad host range, infecting leaves from more than 30 host genera in at least eight plant families: *Amaranthaceae*, *Araceae*, *Asteraceae*, *Fabaceae*, *Malvaceae*, *Plantaginaceae*, *Rosaceae* and *Solanaceae* (Farr and Rossman, 2017; Manaaki Whenua, 2023; Spawton and du Toit, 2024). Nasehi *et al*. (2014) showed that *S. lycopersici* was pathogenic to lettuce, regardless of its original host, and that isolates of this fungus could genetically segregate due to host plant rather than geographic region. As *S. lycopersici* has been isolated from diseased tomato in Algeria (Bessadat *et al*., 2022), phylogenetic segregation by host could be investigated for Algerian isolates of this fungus.

Stemphylium gracilariae also has a broad host range, and has been reported on hosts in six botanical families, including lettuce (Woudenberg *et al*., 2017; Brahmanage *et al*., 2019). Similarly, other fungi such as *S. vesicarium* and *S. eturmiunum* can infect several host species and colonize raw food ingredients (Samson *et al*., 2010; Olsen *et al*., 2018). *Stemphylium vesicarium* and *S. lycopersici* have been identified as causing leaf spot on lettuce in China (Liu *et al*., 2019).

Stemphylium amaranthi was first described from necrotic leaf spots on *Amaranthus retroflexus* (Pei *et al*., 2009), and on several host plants (Poursafar *at al*., 2018; Spawton and du Toit, 2024). The present study has shown that lettuce as a previously unrecognized host for *S. amaranthi*, and this fungus is also identified as a new addition to the recorded mycobiota of Algeria. However, under experimental conditions used in the present study, the tested isolates of *S. vesicarium* and *S. amaranthi* only produced small non-progressing necrotic spots on inoculated lettuce leaves. Although *S. solani* has also been identified as causing lettuce leaf spot in Malaysia and

China (Kim *et al*., 2004; Nasehi *et al*., 2013), none of the isolates collected on symptomatic lettuce leaves in Algeria corresponded to this species.

No synergistic effects were shown for *Alternaria* - *Stemphylium* cross inoculations, indicating that antagonism could reduce disease progression. Tao *et al*. (2021) showed that *Pleospora* was among five fungi that interact directly with pathogenic *Alternaria* on *Nicotina tobaccum* to suppress disease development. O'Neill (2019) considered *Stemphylium* and *Alternaria* as weak pathogens or secondary decay organisms on lettuce. These fungi are polyphagous and can colonize novel environments. Lamichhane and Venturi (2015) reported that co-occurrence of identical pathogens on a single host can lead to antagonistic or synergistic interactions, often determined by the order in which pathogens infect host plants. Modulation of these complex interactions could be influenced by multiple factors (Mishra *et al*., 2024).

The present study has demonstrated that isolates of *S. lycopersici* and *S. gracilariae* obtained from lettuce were primary pathogens of this host, and can cause significant damage under greenhouse conditions. The association of these two fungi is likely to be affected by several external factors, which is not uncommon in closely related pathogens (Bessadat *et al*., 2022).

Although *Stemphylium* and *Alternaria* were widespread fungi causing leaf spot disease on plants (Schlub et al. 2022), this is the first report of natural infections of lettuce plants in Algeria by *Stemphylium* and *Alternaria* fungi. These pathogens may become serious problems because of their broad host ranges and pathogenic variability. International trade of agricultural seeds has moved crops and pathogens away from their original environments, and many fungi causing diseases of leafy vegetables are seed-borne (Gullino *et al*., 2019). Rapid emergence of new diseases is often due to seed contamination, and results in severe economic losses. Greenhouse gases generated by human activities can cause shifts in rainfall patterns and influence development and spread of plant pathogens (Velásquez *et al*., 2018; Gullino *et al*., 2019; Pathak *et al*. 2023).

Foliar diseases of lettuce caused by *Alternaria* or *Stemphylium* spp. could be difficult to manage because these fungi can rapidly produce large amounts of secondary inocula under favorable environmental conditions (Grewling *et al*., 2020; González *et al*., 2024). Conidium production also depends on external factors such as light, photoperiods, pollution, presence of weed hosts, soil chemistry, agronomic practices, and crop density, which can enhance disease spread (Gossen *et al*. 2021; Miranda-Apodaca *et al*. 2023; Waheed *et al*., 2023; Lahlali *et al*., 2024). Some pathogens can infect plant leaves in the field throughout crop growing seasons, and can remain dormant until harvest. However, these pathogens have similar temperature and moisture optima for infection and development, so disease control strategies could be developed according to weather forecasts, for timing of fungicide or other chemical applications. Control measures such as foliar spray applications of fungicides combined with sodium carbonate and/or ammonium sulfate have been shown to be effective inducers of systemic protection against the lettuce pathogens *S. botryosum* and *A. alternata* (Naglaa and Safaa, 2020). Results of the present study emphasize the need for further research to evaluate influences of fungal communities and effect of agronomic practices (chemical fertilizers, pesticides, fungicides, etc.) on *S. gracilariae* and *S. lycopersici*. Additionally, lettuce breeding programmes should aim to develop lettuce cultivars with enhanced resistance to these pathogens.

ACKNOWLEDGMENTS

The authors thank Muriel Marchi (research engineer, French National Institute for Agriculture, Food, and Environment) for her technical support with the molecular analyses of fugal isolates.

AUTHOR CONTRIBUTIONS

Conceptualization: NB and PS. Data curation: PS, JC, and NBS. Formal analysis: NB and PS. Investigation: NBS and NB. Methodology: NBS, NB, and BH. Resources: NB and BH. Supervision: PS and KM. Validation: PS. Visualization: NB. Writing: original draft manuscript; NB; review and editing; NB and PS.

LITERATURE CITED

Algeria Climate Fact Sheet (2023) IFRC. 12pp. Available at: https://prddsgofilestorage.blob.core.windows.net/api/documents/Algeria_Climate_Fact_Sheet/Algeria_Climate_Fact_Sheet_EN.pdf Accessed January5, 2025.

Al Ghafri A., Maharachchikumbura S., Hyde K., Al-Saady N. Al-Sadi A., 2019. A new section and a new species of *Alternaria* encountered from Oman. *Phytotaxa* 405: 279–289. https://doi.org/10.11646/phytotaxa.405.6.1

Ariyawansa H. A., Thambugala K. M., Manamgoda D. S., Jayawardena R., Camporesi E., … Hyde K. D., 2015. Towards a natural classification and backbone tree

for *Pleosporaceae*. *Fungal Diversity* 71: 85–139. https://doi.org/10.1007/s13225-015-0323-z

Basallote-Ureba M. J., Prados-Ligero A. M., Melero-Vara J. M., 1999. Aetiology of leaf spot of garlic and onion caused by *Stemphylium vesicarium* in Spain. *Plant Pathology* 48: 139–145. https://doi.org/10.1046/j.1365-3059.1999.00313.x

Berbee M. L., Pirseyedi M., Hubbard S., 1999. *Cochliobolus* phylogenetics and the origin of known, highly virulent pathogens, inferred from ITS and glyceraldehyde-3-phosphate dehydrogenase gene sequences. *Mycologia* 91: 964–977. https://doi.org/10.1080/00275514.1999.12061106

Bessadat N., Berruyer R., Hamon B., Bataillé-Simoneau N., Benichou S., ... Simoneau, P., 2017. *Alternaria* species associated with early blight epidemics on tomato and other Solanaceae crops in northwestern Algeria. *European Journal of Plant Pathology* 148: 181–197. https://doi.org/0.1007/s10658-016-1081-9.

Bessadat N., Hamon B., Bataillé-Simoneau N., Colou J., Kihal M., Simoneau P., 2022. Characterization of *Stemphylium* spp. Associated with tomato foliar diseases in Algeria. *Phytopathologia Mediterranea* 61(1): 39– 53. https://doi.org/10.36253/phyto-13033

Bessadat N., Hamon B., Bataillé-Simoneau N., Kihal M., Simoneau P., 2019. *Alternaria* foliar diseases of solanaceous crops in Algeria: a multi-species threat? *Acta Horticulturae* 1257: 63–72. https://doi.org/10.17660/ActaHortic.2019.1257.10

Blancard D., 2021. Salads: Diseases and Pests. Ephytia - INRAE. Available at: http://ephytia.inra.fr/en/C/5360/Salads-Salads-List-of-diseases-and-pests Accessed August 28, 2025.

Brahamanage R. S., Hyde K. D., Li X. H., Jayawardena R. S., McKenzie E. H. C., Yan J. Y., 2018. Are pathogenic isolates of *Stemphylium* host specific and cosmopolitan? *Plant Pathology Quarantine* 8(2): 153–164. https://doi.org/10.5943/ppq/8/2/7

Brahmanage R., Wanasinghe D., Dayarathne M., Jeewon R., Yan J., ... Li X., 2019. Morphology and phylogeny reveal *Stemphylium dianthi* sp. nov. and new host records for the sexual morphs of *S. beticola*, *S. gracilariae*, *S. simmonsii* and *S. vesicarium* from Italy and Russia. *Phytotaxa* 411: 243–263. https://doi.org/10.11646/phytotaxa.411.4.1

Câmara M. P., O'Neill N. R., Van Berkum P., 2002. Phylogeny of *Stemphylium* spp. based on ITS and glyceraldehyde– 3–phosphate dehydrogenase gene sequences. *Mycologia* 94: 660–672. https://doi.org/10.1080/15572536.2003.11833194

Campbell C. L., Madden L. V., 1990. Introduction to Plant Disease Epidemiology. John Wiley & Sons, New York City. Available at: https://www.rdocumentation.org/packages/agricolae/versions/1.3-7/topics/audpc. Accessed January 30, 2025.

Crous P.W., Cowan D. A., Maggs-Kolling G., Yilmaz N., Larsson E., ... Groenewald J. Z., 2020. Fungal Planet description sheets: 1112–1181. *Persoonia* 45: 251–409. https://doi.org/10.3767/persoonia.2020.45.10

D'Amico M., Frisullo S., Cirulli M., 2008. Endophytic fungi occurring in fennel, lettuce, chicory, and celery — commercial crops in southern Italy. *Mycological Research* 112(1): 100–107. https://doi.org/10.1016/j.mycres.2007.11.007

Damialis A., Kaimakamis E., Konoglou M. Akritidis I., Traidl-Hoffmann C., Gioulekas, D., 2017. Estimating the abundance of airborne pollen and fungal spores at variable elevations using an aircraft: how high can they fly? *Scientific Reports* **7**: 44535. https://doi.org/10.1038/srep44535

Das A., Dutta S., Jash S., Barman A. R., Das R., Kumar S., Gupta S., 2019. Current Knowledge on Pathogenicity and Management of *Stemphylium botryosum* in Lentils (*Lens culinaris* ssp. *culinaris* Medik). *Pathogens* 8: 225. https://doi.org/10.3390/pathogens8040225

De Mers M., 2022. *Alternaria alternata* as endophyte and pathogen. *Microbiology* 168: 3. https://doi.org/10.1099/MIC.0.001153

Faraway J. J., 2002. Practical Regression and Anova using R. The R project. Available at: https://cran.r-project.org/doc/contrib/Faraway-PRA.pdf. Accessed December 10, 2024, from

Farr D.F., Rossman, A.Y., 2017. Fungal databases, U.S. National Fungus Collections. U.S. Department of Agriculture, Agricultural Research Service. https://nt.ars-grin.gov/fungaldatabases/

Fearnley-Whittingstall H., 2013. Grilled lettuce with goats' cheese. BBC. Available at: https://www.bbc.co.uk/food/recipes/grilledlettucewithgo_14300. Accessed October 6, 2023.

Gannibal P. B., Orina A. S., Gasich E. L., 2022. A new section for *Alternaria helianthiinficiens* found on sunflower and new asteraceous hosts in Russia. *Mycological Progress* 21: 34. https://doi.org/10.1007/s11557-022-01780-6

González M., Barilli E., Rispail N., Rubiales D., 2024. Optimization of inoculum production of *Stemphylium botryosum* for large-scale resistance screening of lentils. *Plant Methods* 20: 51. https://doi.org/10.1186/s13007-024-01177-4

Gossen B. D., Tayviah C. S., McDonald M. R., 2021. The Role of Ascospores and Conidia, in Relation to Weather Variables, in the Epidemiology of Stemphyli-

um Leaf Blight of Onion. *Plant Disease* 105(7): 1912–1918. https://doi.org/10.1094/PDIS-06-20-1283-RE

Grewling Ł., Bogawski P., Szymańska A., Nowak M., Kostecki Ł., Smith, M., 2020. Particle size distribution of the major *Alternaria alternata* allergen, Alt a 1, derived from airborne spores and subspore fragments. *Fungal Biology* 124(3-4): 219–227. https://doi.org/10.1016/j.funbio.2020.02.005

Grum-Grzhimaylo A. A., Georgieva M. L., Bondarenko S. A., Debets A. J. M., Bilanenko, E. N., 2016. On the diversity of fungi from soda soils. *Fungal Diversity* 76(1): 27–74. https://doi.org/10.1007/s13225-015-0320-2

Gullino M. L., Gilardi G., Garibaldi A., 2019. Ready-to-Eat Salad Crops: A Plant Pathogen's Heaven. *Plant Disease* 103(9): 2153–2170. https://doi.org/10.1094/PDIS-03-19-0472-FE

Guo R. T., Shi Y. X., Zhao Q., Li B. J., 2018. Identification of the pathogens causing leaf spot on lettuce. *Acta Phytopathologia Sinica* 48(3): 418–422. https://doi.org/10.13926/j.cnki.apps.000131

Gutiérez-Rodriguez A., Postigo I., Guisantes A. J., Sunen E., Martinez J., 2011. Identification of allergens homologous to Alt a 1 from *Stemphylium botryosum* and *Ulocladium botrytis*. *Medical Mycology* 49: 892–896. https://doi.org/10.3109/13693786.2011.576350

Hay F., Stricker S., Gossen B. D., McDonald M. R., Heck D., … Pethybridge S., 2021. *Stemphylium* Leaf Blight: A Re-Emerging Threat to Onion Production in Eastern North America. *Plant Disease* 105(12): 3780–3794. https://doi.org/10.1094/PDIS-05-21-0903-FE

Inderbitzin P., Mehta Y. R., Berbee M. L. 2009. *Pleospora* species with *Stemphylium* anamorphs: a four locus phylogeny resolves new lineages yet does not distinguish among species in the *Pleospora herbarum* clade. *Mycologia* 101: 329–339. https://doi.org/10.3852/08-071

Institut Technique des Cultures Maraîchères et Industrielles. 2010. Fiches techniques valorisées des cultures maraichères et industrielles, La culture de Laitue. Available at: https://itcmi-dz.org/wp-content/uploads/2022/06/LAITUE.pdf. Accessed January 5, 2025.

Kalyaanamoorthy S., Minh B., Wong T., von Haeseler A., Jermiin, L. S., 2017. ModelFinder: Fast model selection for accurate phylogenetic estimates. *Nature Methods* 14(6): 587–589. https://doi.org/10.1038/nmeth.4285

Katz S. H., Weaver W.W., 2003. Encyclopedia of food and culture. Scribner. 376 pp.

Kim M. J., Moon Y., Tou J. C., Mou B., Waterland, N. L., 2016. Nutritional value, bioactive compounds and health benefits of lettuce (*Lactuca sativa* L.). *Journal of Food Composition and Analysis* 49: 19–34. https://doi.org/10.1016/j.jfca.2016.03.004

Kim B.S., Yu S.H., Cho H.J., Hwang H.S., 2004. Gray leaf spot in peppers caused by *Stemphylium solani* and *S. lycopersici*. *The Plant Pathology Journal* 20, 85–91. https://doi.org/10.5423/PPJ.2004.20.2.085

Koike S. T., Smith R. F., Cahn M. D., Pryor B. M., 2017. Association of the carrot pathogen *Alternaria dauci* with new diseases, *Alternaria* leaf speck, of lettuce and celery in California. *Plant Health Progress* 18(2): 136–143. https://doi.org/10.1094/PHP-12-16-0074-RS

Kornerup A., Wanscher J. H., 1978. *Methuen Handbook of Colour*, 3rd ed. Methuen, London, UK. 252pp.

Kumar S., Stecher G., Tamura K., 2016. MEGA 7: Molecular evolutionary genetics analysis version 7.0 for bigger datasets. *Molecular Biology and Evolution* 33(7): 1870–1874. https://doi.org/10.1093/molbev/msw054

Lahlali R., Taoussi M., Laasli S. E., Gachara G., Ezzouggari R., … Ait Barka, E., 2024. Effects of climate change on plant pathogens and host-pathogen interactions. *Crop Environment* 3(3): 159–170. https://doi.org/10.1016/j.crope.2024.05.003

Lallouche B., Hadj Kouider B., Belloudah A., Ben Madani R., Boutekrabt A., 2020. Phenotypic characterization of some lettuce cultivars (*Lactuca sativa* L.) cultivated in Algeria. *Revue Agrobiologia* 10(1): 1787–96.

Lamichhane J. R., Venturi V., 2015. Synergisms between microbial pathogens in plant disease complexes: a growing trend. Front Plant Sci. 27(6): 385. https://doi.org/10.3389/fpls.2015.00385. PMID: 26074945; PMCID: PMC4445244.

Lawrence D. P., Gannibal P. B., Peever T. L., Pryor B. M., 2013. The sections of *Alternaria*: Formalizing species-groups concepts. *Mycologia* 105: 530–546. https://doi.org/10.3852/12-249

Letunic I., Bork P., 2024. Interactive Tree of Life (iTOL) v6: recent updates to the phylogenetic tree display and annotation tool. *Nucleic Acids Research* 52: 78–82. https://doi.org/10.1093/nar/gkae268

Li J., Jiang H., Jeewon R., Hongsanan S., Bhat D. J., … Phookamsak R., 2023. *Alternaria*: update on species limits, evolution, multi-locus phylogeny, and classification. *Studies in Fungi* 8: 1. https://doi.org/10.48130/SIF-2023-0001

Liu H., Wang H., Zhong J., Lu X., Pan X., T. … Zhou Q., 2019. First Report of *Stemphylium lycopersici* and *Stemphylium vesicarium* causing Leaf Spot on Lettuce (*Lactuca sativa*) in China. *Plant Disease* 103(11): 2957. https://doi.org/10.1094/PDIS-05-19-1052-PDN

Manaaki Whenua - Landcare Research., 2023. New Zealand Fungi Names Databases - *Stemphylium lycopersici* (Enjoji) W. Yamam. 1960. Available at: https://BiotaNZ.landcareresearch.co.nz/scientific-names/1cb1a5ca-36b9-11d5-9548-00d0592d548c. Accessed October 4, 2023.

Marin-Felix Y., Hernandez-Restrepo M., Iturrieta- Gonzalez I., Garcia D., Gene J., ... Crous P. W., 2019. Genera of phytopathogenic fungi: GOPHY 3. *Studies in Mycology* 94: 1–124. https://doi.org/10.1016/j.simyco.2019.05.001

Matić S., Tabone G., Garibaldi A., Gullino M. L., 2020. *Alternaria* Leaf Spot Caused by *Alternaria* Species: An Emerging Problem on Ornamental Plants in Italy. *Plant Disease* 104(8): 2275–2287. https://doi.org/10.1094/PDIS-02-20-0399-RE

Miranda-Apodaca J., Artetxe U., Aguado I., Martin-Souto L., Ramirez-Garcia A., ... Pérez-López U., 2023. Stress Response to Climate Change and Postharvest Handling in Two Differently Pigmented Lettuce Genotypes: Impact on *Alternaria alternata* Invasion and Mycotoxin Production. *Plants* 12: 1304. https://doi.org/10.3390/plants12061304

Mishra S., Srivastava A., Singh A., Pandey G. C., Srivastava G., 2024. An overview of symbiotic and pathogenic interactions at the fungi-plant interface under environmental constraints. *Frontiers in Fungal Biology* 5: 1363460. https://doi.org/10.3389/ffunb.2024.1363460

Moses E., Akrofi S., Beseh P., 2016. *Alternaria* leaf spot on lettuce-Ghana. *Plantwise* https://doi.org/10.1079/pwkb.20177800648

Naglaa A. S. M., Safa E. E., 2020. Salts as controlling agents of lettuce leaf spot diseases. Plant Protection and Pathology Research. Zagazig *Journal of Agricultural Research* 47 (1): 119–133. https://doi.org/10.21608/zjar.2020.70230

Nasehi A., Kadir J. B., Esfahani M. N., Mahmodi F., Ghadirian H., ... Soleimani N., 2013. Leaf Spot on Lettuce (*Lactuca sativa*) Caused by *Stemphylium solani*, a New Disease in Malaysia. *Plant Disease* 97(5): 689. https://doi.org/10.1094/PDIS-10-12-0902-PDN

Nasehi A., Kadir J. B., Nasr-Esfahani M., Abed-Ashtiani F., Wong M. Y., ... Golkhandan E., 2014. Analysis of genetic and virulence variability of *Stemphylium lycopersici* associated with leaf spot of vegetable crops. *European Journal of Plant Pathology* 140: 261–273. https://doi.org/10.1007/s10658-014-0460-3

Nguyen L. T., Schmidt H. A., von Haeseler A., Minh B. Q., 2015. Minh, B.Q. IQ-Tree: A fast and effective stochastic algorithm for estimating maximum likelihood phylogenies. *Molecular Biology and Evolution* 532(1): 268–6274. https://doi.org/10.1093/molbev/msu300

Nischwitz C., 2016. Purple blotch and *Stemphylium* leaf blight. In: Cannon C ed. Utah vegetable production and pest management guide. Utah State University IPM Program, Logan, UT 84322. pp. 103–104.

O'Neill T., 2019. Diseases of lettuce crops. AHDB Horticulture, Stoneleigh Park, Kenilworth, Warwickshire, CV8 2TL. 28 pp. Available at: https://projectblue.blob.core.windows.net/media/Default/Imported%20Publication%20Docs/AHDB%20Horticulture%20/LettuceDiseases1846_190109_WEB.pdf. Accessed October 4, 2023.

Olsen K. J. K., Rossman A., Andersen B., 2018. Metabolite production by species of Stemphylium. *Fungal Biology* 122(2-3): 172–181. https://doi.org/10.1016/j.funbio.2017.12.012

Padhi S., Panda M. K., Das D., Tayung K., 2015. ITS2 RNA secondary structure analysis reveals close affinity between endophytic and pathogenic fungi: a case study in *Fusarium* species. *Annals of Microbiology* 66: 625–633. https://doi.org/10.1007/s13213-015-1142-x

Pathak M., Barik S., Dash S., Moharana D., 2023. Impact of Climate Change on Leafy and Salad Vegetables Production. In: Solankey S.S., Kumari M. (eds) Advances in Research on Vegetable Production Under a Changing Climate Vol. 2. *Advances in Olericulture*. Springer, Cham. https://doi.org/10.1007/978-3-031-20840-9_5

Pegg K., Duff J., Manners A. 2014. *Alternaria* diseases in production nurseries. Agri-science Queensland, Department of Agriculture, Fisheries and Forestry (DAFF). Available at: https://www.vegkit.com.au/globalassets/hort-innovation/resource-assets/ny11001-alternaria-diseases.pdf. Accessed September 29, 2023.

Pei Y. F., Geng Y., Wang Y., Zhang X. G., 2009. Two new species of *Stemphylium* from Sinkiang, China. *Mycotaxon* 109: 493–497. https://doi.org/10.5248/109.493

Poursafar A., Ghosta Y., Javan-Nikkhah M., 2018. An emended description of *Stemphylium amaranthi* with its first record for Iran mycobiota. *Phytotaxa* 371: 93. https://doi.org/10.11646/phytotaxa.371.2.3

Pryor M. B., Gilbertson R. L., 2000. Molecular phylogenetic relationships amongst Alternaria species and related fungi based upon analysis of nuclear ITS and mt SSU rDNA sequences. *Mycological Research* 104 (11): 1312–1321. https://doi.org/10.1017/S0953756200003002

Roberts A. J., Punja, Z. K., 2021. Pathogenicity of seedborne *Alternaria* and *Stemphylium* species and stem-infecting *Neofusicoccum* and *Lasiodiplodia* species to cannabis (*Cannabis sativa* L., marijuana) plants.

Canadian Journal of Plant Pathology 44(2):250–269. https://doi.org/10.1080/07060661.2021.1988712

Saleemi M. K., Khan M. Z., Khan A., Javed I., Ul Hasan Z., ... Mehmood M. A., 2012. Occurrence of toxigenic fungi in maize and maize-gluten meal from Pakistan. *Phytopathologia Mediterranea* 51(1): 219–224. https://doi.org/10.14601/Phytopathol_Mediterr-9858

Samson R. A., Houbraken J., Thrane U., Frisvad J. C., Andersen B., 2010. CBS laboratory manual series 2 - Food and indoor fungi. CBS Fungal Biodiversity Centre, Utrecht, The Netherlands.

Sánchez P., Vélez-del-Burgo A., Suñén E., Martínez J., Postigo I., 2022. Fungal Allergen and Mold Allergy Diagnosis: Role and Relevance of *Alternaria alternata* Alt a 1 Protein Family. *Journal of Fungi* 8(3): 277. https://doi.org/10.3390/jof8030277

Schlub R. L., Hudson J., Hahn E., 2022. Foliar Pathogens in Guam: *Alternaria* and *Stemphylium*: Diseases: Early Blight, Bull's Eye, Leaf Blight, Gray Leaf Spot. University of GUAM, Cooperative Extension & Outreach, Technical Report pp. 2–22.

Shatilov N. V., Razin A. F., Ivanova M. I., 2019. Analysis of the world lettuce market. IOP Conference Series: *Earth and Environmental Science* 395: 012053. https://doi.org/10.1088/1755-1315/395/1/012053

Simmons E.G., 1967. Typification of *Alternaria*, *Stemphylium*, and *Ulocladium*. *Mycologia* 59(1):67-92.

Simmons E.G., 1969. Perfect states of *Stemphylium*. *Mycologia* 61: 1–26.

Simmons E.G., 2001. Perfect states of *Stemphylium*—IV. *Harvard Papers in Botany* 199–208.

Simmons E.G., 2007. *Alternaria*. An identification Manual. CSS Siodiversity Series Io. 6. CSS Fungal Biodiversity Centre, Utrecht, the Netherlands. 775 pp.

Singh V., Shrivastava A., Jadon S., Wahi N., Singh A., Sharma N., 2015. *Alternaria* diseases of vegetable crops and its management control to reduce the low production. *International Journal of Agriculture and Biology* 7(13):834-840.

Spawton K. A., du Toit L. J., 2024. Characterization of *Stemphylium* Species Associated with Stemphylium Leaf Spot of Spinach (*Spinacia oleracea*). *Plant Disease* 108 (12): 3578–3594. https://doi.org/10.1094/PDIS-10-23-2223-RE

Subbarao K. V., Davis R. M., Gilbertson R. L., Raid R. N., 2017. Diseases of Lettuce (*Lactuca sativa* L.). The American Phytopathological Society (APS). Available at: https://www.apsnet.org/edcenter/resources/commonnames/Pages/Lettuce.aspx. Accessed July 26, 2023.

Tao J., Cao P., Xiao Y., Wang Z., Huang Z., Jin J., Liu Y., Yin H., Liu T., Zhou Z., 2021. Distribution of the potential pathogenic *Alternaria* on plant leaves determines foliar fungal communities around the disease spot, *Environmental Research* https://doi.org/10.1016/j.envres.2021.111715

Tayviah C. S., 2017. *Epidemiology and management of Stemphylium leaf blight on onion* (Allium cepa *L.*) *in the Holland Marsh, Ontario.* Master of Science thesis, University of Guelp. Available at: https://atrium.lib.uoguelph.ca/xmlui/bitstream/handle/10214/10430/Tayviah_CyrilSelasi_201704_MSc.pdf?sequence=1. Accessed October 4, 2023.

Thomma B.P. H. J., 2003. *Alternaria* spp.: from general saprophyte to specific parasite. *Molecular Plant Pathology* 4: 225–236. https://doi.org/10.1046/j.1364-3703.2003.00173.x

Velásquez A. C., Castroverde C. D. M., He S. Y., 2018. Plant-Pathogen Warfare under Changing Climate Conditions. *Current Biology* 21-28(10): 619–63. https://doi.org/10.1016/j.cub.2018.03.054

Waheed A., Haxim Y., Islam W., Ahmad M., Muhammad M., ... Zhang D., 2023. Climate change reshaping plant-fungal interaction. *Environmental Research* 238(2):117–282. https://doi.org/10.1016/j.envres.2023.117282

Wang H., Guo Y., Luo Z., Gao L., Li R., ... Chen S., 2022. Recent Advances in *Alternaria* Phytotoxins: A Review of Their Occurrence, Structure, Bioactivity, and Biosynthesis. *Journal of Fungi* 8(2):168. https://doi.org/10.3390/jof8020168

White T. J., Bruns T., Lee S., Taylor J., 1990. Amplification and direct sequencing of fungal ribosomal RNA genes for phylogenetics. In: *PCR Protocols: A Guide to Methods and Applications*. Academic Press, New York, 315–322. https://doi.org/10.1016/B978-0-12-372180-8.50042-1

Woudenberg, J. H. C., Groenewald, J. Z., Binder, M., Crous, P. W., 2013. *Alternaria* redefined. *Studies in Mycology* 75: 171–212. https://doi.org/10.3114/sim0015

Woudenberg J. H. C., Hanse B., van Leeuwen G. C. M., Groenewald J. Z., Crous P. W., 2017. *Stemphylium* revisited. *Studies in Mycology* 87: 77–103. https://doi.org/10.1016/j.simyco.2017.06.001

Yang X., Gil M. I., Yang Q., Tomás-Barberán F. A., 2022. Bioactive compounds in lettuce: Highlighting the benefits to human health and impacts of preharvest and postharvest practices. *Comprehensive Reviews in Food Science and Food Safety* 21: 4– 45. https://doi.org/10.1111/1541-4337.12877

Zhang X.G., Zhang T.Y., 2002. Taxonomic studies of *Stemphylium* from China I. *Mycosystema* 21: 324–326.

Phytopathologia Mediterranea
The international journal of the
Mediterranean Phytopathological Union

Firenze University Press
www.fupress.com/pm

Research Papers

Cultivar-specific effects of physical and biological treatments on grapevine trunk disease control and plant vigour

Ester ABARQUERO[1], María del Pilar MARTÍNEZ-DIZ[2], Angela DÍAZ-FERNÁNDEZ[1], David GRAMAJE[3,*], Emilia DÍAZ-LOSADA[1]

[1] *Estación de Viticultura e Enoloxía de Galicia (AGACAL-EVEGA), Ponte San Clodio s/n 32428-Leiro-Ourense, Spain*
[2] *Centro de Investigacións Agrarias de Mabegondo (CIAM), Mabegondo, 15318 Abegondo, A Coruña, Spain*
[3] *Instituto de Ciencias de la Vid y del Vino (ICVV), Consejo Superior de Investigaciones Científicas - Universidad de la Rioja - Gobierno de La Rioja, Ctra. LO-20 Salida 13, Finca La Grajera, 26071 Logroño, Spain*
*Corresponding author. E-mail: david.gramaje@icvv.es

Summary. Grapevine trunk diseases (GTDs), including black foot and Petri disease, pose threats to young grapevine establishment. Efficacy of hot water treatment (HWT), *Trichoderma atroviride* SC1 (TCH), and their combination (HWT + TCH) was assessed for control of GTDs and promotion of early plant development in nine Galician grapevine cultivars. Treatments were applied either prior to grafting or before planting in the field. The treatments were more effective against Petri disease than black foot, with the HWT + TCH combination reducing Petri disease incidence and severity in several cultivars, particularly when applied at the pre-grafting stage. In contrast, limited efficacy was observed against black foot, indicating that post-planting strategies are likely to be required to manage root-infecting pathogens. Plant performance responses were cultivar- and timing-dependent: early treatments generally improved root biomass, whereas late applications occasionally reduced shoot length and root weight. These results highlight the importance of tailoring integrated disease management strategies to specific grapevine cultivars and propagation stages, to optimize nursery outcomes and grapevine health.

Keywords. Biological control, black foot, hot water treatment, Petri disease, *Trichoderma*, *Vitis vinifera*.

OPEN ACCESS

Citation: Abarquero, E., Martínez-Diz, M. d. P., Díaz-Fernández, A., Gramaje, D., & Díaz-Losada, E. (2025). Cultivar-specific effects of physical and biological treatments on grapevine trunk disease control and plant vigour. *Phytopathologia Mediterranea* 64(3): 513-526. DOI: 10.36253/phyto-16698

Accepted: September 9, 2025

Published: November 3, 2025

Data Availability Statement: All relevant data are within the paper and its Supporting Information files.

Competing Interests: The Author(s) declare(s) no conflict of interest.

Editor: Ilaria Pertot, Centro Agricoltura, Alimenti, Ambiente, University of Trento, Italy.

ORCID:
EA: 0009-0000-0288-6771
MPMD: 0000-0003-0831-0524
AD-F: 0000-0002-3981-7750
DG: 0000-0003-1755-3413
ED-L: 0000-0002-6896-969X

INTRODUCTION

Over the past two decades, there has been a marked increase in decay and progressive mortality among young grapevine plants (Gramaje *et al*., 2018). This situation has been primarily driven by fungal grapevine trunk diseases (GTDs), which pose significant threats to the sustainability of grapevine cultivation (Bertsch *et al*., 2013). GTDs cause substantial economic losses due to reduced

yields, increased costs for disease control, and the premature decline of vineyards (Bertsch *et al*., 2013; Gramaje *et al*., 2018). These diseases, caused by fungal infections, typically originate during growing seasons through the release of pathogen conidia, which germinate to colonize pruning wounds. While most infections occur in vineyards, some plants may be infected prior to planting (Gramaje and Armengol, 2011), because mother plants can harbour GTD pathogens, contributing to disease transmission (Fourie and Halleen, 2004). Nurseries, therefore, may act as reservoirs of infected plant material, and grapevine propagation processes can present increased risks of infection for cuttings (Gramaje and Armengol, 2011).

The most prevalent diseases in nurseries and young grapevines are Petri disease (PD), black foot (BF), and Botryosphaeria dieback. PD is primarily caused by *Cadophora luteo-olivacea*, *Phaeomoniella chlamydospora*, and *Phaeoacremonium* spp., which enter grapevines through wounds or pruning cuts (Gramaje and Armengol, 2011). This disease is characterized by black discolourations of host xylem and accumulation of phenolic compounds in the vessels (Mugnai *et al*., 1999). External symptoms of PD include interveinal leaf chlorosis, leaf necrosis, stunted plant growth and decline, and, in severe cases, dieback (Fourie and Halleen, 2004).

The disease black foot is caused by fungi in the genera *Dactylonectria*, *Cylindrocladiella*, *Ilyonectria*, *Neonectria*, and *Thelonectria*. These pathogens typically infect young grapevines through root wounds or injuries (Agustí-Brisach and Armengol, 2013), leading to black necrotic lesions on roots and brown discolourations at trunk bases (Fourie and Halleen, 2006).

Botryosphaeria dieback, caused by multiple species within *Botryosphaeriaceae* (Úrbez-Torres, 2011), manifests as cordon dieback, characterized by spur losses and wedge-shaped internal necroses in cordon and trunk cross-sections (Gramaje *et al*., 2018). Eradication of GTDs is not possible, so control of these diseases is primarily focused on prevention and mitigation (Gramaje *et al*., 2018). In nurseries, integrated management programmes including physical, chemical, and/or biological controls have been previously implemented to reduce GTD infections (Halleen and Fourie, 2016). In recent years, the number of chemicals authorized for use during grapevine propagation have reduced (Gramaje and Di Marco, 2015), and biological control has then been proposed as a sustainable alternative in grapevine nurseries (Gramaje *et al*., 2018).

Biocontrol agents offer several direct mechanisms of action against pathogens, including competition for space and nutrients, production of hydrolytic enzymes, and parasitism or antibiosis (Thambugala *et al*., 2020). Indirect mechanisms of these agents are associated with plant defense responses after pathogen colonization (Legein *et al*., 2020). *Trichoderma atroviride* SC1 (TCH) has been the most used and effective biocontrol agent against GTD fungi in grapevine nurseries (Pertot *et al*., 2016; Berbegal *et al*., 2020; Leal *et al*., 2023). This *Trichoderma* strain was especially effective in reducing incidence of PD (Pertot *et al*., 2016; Berbegal *et al*., 2020; Leal *et al*. 2023) and Botryosphaeria dieback (Berbegal *et al*., 2020; Leal *et al*., 2021) when applied during the hydration stage of propagation material. Hot-water treatment (HWT) has also been proposed as an environmentally-friendly strategy to reduce GTD infections in grapevine nurseries (Halleen and Fourie, 2016; Eichmeier *et al*., 2018; Lade *et al*., 2022). However, anecdotal reports of unacceptably high rates of vine mortality after HWTs have sometimes resulted in reluctance by nurseries to use them (Gramaje and Di Marco, 2015).

Given that GTD control options are limited in grapevine nurseries, and that TCH and HWT are considered the most effective strategies, the present study aimed to investigate and compare the efficacy of both treatments, applied either individually or in combination, for the control of GTDs. The treatments were applied to two types of plant material at two different time points: (i) rootstock and scion cuttings before grafting, and (ii) grafted plants after the rooting phase in nursery fields. The study also aimed to assess effects of biological and physical treatments on the viability of the plant material. The hypotheses assessed in the study were: (i) that physical and biological treatments reduce the incidence of GTDs compared to untreated controls; (ii) that efficacy of these treatments depends on application timing; (iii) the combination of HWT and TCH enhances effectiveness of disease management, reducing GTD incidence through propagation processes; and (iv) there is variability in susceptibility of rootstock/cultivar combinations to biological and physical treatments.

MATERIALS AND METHODS

Planting material

The experiments described here were carried out in a nursery in O Barco de Valdeorras and a vineyard in Leiro, both located in Ourense, Galicia, Northwestern Spain. Nine native Galician grapevine cultivars were used, including three red grape ('Brancellao', 'Mencía', and 'Merenzao') and six white grape cultivars ('Albariño', 'Branco Lexítimo' 'Dona Branca', 'Loureira' 'Torrontés', and 'Treixadura'). All the cultivars were grafted onto the 110 Richter rootstock (110 R).

Treatments and fungal isolations

The effectiveness of the following treatments was evaluated: HWT at 53°C for 30 min; TCH (Vintec®, Certis Belchim; 2×10^{10} CFU g^{-1} of formulated product) at a dose of 2 g L^{-1}, by immersion in an aqueous suspension for 24 h at room temperature; and a combination of treatments (HWT + TCH), commencing with HWT application followed by maintenance of at 20°C for 24 h before TCH inoculation. The viability of conidia from the fungus TCH was verified to be at least 85% before the trial (Pertot *et al*., 2016). A serial dilution of the conidial suspension was carried out, and the diluted suspensions were plated onto potato dextrose agar (PDA), with colony-forming units counted after 24-48 h of incubation at room temperature.

Before application of treatments and the onset of propagation processes in a nursery, 25 rootstock cuttings and ten scion cuttings of each cultivar were randomly selected and analyzed for the presence of fungal pathogens associated with GTDs. Isolations were carried out from 1 cm-long sections of the cutting stems. These sections were washed with water, surface-disinfected for 1 min in 1.5% sodium hypochlorite solution, and then rinsed twice with sterile distilled water. Wood fragments were then placed on malt extract agar (MEA) supplemented with 0.5 g L^{-1} streptomycin sulfate (Sigma-Aldrich) (MEAS) (five fragments per two Petri dishes). The isolation plates were then incubated at 25°C in darkness for 10-15 d. All developng colonies were transferred to PDA. Preliminary morphological identification of colonies was carried out by observing their macroscopic characteristics to identify potential pathogens.

Identities of fungal species were confirmed using molecular methods. Fungal mycelium from pure cultures grown on PDA for 2-3 weeks at 25°C in darkness was mechanically disrupted using the FastPrep-24™5G system (MP Biomedicals). Total DNA was then extracted following the manufacturer's instructions using the E.Z.N.A. Plant Miniprep Kit (Omega Bio-tek). Identification of all isolates was carried out through analyses of Internal Transcribed Spacer (ITS) regions by amplification with universal fungal primers ITS1F and ITS4. Additional molecular identifications were then carried out for specific fungi. Cylindrocarpon-like asexual morphs were confirmed by sequencing part of the histone H3 gene with primers CYLH3F and CYLH3R (Crous *et al*., 2004). The beta-tubulin (tub2) region was amplified using the T1 (O'Donnell and Cigelnik, 1997) and Bt2b (Glass and Donaldson, 1995) primer set for *Phaeoacremonium* spp., and the BTCadF/BTCadR primer set for *Cadophora* spp. (Travadon *et al*., 2015). Identity of TCH was revealed by using the specific primers developed by Savazzini *et al*. (2008). All PCR products were visualized in 1% agarose gels (agarose D-1 Low EEO, Conda Laboratories) and sequenced in both directions by Eurofins GATC Biotech.

Disease incidence (DI) caused by BF and PD pathogens was determined as the mean percentage of grafted plants infected by these fungi. Disease severity (DS) was assessed as the mean percentage of wood segments (ten segments per stem section) colonized by these fungi, after use of the standard pathogen isolation protocol described for GTDs (Berlanas *et al*., 2020). The wood segments were placed vertically on the agar medium.

Assessments of treatments to cuttings or grafted plantss

Treatments assessed were applied at two critical points in traditional nursery plant production. It is recognized that there is increased risk of contamination by GTD pathogens during pre-grafting hydration (Experiment 1), or after the rooting of plants in a nursery field prior to planting in commercial vineyards (Experiment 2). Two experiments were each repeated for two consecutive years (2021 and 2022).

Experiment 1: Application of treatments to rootstock and scion cuttings prior to grafting. Propagation material was subjected to HWT, TCH, or a combination of both (HWT + TCH) during pre-grafting hydration of the grapevine propagation process, in April 2021. HWT was applied exclusively to rootstock cuttings, while TCH was applied to both rootstock and scion cuttings. Control cuttings (C) underwent the standard nursery hydration using water at room temperature (Gramaje and Armengol, 2011). Grafting and stratification were carried out in May 2021 and repeated in May 2022, followed by field planting in the nursery in, resectively, June 2021 and June 2022. For each trial, the planting material was arranged in a randomized complete block design with three replicates, each of 30 plants per treatment and per cultivar. Standard cultural practices were followed throughout the two growing seasons, and crop maintenance included use of integrated pest management (IPM) strategies.

In March 2022 and March 2023, rooted plants were removed from the nursery field, their roots were trimmed to a uniform length (10 cm), and they were then stored at 4–6°C. In April 2022 and April 2023, the plants were transplanted into an experimental vineyard, maintaining a spacing of 50 cm between plants and 2.5 m between rows. At the end of August 2022 and August 2023, plant viability was assessed as percentage of

sprouted plants (SP), while vegetative development was evaluated by measuring main shoot lengths (SLs). During vegetative dormancy in December 2022 and December 2023, plants were uprooted and transported to the laboratory for fungal isolations and evaluation of the root weight (RW). Three segments (each 1 cm length) were excised from three distinct zones: the graft union, the basal end of the rootstock, or the root system. These segments were surface-washed, disinfected, and processed following the fungal isolation protocol described above. Ten wood fragments from each zone were analyzed (five per Petri dish), totalling 30 fragments per plant. Molecular identification of GTD pathogens and TCH were carried out as described above.

Experiment 2: Application of treatments to grafted plants prior to planting in a commercial vineyard. Grafted plants were produced using 110R rootstock cuttings and scions of the nine grapevine cultivars listed above, following the standard procedure of the production nursery. This included hydration of cuttings for 24 h, grafting using an omega grafting machine, and stratification at 25°C with 75% relative humidity (Gramaje and Armengol, 2011). After stratification, shoots were pruned, plants were waxed, and subsequently planted in the nursery field in June 2021 and June 2022. A total of 90 grafted plants per cultivar were established. Crop maintenance in the nursery followed standard techniques for managing plant growth.

In March 2022 and March 2023, plants were uprooted from the nursery field, roots were trimmed, and shoots were pruned to two buds before being waxed again. The plants were then subjected to HWT, TCH, or HWT + TCH and immediately transplanted into a commercial vineyard. A randomized complete block design was used, with three replicates of ten plants per treatment and cultivar, totalling 360 plants per treatment. The planting arrangement was 0.5 m spacing between plants and 2.5 m between rows. Standard cultural practices were followed throughout the growing season.

At the end of August 2022 and end of August 2023, plant viability was assessed as described in Experiment 1. In December 2022 and December 2023, during vegetative dormancy, plants were uprooted and processed for fungal isolations and RW analysis, as described for Experiment 1.

Data analyses

Before conducting statistical analyses, all data were tested for normality and homogeneity of variances. Since no significant differences ($P > 0.05$) were observed between the two years of experiments (2021 and 2022) for any of the variables analyzed (DI, DS, SP, SL, and RW), and no significant year × treatment interactions were detected, data from both years were pooled for final analyses. Transformations were applied when necessary, with percentage data being converted using the arcsine square root transformation, expressed as arcsin $(DI \text{ or } DS/100)^{1/2}$. Treatment means for variables such as DI, DS, SP, SL, and RW were calculated based on their values at each sampling point. Two-way ANOVA was employed to analyze the experimental results, considering blocks and treatments as independent variables, and DI (%), DS (%), SP (%), SL (cm), and RW (g) as dependent variables. Treatment means were compared using the Student's t-test with the least significant difference (LSD) method, at $P < 0.05$. All analyses were carried out using XLSTAT v24.3 software (Addinsoft).

RESULTS

Analysis of the plant material prior to application of treatments and the onset of nursery propagation processes showed that no fungal pathogens associated with GTDs were present. Specifically, no fungi linked to PD or BF were isolated from 25 rootstock cuttings or ten scion cuttings randomly selected from each cultivar.

Experiment 1: Incidence and severity of fungal grapevine trunk diseases when treatments to rootstock and scion cuttings were applied prior to grafting

No statistically significant effect ($P > 0.05$) year was observed for any of the variables analyzed (DI and DS for both BF and PD); all, and no interactions between year and treatment were detected. Data from both years (2021 and 2022) were therfore pooled for final analyses. Analysis of the plant material at the end of the experiment showed that fungi associated with GTDs were present. For BF, the fungi *Dactylonectria torresensis*, *Dactylonectria macrodidyma* and *Ilyonectria liriodendri* were identified. For PD, the isolated species included *Phaeomoniella chlamydospora*, *Phaeoacremonium minimum* and *Cadophora luto-olivacea*. These results are presented by disease category, grouping the fungi associated with each disease.

Effectiveness of HWT, TCH, and the combined HWT + TCH treatments for reducing BF and PD incidence and severity varied across the different grapevine cultivars (Table 1). Disease incidence was greater for BF than for PD. For BF incidence, no statistically significant differences ($P > 0.05$) were observed among treatments for

Table 1. Incidence and severity of Black Foot and Petri disease in grafted plants of nine grapevine cultivars following HWT, TCH, and HWT+TCH treatments prior to planting in a commercial vineyard (Experiment 1).

Treatments	Albariño	Branco Lexítimo	Brancellao	Dona Blanca	Loureira	Mencía	Merenzao	Torrontés	Traixadura	LSD
BF incidence (%)[a]										
Control	34.0[b] ± 5.9	36.1 ± 9.8	31.9 ± 5.8	38.8 ± 5.5	20.8 ± 12.1	20.1 ± 7.2	42.3 ± 11.6	43.7 ± 12.8	25.0 ± 11.4	0.61
HWT	54.8 ± 15 AB	58.4 ± 16.4 A	29.8 ± 6.7 AB	40.2 ± 10.2 AB	25.6 ± 5.7 B	31.9 ± 7.6 AB	49.3 ± 9.1 AB	44.4 ± 12.5 AB	57.6 ± 10.4 A	0.01
TCH	38.1 ± 16.7	37.5 ± 4.7	27.7 ± 8.6	32.6 ± 8.9	27.0 ± 7.3	26.3 ± 1.4	36.1 ± 9.8	34.7 ± 11.7	39.5 ± 8.4	0.96
HWT+TCH	27.7 ± 10.4	49.3 ± 11.6	27.0 ± 3.0	33.3 ± 7.8	25.0 ± 9.4	33.3 ± 10.8	50.0 ± 10.8	42.3 ± 8.5	34.0 ± 13.8	0.57
LSD[c]	0.5	0.4	0.9	0.9	0.9	0.6	0.7	0.9	0.2	
BF severity (%)										
Control	12.5 ± 7.55	9.5 ± 3.3	5.6 ± 1	8.4 ± 2.3	3.6 ± 2.4	2.3 ± 0.6 b	10.9 ± 3	12.6 ± 3.8	6.2 ± 3.4 b	0.39
HWT	10.9 ± 3.76 ABC	18.6 ± 7.8 AB	6.6 ± 1.6 C	11.3 ± 4.1 ABC	4.7 ± 0.7 C	7.9 ± 2.7 abBC	9.5 ± 2.6 BC	9.7 ± 2.6 BC	21.8 ± 5.3 aA	0.01
TCH	8 ± 3.63 BC	15.8 ± 3.1 A	5.1 ± 2 BC	5.9 ± 2 BC	4 ± 0.7 C	5.1 ± 0.7 abBC	6.5 ± 1.6 aBC	11.3 ± 3.3 AB	7.9 ± 2.8 bBC	0.03
HWT+TCH	4.7 ± 1.67	14.8 ± 6.6	7.6 ± 2.3	8.1 ± 2.6	6.9 ± 2.8	9.4 ± 3 a	12.2 ± 2.2	10.4 ± 2.2	11.5 ± 5.5 ab	0.79
LSD	0.8	0.7	0.7	0.6	0.6	0.02	0.4	0.9	0.04	
PETRI DISEASE incidence (%)										
Control	6.9 ± 4.53 BC	30.5 ± 8.0 aABC	27.7 ± 12 aAB	0 ± 0 C	13.8 ± 9 abBC	8.3 ± 5.2 BC	4.1 ± 4.1 BC	43 ± 14.5 aA	12.5 ± 8.5 BC	0.02
HWT	4.1 ± 4.16	4.1 ± 2.8 b	0 ± 0 b	5.5 ± 5.5	0 ± 0 b	0 ± 0	0.5 ± 0.4	4.1 ± 4.1 b	0 ± 0	0.70
TCH	13.8 ± 9.02 AB	11.1 ± 6.0 bAB	5.5 ± 5.5 abAB	2.7 ± 2.7 AB	18 ± 7.5 aA	6.9 ± 4.5 AB	4.8 ± 3.1 AB	8.3 ± 8.3 bAB	0 ± 0 B	0.02
HWT+TCH	0 ± 0 B	4.1 ± 4.2 bAB	9 ± 4.3 abAB	0 ± 0 B	0 ± 0 bB	2.7 ± 2.7 AB	0 ± 0 B	0 ± 0 bB	12.5 ± 8.5 A	0.03
LSD	0.5	0.009	0.01	0.5	0.04	0.3	0.4	>0.001	0.2	
PETRI DISEASE severity (%)										
Control	1.2 ± 0.86 B	12.2 ± 5.3 aA	9.1 ± 4.2 aAB	0 ± 0B	8.8 ± 7.6AB	2.9 ± 2.4B	0.4 ± 0.4 abB	17 ± 6.5A	5.8 ± 4.1AB	0.01
HWT	2.5 ± 2.49	1.6 ± 1.1 b	0 ± 0 b	3.8 ± 3.8	0 ± 0	0 ± 0	0 ± 0 b	0.8 ± 0.8	0 ± 0	0.62
TCH	7.7 ± 4.98 AB	1.5 ± 0.8 bAB	0.5 ± 0.5 bAB	0.8 ± 0.8 AB	9.2 ± 8.1 AB	1.1 ± 0.8 AB	1.9 ± 1.2 aAB	33.3 ± 33.3 A	0 ± 0 B	0.04
HWT+TCH	0 ± 0	0.4 ± 0.4 b	4.1 ± 2.3 ab	0 ± 0	0 ± 0	0.2 ± 0.2	0 ± 0 b	0 ± 0	4.1 ± 3.2	0.14
LSD	0.3	0.02	0.02	0.4	0.4	0.4	0.05	0.4	0.3	

[a] HWT = Hot Water Treatment; TCH = *Trichoderma atroviride* SC1.

[b] Values expressed as the mean ± SE (Standard error of the mean).

[c] Least significant difference: means followed by the same letter do not differ significantly ($P < 0.05$). Capital letters are for comparison of means in the same row. Small letters are for comparison of means in the same column.

any of the nine cultivars, although a reduction trend was noted for some combinations. For example, the lowest BF incidences were recorded for 'Albariño' (27.7 ± 10.4%) and 'Brancellao' (27.0 ± 3.0%) after the HWT + TCH treatment, compared to the experimental controls (34.0 ± 5.9% for 'Albarino', 31.9 ± 5.8% for 'Brancellao'). However, none of these differences reached statistical significance. For BF severity, significant differences were observed in 'Mencía' (P = 0.02) and 'Treixadura' (P = 0.04). In 'Mencía', BF severity was less in the control (2.3 ± 0.6%) than from the HWT + TCH treatment (9.4 ± 3.0%). Similarly, in 'Treixadura', BF severity was less in the controls (6.2 ± 3.4%) than from the HWT (21.8 ± 5.3%).

For PD incidence, statistically significant differences were observed in several cultivars, including 'Branco Lexítimo' (P = 0.009), 'Brancellao' (P = 0.01), 'Loureira' (P = 0.04), and 'Torrontés' (P = 0.008). The HWT + TCH treatment completely suppressed PD in 'Albariño', 'Loureira', and 'Torrontés, and markedly reduced PD in 'Branco Lexítimo' (4.1 ± 4.2%), compared to the controls (30.5 ± 8.0%). In 'Brancellao', the HWT treatment was particularly effective, fully suppressing detection of the pathogen. For PD severity, significant reductions were recorded in 'Branco Lexítimo' and 'Brancellao' (P = 0.02 in both cases). In 'Branco Lexítimo', the HWT + TCH treatment resulted in the lowest severity (0.4 ± 0.4%) compared to the control (12.2 ± 5.3%). Similarly, in 'Brancellao', both TCH and HWTs led to less severity (0.5 ± 0.5% from TCH, 0 ± 0% from HWT) relative to the control (9.1 ± 4.2%). Statistically significant differences were observed between cultivars for particular treatments and pathogen (Table 1). For BF, HWT gave differences (P < 0.01) between cultivars. Incidence and severity of BF were high in 'Treixadura' compared to those in 'Loureira'. For PD, the TCH treatment showed dependence on the cultivar factor, with differences were detected between cultivars for incidence (P = 0.02) and severity (P = 0.04) (Table 1). 'Loureira' developed greatest incidence and severity, in contrast to these parameters in 'Treixadura'. In addition, intravarietal variations were observed after the HWT + TCH treatment, specifically for incidence of PD.

Experiment 1: Effects of treatments applied prior to grafting on grapevine viability

Effects of the experimental treatments on plant viability and vegetative growth were evaluated, based on the percentage of SP, SL, and RW in grafted grapevine plants following one growing season in the field (Table 2).

Sprouting varied between the cultivars for the control treatments, indicating that this parameter was strongly influenced by genotype (Table 2). The cultivars that showed the highest budburst values were 'Treixadura', 'Torrontés', 'Merenzao', 'Mencía', 'Brancellao', and 'Albariño', in comparison with 'Blanco Lexítimo', which showed lower values. This genotype-dependent behavior was also observed under the HWT, where differences between cultivars persisted. In particular, the 'Dona Branca' cultivar exhibited the lowest budburst after the application of this treatment.

Sprouting rates were generally high across all cultivars and treatments, ranging from 83.3% to 100%. In most cultivars, no statistically significant differences were detected among treatments (P > 0.05). However, in 'Branco Lexítimo', significant differences were observed (P = 0.03), with the control showing a lower sprouting percentage (83.3 ± 4.5%) compared to HWT (100%) and TCH (100%). In 'Loureira', the TCH treatment significantly reduced sprouting (93.3 ± 1.6%) compared to control and other treatments, which all achieved 100% (P = 0.01).

Shoot length proved to be a trait highly dependent on genotype, both in the control treatment and under each of the applied treatments (P < 0.05) (Table 2). In all cases, the 'Brancellao' produced the longest shoots, compared to the cultivars 'Loureira', 'Torrontés', and 'Treixadura', which produced shorter shoots. No differences (P > 0.05) were observed among treatments in any of the cultivars. Nevertheless, trends were noted: for example, in 'Brancellao', the longest shoots were observed after HWT + TCH (67.6 ± 5.3 cm), and less from the control (61.5 ± 6.0 cm). Similar trends favouring HWT + TCH were observed in 'Albariño' mean length = 43.6 ± 0.3 cm) and 'Mencía' (45.9 ± 5.0 cm).

Root weight was not a genotype-dependent trait (P > 0.5) (Table 2). For the treatments, statistically significant differences in RW were found in five cultivars: 'Albariño' (P = 0.03), 'Branco Lexítimo' (P < 0.01), 'Dona Branca' (P < 0.01), and 'Mencía'. The HWT gave the greatest RW, in 'Albariño' (60.2 ± 7.2 g), which was greater than from the control and most of the other treatments. In 'Branco Lexítimo', HWT + TCH gave the greatest RW (72.2 ± 8.3 g), which was greater than the control (50.4 ± 6.3 g). For 'Dona Branca', HWT increased RW to 91.3 ± 8.3 g compared to 67.0 ± 6.5 g from the control. Similarly, the TCH treatment gave the greatest RW in 'Mencía' (92.2 ± 7.8 g), which was greater than from the control and most of the other treatments.

Experiment 2: Incidence and severity of fungal grapevine trunk diseases when treatments were applied to grafted plants prior to planting in a commercial vineyard

Analysis of the plant material at the end of the experiment yielded fungal species associated with GTDs.

Table 2. Average percentage of sprouting (%), shoot length (cm), and root weight (g) of plants from nine grapevine varieties following the treatment of rooted plants with HWT, TCH, or HWT+TCH and cultivation in a commercial vineyard (Experiment 1).

Treatment	Albariño	BrancoLexítimo	Brancellao	DonaBranca	Loureira	Mencía	Merenzao	Torrontés	Treixadura	LSD
SP(%)[a]										
Control	100 A	83.3 ± 4.5 bB	96.6 ± 1.3 A	93.3 ± 2.7 AB	100 aA	100 A	100 A	96.6 ± 1.3 A	100 A	<0.001
HWT	100 A	100 aA	100 A	90.0 ± 2.8 B	100 aA	100 A	100 A	96.6 ± 1.3 AB	100 A	<0.001
TCH	96.6 ± 1.3	100 a	96.6 ± 1.3	96.6 ± 1.3	93.3 ± 1.6 b	96.6 ± 1.3	100	96.6 ± 1.3	100	0.76
HWT+TCH	99.5 ± 0.0	96.6 ± 1.3 ab	100	100	100 a	100	100	100	100	0.09
LSD[c]	0.44	0.03	0.73	0.49	0.01	0.46	0.50	0.66	0.5	
SL(cm)										
Control	28.9 ± 3.5 B	25.5 ± 3.3 B	61.5 ± 6.0 A	35.1 ± 3.0 B	24.3 ± 1.3 B	41.9 ± 4.2 AB	41.7 ± 5.8 AB	27.8 ± 1.3 B	35.2 ± 2.3 B	0.04
HWT	36.9 ± 4.3 AB	31.6 ± 4.2 AB	53.4 ± 4.0 A	29.0 ± 2.2 B	23.7 ± 1.6 B	39.9 ± 3.5 AB	39.1 ± 4.2 AB	28.7 ± 1.3 B	28.3 ± 1.5 B	0.01
TCH	26.8 ± 3.5 B	26.9 ± 4.0 B	57.8 ± 5.2 A	35.7 ± 2.8 AB	22.1 ± 0.8 B	40.2 ± 4.3 AB	40.0 ± 4.3 AB	30.1 ± 2.3 B	28.8 ± 2.0 B	0.04
HWT+TCH	43.6 ± 0.3 AB	34.2 ± 3.6 B	67.6 ± 5.3 A	28.5 ± 2.7 B	23.1 ± 0.8 B	45.9 ± 5.0 AB	41.6 ± 4.0 B	28.2 ± 2.5 B	31.2 ± 2.3 B	0.01
LSD	0.10	0.47	0.44	0.19	0.84	0.14	0.76	0.57	0.15	
RW(g)										
Control	48.0 ± 5.3 b	50.4 ± 6.3 b	86.8 ± 8.0	67.0 ± 6.5 b	70.2 ± 5.8	70.3 ± 6.7 c	62.3 ± 6.2	68.1 ± 7.0	81.2 ± 7.5	0.92
HWT	60.2 ± 7.2 a	49.8 ± 5.8 b	78.9 ± 7.3	91.3 ± 8.3 a	64.0 ± 6.7	83.8 ± 6.8 ab	73.0 ± 8.2	83.7 ± 7.7	73.7 ± 7.0	0.95
TCH	54.1 ± 7.2 ab	55.1 ± 6.8 ab	84.2 ± 7.3	71.1 ± 7.8 b	70.7 ± 6.7	92.2 ± 7.8 a	76.4 ± 7.7	72.2 ± 7.0	80.8 ± 7.7	0.96
HWT+TCH	54.0 ± 0.0 b	72.2 ± 8.3 a	87.5 ± 8.3	71.0 ± 7.2 b	65.4 ± 6.7	79.2 ± 7.3 bc	75.9 ± 7.7	77.6 ± 7.5	81.4 ± 8.0	0.99
LSD	0.03	<0.01	0.81	<0.01	0.61	<0.01	0.19	0.48	0.37	

[a] SP, Sprouting; SL, Shoot Lenght; RW, Root Weight; HWT, Hot Water Treatment; TCH, *Trichoderma atroviride* SC1.
[b] Values expressed as the mean ± SE (Standard error of the mean).
[c] Least significant difference: means followed by the same letter do not differ significantly ($P < 0.05$). Capital letters are for comparison of means in the same row. Small letters are for comparison of means in the same column.

As causes of BF, *D. torresensis*, *Dactylonectria pauciseptata*, and *Dactylonectria novozelandica* were identified. For PD, the isolated species included *Pa. chlamydospora*, *Pm. minimum*, and *C. luteo-olivacea*. These results are presented by disease category, grouping the fungi associated with each category.

In *Experiment 2*, application of HWT, TCH, and HWT + TCH to grafted grapevine plants prior to planting in a commercial vineyard gave variable effects on incidenc and severity of BF and PD across the nine grapevine cultivars (Table 3). For BF incidence and severity, differences among treatments were only observed in 'Branco Lexítimo' (P = 0.01 for incidence; P = 0.03 for severity), and in 'Torrontés' (P = 0.008 and P = 0.03). In 'Branco Lexítimo', HWT (5.5 ± 5.6%) and TCH (4.0 ± 11.3%) both reduced incidence compared with the the control (36.1 ± 9.8%). For BF severity in this cultivar, HWT reduced incidence (1.6 ± 1.7%) compared to the control (9.5 ± 3.3%). In 'Torrontés', none of the treatments significantly reduced DI or DS compared to the control.

Petri disease incidence was different in six of the grapevine cultivars, including 'Albariño' (P = 0.04), 'Branco Lexítimo' (P = 0.005), 'Dona Branca' (P = 0.002), 'Mencía' (P = 0.04), and 'Torrontés' (P = 0.01). In 'Albariño', 'Dona Branca', and 'Mencía', none of the treatments reduced DI compared to the control. In 'Branco Lexítimo', all three treatments reduced incidence from 30.5 ± 8.0% in the control to 2.7 ± 1.8% after HWT. Similarly, for 'Torrontés', HWT (7.5 ± 2.2%), TCH (5.8 ± 2.4%), and HWT + TCH (6.7 ± 3.1%) reduced DI relative to the control (43.0 ± 14.5%). For PD severity, significant treatment effects were observed in 'Albariño' (P = 0.04), 'Branco Lexítimo' (P = 0.005), 'Dona Branca' (P = 0.002), 'Mencía' (P = 0.04), and 'Torrontés' (P = 0.01). However, only in 'Torrontés', all three treatments reduced incidence from 17.0 ± 6.6% in the control to as little as no fungal infection from the TCH. Treatment.

When the effects of each treatment was compared among cultivars, PD exhibited a marked genotype-dependent response (Table 3). From the control treatment, large differences were observed among cultivars, with 'Torrontés' showing high incidence, while 'Dona Branca' displayed no symptoms. Application of HWT reduced disease incidence in some susceptible cultivars (e.g. 'Branco Lexítimo'), but was counterproductive in others, such as 'Albariño', where incidence increased. Similarly, disease severity responded variably: while 'Torrontés' had less severe disease after HWT, disease increased in 'Loureira'.

Experiment 2: Effects on grapevine viability of treatments applied to grafted plants prior to planting in a commercial vineyard

Effects of the experimental treatments on plant viability and growth performance were assessed by measuring the SP, SL, and RW of grafted plants after one growing season in the commercial vineyard (Table 4).

Statistically significant differences in SP were observed between genotypes in some cases, particularly under after the control and TCH treatments (Table 4). The cultivars 'Albariño', 'Loureira', 'Mencía', and 'Treixadura' maintained 100% survival under all conditions, while 'Branco Lexítimo' showed reduced survival after some of the treatments, indicating a specific varietal sensitivity. SP rates were generally high across all cultivars and treatments, ranging from 83.3% to 100%. No differences (P > 0.05) were detected among treatments within each cultivar. However, some trends were observed. In 'Branco Lexítimo', sprouting increased from 83.3 ± 4.5% in the control to 100% after HWT. Conversely, in 'Merenzao', there was a small sprouting reduction after HWT + TCH (83.3 ± 6.9%) compared to the control (100%), although this was not statistically significant.

There were a clear genotype-dependent responses in SL from the treatments (Table 4). 'Brancellao' consistently had the longest shoots, while 'Loureira' and 'Torrontés' had the shortest shoots. Response to the HWT + TCH treatment was variable depending on the cultivar: in 'Albariño', this treatment led increased shoot lengths, whereas for other cultivars (e.g. 'Treixadura' and 'Merenzao'), this effect was less pronounced. This variability reflected a strong interaction between genotype and the applied treatments.

Shoot length was affected by treatments in several of the cultivars (Table 4). In 'Albariño', plants receiving with HWT + TCH developed longer shoots (60.1 ± 4.5 cm) than those in the control group (28.9 ± 3.5 cm) (P < 0.01). In 'Branco Lexítimo', HWT alone resulted in the greatest shoot length (41.1 ± 4.9 cm), which was greater than from the control (25.5 ± 3.3 cm). In contrast, in 'Brancellao' and 'Mencía', the control plants (means, respectively, 61.5 ± 6.1 cm and 41.9 ± 4.1 cm) had longer shoots than those after HWT + TCH (48.8 ± 5.3 cm for 'Brancellao', and 33.5 ± 3.8 cm for 'Mencía') (P < 0.01), indicating a possible negative effect of the combined treatment in these cultivars.

For RW, there was no clear trend of exclusive genotype dependence, as responses varied between treatments within each cultivar (Table 4). Only HWT + TCH caused severe reduction in root weight in 'Albariño' (16.8 g), whereas in other cultivars, including 'Mencía' and 'Branco Lexítimo', effects were less severe or nil.

Table 3. Incidence and severity of Black Foot and Petri disease in grafted plants of nine grapevine cultivars following HWT, TCH, and HWT+TCH treatments prior to planting in a commercial vineyard (Experiment 2).

Treatment	Albariño	Branco Lexítimo	Brancellao	Dona Branca	Loureira	Mencía	Merenzao	Torrontés	Traixadura	LSD
BF incidence (%)[a]										
CONTROL	34.0[b] ± 5.9	36.1 ± 9.8 a	31.9 ± 5.9	38.3 ± 2.8	20.8 ± 12.1	20.1 ± 7.2	42.3 ± 11.6	43.7 ± 12.8 ab	25 ± 11.3	0.61
HWT	33.3 ± 8.3 AB	5.5 ± 5.6 bB	27 ± 7.1 AB	30.5 ± 9.0 AB	20.8 ± 12.1 AB	11.1 ± 5.1 B	26.3 ± 12.4 AB	56.9 ± 4.5 aA	34.7 ± 11.1 AB	0.01
TCH	20.1 ± 5.1	4.0 ± 11.3 b	21.5 ± 5.3	36.1 ± 9.6	19.4 ± 9.0	26.3 ± 12.2	28.5 ± 10.2	36.1 ± 13.8 ab	52.7 ± 8.5	0.50
HWT+TCH	30.5 ± 10.7	20.1 ± 9.6 ab	16.6 ± 5.7	30.5 ± 10.0	27 ± 7.6	27 ± 11.3	29.7 ± 8.5	25 ± 6.8 b	43.7 ± 4.2	0.63
LSD[c]	0.5	0.01	0.3	0.9	0.9	0.6	0.7	0.008	0.4	
BF severity (%)										
CONTROL	12.5 ± 7.6	9.5 ± 3.3 a	5.6 ± 1.0	8.4 ± 1.6	3.6 ± 2.4	2.3 ± 0.7	10.9 ± 3.1	12.6 ± 3.8 ab	6.2 ± 3.4	0.39
HWT	12.5 ± 4.3 AB	1.6 ± 1.7 bB	6.9 ± 3.4 AB	9.5 ± 3.4 AB	3.7 ± 2.0 AB	2.7 ± 1.4 B	4.1 ± 2.1 AB	17.7 ± 3.8 aA	15 ± 4.0 AB	<0.001
TCH	4.5 ± 1.8 BC	10.2 ± 3.6 aC	3.1 ± 0.9 C	9.5 ± 2.2 ABC	3.4 ± 1.6 C	4.5 ± 2.4 BC	5.2 ± 1.7 BC	5.8 ± 2.4 bABC	11.6 ± 3.1 A	0.04
HWT+TCH	12.5 ± 8.0	4.8 ± 2.2 ab	4.0 ± 1.3	6.3 ± 2.2	4.7 ± 2.1	6.9 ± 2.9	9.5 ± 2.8	4.8 ± 1.4 b	10.5 ± 2.2	0.59
LSD	0.7	0.03	0.5	0.8	0.6	0.3	0.1	0.03	0.3	
PETRI incidence (%)										
CONTROL	6.9 ± 4.5 bBCD	30.5 ± 8.0 aAB	27.7 ± 12.2 ABC	0 ± 0.0 cD	13.8 ± 9.0 BCD	8.3 ± 5.3 abBCD	4.1 ± 4.2 CD	43.0 ± 14.5 aA	12.5 ± 8.5 BCD	0.02
HWT	22.7 ± 5.4 aA	2.7 ± 1.8 bD	18.6 ± 6.6 AB	11.3 ± 3.0 abBCD	8.4 ± 2.2 BCD	7.9 ± 1.6 bCD	13.2 ± 3.6 ABC	7.5 ± 2.2 bCD	11.5 ± 2.9 BCD	0.01
TCH	10.3 ± 3.3 b	11.4 ± 2.0 b	13.1 ± 5.5	19.4 ± 4.4 a	9.3 ± 4.1	9.7 ± 2.0 ab	11.9 ± 3.1	5.8 ± 2.4 b	15 ± 3.1	0.63
HWT+TCH	10.6 ± 2.4 bBC	15.2 ± 4.5 bAB	8.6 ± 2.2 C	9.5 ± 2.5 bC	11.9 ± 4.2 BC	18.6 ± 4.0 aA	13.7 ± 3.5 B	6.7 ± 3.1 bC	15.4 ± 2.8 AB	0.01
LSD	0.04	0.005	0.3	0.002	0.8	0.04	0.2	0.01	0.2	
PETRI severity (%)										
CONTROL	1.2 ± 0.9 bB	12.2 ± 5.3 bAB	9.1 ± 4.2AB	0 ± 0.0 bB	8.8 ± 7.6 AB	2.1 ± 2.5 bB	0.4 ± 0.4 B	17 ± 6.6 aA	5.8 ± 4.2 AB	0.01
HWT	7.9 ± 3.7 aABC	15.4 ± 8.1 aAB	15.4 ± 3.8 AB	1.4 ± 1.0 bC	17.8 ± 7.3 A	3 ± 1.6 bC	4.1 ± 2.4 BC	0.4 ± 0.2 bC	1.5 ± 1.0 C	0.01
TCH	3.4 ± 1.6 b	11.5 ± 3.8 b	9 ± 4.4	9.5 ± 3.6 a	2 ± 1.2	2.8 ± 1.6 b	2.5 ± 1.3	0 ± 0.0 b	0 ± 0.0	0.06
HWT+TCH	3.5 ± 1.7 a	8.8 ± 3.8 b	8.1 ± 5.1	5.9 ± 4.0 ab	3.8 ± 1.7	10.5 ± 2.8 a	5.6 ± 3.1	2.9 ± 1.9 b	7.6 ± 3.0	0.83
LSD	0.04	0.005	0.3	0.002	0.8	0.04	0.2	0.01	0.2	

[a] HWT = Hot Water Treatment; TCH = *Trichoderma atroviride* SC1.

[b] Values expressed as the mean ± SE (Standard error of the mean).

[c] Least significant difference: means followed by the same letter do not differ significantly ($P < 0.05$). Capital letters are for comparison of means in the same row. Small letters are for comparison of means in the same column.

Table 4. Average percentage of sprouting (%), shoot length (cm), and root weight (g) of plants from nine grapevine varieties following the treatment of rooted plants with HWT, TCH, or HWT+TCH and cultivation in a commercial vineyard (Experiment 2).

Treatment	Albariño	BrancoLexítimo	Brancellao	DonaBranca	Loureira	Mencía	Merenzao	Torrontés	Traixadura	LSD
SP (%)[a]										
CONTROL	100[b] A	83.3 ± 4.5 B	96.66 ± 1.3 A	93.33 ± 2.7 AB	100 A	100 A	100 A	96.6 ± 1.3 A	100 A	0.01
HWT	100	100	100	100	100	100	100	100	100	1
TCH	100 A	86.6 ± 4.0 B	100 A	90.0 ± 1.8 AB	100 A	100 A	100 A	100 A	96.6 ± 1.3 AB	0.03
HWT+TCH	100	96.6 ± 1.3	100	100	100	100	83.3 ± 6.9	100	100	0.54
LSD[c]	0.52	0.06	0.43	0.06	0.35	0.75	0.43	0.14	0.43	
SL (cm)										
CONTROL	28.9 ± 3.5 bB	25.5 ± 3.3 bB	61.5 ± 6.1 aA	35.1 ± 3.0 B	24.3 ± 1.3 B	41.9 ± 4.1 aAB	41.7 ± 5.3 AB	27.8 ± 1.3 B	35.2 ± 2.3 B	0.01
HWT	37.6 ± 4.5 bAB	41.1 ± 4.9 aAB	56.9 ± 5.3 abA	39.2 ± 4.5 AB	28.7 ± 2.3 AB	42.4 ± 4.5 aAB	39.6 ± 5.3 AB	21.3 ± 2.3 B	29.0 ± 1.5 AB	<0.001
TCH	37.9 ± 4.5 bAB	31.4 ± 3.7 abAB	54.8 ± 5.3 abA	28.9 ± 2.5 B	28.1 ± 2.3 B	40.6 ± 3.8 abAB	39.1 ± 4.5 AB	28.2 ± 1.8 B	31.6 ± 2.0 AB	<0.001
HWT+TCH	60.1 ± 4.5 aA	29.1 ± 4.1 abAB	48.8 ± 5.3 bAB	31.4 ± 9.0 AB	22.7 ± 2.3 B	33.5 ± 3.8 bAB	28.2 ± 4.9 AB	26.9 ± 2.2 B	28.4 ± 2.3 AB	0.02
LSD	<0.01	<0.01	<0.01	0.14	0.06	<0.01	0.14	0.12	0.26	
RW (g)										
CONTROL	48.0 ± 5.3 b	55.4 ± 6.5 a	86.8 ± 8.2	67.0 ± 6.5	70.2 ± 5.7	70.3 ± 6.5	62.3 ± 6.1	68.0 ± 6.9 a	81.2 ± 7.5 a	0.77
HWT	67.5 ± 7.3 a	61.8 ± 6.9 a	85.8 ± 7.3	71.7 ± 6.5	65.3 ± 5.7	72.9 ± 6.9	62.0 ± 6.5	49.4 ± 7.3 b	60.4 ± 7.0 b	0.93
TCH	61.3 ± 6.9 a	36.3 ± 4.9 b	79.2 ± 7.3	69.2 ± 6.9	67.8 ± 6.5	81.9 ± 6.5	68.6 ± 7.8	74.0 ± 6.9 a	68.0 ± 7.7 b	0.74
HWT+TCH	16.8 ± 7.3 cB	55.3 ± 5.7 aAB	74.6 ± 7.3 A	67.8 ± 7.3 AB	64.5 ± 7.3 AB	73.9 ± 7.3 AB	67.5 ± 6.5 AB	72.6 ± 7.3 aAB	59.3 ± 8.0 bAB	0.01
LSD	<0.01	<0.01	0.56	0.91	0.15	0.09	0.96	<0.01	<0.01	

[a] SP: Sprouting; SL: Shoot Lenght; RW: Root Weight; HWT = Hot Water Treatment; TCH = *Trichoderma atroviride* SC1.
[b] Values expressed as the mean ± SE (Standard error of the mean).
[c] Least significant difference: means followed by the same letter do not differ significantly ($P < 0.05$). Capital letters are for comparison of means in the same row. Small letters are for comparison of means in the same column.

Root weight responses to the treatments varied across cultivars. In 'Albariño', Treatments of HWT and TCH increased RW compared to the control (48.0 ± 5.3 g), with the greatest RW after HWT (67.5 ± 7.3 g; $P < 0.01$). In contrast, treatments resulted in reductions in RWs ($P < 0.01$) in 'Branco Lexítimo', 'Torrontés', and 'Treixadura' compared to the control, indicating potentially detrimental effects of these treatments on root development in these cultivars.

DISCUSSION

This study evaluated the potential effectiveness of different treatments (HWT, TCH, and their combination, HWT + TCH for controlling GTDs, specifically black foot (BF) and Petri disease (PD), and their influence on plant viability and early development for nine Galician grapevine cultivars. Results obtained indicated variable responses to the treatments, depending on cultivar, particular pathogen, and timing of applications.

The treatments were more effective against PD than BF. In Experiment 1 (pre-grafting host stage), the combination of HWT + TCH reduced PD incidence and severity in several cultivars, including complete suppression in 'Albariño', 'Loureira', and 'Torrontés'. Reductions in severity were also observed in 'Branco Lexítimo' and 'Brancellao' following the combined or individual treatments. These results are consistent with previous research showing that the early application of HWT and/or biocontrol agents can effectively suppress internal wood-colonizing pathogens such as *Pa. chlamydospora* and *Pm. minimum* during pre-planting hydration and stratification phases (Gramaje *et al*., 2009; Pertot *et al*., 2016; Berbegal *et al*., 2020). This reinforces the concept of combining physical and biological control strategies can enhance disease suppression, as previously reported by Fourie and Halleen (2006), Halleen and Fourie (2016), and Martínez-Diz *et al*. (2021). While HWT physically reduces inoculum loads by eliminating fungal propagules (Gramaje *et al*., 2009; Pertot *et al*., 2016; Lade *et al*., 2022), TCH provides long-term protection through competitive colonization, induction of host defenses, and antifungal metabolite production (Pertot *et al*., 2016; Leal *et al*., 2024).

In contrast, the treatments had limited efficacy against BF in both experiments, with differences observed only in specific cultivars such as 'Branco Lexítimo' and 'Torrontés' in Experiment 2 (post-rooting stage). These results align with the known biology of BF pathogens, which primarily infect host plants through root systems, and may not be fully reached by treatments applied prior to or shortly after grafting (Fourie and Halleen, 2006; Leal *et al*., 2023). This indicates that post-planting interventions may also be necessary to more effectively target BF pathogens during the early grapevine establishment in the field, when the risks of soilborne infections are is greatest (Mártinez-Diz *et al*., 2021; Labarga *et al*., 2025). Similar limited efficacy of TCH against BF pathogens was reported by Berbegal *et al*. (2020), who observed that although TCH reduced incidence and severity of PD and Botryosphaeria dieback in nursery and vineyard conditions, the reduction in BF was not statistically significant despite decreased pathogen recovery from treated plants.

For plant development, treatment effects were most evident on root weights (RW), with differences observed among cultivars. In Experiment 1, treatments, particularly HWT or HWT + TCH, gave increased RW in 'Albariño', 'Branco Lexítimo', 'Dona Branca', and 'Mencía'. This indicates potential stimulatory effects of these treatments on root development, when applied early. However, in Experiment 2, the same treatments led to reductions in RW in several cultivars, including 'Branco Lexítimo', 'Torrontés', and 'Treixadura'. These contrasting results indicate that treatment timing is likely to play a crucial role in determining plant responses, and late application may exert stress on developing root systems, particularly in sensitive cultivars. Shoot length (SL) responses also varied with timing and cultivar. While in Experiment 1 SL remained largely unaffected by the treatments, in Experiment 2, differences emerged. For example, 'Albariño' showed increased SL after HWT + TCH, but 'Brancellao', 'Mencía', and 'Treixadura' had short shoots following HWT + TCH treatment. These result indicate that combined treatments applied at advanced plant developmental stages can adversely affect vegetative growth in some genotypes, likely due to additive stress effects (Waite and May, 2005; Waite and Morton, 2007). Sprouting percentages (SP) were generally unaffected by treatments in both experiments, although minor cultivar-specific variations were noted. This is consistent with previous results showing that HWT, when adequately managed, does not impair grapevine bud viability (Waite and Morton, 2007; Gramaje *et al*., 2014; Soltekin and Altindisli, 2017).

The differential cultivar responses highlight the importance of considering genotype-specific tolerance and physiological traits. For example, 'Branco Lexítimo' benefitted from all treatments, in terms of PD suppression and root biomass in Experiment 1, but had showed reduced growth parameters under the same treatment in Experiment 2. Conversely, 'Albariño' was less affected by treatment stress overall, and had increased vegetative

vigour in some cases. These results are similar to those of previous studies, indicating that grapevine varietal differences influence tolerance to HWT, and colonization success by biological agents (Waite and May, 2005; Mutawila *et al*., 2011; Eichmeier *et al*., 2018; Işçi *et al*., 2019). These differences may be due to variations among cultivars in tissue tolerance, metabolic recovery, and hydration status. Waite and Morton (2007), Gramaje *et al*. (2009), Gramaje and Armengol (2012), and Soltekin and Altindisli (2017) emphasized that effects of HWT on rooting and sprouting can vary according to the rootstock–scion combination and the timing of HWT application. The reduced root biomass observed in some cultivars following HWT + TCH, particularly in Experiment 2, could reflect additive stress effects when thermally treated plants are subsequently exposed to microbial colonization during later metabolically demanding growth phases. These results underline the importance of optimizing timing and combinations of treatments to avoid unintended negative impacts on plant vigour in sensitive genotypes.

Use of TCH showed promise as a biostimulant for some cultivars, increasing RW and SL, particularly when applied early. This indicates potential biostimulatory effects in the cultivars consistent with previous results demonstrating that *Trichoderma* spp. can promote plant growth through endophytic colonization, production of phytohormones such as indole-3-acetic acid (IAA), and improved nutrient uptake (Mutawila *et al*., 2011; Leal *et al*., 2021; Leal *et al*., 2024). However, in other cases, especially following HWT in Experiment 2, TCH had neutral or even negative effects. These results support previous observations that efficacy of *Trichoderma*-based products is context-dependent, influenced by plant physiological status, environmental conditions, and timing of applications (Leal *et al*., 2021; Lade *et al*., 2022).

While HWT + TCH can offer an effective strategy for managing PD, especially during early grapevine propagation phases, its application must be tailored to each cultivar and propagation stage, to avoid unintended impacts on plant vigour. For BF, post-rooting interventions may be more appropriate, though additional complementary strategies may be needed to enhance disease control. From a practical standpoint, integrating physical and biological treatments into nursery practices requires genotype-informed protocols. Early application of HWT + TCH may be recommended for cultivars with high susceptibility to PD and greater resilience to stress, while alternative approaches may be preferable for more sensitive genotypes, or for managing BF pathogens. These results reinforce the value of flexible and adaptive nursery management, as well as the need for continued research on cultivar-specific physiological responses to integrated disease management strategies.

ACKNOWLEDGEMENTS

This research was funded within the framework of demonstration and information activities for the Galician agricultural sector from 2021 to 2023 (References TT-2021-083 and TT-2022-100), and co-financed by the European Agricultural Fund for Rural Development (EAFRD) through the Rural Development Program (RDP) of Galicia. Ester Abarquero acknowledges financial support of her predoctoral contract (Ref. INIA-2020-0012), granted by the Agencia Estatal de Investigación (AEI) within the State Training Subprogram of the State Program for the Development, Attraction, and Retention of Talent, under the framework of the 2017-2020 State Plan for Scientific, Technical, and Innovation Research.

LITERATURE CITED

Agustí-Brisach C., Armengol J., 2013. Black-foot disease of grapevine: an update on taxonomy, epidemiology and management strategies. *Phytopathologia Mediterranea* 52(2): 245–261. https://doi.org/10.14601/Phytopathol_Mediterr-12662

Berbegal M., Ramón-Albalat A., León M., Armengol J., 2020. Evaluation of long-term protection from nursery to vineyard provided by *Trichoderma atroviride* SC1 against fungal grapevine trunk pathogens. *Pest Management Science* 76: 967–977. https://doi.org/10.1002/ps.5605

Berlanas C., Ojeda S., López-Manzanares B., Andrés-Sodupe M., Bujanda R., Gramaje D., 2020. Occurrence and diversity of black-foot disease fungi in symptomless grapevine nursery stock in Spain. *Plant Disease* 104: 94-104 https://doi.org/10.1094/PDIS-03-19-0484-RE

Bertsch C., Ramírez-Suero M., Magnin-Robert M., Larignon P., Chong J., Abou-Mansour E., Fontaine F., 2013. Grapevine trunk diseases: complex and still poorly understood: Grapevine trunk diseases. *Plant Pathology* 62: 243–265. https://doi.org/10.1111/j.1365-3059.2012.02674.x

Crous P. W., Gams W., Stalpers J. A., Robert V., Stegehuis G. 2004. MycoBank: an online initiative to launch mycology into the 21st century. *Studies in Mycology* 50(1): 19-22. https://doi.org/10.4236/aim.2015.52014

Eichmeier A., Pečenka J., Peňázová E., Baránek M., Català-García S., Gramaje D., 2018. High-throughput

amplicon sequencing-based analysis of active fungal communities inhabiting grapevine after hot-water treatments reveals unexpectedly high fungal diversity. *Fungal Ecology* 36: 26–38. https://doi.org/10.1016/j.funeco.2018.07.011

Fourie P. H., Halleen F., 2004. Proactive control of Petri disease of grapevine through treatment of propagation material. *Plant Disease* 88(11): 1241–1245. https://doi.org/10.1094/PDIS.2004.88.11.1241

Fourie P. H., Halleen F. 2006. Chemical and biological protection of grapevine propagation material from trunk disease pathogens. *European Journal of Plant Pathology* 116: 255–265. https://doi.org/10.1007/s10658-006-9057-9

Glass N. L., Donaldson G. C. 1995. Development of primer sets designed for use with the PCR to amplify conserved genes from filamentous ascomycetes. *Applied and Environmental Microbiology* 61(4): 1323–1330. https://doi.org/10.1128/aem.61.4.1323-1330.1995

Gramaje D., Armengol J., 2011. Fungal trunk pathogens in the grapevine propagation process: Potential inoculum sources, detection, identification, and management strategies. *Plant Disease* 95: 1040–1055. https://doi.org/10.1094/PDIS-01-11-0025

Gramaje D., Armengol J., 2012. Effects of hot-water treatment, post-hot-water-treatment cooling and cold storage on the viability of dormant grafted grapevines under field conditions. *Australian Journal of Grape and Wine Research* 18: 158–163. https://doi.org/10.1111/j.1755-0238.2012.00185.x

Gramaje D., Di Marco S., 2015. Identifying practices likely to have impacts on grapevine trunk disease infections: a European nursery survey. *Phytopathologia Mediterranea* 54(2): 313–324. https://doi.org/10.14601/Phytopathol_Mediterr-16317

Gramaje D., Armengol J., Salazar D., López-Cortés I., García-Jiménez J., 2009. Effect of hot-water treatments above 50°C on grapevine viability and survival of *Petri* disease pathogens. *Crop Protection* 28(3): 280–285. https://doi.org/10.1016/j.cropro.2008.11.002

Gramaje D., Mañas F., Lerma M. L., Muñoz R. M., García-Jiménez J., Armengol J. 2014. Effect of hot-water treatment on grapevine viability, yield components and composition of must. *Australian Journal of Grape and Wine Research* 20(1): 144–148. https://doi.org/10.1111/ajgw.12052

Gramaje D., Úrbez-Torres J. R., Sosnowski M. R.. 2018. Managing grapevine trunk diseases with respect to etiology and epidemiology: current strategies and future prospects. *Plant Disease* 102: 12–39. https://doi.org/10.1094/PDIS-04-17-0512-FE

Halleen F., Fourie P.H., 2016. An integrated strategy for the proactive management of grapevine trunk disease pathogen infections in grapevine nurseries. S*outh African Journal of Enology and Viticulture* 37(2): 104–114. https://doi.org/10.21548/37-2-825

Işçi B., Kacar E., Altindisli A., 2019. Relationship between hot water treatment (HWT) and vitality criteria on dormant cuttings of *Vitis Vinifera* cultivars and rootstocks. *Erwebs-Obstbau* 61: 61–66. https://doi.org/10.1007/s10341-019-00453-1

Labarga D., Mairata A., Puelles M., Tronchoni J., Eichmeier A., Pou. A, 2025. Vineyard mycobiota shows a local and long-term response to the organic mulches application. *Agriculture, Ecosystems and Environment* 382: 109506. https://doi.org/10.1016/j.agee.2025.109506

Lade S. B., Štraus D., Oliva J., 2022. Variation in Fungal Community in Grapevine (*Vitis vinifera*) Nursery Stock Depends on Nursery, Cultivar, and Rootstock. *Journal of Fungi* 8(1): 47. https://doi.org/10.3390/jof8010047

Leal C., Richet N., Guise J.-F., Gramaje D., Armengol J., Trotel-Aziz P., 2021. Cultivar contributes to the beneficial effects of *Bacillus subtilis* PTA-271 and *Trichoderma atroviride* SC1 to protect grapevine against *Neofusicoccum parvum*. *Frontiers in Microbiology* 12: 726132. https://doi.org/10.3389/fmicb.2021.726132

Leal C., Gramaje D., Fontaine F., Richet N., Trotel-Aziz P., Armengol J., 2023. Evaluation of *Bacillus subtilis* PTA-271 and *Trichoderma atroviride* SC1 to control *Botryosphaeria* dieback and black-foot pathogens in grapevine propagation material. *Pest Management Science* 79(5): 1674–1683. https://doi.org/10.1002/ps.7339

Leal L., Eichmeier A., Stuskova K., Armengol J., Bujanda R., Gramaje D., 2024. Establishment of biocontrol agents and their impact on rhizosphere microbiome and induced grapevine defenses are highly soil-dependent. *Phytobiomes Journal* 8: 111–127. https://doi.org/10.1094/PBIOMES-08-23-0077-R

Legein M., Smets W., Vandenheuvel D., Eilers T., Muyshondt B., Prinsen E., Lebeer S., 2020. Modes of action of microbial biocontrol in the phyllosphere. *Frontiers in Microbiology* 11: 1619. https://doi.org/10.3389/fmicb.2020.01619

Martínez-Diz M. P., Díaz-Losada E., Díaz-Fernández Á., Bouzas-Cid Y., Gramaje D., 2021. Protection of grapevine pruning wounds against *Phaeomoniella chlamydospora* and *Diplodia seriata* by commercial biological and chemical methods. *Crop Protection* 143: 105465. https://doi.org/10.1016/j.cropro.2020.105465

Mugnai L., Graniti A., Surico G., 1999. Esca (Black Measles) and brown wood-streaking: Two old and elusive diseases of grapevines. *Plant Disease* 83: 404–418. https://doi.org/10.1094/PDIS.1999.83.5.404

Mutawila C., Fourie P. H., Halleen F., Mostert L., 2011. Grapevine cultivar variation to pruning wound protection by *Trichoderma* species against trunk pathogens. *Phytopathologia Mediterranea 50*: S264–S276. https://doi.org/10.14601/Phytopathol_Mediterr-8981

O'Donnell K., Cigelnik E., 1997. Two divergent intragenomic rDNA ITS2 types within a monophyletic lineage of the fungusfusariumare nonorthologous. *Molecular phylogenetics and evolution* 7(1): 103–116. https://doi.org/10.1006/mpev.1996.0376

Pertot I., Prodorutti D., Colombini A., Pasini L., 2016. *Trichoderma atroviride* SC1 prevents *Phaemoniella chlamydospora* and *Phaeoacremonium aleophilum* infection of grapevine plants during the grafting process in nurseries. *BioControl* 61: 257–267. https://doi.org/10.1007/s10526-016-9723-6

Savazzini F., Longa C. M. O., Pertot I., Gessler C., 2008. Real-time PCR for detection and quantification of the biocontrol agent *Trichoderma atroviride* strain SC1 in soil. *Journal of Microbiological Methods* 73(2): 185–194. https://doi.org/10.1016/j.mimet.2008.02.004

Soltekin O., Altindisli A., 2017. Effects of hot water treatments on dormant grapevine propagation materials used for grafter vine production. *BIO Web of Conferences* 9: 01003.

Thambugala K. M., Daranagama D. A., Phillips A. J. L., Kannangara S. D., Promputtha I., 2020. Fungi vs. Fungi in Biocontrol: An overview of fungal antagonists applied against fungal plant pathogens. *Frontiers in Microbiology* 10. https://doi.org/10.3389/fcimb.2020.604923

Travadon R., Lawrence D. P., Rooney-Latham S., Gubler W. D., Wilcox W. F., Baumgartner K. 2015. *Cadophora* species associated with wood-decay of grapevine in North America. *Fungal Biology* 119(1): 53–66. https://doi.org/10.1016/j.funbio.2014.11.002

Úrbez-Torres J. R., 2011. The status of Botryosphaeriaceae species infecting grapevines. *Phytopathologia Mediterranea* 50: S5–S45. https://doi.org/10.14601/Phytopathol_Mediterr-9316

Waite H., May P., 2005. The effects of hot water treatment, hydration and order of nursery operations on cuttings of *Vitis vinifera* cultivars. *Phytopathologia Mediterranea* 44(2): 144–152. https://doi.org/10.14601/Phytopathol_Mediterr-1791

Waite H., Morton L., 2007. Hot water treatment, trunk diseases and other critical factors in the production of high-quality grapevine planting material. *Phytopathologia Mediterranea* 46: 5–17. https://doi.org/10.3390/jof8050485

Phytopathologia Mediterranea
The international journal of the
Mediterranean Phytopathological Union

Firenze University Press
www.fupress.com/pm

Research Papers

Validation of a duplex TaqMan real-time PCR for detection of *Colletotrichum coccodes* and *Rhizoctonia solani* AG-3 on potato tubers

Martina SANNA, Vladimiro GUARNACCIA*, Davide SPADARO, Monica MEZZALAMA

Department of Agricultural, Forestry and Food Sciences (DISAFA), University of Torino, Largo Paolo Braccini 2, 10095, Grugliasco, Italy
Interdepartmental Center for Innovation in the Agri-Environmental Field – AGROINNOVA, University of Turin, Largo Paolo Braccini 2, 10095, Grugliasco, Italy
*Corresponding author. E-mail: vladimiro.guarnaccia@unito.it

Summary. The potato pathogens *Colletotrichum coccodes*, (causing black dot), and *Rhizoctonia solani* anastomosis group 3 (AG-3) (causing black scurf and stem canker) are economically important, and are common in potato production regions, including Northern Italy. A duplex TaqMan quantitative real-time PCR, based on two previously validated singleplex methods, was tested for identification of these species in potato propagation material. This validation was carried out according to EPPO PM 7/98 standard guidelines. The limit of detection (LOD) for the method, assessed using serial dilutions of targets DNA, was 10 fg. Specificity was assessed by testing ten *C. coccodes* and four *R. solani* AG-3 isolates, and 19 non-target species including other *Colletotrichum* and *Rhizoctonia* spp. and potato pathogens, respecting inclusivity and exclusivity criteria. Selectivity of the test showed no influence of DNA obtained from potato tubers. Repeatability and reproducibility of the duplex qPCR were also validated. The assay was able to detect and distinguish, within a single run, the two fungi allowing early detection in potato tubers.

Keywords. Quantitative PCR, diagnostics, black dot, black scurf, stem canker, *Solanum tuberosum* L.

OPEN ACCESS

Citation: Sanna, M., Guarnaccia, V., Spadaro, D., & Mezzalama, M. (2025). Validation of a duplex TaqMan real-time PCR for detection of *Colletotrichum coccodes* and *Rhizoctonia solani* AG-3 on potato tubers. *Phytopathologia Mediterranea* 64(3): 527-536. DOI: 10.36253/phyto-16094

Accepted: August 28, 2025

Published: November 3, 2025

Data Availability Statement: All relevant data are within the paper and its Supporting Information files.

Competing Interests: The Author(s) declare(s) no conflict of interest.

Editor: Epaminondas Paplomatas, Agricultural University of Athens, Greece.

ORCID:
MS: 0000-0002-4917-7654
VG: 0000-0003-3188-7743
DS: 0000-0001-5207-9345
MM: 0000-0003-2558-8878

INTRODUCTION

Potatoes (*Solanum tuberosum* L.) are one of the most consumed human food crops, with rice and wheat. Asia produces most potatoes, followed by Europe, where five countries are among the ten greatest producers (FAO, 2022; Europatat, 2023). Italy is the fifth largest producer in Europe with approx. 33,000 ha grown, and total production of 10 million tons in 2024 (Çalışkan *et al.*, 2023; ISTAT, 2024).

Potato crops can be affected by several diseases caused by air- or soil-borne pathogens, which can cause severe damage on all parts of potato plants, especially tubers which are economically important plant organ (Fiers *et al.*,

2012). *Colletotrichum coccodes* and *Rhizoctonia solani*, among the most important pathogens of potato, occur commonly in potato-producing regions, and cause, respectively, black dot and black scurf/stem canker.

Colletotrichum coccodes has a wide host range, affecting several horticultural species of *Cucurbitaceae*, *Fabaceae* and *Solanaceae*. Tuber blemish, stem and root lesions are the main symptoms caused by this pathogen (Tsor, 2004; Aqeel *et al*., 2008; Fiers *et al*., 2012). The first record of this fungus in Italy was reported by Buonaurio *et al.* (2002), after detection of black dot symptoms on potato tubers, with incidence ranging from 50 to 100%. *Rhizoctonia solani* causes potato symptoms of tuber blemish and stem lesions (Woodhall *et al*., 2008; Fiers *et al*., 2012), and losses related to *R. solani* in potato crops range from 10 to 30% (Banville *et al*., 1996). Hyphae of *Rhizoctonia* spp. can anastomose with isolates of other anastomosis groups (AGs), and previous studies have shown that *R. solani* AG-3 is the predominant anastomosis group affecting potato crops (Anderson, 1982; Banville *et al*., 1996). Both *C. coccodes* and *R. solani* colonize the surfaces of potato tubers, and can also infect potato plant vascular systems in roots and stems (Stevenson *et al*., 2001; Lehtonen *et al*., 2008; Fiers *et al*., 2012).

Northern Italy is an intensive potato cultivation area, and these pathogens are important causes of potato yield decline. Surveys carried out in specialized potato farms have confirmed *C. coccodes* and *R. solani* as endemic pathogens in this region (Manici and Caputo, 2009; Manici *et al*., 2016). Early detection of these pathogens, in the field and in seed potato material, is important for reducing pathogen spread, and to assist disease management and reduce yield losses.

Detection of *C. coccodes* and *R. solani* was originally based on isolation methods, use of selective media, and morphological characterization, but these methods are not providing quantification of pathogen incidence. These methods are also time-consuming, and are biased by the operator competence (Lees and Hilton, 2003). Polymerase chain reactions (PCRs) are molecular methods widely used for disease diagnoses and identification of several potato pathogens, including *Helminthosporium solani* (Cullen *et al*., 2001), *Alternaria solani* (Niu *et al*., 2022), and *Fusarium coeruleum* (Heltoft *et al*., 2016), and they can be used to assess asymptomatic plant samples.

Several diagnostic methods were developed for specific individual detection of *C. coccodes* and *R. solani*. Specific primer pairs for *C. coccodes* detection were designed for conventional PCR by Cullen *et al.* (2002), and two TaqMan qPCR protocols were developed targeting the ribosomal internal transcribed spacer (ITS) region (Cullen *et al*., 2002) and the glycerol-3-phosphate dehydrogenase (*gapdh*) gene (Ryazantsev *et al*., 2023), to detect *C. coccodes* in potato tubers and soil. The method described by Ryazantsev *et al.* (2023) was developed considering the high variability of this fungus, that can lead to false negatives if a single DNA sequence is used for detection. However, analyses performed in other laboratories using the primers and the probe used by Cullen *et al.* (2002) gave good accuracy for detecting *C. coccodes* (Belov *et al*., 2018). A conventional PCR protocol, specific for *R. solani* AG-3 detection, was validated by Lees *et al.* (2002), while specific quantitative real-time PCR, using SYBR Green and TaqMan chemistries, were developed based on the ribosomal internal transcribed spacer (ITS) by Lees *et al.* (2002), Woodhall *et al.* (2013), and Salamone and Okubara (2020).

Simultaneous presence of multiple pathogens on potatoes is challenging for farmers, and time-consuming for laboratories testing for potato pathogens. Given the challenges in distinguishing and accurately identifying symptoms and the pathogens responsible, development of multiplex qPCR assays could speed up analyses, allowing rapid monitoring and detection of pathogens in the field, and assisting disease management in the field and certification of the propagation material that could be sources of pathogen inoculum. To date, no duplex qPCR protocols have been developed for detection of *C. coccodes* and *R. solani* AG-3 detection.

The aim of the present study was to test and validate a method for detecting and quantifying these two pathogens on potato tubers.

MATERIALS AND METHODS

Fungus isolates

During 2022 and 2023, monitoring activities were carried out on potato crops (cv. 'Monique'), both on seed potatoes and on field-grown plants. For the propagation material, 100 tubers were examined each year. Field monitoring was conducted during the cropping cycle in both years, in two sites located in the province of Alessandria, Piedmont (Northwest Italy), at coordinates 44.9328, 8.9369 and 44.9358, 8.9351, respectively. In addition, observations were extended to the storage phase. Symptomatic tubers and plant portions, collected during the monitoring activities, were surface disinfected with 1% sodium hypochlorite water solution for 1 min, rinsed in sterile deionized water, dried, then cut into small sections (0.2–0.3 cm long) which were placed into Petri dishes containing potato dextrose agar (PDA; Merck) amended with 25 mg L^{-1} of streptomycin sulphate. These plates were then incubated in a cli-

mate chamber at 25±1°C for 72 h, after which resulting colonies were transferred and grown on PDA plates, and were then purified to obtain single conidium or monohyphal cultures.

Selected isolates of *C. coccodes* (eight) and *R. solani* (three) were morphologically and molecularly characterized (as described below), and used in the validation process. One reference isolate (*R. solani* AG-3 MUCL 51930) for comparisons was provided by the *Mycothèque de l'Université Catholique de Louvain* (BCCM/MUCL). Two *C. coccodes* isolates, and 16 isolates of species phylogenetically related to the target species and potato pathogens were provided by the Università di Torino (Agroinnova collection), and isolates of *C. destructivum complex* (CBS 136232) and *C. lentis* (CBS 127604) were provided by the Westerdijk Fungal Biodiversity Institute. Isolates used in this study are reported in Table 1. Monoconidial cultures of the isolates obtained in the present study were stored in tubes of PDA at 4°C.

DNA extraction and molecular identification of Colletotrichum coccodes *and* Rhizoctonia solani *AG-3 isolates*

Eight isolates morphologically identified as *C. coccodes*, and three isolates of *R. solani* were grown on PDA for 7 d at 25±1°C, and 100 mg of mycelium was gently scraped from respective colony surfaces for DNA extraction, using the Omega E.Z.N.A. Fungal DNA Mini Kit (Omega Bio-Tek), following the manufacturer's instruc-

Table 1. Fungal species used in this study for the validation of a TaqMan duplex qPCR assay.

Species	Strain ID	Host	Source	Origin
Colletotrichum coccodes	P178	*Solanum tuberosum*	Tuber	Italy
C. coccodes	P180	*Solanum tuberosum*	Tuber	Italy
C. coccodes	P181	*Solanum tuberosum*	Tuber	Italy
C. coccodes	TS1	*Solanum tuberosum*	Tuber	Italy
C. coccodes	TS2	*Solanum tuberosum*	Tuber	Italy
C. coccodes	TS3	*Solanum tuberosum*	Tuber	Italy
C. coccodes	TS5	*Solanum tuberosum*	Tuber	Italy
C. coccodes	TS11	*Solanum tuberosum*	Tuber	Italy
C. coccodes	T126	*Solanum lycopersicum*	Roots	Italy
C. coccodes	T125.1	*Solanum lycopersicum*	Roots	Italy
C. nigrum	CVG 171	*Salvia greggii*	Leaves	Italy
C. nigrum	CVG 173	*Salvia greggii*	Leaves	Italy
C. karsti	KUM6	*Citrus sinensis*	Fruit	Italy
C. fioriniae	CVG 268	*Origanum vulgare*	Leaves	Italy
C. fructicola	CVG 170	*Salvia greggii*	Leaves	Italy
C. ocimi	CVG 200	*Ocimum basilicum*	Leaves	Italy
C. americae-borealis	CBS 136232	*Medicago sativa*	Stems	United States of America
C. lentis	CBS 127604	*Lens culinaris*	Seeds	Canada
C. lineola	CVG 207	*Campanula trachelium*	Leaf	Italy
C. gloeosporioides	CVG 1940	*Citrus sinensis*	Fruit	Italy
Rhizoctonia solani AG-3	MUCL 51930	*Solanum tuberosum*	Plant tissue	Belgium
R. solani AG-3	P37	*Solanum tuberosum*	Tuber	Italy
R. solani AG-3	P38	*Solanum tuberosum*	Tuber	Italy
R. solani AG-3	P257	*Solanum tuberosum*	Tuber	Italy
R. solani AG-2	St 11.6	*Fragaria ananassa*	Roots	Italy
R. solani	RS 230	*Fragaria ananassa*	Roots	Italy
R. solani	RS 232	*Fragaria ananassa*	Roots	Italy
R. solani	RS 256	*Fragaria ananassa*	Roots	Italy
R. solani	C22	*Allium cepa*	Roots	Italy
Fusarium oxysporum	P149	*Solanum tuberosum*	Tuber	Italy
F. oxysporum	P153	*Solanum tuberosum*	Tuber	Italy
Alternaria alternata	P150	*Solanum tuberosum*	Tuber	Italy
A. alternata	P154	*Solanum tuberosum*	Tuber	Italy

tions. Quality and the concentration of the DNA were checked with a Nanodrop 2000 Spectrophotometer (Thermo Fisher Scientific). Isolates of *Colletotrichum* spp. were identified through amplification of the partial glyceraldehyde-3-phosphate dehydrogenase gene (*gapdh*), using GDF1 and GDR1 primers (Guerber *et al.* 2003), and the primers ITS1 and ITS4 (White *et al.* 1990) were used to amplify the internal transcribed spacer regions (ITS) for the *Colletotrichum* spp. and *R. solani* isolates.

For both fungi, PCRs were performed with a Taq DNA polymerase kit (Qiagen), following amplification mixtures and relative cycling conditions described by Damm *et al.* (2012). Amplicons generated were checked by electrophoresis on 1% agarose (VWR), and both strands of the PCR products were sequenced by Eurofins Genomics Service. The generated sequences were analysed and assembled using the program Geneious v. 11.1.5 (Auckland, New Zealand).

Specific primers and duplex qPCR optimization

Specific primers and probes for *C. coccodes* and *R. solani* AG-3 used in this study, both designed on ITS regions, were described, respectively, by Cullen *et al.* (2002) and Lees *et al.* (2002) (Table 2). For each target, qPCR assay optimization and validation were carried out in previous studies (Cullen *et al.* 2002; Lees *et al.* 2002), and were then verified in the present study following the EPPO PM 7/98 guidelines (EPPO, 2021).

Optimum conditions for the duplex amplification of the two target species were evaluated by applying a thermal gradient from 56 to 62°C to assess the optimum annealing temperature, and using different concentrations of primers and probes (from 0.1 to 0.3 μM).

Duplex qPCR assays were carried out with the StepOnePlus qPCR system (Applied Biosystems), using 2× TaqMan Universal Master Mix (Applied Biosystems). Each reaction was carried out in 10 μL total volume, using 2 μL of DNA (10 ng), extracted as described above, and each plate was loaded with standard DNA, a positive control (target pathogen DNA), and a negative control (nuclease-free water), in triplicate. Data collected by the assay instrument were analysed, and presence and quantities of target DNA were assumed by interpolating Ct values from the standard curves generated.

Validation of the duplex qPCR for Colletotrichum coccodes *and* Rhizoctonia solani *AG-3*

The analytical sensitivity, specificity, selectivity, repeatability, and reproducibility of the duplex qPCR assay were assessed, according to the EPPO PM 7/98 standard (EPPO, 2021).

Analytical sensitivity of the reaction was assessed using ten-fold serial dilutions (from 1 ng to 1 fg) obtained from genomic DNA of the targets. The analysis was performed in triplicate, and target DNA was quantified in the samples using the regression line. Analytical sensitivity was assessed both for fungal DNA and inoculated potatoes.

Target and non-target DNA were used to validate analytical specificity of the method. All samples were first analysed with singleplex qPCR, during the verification of the protocols, then the same samples were used in duplex assays to assess any differences in results from the two methods. Ten isolates of *C. coccodes* (eight from potato tubers and plants in this study, and two from *Solanum lycopersicum*), four isolates of *R. solani* AG-3 (three isolated from potato tubers in the present study, and one provided by the *Mycothèque de l'Université Catholique de Louvain* (BCCM/MUCL)), as well as 19 non-target species (Table 2), were used. The non-target isolates included different *Colletotrichum* and *Rhizoctonia* spp. and other potato pathogens.

Selectivity of the assay was evaluated to establish the influence of the host DNA. Healthy potato DNA was added to DNA from *C. coccodes* and *R. solani* AG-3, each at a concentration of 1 ng μL^{-1}. Repeatability was assessed

Table 2. Primer pairs and probes used in this study for the detection of *Colletotrichum coccodes* and *Rhizoctonia solani* AG-3 with the TaqMan quantitative PCR assay.

Primer pairs and probes	Sequence (5'-3')	Target DNA	Reference
CcTqF1	TCTATAACCCTTTGTGAACATACCTAACTG		
CcTqR1	CACTCAGAAGAAACGTCGTTAAAATAGAG	ITS1	Cullen et al. (2002)
CcTqP1	[VIC]-CGCAGGCGGCA CCCCCT-[TAMRA]		
RsTqF1	AAGAGTTTGGTTGTAGCTGGTCTATTT		
RsTqR1	AATTCCCCAACTGTCTCACAAGTT	ITS1	Lees et al. (2002)
RQP1	[FAM]-TTTAGGCATGTGCACACCTCCCTCTTTC-[TAMRA]		

by running three independent duplex qPCRs in the same laboratory on different days, while the reproducibility was evaluated by performing the assay by different operators on different days, in the same laboratory.

Validation of duplex qPCR in artificially inoculated potato samples (cv. 'Monique')

The *C. coccodes* (P178) and *R. solani* AG-3 (MUCL 51930) isolates were grown on PDA plates at 25±1°C for 7 d. Seven potato tubers (cv. 'Monique') were surface disinfected with 5% sodium hypochlorite solution for 5 min, then rinsed twice with sterile deionized water, air dried, and then tested with the assay to confirm absence of pathogens. Five tubers were each inoculated with 5 mm diam. mycelium plugs of both pathogens, taken from 7-d-old PDA cultures, and sealed with parafilm, while two tubers were used as negative controls (one inoculated with the non-target pathogens *C. gloeosporioides* and *R. solani* AG-2, and one inoculated with water). These tubers were then incubated at 25°C for 15 d. The mycelium plugs were removed, and symptomatic portions of the tubers were cut and disinfected to proceed with molecular analyses. The tissues from the inoculated and negative controls were ground with liquid nitrogen, and DNA was extracted with the E.Z.N.A. Plant DNA kit (VWR), following the manufacturer's instructions. Each sample was analysed with duplex qPCR assay in triplicate, and quantities (pg μL^{-1}) of detected *C. coccodes* and *R. solani* AG-3 DNA were determined.

Data analyses

StepOne software automatically generated threshold cycle (Ct) values, baseline range, and real-time PCR standard curves. Data were statistically analysed by variance analysis ANOVA, using Tukey's test ($P \leq 0.05$), with the Statistical Package for Social Science, Version 29.0 (SPSS; IBM, Chicago, Illinois, United States of America).

RESULTS

Isolation and molecular identification of the isolates

During monitoring activities, eight *Colletotrichum* spp. and three *R. solani* isolates obtained from symptomatic potato plants and tubers of cv. 'Monique' were morphologically and molecularly analysed. For molecular identification, all DNA sequences obtained were aligned with reference sequences deposited in the NCBI database, showing similarity percentages from 99% to 100% for all the isolates tested. *Colletotrichum* isolates were all identified as *C. coccodes*, while the three *R. solani* isolates were identified as within the anastomosis group 3. All the isolates were used for the duplex qPCR protocol validation.

Specific primers and duplex qPCR optimization

The specificity of the two sets of primers and probes was verified following EPPO PM 7/98 guidelines (EPPO, 2021).

Optimum conditions for duplex qPCR amplification with 2× TaqMan Universal Master Mix (Applied Biosystems) were: 0.3 μM for CcTqF1/CcTqR1, 0.1 μM CcTqP1, and 0.2 μM for RsTqF1/RsTqR1 and RsP1, and annealing temperature of 60°C for 1 min. Duplex reactions were each carried out in a final volume of 10 μL, using the following thermal protocol: 50°C for 2 min, 95°C for 10 min, followed by 40 cycles at 95°C for 15 sec, and 60°C for 1 min.

Duplex qPCR validation

Analytical sensitivity, analytical specificity, selectivity repeatability, and reproducibility of the duplex qPCR protocol were evaluated according to EPPO PM7/98 standard (EPPO, 2021).

Seven serial dilutions, ranging from 1 ng to 1 fg, of the two target DNA were tested to assess the analytical sensitivity of the assay, showing a LOD of 10 fg, for both pathogens. Average values obtained performing the analysis in triplicate were included in the regression line, obtained with the determination coefficient (R^2) values of 0.9977 for *C. coccodes* and of 0.999 for *R. solani* AG-3, and then used to quantify targets DNA in samples tested (Figure 1). The average reaction efficiencies, calculated from the slopes of the regression lines obtained, were of 93% for *C. coccodes* and 90% for *R. solani* AG-3.

In duplex real-time PCR, seven ten-fold serial dilutions of samples containing 1 ng μL^{-1} of both target DNAs, were spiked with healthy potato DNA. Selectivity of the method was validated showing no influence of the host DNA in the duplex qPCR assay, and this showed reliable reaction efficiencies and correlations between the quantities of target DNA and the Ct values detected by the instrument, both when target pathogen DNA was spiked or not with potato DNA (Figure 2).

The duplex assay showed analytical specificity of 100% when tested with a panel of fungal isolates that considered inclusivity and exclusivity criteria, detecting

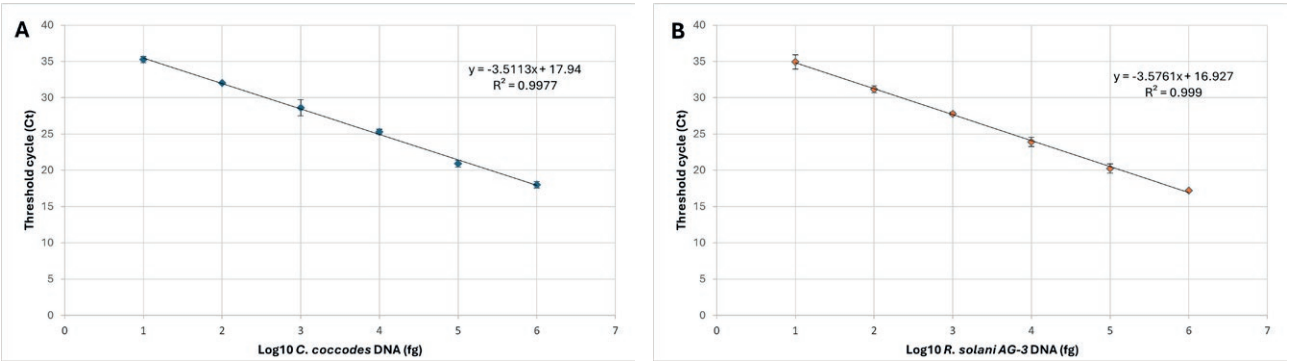

Figure 1. Standard curves obtained in duplex qPCR, running 1:10 serial dilutions (from 1 ng to 10 fg) of DNA of *Colletotrichum coccodes* (A) and *Rhizoctonia solani* AG-3 (B). The coefficients of determination (R2) are indicated, and the standard deviation bars are shown for each mean value in the graphs. Each point of the regression lines was run in triplicate.

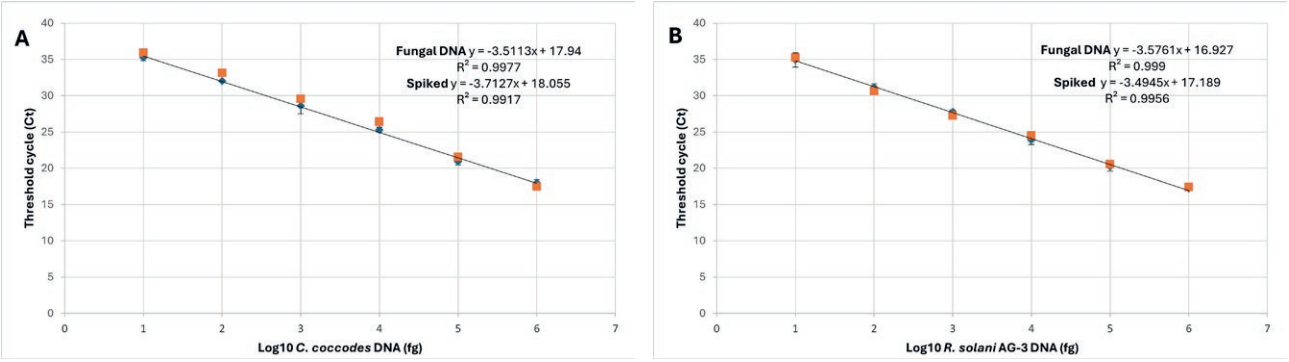

Figure 2. Standard curves obtained in duplex qPCR, running 1:10 serial dilutions (from 1 ng to 10 fg) of DNA of *Colletotrichum coccodes* (A) and *Rhizoctonia solani* AG-3 (B), both spiked with potato tuber DNA. The coefficients of determination (R^2) are indicated, and the standard deviation bars are shown for each mean value in the graphs. Each point of the regression lines was run in triplicate.

amplifications only in DNA samples from target species. The specificity of the assays was compared with the singleplex tests, showing non-significant differences among the Ct values detected (Table 3).

Repeatability and reproducibility of the method were assessed by producing reliable amplifications among biological and technical replications, with no statistically significant differences ($P > 0.05$), when analysed under unchanged or modified test conditions, as described in the EPPO standard PM 7/98.

Validation of duplex qPCR in artificially inoculated potato samples (cv. 'Monique')

Analyses carried out on artificially inoculated potato tubers cv. 'Monique' showed the efficacy of the validated method for detecting and distinguishing true positive and true negative samples. The duplex qPCR assay gave positive amplifications, with Ct values ranging from 21.3 to 33, only for DNA samples extracted from artificially inoculated potato tubers, while no amplifications were observed for negative controls (Table 4).

DISCUSSION

Molecular tools are commonly used for detection of plant pathogens, allowing rapid, accurate and specific identification and quantification of target species affecting crops, even in early stages of plant growth in propagation material and, when more than one species occurs in the same sample, controlling the spread of plant pathogens and the diseases they cause (McCartney *et al.*, 2003; Capote *et al.*, 2012; Hariharan and Prasannath, 2021). In the present study, a sensitive and specific duplex TaqMan qPCR assay was tested and validated for detection and quantification of *C. coccodes* and *R. solani* AG-3 in potato samples.

Currently, two TaqMan qPCR assays based on amplification of the ITS1 region of rDNA, developed by,

Table 3. Fungus isolates used in this study to check specificity of the duplex qPCR assay for detection of *Colletotrichum coccodes* and *Rhizoctonia solani AG-3*, and *Ct* values acquired in singleplex and duplex reactions. Standard deviations are included for each Ct.

Species	Strain ID	Host	Source	Origin	Singleplex *C. coccodes* (Ct)	Singleplex *R. solani* AG-3 (Ct)	Duplex Real-time PCR (Ct)
Colletotrichum coccodes	P178	*Solanum tuberosum*	Tuber	Italy	15.72±0.65	Not detected	15.12±0.11
C. coccodes	P180	*Solanum tuberosum*	Tuber	Italy	15.16±0.08	Not detected	15.27±0.14
C. coccodes	P181	*Solanum tuberosum*	Tuber	Italy	16.15±0.51	Not detected	16.65±0.31
C. coccodes	TS1	*Solanum tuberosum*	Tuber	Italy	18.92±0.27	Not detected	18.51±0.24
C. coccodes	TS2	*Solanum tuberosum*	Tuber	Italy	16.39±0.34	Not detected	16.33±0.46
C. coccodes	TS3	*Solanum tuberosum*	Tuber	Italy	18.73±0.61	Not detected	18.66±0.79
C. coccodes	TS5	*Solanum tuberosum*	Tuber	Italy	15.51±0.24	Not detected	15.82±0.02
C. coccodes	TS11	*Solanum tuberosum*	Tuber	Italy	18.58±0.36	Not detected	18.62±0.23
C. coccodes	T126	*Solanum lycopersicum*	Roots	Italy	17.32±0.22	Not detected	17.26±0.16
C. coccodes	T125.1	*Solanum lycopersicum*	Roots	Italy	16.20±0.34	Not detected	16.32±0.01
C. nigrum	CVG 171	*Salvia greggii*	Leaves	Italy	Not detected	Not detected	Not detected
C. nigrum	CVG 173	*Salvia greggii*	Leaves	Italy	Not detected	Not detected	Not detected
C. kartsi	KUM6	*Citrus sinensis*	Fruit	Italy	Not detected	Not detected	Not detected
C. fioriniae	CVG 268	*Origanum vulgare*	Leaves	Italy	Not detected	Not detected	Not detected
C. fructicola	CVG 170	*Salvia greggii*	Leaves	Italy	Not detected	Not detected	Not detected
C. ocimi	CVG 200	*Ocimum basilicum*	Leaves	Italy	Not detected	Not detected	Not detected
C. americae-borealis	CBS 136232	*Medicago sativa*	Stems	USA	Not detected	Not detected	Not detected
C. lentis	CBS 127604	*Lens culinaris*	Seeds	Canada	Not detected	Not detected	Not detected
C. lineola	CVG 207	*Campanula trachelium*	Leaf	Italy	Not detected	Not detected	Not detected
C. gloeosporioides	CVG 1940	*Citrus sinsensis*	Fruit	Italy	Not detected	Not detected	Not detected
Rhizoctonia solani AG-3	MUCL 51930	*Solanum tuberosum*	Plant tissue	Belgium	Not detected	19.22±0.41	20.40±0.04
R. solani AG-3	P37	*Solanum tuberosum*	Tuber	Italy	Not detected	19.90±0.63	20.53±0.12
R. solani AG-3	P38	*Solanum tuberosum*	Tuber	Italy	Not detected	19.92±0.15	20.36±0.12
R. solani AG-3	P257	*Solanum tuberosum*	Tuber	Italy	Not detected	19.58±0.88	20.22±0.04
R. solani AG-2	St 11.6	*Fragaria ananassa*		Italy	Not detected	Not detected	Not detected
R. solani	RS 230	*Fragaria ananassa*	Roots	Italy	Not detected	Not detected	Not detected
R. solani	RS 232	*Fragaria ananassa*	Roots	Italy	Not detected	Not detected	Not detected
R. solani	RS 256	*Fragaria ananassa*	Rootss	Italy	Not detected	Not detected	Not detected
R. solani	C22	*Allium cepa*	Roots	Italy	Not detected	Not detected	Not detected
Fusarium oxysporum	P149	*Solanum tuberosum*	Tuber	Italy	Not detected	Not detected	Not detected
F. oxysporum	P153	*Solanum tuberosum*	Tuber	Italy	Not detected	Not detected	Not detected
Alternaria alternata	P150	*Solanum tuberosum*	Tuber	Italy	Not detected	Not detected	Not detected
A. alternata	P154	*Solanum tuberosum*	Tuber	Italy	Not detected	Not detected	Not detected

respectively, Cullen *et al.* (2002) and Lees *et al.* (2002), are used for the detection of *C. coccodes* and *R. solani* AG-3, also gave reliable results in testing the isolates obtained in the present study. A specific duplex TaqMan qPCR was tested and validated, based on the above methods, to detect both pathogens using a a single run.

Other singleplex assays have been designed and validated for *C. coccodes* and *R. solani* AG-3, giving similar detection sensitivity. A TaqMan Real-Time PCR was developed for *C. coccodes* detection by the amplification of the *gapdh* genomic locus, to reduce false negatives results, due to the high variability of this fungus (Ryazantsev *et al.*, 2023). However, all the isolates used in the present showed positive amplifications with both, the assay developed by Cullen *et al.* (2002), and the duplex qPCR assay validated in the present study, as observed for isolates tested with Cullen *et al.* (2002) protocol in other studies (Belov *et al.*, 2018). The assay was also able to distinguish *C. coccodes* from *C. nigrum*, a closely related species which has been reported as an important pathogen of solanaceous hosts (Liu *et al.*, 2013). A specific qPCR protocol was also validated for *R. solani* AG-3 by Salamone and Okubara (2020), with the primers designed on a portion of the ITS1 region for the forward primer, and on a conserved portion of the 5.8S rRNA gene for the reverse primer. This allowed identification

Table 4. Mean numbers of cells µL-1 of *Colletotrichum coccodes* and pg DNA µL-1 of *Rhizoctonia solani* AG-3 detected in five artificially inoculated tuber samples. Two tubers inoculated with non-target *Colletotrichum* and *Rhizoctonia* species (*C. gloeosporioides* and *R. solani* AG-2) and with sterile deionized water were used as negative controls.

Sample ID	Ct mean ± SD *C. coccodes*	Concentration of *C. coccodes* (pg DNA µL^{-1})	Ct mean ± SD R. solani AG-3	Concentration of R. solani AG-3 (pg DNA µL^{-1})
PAT_IN_1	23.12±0.24	32.80±0.07	22.10±0.30	35.90±0.08
PAT_IN_2	24.03±0.02	18.00±0.01	23.21±0.06	17.50±0.02
PAT_IN_3	29.00±0.19	0.69±0.05	29.95±0.15	0.23±0.04
PAT_IN_4	21.30±0.38	108.00±0.11	17.90±0.14	536.00±0.04
PAT_IN_5	22.97±0.08	36.10±0.02	29.90±0.10	0.24±0.03
PAT_IN_NCF	Not detected	Not detected	Not detected	Not detected
PAT_IN_NC_water	Not detected	Not detected	Not detected	Not detected

of Pacific Northwest (United States of America) isolates, which were not detectable by Lees *et al.* (2002). The strains revealed as undetectable by the Lees *et al.* (2002) assay were all isolated in Washington State. However, no issues were observed in detecting strains from other origins, indicating the high specificity of the validated assay. In the present study, all analysed isolates were successfully detected and quantified using the validated assay.

Specificity of the duplex qPCR assay was assessed testing ten *C. coccodes* and four *R. solani* AG-3 DNA samples extracted from pure cultures of these fungi, including target isolates from hosts other than potato and coming from other countries, showing positive amplifications for all the tested isolates. No false positive results were observed when phylogenetically related strains or other *Colletotrichum* and *Rhizoctonia* species were analyzed. Low differences were observed in Ct values among the tested isolates.

The LOD of the method was approx. 10 fg for both *C. coccodes* and *R. solani* AG-3 detection, yielding reliable and reproducible results comparable to those obtained in simplex qPCR assays (LOD 10 fg) as reported by Cullen *et al.* (2002) and Lees *et al.* (2002).Furthermore, this method was more sensitive for detecting the target species than the method reported by Ryazantsev *et al.* (2023) with a LOD of 500 fg, while comparable analytical sensitivity results were obtained by Salamone and Okubara, (2020) for *R. solani* AG-3 detection (LOD 10 fg). The results obtained in the present study are similar to those obtained by other TaqMan qPCR methods (Prencipe *et al.*, 2020; Ortega *et al.* 2020) and duplex qPCR assays used for other fungi such as *Botryosphaeriaceae* (*Neofusicoccum parvum* and *Botryosphaeria dothidea*) causing canker diseases in woody crops (Romero-Cuadrado, *et al.*, 2023); *Caliciopsis pinea* and *Fusarium circinatum* in pine samples (Luchi *et al.*, 2018), and for the biocontrol agents *Trichoderma asperellum* and *Trichoderma gamsii* (Gerin *et al.*, 2018).

Colletotrichum coccodes and *R. solani* AG-3 DNA were detected and quantified in the presence of DNA of healthy potato tubers, showing no effects on the sensitivity of the assay, and allowing detection and quantification of both pathogens in artificially inoculated samples, discriminating true negative and true positive samples. The results showed no influence on selectivity of the assay for both pathogens, with concentrations ranging from 1.99×10^3 cells µL^{-1} to 12.8 cells µL^{-1} for *C. coccodes,* and ranging from 0.23 pg DNA µL^{-1} to 536.00 pg DNA µL^{-1} for *R. solani* AG-3.

In conclusion, the assay developed and validated in the present study was able to simultaneously detect *C. coccodes* and *R. solani* AG-3 in infected potato samples. The assay could be used to speed up detection of both pathogens in symptomatic samples during potato cropping cycles, to assess seed tubers allowing quantification of the pathogens, and to promptly intervene in managing the disease in the field, as these pathogens can rapidly infect stems, stolons and roots of potato plants grown from infected propagation material (Lees and Hilton, 2003).

ACKNOWLEDGEMENTS

The Authors thank the National Operational Programme Research and Innovation 2014-2020 (CCI-2014IT16M2OP005), that co-financed the doctoral scholarship awarded to Martina Sanna, through FSE REACT-EU resources, under Action IV.5 'Doctorates on Green Topics', with the collaboration of SATA Srl.

LITERATURE CITED

Anderson N.A., 1982. The genetics and pathology of *Rhizoctonia solani*. *Annual Review of Phytopathol-*

ogy 20: 329–347. https://doi.org/10.1146/annurev.py.20.090182.001553

Aqeel A.M., Pasche J.S., Gudmestad, N.C., 2008. Variability in morphology and aggressiveness among North American vegetative compatibility groups of *Colletotrichum coccodes*. *Phytopathology* 98(8): 901–909. https://doi.org/10.1094/PHYTO-98-8-0901

Banville G.J., Carling D.E., Otrysko B.E., 1996. *Rhizoctonia* diseases on potato. In: *Rhizoctonia Species: Taxonomy, Molecular Biology, Ecology, Pathology and Disease Control* (B. Sneh, S. Jabaji-Hare, S. Neate, G. Dijst, ed.), Kluwer Academic Publishers, Dordrecht, Netherlands, 321–330.

Belov G.L., Belosokhov A.F., Kutuzova I.A., Statsyuk N.V., Chudinova E.M., … Elansky, S.N., 2018. *Colletotrichum coccodes* in potato and tomato leaves in Russia. *Journal of Plant Diseases and Protection* 125: 311–317. https://doi.org/10.1007/s41348-017-0138-0

Buonaurio R., Natalini G., Covarelli L., Cappelli C., 2002. Occurrence of black dot of potato caused by *Colletotrichum coccodes* in central Italy. *Plant Disease* 86(5): 562–562. https://doi.org/10.1094/PDIS.2002.86.5.562C

Çalışkan M.E., Yousaf M.F., Yavuz C., Zia M.A.B., Çalışkan S., 2023. History, production, current trends, and future prospects. In: *Potato production worldwide* (M. E. Çalişkan, A. Bakhsh, K. Jabran, ed.), Academic Press, 1–18. https://doi.org/10.1016/B978-0-12-822925-5.00016-5

Capote N., Pastrana A.M., Aguado A., Sánchez-Torres, P., 2012. Molecular tools for detection of plant pathogenic fungi and fungicide resistance. *Plant Pathology* 7: 151–202.

Cullen D.W., Lees A.K., Toth I.K., Duncan J.M., 2001. Conventional PCR and real-time quantitative PCR detection of *Helminthosporium solani* in soil and on potato tubers. *European Journal of Plant Pathology* 107(4): 387–398. https://doi.org/10.1023/A:1011247826231

Cullen D.W., Lees A.K., Toth I.K., Duncan J.M., 2002. Detection of *Colletotrichum coccodes* from soil and potato tubers by conventional and quantitative real-time PCR. *Plant Pathology* 51(3): 281–292. https://doi.org/10.1046/j.1365-3059.2002.00690.x

Damm U., Cannon P. F., Woudenberg J. H. C., Johnston P. R., Weir B. S., … Crous P.W. 2012. The *Colletotrichum boninense* species complex. *Studies in Mycology* 73(1): 1–36. https://doi.org/10.3114/sim0002

EPPO, 2021. PM 7/98 (5) Specific requirements for laboratories preparing accreditation for a plant pest diagnostic activity. *EPPO Bulletin* 51: 468–498.

Europatat, 2023. The EU potato sector in 2020: statistics on production & trade. European Potato Trade Association (Europatat). Accessed February 26, 2025, from https://europatat.eu/activities/the-eu-potato-sector/

FAO, 2022. Food and agriculture data, Food and Agriculture Organization of the United Nations. Accessed February 26, 2025, from https://www.fao.org/faostat/en/#home

Fiers M., Edel-Hermann V., Chatot C., Le Hingrat Y., Alabouvette C., Steinberg C., 2012. Potato soil-borne diseases. A review. *Agronomy for Sustainable Development* 32(1): 93–132. https://doi.org/10.1007/s13593-011-0035-z

Gerin D., Pollastro S., Raguseo C., De Miccolis Angelini R.M., Faretra F., 2018. A ready-to-use single- and duplex-TaqMan-qPCR assay to detect and quantify the biocontrol agents *Trichoderma asperellum* and *Trichoderma gamsii*. *Frontiers in Microbiology* 9: 2073. https://doi.org/10.3389/fmicb.2018.02073

Guerber J.C., Liu B., Correll J.C., Johnston P.R., 2003. Characterization of diversity in *Colletotrichum acutatum sensu lato* by sequence analysis of two gene introns, mtDNA and intron RFLPs, and mating compatibility. *Mycologia* 95(5): 872–895. https://doi.org/10.1080/15572536.2004.11833047

Hariharan G., Prasannath K., 2021. Recent advances in molecular diagnostics of fungal plant pathogens: a mini review. *Frontiers in Cellular and Infection Microbiology* 10: 600234. https://doi.org/10.3389/fcimb.2020.600234

Heltoft P., Brurberg M.B., Skogen M., Le V.H., Razzaghian J., Hermansen A., 2016. *Fusarium* spp. causing dry rot on potatoes in Norway and development of a real-time PCR method for detection of *Fusarium coeruleum*. *Potato Research* 59: 67–80. https://doi.org/10.1007/s11540-015-9313-5

ISTAT, 2024. Coltivazioni: Cereali, Legumi, Radici Bulbi e Tuberi. Accessed February 26, 2025, from http://dati.istat.it/Index.aspx?QueryId=33702

Lees A.K., Cullen D.W., Sullivan L., Nicolson M.J., 2002. Development of conventional and quantitative real-time PCR assays for the detection and identification of *Rhizoctonia solani* AG-3 in potato and soil. *Plant Pathology* 51(3): 293–302. https://doi.org/10.1046/j.1365-3059.2002.00712.x

Lees A.K., Hilton A.J., 2003. Black dot (*Colletotrichum coccodes*): an increasingly important disease of potato. *Plant Pathology* 52(1): 3–12. https://doi.org/10.1046/j.1365-3059.2003.00793.x

Lehtonen M.J., Somervuo P., Valkonen J.P.T., 2008. Infection with *Rhizoctonia solani* induces defense genes and systemic resistance in potato sprouts grown without light. *Phytopathology* 98: 1190–1198. https://doi.org/10.1094/PHYTO-98-11-1190

Liu F., Cai L., Crous P.W., Damm U., 2013. Circumscription of the anthracnose pathogens *Colletotrichum lindemuthianum* and *C. nigrum*. *Mycologia* 105: 844–860. https://doi.org/10.3852/12-315

Luchi N., Pepori A.L., Bartolini P., Ioos R., Santini, A., 2018. Duplex real-time PCR assay for the simultaneous detection of *Caliciopsis pinea* and *Fusarium circinatum* in pine samples. *Applied Microbiology and Biotechnology* 102: 7135–7146. https://doi.org/10.1007/s00253-018-9184-1

Manici L.M., Caputo F., 2009. Fungal community diversity and soil health in intensive potato cropping systems of the east Po valley, northern Italy. *Annals of Applied Biology* 155(2): 245–258. https://doi.org/10.1111/j.1744-7348.2009.00335.x

Manici L.M., Caputo F., Nicoletti F., 2016. Potato root infection by *Rhizoctonia solani* anastomosis group-3 and *Colletotrichum coccodes* under current and future spring weather in northern Italy. *The Journal of Agricultural Science* 154(8): 1413–1424. https://doi.org/10.1017/S0021859615001343

McCartney H.A., Foster S.J., Fraaije B.A., Ward, E., 2003. Molecular diagnostics for fungal plant pathogens. *Pest Management Science: formerly Pesticide Science* 59(2): 129–142.

Niu Z., Zheng L., Yang P., Wang J., Tian M., ... Zhu J., 2022. Detection of *Alternaria solani* with high accuracy and sensitivity during the latent period of potato early blight. *Frontiers in Microbiology* 13: 1016996. https://doi.org/10.3389/fmicb.2022.1016996

Ortega S.F., Siciliano I., Prencipe S., Gullino M.L., Spadaro D., 2020. Development of PCR, LAMP and qPCR Assays for the Detection of Aflatoxigenic Strains of *Aspergillus flavus* and *A. parasiticus* in Hazelnut. *Toxins* 12(12): 757. https://doi.org/10.3390/toxins12120757

Prencipe S., Sillo F., Garibaldi A., Gullino M.L., Spadaro D., 2020. Development of a sensitive TaqMan qPCR assay for detection and quantification of *Venturia inaequalis* in apple leaves and fruit and in air samples. *Plant Disease* 104(11): 2851–2859. https://doi.org/10.1094/PDIS-10-19-2160-RE

Romero-Cuadrado L., López-Herrera C.J., Aguado A., Capote N., 2023. Duplex real-time PCR assays for the simultaneous detection and quantification of *Botryosphaeriaceae* species causing canker diseases in woody crops. *Plants* 12(11): 2205. https://doi.org/10.3390/plants12112205

Ryazantsev D.Y., Chudinova E.M., Kokaeva L.Y., Elansky S.N., Balabko P. N., ... Zavriev S.K., 2023. Detection of *Colletotrichum coccodes* by Real-Time PCR. *Biology Bulletin Reviews* 13(1): S108-S113. https://doi.org/10.1134/S2079086423070101

Salamone A.L., Okubara P.A., 2020. Real-time PCR quantification of *Rhizoctonia solani* AG-3 from soil samples. *Journal of Microbiological Methods* 172: 105914. https://doi.org/10.1016/j.mimet.2020.105914

Stevenson W.R., Loria R., Franc G.D., Weingartner D.P., 2001. *Compendium of Potato Diseases*. 2nd ed. The American Phytopathological Society, St. Paul, MN, USA. 520 pp.

Tsror L., 2004. Effect of light duration on severity of black dot caused by *Colletotrichum coccodes* on potato. *Plant Pathology* 53: 288–293. https://doi.org/10.1111/j.0032-0862.2004.01011.x

White T.J., Bruns T., Lee S.J.W.T., Taylor J., 1990. Amplification and direct sequencing of fungal ribosomal RNA genes for phylogenetics. In: *PCR protocols: a Guide to methods and applications* (M.A. Innis, D.H. Gelfand, J.J. Sninsky, T.J. White ed.), Academic Press, New York, 315-322.

Woodhall J.W., Lees A.K., Edwards S.G., Jenkinson P., 2008. Infection of potato by *Rhizoctonia solani*: effect of anastomosis group. *Plant Pathology* 57(5): 897–905. https://doi.org/10.1111/j.1365-3059.2008.01889.x

Woodhall J.W., Adams I.P., Peters J.C., Harper G., Boonham N., 2013. A new quantitative real-time PCR assay for *Rhizoctonia solani* AG3-PT and the detection of AGs of *Rhizoctonia solani* associated with potato in soil and tuber samples in Great Britain. *European journal of plant pathology* 136: 273–280. https://doi.org/10.1007/s10658-012-0161-8

Phytopathologia Mediterranea
The international journal of the
Mediterranean Phytopathological Union

Firenze University Press
www.fupress.com/pm

Research Papers

Fungi associated with table grape propagation material, with emphasis on *Neoscytalidium dimidiatum* and *Quambalaria cyanescens* in Italy

Daniel MATTIA[1,†], Simone MAVICA[1,†], Chiara DI PIETRO[1], Styliana EFSTATHIOU[2], Georgios MAKRIS[2], Loukas I. KANETIS[2], Dalia AIELLO[1,*]

[1] *Department of Agriculture, Food and Environment, University of Catania, Via Santa Sofia 100, 95123 Catania, Italy*
[2] *Department of Agricultural Sciences, Biotechnology and Food Science, Cyprus University of Technology, Limassol 3036, Cyprus*
[†] These authors contributed equally to the research reported in this paper.
*Corresponding author. E-mail: dalia.aiello@unict.it

Summary. Italy is the leading producer and the main exporting country of table grapes in the European Union. However, table grape production is affected by Grapevine Trunk Diseases (GTDs) which cause serious economic losses to grape growers. Aetiology of GTDs is crucial for application of effective management strategies, particularly regarding the quality of the grapevine propagation material. During 2022-23, four nurseries in Eastern Sicily, Southern Italy, were surveyed, and high incidence of propagation material with GTDs symptoms was found. Over 100 fungal isolates were collected from 80 symptomatic cuttings of 'Italia' and 'Victoria' cultivars grafted on rootstock 140RU. Of these isolates, 82 were molecularly analysed, and were found to belong to 22 genera. Isolation results highlighted the presence of well-known GTDs-related pathogens, including species within the *Botryosphaeriaceae*, and *Phaeomoniella chlamydospora*, *Phaeoacremonium minimum,* and *Cylindrocarpon*-like species. Less common fungi, including *Neoscytalydium dimidiatum* and *Quambalaria cyanescens*, were also isolated and characterized by molecular, morphological and phylogenetic analyses, and Koch's postulates were fulfilled for these two species. This is the first study to associate *N. dimidiatum* and *Q. cyanescens* with table grape propagation material in Europe.

Keywords. Grapevine Trunk Diseases, nursery material, isolate characterization, pathogenicity.

OPEN ACCESS

Citation: Mattia, D., Mavica, S., Di Pietro, C., Efstathiou, S., Makris, G., Kanetis, L. I., & Aiello, D. (2025). Fungi associated with table grape propagation material, with emphasis on *Neoscytalidium dimidiatum* and *Quambalaria cyanescens* in Italy. *Phytopathologia Mediterranea* 64(3): 537-558. DOI: 10.36253/phyto-16099

Accepted: September 14, 2025

Published: November 3, 2025

Data Availability Statement: All relevant data are within the paper and its Supporting Information files.

Competing Interests: The Author(s) declare(s) no conflict of interest.

Editor: Josep Armengol Forti, Polytechnical University of Valencia, Spain.

ORCID:
DM: 0009-0006-4681-0860
SM: 0009-0008-0073-2478
CDP: 0009-0005-5746-8389
SE: 0009-0006-4596-1122
GM: 0000-0001-6688-293X
LIK: 0000-0002-1869-558X
DA: 0000-0002-6018-6850

INTRODUCTION

Table grape (*Vitis vinifera* L.) is an important and widely cultivated crop plant, showing positive production trends in the last 20 years. Italy is the leading producer and the main exporting country of table grapes in the European Union, with annual production of 925.472 t produced from 40.705 ha. Most (94.4%) of this production is from southern Apulia (610.555 t from 25.285 ha) and Sicily (262.846 t from 12.075 ha) (Istat 2025). Italy occupies a

prominent commercial position with a long production season from late May to December (> 7 months). 'Italia' and 'Victoria' are the main cultivars produced, (respective proportions of production of approx. 40% and 15%), followed by 'Red Globe', 'Black Magic', and an increasing number of seedless cultivars, including 'Sugraone', 'Crimson Seedless', and 'Regal Seedless' (Pisciotta *et al*., 2022). The major rootstocks for these cultivars are 140RU, 1103 Paulsen, and 775 P.

As a highly profitable crop, it is important to incorporate effective vine health practices throughout grape production to prolong longevity and productive lifespans of vineyards. Grapevine trunk diseases (GTDs) are a disease aggregate of fungal diseases that are the most destructive biotic factor of grapevines (Guerin-Dubrana *et al.,* 2019; Azevedo-Nogueira *et al.,* 2022). Multifaceted adverse effects due to GTDs include reduced plant longevity, cumulative yield losses, increased costs due to required disease management practices, and premature replanting of severely affected vineyards (Gramaje *et al*., 2018). According to their aetiology and symptomatology, GTDs can be grouped in different syndromes: Black Foot (BF), Eutypa, Botryosphaeria and Phomopsis dieback, and the Esca and Petri disease (PD) complexes.

The first report of BF of grapevines in Italy was by Grasso and di San Lio (1975), and Grasso (1984) associated this disease with death of young grapevines in Sicily. Carlucci *et al.,* (2017) studied BF occurrence on young grapevines and nursery material, reporting *Dactylonectria torresensis* to be the most prevalent pathogenic fungus associated with GTDs in Italy. Therefore, these diseases have caused problems in Italian grapevine production for many years, especially in young plants, originating from nurseries. However, since those publications, no further studies on GTDs in young grapevine plants in Italy have been reported.

Eutypa dieback was first reported on grapevines in Italy in 1983 (Bisiach and Minervini, 1985). Sexual structures of *Eutypa lata*, the most common pathogen associated with this disease, were reported by Cortesi and Milgroom (2001). This pathogen is widespread in all regions of Italy except Sicily, probably due to the low amount of rainfall on the island, which plays a key role in the dispersal of *E. lata* inoculum. Damage caused by this pathogen is limited (Guerin-Dubrana *et al*., 2019).

Phomopsis dieback, also known as cane blight and leaf spot, was first reported in Italy with the description of the teleomorph *Diaporthe silvestris* on grapevines by Saccardo and Berlese (1885). *Phomopsis viticola*, the *D. silvestris* anamorph (originally described as *P. cordifolia*), was first reported by Uecker and Johnson (1991). *Diaporthe eres* is one of the most detected species in Italy, isolated for the first time from 1-year-old canes of grapevines in Tuscany by Cinelli *et al*., (2016). Phomopsis cane and leaf spot have been reported from all Italian regions, but is widespread in Apulia, Veneto, and Piedmont (Guerin-Dubrana *et al*., 2019).

Botryosphaeria dieback has been a significant problem in Italian viticulture since the end of the 1970s, with the first tentative association of bark cankers, dieback, and leaf chlorosis on grapevines with *Botryosphaeriaceae* fungi by Cristinzio (1978). Many studies have since been reported, and to date 16 species in *Botryosphaeriaceae* have been reported in association with grapevines in Italy (Rovesti and Montermini, 1987; Burruano *et al.,* 2008; Carlucci *et al.,* 2009; Mondello *et al.,* 2013; Carlucci *et al.,* 2015b). Nowadays, the most common and abundantly isolated species is *Diplodia seriata,* although it appears that this fungus is among the least virulent of the dieback pathogens (Carlucci *et al.,* 2015b; Aiello *et al*., 2023).

Esca and the PD complex are probably as old as grapevine cultivation, but studies on their aetiology have intensified since the 1990s (Mugnai *et al.,* 1999). Lionel Petri was the first to fulfil Koch's postulates in 1912, demonstrating that *Cephalosporium* and *Acremonium* spp. were responsible for the vascular necroses in young vineyards and nurseries, in the Sicilian provinces of Palermo, Messina and Trapani (Petri, 1912). Since then, many studies have been carried out and the main associated species are *Phaeomoniella chlamydospora*, *Phaeoacremonium* spp., and *Fomitiporia mediterranea* (Bertelli *et al.,*1998; Mugnai *et al.,* 1999; Cortesi *et al.,* 2000; Tegli *et al.,* 2000; Ciccarone *et al.,* 2004; Essakhi *et al.,* 2008; Raimondo *et al.,* 2014; Carlucci *et al.,* 2015a; Carlucci *et al.,* 2017).

Although GTDs have been extensively studied on wine grape plants, the causal agents associated with GTDs on table grape plants remain less studied in Italy. Graniti (1960) already knew about Esca in Apulia, and reported a diseased young vineyard of cultivar 'Regina' at two years after grafting. During 1995, young plants of cultivar 'Italia' in the areas of Canicattì and Mazzarrone (eastern Sicily) exhibited Esca symptoms with incidences of 9% in Canicatti and 17% in Mazzarrone, while 42% of the affected plants died (Schiliro *et al*., 1996). Also in Sicily, Sidoti *et al.* (2000) reported symptoms of decline on young vines of cultivar 'Victoria', with high mortality in the first year after planting. During the same year in Apulia, Pollastro *et al.* (2000) reported severe infections of 18-year-old cultivar 'Italia' vines, with 84% incidence of diseased wood, and 17% incidence of esca symptoms on the leaves or bunches. Sparapano *et al.* (2000a; 2000b; 2001) reported *Fomitiporia punctata* as the pri-

mary pathogen causing white rot of wood, and 'Italia' as the most susceptible cultivar. Since then, increased GTD incidence and severity have been seen in different vineyards (Pichierri *et al*., 2009; Guerin-Dubrana *et al*., 2019). This is commonly attributed to factors including the expanded planted area, increased vineyard productivity, changes in cultural practices, following of market requirements, and the poor quality of table grape propagation material produced in nurseries (Surico *et al*., 2004; Pichierri *et al*., 2009).

Knowledge of disease aetiology and epidemiology is important for developing effective control strategies that aim to minimize the economic impact of fungal pathogens in young vines, especially originating from nursery material. Effective control of the diseases is important for the future of vineyards.

To date, the quality of propagation material destined for table grape production has been little studied in Italy. To document GTDs in Sicilian cuttings of table grapes, nurseries in Comiso and Mazzarrone were surveyed from May 2022 to September 2023. The objectives in the present study were to: (a) identify the causal agents associated with GTDs on propagation material coming from Sicilian nurseries, using molecular analyses; (b) calculate isolation frequencies of these pathogens, depending on isolation points; and (c) characterize the species associated for the first time with GTDs on table grape plants in Italy, using morphology and multi-locus phylogenetic analyses, and determine their pathogenicity.

MATERIALS AND METHODS

Field surveys, sampling, and fungus isolations

Surveys were conducted in 2022 and 2023 in four nurseries in Comiso (36°57′N, 14°36′E) and Mazzarrone (37°05′N, 14°34′E), located in the Ragusa and Catania provinces of eastern Sicily, Italy, respectively. A total of 80 5- to 7-month-old cuttings of 'Italia' and 'Victoria' cultivars grafted onto 140RU rootstock (ten samples for each cultivar from each nursery) were collected and brought to the Plant Pathology laboratory at the Department of Agriculture, Food and Environment, University of Catania, for isolation and further analyses. Fungal strains were isolated from symptomatic wood tissue from different parts of the cuttings, including: (a) the graft union, (b) 15 cm from the base, and (c) the base of the rootstock. From each part, a wood segment was excised, and then fragmented in five to six pieces (each 5 mm thick). These pieces were then surface-sterilized in a 1.5% sodium hypochlorite (NaClO) solution for 1 min, rinsed in sterile water, dried on sterilized absorbent paper, and then placed onto potato dextrose agar (PDA; Lickson) in Petri plates, that was amended with 100 mg L^{-1} of streptomycin sulphate (Sigma-Aldrich) to prevent bacterial growth. The plates were then incubated in the dark at 25 ± 1°C for 7 to 14 d until fungal colonies grew sufficiently to be examined. Representative colonies were then transferred onto fresh PDA plates, and subsequently, single hypha isolates were obtained from pure cultures. These isolates were then stored as mycelial plugs in sterile water in the collection of the Plant Pathology laboratory.

Isolation frequencies (%) were estimated for the main fungal morphotypes recovered from each isolation point on the symptomatic cuttings. Each value was calculated as the average obtained from the four nurseries investigated, and a single value from each nursery was calculated as the number of isolation positive tissue pieces (from which each morphotype was isolated) divided by the total number of analyzed tissue pieces (Šišić *et al*., 2018; Dastogeer *et al*., 2020).

DNA extractions and PCR

Eighty-two of the collected isolates were grown on Malt Extract Agar (MEA) plates incubated at room temperature (20°C) for 7–15 d. Mycelium from each isolate was then collected in a 1.5 mL sterile Eppendorf tube using a sterile scalpel blade. Genomic DNA was extracted from these samples using the Wizard® Genomic DNA Purification Kit (Promega Corporation), following the manufacturer's protocol. DNA amplification and sequencing of partial regions of various genetic loci were carried out for identification purposes. Specifically, the universal oligonucleotide primers ITS4 and ITS5 (White *et al*., 1990) were used to amplify the ITS1-5.8S-ITS2 region of the rDNA for each isolate (Supplementary Tables S1), while a partial region of the translation elongation factor 1-alpha (*tef1-a*) gene was also amplified for representative isolates of the collection (Supplementary Table S1). Furthermore, for ten *Quambalaria* isolates, fragments of the large subunit (LSU) of the rDNA were amplified using the primer sets NL1 and NL4 (Boekhout *et al*., 1995), and the second largest subunit of RNA polymerase II (*rpb2*) was amplified using the primer sets bRPB2-6F and bRPB2-7R (Matheny, 2005). Similarly, for five *Neoscytalidium* isolates, the *tef1-α* gene was amplified using the primer sets EF1-728F and EF1-986R (Carbone and Kohn, 1999), and the beta-tubulin (*β-tub*) gene was amplified using T1 and Bt-2b (Glass and Donaldson, 1995). All PCR reactions were each carried out in a final volume of 20 µL, containing: 1 µL of each primer (10 µM), 4 µL of the

appropriate buffer, 2 µL $MgCl_2$, 0.4 µL dNTPs, 0.2 µL Taq polymerase (5 U μL^{-1}; KAPA Taq 500 U), 10.4 µL sterile water, and 1 µL DNA template (5 µg µL). The amplifications were performed using the following programme: an initial denaturation at 94°C for 5 min; followed by 35 cycles each of denaturation at 94°C for 30 sec, primer annealing for 1 min at 52°C for ITS, 51°C for *rpb2,* 56°C for LSU, or 30 sec at 60°C for *tef1-a* and *β-tub*; extension at 72°C for 1 min; and a final extension at 72°C for 8 min. PCR products were resolved on 1.5% agarose gels in Tris-acetate-EDTA buffer, stained with SYBR™ Safe DNA gel stain (Invitrogen), and were visualized under UV light. After confirmation by agarose gel electrophoresis, the PCR products were sequenced in both directions using the same primer pairs used for amplification, by Macrogen Inc. (Seoul, South Korea). The retrieved nucleotide sequences were assembled and edited with MEGA X (Kumar *et al.,* 2018).

Morphological descriptions of Quambalaria cyanescens *and* Neoscylalidium dimidiatum *isolates*

Two representative isolates of *Q. cyanescens* (GP9 and GP15) and of *Neos. dimidiatum* (GP33 and GP40), were selected for morphological characterization. Mycelium plugs (4 mm in diam.) were placed into 85 mm-diam. Petri dishes containing PDA, and were incubated at 25°C in the dark for 1–3 weeks. Actively growing colonies of *Neos. dimidiatum* were transferred to plates containing water agar (WA) supplemented with sterile pine needles to allow pycnidium formation (Smith *et al*., 1996). The inoculated Petri dishes were then incubated at room temperature (24 ± 2°C) under a 12 h/12 h fluorescent light/dark regime for 3–4 weeks. For microscopic characterization, pycnidia, pycnidiospores and arthroconidia produced by the hyphomycetous and coelomycetous morphs of *Neos. dimidiatum*, and conidiophores and conidia of *Q. cyanescens*, were mounted in sterile lactic acid. Morphology of all reproductive structures was determined at appropriate magnifications using an Olympus BZX16 dissecting microscope and Olympus ColorView I camera, or a Zeiss AX10 compound microscope and Zeiss AxionCam MRc 5 camera. Mean, maximum, and minimum dimensions (± standard deviations) of *Neos. dimidiatum* and *Q. cyanescens* reproductive structures were calculated, as well as the conidium length-to-width ratios (L/W). Colony morphologies of the respective isolates were described on PDA, malt extract agar (MEA; Sigma-Aldrich), oatmeal agar (OA; Sigma-Aldrich), and corn meal agar (CMA; Sigma-Aldrich), while colony colours were also determined for each medium, based on Rayner's (1970) charts.

Effects of temperature on mycelium growth

Optimum temperatures for mycelium growth of *Q. cyanescens* (isolates GP9 and GP15) and *Neos. dimidiatum* (isolates GP33 and GP40) were determined. Mycelium plugs (each 4 mm diam.) from the margins of actively growing cultures were transferred into the centre of Petri dishes containing PDA, and were incubated in the darkness at constant temperatures from 5 to 35°C (5°C intervals). Two perpendicular diameters of resulting colonies were recorded daily for *Neos. dimidiatum* over 2 d, and for *Q. cyanescens* over 14 d. Three replicates were prepared per isolate and the experiment was repeated once.

Regression curves were fitted for each isolate at the different temperatures and the data were analyzed using the Kruskal-Wallis test (non-parametric). The optimum growth temperature and the mycelium growth rate (mm d^{-1}) were calculated for each isolate, and means per fungus species were compared using Dunn's test for multiple comparisons ($P \leq 0.05$). Statistical analyses of data were carried out using SPSS (v. 25, IBM Corporation,) and graphically presented with GraphPad Prism (v. 10.1.0, GraphPad Software).

Phylogenetic analyses of Quambalaria *and* Neoscytalidium *isolates*

Raw sequence chromatograms of each locus (forward and reverse) generated for *Quambalaria* and *Neoscytalidium* isolates were retrieved, and their quality was evaluated using the FinchTV software (version 1.4.0) (Geospiza Inc.). Consensus sequences were assembled using MEGA software (version 7.0.26) (Kumar *et al*., 2018) with ClustalW (Thompson *et al*., 1994). All the sequences generated in this study, along with reference sequences from NCBI (Tables 3 and 4) were aligned with MAFFT v. 7.110 (Katoh *et al*., 2019), using the default parameters. Manual adjustments were made, when necessary, using MEGA software (version 7.0.26) (Kumar *et al*., 2018). The alignments of each locus were concatenated in Sequence Matrix v.1.8 software (Vaidya *et al*. 2011). The concatenated sequence alignments were analyzed using Maximum Likelihood (ML) in IQ-TREE software (version 2.3.4) (Minh *et al*., 2020), with the best evolutionary model selected using ModelFinder (Kalyaanamoorthy *et al*., 2017). Branch support was estimated using 1000 replicates of the ultrafast approximation (UFBoot2) (Hoang *et al*., 2018). Bayesian inference (BI) was carried out using MrBayes v3.2.7 (Ronquist *et al*., 2012). Two independent Markov Chain Monte Carlo (MCMC) runs (each with one cold and three heated chains) were conducted for 1,000,000 generations, and

trees and parameters were sampled every 100 generations. Convergence was monitored using the average standard deviations of split frequencies, with a target value of <0.01, assessed every 1,000 generations. The first 25% of samples were discarded as burn-in, and a 50% majority-rule consensus tree was generated from the remaining trees, with posterior probabilities (PP) used as nodal support values. For *Quambalaria* species, no *rpb2* sequence was available for their type strains.

Pathogenicity tests

To determine abilities to infect and induce symptoms on host plants, pathogenicity tests were carried out using isolate GP9 of *Q. cyanescens* and isolate GP40 of *Neos. dimidiatum*. Inoculations were carried out *in vivo* on asymptomatic cuttings of 'Italia' grafted onto 140RU rootstock. Each isolate was inoculated onto 12 green and 12 woody shoots of scion and onto six rootstocks, using a mycelial plug in each case. Before inoculations, the shoots and rootstocks were surface-disinfected with a 70% aqueous solution of ethanol. For each inoculation, the bark was gently scraped using a sterile blade, and an agar plug (5 mm diam.) from a 20-d-old fungal culture grown on PDA supplemented with lactic acid (2.5 mL of 25% [v:v] per L; APDA) at 25 ± 1 °C was inserted into each wound. The wounds were then sealed with Parafilm® (Pechney Plastic Packaging Inc.) to prevent contamination and dehydration. Controls consisted of 12 plants each inoculated with a sterile APDA plug. All the plants were then moved to a growth chamber set with a 12 h light 12 h dark daily cycle, and maintained at 25°C. The plants were regularly watered and monitored weekly for development of symptoms. Symptom evaluation on the scions was carried out after 1 month for half of the inoculated shoots, and at 3 months for the remaining shoots. For the rootstock, symptom evaluation was performed at 3 months post-inoculation. Mean lengths of necrotic lesions (external or internal) extending both upward and downward from each inoculation site were determined. The experiment was carried out twice. Isolations of fungal species from diseased plant tissues were carried out to assess fulfilment of Koch's postulates.

RESULTS

Field surveys, sampling and fungus isolations

In the four surveyed nurseries, 95% of the sampled rooted and grafted table grape cuttings were symptomatic (76 of 80 cuttings examined). The symptoms included necroses and discolourations at the graft points extending upward the scions, wood necroses and black streaking at the rootstock bases, as well as pith necroses and black streaking on vascular tissues (Figure 1). More than 100 isolates were collected from symptomatic cuttings, and 82 representative strains from different nurseries and plant parts were characterized using molecular analyses.

Figure 1. Symptoms observed on table grape propagation material in nurseries. **A** and **B**, views of two of the table grape nurseries investigated. **C** and **D**, vertical sections of symptomatic cuttings. **E**, **F** and **G**, necroses and discolouration at graft unions. **H**, vascular discolouration. **I**, pith necrosis. **J**, black streaking and wood necrosis at bases of rootstock plants.

Fungus identifications

Initial molecular identification of the 82 representative isolates was based on their ITS sequences. These identifications were then supported by the *tef1-a* sequences for 28 representative isolates of the main species recovered from the propagation material. BLASTn analysis identified 22 genera: *Acremonium*, *Alternaria*, *Arthrinium*, *Aspergillus*, *Botryosphaeria*, *Cadophora*, *Cladosporium*, *Clonostachys*, *Dactylonectria*, *Diaporthe*, *Diplodia*, *Entoleuca*, *Fusarium*, *Idriella*, *Ilyonectria*, *Neofusicoccum*, *Neoscytalidium*, *Phaeoacremonium*, *Phaeomoniella*, *Paraphoma*, *Quambalaria* and *Trichoderma* (Supplementary Table S1). Fungi recovered at low frequency in the present survey and/or generally considered as saprophytes or antagonists (*Acremonium* sp., *Alternaria* sp., *Aspergillus* spp., *Cladosporium* spp., *Entoleuca* spp., *Idriella* sp., *Paraphoma* sp., *Clonostachys* sp. and *Trichoderma* spp.) were not examined further. Sequences of *tef1-α* confirmed the identity of 16 species. Some of these are well-known GTDs pathogens, including *Botryosphaeriaceae* (*N. parvum*, *D. seriata*, *N. australe*, *N. luteum, B. dothidea*), *Ph. chlamydospora*, *P. minimum*, *Cadophora luteo-olivacea*, and *Cylindrocarpon*-like species (*I. liriodendri*, *I. destructans*, *D. macrodidyma*, *D. torresensis*). Other usually less common fungi (*F. proliferatum*, *F. oxysporum*, *Neos. dimidiatum*, *Q. cyanescens*) were also identified. The ITS and *tef1-a* sequences generated in this study were deposited in GenBank (Supplementary Table S1).

For isolation frequencies, fungal colonies obtained were classified into seven morphotypes, based on colony morphology, *Botryosphaeriaceae*, *Fusarium* spp., *Cylindrocarpon*-like spp., *Q. cyanescens*, *Neos. dimidiatum*, *Ph. chlamydospora* and *P. minimum*. Morphological identifications of fungal morphotypes were confirmed from molecular analyses (Table 1).

Isolation results indicated that fungus incidence varied between the different parts of the plant cuttings. Isolation frequency (%) at the graft unions showed a prevalence of *Q. cyanescens*, followed by *Neos. dimidiatum*, other *Botryosphaeriaceae* and *Fusarium* spp. Isolations at 15 cm from rootstock base showed prevalence of *Ph. chlamydospora* followed by *Q. cyanescens* and *Neos. dimidiatum*, while from the rootstock base, the dominant species were similar to those from the graft unions (Table 1).

Morphological analyses of Neoscytalidium *and* Quambalaria *isolates*

Colonies of *Q. cyanescens* (isolates GP9 and GP15) were white, flat, with smooth margins and slow growth on PDA, MEA, CMA, and OA media, after 7 d incubation at 25°C in darkness. On OA, pale vinaceous grey-purple haloes developed around the colonies (Figure 2). Conidiogenous cells for both isolates developed at the ends along the sides of conidiophores, which were indistinguishable from the vegetative hyphae. Primary conidia of the *Q. cyanescens* isolates were ellipsoidal to subcylindrical, hyaline, often guttulate, and aseptate; secondary conidia were obovoid to guttiform, hyaline, often guttulate, and aseptate (Figure 3). Characteristics of conidium and conidiogenous cells are reported in the Supplementary Table S2. Overall, their morphologies were in line with the original description of *Q. cyanescens* by de Hoog and de Vries (1973) and earlier descriptions of the species. No sexual morphs were observed.

Both isolates of *Neos. dimidiatum* (GP33 and GP40) had characteristics consistent with the description of the type-strain of this species described by Campbell and Mulder (1977) (Supplementary Table S3). The two isolates grew rapidly at 25°C, with mycelium covering the surfaces of 85 mm diam. plates of PDA, MEA, and OA in less than 72 h, and after 4 d on CMA. The colonies were initially hyaline to white with smooth margins on the four media, and with aerial mycelium on OA and MEA. With time, colonies on PDA turned smoke grey and grey olivaceous to black, beginning from their centres, while on MEA they developed olivaceous grey to pale greyish colours, both with powdery texture. On OA, the colonies turned grey olivaceous to olivaceous black and cottony, whereas on CMA, they

Table 1. Isolation frequencies (%) of the main fungi recovered from different parts of symptomatic table grape propagation material.

Fungal species/taxon	Isolation frequency (%) per plant part [a]		
	Graft point	15 cm from the base	Rootstock base
Quambalaria cyanescens	20.5	11.1	18.3
Neoscytalidium dimidiatum	13.1	11	15.1
Other *Botryosphaeriaceae*	10.1	3.5	12.1
Fusarium spp.	6.4	5.1	1.3
Phaeomoniella chlamydospora	0.6	16.8	8.2
Phaeoacremonium minimum	1.7	2.1	0.6
Cylindrocarpon-like species	-	-	2.0
other	1.1	2.9	1.7
Total	53.5	52.5	59.3

[a] Each isolation frequency is the average of frequencies obtained from four table grape nurseries. The frequency from each nursery was calculated as the number of positive tissue pieces from which each morphotype was isolated, divided by the total number of analyzed tissue pieces.

were flat and progressed from hyaline to white to grey olivaceous (Figure 2). Pycnidia were irregular dark brown to black, and pycnidiospores were also irregular in shape, and dark brown to black. Arthroconidia were produced by hyphal disarticulation, and were hyaline to pale brown, 0 to 1 (rarely 2) septate and cylindrical, and were produced singly or in arthric chains (Figure 3). No sexual morphs were observed.

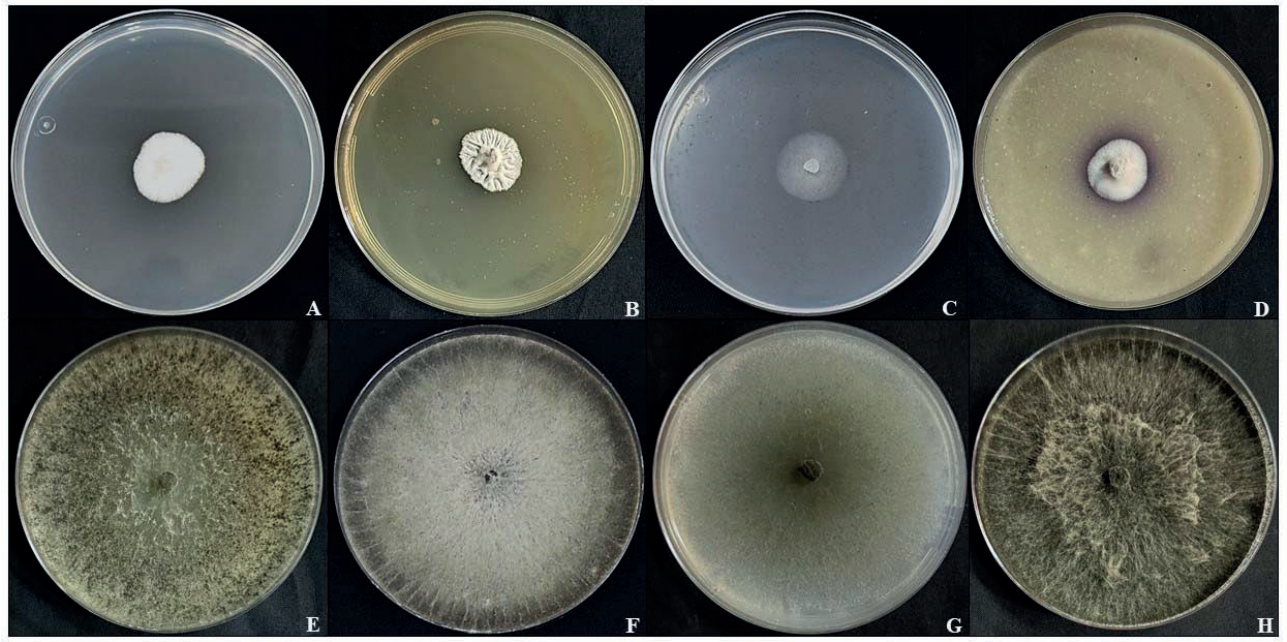

Figure 2. A to **D**, colonies of *Quambalaria cyanescens* (isolate GP9). **E to H**, colonies of *Neoscytalidium dimidiadum* (isolate GP40). Both isolates were grown for 7 d at 25°C in darkness on PDA (**A** and **E**), MEA (**B** and **F**), CMA (**C** and **G**), and OA (**D** and **H**).

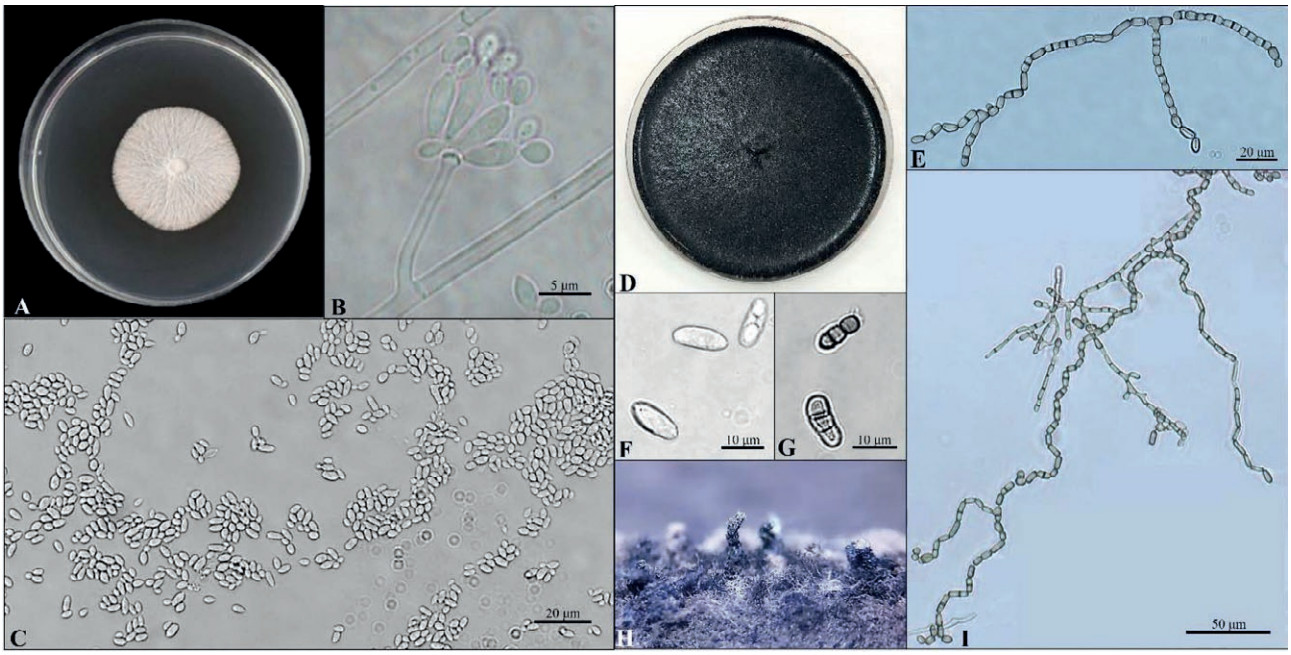

Figure 3. Morphological characteristics of *Quambalaria cyanescens* and *Neoscytalidium dimidiatum*. **A**, colony of *Q. cyanescens* (isolate GP9; 2 weeks old). **B**, conidiophore with primary and secondary conidia. **C**, general view of conidia. **D**, colony of *Neos. dimidiatum* (isolate GP40; 3 weeks old). **E** and **I**, chains of arthroconidia. **F** and **G**, pycnidiospores without (F) and with one or two septa (G). **H**, pycnidia.

Effects of temperature on mycelium growth

Analysis of variance showed no differences ($P < 0.05$) in mycelium growth among experiments, allowing data to be pooled. Relationships between temperature and growth were modelled using a cubic response model ($y = aT^3 + bT^2 + cT + d$), with R^2 values ranging from 0.95 to 0.98, indicating excellent fit (Table 2).

Maximum mycelium growth was recorded after 2d for the two *Neos. dimidiatum* isolates and 14 d for the two *Q. cyanescens* isolates. The *Neos. dimidiatum* isolates had optimum growth temperatures between 30 and 35°C, with no growth observed at 5 and 10°C after 14 d. Although no significant differences were found for optimum growth temperature between the two isolates (GP33, 31.93°C; GP40, 32.86°C), maximum growth rates (approx. 41 mm d^{-1}) did not differ ($P > 0.05$). Colony diameters after 48 h ranged from 8.6 mm at 15°C to 64.6 mm at 25°C.

The two *Q. cyanescens* isolates had optimum growth at 25.17°C and 27.06°C, with maximum daily growth rates of 2.56 to 3.42 mm, and no differences ($P > 0.05$) between the isolates. After 14 d, mean colony diameters were from 5.3 mm at 5°C to 41.5 mm at 30°C (Figure 4).

Phylogenetic analyses of Quambalaria *and* Neoscytalidium

Sequence alignment of the three genetic loci (ITS, LSU, and *rpb2*) prepared for *Quambalaria* isolates consisted of a 2020 character dataset, of which 1389 were constant, 442 were parsimony-informative, and 189

Table 2. Temperature-mycelium growth relationships for *Neoscytalidium dimidiatum* and *Quambalaria cyanescens* isolates obtained from table grape propagation material w.

Species	Isolate	Adjusted model[x]					Optimum temperature (°C)[y]	Growth rate (mm/day)[z]
		R^2	*a*	*b*	*c*	*d*		
Neos. dimidiatum	GP33	0.98	-0.0071	0.434	-59.99	21.10	31.93 a	40.89 a
Neos. dimidiatum	GP40	0.98	-0.0066	0.415	-59.15	21.30	32.86 a	41.18 a
Q. cyanescens	GP9	0.95	-0.0007	0.034	-0.361	15.29	25.17 b	2.56 b
Q. cyanescens	GP15	0.96	-0.0007	0.035	-0.371	15.79	27.06 b	3.42 b

[w] Data are means of six replicates per isolate. Means in each column accompanied by the same letter, are not different ($P = 0.05$), according to Kruskal-Wallis and Dunn's test for multiple comparisons.
[x] Mycelium growth of PDA at 5 to 35°C (5°C increments) was adjusted to a quadratic model of $y = aT^3 + bT^2 + cT + d$: where y = mycelium growth (mm d^{-1}); a, b, c, d = regression coefficients; and R^2 = coefficient of determination.
[y] Optimum temperatures for each isolate were estimated using the adjusted model.
[z] Maximum growth rate per isolate estimated using the adjusted model.

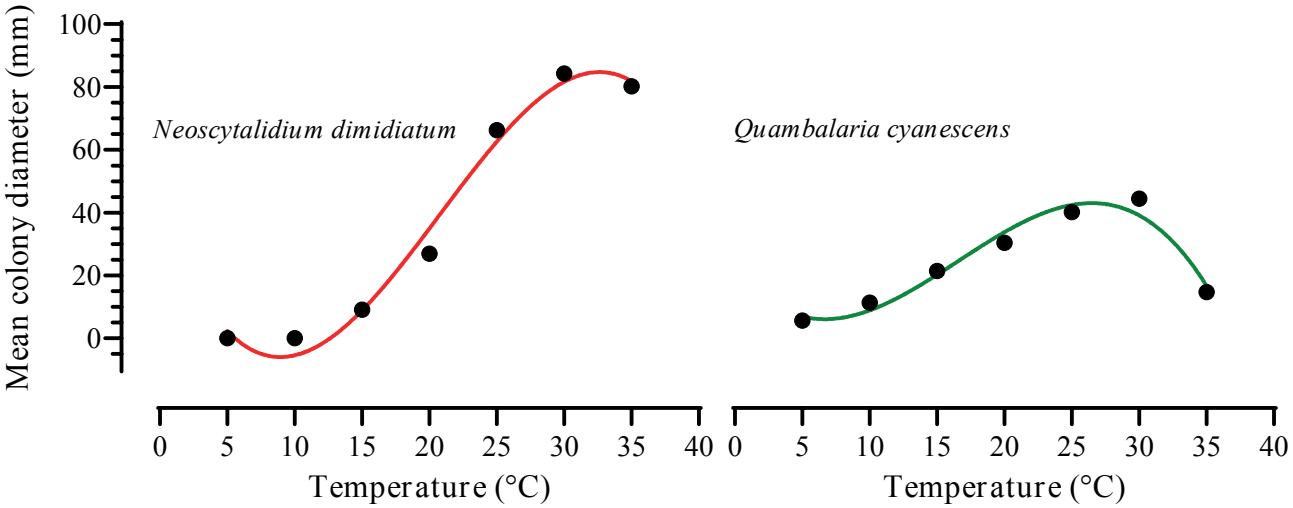

Figure 4. Mean colony diameters (mm) at seven temperatures (5 to 35°C) for two isolates each of *Neoscytalidium dimidiatum* (after 2 d) and *Quambalaria cyanescens* (after 14 d). The isolates were obtained from table grape propagation material in Catania, Italy.

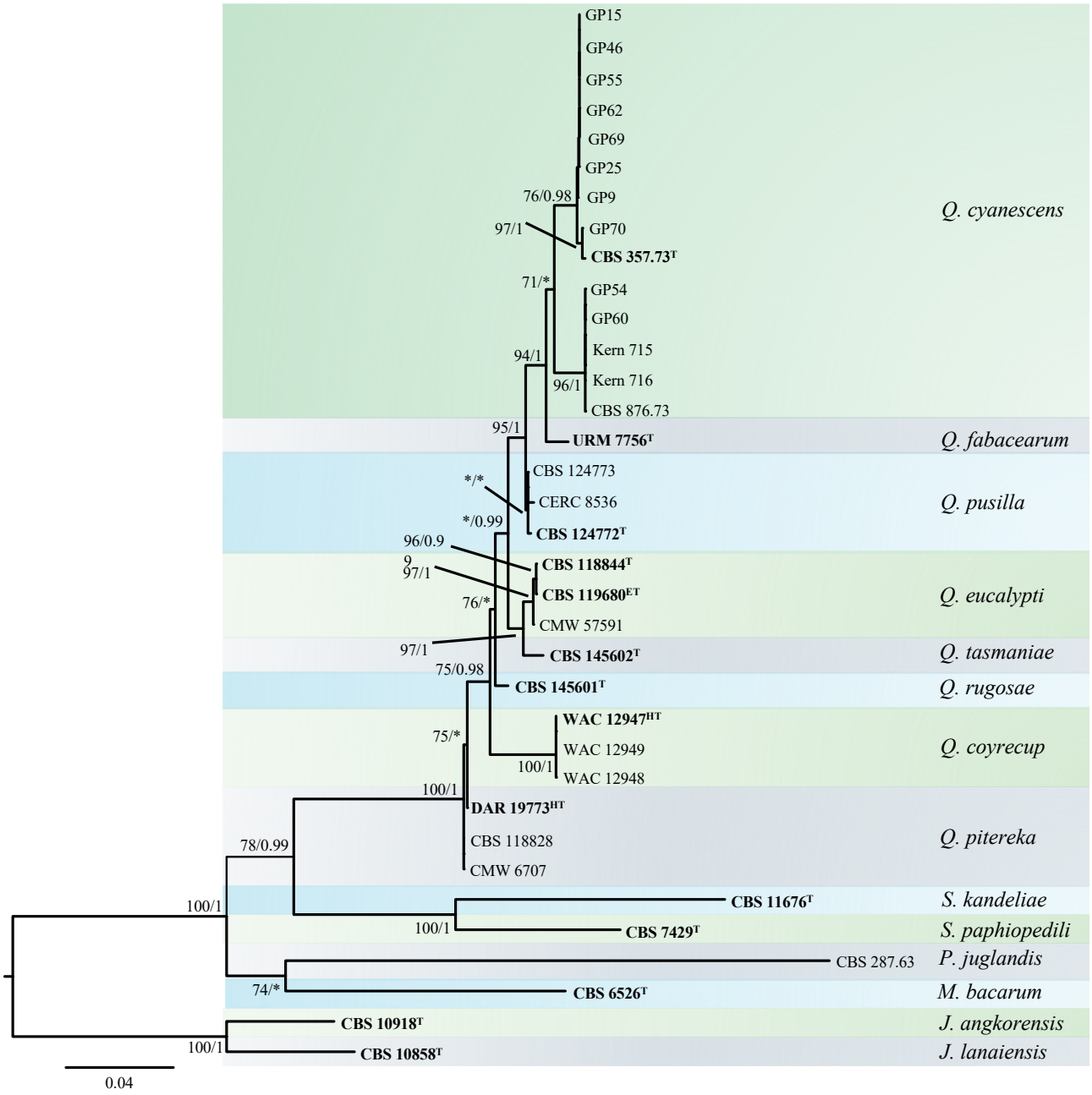

Figure 5. Phylogenetic tree inferred from Maximum Likelihood (ML) and Bayesian Inference (BI) analyses, based on aligned and concatenated ITS, LSU, and *rpb2* sequences of 35 isolates in *Quambalariaceae*. Strains CBS 10918T (*Jaminaea angkorensis*) and CBS 10858T (*Jaminaea lanaiensis*) were used as the outgroup taxa. Numbers at branches indicate support values: Ultrafast bootstrap (UFBoot2) ≥70% and Bayesian posterior probability (B-PP) ≥0.95, with asterisks (*) indicating values <70% and <0.95, respectively. Ex-type, and ex-epitype isolates are indicated in bold. The scale bar represents the expected number of changes per site.

were singleton sites, with 614 distinct patterns. For maximum likelihood (ML) analysis, the ModelFinder determined SYM + I + G4 as the best-fit model. ML and BI phylogenetic analyses with strong supports (respectively 94% and 1) clustered all the *Quambalaria* isolates obtained in the present study in the same clade with other *Q. cyanescens* isolates and *Q. fabacearum* (URM 7756) (Figure 5).

Sequence alignment prepared for the three loci (ITS, *β-tub*, and *tef1-a*) of *Neoscytalidium* isolates consisted of a dataset of 1321 characters, of which 832 were constant, 447 were parsimony-informative, and 42 were singleton

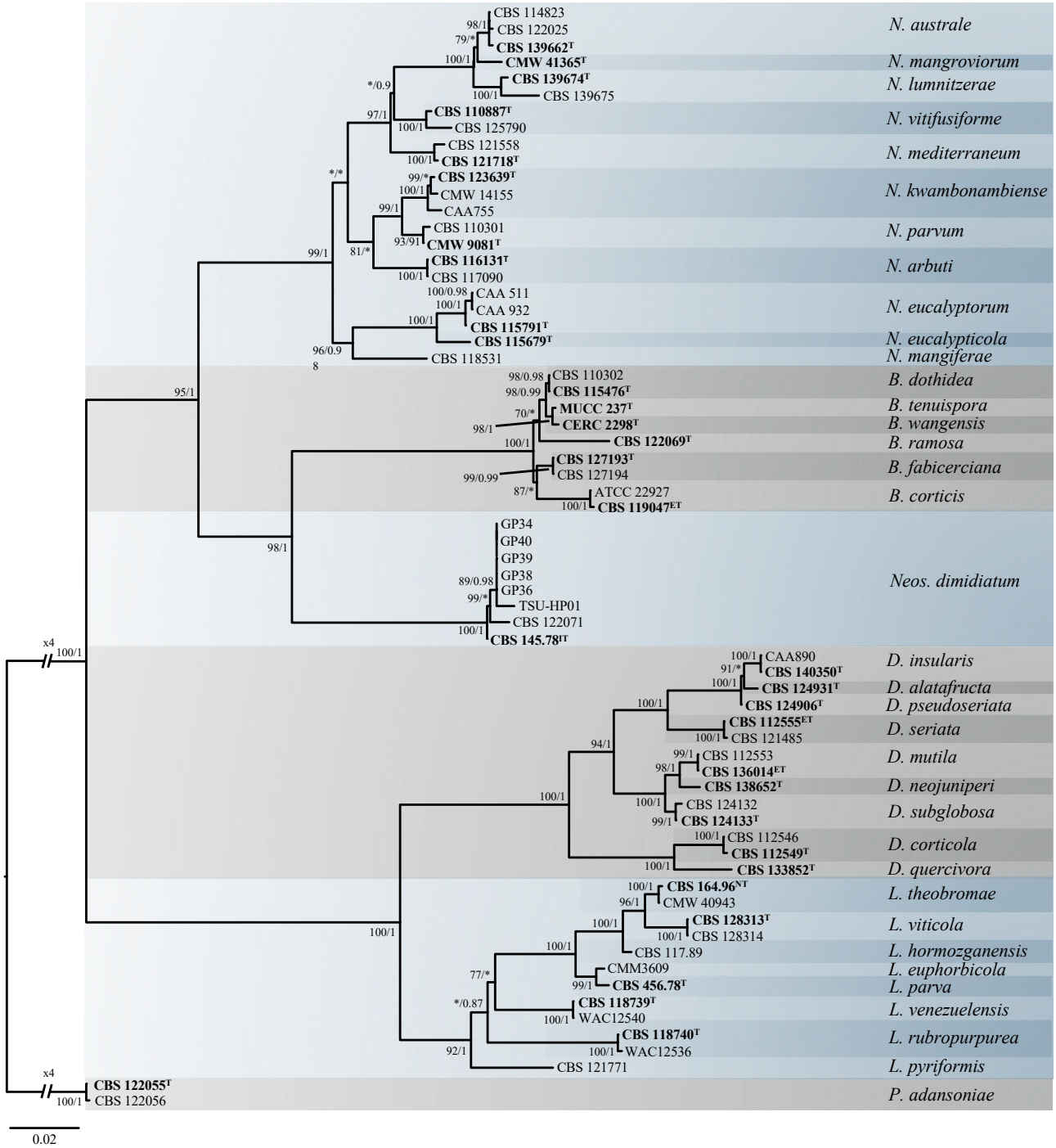

Figure 6. Phylogenetic tree inferred from Maximum Likelihood (ML) and Bayesian Inference (BI) analyses, based on aligned and concatenated ITS, *β-tub*, and *tef1-a* sequences of 67 isolates belonging to *Botryosphaeriaceae*. The strains CBS 122055T and CBS 122056 (*Pseudofusicoccum adansoniae*) were used as the outgroup taxa. Numbers at branches indicate support values: Ultrafast bootstrap (UFBoot2) ≥70% and Bayesian posterior probability (B-PP) ≥0.95; with asterisks (*) indicating values <70% and <0.95, respectively. Ex-type, ex-epitype, ex-isotype, and ex-neotype strains are indicated in bold. The scale bar represents the expected number of changes per site.

sites, with 577 distinct patterns. For maximum likelihood (ML) analysis, the ModelFinder determined TIM + F + I + G4 as the best-fit model. ML and BI phylogenetic analyses with strong support (respectively 100% and 1) clustered all the present study *Neoscytalidium* isolates in the same clade as *Neos. dimidiatum* reference isolates (Figure 6).

Table 3. Phylogenetic analysis of *Quambalaria cyanescens* isolates assessed in the present study, with details of their geographic origins, hosts, and GenBank accession numbers a.

Species	Strain code[c,d]	Host	Country	GenBank Accession Number[b]		
				ITS	LSU	*rpb2*
Jaminaea angkorensis	CBS 10918^{T}=CCY 88-1-1=C5b	Decaying leaves	Cambodia	KY103614	KY107895	KP323082
Jaminaea lanaiensis	CBS 10858^{T}=BCRC 23177=LM418	Driftwood	USA	KY105576	KY109812	KP323080
Microstroma bacarum	CBS 6526^{T}=IGC4391=CGMCC2.3190	*Ribes nigrum*	UK	DQ317629	AF352055	KP323098
Pseudomicrostroma juglandis	CBS 287.63	*Juglans regia*	The Netherlands	DQ789989	AF009867	DQ789989
Quambalaria cyanescens	CBS 357.73^{T}=CMW 5583=MUCL 19329	Skin of man	The Netherlands	DQ317622	DQ317615	-
Q. cyanescens	CBS 876.73=CMW 5584	*Eucalyptus pauciflora*	Australia	DQ317623	DQ317616	-
Q. cyanescens	Kern 715	*Vitis vinifera*	USA	OP038078	OP076927	OP095256
Q. cyanescens	Kern 716	*V. vinifera*	USA	OP038079	OP076928	OP095257
Q. cyanescens [b]	**GP9**	***V. vinifera***	**Italy**	**PV440727**	**PV466206**	**PV469421**
Q. cyanescens	**GP15**	***V. vinifera***	**Italy**	**PV440730**	**PV466207**	**PV469422**
Q. cyanescens	**GP25**	***V. vinifera***	**Italy**	**PV440801**	**PV466208**	**PV469423**
Q. cyanescens	**GP46**	***V. vinifera***	**Italy**	**PV440732**	**PV466209**	**PV469424**
Q. cyanescens	**GP54**	***V. vinifera***	**Italy**	**PV440733**	**PV466210**	**PV469425**
Q. cyanescens	**GP55**	***V. vinifera***	**Italy**	**PV440734**	**PV466211**	**PV469426**
Q. cyanescens	**GP60**	***V. vinifera***	**Italy**	**PV440736**	**PV466212**	**PV469427**
Q. cyanescens	**GP62**	***V. vinifera***	**Italy**	**PV521998**	**PV466213**	**PV469428**
Q. cyanescens	**GP69**	***V. vinifera***	**Italy**	**PV440738**	**PV466214**	**PV469429**
Q. cyanescens	**GP70**	***V. vinifera***	**Italy**	**PV440803**	**PV466215**	**PV469430**
Quambalaria eucalypti	CBS 118844^{T}=CMW 1101	*Eucalyptus grandis*	South Africa	DQ317625	DQ317618	-
Q. eucalypti	CBS 119680^{ET}=CMW 11678	*E. grandis*	South Africa	DQ317626	DQ317619	-
Q. eucalypti	CMW 57591	*E. pellita*	Indonesia	OR345271	OR345280	-
Quambalaria pitereka	CBS 118828=CMW 5318	*Corymbia citriodora* subsp. *Variegata*	Australia	DQ317628	DQ317621	-
Q. pitereka	CMW 6707	*Corymbia maculata*	Australia	DQ317627	DQ317620	-
Q. pitereka	DAR 19773^{HT}	*Corymbia eximia*	Australia	DQ823423	DQ823438	-
Quambalaria pusilla	CBS 124773	*Eucalyptus* sp.	Thailand	GQ303291	GQ303322	-
Q. pusilla	CERC 8536	*E. urophylla* x *E. grandis*	China	KY615046	KY615061	-
Q. pusilla	CBS 124772^{T}=CPC 14499	*Eucalyptus tintinnans*	Australia	GQ303290	GQ303321	-
Quambalaria tasmaniae	CBS 145602^{T}=CPC 25464	*Eucalyptus* spp.	Australia	MN162015	MN162213	-
Quambalaria rugosae	CBS 145601^{T}=CPC 20162	*Eucalyptus rugosa*	Australia	MN162014	MN162212	-
Quambalaria coyrecup	WAC 12947^{HT}	*Corymbia calophylla*	Australia	DQ823431	DQ823444	-
Q. coyrecup	WAC 12948	*Corymbia calophylla*	Australia	DQ823433	DQ823446	-
Q. coyrecup	WAC 12949	*Corymbia calophylla*	Australia	DQ823432	DQ823445	-
Quambalaria fabacearum	URM 7756^{T}	*Mimosa tenuiflora*	Brazil	MG253664	MG253665	
Sympodiomycopsis kandeliae	CBS 11676^{T}=BCRC 23165=FIRDI 007	*Kandelia candel*	Taiwan	KY105575	KY109811	KP323077
Sympodiomycopsis paphiopedili	CBS 7429^{T}=IGC5543=CGMCC2.1398	*Paphiopedilum primurinum*	Japan	KY105577	AF190005	KP323099

[a] GenBank accession numbers for the sequences of four loci: internal transcribed spacer regions and intervening 5.8S rRNA gene (ITS), large subunit of the rRNA (LSU), and the second largest subunit of RNA polymerase II (*rpb2*) that were generated in the present study or from others.

[b] Sequences from isolates in our collection are highlighted in bold.

[c] **BCRC:** Bioresources Collection and Research Center, Food Industry Research and Development Institute, Hsinchu, Taiwan (same as CCRC); **CBS:** Culture collection of the Westerdijk Fungal Biodiversity Institute, Utrecht, The Netherlands; **CGMCC:** China General Microbiological Culture Collection Center, Institute of Microbiology, Chinese Academy of Sciences, Beijing, China; **CMW:** Culture collection of the Forestry and Agricultural Biotechnology Institute (FABI) at the University of Pretoria, South Africa; **CPC:** Culture collection of Pedro Crous, housed at the Westerdijk Institute; **DAR:** Plant Pathology Herbarium, Orange Agricultural Institute, Orange, New South Wales, Australia; **FIRDI:** Food Industry Research and Development Institute, Hsin-Chu, Taiwan; **MUCL:** Belgian Coordinated Collections of Microorganisms, Université Catholique de Louvain, Earth and Life Institute, Belgium; **URM:** Culture collection at the Universidade Federal de Pernambuco, Recife, Brazil; **WAC:** Western Australian Plant Pathology Reference Culture Collection, Perth, Australia.

[d] Status of the isolates = ET: ex-epitype; HT: ex-holotype; T: ex-type. Sequences in bold indicate isolates collected and characterized in the present study.

Table 4. Isolates used in this study for the phylogenetic analysis of *Neoscytalidium dimidiatum*, with details of their geographic origins, hosts, and GenBank accession numbers a.

Species	Strain[c,d]	Host	Country	GenBank Accession Numbers[b]		
				ITS	*β-tub*	*tef1-a*
Botryosphaeria corticis	CBS 119047^{ET}	*Vaccinium corymbosum*	USA	DQ299245	EU673107	EU017539
B. corticis	ATCC 22927	*Vaccinium* sp.	USA	DQ299247	EU673108	EU673291
Botryosphaeria dothidea	CBS 115476^{T}=CMW 8000	*Prunus* sp.	Switzerland	AY236949	AY236927	AY236898
B. dothidea	CBS 110302	*Vitis vinifera*	Portugal	AY259092	EU673106	AY573218
Botryosphaeria. fabicerciana	CBS 127193^{T}=CMW 27094	*Eucalyptus* sp.	China	HQ332197	KF779068	HQ332213
B. fabicerciana	CBS 127194	*Eucalyptus* sp.	China	HQ332198	KF779069	HQ332214
Botryosphaeria ramosa	CBS 122069^{T}=CMW 26167	*Eucalyptus camaldulensis*	Australia	EU144055	KF766132	EU144070
Botryosphaeria tenuispora	MUCC 237^{T}	*Leucothoe catesbaei*	Japan	LC585278	LC585174	LC585150
Botryosphaeria wangensis	CERC 2298=CGMCC3.18744^{T}	*Cedrus deodara*	China	KX278002	KX278211	KX278107
Diplodia alatafructa	CBS 124931^{T}=CMW 22627	*Pterocarpus angolensis*	South Africa	FJ888460	MG015799	FJ888444
Diplodia corticola	CBS 112549^{T}	*Quercus suber*	Portugal	AY259100	DQ458853	AY573227
D. corticola	CBS 112546	*Quercus ilex*	Spain	AY259090	EU673117	EU673310
Diplodia insularis	CBS 140350^{T}	*Pistacia lentiscus*	Italy	KX833072	MG015809	KX833073
D. insularis	CAA890	*Eucalyptus globulus*	Portugal	MK940299	MT309385	MT309406
Diplodia mutila	CBS 136014^{ET}	*Populus alba*	Portugal	KJ361837	MG015815	KJ361829
D. mutila	CBS 112553	*V. vinifera*	Portugal	AY259093	MZ073931	AY573219
Diplodia neojuniperi	CBS 138652^{T}=CPC 22753	*Juniperus chinensis*	Thailand	KM006431	MT592516	KM006462
Diplodia pseudoseriata	CBS 124906^{T}=CMW 26771	*Blepharocalyx salicifolius*	Uruguay	EU080927	MG015820	EU863181
Diplodia quercivora	CBS 133852^{T}	*Quercus canariensis*	Tunisia	JX894205	MG015821	JX894229
Diplodia seriata	CBS 112555^{ET}=HAP 052=CAP 063	*V. vinifera*	Portugal	AY259094	DQ458856	AY573220
D. seriata	CBS 121485	*V. vinifera*	Spain	EU650671	MT592556	MT592093
Diplodia subglobosa	CBS 124133^{T}	*Lonicera nigra*	Spain	GQ923856	MT592576	GQ923824
D. subglobosa	CBS 124132	*Fraxinus excelsior*	Spain	DQ458887	DQ458852	DQ458871
Lasiodiplodia euphorbicola	CMM3609	*Jatropha curcas*	Brazil	KF234543	KF254926	KF226689
Lasiodiplodia hormozganensis	CBS 117.89	*Quercus cerris*	Italy	KX464134	MT592620	KX464627
Lasiodiplodia parva	CBS 456.78^{T}	Cassava field soil	Colombia	EF622083	KU887523	EF622063
Lasiodiplodia pyriformis	CBS 121771	*Acacia mellifera*	Namibia	EU101308	KU887528	EU101353
Lasiodiplodia rubropurpurea	CBS 118740^{T}=WAC12535	*Eucalyptus grandis*	Australia	DQ103553	EU673136	DQ103571
L. rubropurpurea	WAC12536	*E. grandis*	Australia	DQ103554	KU887530	DQ103572
Lasiodiplodia theobromae	CBS 164.96^{NT}	fruit along coral reef coast	Papua New Guinea	AY640255	KU887532	AY640258
L. theobromae	CMW 40943	*Myrtales* plant	South Africa	MG367178	KP872426	MG367173
Lasiodiplodia venezuelensis	CBS 118739^{T}=WAC12539	*Acacia mangium*	Venezuela	DQ103547	KU887533	EU673305
L. venezuelensis	WAC12540	*A. mangium*	Venezuela	DQ103548	KU887534	DQ103569
Lasiodiplodia viticola	CBS 128313^{T}	*Vitis* sp.	USA	HQ288227	HQ288306	HQ288269
L. viticola	CBS 128314	*V. vinifera*	USA	HQ288228	HQ288307	HQ288270
Neofusicoccum arbuti	CBS 116131^{T}	*Arbutus menziesii*	USA	AY819720	KF531793	KF531792

(Continued)

Table 4. (Continued).

Species	Strain[c,d]	Host	Country	GenBank Accession Numbers[b]		
				ITS	*β-tub*	*tef1-a*
N. arbuti	CBS 117090	*A. menziesii*	USA	AY819724	KF531794	KF531791
Neofusicoccum australe	CBS 139662^{T}=CMW 6837	*Acacia* sp.	Australia	AY339262	AY339254	AY339270
N. australe	CBS 122025	*Eucalyptus* sp.	Spain	KX464160	KX464949	KX464672
N. australe	CBS 114823	*Eucalyptus* sp.	South Africa	KX464159	KX464947	KX464671
Neofusicoccum eucalypticola	CBS 115679^{T}	E. grandis	Australia	AY615141	AY615125	AY615133
Neofusicoccum eucalyptorum	CBS 115791^{T}	*E. grandis*	South Africa	AF283686	AY236920	AY236891
N. eucalyptorum	CAA 932	*E. globulus*	Portugal	MK940311	MT309396	MT309422
N. eucalyptorum	CAA 511	*E. globulus*	Portugal	KX505907	KX505919	KX505896
Neofusicoccum kwambonambiense	CBS 123639^{T}	*Syzygium cordatum*	South Africa	EU821900	EU821840	EU821870
N. kwambonambiense	CAA755	*E. globulus*	Portugal	KT440946	KX505917	KT441006
N. kwambonambiense	CMW 14155	-	-	EU821923	EU821863	EU821893
Neofusicoccum lumnitzerae	CBS 139674^{T}=CMW 41469	*Lumnitzera racemosa*	South Africa	KP860881	KP860801	KP860724
N. lumnitzerae	CBS 139675=CMW 41228	*L. racemosa*	South Africa	KP860882	KP860802	KP860725
Neofusicoccum mangiferae	CBS 118531=CMW 7024	*Mangifera indica*	Australia	AY615185	AY615172	DQ093221
Neofusicoccum mangroviorum	CMW 41365^{T}	*Avicennia marina*	South Africa	KP860859	KP860779	KP860702
Neofusicoccum mediterraneum	CBS 121718^{T}	*Eucalyptus* sp.	Greece	GU251176	GU251836	GU251308
N. mediterraneum	CBS 121558	*V. vinifera*	USA	GU799463	GU799461	GU799462
Neofusicoccum parvum	ATCC 58191=CMW 9081^{T}	*Populus nigra*	New Zealand	AY236943	AY236917	AY236888
N. parvum	CBS 110301	*V. vinifera*	Portugal	AY259098	EU673095	AY573221
Neofusicoccum vitifusiforme	CBS^{T} 110887 ^{T}	*V. vinifera*	South Africa	AY343383	KX465061	AY343343
N. vitifusiforme	CBS 125790	*Acacia mearnsii*	-	MH863762	MT592749	MT592257
Neoscytalidium dimidiatum	IMI 198935 = CBS 145.78^{IT}	*Homo sapiens*	USA	KF531816	KF531796	KF531795
Neos. dimidiatum	TSU-HP01	*Hylocereus polyrhizus*	Thailand	LC590860	LC647833	LC590863
Neos. dimidiatum	CBS 122071	*Crotalaria medicaginea*	Australia	KF766207	MT592760	EF585580
Neos. dimidiatum	**GP34**	***V. vinifera***	**Italy**	**PV440740**	**PV541662**	**PV591900**
Neos. dimidiatum	**GP36**	***V. vinifera***	**Italy**	**PV440742**	**PV541663**	**PV591901**
Neos. dimidiatum	**GP38**	***V. vinifera***	**Italy**	**PV440744**	**PV541664**	**PV591902**
Neos. dimidiatum	**GP39**	***V. vinifera***	**Italy**	**PV440745**	**PV541665**	**PV591903**
Neos. dimidiatum	**GP40**	***V. vinifera***	**Italy**	**PV392803**	**PV541666**	**PV591904**
Pseudofusicoccum adansoniae	CBS 122055^{T}=CMW 26147	*Adansonia gibbosa*	Australia	EF585523	MT592771	EF585571
P. adansoniae	CBS 122056=CMW 26148	*Ficus opposita*	Australia	EF585524	MT592772	MT592279

[a] GenBank accession numbers for the sequences of four loci: internal transcribed spacer regions and intervening 5.8S nrRNA gene (ITS), β-tubulin (*β-tub*), and translation elongation factor 1-a (*tef1-a*) that were generated in this study or from others.

[b] Sequences from isolates obtained in the present study are highlighted in bold.

[c] **ATCC:** American Type Culture Collection, Manassas, Virginia, USA; **CBS:** Culture collection of the Westerdijk Fungal Biodiversity Institute, Utrecht, The Netherlands; **CGMCC:** China General Microbiological Culture Collection Center, Institute of Microbiology, Chinese Academy of Sciences, Beijing, China; **CMW:** Culture collection of the Forestry and Agricultural Biotechnology Institute (FABI) at the University of Pretoria, South Africa; **CPC:** Culture collection of Pedro Crous, housed at the Westerdijk Institute; **MUCC:** Culture Collection, Laboratory of Plant Pathology, Mie University, Tsu, Mie Prefecture, Japan; **WAC:** Western Australian Plant Pathology Reference Culture Collection, Perth, Australia.

[d] Status of the isolates. NT = ex-neotype; ET = ex-epitype; IT = ex-isotype; T = ex-type.

All the sequences generated in the present study were deposited in GenBank (Tables 3 and 4).

Pathogenicity tests

Quambalaria cyanescens and *Neos. dimidiatum* both caused symptoms on inoculated 'Italia' cuttings. One month after inoculations with the *Q. cyanescens* isolate, the mean external lesion length on green shoots was 2.83 ± 1.33 cm, and that with the *Neos. dimidiatum* isolate was 2.63 ± 0.47 cm. The two fungi were more virulent to woody shoots, causing lesions that extended under the bark as internal wood discolourations. The mean lesion length was 3.2 ± 1.26 for *Q. cyanescens* isolates, and 3.4 ± 0.51 cm for *Neos. dimidiatum* (Figure 7). After 3 months, inoculated green and woody shoots were wilted, and the rootstocks also had internal necrotic lesions above and below the inoculation points and extending under the bark. The mean internal lesions lengths were 3.30 ± 1.43 cm for *Q. cyanescens* and 3.37 ± 0.9 cm for *Neos. dimidiatum* (Figure 7). Colonies of the respective fungi were obtained from necrotic tissues of plants inoculated with one or other of the fungi, and identified based on morphology. Control plants did not show any symptoms except those due to wound oxidation.

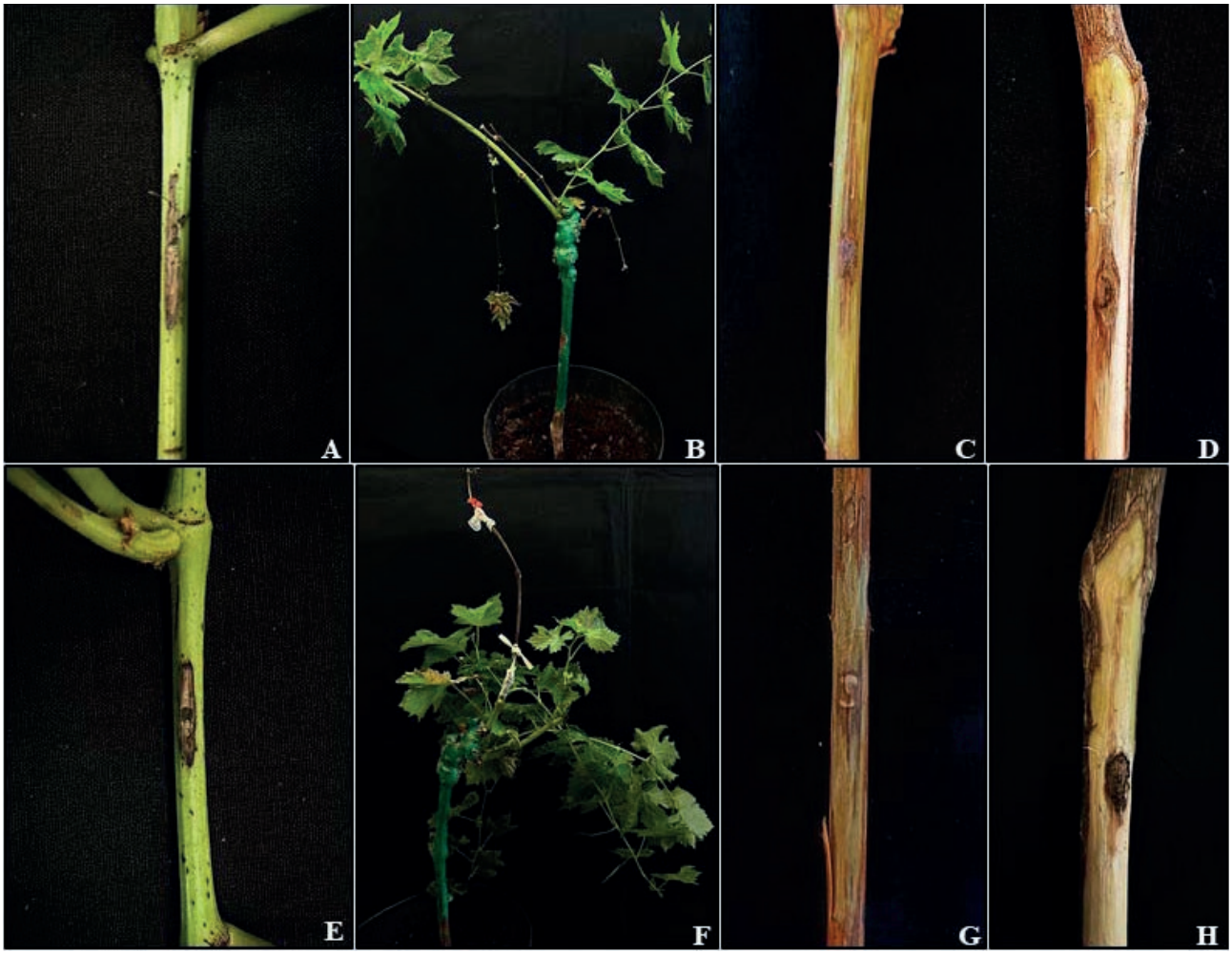

Figure 7. Results of pathogenicity tests with representative isolates of *Quambalaria cyanescens* and *Neoscytalidium dimidiatum*. **A**, external necrotic lesion caused by *Q. cyanescens* on a green shoot at 1 month after inoculation with *Q. cyanescens*. **B**, wilted green shoots caused by *Q. cyanescens* at 3 months post inoculation. **C**, internal necrotic lesion caused by *Q. cyanescens* on a woody shoot at 1 month post inoculation. **D**, internal necrotic lesion caused by *Q. cyanescens* on a rootstock plant 3 months post inoculation. **E**, external necrotic lesion caused by *Neos. dimidiatum* on a green shoot at 1 month post inoculation. **F**, a wilted green shoot caused by *Neos. dimidiatum* at 3 months post inoculation. **G**, internal necrotic lesion caused by *Neos. dimidiatum* on woody shoot at 1 month post inoculation. **H**, internal necrotic lesion caused by *Neos. dimidiatum* on a rootstock plant 3 three months post inoculation.

DISCUSSION

The impacts of fungal pathogens in grapevine propagation material, and within nursery management processes, have been well documented (Gramaje and Armengol, 2011; Gramaje *et al*., 2018). The present study investigated fungi associated with symptomatic table grape cuttings from four Sicilian nurseries exhibiting a high incidence of GTD symptoms. Some of these fungi have been previously associated with these symptoms on grapevines in Italy, and are known to be GTD causal agents in other countries. The isolation frequency from rootstock bases and cutting graft unions showed higher proportions of *Botryosphaeriaceae* species, than isolations from cane bases. It is probable that the large numbers of cuts made during the propagation process in nurseries expose the planting material to infections (Carlucci *et al*., 2015b; Aiello *et al*., 2020).

Sixteen species of *Botryosphaeriaceae* have been reported to be associated with grapevines in Italy (Carlucci *et al*., 2009: Linaldeddu *et al*., 2010; Carlucci *et al*., 2015b; Aiello *et al*., 2023), some of these fungi match those found in the present study (i.e. *N. parvum*, *D. seriata*, *N. australe*, *N. luteum* and *B. dothidea*). These species are important in Italy, as they are increasingly isolated from diseased wood of different plant species, including ornamentals, as reported especially for *N. parvum* (Ismail *et al*., 2013; Guarnaccia *et al*., 2016; Aiello *et al*., 2020; Gusella *et al*., 2020; Bezerra *et al*., 2021; Guselle *et al*., 2021; Aiello *et al*., 2022; Fiorenza *et al*., 2022; Gusella *et al*., 2022).

Phaeomoniella chlamydospora was present in all assessed parts of grapevine cuttings, and this was the predominant species obtained at 15 cm from the cutting bases, while *P. minimum* was isolated less frequently. Both fungi are commonly isolated from grapevine cuttings (Bertelli *et al*.,1998; Mugnai *et al*., 1999; Tegli *et al*., 2000).

Fusarium o*xysporum* and *F. proliferatum* were isolated at relatively high frequencies, mainly from grafting points of young plants, highlighting the role of these points for pathogen access to initiate plant infections (Úrbez-Torres *et al*., 2023). *Fusarium* spp. are common inhabitants in asymptomatic and symptomatic grapevines (Lorenzini and Zapparoli, 2015; Lorenzini *et al*., 2016). These fungi have been reported producing vascular discolourations in California in young grapevines and in association with vines exhibiting trunk disease symptoms California and Mexico (Bustamante *et al*., 2022; Travadon *et al*., 2022; Argüelles-Moyao *et al*., 2024). However, other reports from France and Spain have highlighted the potential role of *Fusarium* spp. as biocontrol agents, showing strain-dependent abilities of the genus (González and Tello, 2011; Bruez *et al*., 2014).

For *Cylindrocarpon*-like species causing black foot of grapevine, *I. lirioendri*, *I. destructans, D. torresensis*, and *D. macrodidyma* were only isolated from rootstock bases, and then only at low frequency (2%). These fungi have been mainly reported on mature grapevines, but in recent years they have become more commonly identified in young nursery plants in Italy (Carlucci *et al.,* 2017).

Well-recognised antagonistic fungi were infrequently isolated, including *Clonostachys rosea*, *Trichoderma* spp., as well as saprophytic and endophytic species of *Entoleuca*, *Aspergillus*, *Alternaria*, *Acremonium* and *Cladosporium*, previously found in association with grapevine (Lo Piccolo *et al*., 2015; Silva-Valderrama *et al*., 2021; Úrbez-Torres *et al*., 2020; Zhu *et al*., 2021). Some of these fungi have been reported to infect grapevine under favourable conditions (Latorre *et al*., 2011; Somma *et al*., 2012; Kizis *et al*., 2014; Bustamante *et al*., 2024; Yurchenko *et al*., 2024). Other fungi recovered at low frequency included *Cadophora* spp., which have been previously reported as grapevine pathogens (Mondello *et al*., 2020; Travadon *et al*., 2022), while *A. xenocordella* has been reported as a causal agent of fruit blight of *Pistacia vera* in Italy (Aiello *et al*., 2018).

Neoscytalidium dimidiatum and *Q. cyanescens* were the most isolated species in the present study, and were obtained from all three isolation points of the investigated cuttings. *Neoscytalidium dimidiatum* (Penz.) Crous & Slippers, 2006 is a polyphagous and cosmopolitan plant and human-associated pathogen. This species has a wide host range and has been reported in 37 countries, associated with 126 plant species belonging to 46 families and 84 genera, including six asymptomatic hosts (Derviş and Özer, 2023). To date, *Neos. dimidiatum* has been reported in associations with grapevine in Africa, North and South America, and Asia (Al-Saadoon *et al*., 2012; Rolshausen *et al*., 2013; Correia *et al*., 2016; Kenfaoui *et al*., 2024). The only data for Italy was from Sicily in 1991, where this fungus was reported as *Natrassia toruloidera* (synonym of *Neos. dimidiatum*) on different wine grape cultivars grafted onto 140 RU rootstocks (Granata and Sidoti, 1991), where the pathogen identification was based only on morphological characters. The fungus was later isolated from symptomatic *Citrus sinensis* (sweet orange) plants showing blight, canker and gummosis symptoms, and from branch canker and dieback of *Meryta denhamii* plants, and was identified through molecular analysis (Polizzi *et al*., 2009; Gusella *et al*., 2023).

Quambalaria cyanescens (de Hoog & G.A. de Vries) Z.W. de Beer, Begerow & R. Bauer is a ubiquitous fun-

gus, isolated from a broad range of ecological niches. In Italy, this fungus has only been reported amongst mycobiota of withered grapes, but its role in the development of GTDs was not assessed (Lorenzini *et al*., 2016). This fungus has also been isolated from human skin and air samples (Sigler *et al*., 1990). Successively, *Q. cyanescens* and other *Quambalaria* spp., have been reported as pathogens on *Eucalyptus* and *Corymbia* plants (de Beer *et al*., 2006; Paap *et al*., 2008). In 2012, *Q. cyanescens* was found in association with GTDs in north-western Iran (Narmani and Arzanlou, 2019), and was isolated from dormant and healthy grapevine cuttings in Turkey (Görür and Akgül, 2019). More recently, Travadon *et al*., (2022) and Argüelles-Moyao *et al*., (2024) reported *Q. cyanescens* from plants exhibiting GTDs in, respectively, California and Mexico. This fungus has been reported from Russia as pollen endophyte of silver birch (*Betula pendula*), as well as in woody hosts, including in flowers of healthy pomegranate and pistachio, in Iran (Antropova *et al*., 2014; Vahedi-Darmiyan *et al*., 2017; Kari Dolatabad *et al*., 2019). However, *Q. cyanescens* has also been associated with diseased vascular tissues of declining almond trees in Iran (Baradaran Bagheri *et al*., 2015). This species was recently reported in association with larvae and pupae of the phyllophagous olive moth, the skins of healthy green frogs, and faeces and larval debris of codling moths on walnut kernels (Oliveira *et al*., 2012; Mahdizadeh *et al*., 2023; Stupar *et al*., 2023). In addition, *Q. cyanescens* has been reported for its broad-spectrum antimicrobial activity against *Aspergillus fumigatus* and *Beauveria bassiana*, pathogens of *Pistacia vera*, and *Colletotrichum acutatum* (Stodůlková *et al*., 2015; Dolatabad *et al*., 2017; Preto *et al*., 2017).

The phylogenetic analysis of the *Neoscytalydium* and *Quambalaria* isolates obtained in the present study confirmed that they belonged, respectively, to *Neos. dimidiatum* and *Q. cyanescens*. All the *Q. cyanescens* isolates were also found to be closely related to *Q. fabacearum*, as previously reported by Narmani and Arzanlou (2019). However, based on the type strains of the two species, *Q. cyanescens* has shorter conidiogenous cells than *Q. fabacearum*, and unlike *Q. fabacearum*, lacks chlamydospores (Bezerra *et al*., 2018; de Hoog and de Vries 1973). Furthermore, the molecular analyses in the present study have shown that the LSU locus is identical in these two species, while six base differences were observed at the ITS region of the *Q. fabacearum* type strain compared to the *Q. cyanescens*.

The growth temperature studies showed that *Neos. dimidiatum* and *Q. cyanescens* both had greatest growth at high temperature. These results explain the increasing spread and incidence of these pathogens in the context of climate change. *Neoscytalydium dimidiatum* was did not grow at 5 and 10°C, and had greatest mycelial approx. 33°C, and also grew very rapidly at that temperature. In contrast, *Q. cyanescens* was able to grow at all the temperatures tested, although growth was slow.

The pathogenicity assessments fulfilled Koch's postulates for isolates of *Neos. dimidiatum* and *Q. cyanescens*, confirming abilities of these fungi to cause disease symptoms on green and woody tissues, both at the grapevine scions and the rootstocks.

GTDs are an aggregate of fungal diseases that are currently considered to be the most destructive biotic factor affecting grapevines (Kanetis *et al*., 2022). Besides their adverse effects on longevity and productivity of established vineyards, GTD pathogens affect the phytosanitary status of grapevine propagation material, resulting in pathogen dissemination and costs associated with vine replanting. The present study results have shown high incidence of GTD pathogens in nursery plants and identified, for the first time, *Neos. dimidiatum* and *Q. cyanescens* as further causal agents within complex of fungi that cause GTDs in Europe, particularly in Italian nurseries. These results highlight the importance of implementing sustainable management strategies for emerging polyphagous plant pathogens that can infect an increasing number of plant species, especially in the context of climate warming. This could contribute to favourable conditions for development and spread of these pathogens in temperate regions.

Further investigations within the GTD complex are required to determine what triggers latent pathogens to transition from endophytic to a pathogenic state, and to cause symptoms on young plants. As the roles of endophytic fungi remain poorly understood, further studies are required elucidate the pathogenicity of *Fusarium* spp. and to investigate the spread of fungi such as *Q. cyanescens* and *Neos. dimidiatum* in table grape plants. The present study results, along with relevant future research, will be valuable for the early detection of fungi involved in GTDs, and for development of increasingly efficient and sustainable disease management strategies.

FUNDING

This study was funded by Piano di incentivi per la ricerca di Ateneo DIME-SIECO 2024-2026 University of Catania (Italy) and PRIN project 2022 PNRR 'New Therapeutic Approaches to Reinforce the Natural Grapevine Microbiome Against Grapevine Trunk Diseases (TARGET_GTDs)'.

DATA AVAILABILITY

Nucleotide sequences of this study are deposited with NCBI GenBank and the accession numbers are reported within this text.

LITERATURE CITED

Aiello D., Gulisano S., Gusella G., Polizzi G., Guarnaccia V., 2018. First report of fruit blight caused by *Arthrinium xenocordella* on *Pistacia vera* in Italy. *Plant Disease* 102(9): 1853. https://doi.org/10.1094/PDIS-02-18-0290-PDN

Aiello D., Gusella G., Fiorenza A., Guarnaccia V., Polizzi G., 2020. Identification of *Neofusicoccum parvum* causing canker and twig blight on *Ficus carica* in Italy. *Phytopathologia Mediterranea* 59(1): 213–218. https://www.jstor.org/stable/27015409

Aiello D., Guarnaccia V., Costanzo M.B., Leonardi G.R., Epifani F., … Polizzi G., 2022. Woody Canker and Shoot Blight Caused by *Botryosphaeriaceae* and *Diaporthaceae* on Mango and Litchi in Italy. *Horticulturae* 8(4): 330. https://doi.org/10.3390/horticulturae8040330

Aiello D., Bregant C., Carlucci A., Guarnaccia V., Gusella G., … Polizzi G., 2023. Current status of *Botryosphaeriaceae* species in Italy: Impacts on agricultural crops and forest ecosystems, *Phytopathologia Mediterranea*, 62(3): 381–412. https://doi.org/10.36253/phyto-14711

Al-Saadoon A. H., Ameen M. K., Hameed M. A. M., Al-Badran A., Ali Z., 2012. First report of grapevine dieback caused by *Lasiodiplodia theobromae* and *Neoscytalidium dimidiatum* in Basrah, Southern Iraq. *African Journal of Biotechnology* 11(95): 16165–16171. https://doi.org/10.5897/AJB12.010

Antropova A. B., Bilanenko E. N., Mokeeva V. L., Chekunova L. N., Kachalkin A. V., … Kamzolkina O. V., 2014. Report of *Quambalaria cyanescens* in association with the birch (*Betula pendula*). *Microbiology* 83: 690–698. https://doi.org/10.1134/S0026261714050038

Argüelles-Moyao A., Ángeles-Argáiz R., Garibay-Orijel R., Pacheco-Aguilar J. R., 2024. Isolation and enzymatic characterization of fungal strains from grapevines with grapevine trunk diseases symptoms in Central Mexico. *Current Microbiology* 81(7): 200. https://doi.org/10.1007/s00284-024-03709-6

Azevedo-Nogueira F., Rego C., Gonçalves H.M.R., Fortes A.M., Gramaje D., Martins-Lopes P., 2022. The road to molecular identification and detection of fungal grapevine trunk diseases. *Frontiers in plant science* 13: 960289. https://doi.org/10.3389/fpls.2022.960289

Baradaran Bagheri M., Arzanlou M., Babai-Ahari A., 2015. Identification of the fungal agents associated with almond Trunk Diseases in East Azerbaijan Province. *Journal of Applied Research in Plant Protection* 4(1): 13–27.

Bertelli E., Mugnai L., Surico G., 1998. Presence of *Phaeoacremonium chlamydosporium* in apparently healthy rooted grapevine cuttings. *Phytopathologia Mediterranea* 37(2): 79–82.

Bezerra J.D.P., Machado A.R., Firmino A.L., Rosado A.W.C., de Souza C.A.F., … Fan X., 2018. Mycological Diversity Description I. *Acta Botanica Brasilica* 32(4): 656–666. https://doi.org/10.1590/0102-33062018abb0154

Bezerra J.D.P., Crous P.W., Aiello D., Gullino M.L., Polizzi G., Guarnaccia V., 2021. Genetic diversity and pathogenicity of *Botryosphaeriaceae* species associated with symptomatic *Citrus* plants in Europe. *Plants* 10(3): 492. https://doi.org/10.3390/plants10030492

Bisiach M., Minervini G., 1985. *Libertella blepharis* A.L. Smith e altri funghi associati ad una sindrome atipica della vite. *Vignevini* 12: 31–35.

Boekhout T., Fell J., O'Donnell K., 1995. Molecular systematics of some yeast-like anamorphs belonging to the Ustilaginales and Tilletiales. *Studies in Mycology* 38: 175–183.

Bruez E., Vallance J., Gerbore J., Lecomte P., Da Costa J-P., … Rey P., 2014. Analyses of the temporal dynamics of fungal communities colonizing the healthy wood tissues of Esca leaf-symptomatic and asymptomatic vines. *PLoS ONE* 9(5): e95928. https://doi.org/10.1371/journal.pone.0095928

Burruano S., Mondello V., Conigliaro G., Alfonzo A., Spagnolo A., Mugnai L., 2008. Grapevine decline in Italy caused by *Lasiodiplodia theobromae*. *Phytopathologia Mediterranea* 47(2): 132–136. https://doi.org/10.14601/Phytopathol_Mediterr-2616

Bustamante M. I., Elfar K., Smith R. J., Bettiga L. J., Tian T., … Eskalen A., 2022. First report of *Fusarium annulatum* associated with young vine decline in California. *Plant Disease* 106(10): 2752. https://doi.org/10.1094/PDIS-12-21-2790-PDN

Bustamante M. I., Elfar K., Kuzmenko J., Zaninovich T., Arreguin M., … Eskalen, A., 2024. Reassessing the etiology of *Aspergillus* vine canker and summer bunch rot of table grapes in California. *Plant Disease* 108(4): 941–950. https://doi.org/10.1094/PDIS-06-23-1137-RE

Campbell C.K., Mulder J.L., 1977. Skin and nail infection by *Scytalidium hyalinum* sp. nov. *Sabouraudia*. 15: 161–166. https://doi.org/10.1080/00362177785190241

Carbone I., Kohn L.M., 1999. A method for designing primer sets for speciation studies in filamentous ascomycetes. *Mycologia* 91: 553–556. https://doi.org/10.1080/00275514.1999.12061051

Carlucci A., Lops F., Raimondo M.L., Gentile V., Mucci M., Frisullo S., 2009. The Botryosphaeria species from vineyards of Apulia. *Phytopathologia Mediterranea* 48(1): 180.

Carlucci A., Cibelli F., Lops F., Phillips A.J.L., Ciccarone C., Raimondo M.L., 2015a. *Pleurostomophora richardsiae* associated with trunk diseases of grapevines in southern Italy. *Phytopathologia Mediterranea* 54(1): 109–123. https://doi.org/10.14601/Phytopathol_Mediterr-15257

Carlucci A., Cibelli F., Lops F., Raimondo M.L., 2015b. Characterization of *Botryosphaeriaceae* species as causal agents of trunk diseases on grapevines. *Plant Disease* 99(12): 1678–1688. https://doi.org/10.1094/PDIS-03-15-0286-RE

Carlucci A., Lops F., Mostert L., Halleen F., Raimondo M. L., 2017. Occurrence fungi causing black foot on young grapevines and nursery rootstock plants in Italy. *Phytopathologia Mediterranea* 56(1):10-39. https://doi.org/10.14601/Phytopathol_Mediterr-18769

Ciccarone C., Graniti A., Schiaffino A., Marras F., 2004. Molecular analysis of *Fomitiporia mediterranea* isolates from esca-affected grapevines in southern Italy. *Phytopathologia Mediterranea* 43(2): 268–272.

Cinelli T., Mondello V., Marchi G., Burruano S., Alves A., Mugnai L., 2016. First report of *Diaporthe eres* associated with cane blight of grapevine (*Vitis vinifera*) in Italy. *Plant Disease* 100(2): 532. https://doi.org/10.1094/PDIS-08-15-0872-PDN

Correia K.C., Silva M.A., Netto M.S.B., Vieira W.A.S., Câmara M.P.S., Michereff S.J., 2016. First report of grapevine dieback caused by *Neoscytalidium hyalinum* in Brazil. *Plant Disease* 100(1): 213. https://doi.org/10.1094/PDIS-03-15-0366-PDN

Cortesi P., Fischer M., Milgroom M.G., 2000. Identification and spread of *Fomitiporia punctata* associated with wood decay of grapevine showing symptoms of esca. *Phytopathology* 90(9): 967–972. https://doi.org/10.1094/PHYTO.2000.90.9.967

Cortesi P., Milgroom M.G., 2001. Outcrossing and diversity of vegetative compatibility types in populations of *Eutypa lata* from grapevines. *Journal of Plant Pathology* 83(2): 79–86.

Cristinzio G., 1978. Gravi attacchi di *Botryosphaeria obtusa* su vite in provincia di Isernia. *Informatore Fitopatologico* 6: 21–23.

Crous P.W., Slippers B., Wingfield M.J., Rheeder J., Marasas W.F., … Groenewald J.Z., 2006. Phylogenetic lineages in the *Botryosphaeriaceae*. *Studies in Mycology* 55(1): 235–253. https://doi.org/10.3114/sim.55.1.235

Dastogeer Mohammad Golam K., Oshita Y., Yasuda M., Kanasugi M., Matsuura E., … Host S., 2020. Specificity of Endophytic Fungi from Stem Tissue of Nature Farming Tomato (*Solanum lycopersicum* Mill.) in Japan. *Agronomy* 10: 1019. https://doi.org/10.3390/agronomy10071019

de Beer Z.W., Begerow D., Bauer R., Pegg G.S., Crous P.W., Wingfield M.J., 2006. Phylogeny of the Quambalariaceae fam. nov., including important *Eucalyptus* pathogens in South Africa and Australia. *Studies in mycology* 55(1): 289–298. https://doi.org/10.3114/sim.55.1.289

de Hoog G.S., de Vries G.A., 1973. Two new species of *Sporothrix* and their relation to *Blastobotrys nivea*. *Antonie van Leeuwenhoek* 39: 515–520. https://doi.org/10.1007/BF02578895

Derviş S., Özer G., 2023. Plant-associated *Neoscytalidium dimidiatum*-taxonomy, host range, epidemiology, virulence, and management strategies: A comprehensive review. *Journal of Fungi* 9(11): 1048. https://doi.org/10.3390/jof9111048

Dolatabad H.K., Javan-Nikkhah M., Shier W.T., 2017. Evaluation of antifungal, phosphate solubilisation, and siderophore and chitinase release activities of endophytic fungi from *Pistacia vera*. *Mycological Progress* 16: 777–790. https://doi.org/10.1007/s11557-017-1315-z

Essakhi S., Mugnai L., Crous P.W., Groenewald J.Z., Surico G., 2008. Molecular and phenotypic characterisation of novel *Phaeoacremonium* species isolated from esca diseased grapevines. *Persoonia-Molecular Phylogeny and Evolution of Fungi* 21(1): 119–134. https://doi.org/10.3767/003158508X374385

Fiorenza A., Aiello D., Costanzo M.B., Gusella G., Polizzi G., 2022. A New Disease for Europe of *Ficus microcarpa* Caused by *Botryosphaeriaceae* Species. *Plants* 11(6): 727. https://doi.org/10.3390/plants11060727

Glass N.L., Donaldson G.C., 1995. Development of primer sets designed for use with the PCR to amplify conserved genes from filamentous ascomycetes. *Applied and Environmental Microbiology* 61(4): 1323–1330. https://doi.org/10.1128/aem.61.4.1323-1330.1995

González V., Tello M.L., 2011. The endophytic mycota associated with *Vitis vinifera* in central Spain. *Fungal Diversity* 47(1): 29–42. https://doi.org/10.1007/s13225-010-0073-x

Görür V., Akgül D.S., 2019. Fungicide suspensions combined with hot-water treatments affect endogenous *Neofusicoccum parvum* infections and endophytic fungi in dormant grapevine canes. *Phytopatho-*

logia Mediterranea 58(3): 559–571. https://doi.org/10.14601/Phyto-10822

Gramaje D., Armengol J., 2011. Fungal trunk pathogens in the grapevine propagation process: potential inoculum sources, detection, identification, and management strategies. *Plant Disease* 95(9):1040-1055. https://doi.org/10.1094/PDIS-01-11-0025

Gramaje D., Úrbez-Torres J. R., Sosnowski M. R., 2018. Managing grapevine trunk diseases with respect to etiology and epidemiology: Current strategies and future prospects. *Plant Disease* 102(1): 12–39. https://doi.org/10.1094/PDIS-04-17-0512-FE

Granata G., Sidoti A., 1991. Grapevine death caused by *Nattrassia toruloidea*. *Vitis* 30: 219–222.

Graniti A., 1960. Il "mal dell'esca" della vite in Puglia. *Italia Agricola* 97: 543–550.

Grasso S., Di San Lio G. M., 1975. Infezioni di *Cylindrocarpon obtusisporum* su piante di vite in Sicilia. *Vitis* 14: 8–39.

Grasso S., 1984. Infezioni di *Fusarium oxysporum* e di *Cylindrocarpon destructans* associate a una moria di giovani piante di vite in Sicilia. *Informatore Fitopatologico* 36(1): 59–63.

Guarnaccia V., Vitale A., Cirvilleri G., Aiello D., Susca A., … Polizzi G. 2016. Characterisation and pathogenicity of fungal species associated with branch cankers and stem-end rot of avocado in Italy. *European Journal of Plant Pathology* 146(4): 963–976. https://doi.org/10.1007/s10658-016-0973-z

Guerin-Dubrana L., Fontaine F., Mugnai L., 2019. Grapevine trunk disease in European and Mediterranean vineyards: occurrence, distribution and associated disease-affecting cultural factors. *Phytopathologia Mediterranea* 58(1): 49–71. https://doi.org/10.13128/Phytopathol_Mediterr-25153

Gusella G., Aiello D., Polizzi G., 2020. First report of leaf and twig blight of Indian hawthorn (*Rhaphiolepis indica*) caused by *Neofusicoccum parvum* in Italy. *Journal of Plant Pathology* 102: 275. https://doi.org/10.1007/s42161-019-00412-5

Gusella G., Costanzo M. B., Aiello D., Polizzi G., 2021. Characterization of *Neofusicoccum parvum* causing canker and dieback on *Brachychiton* species. *European Journal of Plant Pathology* 161: 999–1005. https://doi.org/10.1007/s10658-021-02379-5

Gusella G., Lawrence D.P., Aiello D., Luo Y., Polizzi G., Michailides T., 2022. Etiology of Botryosphaeria Panicle and Shoot Blight of Pistachio (*Pistacia vera*) caused by *Botryosphaeriaceae* in Italy. *Plant Disease* 106(4): 1192–1202. https://doi.org/10.1094/PDIS-08-21-1672-RE

Gusella G., Di Pietro C., Vecchio L., Campo G., Polizzi G. 2023. Branch canker and dieback of *Meryta denhamii* caused by *Neofusicoccum parvum* and *Neoscytalidium dimidiatum* in Italy. Australasian Plant Disease Notes 18(1): 31. https://doi.org/10.1007/s13314-023-00515-0

Hoang D.T., Chernomor O., von Haeseler A., Minh B.Q., Vinh L.S., 2018. UFBoot2: Improving the Ultrafast Bootstrap Approximation. *Molecular Biology and Evolution* 35(2): 518–522. https://doi.org/10.1093/molbev/msx281

Ismail A.M., Cirvilleri G., Lombard L., Crous P.W., Groenewald J.Z., Polizzi G., 2013. Characterisation of *Neofusicoccum* species causing mango dieback in Italy. *Journal of Plant Pathology* 95(3): 549–557. https://www.jstor.org/stable/23721576

Istituto Nazionale di Statistica. Agriculture in 2025. Available online: https://dati.istat.it/ (accessed on 19 April 2025).

Kalyaanamoorthy S., Minh B.Q., Wong T.K.F., von Haeseler A., Jermiin L.S., 2017. ModelFinder: fast model selection for accurate phylogenetic estimates. *Nature Methods* 14(6): 587–589. https://doi.org/10.1038/nmeth.4285

Kanetis L.I., Taliadoros D., Makris G., Christoforou M., 2022. A Novel *Seimatosporium* and Other Sporocadaceae Species Associated with Grapevine Trunk Diseases in Cyprus. *Plants* 11: 2733. https://doi.org/10.3390/plants11202733

Kari Dolatabad H., Asadi Rahmani H., Rejali F., 2019. Identification and evaluation of growth promoting and biocontrol properties of isolated endophytic fungi from the leaves and fruits of Pistacia vera. *Journal of Sol Biology* 7(1): 53–71. https://doi.org/10.22092/sbj.2019.118973

Katoh K., Rozewicki J., Yamada K.D., 2019. MAFFT online service: multiple sequence alignment, interactive sequence choice and visualization. *Briefings in Bioinformatics* 20(4): 1160–1166. https://doi.org/10.1093/bib/bbx108

Kenfaoui J., Amiri S., Goura K., Radouane N., Mennani M., … Lahlali R., 2024. Uncovering the hidden diversity of fungi associated with grapevine trunk diseases in the Moroccan vineyards. *Tropical Plant Pathology* 49: 662–688. https://doi.org/10.1007/s40858-024-00656-2

Kizis D., Natskoulis P., Nychas G.J.E., Panagou E.Z., 2014. Biodiversity and ITS-RFLP characterisation of *Aspergillus* section *Nigri* isolates in grapes from four traditional grape-producing areas in Greece. *PLoS ONE* 9(4): e93923. https://doi.org/10.1371/journal.pone.0093923

Kumar S., Stecher G., Li M., Knyaz C., Tamura K., 2018. MEGA X: Molecular evolutionary genetics analysis

across computing platforms. *Molecular Biology and Evolution* 35: 1547–1549. https://doi.org/10.1093/molbev/msy096

Latorre B.A., Briceño E.X., Torres R., 2011. Increase in *Cladosporium* spp. populations and rot of wine grapes associated with leaf removal. *Crop Protection* 30(1): 52–56. https://doi.org/10.1016/j.cropro.2010.08.022

Linaldeddu B.T., Scanu B., Schiaffino A., Serra S. 2010. First report of *Neofusicoccum australe* associated with grapevine cordon dieback in Italy. *Phytopathologia Mediterranea* 49: 417–420. https://doi.org/10.14601/Phytopathol_Mediterr-8727

Lo Piccolo S., Alfonzo A., Giambra S., Conigliaro G., Lopez-Llorca L.V., Burruano S. 2015. Identification of *Acremonium* isolates from grapevines and evaluation of their antagonism towards *Plasmopara viticola*. *Annals of Microbiology* 65: 2393–2403. https://doi.org/10.1007/s13213-015-1082-5

Lorenzini M., Zapparoli G. 2015. Occurrence and infection of *Cladosporium*, *Fusarium*, *Epicoccum* and *Aureobasidium* in withered rotten grapes during post-harvest dehydration. *Antonie Van Leeuwenhoek* 108: 1171–1180. https://doi.org/10.1007/s10482-015-0570-8

Lorenzini M., Cappello M.S., Logrieco A., Zapparoli G. 2016. Polymorphism and phylogenetic species delimination in filamentous fungi from predominant mycobiota in withered grapes. *International Journal of Food Microbiology* 238: 56–62. https://doi.org/10.1016/j.ijfoodmicro.2016.08.039

Mahdizadeh Z., Narmani A., Arzanlou M., 2023. Phenotypic and molecular characterization of *Quambalaria cyanescens* from walnut kernels infested with codling moth (*Cydia pomonella*) in Iran. *Mycologia Iranica* 10(2): 131–140. https://doi.org/10.22043/MI.2024.365215.1278

Matheny P. B., 2005. Improving phylogenetic inference of mushrooms with RPB1 and RPB2 nucleotide sequences (*Inocybe*; Agaricales). *Molecular Phylogenetics and Evolution* 35(1): 1–20. https://doi.org/10.1016/j.ympev.2004.11.014

Minh B.Q., Schmidt H.A., Chernomor O., Schrempf D., Woodhams M.D., … Lanfear R., 2020. IQ-TREE 2: New models and efficient methods for phylogenetic inference in the genomic era. *Molecular Biology and Evolution* 37(5): 1530–1534. https://doi.org/10.1093/molbev/msaa015

Mondello V., Lo Piccolo S., Conigliaro G., Alfonzo A., Torta L., Burruano S., 2013. First report of *Neofusiccoccum vitifusiforme* and presence of other *Botryosphaeriaceae* species associated with Botryosphaeria dieback of grapevine in Sicily (Italy). *Phytopathologia Mediterranea* 52(2): 388–396. https://www.jstor.org/stable/42685416

Mondello V., Giambra S., Conigliaro G., Francesca N., Burruano S., 2020. Fungal pathogens associated with grapevine trunk diseases in young vineyards in Sicily. *Phytopathologia Mediterranea* 59(3): 453–463. https://doi.org/10.14601/Phyto-11169

Mugnai L., Graniti A., Surico G., 1999. Esca (black measles) and brown wood-streaking: Two old and elusive diseases of grapevines. *Plant Disease* 83(5): 404–418. https://doi.org/10.1094/PDIS.1999.83.5.404

Narmani A., Arzanlou M., 2019. *Quambalaria cyanescens*, a new fungal trunk pathogen associated with grapevine decline in Iran. *Crop Protection* 124: 104875. https://doi.org/10.1016/j.cropro.2019.104875

Oliveira I., Pereira J. A., Lino-Neto T., Bento A., Baptista P., 2012. Fungal diversity associated to the olive moth, *Prays oleae* Bernard: a survey for potential entomopathogenic fungi. *Microbial Ecology* 63: 964–974. https://doi.org/10.1007/s00248-011-9955-z

Paap T., Burgess T.I., McCOMB J.A., Shearer B.L., Hardy G.E.S.J., 2008. *Quambalaria* species, including *Q. coyrecup* sp. nov., implicated in canker and shoot blight diseases causing decline of *Corymbia* species in the southwest of Western Australia. *Mycological Research* 112(1): 57–69. https://doi.org/10.1016/j.mycres.2007.10.005

Petri L., 1912. Osservazioni sopra le alterazioni del legno della vite in seguito a ferite. *Stazioni Sperimentali Agrarie Italiane* 45: 501–547.

Pichierri A., Habib W., Masiello N., Pollastro S., Faretra F., 2009. Occurrence of *Phaemoniella chlamydospora* in grapevine rootstocks and grafted rootstocks: results of a three-year monitoring. *Phytopathologia Mediterranea* 48: 178. https://hdl.handle.net/11586/136234

Pisciotta A., Barone E., Di Lorenzo R., 2022. Table-Grape Cultivation in Soil-Less Systems: A Review. *Horticulturae* 8(6): 553. https://doi.org/10.3390/horticulturae8060553

Polizzi G., Aiello D., Vitale A., Giuffrida F., Groenewald J.Z., Crous P.W., 2009. First Report of shoot blight, canker, and gummosis caused by *Neoscytalidium dimidiatum* on citrus in Italy. *Plant Disease* 93(11): 1215. https://doi.org/10.1094/PDIS-93-11-1215A

Pollastro S., Faretra F., Abbatecola A., Dongiovanni C., 2000. Observations on the fungi associated with esca and on spatial distribution of esca-symptomatic plants in Apulian (Italy) vineyards. *Phytopathologia Mediterranea* 39: 206–210. http://digital.casalini.it/10.1400/57845

Preto G., Martins F., Pereira J. A., Baptista P., 2017. Fungal community in olive fruits of cultivars with different susceptibilities to anthracnose and selection of isolates to be used as biocontrol agents. *Biological Control* 110: 1–9. https://doi.org/10.1016/j.biocontrol.2017.03.011

Raimondo M.L., Lops F., Carlucci A., 2014. *Phaeoacremonium italicum* sp. nov., associated with esca of grapevine in southern Italy. *Mycologia* 106(6): 1119–1126. https://doi.org/10.3852/14-080

Rayner R.W., 1970. A Mycological Colour Chart. *Kew*, Commonwealth Mycological Institute.

Rehner S. A., Buckley E., 2005. A *Beauveria* phylogeny inferred from nuclear ITS and EF1-α sequences: evidence for cryptic diversification and links to *Cordyceps* teleomorphs. *Mycologia* 97(1): 84–98. https://doi.org/10.1080/15572536.2006.11832842

Rolshausen P.E., Akgül D.S., Perez R., Eskalen A., Gispert C., 2013. First report of wood canker caused by *Neoscytalidium dimidiatum* on grapevine in California. *Plant Dis*ease 97(11): 1511. https://doi.org/10.1094/PDIS-04-13-0451-PDN

Ronquist F., Teslenko M., van der Mark P., Ayres D.L., Darling A., … Huelsenbeck. J.P., 2012. MrBayes 3.2: efficient Bayesian phylogenetic inference and model choice across a large model space. *Systematic Biology* 61(3): 539–542. https://doi.org/10.1093/sysbio/sys029

Rovesti L., Montermini A., 1987. Un deperimento della vite causato da *Sphaeropsis malorum* diffuso in provincia di Reggio Emilia. *Informatore Fitopatologico* 37(1): 59–61.

Saccardo P.A., Berlese A.N., 1885. Miscellanea mycologica. Ser. II. Atti dell'Istituto Veneto di Scienze, Lettere ed Arti 6: 711–742.

Schiliro E., Sidoti A., Buonocore E., Di Natale A., Zaffuto G., 1996. Incidenza del mal dell'esca della vite nella Sicilia centro-orientale. *Tecnica agricola*, Anno XLVI-II 2(3): 71–79.

Sidoti A., Buonocore E., Serges T., Mugnai L., 2000. Decline of young grapevines associated with *Phaeoacremonium chlamydosporum* in Sicily (Italy). *Phytopathologia Mediterranea* 39: 87–91.

Sigler L., Harris J.L., Dixon D.M., Flis A. L., Salkin I. F., … Duncan R. A., 1990. Microbiology and potential virulence of *Sporothrix cyanescens*, a fungus rarely isolated from blood and skin. *Journal of Clinical Microbiology* 28(5): 1009–1115. https://doi.org/10.1128/jcm.28.5.1009-1015.1990

Silva-Valderrama I., Toapanta D., Miccono M.L.A., Lolas M., Díaz G.A., … Castro A., 2021. Biocontrol Potential of Grapevine Endophytic and Rhizospheric Fungi Against Trunk Pathogens. *Frontiers in Microbiology* 11: 614620. https://doi.org/10.3389/fmicb.2020.614620

Šišić A., Baćanović-Šišić J., Karlovsky P., Wittwer R., Walder F., … Finckh M.R., 2018. Roots of symptom-free leguminous cover crop and living mulch species harbor diverse *Fusarium* communities that show highly variable aggressiveness on pea (*Pisum sativum*). *PLoS ONE* 13(2): e0191969. https://doi.org/10.1371/journal.pone.0191969

Smith H., Wingfield M.J., Coutinho T.A., Crous P.W., 1996. *Sphaeropsis sapinea* and *Botryosphaeria dothidea* endophytic in *Pinus* spp. and *Eucalyptus* spp. in South Africa. *South African Journal of Botany* 62(2): 86–88. https://doi.org/10.1016/S0254-6299(15)30596-2

Somma S., Perrone G., Logrieco A. F., 2012. Diversity of black Aspergili and mycotoxin risks in grape, wine, and dried vine fruits. *Phytopathologia Mediterranea* 51(1): 131–147. http://www.jstor.org/stable/43872362

Sparapano L., Bruno G., Ciccarone C., Graniti A., 2000a. Infection of grapevines by some fungi associated with esca. I. *Fomitiporia punctata* as a wood-rot inducer. *Phytopathologia mediterranea* 39(1): 46–52. http://digital.casalini.it/10.1400/57810

Sparapano L., Bruno G., Ciccarone C., Graniti A., 2000b. Infection of grapevines by some fungi associated with esca. II. Interaction among *Phaeoacremonium chlamydosporum*, *P. aleophilum* and *Fomitiporia punctata*. *Phytopathologia Mediterranea* 39(1): 53–58. http://digital.casalini.it/10.1400/57811

Sparapano L., Graniti A., Bruno G., 2001. Three-year observation of grapevines cross-inoculated with esca-associated fungi. *Phytopathologia mediterranea* 40: Supplement, S376-S386. http://digital.casalini.it/10.1400/14653

Stodůlková E., Císařová I., Kolařík M., Chudíčková M., Novák P., … Flieger M., 2015. Biologically active metabolites produced by the basidiomycete *Quambalaria cyanescens*. *PLoS One* 10(2): e0118913. https://doi.org/10.1371/journal.pone.0118913

Stupar M., Savković Ž., Breka K., Stamenković S., Krizmanić I., … Grbić M. L., 2023. A variety of fungal species on the green frogs' skin (*Pelophylax esculentus* complex) in South Banat. *Microbial Ecology* 86(2): 859–871. https://doi.org/10.1007/s00248-022-02135-0

Surico G., Bandinelli R., Braccini P., Di Marco S., Marchi G., Mugnai L., Parrini C., 2004. On the factors that may have influenced the esca epidemic in Tuscany in the eighties. *Phytopathologia Mediterranea* 43: 136–143. https://hdl.handle.net/2158/21466

Tegli S., Santilli E., Bertelli E., Surico G., 2000. Genetic variation within *Phaeoacremonium aleophilum* and *P. chlamydosporum* in Italy. *Phytopathologia Mediterranea* 39(1): 125–133.

Thompson J.D., Higgins D.G., Gibson T.J., 1994. CLUSTAL W: improving the sensitivity of progressive multiple sequence alignment through sequence weighting, position-specific gap penalties and weight matrix choice. *Nucleic Acids Research* 22(22): 4673–80. https://doi.org/10.1093/nar/22.22.4673

Travadon R., Lawrence D.P., Moyer M.M., Fujiyoshi P.T., Baumgartner K., 2022. Fungal species associated with grapevine trunk diseases in Washington wine grapes and California table grapes, with novelties in the genera *Cadophora*, *Cytospora*, and *Sporocadus*. *Frontiers in Fungal Biology* 3: 1018140. https://doi.org/10.3389/ffunb.2022.1018140

Uecker F. A., Johnson D.A., 1991. Morphology and taxonomy of species of *Phomopsis* on *Asparagus*. *Mycologia* 83(2):192-199. https://doi.org/10.1080/00275514.1991.12025995

Úrbez-Torres J.R., Tomaselli E., Pollard-Flamand J., Boulé J., Gerin D., Pollastro S., 2020. Characterization of *Trichoderma* isolates from southern Italy, and their potential biocontrol activity against grapevine trunk disease fungi. *Phytopathologia Mediterranea* 59(3): 425–439. https://doi.org/10.14601/Phyto-11273

Úrbez-Torres J.R., Boulé J., Hrycan J., O'Gorman D.T. 2023. Potential role of *Fusarium* spp. in grapevine decline. *Phytopathologia Mediterranea* 62(2): 269–281. https://doi.org/10.36253/phyto-14679

Vahedi-Darmiyan M.E., Jahani M., Mirzaee M.R., Asgari B., 2017. A noteworthy record of endophytic *Quambalaria cyanescens* from *Punica granatum* in Iran. *Czech Mycology* 69(2): 113–123. https://doi.org/10.33585/cmy.69201

Vaidya G., Lohman D.J., Meier R., 2011. SequenceMatrix: concatenation software for the fast assembly of multigene datasets with character set and codon information. *Cladistics* 27: 171–180. https://doi.org/10.1111/j.1096-0031.2010.00329.x

White T.J., Bruns T., Lee S.J.W.T., Taylor J.L., 1990. Amplification and direct sequencing of fungal ribosomal RNA genes for phylogenetics. In: PCR Protocols: A guide to methods and applications (M.A. Innis, D.H. Gelfand, J.J. Sninsky, T.J. White, Ed.), Academic Press, New York, 315–321. https://doi.org/10.1016/B978-0-12-372180-8.50042-1

Yurchenko E, Karpova D, Burovinskaya M, Vinogradova S., 2024. Leaf Spot Caused by *Alternaria* spp. is a new disease of grapevine. *Plants* (Basel)13(23): 3335. https://doi.org/10.3390/plants13233335

Zhu L., Li T., Xu X., Shi X., Wang B., 2021. Succession of fungal communities at different developmental stages of Cabernet Sauvignon grapes from an organic vineyard in Xinjiang. *Frontiers of Microbiology* 12: 718261. https://doi.org/10.3389/fmicb.2021.718261

Phytopathologia Mediterranea
The international journal of the
Mediterranean Phytopathological Union

Firenze University Press
www.fupress.com/pm

Short Notes

Phytophthora hibernalis, *P. lacustris* and *P. multivora* associated with declining *Ligustrum lucidum* trees in an urban park in Portugal

Carlo BREGANT[1,*], Benedetto Teodoro LINALDEDDU[1], Michele NARDUZZI[2], Anna Maria VETTRAINO[2], Artur ALVES[3]

[1] *Dipartimento Territorio e Sistemi Agro-Forestali, Università degli Studi di Padova, Viale dell'Università, 16, 35020 Legnaro, Italy*
[2] *Department for Innovation in Biological, Agro-Food and Forest Systems (DIBAF), University of Tuscia, Viterbo 01100, Italy*
[3] *Centre for Environmental and Marine Studies (CESAM) and Department of Biology, University of Aveiro, 3810-193 Aveiro, Portugal*
*Corresponding author. E-mail: carlo.bregant@unipd.it

Summary. During a monitoring survey carried out in a park in Aveiro, Portugal, typical *Phytophthora* symptoms of root rot, stem bleeding cankers and extensive canopy dieback were observed on mature ornamental glossy privet trees (*Ligustrum lucidum*). A study carried out in spring 2022 aimed to isolate the causal agents, as there is was no available knowledge on potential root pathogens of this host. Thirty-two *Phytophthora* isolates were obtained from inner bark tissues and/or rhizosphere samples (soil and fine roots) collected from 27 declining glossy privet trees. Based on morpho-biometric data and phylogeny of concatenated ITS and *cox*1 sequences, *Phytophthora* isolates were identified as *P. hibernalis* (14 isolates), *P. multivora* (12) and *P. lacustris* (6). Pathogenicity tests confirmed the virulence of the three species on glossy privet. *Phytophthora lacustris* was the most aggressive species, while *P. hibernalis* was most abundant. These results give new insights into emerging *Phytophthora*-related tree diseases in urban areas, and highlight the importance of enhancing biosecurity measures against these invasive pathogens.

Keywords. Emerging disease, *Oomycetes*, urban green areas.

OPEN ACCESS

Citation: Bregant, C., Linaldeddu, B. T., Narduzzi, M., Vettraino, A. M., & Alves, A. (2025). *Phytophthora hibernalis*, *P. lacustris* and *P. multivora* associated with declining *Ligustrum lucidum* trees in an urban park in Portugal. *Phytopathologia Mediterranea* 64(3): 559-566. DOI: 10.36253/phyto-16637

Accepted: September 16, 2025

Published: November 3, 2025

Data Availability Statement: All relevant data are within the paper and its Supporting Information files.

Competing Interests: The Author(s) declare(s) no conflict of interest.

Editor: Matteo Garbelotto, University of California, Berkeley CA, USA.

ORCID:
CB: 0000-0003-1353-7993
BL: 0000-0003-2428-9905
MN: 0009-0004-2205-8649
AV: 0000-0003-0797-3297
AA: 0000-0003-0117-2958

INTRODUCTION

Urban forests and green areas are important components of city life, contributing to a wide range of ecosystem services as well as environmental quality and social well-being (Kabisch *et al*., 2015). However, urban vegetation is particularly vulnerable to disturbances and imbalances arising from biotic, abiotic or anthropogenic factors (Stenhouse, 2005; Threlfall *et al*., 2016). Some external abiotic and anthropogenic stresses, such as air pollution, climate change, limited soil availability, pruning activities and other mechanical damage, can increase plant susceptibility to pathogens and pests

(Oldfield *et al*., 2013; Vettraino *et al*., 2025). Close proximity of ornamental plants with different origins can also facilitate host jumps of pathogens and emergence of new diseases, which can be further promoted by the introduction of infected nursery material (Laurence *et al*., 2024).

Phytophthora species are major pathogens threatening plant health (Scott *et al*., 2019). Research on *Phytophthora* has mainly focused on forest ecosystems, nurseries and agricultural systems (Bose *et al*., 2023; Bregant *et al*., 2023a), whereas urban areas have been relatively understudied for *Phytophthora* presence and impacts on trees. Recent studies have highlighted how urban vegetation is susceptible to root infections by *Phytophthora* (Khdiar *et al*., 2020; Antonelli *et al*., 2023, Laurence *et al*., 2024). Urban areas can be unintentionally exposed to *Phytophthora* pathogens through introduction of infected nursery plants, which may lead to widespread disease outbreaks (Laurence *et al*., 2024). In cities, close proximity of exotic and native species for ornamental purposes may also facilitate host jumps and new diseases. Urban green areas may also serve as reservoirs of *Phytophthora* diversity, and function as entry points for the spread of *Phytophthora* into managed and natural ecosystems. These pathogens are easily moved by human activities, and their abilities to infect plants under a variety of conditions poses challenges for management of urban green spaces (Hulbert *et al*., 2017).

In Portugal, the impact of *Phytophthora* species has been studied in natural ecosystems, forest plantations and nurseries, showing a wide diversity of these organisms, many of which are invasive and polyphagous (Diogo *et al*., 2022; Bregant *et al*., 2023b, 2025; Horta Jung *et al*., 2024). However, no study has investigated the occurrence of these pathogens in urban green spaces in Portugal.

Severe and unusual decline of mature glossy privet trees (*Ligustrum lucidum*) was discovered in a public park in the city of Aveiro (northern Portugal). Research carried out to isolate and characterize the pathogens involved is outlined in the present paper.

MATERIAL AND METHODS

A survey was carried out during winter and spring 2022 in a public park in Aveiro, Portugal (40°38'05.4"N, 8°39'11.0"W). The area includes a series of wetlands and lakes, with many ornamental plant species and a dominance of symptomatic glossy privet (*Ligustrum lucidum*). Disease incidence and mortality rate were estimated along two 25 m transects as described by Bregant *et al*., (2023b). Rhizosphere soil samples including soil and symptomatic fine roots were collected from 27 declining glossy privet trees. Among these, seven trees were randomly chosen for the collection of inner bark tissue samples, which were taken from margins of necrotic lesions at the lower part of trunks.

Phytophthora colonies were isolated using the zoospore trap method of Linderman and Zeitoun (1977), with small changes. Soil plus fine root samples (each of 300 g) were placed in conical flasks and 0.8 L of distilled water was added to each flask. After 24 h, fresh cork oak and *Pittosporum* leaves were placed on the clean water surface and used as baits to capture *Phytophthora* zoospores. The flasks were kept at 18–20°C in laboratory conditions for 5 d. Leaves showing necrotic lesions were then washed in sterile water, cut in small pieces (5 mm^2) and placed in Petri dishes containing the selective substrate PDA+ (Bregant *et al*., 2020). *Phytophthora* isolations were also carried out from inner bark samples taken at tree collars. For each of these samples, outer bark was removed, and ten small fragments were aseptically cut from the lesion margin with a disinfected scalpel and were placed into a Petri dish containing PDA+. All plates were kept at 20°C in the dark. and examined every 12 h. Hyphal tips from emerging mycelium were sub-cultured onto carrot agar (CA) (Erwin and Ribeiro, 1996), and kept at 20°C in the dark.

All isolates obtained were initially grouped into morphotypes, based on colony appearance after 7 d incubation, and morpho-biometric data of reproductive structures (oogonia and sporangia) were recorded using a Motic BA410E microscope. Representative isolates of isolated species were stored on CA slants at -80 °C under 15% glycerol, in the culture collection of Prof Linaldeddu, at the University of Padova, Italy and in the Department of Biology, University of Aveiro, Portugal.

Identities of all isolates were confirmed by molecular analyses. Genomic DNA was extracted from mycelium of 5-d-old pure cultures (Bregant *et al*., 2023a), and internal transcribed spacer regions (ITS) for all isolates were amplified and sequenced using the primers ITS1 and ITS4 (White *et al*., 1990) according to Linaldeddu *et al*. (2023). The primer-pairs FM83/FM84 (Martin and Tooley, 2003) were also used to amplify and sequence a portion of the mitochondrial cytochrome c oxidase subunit I (*cox*1) regions. Amplicons were purified using a EUROGOLD gel extraction kit (EuroClone S.p.A.), following the manufacturer's instructions, and were sequenced by BMR Genomics (University of Padova). Forward and reverse DNA sequences were read and analysed with FinchTV 1.4.0 (Geospiza Inc.). Resulting consensus sequences were then compared though BLAST analysis with reference sequences (ex-type culture or

representative strains) available in GenBank (Altschul *et al*., 1990). Identities of the isolates from glossy privet trees were confirmed when the DNA sequences showed 100% similarity with those of ex-type or representative cultures. Representative ITS and *cox*1 sequences were register at GenBank (Accession numbers: *P. hibernalis* isolate CBP19: PV570382, PV611059; *P. lacustris* isolate CBP161: PV570383, PV611061; *P. multivora* isolate CBP157: PV570384, PV611060).

Concatenated ITS and *cox*1 sequences of three representative *Phytophthora* isolates obtained from glossy privet were analyzed together 24 sequences of nine other *Phytophthora* species representative of the major clades 2, 6 and 8 available in GenBank. Sequence alignments and phylogenetic analyses were carried out as described by Bregant *et al.* (2023a).

Koch's postulates were assessed by inoculating one representative isolate of each *Phytophthora* species (*P. hibernalis* CBP19, *P. lacustris* CBP161, *P. multivora* CBP157) onto the stems of asymptomatic 1-year-old glossy privet seedlings. Inoculations were carried out using the protocol of Linaldeddu *et al*., (2023). Individual inoculation points were each wrapped with sterile damp cotton wool and covered with aluminium foil. Six seedlings were inoculated with each isolate, and six seedlings were each inoculated with a sterile plug of potato dextrose agar (PDA, Oxoid Ltd) as controls. The seedlings were then maintained in natural conditions at 22°C and watered every 2 d. After 15 d, the seedlings were inspected for external and internal disease symptoms, and the extent of necrotic lesions on the stems were assessed. Re-isolations were carried out by placing ten small inner bark samples taken from the margin of each necrotic lesion onto PDA+. Resulting colonies were transferred into PDA and CA plates, and resulting organisms were identified as described above.

Data of necrotic lesion size were checked for normality, then subjected to analysis of variance (one-way ANOVA). Statistically significant differences ($P \leq 0.05$) among mean values were evaluated using Fisher's least significant difference multiple range test in XLSTAT 2008 software (Addinsoft).

RESULTS AND DISCUSSION

The field survey conducted in the public green urban area of Aveiro showed severe decline symptoms and death of ornamental glossy privet trees, including root and collar rot related to soilborne *Phytophthora* infections. Loss of the fine root systems was reflected on the tree canopies by the leaf chloroses, stunted growth, progressive branch dieback, and secondary sudden death (Figure 1). Symptoms were most evident on mature plants, particularly those growing placed close to water. Average disease incidence was 88% of trees affected, with 25% of trees dead.

Direct and indirect (baiting) isolations from glossy privet samples yielded 32 *Phytophthora* isolates belonging to three species (Figure 2). Of these isolates, 27 were from rhizosphere samples and five were from inner bark tissues collected at collar. Based on biometric data of sporangia, colony appearance, and nuclear and mitochondrial sequence data, the 32 isolates were identified as *Phytophthora hibernalis* (14 isolates), *Phytophthora multivora* (12) and *Phytophthora lacustris* (6). *Phytophthora hibernalis* was obtained from 12 rhizosphere samples and two inner bark samples, *P. multivora* was identified from nine rhizosphere samples and three inner bark samples, and *P. lacustris* was identified from six rhizosphere samples. Five of the sampled plants were positive for *P. hibernalis* and *P. multivora*.

Phylogenies obtained using concatenated ITS and *cox*1 sequences placed the isolates in three terminal clades including the ex-type strains of *P. multivora, P. lacustris* and *P. hibernalis* confirming the identifications (Figure 3).

Fifteen days after inoculations the three *Phytophthora* species were pathogenic on glossy privet seedlings, causing dark brown inner bark lesions that spread up and down from the stem inoculation points (Figure 4). Mean lesion sizes differed ($P \leq 0.05$) according to species. The lesions caused after *P. lacustris* inoculations (mean length = 32 ± 5 mm) were larger than those induced by *P. multivora* (19 ± 2 mm) or *P. hibernalis* (14 ± 4 mm). Control seedlings showed oxidative browning at the inoculation sites. *Phytophthora hibernalis, P. lacustris* and *P. multivora* were re-isolated from all the respective inoculated seedlings. No fungi or oomycete colonies were obtained from control seedlings.

The results from this study are the first to demonstrate susceptibility of glossy privet to three *Phytophthora* species which have been associated with the decline of different riparian ecosystems in Europe (Bregant *et al*., 2024). Glossy privet was introduced into Europe for ornamental purposes in the 16th century from China (Fernandez *et al*., 2020). This tree is now naturalized and considered invasive in many European countries, including Portugal (Fernandez *et al*., 2020; Silva *et al*., 2023). Although many biotic threats have been reported for glossy privet, the impacts of *Phytophthora* were unknown (Shaw *et al*., 2018).

Phytophthora hibernalis, *P. lacustris* and *P. multivora* are reported here for the first time in an urban environment of Portugal, although the occurrence of these

Figure 1. Overview of *Phytophthora*-related symptoms observed on *Ligustrum lucidum* (glossy privet). **a** and **b**, photographs of the declining stand near water, examined in the present study. **c**, trees with chlorosis, and **d** and **e**, progressive canopy dieback. **f**, trunk base rot with exudates.

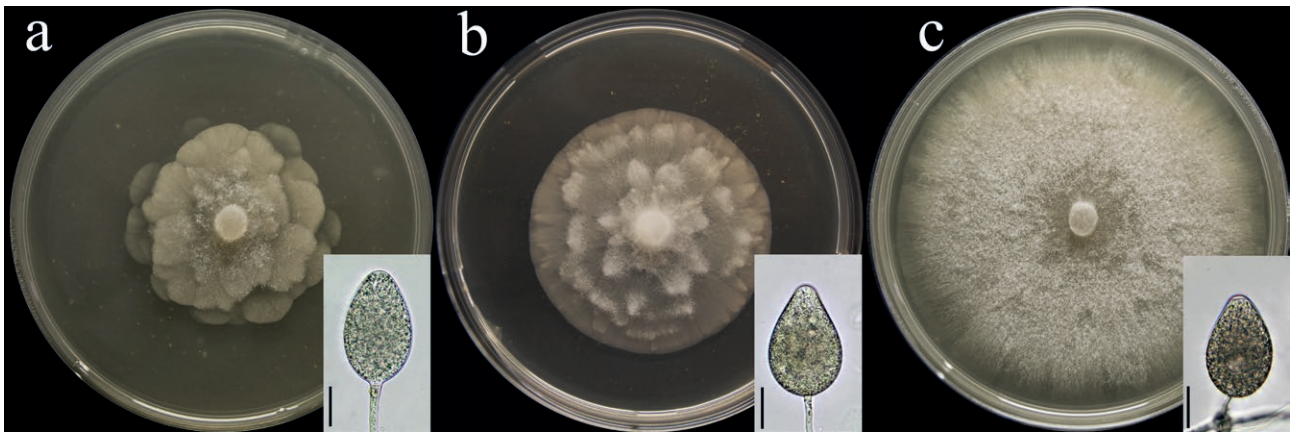

Figure 2. Colony morphologies of *Phytophthora hibernalis* (**a**), *P. lacustris* (**b**) and *P. multivora* (**c**), after 7 d on CA at 20°C in the dark. The insets accompanying the culture photographs show mature sporangia of the respective *Phytophthora* species. Scale bars = 20 µm.

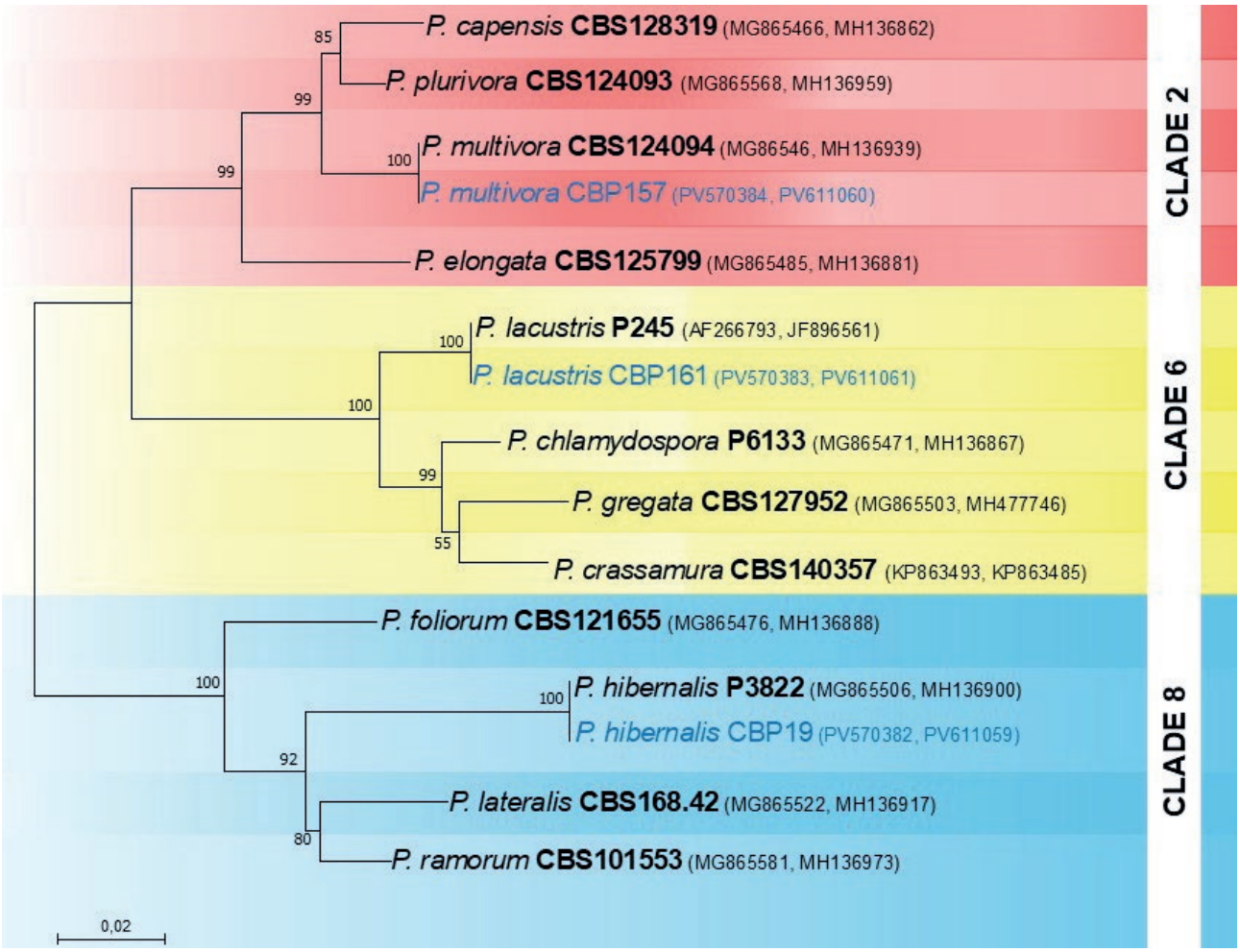

Figure 3. Maximum likelihood tree obtained from concatenated ITS and *cox*1 sequences of selected *Phytophthora* species belonging to the clades 2, 6 and 8. The data are based on the General Time Reversible model. A discrete Gamma distribution was used to model evolutionary rate differences among sites. The tree is drawn to scale, with branch lengths equivalent to numbers of substitutions per site. Bootstrap support values in percentages (1000 replicates) are given at the nodes. Ex-type cultures are in bold font, and isolates obtained in the present study in blue font.

organisms has been extensively documented in several Portuguese forests (Bregant *et al*., 2025). All three species artificially inoculated on asymptomatic glossy privet seedlings colonized and necrotized inner bark tissues of glossy privet. *Phytophthora lacustris* was the most aggressive of these species, while *P. hibernalis* was the most widespread at the investigation site.

Phytophthora hibernalis is a pathogen with broad international distribution although a few records are available (Álvarez *et al*., 2007; Schlenzig *et al*., 2015). Originally, this organism has been associated with collar, root and fruit rots of *Citrus* spp., and recently also in *Eucalyptus globulus* plantations in Portugal near Aveiro (Carne, 1925; Nadel-Schiffmann, 1947; Graham and Feichtenberger, 2015; Bregant *et al*., 2023c). *Phytophthora hibernalis* was the most frequently isolated species in the present study from the monitored site, suggesting an adaptability and potential epidemiological relevance in urban conditions.

Phytophthora lacustris is a widespread species in wet and aquatic environments across Europe (Nechwatal *et al*., 2013). It has been commonly reported as an opportunistic pathogen, but can also be aggressive on some susceptible riparian trees such as *Alnus* spp. (Kanoun-Boulé *et al*., 2016; Bregant *et al*., 2023b; Rial-Martínez *et al*., 2023). Although this species was isolated from rhizosphere soil, it was aggressive towards glossy privet, suggesting requirement for further investigation into the susceptibility of trees used in urban green areas and forests towards this water-borne *Phytophthora* species.

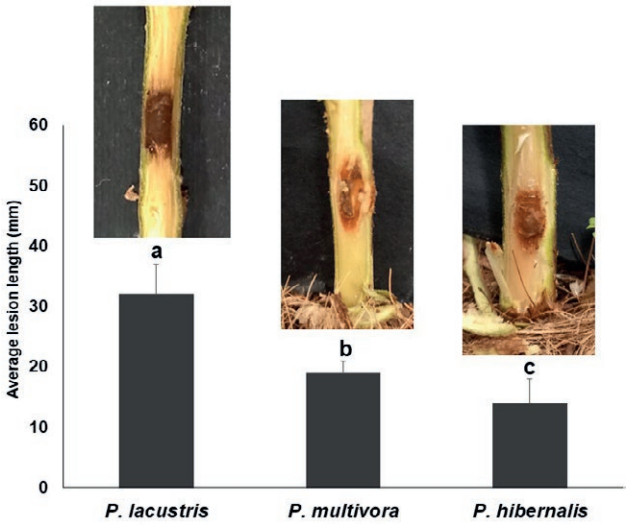

Figure 4. Mean lesion lengths (± standard deviations), and symptoms on 1-year-old *Ligustrum lucidum* seedlings, 15 d after inoculation with *Phytophthora hibernalis* (CBP19) (left), *P. lacustris* (CBP161) (centre), or *P. multivora* (CBP157) (right). The letters accompanying the means indicate differences ($P \leq 0.05$) according to LSD multiple range tests.

Phytophthora multivora is a polyphagous and invasive organism with broad international distribution (Scott *et al*., 2009). In Australia, *P. multivora* has contributed to destruction of many natural habitats dominated by *Eucalyptus* and *Banksia* host species, and several other plants have been reported as hosts, including urban ornamental trees (Burgess *et al*., 2021). In addition to natural environments, *P. multivora* is also widespread in nurseries and urban systems in Australia, where it is the dominant species (Khdiar *et al*., 2020; Burgess *et al*., 2021). The present study is the first to report *P. multivora* in an urban environment of Europe. This species is an emerging organism in Europe and North America with a wide distribution in areas with Mediterranean climate (Tsykun *et al*., 2022; Sims and Garbelotto, 2021; Bregant *et al*., 2023b). In Portugal, *P. multivora* is widespread and is a growing threat to natural ecosystems, timber plantations, and urban green areas as demonstrated in the present study.

In conclusion, results outlined here are the first to demonstrate occurrence of three *Phytophthora* species in an urban area of Portugal. Although interest in plant health within urban environments is increasing, studies addressing the impacts of *Oomycetes* on trees and shrubs used for ornamental proposes in urban contexts have been few (Khdiar *et al*., 2020; Antonelli *et al*., 2024; Laurence *et al*., 2024). These environments may be important for introduction and dissemination of invasive pathogens, and be significant reservoirs of inoculum. The global trade in ornamental plants, together with effects of climate change, may facilitate the spread of invasive species such as *P. multivora* into natural habitats and agroecosystems, posing serious ecological and economic issues.

ACKNOWLEDGEMENTS

This research has been financially supported by the Land Environment Resources and Health (L.E.R.H.) doctoral course (University of Padova) and by national funds through FCT – Fundação para a Ciência e a Tecnologia I.P., under the project/grant UID/50006 + LA/P/0094/2020 (https:// doi.org/10.54499/LA/P/0094/2020).

LITERATURE CITED

Álvarez L.A., Pérez-Sierra A., García-Jiménez J., Abad-Campos P., Landeras E., Alzugaray R., 2007. First report of leaf spot and twig blight of *Rhododendron* spp. caused by *Phytophthora hibernalis* in Spain. *Plant Disease* 91(7): 909. https://doi.org/10.1094/PDIS-91-7-0909A

Antonelli C., Biscontri M., Tabet D., Vettraino A.M., 2023. The never-ending presence of *Phytophthora* species in Italian nurseries. *Pathogens* 12(1): 15. https://doi.org/10.3390/pathogens12010015

Antonelli C., Soulioti N., Linaldeddu B.T., Tsopelas P., Biscontri M., … Vettraino A.M., 2024. *Phytophthora nicotianae* and *Ph. mediterranea*: A biosecurity threat to *Platanus orientalis* and *P. x acerifolia* in urban green areas in Greece. *Urban Forestry and Urban Greening* 95: 128281. https://doi.org/10.1016/j.ufug.2024.128281

Altschul S.F., Gish W., Miller W., Myers E.W., Lipman D. J., 1990. Basic local alignment search tool. *Journal of Molecular Biology* 215(3): 403–410.

Bose T., Spies C.F.J., Hammerbacher A., Coutinho T.A. 2023. *Phytophthora*: an underestimated threat to agriculture, forestry, and natural ecosystems in sub-Saharan Africa. *Mycological Progress* 22(11): 78. https://doi.org/10.1007/s11557-023-01926-0

Bregant C., Sanna G. P., Bottos A., Maddau L., Montecchio L., Linaldeddu B.T., 2020. Diversity and pathogenicity of *Phytophthor*a species associated with declining alder trees in Italy and description of *Phytophthora alpina* sp. nov. *Forests* 11(8), 848. https://doi.org/10.3390/f11080848

Bregant C., Rossetto G., Meli L., Sasso N., Montecchio L., … Linaldeddu B.T. 2023a. Diversity of *Phytophthora*

Species Involved in New Diseases of Mountain Vegetation in Europe with the Description of *Phytophthora pseudogregata* sp. nov. *Forests* 14(8): 1515. https://doi.org/10.3390/f14081515

Bregant C., Batista E., Hilário S., Linaldeddu B.T., Alves A., 2023b. *Phytophthora* species involved in *Alnus glutinosa* decline in Portugal. *Pathogens* 12(2): 276. https://doi.org/10.3390/pathogens12020276

Bregant C., Batista E., Hilário S., Linaldeddu B.T., Alves A., 2023c. First report of *Phytophthora hibernalis*, *P. multivora* and *P. niederhauserii* causing root rot and bleeding cankers on *Eucalyptus globulus* in Portugal. *New Disease Report*s 47(2): e12171. https://doi.org/10.1002/ndr2.12171

Bregant C., Rossetto G., Sasso N., Montecchio L., Maddau L., Linaldeddu B.T., 2024. Diversity and distribution of *Phytophthora* species across different types of riparian vegetation in Italy with the description of *Phytophthora heteromorpha* sp. nov. *International Journal of Systematic and Evolutionary Microbiology* 74: 006272. https://doi.org/10.1099/ijsem.0.006272

Bregant C., Batista E., Hilário S., Linaldeddu B.T., Alves A., 2025. Diversity and Distribution of *Phytophthora* Species Along an Elevation Gradient in Natural and Semi-Natural Forest Ecosystems in Portugal. *Pathogens* 14(1): 103. https://doi.org/10.3390/pathogens14010103

Burgess T.I., Edwards J., Drenth A., Massenbauer T., Cunnington J., … Tan Y.P., 2021. Current status of *Phytophthora* in Australia. *Persoonia* 47(27): 151–177.

Carne W.M., 1925. A brown rot of Citrus in Australia (*Phytophthora hibernalis* n. sp.). CABI Database 12, 13–41.

Diogo E., Machado H., Reis A., Valente C., Phillips A.J., Bragança H., 2023. *Phytophthora alticola* and *Phytophthora cinnamomi* on Eucalyptus globulus in Portugal. *European Journal of Plant Pathology* 165: 255–269. https://doi.org/10.1007/s10658-022-02604-9

Erwin D.C., Ribeiro O.K., 1996. *Phytophthora* diseases worldwide. American Phytopathological Society, Saint Paul, Minnesota, USA. (pp. xii+562).

Fernandez R.D., Ceballos S.J., Aragón R., Malizia A., Montti L., … Grau H.R., 2020. A global review of *Ligustrum lucidum* (*Oleaceae*) invasion. *The Botanical Review* 86: 93–118. https://doi.org/10.1007/s12229-020-09228-w

Graham J., Feichtenberger E., 2015. *Citrus Phytophthora* diseases: management challenges and successes. *Journal of Citrus Pathology* 27203. https://doi.org/10.5070/C421027203

Horta Jung M., Maia C., Mora-Sala B., Abad-Campos P., Schena L., … Jung T., 2025. High diversity of *Phytophthora* species in natural ecosystems and nurseries of Portugal: Detrimental side effect of plant introductions from the age of discovery to modern globalization. *Plant Pathology* 74: 330–362. https://doi.org/10.1111/ppa.14022.

Hulbert J.M., Agne M.C., Burgess T.I., Roets F., Wingfield M.J. 2017. Urban environments provide opportunities for early detections of *Phytophthora* invasions. *Biological Invasions* 19: 3629–3644. https://doi.org/10.1007/s10530-017-1585-z

Kabisch N., Qureshi S., Haase D., 2015. Human–environment interactions in urban green spaces—A systematic review of contemporary issues and prospects for future research. *Environmental Impact Assessment Review* 50(1): 25–34. https://doi.org/10.1016/j.eiar.2014.08.007

Kanoun-Boulé M., Vasconcelos T., Gaspar J., Vieira S., Dias-Ferreira C., Husson C., 2016. *Phytophthora* ×*alni* and *Phytophthora lacustris* associated with common alder decline in Central Portugal. *Forest Pathology* 46(2): 174–176. https://doi.org/10.1111/efp.12273

Khdiar M.Y., Barber P.A., Hardy G.E.S.J., Shaw C., Steel E.J., McMains C., Burgess T.I., 2020. Association of *Phytophthora* with declining vegetation in an urban forest environment. *Microorganisms* 8(7): 973. https://doi.org/10.3390/microorganisms8070973

Laurence M.H., Mertin A.A., Scarlett K., Pang C., Tabassum S., … Summerell B.A., 2024. *Phytophthora* in urban tree planting stock: Are we managing the risk to the urban forest and natural ecosystems? *Plant Pathology* 73(8): 2030–2042. https://doi.org/10.1111/ppa.13960

Linaldeddu B.T., Rossetto G., Maddau L., Vatrano T., Bregant C., 2023. Diversity and pathogenicity of *Botryosphaeriaceae* and *Phytophthora* species associated with emerging olive diseases in Italy. *Agriculture* 13(8): 1575. https://doi.org/10.3390/agriculture13081575

Linderman R.G., Zeitoun F. 1977. *Phytophthora cinnamomi* causing root rot and wilt of nursery-grown native Western azalea and Salal. *Plant Disease Reports* 61: 1045–1048.

Martin F.N., Tooley P.W., 2003. Phylogenetic relationships among P*hytophthora* species inferred from sequence analysis of mitochondrially encoded cytochrome oxidase I and II genes. *Mycologia* 95(2): 269–284.

Nadel-Schiffmann M., 1947. *Phytophthora hibernalis*. *CABI Databases* 1-2, 148–157.

Nechwatal J., Bakonyi J., Cacciola S.O., Cooke D.E.L., Jung T., … Brasier C.M., 2013. The morphology,

behaviour and molecular phylogeny of *Phytophthora* taxon Salixsoil and its redesignation as *Phytophthora lacustris* sp. nov. *Plant Pathology* 62: 355–369. https://doi.org/10.1111/j.1365-3059.2012.02638.x

Oldfield E.E., Warren R.J., Felson A.J., Bradford M.A., 2013. Challenges and future directions in urban afforestation. *Journal of Applied Ecology* 50(5): 1169–1177. https://doi.org/10.1111/1365-2664.12124

Rial-Martínez C., Souto-Herrero M., Piñón-Esteban P., García-González I., Aguín-Casal O., Salinero-Corral C., Vázquez-Ruiz R.A., 2023. First report of root rot caused by *Phytophthora lacustris* on alder (*Alnus lusitanica*) in Spain. *Plant Disease* 107(19): 3322. https://doi.org/10.1094/PDIS-04-23-0793-PDN

Schlenzig A., Campbell R., Chard J., 2015. *Phytophthora* species infecting hardy ornamentals in nurseries and the managed environment in Scotland. *Journal of Phytopathology* 163(7-8): 686–689. https://doi.org/10.1111/jph.12308

Scott P.M., Burgess T.I., Barber P.A., Shearer B.L., Stukely M.J.C., … Jung T., 2009. *Phytophthora multivora* sp. nov., a new species recovered from declining *Eucalyptus, Banksia, Agonis* and other plant species in Western Australia. *Persoonia* 22(3): 1–13. https://doi.org/10.1111/ppa.13312

Scott P., Bader M.K.F., Burgess T.I., Hardy G., Williams N., 2019. Global biogeography and invasion risk of the plant pathogen genus *Phytophthora*. *Environmental Science & Policy* 101(11): 175–182. https://doi.org/10.1016/j.envsci.2019.08.020.

Shaw R.H., Cock M.J., Evans H.C., 2018. The natural enemies of privets (*Ligustrum: Oleaceae*): a literature review, with particular reference to biological control. *CABI Reviews* 13(11): 1–24. https://doi.org/10.1079/PAVSNNR201813011

Silva V., Laguna E., Guillot D., 2023. Novos dados sobre neófitos em Portugal. *Bouteloua* 33: 312–328.

Sims L.L., Garbelotto M., 2021. *Phytophthora* species repeatedly introduced in Northern California through restoration projects can spread into adjacent sites. *Biological Invasions* 23: 2173–2190.

Stenhouse R.N., 2005. Assessing disturbance and vegetation conditions in urban bushlands. Australasian *Journal of Environmental Management* 12: 16–26. https://doi.org/10.1080/14486563.2005.10648630

Threlfall C.G., Ossola A., Hahs A.K., Williams N.S., Wilson L., Livesley S.J., 2016. Variation in vegetation structure and composition across urban green space types. *Frontiers in Ecology and Evolution* 4: 66. https://doi.org/10.3389/fevo.2016.00066

Tsykun T., Prospero S., Schoebel C.N., Rea A., Burgess T.I. 2022. Global invasion history of the emerging plant pathogen *Phytophthora multivora*. *BMC genomics* 23: 153. https://doi.org/10.1186/s12864-022-08363-5

Vettraino A.M., Soulioti N., Matosevic D., Lehtijarvi H.T.D., Woodward S., Santini A., Luchi N., 2025. Management of fungal diseases of *Platanus* under changing climate conditions: case studies in urban areas. *Urban Forestry and Urban Greening* 128750. https://doi.org/10.1016/j.ufug.2025.128750

White T.J., Bruns T., Lee S.J.W.T., Taylor J., 1990. Amplification and direct sequencing of fungal ribosomal RNA genes for phylogenetics. In: (Innis, M.A., Gelfand, D.H., Sninsky, J.J. and White, T.J., ed.)., *PCR Protocols: A Guide to Methods and Applications*, Academic Press, New York, 315-322. https://doi.org/10.1016/B978-0-12-372180-8.50042-1

Phytopathologia Mediterranea
The international journal of the
Mediterranean Phytopathological Union

Firenze University Press
www.fupress.com/pm

Research Papers

Evaluation of silver nanoparticle antifungal activity biosynthesized from *Nigella sativa* extract, against *Aspergillus* species

Abdulrahman S. BAZAID[1,2,*], Husam QANASH[1,2], Ghaida ALSAIF[1,2], Ali Saud ALMALAQ[1,2], Sghair AL-KASEB[1,2], Ahmed M. ABDULFATTAH[3,4], Mohammed F. ABUZINADAH[3,4], Faisal AL-SARRAJ[5], Majid AL-ZAHRANI[6]

[1] *Department of Medical Laboratory Science, College of Applied Medical Sciences, University of Ha'il, Hail 55476, Saudi Arabia*
[2] *Medical and Diagnostic Research Center, University of Ha'il, Hail 55473, Saudi Arabia*
[3] *Department of Medical Laboratory Sciences, Faculty of Applied Medical Sciences, King Abdulaziz University, Jeddah 21589, Saudi Arabia*
[4] *Embryonic Stem Cell Unit, King Fahd Medical Research Center, King Abdulaziz University, Jeddah 21589, Saudi Arabia*
[5] *Department of Biological Sciences, Faculty of Science, King Abdulaziz University, P.O. Box 80203, Jeddah,21589, Saudi Arabia*
[6] *Biological Science Department, College of Science and Art, King Abdulaziz University, Rabigh, Saudi Arabia*
*Corresponding author. E-mail: ar.bazaid@uoh.edu.sa

Summary. Addressing emergent antifungal resistance associated with *Aspergillus* species and public health concerns posed by aflatoxin contamination requires new antifungal strategies. *Nigella sativa* (black seed) has shown promise when integrated with nanotechnology, making it a candidate for reducing aflatoxin risks. Antifungal activity of silver nanoparticles (AgNPs) synthesized using *N. sativa* was assessed against pathogenic *Aspergillus* species, and AgNP effects were assessed on expression of fungal genes related to toxin biosynthesis, membrane integrity, oxidative stress, and apoptosis. Silver nanoparticles were synthesized using aqueous extracts from *N. sativa*, and were spectroscopically characterized, confirming the functional groups involved in nanoparticle stabilization. Antifungal activity and gene expression were demonstrated *in vitro* and *in vivo* against *Aspergillus flavus*, *A. fumigatus*, and *A. niger*. The Ag-NPs biosynthesized by *N. sativa* had antifungal activity (MICs = 40–60 µg mL-1; MFCs = 90–120 µg mL^{-1}), and *A. fumigatus* was the most sensitive strain. Downregulation of aflR was reduced by 68% in *A. flavus*, erg11 by 42–55% in the three fungi, and catA was upregulated by 85–110%. These results indicate that Ag-NPs derived from *N. sativa* exert antifungal activity against *Aspergillus* species by at least two actions, suppression of aflatoxin biosynthesis and antifungal activity. This nanotechnology approach offers promise as a safe and effective alternative to traditional fungicide medications, which requires further in vivo evaluation.

Keywords. Aflatoxin, ergosterol, RT-PCR.

OPEN ACCESS

Citation: Bazaid, A. S., Qanash, H., Alsaif, G., Almalaq, A. S., Al-Kaseb, S., Abdulfattah, A. M., Abuzinadah, M. F., Al-Sarraj, F., & Al-Zahrani, M. (2025). Evaluation of silver nanoparticle antifungal activity biosynthesized from Nigella sativa extract, against Aspergillus species. *Phytopathologia Mediterranea* 64(3): 567-577. DOI: 10.36253/phyto-16620

Accepted: September 30, 2025

Published: December 11, 2025

Data Availability Statement: All relevant data are within the paper and its Supporting Information files.

Competing Interests: The Author(s) declare(s) no conflict of interest.

Editor: Mario Masiello, National Research Council, (CNR), Bari, Italy.

ORCID:
ASB: 0000-0002-5884-0278
HQ: 0000-0002-3068-0313
GA: 0000-0002-9619-8538
AMA: 0009-0002-7822-9537
FAS: 0000-0002-5017-3570
MAZ: 0000-0003-0781-0121

INTRODUCTION

Mycotic infections are important in human and animal health and agriculture, particularly those caused by *Aspergillus* spp., which are important fungal pathogens. The most common and invasive species are *A. flavus*, *A. fumigatus*, and *A. niger*. These species are also plant pathogens, infecting agricultural crops both in the field and post-harvest. These fungi infect different crops and human foods, and contaminate food with mycotoxins (Zakaria, 2024). Aflatoxins, primarily associated with *A. flavus*, are the most potent natural carcinogens, causing immunosuppression, liver cancer and growth retardation in humans and animals (Mallmann *et al*., 2015; Awuchi *et al*., 2021).

Current antifungal treatments mostly rely on chemical compounds that target fungal cells through various mechanisms, including azoles, which inhibit ergosterol synthesis,echinocandins, which disrupt cell wall formation, and polyenes, which damage membrane-bound structures. Despite these options, treating fungal infections remains challenging due to increasing drug resistance, high cost of treatments, potential drug toxicity, and narrow ranges of effectiveness of available medications (Gupta and Tomas, 2003; Berger *et al*., 2017; Machado *et al*., 2017).

Azoles, polyenes, and echinocandins are the primary fungicides used, although there is increasing concern due to the increasing resistance in pathogens to these treatments which weakens treatment strategies and increases requirement for development of new antifungal compounds (Gupta and Tomas, 2003; Machado *et al*., 2017). Alongside human medicine, application of chemical fungicides has contributed to the development of pathogenic fungi that are resistant to these compounds, along with other ecological problems (Atanda *et al*., 2005; Berger *et al*., 2017).

Research has shown that common fungal infections, especially those caused by *Aspergillus*, are becoming increasingly difficult to treat with the usually used azoles (Gupta and Tomas, 2003). In agronomy, overuse of fungicides such as triazoles and benzimidazoles has led to emergence of resistant fungal strains, and has contributed to environmental pollution, posing potential human health risks (Berger *et al*., 2017; Machado *et al*., 2017).

For these reasons herbal plants are becoming popular as sources for new medicines that have antimicrobial and antifungal properties. *Nigella sativa* (black cumin) is a traditional herb that is widely used in Egypt and other regions. This plant has pharmacological properties including antimicrobial, antioxidant, anti-inflammatory, anticancer, and immunomodulatory effects (Vijayakumar *et al*., 2021; Mossa *et al*., 2023; Abbas *et al*., 2024). The seeds of *N. sativa* are rich in bioactive compounds including thymoquinone, p-cymene, carvacrol, thymohydroquinone, and flavonoids, which are medicinally important (Vijayakumar *et al*., 2021; Abbas *et al*., 2024).

Research has shown that phytochemicals of *N. sativa* are active against a range of gram negative and gram positive bacteria, viruses and fungi (Mossa *et al*., 2023; Abbas *et al*., 2024), and antifungal properties of these compounds have been reported against filamentous fungi, including *Aspergillus* spp. (Vijayakumar *et al*., 2021; Mossa *et al*., 2023). The phytochemicals of *N. sativa* disrupt microbial cell membranes and metabolism, and cause oxidative stress which has antimicrobial effects (Abbas *et al*., 2024).

Nanotechnology offers effective methods for enhancing the antimicrobial properties of plant-based compounds. The antifungal activity of silver nanoparticles (AgNPs) has gained particular attention because of their multiple antimicrobial properties (Franci *et al*., 2015; Gholamnezhad *et al*., 2016). Synthesis of AgNPs using plant extracts ("biogenic synthesis,") is beneficial when compared to physical and chemical syntheses, because it is economical, environmentally-friendly, and the particles are biologically active (Gopinath *et al*., 2017; Vijayakumar *et al*., 2021; El-Seedi *et al*., 2024; Pirbalouti *et al*., 2024; Badmos et al., 2025). AgNPs can be synthesized from various plant extracts (Mallmann *et al*., 2015; Gibała *et al*., 2021; Hashem *et al*., 2022; Pirbalouti *et al*., 2024). These plant-mediated AgNPs contain silver ions which are combined with bioactive molecules from plants (El-Seedi *et al*., 2024).

Although research has examined the use of AgNPs as antifungal agents, their molecular mechanisms of action against fungi have not been elucidated. Important molecular markers for antifungal action include the aflatoxin regulatory gene *aflR*, *erg11* which encodes lanosterol 14α-demethylase involved in ergosterol biosynthesis, and *catA* the oxidative stress contributing catalase gene. These genes are useful for probing antifungal responses in fungi (Deabes *et al*., 2018; Peng *et al*., 2018).

Downregulation of *aflR* probably causes aflatoxin production to be blocked. Similarly, suppressing *erg11* probably disrupts ergosterol biosynthesis, which is a key membrane component in fungi. Upregulation of *catA* may result in increased nanoparticle exposure and heightened oxidative stress (Franci *et al*., 2015). RT-PCR allows monitoring of changes in gene expression in fungi due to treatments with antifungal agents, thus enabling real time tracking of gene expression changes in these organisms.

The present study has addressed two major problems: the growing resistance of *Aspergillus* species to

antifungal compounds, and the dangers posed by aflatoxins. By observing molecular markers, this research aimed to determine how AgNPs synthesized from *N. sativa* exert antifungal effects. This knowledge could allow the design of new and safe antifungal therapies.

MATERIALS AND METHODS

Preparation of Nigella sativa *extract*

Nigella sativa seeds were procured from a certified herbal outlet in Alexandria, Egypt. The seeds were washed with distilled water and air dried at room temperature (25 ± 2°C), then finely ground using a laboratory grinder. An extraction was carried out from 10 g of powdered seeds, using 100 mL of double distilled water, which was stirred continuously at 60°C for 60 min. The mixture was then filtered through Whatman No.1 filter paper, and the clear filtrate was kept at 4°C until used for nanoparticle synthesis.

Biosynthesis of silver nanoparticles

The green synthesis was performed by mixing 10 mL of the aqueous extract of *N. sativa* with 90 mL of 1mM solution of silver nitrate ($AgNO_3$) in sterile tubes. The reaction mixture was incubated at room temperature (25°C) in the dark with 150 rpm shaking for 24 h. The silver nanoparticles were visually confirmed by colour change from pale yellow to dark brown (Figure 1), which indicates surface plasmon resonance (SPR) of silver nanoparticles (Ahmed *et al*., 2016).

The synthesized nanoparticles were collected and concentrated by centrifugation at 12,000 rpm for 15 min. They were then washed three times with distilled water plus ethanol to remove unreacted residues, and were then dried in a vacuum desiccator. The dried nanoparticles were stored in sterile containers at 4°C, until characterization and bioactivity assessments were carried out.

Figure 1. The synthesized silver nanoparticles showed a dark colour in solution (left).

Characterization of synthesized silver nanoparticles

The biosynthesized silver nanoparticles were characterized using the following techniques:

UV–Visible spectroscopy. Absorption spectra within the range of 300–700 nm were recorded on a UV-Vis spectrophotometer (Shimadzu), for confirmation of nanoparticle synthesis and stability.

Fourier Transform Infrared Spectroscopy (FTIR). FTIR was used to detect functional groups for reduction and stabilization of the biosynthesized nanoparticles. The dried nanoparticle powder was mixed with potassium bromide (KBr) in a 1:100 ratio, and a Shimadzu FTIR (Shimadzu 8400S) spectrophotometer was used to scan the resulting spectra. The resulting FTIR spectrum was scanned in wave numbers from 500 cm^{-1} to 4000 cm^{-1}.

X-ray Diffraction (XRD). The crystallinity of the nanoparticles was assessed by recording of XRD patterns.

Transmission Electron Microscopy. Morphology, size and shape of the selenium nanoparticles were analyzed using a transmission electron microscope (TEM) (JEOL model JEM-2100), The aqueous suspension of AgNPs was ultrasonically dispersed, and the sample was prepared by adding a drop of the suspension onto a carbon-coated copper grid, and this was then dried using an IR lamp. Micrographs were capture using 80 kV accelerating voltage. The pattern of size distribution for the particles was determined by measuring and counting of 200 separate particles from TEM images.

Fungus cultivation and inoculum preparation

A collection of previously identified fungi was provided by Dr Elsayed Shabaan, Plant Protection and Biodiagnostics Department, Arid Land Cultivation Research Institute (ALCRI), City of Scientific Research and Technological Applications (SRTA-CITY), Alexandria, Egypt. This included *Aspergillus flavus* (KJ831193), *Aspergillus fumigatus* (KJ831194), and *Aspergillus niger* (ATCC 16888).

The *Aspergillus* species were grown on Sabouraud Dextrose Agar (SDA) plates for 5 to 7 d at 28°C. Resulting conidia were collected by rinsing the plates with sterile saline containing 0.1% Tween 80, which was then filtered through sterile gauze to remove mycelium debris. Using a hemocytometer, the conidium concentration was adjusted to 1×10^6 conidia mL^{-1}.

In vitro *assessments of antifungal activity*

Disk diffusion assay

Based on CLSI M38-A2 guidelines (Clinical and Laboratory Standards Institute, 2015), the antifungal activity of the synthesized AgNP was assessed using the disk diffusion method. Fungal spore suspension (100 µL) was evenly spread on the surface of each SDA plate. Sterile paper disks (6 mm diam.) previously loaded with 50 µL of AgNPs at concentrations between 25 and 200 µg mL^{-1} were then placed on the inoculated plates. The plates were then incubated at 28°C for 48 h, after which resulting zones of inhibition were measured.

Minimum Inhibitory Concentrations (MIC) and Minimum Fungicidal Concentrations (MFC)

MICs and MFCs were analyzed using the broth microdilution method, following CLSI guidelines (M38-A2). In 96-well microtiter plates containing Sabouraud Dextrose Broth (SDB), two-fold serial dilutions of AgNPs (from 5 to 200 µg mL^{-1}) were prepared. Each well was then inoculated with 100 µL of conidium suspension (1×10^4 conidia mL^{-1}). The plates were then incubated at 28°C for 48 h. The MIC was defined as the lowest AgNP concentration at which no fungal growth was observed. For MFC determination, aliquots (as above) were sub-cultured onto SDA plates, and the lowest concentration at which no fungal colonies were observed after 72 h incubation at 28°C was recorded as the MFC.

Bioactive compound analysis using GC-MS

A Gas Chromatography-Mass Spectrometry (GC-MS) analysis was carried out to identify the phytochemical constituents responsible for antifungal activities of *N. sativa* extract. Chemical profiling of *N. sativa* aqueous extract was carried out after freeze-drying to yield a 10 mL portion. This was re-dissolved in 2 mL of methanol, and the solution was filtered using a 0.22 µm syringe filter. The solution was then analyzed using a GC-MS system (Agilent 7890A) with a 5975C MS detector. The separation was carried out in an HP-5MS capillary column (30 m × 0.25 mm, 0.25 µm film thickness). The oven temperature was set to rise from 60°C (3 min hold) to 280°C with a ramp of 10°C min^{-1}. The carrier gas was helium with constant flow of 1.0 mL min^{-1}, the injector was set at 250°C, and a volume of 1 µL was used for injection in splitless mode. Mass spectra were collected in EI mode at 70 eV. Items in the sample were identified from elative indices and mass spectra (RI-MS) matching against WILEY and National Institute of Standards and Technology (NIST08) library data (http://webbook.nist.gov; accessed 20 November 2021), supplied with the computer-controlled GC-MS system.

RNA extraction and cDNA synthesis

Aspergillus cultures were treated with sub-inhibitory concentrations of AgNPs (at MIC/2), and were then incubated for 24 h. Total RNA was extracted from treated and untreated cultures using TRIzol reagent (Invitrogen). RNA purity and concentrations were assessed using NanoDrop spectrophotometry (Thermo Fisher Scientific). High-quality RNA (A260/A280 ratio between 1.8 and 2.0) underwent cDNA synthesis using the RevertAid First Strand cDNA Synthesis Kit (Thermo Fisher Scientific).

Real-Time quantitative PCR (RT-qPCR)

Expressions of *aflR*, *erg11*, and catA genes were analyzed using RT-qPCR with SYBR Green detection on an Applied Biosystems StepOnePlus Real-Time PCR System (Thermo Fisher Scientific). Each reaction contained 10 µL of SYBR Green Master Mix, 1 µL each of forward and reverse primers (10 µM), 2 µL of cDNA template, and 6 µL of nuclease free water, in a total volume of 20 µL. The β-actin gene was used as an internal control. The thermal cycling conditions were as follows: initial denaturation at 95°C for 5 min; 40 cycles each of denaturation at 95°C for 15 sec, annealing at 60°C for 30 sec, and extension at 72°C for 30 sec. All reactions were carried out in triplicate. Relative gene expression was calculated using the 2^−ΔΔCt method (Livak and Schmittgen, 2001).

In planta *biocontrol assay using banana tissue culture*

Banana plantlets (*Musa* spp.) were used for the *in planta* assay, to replicate post-harvest scenarios where *A. flavus* is known to grow on a variety of fruits and stored foods which are left unprotected. The technique using banana tissue culture allows for the observation of fungal colonization and antifungal activity under conditions of fungal infection devoid of contamination, using a standardized tissue culture method. *Aspergillus flavus* is not a classical pathogen of the banana, yet, in the present study experiments, banana plantlets inoculated with this fungus exhibited chlorosis, necrosis and browning at

the bases of pseudostems. This model system provided a repeatable process for determining *in planta* biocontrol activity of AgNPs against *A. flavus*. An *in vitro* assay to test the antifungal activity of *N. sativa*-mediated AgNPs was also carried out using sterile tissue cultured banana plantlets (*Musa* spp.).

Banana shoot tips were procured from healthy suckers and were surface sterilized using 70% ethanol for 1 min followed by 20% sodium hypochlorite for 15 min, and then rinsing three times in sterilized distilled water. The explants were then inoculated onto Murashige and Skoog (MS) medium containing 3% sucrose and 2 mg L^{-1} 6-benzylaminopurine (BAP), for shoot multiplication. The shoots were then incubated at 25°C in 16 h light/8 h darkness. After 3 weeks, healthy banana plantlets were each inoculated at the pseudostem base with 10 µL of *A. flavus* conidium suspension (1×10^6 conidia L^{-1}), using a sterile micropipette. Inoculated plants were then maintained for 24 h before interventions were made. AgNPs were administered through a sterile micropipette tip just proximal to the *A. flavus* inoculation sites.

Experimental designs

The experiments were of randomized layouts. For all *in vitro* analyses (disk diffusion, MIC, and MFC), treatments were applied in a fully random fashion across microtiter plates and culture dishes. Each treatment was applied to three independent biological replicates, each of which had three technical repeats. For the *in planta* banana experiment, plantlets were randomly assigned to treatment groups (infected only, infected + 50 µg mL^{-1} AgNPs, infected + 100 µg mL^{-1} AgNPs). Each treatment group consisted of ten plantlets, and the experiment was independently conducted twice. The following parameters were recorded at 7 d following treatments: symptom scoring (yellowing and necrosis) on a 0 to 5 scale; fungal re-isolation on PDA to confirm colonization; tissue aflatoxin B1 quantification by ELISA; and photographic documentation of disease phenotypes.

Statistical analyses

All data were analyzed using SPSS software (Version 22.0; IBM Corp.). Results were expressed as means ± standard deviations (SD). Differences between treated and control groups were analyzed using Student's t-test at $P < 0.05$. Mean values, each from two replicates, were recorded.

RESULTS

GC-MS profile of Nigella sativa *extract*

Analysis by GC-MS of the aqueous extract from *N. sativa* showed several bioactive compounds. The most important constituents are described in Table 1.

Characterization of biosynthesized silver nanoparticles

The successful synthesis of AgNPs using *N. sativa* extract was confirmed by multiple characterization techniques. UV-Visible Spectroscopy gave an absorption peak at 428 nm, indicating presence of surface plasmon resonance for silver ions, confirming formation of the AgNPs (Figure 2A). FTIR analysis showed characteristic peaks corresponding to -OH, C=O, and -NH bonds, indicating secondary metabolites responsible for stabilization of the nanoparticles (Figure 2B).

The AgNPs produced by the biological method were first examined by X-ray diffraction (XRD) (Figure 3). The resulting pattern had four sharp peaks with respective approx. 2θ values of 36°, 42°, 60°, and 74°. These correspond, respectively, to the (111), (200), (220), and (311) crystal planes of silver. These reflections confirm that the nanoparticles had a face-centered cubic (fcc) lattice, verifying that well-formed crystalline AgNPs had been synthesized. The strongest (111) peak indicates that most particles preferentially grew along this direction, a behaviour frequently observed in metal nanoparticles made with plant extracts.

Table 1. Major bioactive compounds identified from *Nigella sativa* using GC-MS.

Mean retention time (min)	Compound name	Molecular formula	Mean peak area (%)	Reported biological activity	References
7.85	Thymoquinone	$C_{10}H_{12}O_2$	29.4	Antifungal, antioxidant, anti-inflammatory	Khader and Eckl (2014)
9.14	p-Cymene	$C_{10}H_{14}$	17.6	Antimicrobial, membrane disruption	Burt *et al.*, 2007
10.62	α-Thujene	$C_{10}H_{16}$	11.2	Antioxidant, antifungal	Kanika and Satyawati, (2022)
11.45	Carvacrol	$C_{10}H_{14}O$	9.8	Antifungal, anti-biofilm	Gómez-Sequeda *et al.*, (2020)
13.71	Thymol	$C_{10}H_{14}O$	6.3	Antiseptic, antifungal	Jung *et al.*, (2021)
16.27	Linoleic acid	$C_{18}H_{32}O_2$	5.1	Membrane disruption, anti-aflatoxin	Wu *et al.*, (2022)

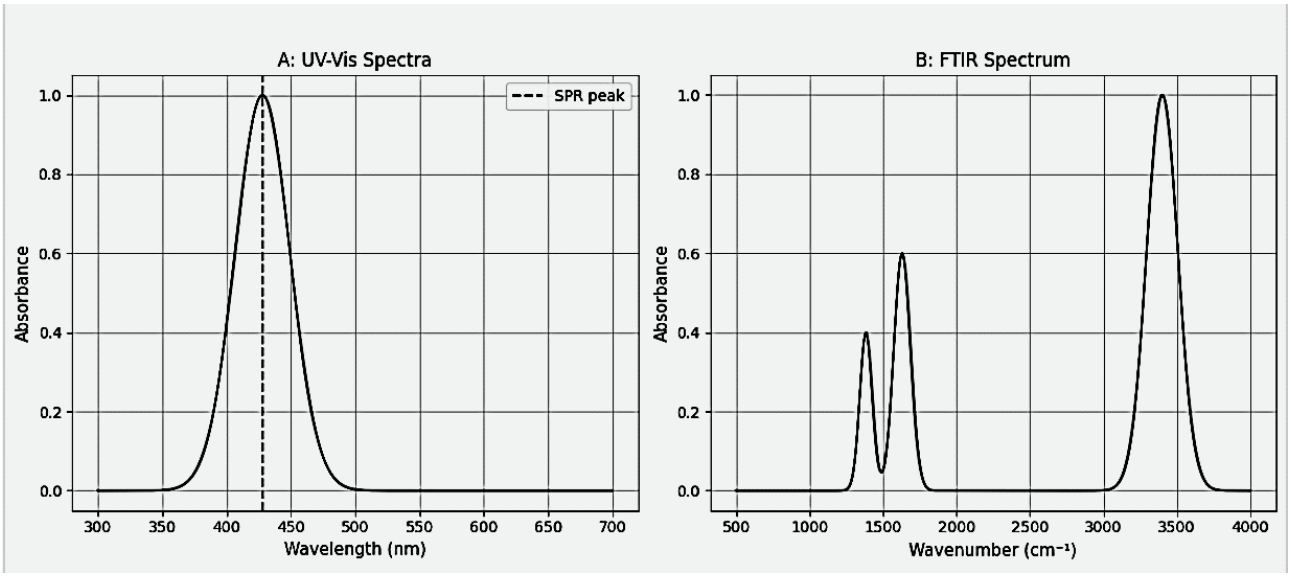

Figure 2. Spectra for characterization of silver nanoparticles.

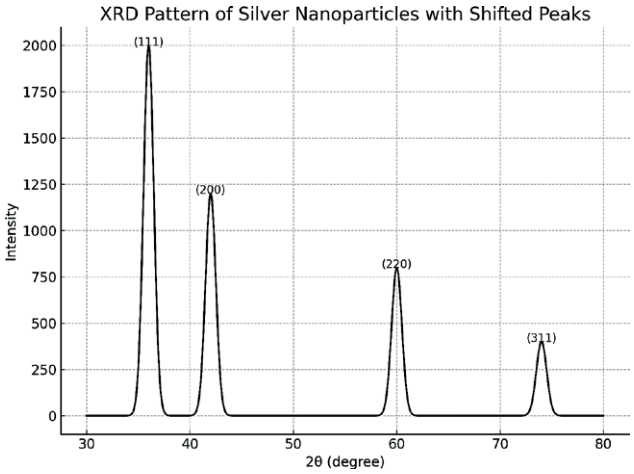

Figure 3. X-ray Diffraction (XRD) pattern for silver nanoparticles.

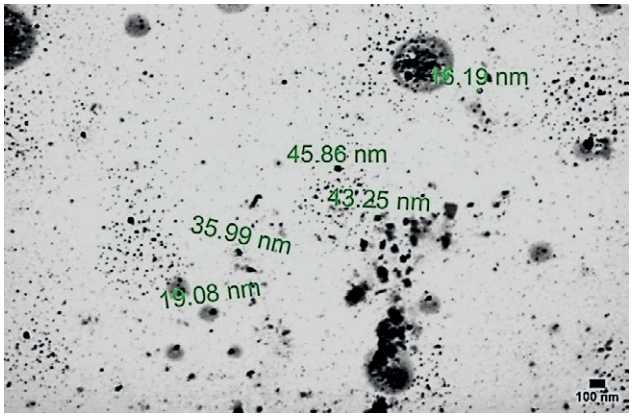

Figure 4. Nanoparticle sizes and shapes shown using transmission electron microscopy.

The minor shifts of the peaks away from standard positions probably arose from internal strain or small crystal size, features typical of biosyntheticized and low-temperature materials. No extra peaks appeared in the pattern, confirming that the product was phase-pure and free of detectable impurities from other silver allotropes.

TEM images (Figure 4) showed that the nanoparticles are mostly spherical or nearly so, and were evenly distributed with little clustering. Size annotations in Figure 4 indicate nanoparticle diameters from approx. 16.19 nm to 45.86 nm, affirming that the particles occupy the nanoscale needed for strong biological activity. This size range matches the histogram generated by image analysis software, which identified an average diameter of approx. 27 nm.

Antifungal activity of Nigella sativa*-mediated silver nanoparticles*

Diameters of inhibition zones increased with increasing AgNP concentrations in a dose-dependent manner (Figure 5). The antifungal effects of the synthesized AgNPs on the isolates of *A. flavus, A. fumigatus,* and *A. niger* assessed in the disk diffusion, MIC and MFC assays are summarized in Table 2. *Aspergillus fumigatus* (KJ831194) was the most sensitive isolate to

Table 2. The minimum inhibitory concentrations (MIC) and minimum fungicidal concentrations (MFC) against three *Aspergillus* spp. isolates.

Fungus isolate	MIC (μg mL^{-1})	MFC (μg mL^{-1})
A. flavus (KJ831193)	50	100
A. fumigatus (KJ831194)	40	90
A. niger (ATCC 16888)	60	120

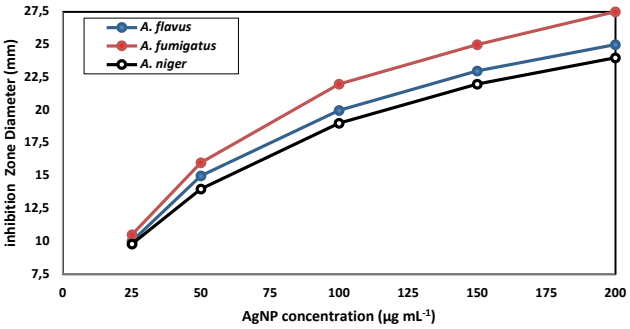

Figure 5. Mean diameters of culture inhibition zones for three Aspergillus spp. isolates grown in cultures containing different AgNP concentrations.

AgNPs, while *A. niger* (ATCC 16888) had comparatively greater MIC and MFC values.

Antifungal effects on banana plantlets

Quantification of *in planta* fungus recovery relied on banana tissue colonization by *A. flavus* assessed from re-isolation frequency. A piece of surface sterilized pseudostem base tissue was removed from each plantlet at 1 week intervals, and *A. flavus* re-isolation frequency was determined on PDA plates. Each treatment yielding *A. flavus* was recorded and the frequency of recovery of *A. flavus* was computed (Figure 6). This metric, in conjunction with *A. flavus* sample populations, determined the degree of colonization and the effectiveness of AgNP treatment in mitigating fungal persistence.

In untreated cultures, *A. flavus* (KJ831193)-inoculated banana plantlets developed severe chloroses and pseudostem tissue browning necroses, with a mean symptom score of 4.5 ± 0.3. AgNP treatment induced a dose-dependent protective response. Plantlets treated with 50 μg mL^{-1} AgNPs had mild necroses, with a symptom score of 2.3 ± 0.4, while those treated with 100 μg mL^{-1} AgNPs displayed almost normal morphology, with a symptom score of 1.1 ± 0.3. Fungus re-isolations assays resulted in dense fungal growth from untreated samples,

Table 3. Mean concentrations of aflatoxin B1 in banana plantlets treated with different amounts of AgNPs after inoculation with Aspergillus flavus.

Treatment	Mean aflatoxin B1 concentration (ppb)*
Inoculated only	142.7 ± 5.9
Inoculated, + 50 μg /mL^{-1} AgNPs	52.1 ± 3.4
Inoculated, + 100 μg mL^{-1} AgNPs	19.6 ± 2.8

*All differences in means were statistically significant ($P < 0.01$).

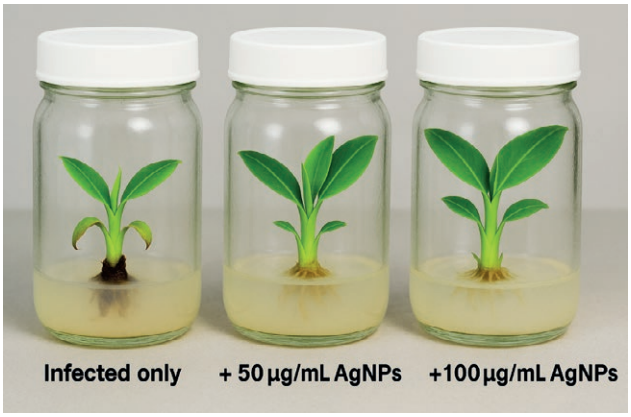

Figure 6. Banana plantlets treated with different concentrations of AgNPs.

whereas plantlets treated with AgNPs gave reduced fungus recovery.

RT-qPCR gene expression results

Expression of genes related to aflatoxin biosynthesis (*aflR*), ergosterol synthesis (*erg11*), and oxidative stress response (*catA*) after treatment with sub-inhibitory concentrations (MIC/2) of AgNPs are summarized in Table 3. Figure 7 summarizes data of gene expression in response to the three *Aspergillus* spp. isolates.

After AgNPs treatment, *A. flavus* showed substantial downregulation of the *aflR* gene, which indicated reduced aflatoxin biosynthesis. The mean down regulation fold change was 0.32 (68% downregulation; $P < 0.01$).

Expression levels of the *erg11* gene were also downregulated in all three *Aspergillus* spp. isolates. This indicated disruption of ergosterol biosynthesis, which is important for structural integrity of fungal cell membranes. Mean downregulation fold changes were: for *A. flavus*, 0.45 (55% downregulation; $P < 0.01$); *A. fumigatus*, 0.52 (48% downregulation; $P < 0.01$), and for *A. niger*, 0.58 (42% downregulation; $P < 0.01$).

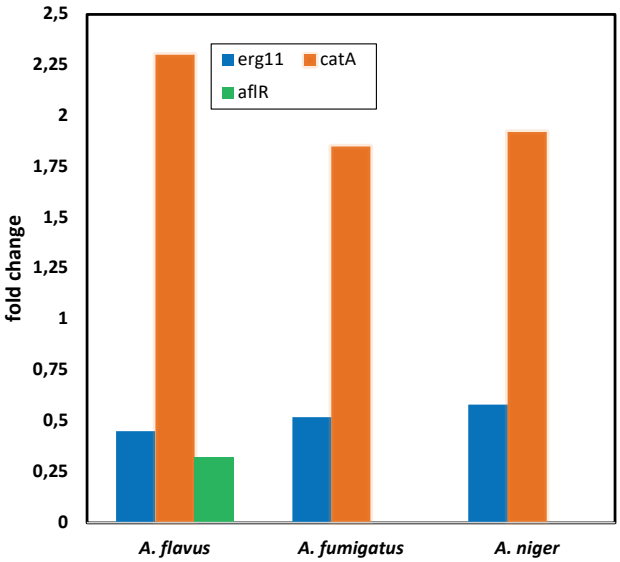

Figure 7. Mean expression fold changes for three genes in three Aspergillus species isolates, after AgNP treatments.

The stress response gene *catA* associated with oxidative stress was overexpressed in all three fungal species, indicating production of reactive oxygen species (ROS) due to the AgNPs. Mean fold changes were: *A. flavus*, 2.10 (110% upregulation; $P < 0.01$); *A. fumigatus,* 1.85 (85% upregulation; $P < 0.01$), and *A. niger*, 1.92 (92% upregulation; $P < 0.01$).

DISCUSSION

This study aimed to assess the potential antifungal activity of silver nanoparticles (AgNPs), synthesized using aqueous extract of *N. sativa*, against isolates of *A. flavus*, *A. fumigatus*, and *A. niger*. Pirbalouti *et al*., (2024) and Gopinath *et al*., (2017) reported that colour change from pale yellow to dark brown marked the initial stages in the synthesis of AgNPs, and indicated their formation. In the present study, XRD analyses did not detect extra peaks, verifying that the product obtained was phase-pure with no other impurities of other silver allotropes.

These results are similar to those in past reports of AgNP synthesis through *N. sativa* extracts (Vijayakumar *et al*., 2021; Mossa *et al*., 2023), and further indicate an environmentally acceptable route to quality silver crystallites. The AgNPs were confirmed to have been formed, as SPR peaks were recorded at 428 nm using UV-Vis spectrometry (Franci *et al*., 2015). FTIR analysis confirmed some functional groups as hydroxyl, carbonyl, and amine groups. These probably arose from thymoquinone, flavonoids, and proteins in the extract from *N. sativa*, which served as the reducing and stabilizing agents (Vijayakumar *et al*., 2021; Abbas *et al*., 2024).

This method of biosynthesis fits with the principles of "green nanotechnology", which has garnered increasing attention due to emphasis on minimizing the use of toxic chemicals in production of nanoparticles (El-Seedi *et al*., 2024).

Results from the disk diffusion and MIC/MFC assays confirmed that all the assessed *Aspergillus* isolates were sensitive to the AgNPs, with activity being dose dependent. AgNP MIC values of 40-60 μg mL^{-1} and MFC values of 90-120 μg mL^{-1} are within ranges documented for silver nanoparticles synthesized from plant extracts (Mallmann *et al*., 2015; Hashem *et al*., 2022).

Among the three fungus isolates assessed, *A. fumigatus* displayed the greatest sensitivity, while *A. niger* showed the greatest MIC and MFC values, indicating species-dependent susceptibility. A diverse array of AgNP antifungal actions is probable, including disruption of membrane integrity of the fungus through generation of reactive oxygen species (ROS), blockage of essential metabolic pathways, and interference with DNA and protein synthesis (Franci *et al*., 2015; Gholamnezhad *et al*., 2016). Among the tested species, *A. fumigatus* had the greatest sensitivity to AgNP treatment, which could be due cell wall composition and membrane physiology of this fungus (Vanlalveni *et al*., 2024). Previous studies have shown that *A. fumigatus* has greater membrane permeability and thinner cell walls compared to other *Aspergillus* species, making it more vulnerable to nanoparticle penetration and oxidative stress. In addition, the downregulation of *erg11* observed in *A. fumigatus* suggests a strong disruption of ergosterol biosynthesis, which affects membrane stability and enhances antifungal susceptibility. These structural and molecular characteristics may explain why *A. fumigatus* responded more sensitively to AgNP exposure than *A. flavus* and *A. niger*.

These results align with previously reported synergistic effects of silver ions and *N. sativa* phytochemicals, which had strong antifungal activities. This indicates increased enhancement of bioactivity of the nanoparticles (Atanda *et al*., 2005; Badmos *et al*., 2025).

Further investigations of response of *Aspergillus* species to AgNP exposure could be conducted based on RT-qPCR outcomes. The pronounced downregulation of *aflR* in *A. flavus* signals disrupted aflatoxin biosynthesis, which confirms previous findings indicating nanoparticle treatments may reduce mycotoxin production (Deabes *et al*., 2018). The *aflR* blockade supports the assump-

tion that AgNPs could be utilized to mitigate risks of fungal mycotoxins in contaminated food products, to reduce the threats aflatoxin poses to food safety.

All three assessed *Aspergillus* species had *erg11* downregulation, indicating that AgNPs interfere with the ergosterol biosynthesis crucial for the structural integrity of the fungal cell membranes. Disruption of ergosterol synthesis is a well-documented antifungal mechanism, as occurs for azole compounds (Gupta and Tomas, 2003). AgNP induced downregulation of *erg11* has also been shown in other fungi (Deabes *et al*., 2018). Toxicity of AgNPs may also stem from their effects on the catalase enzyme, demonstrated in the upregulation of *catA*. More specifically, silver nanoparticles are well known for their powerful antifungal activity through cell wall and membrane destruction, generation of reactive oxygen species (ROS), interactions with important cellular macromolecules including DNA and proteins, and inhibition of key enzymes (Franci *et al*., 2015; Gholamnezhad *et al*., 2016).

The azole class of antifungal chemicals have induced development of resistance in fungi to these compounds, which created need for alternative therapies (Gupta and Tomas, 2003; Machado *et al*., 2017). The new "green-synthesized" AgNPs have multi-targeted mechanisms of action and low probability of inducing pathogen resistance, which is an advantage over previously developed antifungal chemicals (Deabes *et al*., 2018; El-Seedi *et al*., 2024).

Nigella sativa is also a safe plant, and may enhance biocompatibility along with stability of nanoparticles previously synthesized (Vijayakumar *et al*., 2021; Abbas *et al*., 2024).

Application of *N. sativa*-based AgNPs to combat *Aspergillus flavus* infections in horticultural systems has promise, as indicated by their activity in controlling infections in banana plantlets. Aflatoxins, especially those from *A. flavus*, are among the most toxic natural compounds. They can cause severe short- and long-term health problems in animals and humans (Mallmann *et al*., 2015; Awuchi *et al*., 2021). Aflatoxin is a widespread human and animal food safety issue, especially in tropical and subtropical regions (Atanda *et al*., 2005; Peng *et al*., 2018). Aflatoxin causes hepatocellular carcinoma, growth impairment, and immunosuppression from chronic exposure. The decrease in aflatoxin B1, along with reduced fungal growth and tissue damage, indicate that synthesized silver nanoparticles could provide effective biological control for toxin-producing fungi.

The tissue culture system used in the present study was chosen because it usually remains free of contaminants, thus providing a balanced environment to test the AgNP effectiveness on banana, which may be prone to postharvest mycotoxin development. Plant-based nanotechnology applied in agriculture is likely to broaden scope of the technology. Greenhouse and field experiments would be worthwhile to assess sprays and coatings of AgNPs on banana bunches for suppression of fruit pathogens.

Limitations in the scope of the present study are recognized. Only clinical and laboratory strains of *Aspergillus* spp. were used; responses from environmental isolates may differ from those recorded here. Safety, pharmacokinetics, and therapeutic efficacy of nanoparticles require validations through *in vivo* studies prior to clinical or agricultural uses. As well, evaluations are required to determine long-term stability, mammalian cell cytotoxicity, and potential environmental impacts of these materials (Gholamnezhad *et al*., 2016; Vignesh *et al*., 2025). Focus should also be directed at functionalization of nanoparticle surfaces, optimization of large-scale synthesis, and exploration of synergism of these materials with other antifungal agents.

CONCLUSIONS

The present study has indicated that AgNPs biosynthesized using aqueous extract from *N. sativa* had antifungal activity against *A. flavus*, *A. fumigatus*, and *A. niger*. The nanoparticles exerted dose-dependent antifungal effects causing inhibition in cultures, low MICs and MFCs, and suppression of fungal growth *in vitro*. At molecular level, RT-qPCR analysis showed that AgNP treatments downregulated genes responsible for aflatoxin biosynthesis and ergosterol, which are important aspects for sustaining activity and pathogenicity of these fungi. At the same time, the increase of *catA* suggests that AgNPs exert antifungal activity mainly through oxidative damage. This research provides knowledge supporting the "green synthesis" approach, which has ecological advantage, as it is low cost and is unlikely to cause environmental damage. The combined antimicrobial effect of *N. sativa* phytochemicals and silver nanoparticles may provide an effective alternative to conventional antifungal therapies. This research has contributed to nanobiocontrol, and particularly provides direction for addressing threats of antifungal resistance and aflatoxin contamination of foodstuffs.

Further research is required to make safety assessments, and assess practical applications, to tailor nanoparticle formulations for clinical and agricultural applications.

ACKNOWLEDGEMENT

The authors thank the Scientific Research Deanship at University of Ha'il, Saudi Arabia, for funding this research through, number RCP-24 206.

LITERATURE CITED

Abbas M., Gururani M.A., Ali A., Alsahli A.A., Almatroudi A., ….. El Ansari F., 2024. Antimicrobial properties and therapeutic potential of bioactive compounds in *Nigella sativa*: A review. *Molecules* 29(20): 4914. https://doi.org/10.3390/molecules29204914

Ahmed S., Ahmad M., Swami B.L., Ikram S., 2016. A review on plants extract mediated synthesis of silver nanoparticles for antimicrobial applications: A green expertise. *Journal of Advanced Research* 7(1): 17–28.

Atanda O.O., Akpan I., Rati E.R., Ozoje M., 2005. Palm kernel: A potential substrate for rapid detection of aflatoxin in agricultural commodities. *African Journal of Biotechnology* 5: 1029–1034.

Awuchi C.G., Echeta K.A., Ngwu E.K., Obayiuwana E., Amagwula I.O., Okpala C.O.R., 2021. Mycotoxins affecting animals, foods, humans, and plants: Types, occurrence, toxicities, action mechanisms, prevention, and detoxification strategies—A revisit. *Foods* 10(6): 1279.

Badmos A., Oni E., Ojewale I., Oluwafemi F., 2025. Evaluating the potency of Nigella sativa-mediated silver nanoparticles against aflatoxigenic fungi in planting soil. *Food and Environment Safety* 24(1): 33–44. https://doi.org/10.4316/fens.2025.004

Berger S., El Chazli Y., Babu A.F. and Coste A.T., 2017. Azole Resistance in *Aspergillus fumigatus*: A Consequence of Antifungal Use in Agriculture? *Frontier of Microbiology* 8: 1024. https://doi.org/10.3389/fmicb.2017.01024

Burt S.A., Van Der Zee R., Koets A.P., De Graaff A.M., Van Knapen F., … Veldhuizen E.J.A., 2007. Carvacrol induces heat shock protein 60 and inhibits synthesis of flagellin in *Escherichia coli* O157:H7. *Applied and Environmental Microbiology* 73: 4484–4490. https://doi.org/10.1128/AEM.00340-07.

Clinical and Laboratory Standards Institute (CLSI), 2015. *Performance Standards for Antimicrobial Disk Susceptibility Tests; Approved Standard - Twelfth Edition* M02- A12., CLSI, (ISBN 1-56238-985-8 (print); ISBN 1-56238-986-6 (Electronic). Clinical and Laboratory Standards Institute, 950 West Valley Road, Suite 2500, Wayne, PA, 19087 USA.

Deabes M.M., Khalil W.K.B., Attallah A.G., El-Desouky T.A., Naguib K.M., 2018. Impact of Silver Nanoparticles on Gene Expression in *Aspergillus flavus* Producer Aflatoxin B1. *Open Access Macedonian Journal of Medical Sciences* 6(4): 600–605. https://doi.org/10.3889/oamjms.2018.117

El-Seedi H.R., Omara M.S., Omar A.H., Elakshar M.M., Shoukhba Y.M., … S. A. M. Khalifa, 2024. Updated Review of Metal Nanoparticles Fabricated by Green Chemistry Using Natural Extracts: Biosynthesis, Mechanisms, and Applications. *Bioengineering* 11: 1095. https://doi.org/10.3390/bioengineering11111095

Franci G., Falanga A., Galdiero S., Palomba L., Rai M., ….. Galdiero M., 2015. Silver nanoparticles as potential antibacterial agents. *Molecules* 18: 20(5): 8856–8874. https://doi.org/10.3390/molecules20058856.

Gholamnezhad Z., Havakhah S., Boskabady M.H., 2016. Preclinical and clinical effects of *Nigella sativa* and its constituent, thymoquinone: A review. *Journal of Ethnopharmacology* 22(190): 372–386. https://doi.org/10.1016/j.jep.2016.06.061

Gibała A., Żeliszewska P., Gosiewski T., Krawczyk A., Duraczyńska D., …. Oćwieja M., 2021. Antibacterial and antifungal properties of silver nanoparticles-effect of a surface-stabilizing agent. *Biomolecules* 7: 11(10): 1481. https://doi.org/10.3390/biom11101481 PMID: 34680114; PMCID: PMC8533414

Gómez-Sequeda N., Cáceres M., Stashenko E.E., Hidalgo W., Ortiz C., 2020. Antimicrobial and Antibiofilm Activities of Essential Oils against *Escherichia coli* O157:H7 and Methicillin-Resistant *Staphylococcus aureus* (MRSA). *Antibiotics* 9(11): 730. https://doi.org/10.3390/antibiotics9110730

Gopinath V., Priyadarshini S., Loke M.F., Arunkumar J., Marsili E., Velusamy P., 2017. Biogenic synthesis, characterization of antibacterial silver nanoparticles and its cell cytotoxicity. *Arabian Journal of Chemistry* 10: 1107–1117. https://doi.org/10.1016/j.arabjc.2015.11.011

Gupta A.K., Tomas E., 2003. New antifungal agents. *Dermatologic Clinics* 21(3): 565–576. https://doi.org/10.1016/S0733-8635(03)00024-X

Hashem A.H., Albader N.M., Khan A.Q., F. O. Alotibi, A. Al-Askar, A… Elbahnasawy M. A., 2022. Antifungal Activity of biosynthesized silver nanoparticles using cell-free extract of *Bacillus thuringiensis* against *Aspergillus* species. *Journal of Functional Biomaterials* 2022: 13(4): 242. https://doi.org/10.3390/jfb13040242

Jung K.W., Chung M.S., Bai H.W., Chung B.Y., Lee S., 2021. Investigation of Antifungal Mechanisms of Thymol in the Human Fungal Pathogen, *Cryptococcus neoformans*. *Molecules* 26(11): 3476. https://doi.org/10.3390/molecules26113476

Kanika C. and Satyawati S., 2022. Chemical composition, antioxidant and antifungal activity of essential oil of *Trachyspermum ammi* seeds. *International Journal of Advanced Research* 10(4): 592–596.

Khader M. and Eckl P.M., 2014. Thymoquinone: an emerging natural drug with a wide range of medical applications. *Iranian Journal of Basic Medical Science* 17(12): 950–957.

Livak K.J. and Schmittgen T.D., 2001 Analysis of relative gene expression data using real-time quantitative PCR and the 2^{-}^^CT method. *Methods* 25: 402–408.

Machado F.J., Santana F.M., Lau D., Ponte E.M., 2017. Quantitative review of the effects of triazole and benzimidazole fungicides on Fusarium head blight and wheat yield in Brazil. *Plant Disease* 101(9): 1633–1641. https://doi.org/10.1094/PDIS-03-17-0340-RE

Mallmann E.J., Cunha F.A., Castro B.N., Maciel A.M., Menezes E.A., Fechine P.B., 2015. Antifungal activity of silver nanoparticles obtained by green synthesis. *Revista do Instituto de Medicina Tropical de São Paulo* 57(2): 165-167. https://doi.org/10.1590/S0036-46652015000200011. PMID: 25923897; PMCID: PMC4435016.

Mossa M.I., El-Sharkawy E.E., ElSharawy A.A., 2023. Antifungal activity of silver nanoparticles green biosynthesis from the extract of *Zygophyllum album* (L.f.) on Fusarium wilt. *Journal of Plant Protection Research* 63(3): 340–349. https://doi.org/10.24425/jppr.2023.146874.

Peng Z., Chen, L., Zhu, Y., Huang, Y., Hu, X.,... Yang W., 2018. Current major degradation methods for aflatoxins: A review. *Trends in Food Science & Technology* 80: 155–166. https://doi.org/10.1016/j.tifs.2018.08.009

Pirbalouti M.A., Shahbazi S., Shahrokh S.S., Reiisi S., Mokhtari A., 2024. Study the antifungal effects of green synthesized silver nanoparticles on the *Aspergillus niger*, *Microsporum canis*, and *Candida albicans*. *Journal of Microbiota* 1(3): e154535. https://doi.org/10.5812/jmb-154535

Vanlalveni C., Ralte V., Zohmingliana H., Das S., Anal J.M.H., … Rokhum S.L., 2024. A review of microbes mediated biosynthesis of silver nanoparticles and their enhanced antimicrobial activities. *Heliyon* 10(11): e32333. https://doi.org/10.1016/j.heliyon.2024.e32333

Vignesh A., Menaka C., Amal T.C., Selvakumar S., Vasanth K., 2025. Exploring the dual impact of nanoparticles on human well-being: A comprehensive review of risks and benefits. *Next Nanotechnology* (8): 100223. https://doi.org/10.1016/j.nxnano.2025.100223

Vijayakumar S., Malaikozhundan B., Shanthi S., Vaseeharan B., Thajuddin N., 2021. Biological compound capping of silver nanoparticles with the seed extracts of black cumin (*Nigella sativa*): a potential antibacterial, antidiabetic, anti-inflammatory, and antioxidant. *Journal of Inorganic and Organometallic Polymers and Materials* 31: 624–635. https://doi.org/10.1007/S10904-020-01713-4

Wu S., Zhang Q., Zhang W., Huang W., Kong O., ….. Yan S., 2022. Linolenic Acid-Derived Oxylipins Inhibit Aflatoxin Biosynthesis in *Aspergillus flavus* through Activation of Imizoquin Biosynthesis. *Journal of Agricultural and Food Chemistry* 70(50): 15928–15944. https://doi.org/10.1021/acs.jafc.2c06230

Zakaria L., 2024. An overview of *Aspergillus* species associated with plant diseases. *Pathogens* 20: 13(9): 813. https://doi.org/10.3390/pathogens13090813. PMID: 39339004; PMCID: PMC11435247.

Phytopathologia Mediterranea
The international journal of the
Mediterranean Phytopathological Union

Firenze University Press
www.fupress.com/pm

Short Notes

First report of strawberry mild yellow edge virus in Bosnia and Herzegovina

Armin VUKOJEVIC[1], Amani BEN SLIMEN[2], Mirsad MUJKOVIC[1], Emina KRAJINA-IBRULJ[1], Toufic ELBEAINO[2,3,*]

[1] *Department of Quality Control of Seeds, Pest Diagnosis and the Presence of GMOs of Federal Institute of Agriculture, Sarajevo, Butmirska cesta 18, Ilidza 71210, Bosnia & Herzegovina*
[2] *Department of Integrated Pest Management, Istituto Agronomico Mediterraneo di Bari, Via Ceglie 9, 70010 Valenzano, Bari, Italy*
[3] *National Research Council of Italy (CNR), Institute for Sustainable Plant Protection (IPSP), Naples, Italy*
*Corresponding author. E-mail: elbeaino@iamb.it

Summary. In 2023, a survey assessed 120 strawberry leaf samples collected from regions of Bosnia and Herzegovina (BiH) for presence of arabis mosaic virus (ArMV), strawberry mottle virus (SMoV), strawberry latent ringspot virus (SLRSV), and strawberry mild yellow edge virus (SMYEV), which are among the most common and internationally widespread viruses affecting strawberry plants. All samples were tested using Double Antibody Sandwich ELISA (DAS-ELISA) and RT-PCR. SMYEV was detected in 19 samples, 17 of which were from the variety Clery and two from Alba. ArMV, SLRSV, and SMoV were not detected in any of the samples. Sequence analyses of 405 nucleotides within the replicase and 25k triple gene block protein genes from 19 SMYEV isolates showed nine sequence variants. The least nucleotide similarity (83%) was observed with a Chinese SMYEV isolate, FJ1 (GenBank accession number OK562580), while greatest similarity (99.3%) was found with a German isolate, MY-18 (GenBank accession number NC_003794). Phylogenetic analysis showed that the BiH SMYEV isolates formed a distinct cluster closely related to the Argentinian isolate Berra-2 (GenBank accession number KX150372) and the German isolate, MY-18 (GenBank accession number NC_003794). This is the first report of SMYEV in BiH. Further research is required to determine whether additional viruses or other pathogens may be contributing to the symptoms observed in the field.

Keywords. Strawberry, DAS-ELISA, RT-PCR, sequence analysis.

OPEN ACCESS

Citation: Vukojevic, A., Ben Slimen, A., Mujkovic, M., Krajina-Ibrulj, E., & Elbeaino, T. (2025). First report of strawberry mild yellow edge virus in Bosnia and Herzegovina. *Phytopathologia Mediterranea* 64(3): 579-583. DOI: 10.36253/phyto-16227

Accepted: October 15, 2025

Published: December 11, 2025

Data Availability Statement: All relevant data are within the paper and its Supporting Information files.

Competing Interests: The Author(s) declare(s) no conflict of interest.

Editor: Assunta Bertaccini, Alma Mater Studiorum, University of Bologna, Italy.

ORCID:
AV: 0009-0008-2710-0892
ABS: 0000-0001-8070-5120
MM: 0009-0009-2435-769X
EKI: 0009-0008-9415-2115
TE: 0000-0003-2211-7907

INTRODUCTION

Strawberry (*Fragaria* × *ananassa* Duch.) is an important crop in Bosnia and Herzegovina (BiH). In 2020, the 1,337 hectares, with an average yield of 8.5 tonnes ha^{-1}. More than 30 viruses and phytoplasmas are known to infect strawberries, often causing poorly defined or latent symptoms in single infections. However, mixed infections are also frequently associated with stunted

plant growth and substantial yield losses (Maas, 1998; Babini *et al*., 2004; Kwon *et al*., 2019). Among the most economically significant strawberry viruses are arabis mosaic virus (ArMV; *Secoviridae*, *Nepovirus*, *Nepovirus arabis*), strawberry mottle virus (SMoV; *Secoviridae*, *Sadwavirus*, *Sadwavirus fragariae*), strawberry latent ringspot virus (SLRSV; *Secoviridae*, *Stralarivirus*, *Stralarivirus fragariae*), and strawberry mild yellow edge virus (SMYEV; *Alphaflexiviridae*, *Potexvirus, Potexvirus fragariae*). These viruses can cause severe damage, particularly when occurring in mixed infections with other viruses.

Strawberry cultivation is widespread in BiH, with the regions of Ilidža, Čelić, Gornji Vakuf, Čapljina, and Živinice recognized as key production areas. In 2023, virus-like symptoms and significant decline in strawberry yields were observed in several locations of these regions. In response, a preliminary laboratory investigation was conducted to assess the presence of major viruses known to infect strawberries. The results from this diagnostic survey are presented in this paper.

MATERIALS AND METHODS

Source of plant material

A total of 120 strawberry leaf samples were collected from 6-month-old plants from Ilidža, Čelić, Gornji Vakuf, Čapljina and Živinice. The samples were from several strawberry varieties: 62 from Clery, 28 from Mjesecarke, 12 from Alba, and ten from Asia. Additionally, two samples were collected from each of the varieties Senga Sengana, Elsanta, Joly, and Arosa. Most of the sampled plants were asymptomatic, while 32 plants had virus-like symptoms, including vein clearing, and leaf mottling, and yellowing. During field inspections, all plant samples were carefully examined, using a hand lens in the field and a stereomicroscope in the laboratory, for the presence of insects, particularly strawberry mites which commonly infest this crop, but no mites were detected. The collected samples were brought to the laboratory for serological and molecular analyses to detect virus presence.

DAS-ELISA, RT-PCR and bioinformatic analysis

All the strawberry leaf samples were initially screened serologically using the Double Antibody Sandwich Enzyme-Linked Immunosorbent Assay (DAS-ELISA), as described by Clark and Adams (1977). Polyclonal antibodies specific to ArMV, SLRSV, and SMYEV were used according to the manufacturer's protocol (BIOREBA AG). For molecular detections, total RNA was extracted from 100 mg of leaf vein tissue, which was homogenized in 1 mL of grinding buffer containing 4.0 M guanidine thiocyanate, 0.2 M sodium acetate (pH 5.2), 25 mM EDTA, 1.0 M potassium acetate, and 2.5% (w/v) polyvinylpyrrolidone-40 (PVP-40). RNA purification was carried out using silica particle-based extraction, following the protocol described by Foissac *et al.* (2001). Total RNAs were extracted from grapevines infected with SLRSV (isolate T-29, France) and ArMV (isolate Fr2-, Germany), both previously characterized by Digiaro *et al*. (2007) and maintained in the grapevine collection at IAM Bari, Italy, as well as from the SMoV DSMZ isolate PV-1268. These samples were used as positive controls in the RT-PCR assays. In parallel, healthy plant material derived from certified grapevine and strawberry plants was used as negative controls in the RT-PCR assays. RNA samples with A260/280 ratios between 1.8 and 2.1, A260/230 ratios >1.8, and concentrations above 50 ng μL^{-1} were employed for downstream complementary DNA (cDNA) synthesis.

Reverse transcription was carried out performed using 0.5 µg of total RNA and 0.5 µg of random hexamer primers (Sigma-Aldrich) and 200 U of Moloney murine leukemia virus (M-MLV) reverse transcriptase (Thermo Fisher Scientific), incubated at 39°C for 1 h, followed by enzyme inactivation at 70°C for 10 min. The resulting cDNA was subjected to RT-PCR using virus-specific primers targeting all four viruses (Thermo Fisher Scientific) (Table 1), using the PCR conditions detailed in Table 1. Amplification products were analyzed by electrophoresis on 1.2% agarose gel with 1× Tris-Borate-EDTA buffer. After purification, the PCR amplicons were bidirectionally sequenced at Eurofins Genomics (Konstanz, Germany), by Sanger sequencing using both forward and reverse primers. The obtained sequences were compared using the BLASTn algorithm on the NCBI platform (Altschul *et al*., 1990). Sequence similarity matrices and a phylogenetic tree were constructed using the Maximum likelihood method with 1000 bootstrap replicates, implemented in Geneious Prime v2020.2.5 program (Dotmatics, Boston, United States of America, Auckland, New Zealand).

RESULTS AND DISCUSSION

Virus detection and sequence analysis

ELISA and RT-PCR assays exclusively detected SMYEV. ArMV, SLRSV, and SMoV were not detected by DAS-ELISA, and were also not detected when RT-PCR was used as a supplementary method to detect potentially

Table 1. List of primers used in RT-PCR assays for amplifying partial genome sequences of SMYEV, ArMV, SLRSV and SMoV.

Virus	Primers	Sequence (5′ to 3′)	Amplicon size (bp)	Reference
SMYEV	SMYEV-C	TGCACTCTGTGTTGACCTTC	405	Kaden-Kreuziger *et al.* (1995)
	SMYEV-B	ATACTCGTCTACGAAGGCT		
ArMV	ArMV-5A	TACTATAAGAAACCGCTCCC	302	Faggioli *et al.* (2005)
	ArMV-3A	CATCAAAACTCATAACCCAC		
SLRSV	SLRSV-5D	CCCTTGGTTACTTTTACCTCCTCATTGTCC	291	Faggioli *et al.* (2002)
	SLRSV-3D	AGGCTCAAGAAAACACAC		
SMoV	Smdetncr4a	TAAGCGACCACGACTGTGACAAAG	460	Thompson & Jelkmann (2003)
	Sm2ncr1b	ATTCGGTTCACGTCCTAGTCTCAC		

low virus concentrations. Both methods yielded consistent results, identifying 19 of the 120 samples as SMYEV-positive, corresponding to an infection rate of 16 %, of which six (32%) were symptomatic. The variety Clery accounted for most of the SMYEV infections (17 samples), while only two infected samples were detected in the Alba variety.

All sequences obtained in this study have been deposited in GenBank under accession numbers PP489404 and PP530291 to PP530298. Comparative nucleotide analyses gave the lowest sequence similarity (83%) with the Chinese SMYEV isolate, FJ1 (GenBank accession number OK562580), and greatest similarity with the German SMYEV isolate, MY-18 (GenBank accession number NC_003794). Among the 19 SMYEV-positive samples, nine sequence types were distinguished, partly spanning the replicase and the 25k triple gene block protein genes. The intra comparison of the nucleotide sequences resulted in similarities from 89.4% to 99.3%, indicating the coexistence of genetically divergent and closely related viral strains in BiH.

SMYEV prevalence in BiH strawberries

SMYEV was detected in Ilidža, Čelić, and Živinice. The predominance of infections in the Clery variety may indicate greater susceptibility of this variety to virus infections, or reflect effects of regional propagation practices, such as the exchange of infected monovarietal plant material, on virus spread. The absence of ArMV, SLRSV, and SMoV in all tested samples indicates either limited presence of these viruses in the surveyed areas or the effectiveness of current disease management strategies, as these viruses are typically associated with severe symptoms in strawberry crops and growers often remove affected plants at the first signs of infection.

The two SMYEV-infected strawberry plants of the Alba variety, as well as 11 infected Clery plants, all had no visible symptoms. Only six infected plants exhibited mild leaf yellowing, which resembled symptoms typically associated with SMYEV (Figure 1). The causal agent of the virus-like symptoms observed in the other 13 symptomatic plants were unclear, as none of the four assessed viruses tested were detected in these samples. Involvement of other potential pathogens, such as strawberry-infecting viruses not assessed in this study, as well as phytoplasmas or viroids, cannot be excluded. Hence, further investigations are required to clarify the underlying etiology of the symptomatic plants that gave negative virus detections.

Phylogenetic analyses

The phylogenetic analyses based on the nucleotide sequences of SMYEV isolates showed presence of two distinct clusters (Figure 2). All the BiH SMYEV isolates grouped within Cluster II, alongside the German isolate MY-18 (GenBank accession number NC_003794). This clustering pattern, derived from partial RNA replicase and 25K triple gene block sequences, aligned with previously reported phylogenetic groupings. Notably, similar genetic stratification into two major groups has also been observed when analyses are based on coat protein (CP) sequences of SMYEV (Cho *et al*., 2011). This consistent clustering, supported by RNA replicase and 25K triple gene block sequences, reinforces previous findings, and highlights the genetic stability of SMYEV differentiation into two major phylogenetic groups. These groups probably reflect geographic origins rather than differences in host ranges or pathogenicity. Further research is required to determine whether these genetic clusters correlate with biological virus traits, such as virulence or transmission dynamics.

The present study is the first to record occurrence of SMYEV in BiH. Although SMYEV infection alone is generally not considered highly detrimental to most

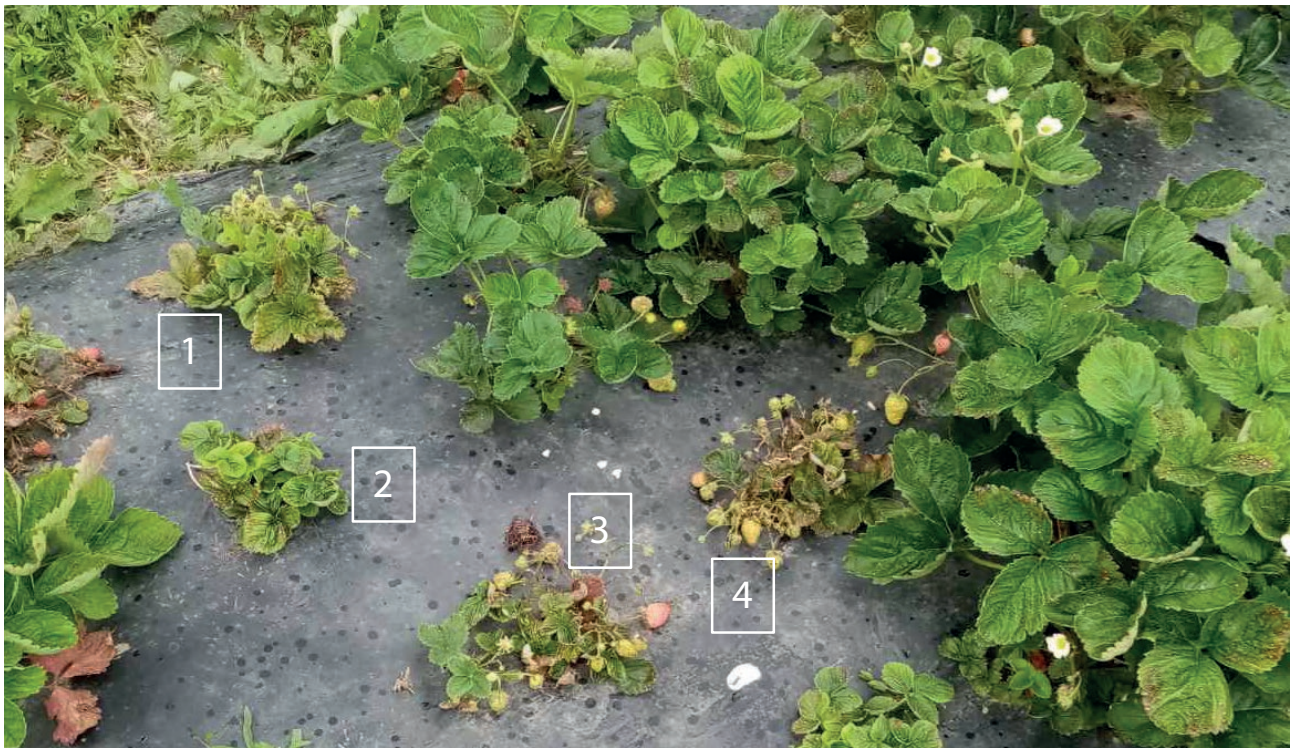

Figure 1. Strawberry plants (variety Cleary) infected with SMYEV, confirmed by DAS-ELISA and RT-PCR, showing leaf yellowing and stunting.

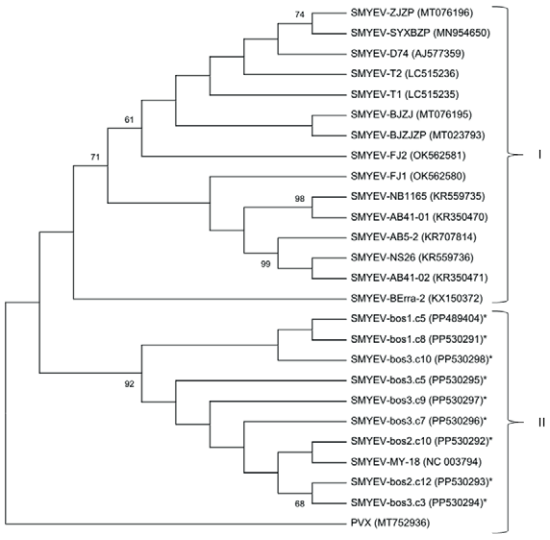

Figure 2. Maximum-likelihood phylogenetic tree constructed based on the nucleotide sequence alignment of partial RNA replicase and 25K triple gene block regions from SMYEV isolates originating from Bosnia and Herzegovina (indicated by asterisks), and for homologous sequences retrieved from the GenBank. Sequence accession numbers are shown in parentheses. Potato virus X (PVX) was included as an outgroup. Bootstrap support values greater than 60% (based on 1,000 replicates) are indicated at the corresponding branch nodes; values below <60% are not shown.

strawberry varieties, it rarely occurs as a single infection, thereby complicating the assessment of its actual economic impact. This is reflected in the findings of 19 SMYEV-infections, of which only 6 (32%) exhibited SMYEV-like symptoms, while the remaining 13 plants were asymptomatic. Consequently, further research is needed to investigate potential mixed infections involving other common strawberry-infecting pathogens (viruses, phytoplasmas and viroids), to better understand the overall pathological landscape and its implications for the strawberry production in the country.

FUNDING

This research was conducted in the frame of a bilateral project (PHYTO BiH, AID 011681): "*New Actions to Support the Phytosanitary Sector in Bosnia and Herzegovina for the Harmonization with EU Standards*", funded by the General Directorate for Development Cooperation – Italian Ministry of Foreign Affairs and International Cooperation (AICS).

LITERATURE CITED

Altschul S.F., Gish W., Miller W., Myers E.W., Lipman D.J., 1990. Basic local alignment search tool. *Journal of Molecular Biology* 215(3): 403–410.

Babini A.R., Cieślińska M., Karešová R., Thompson J.R., Cardoni M., 2004. Occurrence and identification of strawberry viruses in five European countries. *Acta Horticulturae* 656: 39–43.

Cho J.D., Choi G.S., Chung B.N., Kim J.S., Choi H.S., 2011. Strawberry mild yellow edge potexvirus from strawberry in Korea. *The Plant Pathology Journal* 27(2): 187–190.

Clark M.F., Adams A.N., 1977. Characteristics of the microplate method of enzyme-linked immunosorbent assay for the detection of plant viruses. *Journal of General Virology* 34(3): 475–483.

Digiaro M., Elbeaino T., Martelli G.P., 2007. Development of degenerate and species-specific primers for the differential and simultaneous RT-PCR detection of grapevine-infecting nepoviruses of subgroup A, B, and C. *Journal of Virological Methods* 141: 34–40.

Faggioli F., Ferretti L., Pasquini G., Barba M., 2002. Detection of strawberry latent ring spot virus in leaves of olive trees in Italy using one-step RT-PCR. *Journal of Phytopathology* 150(11-12): 636–639.

Faggioli F., Ferretti L., Albanese G., Sciarroni R., Pasquini G., Lumia V., Barba M., 2005. Distribution of olive tree viruses in Italy as revealed by one-step RT-PCR. *Journal of Plant Pathology* 87(1): 49–55.

Foissac X., Svanella-Dumas L., Gentit P., Dulucq M.J., Candresse T., 2001. Polyvalent detection of fruit tree *tricho, capillo and foveavirus* by nested RT-PCR using degenerated and inosine containing primers (DOP RT-PCR). *Acta Horticulturae* 550: 37–43.

Kaden-Kreuziger D., Lamprecht S., Martin R.R., Jelkmann W., 1995. Immunocapture polymerase chain reaction assay and ELISA for the detection of strawberry mild yellow edge associated potexvirus. *Acta Horticulturae* 385: 33–38.

Kwon S.J., Yoon J.B., Cho I.S., Yoon J.Y., Kwon T.R., 2019. Incidence of aphid-transmitted strawberry viruses in Korea and phylogenetic analysis of Korean isolates of strawberry mottle virus. *Research in Plant Disease* 25(4): 226–232.

Maas J.L., 1998. Opportunities to reduce the potential for disease infection and spread with strawberry plug plants. In *XXV International Horticultural Congress, Part 3: Culture Techniques with Special Emphasis on Environmental Implications* 513: 409–416.

Thompson J.R., Jelkmann W., 2003. The detection and variation of strawberry mottle virus. *Plant Disease* 87(4): 385–390.

Phytopathologia Mediterranea
The international journal of the
Mediterranean Phytopathological Union

Firenze University Press
www.fupress.com/pm

Research Papers

Virome analysis of melon with yellowish symptoms reveals mixed infections of known and emerging viruses in Southern Italy

Myeonghwan KWAK[1], Cecile DESBIEZ[2], Eui-Joon KIL[1], Giuseppe PARRELLA[3,*]

[1] *Department of Plant Medicals, Gyeongkuk National University, 36729 Andong, Republic of Korea*
[2] *Institute for Agriculture, Food, and Environment (INRAe), Pathologie Végétale, F-84140, Montfavet, France*
[3] *Institute for Sustainable Plant Protection, National Research Council (IPSP-CNR), 80055 Portici, Italy*
*Corresponding author. Email: giuseppe.parrella@ipsp.cnr.it

Summary. New viruses and virus strains have emerged with increasing frequencies in cucurbit cropping systems, and surveillance for these pathogens requires effective techniques. Virus diversity was assessed in a melon leaf sample from one field in the Campania region of Southern Italy. Four viruses were identified in melon presenting yellowish symptoms, including: cucurbit chlorotic yellows virus (CCYV), cucumis melo endornavirus (CmEV), tomato leaf curl New Delhi virus (ToLCNDV), and cucurbit aphid-borne yellows virus (CABYV). De novo assemblies reconstructed near-complete genomes of these viruses, and using data available in GenBank, whole genome phylogenetic relationships were determined. Based on the HTS results, a virus survey was then carried out in the same melon field, using 108 symptomatic and non-symptomatic leaf samples and RT-PCR/PCR for specific virus detections. Results obtained confirmed presence of the four viruses, with incidences of 78% for CmEV, 78% for ToLCNDV, 69% for CCYV and 52% for CABYV in the field. Most samples had mixed infections, with from two to four viruses in individual samples. Multiple infections comprised 41% infected with CABYV + ToLCNDV + CCYV + CmEV, 28% with ToLCNDV + CCYV + CmEV, 9% with CABYV + ToLCNDV and 2 % of CMV+CABYV. ToLCNDV and CmEV were the most abundant virus detected. This record of CCYV and CmEV is the first for these two viruses in Italy, with CCYV detected with high incidence. CABYV also had high incidence compared to previous reports for this virus. Further research is required, including with other cucurbit hosts, to determine incidence of emerging virus complexes causing yellowing disease in melon.

Keywords. Cucumis melo, whitefly-transmitted viruses, HTS, CCYV, CmEV.

OPEN ACCESS

Citation: Kwak, M., Desbiez, C., Kil, E.-J., & Parrella, G. (2025). Virome analysis of melon with yellowish symptoms reveals mixed infections of known and emerging viruses in Southern Italy. *Phytopathologia Mediterranea* 64(3): 585-596. DOI: 10.36253/phyto-16655

Accepted: November 1, 2025

Published: December 11, 2025

Data Availability Statement: All relevant data are within the paper and its Supporting Information files.

Competing Interests: The Author(s) declare(s) no conflict of interest.

Editor: Safaa Kumari, International Center for Agricultural Research in the Dry Areas (CARDA), Terbol Station, Lebanon.

ORCID:
MK: 0009-0008-9662-9044
CD: 0000-0001-8691-7423
EJK: 0000-0002-7256-3879
GP: 0000-0002-0412-4014

INTRODUCTION

Melon (*Cucumis melo* L.) is one of the most economically important vegetable crops in Italy, covering approx. 14,000 ha, mainly (88%) in open fields,

with total annual production of approx. 500,000 tons (Utili, 2023). During the last 20 years there has been a steady contraction both in the areas of melon cultivated and in melon production, especially for the protected crops (ISTAT, 2024). The main causes of reduced production are most likely associated with climate changes, which expose plants to multiple abiotic stresses, and have favoured the spread of new diseases in the Mediterranean region. Spread of new viruses or new variants of known viruses may threaten cucurbit production, especially in Southern Italy, reducing yields and organoleptic quality of crop production, including melon.

Several viruses have been reported in melon in Italy, but cucurbit production has become difficult due to high populations of whiteflies (*Bemisia tabaci* complex) and associated high incidence of whitefly-transmitted viruses. This occurs mainly in summer and autumn crops, even at higher latitudes than in the past, due to the recent northward movement and stabilization of *B. tabaci* (Bertin *et al*., 2018; Bertin *et al*., 2021).

Beet pseudoyellows virus (BPYV), causing leaf yellowing in melon and transmitted by the whitefly *Trialeurodes vaporariorum*, was detected in Sardinia (Southern Italy) by Tomassoli *et al*. (2003), while cucurbit yellow stunting disorder virus (CYSDV, genus *Crinivirus*) was the first *B. tabaci* transmitted virus detected in melon in Italy (Manglli *et al*., 2016). Almost at the same time the cucurbit cultivations in central-southern Italy were shown to be infected by the Mediterranean variant of tomato leaf curl New Delhi virus (ToLCNDV-ES), efficiently transmitted by the local populations of *B. tabaci* (Parrella *et al*., 2018; Panno *et al*., 2019; Luigi *et al*., 2019; Parrella *et al*., 2020). This variant had different infectivity in cucurbit crops compared to the Southern Asian tomato leaf curl New Delhi virus (ToLCNDV-In) (Vo *et al*., 2022a; Vo *et al*., 2022b). Several viruses can induce similar symptoms on cucurbits, and since each virus is often identified using a specific method, the presence of unsuspected or novel viruses is unknown.

Analyses of virus populations in plant samples using high throughput sequencing (HTS) has become established for detecting and identifying plant viruses and viroids introduced into agroecosystems (Barba *et al*., 2014; Maina *et al*., 2024). This method can potentially detect all viruses and viroids present in a plant sample, including those that are unknown. Thus, HTS is a powerful tool for plant disease management, because it can detect and characterize many viruses in individual plant samples.

The present study included a survey carried out in summer 2021 in a melon growing area of the Campania region (south Italy), and viruses present in a representative plant sample were identified by HTS. Viruses were then identified in several plant samples using specific PCR or RT-PCR. Near complete genome sequences of detected viruses were assembled from HTS data, and their characteristics and phylogeny were determined. Using unbiased small RNA sequencing and de-novo assemblies, aphid- and whitefly-transmitted viruses infecting melon in Campania were identified, showing high incidence of mixed infections with up to four viruses in some samples. Some of these viruses had not been previously reported in Italy.

MATERIALS AND METHODS

Sample collection

In July 2021, during field monitoring for cucurbit viruses, a *c.a.* 1000 m^2 melon field of the "Rodrigues" variety, located in Caserta province (Campania region, south Italy), was noticed, because of the intense yellowing of the leaves on almost all plants in the crop (Figure 1A). A single representative plant, labelled Cume-533-21, was chosen for HTS analysis (Figure 1B). Further, a small survey was conducted in the same melon field on one hundred eight leaf samples (around 20% of total plants). In detail, one plant was collected within each of fifty-four 1 m^2 plots on diagonals transect across the 1000 m^2 melon field.

Proportional incidence of symptomatic plants, showing generalized yellowing disease (YD), was assessed by counting the number of plants with symptoms out of the total number of plants observed in the field, using the following formula:

$$\% \quad \text{disease} \quad \text{incidence} = \frac{\text{No.} \quad \text{of} \quad \text{symptomatic} \quad \text{plants}}{\text{No.} \quad \text{of} \quad \text{plants} \quad \text{observed}}$$

Collected samples were kept on ice and brought to the Portici section of the Institute for Sustainable Plant Protection of National Research Council (IPSP-CNR). All samples were annotated in the IPSP-CNR virus collection and kept both in calcium chloride at 5°C and at –80 °C until further analysis. In addition, the presence of *B. tabaci* was verified, and individual adult insects were randomly collected from different plants, with the aim to identify the vector genotype associated with the melon crop, using the method described by Parrella *et al*. 2012.

RNA isolation and library preparation

The Cume-533-21 sample was chosen for HTS analysis, using a bulk of leaf disks (each approx. 1 cm diam.

Figure 1. A, Melon field showing yellowing symptoms on almost all the plants (sampling site: 40°58'28''N 14°07'28''E). B,)The plant, subsequently designated Cume-533-21, was chosen for HTS virus analysis.

and taken from the top, middle and basal portion of the plant. Extraction of total RNA was carried out with the NucleoSpin RNA Plant Kit (Macherey-Nagel), using 100 mg of fresh leaves to obtain enough RNA to submit to RT-PCR and HTS analysis. RNA samples were checked for their quality and quantity using a NanoDrop 2000c UV-vis spectrophotometer (Thermo Fisher Scientific Inc.). One microgram total RNA was used for library preparation. Ribosomal RNA was depleted from the purified RNA using the RiboMinus Plant Kit for RNA-Seq (Thermo Fisher Scientific), and sequencing libraries were prepared by using TruSeq stranded total RNA of the RiboZero Plant kit (Illumina). High-throughput sequencing was carried out by Macrogen (Republic of Korea), using the Illumina NovaSeq 6000 platform with 101 nt paired-end chemistry.

High Throughput Sequencing (HTS) analyses

The bioinformatics analysis of the obtained raw data was carried out using the CLC Genomics Workbench (Qiagen). Reads were trimmed and filtered (reads with Q ≤ 0.05 and shorter than 15 bp were discarded). Host transcripts were filtered using collection reads that were not mapped to the host genome (GCF_025177605.1). Filtered sequencing reads were assembled into contigs using *de novo* assembly, with a minimum contig length cutoff of 200 bp, and using the following for the graph parameters: word size = 20, bubble size = 50. To map the reads back to contigs the parameters were: mismatch cost = 2, insertion cost = 3, deletion cost = 3, length fraction = 0.5 and similarity fraction = 0.8. Assembled contigs were subjected to BLASTn and tBLASTx analyses against the NCBI online database and viral RefSeq (November 2023). BLASTn *E*-value was set as default (1e-5), and for tBLASTx, the parameter was adjusted for optimization. Contigs that mapped with the individual viral genome sequences from the NCBI database were used to identify candidate viruses present in analyzed melon samples. Scaffolds were finally assembled by mapping each specific virus contig and residual reads on the reference genomes. The consensus viral genomes were deposited in NCBI GenBank, and were used for further analyses. The open reading frames (ORFs) of the identified viruses were found using the ORF finder NCBI (https://www.ncbi.nlm.nih.gov/orffinder/). The schematic representation of the workflow followed for the entire virome analysis, consisting of the three main steps of HTS, data processing, and in-depth data analysis, is reported in Supplementary Figure S1A.

Confirmation of identified viruses using RT-PCR

Specific pairs of primers were also designed on the viral sequences obtained by HTS, to confirm the presence of the viruses within the infected melon plant (sample Cume-533-21) (Supplemetary Table S1). The cDNAs were produced as described above, while PCR amplifications were carried out using the proofreading Platinum SuperFi II DNA Polymerase (Thermo Fisher Scientific Inc.) under the following cycling conditions: initial denaturation at 94°C for 4 min; 35 cycles, each at 94°C for 30 s, 56°C for 30 s, and 72°C for 1 min; and a final extension step at 72°C for 10 min. The amplicons were controlled on 1% agarose gel and were directly sequenced in both orientations with the primers used for PCR (Microsynth, Seqlab GmbH).

RT-PCR determination of field incidence of identified viruses

Additional leaf samples (n = 108) from distinct melon plants of the same field were analyzed for the presence of zucchini yellow mosaic virus (ZYMV; Family *Potyviridae*), watermelon mosaic virus (WMV; Family *Potyviridae*), papaya ringspot virus (PRSV; Family *Potyviridae*), poleroviruses, cucurbit chlorotic yellows virus (CCYV; Family *Closteroviridae*), cucurbit yellow stunting disorder virus (CYSDV; Family *Closteroviridae*), and cucumber mosaic virus (CMV; Family *Bromoviridae*), through virus-specific RT-PCR assays (Supplementary Table S2).

cDNA was synthesized from the extracted RNAs using the ImProm-II reverse transcriptase system (Promega), according to the manufacturer's instructions. Reactions were performed at 42°C for 60 min, followed by incubation at 70°C for 5 min. References for the specific PCR conditions and cycles of each virus are reported in Supplementary Table S2. The amplicons of all samples shown to be positive with the poleroviruses generic primers were sequenced by Sanger sequencing, to determine the virus species present.

Pairwise and phylogenetic analysis

The assembled virus genomes identified in this study from HTS were subjected to Blastn search of the NCBI database. Only the near complete genomes that mapped with the assembled virus genomes found in the present study were used to determine the pairwise identity and phylogenetic relationships. The genomes were trimmed to equal sizes and aligned using the ClustalW multiple alignment program in BioEdit version 7.2.5 (Hall, 1999). Pairwise nucleotide identities were calculated using the sequence demarcation tool (SDTv1.2) (Muhire *et al*., 2014), and identity scores were generated using colour coded matrix. The maximum likelihood method was used to establish phylogenetic relationships among the aligned sequences, with 1000 bootstrap replications, and adopting the nucleotide substitution models with the lowest Bayesian Information Criterion (BIC) scores to describe best substitution patterns implemented in the MEGA X software (Kumar *et al*., 2018).

RESULTS

Incidence of symptomatic plants, and identification of the Bemisia tabaci *genotypes*

Symptoms of YD were observed on almost 80% of the plants inspected. Seven *B. tabaci* adults collected from symptomatic melon plants and analysed by the method of Parrella *et al*., (2012) were all of the MED Q2 mitotype (Supplementary Figure S4).

HTS results from one melon plant

The RNA extracted from the pooled leaves of the Cume-533-21 plant passed the quality control (QC) showing an RNA integrity number (RIN) of 5.3. To guarantee reliability of the data, QC was assessed at each step of the procedure. A total of 16.9 GB of sequence data was obtained from Illumina sequencing of constructed cDNA libraries, with 69,898,104 raw reads and 14,119,417,008 bases. After trimming, 61,111,634 trimmed reads and 5,605,609,577 bases were obtained, with quality scores of Q30 and 49% GC content. Of these, 3,100,867 were related to viruses (Supplementary Figure S1B). Overall, the raw data with average length of 101 bp became of 91.73 bp after trimming. The *de novo* assembly and BLASTn results generated nine contigs related to partial/near-complete genomes of these viruses: two related to CCYV, one related to cucumis melo alphaendornavirus (CmEV, genus *Alphaendornavirus*), two to ToLCNDV, and four to CABYV (Supplementary Figure S2). The near complete genome of one isolate of CCYV (named Cume-533-21-CY), one isolate of CmEV (named Cume-533-21-Alpha), one isolate of ToLCNDV (named Cume-533-21-ND), and one isolate of CABYV (named Cume-533-21-CAB), were assembled. A quantitative analysis of viral reads was carried out by mapping the trimmed reads with over 99% similarity to each assembled virus genome. The most abundant was Cume-533-21-CY with 543,277 reads for RNA1 and 1,706,894 for RNA2, followed by Cume-533-21-Alpha with 724,271 reads, Cume-533-21-ND with 59,181 reads for DNA-A and 66,353 for DNA-B, and only 891 reads for Cume-533-21-CAB. The classification results showed that most of virus sequences were derived from CCYV, representing 66% of total viral reads. CmEV was 23% of the reads, ToLCNDV was 11%, and CABYV was 1 % of the reads (Supplementary Figure S1C). The CABYV genome was then definitely assembled to complete genome by the overlapping contigs obtained by HTS, with amplicons sequences obtained by Sanger sequencing and using a primer set for genome walking (Table S3). The genomic sequences were subsequently deposited in the GenBank database, with accession numbers OQ190463 (RNA1) and OQ190464 (RNA2) for Cume-533-21-CY; PP977196 for Cume-533-21-Alpha; PQ115115 (DNA-A) and PQ115116 (DNA-B) for Cume-533-21-ND; and PV165535 for Cume-533-21-CAB (of 5,672 nt).

Genome organization, pairwise nucleotide comparisons, and phylogenetic analysis of detected viruses

The entire sequence of RNA1 and RNA2 of isolate Cume-533-21-CY of CCYV were of lengths, respectively, 8,606 and 8,032 nucleotides. Overall, the genome organization was consistent to that described for CCYV (Okuda *et al*., 2010; Supplementary Figure S2). In particular, the lengths of the 5' untranslated region (UTR) for RNA1 was 73 nt, and for RNA2 was 1,026 nt, both showing individual high similarity, and the lengths of the 3' UTR were 250 nt for RNA1 and 221 nt for RNA2, Four ORFs were found in Cume-533-21-CY RNA1. These were: ORF1a, with predicted methyltransferase and helicase motifs; ORF1b, with predicted RNA dependent RNA polymerase (RdRp) motif; ORF2, encoding a predicted protein of 6.04 kDa (p6), and ORF3, encoding a predicted protein of 22.11 kDa (p22). The ORF1a could be fused with ORF1b via a ribosomal frameshift, as reported for other criniviruses (Karasev, 2000). The RNA2 encoded eight ORFs (designated ORF1 to ORF8, from 5' to 3' end), and the relative proteins are shown in Supplementary Figure S2. The BLASTn analysis showed that the RNA 1 of Cume-533-21-CY had the greatest nucleotide similarity with isolates Beijing (Acc. No. JQ904628) from China and TW (Acc. No. JN641883) from Taiwan, with 99.8% similarity and 100% genomic cover for both isolates. The RNA2 had the greatest nucleotide similarity with a Japanese isolate (Acc. No. AB523789), with 99.8% of similarity 100% of genomic cover. The pairwise nucleotide identity of Cume-533-21-CY with all the other complete genomic sequences of CCYV isolates (n = 32) available in GenBank (October 2024) ranged from 99.8% to 99.4%, for both RNA1 and RNA2 (Supplementary Figures S3A and S3B). Consequently, phylogenetic trees obtained for both RNA1 and RNA2 did not detected any clear evolutionary relationships among the CCYV isolates (Figure 2, A and B).

The near full genome size of Cume-533-21-Alpha isolate of CmEV was of 15,074 nt, while the ORF comprising 1,5035 nt, which encodes a predicted polyprotein of 5,011 aa (Supplementary Figure S2). The two untranslated regions (UTR) at the 5' and 3' ends of genomic RNA consisted, respectively, of 3 nt and 35 nt. The greatest nucleotide identity of 99% was shared with the sequence of isolate MVU2/21 (Acc. No. OL957252) from

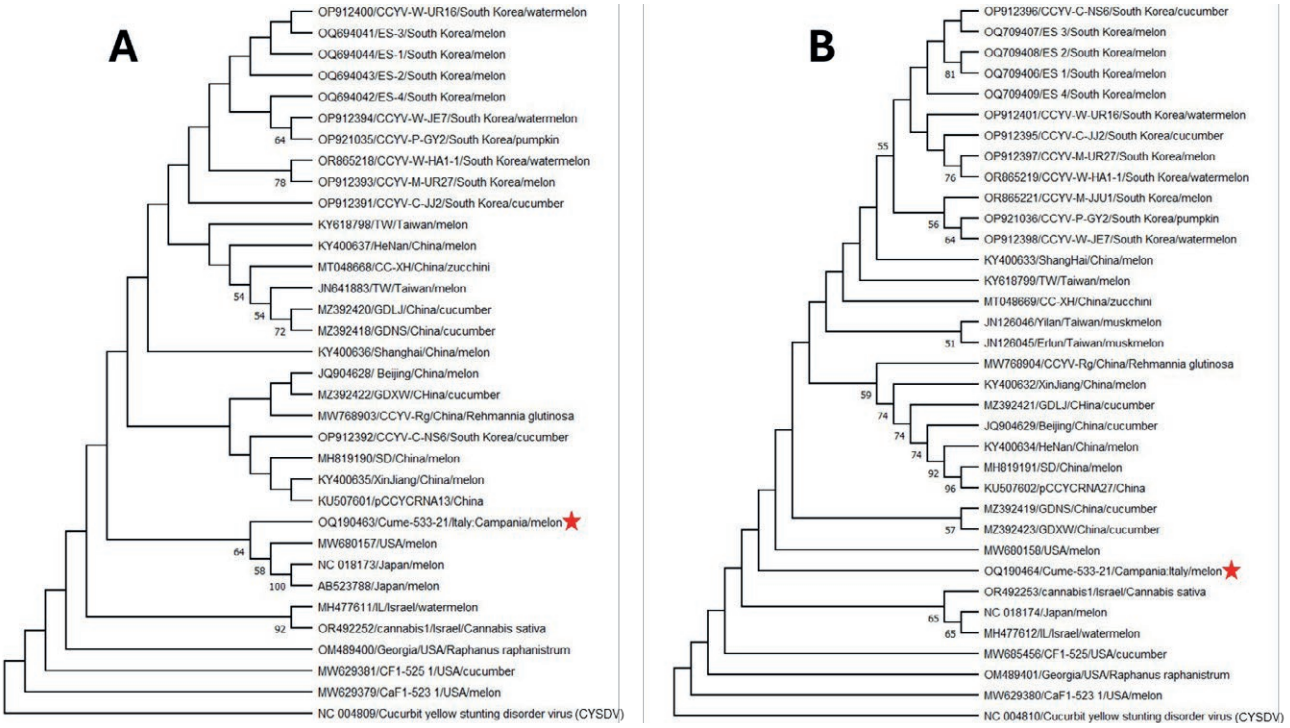

Figure 2. Maximum-likelihood trees obtained for complete RNA1 (A) and RNA2 (B) of CCYV sequences retrieved from GenBank. Based on the best substitution model obtained, the Hasegawa-Kishino-Yano (1985) model of nucleotide substitutions was used. The tree with the greatest log likelihood (-24,028.46) is shown. Percentages of replicate trees (1,000 replicates) are shown next to the branches. The sequence corresponding to the Italian isolate from the present study survey is marked with a red star. Cucurbit yellow stunting disorder virus (CYSDV) was used as the outgroup.

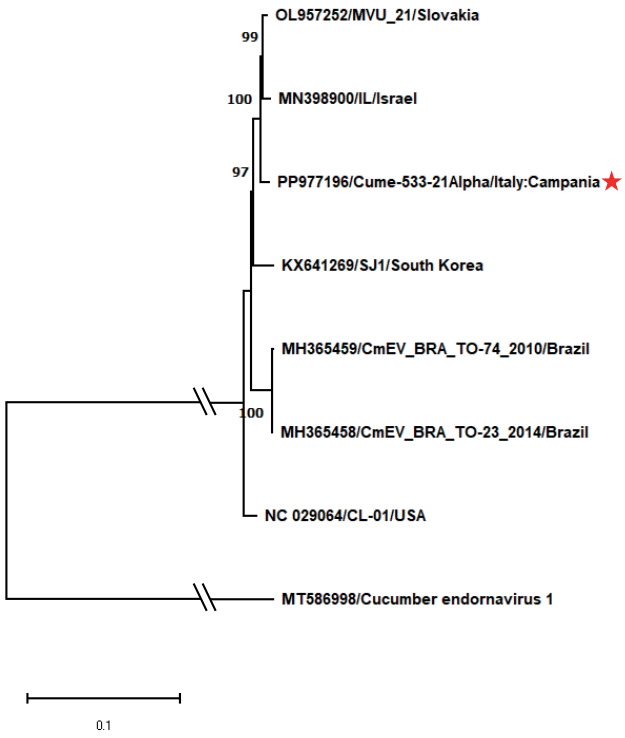

Figure 3. Phylogenetic tree obtained for CmEV complete sequences using the Maximum Likelihood method and General Time Reversible model (Nei and Kumar, 2000) of nucleotide substitutions. The tree with the greatest log likelihood (-38,882.00) is shown. The bootstrap values (1,000 replicates) above 75% are shown next to the branches. The sequence corresponding to the Italian isolate from the present study survey is marked by a red star. Cucumber endornavirus 1 was used as the outgroup.

Slovakia, while pairwise nucleotide identity of isolates Cume-533-21-Alpha with the other CmEV isolates available at GenBank (n = 7; February 2025) ranged from 97.6% to 99% (97–100% of genomic cover). The phylogenetic analysis showed a similar trend as indicated by pairwise analysis. The isolate Cume-533-21-Alpha clustered with the MVU2/2 isolate from Slovakia and the IL isolate from Israel (Acc. No. MN398900) (Figure 3 and Supplementary Figure S3F).

The DNA-A and DNA-B of Cume-533-21-ND isolate were of lengths, respectively, 2738 nt and 2686 nt. The genomes exhibited typical organization of Old World bipartite begomoviruses (Brown *et al*., 2015). The DNA-A contained the AV1 and AV2 genes, in the virion sense orientation, which encode, respectively, the coat protein (CP) and pre-coat protein. In the complementary sense orientation, AC1 encoded the replication-associated protein (Rep), AC2 the transcriptional activator protein (TrAP), AC3 encoded the replication enhancer protein (REn), and AC4 encoded the viral effector. The DNA-B encoded the BV1 gene, in the virion sense orientation which functions as a nuclear shuttle protein (NSP), and the BC1 gene which functions as a movement protein (MP) (Supplementary Figure S2). Both DNAs clustered within the subgroup I of ToLCNDV-ES isolates (the pink clades in Figure 4, A and B) (Panno *et al*., 2019; Troiano and Parrella, 2023). The DNA-A showed greatest nucleotide similarity (99.8%) with isolate Z366 (Acc. No. PP526249), and the DNA-B had 99.7% similarity with isolate Cum-45/16 (Acc. No. MF688671).

The near full-length genome of the CABYV isolate Cume-533-21-CAB was composed of 5,672 nt, and had genomic organization typical of poleroviruses, consisting of single positive-strand RNA, organized in two regions separated by a non-coding internal region (IR) of 200 nucleotides (Supplementary Figure S2). The two genomic regions each had three overlapping open reading frames (ORFs) encoding, respectively, the P0, P1, P1-P2 and the MP, CP, P3-P5 proteins (Supplementary Figure S2) (La Tourrette *et al*., 2021). Phylogenetic relationships based on the near full-length genome of non-recombinants CABYV isolates (n = 85), showed three main groups, according with the geographic origins of isolates: Brazil, the Mediterranean region, and Asia. The Cume-533-21-CAB isolate clustered within the Mediterranean group (Figure 5). Isolates of the Mediterranean group were further grouped into two clades: one composed of Spanish and also isolates from other Mediterranean regions, including the Italian isolate from the present study (Figure 5, pink box), and the other only with Spanish isolates (Figure 5, green box). The Brazilian group (Figure 5, yellow box) was composed only of isolates from *Passiflora* spp., and was most related to the Mediterranean group. The Asian group included two sister clades: a monophyletic clade containing mostly Korean isolates (Figure 5, orange box) and two isolates from China and Japan, and the second, more basal (Figure 5, blue box) containing isolates from different Asian countries.

Confirmation of identified viruses by RT-PCR and PCR

Viruses identified by HTS were confirmed by RT-PCR and PCR (for ToLCNDV) using specific primers for each virus against the same sample used for RNA-Seq. Four virus-specific primers designed were used (Supplementary Table S2). Presence of all four viruses was confirmed, with expected amplicon sizes of 509 bp for CCYV, 581 bp for CmEV, 632 bp for ToLCNDV, and 787bp for CABYV. RT-PCR/PCR amplified virus-derived fragments were assessed on agarose gel (Supplementary Figure S5), and further confirmed by Sanger sequencing. The sequencing results showed 100% similarities with

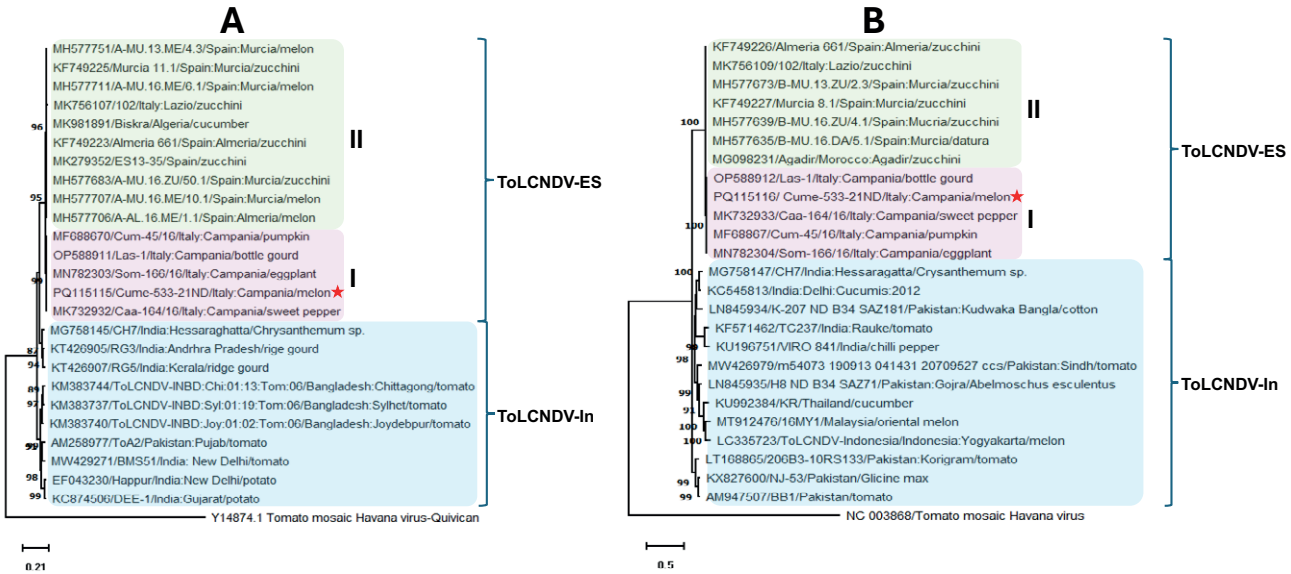

Figure 4. Phylogenetic analyses based on the complete nucleotide sequences of DNA-A (A) and DNA-B (B) components of different ToLCNDV isolates from the Mediterranean region (ToLCNDV-ES) and Asia (ToLCNDV-In). Bootstrap values >75% (n = 1,000 bootstraps) are indicated for each node. In both trees, the ToLCNDV isolate Cume-533-21-ND (red star) groups together with the other four isolates identified in the Italian region Campania, forming a distinct subgroup (pink box), within the ToLCNDV-ES major clade. The green box groups ToLCNDV isolates belonging to subgroup II (from Spain and central Italy) within the ToLC-NDV-ES major clade. The blue box highlights the ToLCNDV-In clade, including isolates from Asia.

the contig sequences derived from the HTS data. The RT-PCR/PCR and HTS results both indicated that all the viruses identified by HTS were present in the melon sample Cume-533-21 used for HTS sequencing.

RT-PCR/PCR-based incidence of identified viruses

Approximately 80% of collected plants showed symptoms (i.e. 86 plants). Ninety-six of the 108 samples were positive for viral pathogens, with CmEV present in 84 (78%) of the samples, ToLCNDV in 84 (78%), CCYV in 74 (69%) and CABYV in 56 (52%) of the samples. CMV was detected only in two plants, while WMV, ZYMV and PRSV were not detected in any of the sampled plants. Of the 22 asymptomatic plants, ten were infected by CmEV and twelve were negative to all the viruses assayed.

Most of the symptomatic samples showed positive reactions for more than one virus, and mixed infections were present in all the symptomatic samples. The mixed infection rate was greatest among CABYV, ToLCNDV, CCYV and CmEV, with 44 samples (41%) having these quadruple infections. Thirty plants (28%) were infected by ToLCNDV + CCYV + CmEV. Double infections by CABYV + ToLCNDV were identified in ten samples (9%), and by CMV + CABYV in two samples (2%) (Figure 6). CABYV, ToLCNDV and CCYV were detected in all of the mixed infections.

DISCUSSION

Spring-summer production of melons in Southern Italy has been severely affected by heavy infestations of whiteflies and aphids, probably associated with ongoing climate changes, which favour thermophilic virus vectors such as *B. tabaci*, and with the increasing difficulties in controlling insects. This has resulted in increased field incidence of symptoms probably caused by viruses, and emergence of yellows symptoms associated with decline of melon crops in Southern Italy. However, the causal agents responsible for melon yellows in the main growing areas of Italy had not been previously identified.

Data presented here, based on HTS results from one melon plant and a following survey in the same field using RT-PCR/PCR with virus-specific primers, showed that whitefly-transmitted viruses, particularly ToLCNDV and CCYV, with this record of CCYV being the first in Italy, were probably more established in the field inspected than viruses transmitted by aphids. CABYV, with incidence of 52% was the most prevalent aphid-transmitted virus in the assessed field. The other aphid-transmitted viruses (WMV, ZYMV and PRSV), except for CMV found in two

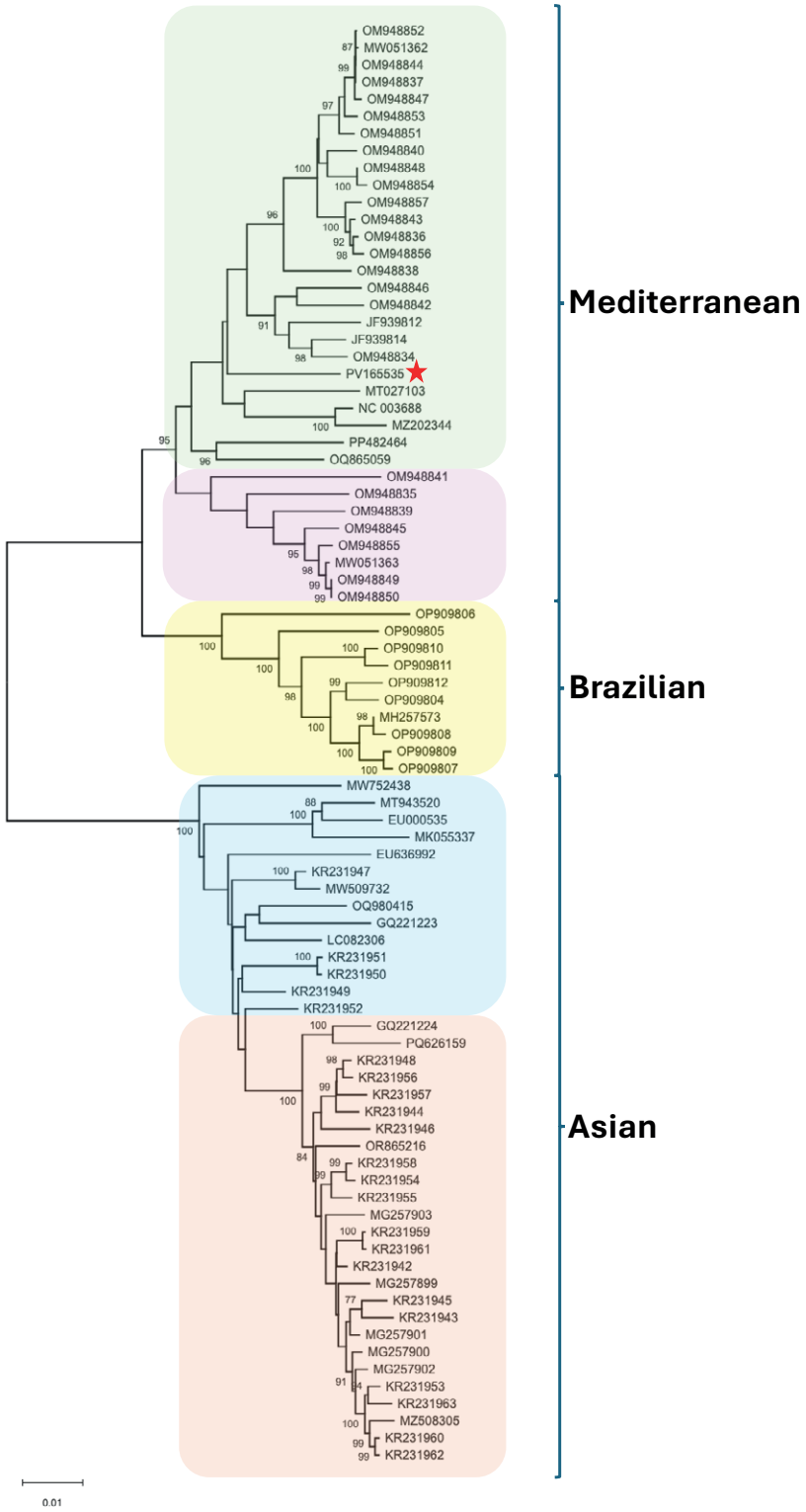

Figure 5. Maximum likelihood tree obtained with the whole genome of CABYV international isolates. Bootstrap values (n = 1000 replicates) >75% are indicated. Phylogeny reconstruction showed that Mediterranean clade was composed of a major (green box) and a minor (pink box) subgroup. Similarly, the Asian clade was composed by two sister subclades (blue and orange boxes). The Brazilian clade (yellow box) was related to the Mediterranean clade. The CABYV isolate Cume-533-21-CAB (PV165535) (red star) clustered within the major subgroup (green box) of the Mediterranean clade.

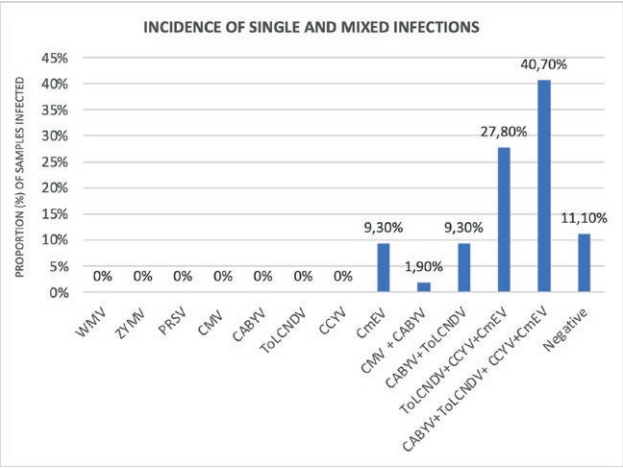

Figure 6. Proportions of 108 sampled melon plants that were infected by four viruses, as shown by RT-PCR results. WMV, watermelon mosaic virus; ZYMV, zucchini yellow mosaic virus; PRSV, papaya ring spot virus; CMV, cucumber mosaic virus; CABYV, cucurbit aphid-borne yellows virus; ToLCNDV, tomato leaf curl New Delhi virus; CCYV, cucurbit chlorotic yellows virus; CmEV, cucumis melo alphaendornavirus.

plants, were not detected (Figure 6). Since only one melon field was sampled, these results may not reflect virus prevalence in melon crops in the Campania region.

ToLCNDV has been considered the main emerging virus in cucurbit cultivations of the Mediterranean region (Moriones *et al*., 2017; Vo *et al*., 2025), and this was found to be the most prevalent virus (78% of the tested samples) in the present study. The MEAM1 and MED genotypes of the *B. tabaci* complex are involved in the transmission and spread of the ToLCNDV-ES strain in the Mediterranean region (Moriones *et al*., 2017; Janssen *et al*., 2017; Bertin *et al*., 2018). From the phylogenetic point of view, the subgroup I and II of this virus have been described in ToLCNDV-ES populations. Based on CP phylogeny, subgroup II comprises isolates from Spain, Italy and other Mediterranean countries, while subgroup I comprises only Italian isolates from the central and southern Italy (Panno *et al*., 2019; Troiano and Parrella, 2023). Phylogenetic relationships of the ToLCNDV-ES isolate from Campania region, based on both DNA components, showed that the Cume-533-21-ND isolate grouped within subgroup I (Figure 4, A and B). Using an infectious clone of a ToLCNDV-ES isolate identified from Campania region and belonging to subgroup I (Parrella *et al*., 2018; Troiano and Parrella, 2023), Vo *et al*. (2022b) demonstrated that this isolate was able to infect only cucurbit hosts, although reported that infection in tomato could be enhanced by tomato yellow leaf curl virus (TYLCV). The continuous overlapping of cucurbit cultivations, particular courgette, from spring until late autumn, which occurs in some cultivation areas of the Campania region, may have resulted in biological adaptation of subgroup I to cucurbits, although further evidence is required to support this hypothesis.

The consistent detection of ToLCNDV on symptomatic cucurbits led to the assumption that this was the only virus responsible for losses on cucurbits in southern Italy. However, two poleroviruses, CABYV and recently PABYV, have been detected on cucurbits, responsible of YD in Italy. CABYV has been present for at least 20 years (Tomassoli and Meneghini, 2007) and has been recently detected with high incidence in the Campania region, associated with yellowing of the older leaves of courgette (Desbiez *et al*., 2023), whereas Parrella *et al*. (2023) detected PABYV at low frequency in the same area. In the present study we also detected CABYV infecting melon. The CABYV isolate Cume-533-21-CAB, here identified by HTS analysis, was completely sequenced, and it grouped within the Mediterranean clade (Figure 5). The incidence of CABYV was high (52% of the sampled plants), and always found in mixed (double or quadruple) virus infections (Figure 6). CABYV is persistently transmitted by cucurbit-colonizing aphids (e.g., *Aphis gossypii*, *Myzus persicae*). Since the number and frequency of use of insecticides allowed for a sustainable crop management have been reduced in recent years, this could lead to increased incidence of persistent-transmitted viruses in susceptible crops including cucurbits.

The present study is also the first to identify CCYV infecting melon in Italy. However, CCYV has been reported in the Mediterranean region for several years, particularly in Spain, Greece, Turkey, Algeria and Israel (EPPO, 2022), and this virus has probably also been present in Italy for some time. CCYV in melon produces symptoms that are very similar to those of caused by CYSDV and BPYV, consisting of yellowing of host plant leaves. CCYV, CYSDV and BPYV are criniviruses (or: belong to the genus *Crinivirus*), and are part of the complex of emerging whitefly-transmitted viruses causing yellows diseases in cucurbits responsible for severe losses (Kavalappara *et al*., 2021). Whereas BPYV is transmitted by *T. vaporariorum*, both MEAM1 and MED genotypes of *B. tabaci* transmit CCYV and CYSDV, although the MED genotype can transmit CCYV more efficiently than CYSDV (Lu *et al*., 2017). Since the MED genotype was found to be much more widespread than the MEAM1 genotype in Campania (Parrella *et al*., 2014 and the present study) this could partly explain the high incidence of CCYV found in melon in the present survey. From a phylogenetic viewpoint, the RNA 1 sequence of the new CCYV isolate clustered with sequences of isolates from the United States of

America (USA) and Japan, although this grouping was not well supported statistically (Figure 1A). For the RNA 2, no clear grouping was shown by the phylogenetic reconstruction (Figure 1B). This is not surprising since criniviruses show limited genetic diversity even among geographically distant isolates (Rubio *et al*., 2001; Orilio and Navas-Castillo, 2009). CCYV has already been shown to have low genetic variability in the RNA-dependent RNA polymerase, coat protein, and minor coat protein genes of different virus isolates (Orfanidou *et al*., 2017).

The present study is also the first to report CmEV in Italy, with high incidence (78%) among the viruses detected. This is not surprising, since endornaviruses are vertically transmitted, infecting host germ line, and remaining permanently associated with that host (Sabanadzovic *et al*., 2016). This is consistent with division of CmEV isolates into two phylogenetic groups based on partial sequences identified, respectively, in *Cucumis melo* subsp. *melo* and *C. melo* subsp. *agrestis* (Sabanadzovic *et al*., 2016). Nevertheless, this phylogenetic reconstruction was based on partial sequences of CmEV isolates. In the present study, the phylogenetic reconstruction shown in Figure 3 was based on the whole CmEV genomes available in Genbank, including the new isolate Cume-533-21-Alpha, and concerns only isolates from *C. melo* subsp. *melo*. Phylogenetic relationships among CmEV genomic sequences available in GenBank showed that the Italian isolate was more related to two isolates from the Mediterranean/European region (one from Israel and the other from Slovakia) compared to isolates from Brazil and the USA), suggesting possible phylogeographic distribution of CmEV isolates. Nevertheless, these data should be supported by additional large-scale CmEV phylogenetic reconstruction, including genomic sequences of geographically different isolates.

Plant viruses can influence behaviour of their vectors by increasing efficiency of their transmission, as reported in CCYV-*B. tabaci* interactions (Lu *et al*., 2019). Virus-virus interactions in mixed infections can also influence population dynamics of particular component viruses in their hosts (Wintermantel *et al*., 2008; Gautam *et al*., 2020). For example, for the CCYV-CYSDV pathosystem, CYSDV and CCYV tend to accumulate at lower level in zucchini plants infected with the two viruses than in singly infected plants (Orfanidou *et al*., 2021). Also in *Begomovirus-Crinivirus* pathosystem of cucurbit leaf crumple virus (CuLCrV)-CYSDV, *B. tabaci* acquires the same levels of the CuLCrV but reduced levels of CYSDV from double infected plants compared to plants infected by any one of these viruses (Gadhave *et al*., 2020; Gautam *et al*., 2020). This could partially explain the greater incidence of ToLCNDV compared to that of CCYV observed in melon in the present study.

Virus infections of melon can cause important economic losses. Field monitoring of major production areas is important for identifying emerging and spreading viruses. In the present study two previously unreported viruses (CCYV and CmEV) were deteted in an Italian melon crop. In addition to these viruses, most of the plants were doubly or multiply infected with other viruses including ToLCNDV and CABYV, confirming the trend for YD described in melon in some regions of Spain, where CmEV, CABYV, ToLCNDV as well as WMV were the most abundant viruses detected (Maachi *et al*., 2022), and in other cucurbit crops in Mediterranean region (Radouane *et al*., 2021; López-Martín *et al*., 2023). The results of the present study, although temporally and spatially limited, indicate that these emerging viruses, forming a complex in association with other known cucurbit viruses, represent new threats of YD to melon crops in southern Italy. However, future impacts of these diseases are likely to be influenced by success of global and national efforts to create effective surveillance and response systems, based on accurate diagnostic tools and regular field monitoring. Extensive and frequent surveys of winter and spring crops, of melon, other cucurbits and wild plants, will elucidate aspects of the epidemiology of the viral yellowing complex, including the identification of the hosts allowing virus overwintering and the role of the different vector genotypes in disease spread. This information will assist definition of useful strategies to mitigate the disease impacts of viruses on host crops.

ACKNOWLEDGEMENTS

This research was part of the Short Term Mobility (STM) 2020 and 2024 programmes, financed by the National Research Council (CNR) of Italy. The authors thank Mr Gaetano Mennella (IPSP-CNR) for his administrative support.

LITERATURE CITED

Barba M., Czosnek H., Hadidi A., 2014. Historical perspective, development and applications of next-generation sequencing in plant virology. *Viruses* 6: 106–136. https://doi.org/10.3390/v6010106

Bertin S., Luigi M., Parrella G., Giorgini M., Davino S., Tomassoli L., 2018. Survey of the distribution of *Bemisia tabaci* (*Hemiptera*: *Aleyrodidae*) in Lazio region (Central Italy): a threat for the northward

expansion of tomato leaf curl New Delhi virus (*Begomovirus*: *Geminiviridae*) infection. *Phytoparasitica* 46: 171–182. https://doi.org/10.1007/s12600-018-0649-7

Bertin S., Parrella G., Nannini M., Guercio G., Troiano E., Tomassoli L., 2021. Distribution and genetic variability of *Bemisia tabaci* cryptic species (*Hemiptera: Aleyrodidae*) in Italy. *Insects* 12: 521. https://doi.org/10.3390/ insects12060521

Brown J.K., Zerbini F.M., Navas-Castillo J., Moriones E., Ramos-Sobrinho R., *et al.,* 2015. Revision of *Begomovirus* taxonomy based on pairwise sequence comparisons. *Archives of Virology* 160: 1593–1619.

Desbiez C., Troiano E., Kwak M., Kil E-J., Parrella G., 2023. Identification and characterization of the viruses responsible for recent epidemics on cucurbits in Southern Italy. 19th Plant Virology Conference, Aussois, France, P-17.

EPPO, 2022. Cucurbit chlorotic yellows virus, an emerging virus of cucurbits spreading worldwide. EPPO Reporting Service no. 02 – 2022; Num. article: 2022/043.

Gadhave K.R., Gautam S., Dutta B., Coolong T., Adkins S., Srinivasan R., 2020. Low frequency of horizontal and vertical transmission of cucurbit leaf crumple virus in whitefly *Bemisia tabaci* Gennadius. *Phytopathology* 110: 1235–1241. https://doi.org/10.1094/PHYTO-09-19-0337-R

Gautam S., Gadhave K.R., Dutta B., Coolong T., Adkins S., Srinivasan R., 2020b. Virus-virus interactions in a plant host and in a hemipteran vector: implication for vector fitness and virus epidemics. *Virus Research* 286: 198069.

Hall T.A., 1999. BioEdit: A user-friendly biological sequence alignment editor and analysis program for Windows 95/98/NT. *Nucleic Acids Symposium Series* 41: 95–98.

Hasegawa M., Kishino H., and Yano T., 1985. Dating the human-ape split by a molecular clock of mitochondrial DNA. *Journal of Molecular Evolution* 22: 160–174.

Janssen D., Simon A., Crespo O., Ruiz L., 2017. Genetic population structure of *Bemisia tabaci* in Spain associated with Tomato leaf curl New Delhi virus. *Plant Protection Science* 53: 25–31.

Karasev A. V., 2000. Genetic diversity and evolution of closteroviruses. *Annual Review of Phytopathology* 38: 293–324.

Kavalappara S.R., Milner H., Konakalla N.C., Morgan K., Sparks A.N., … Bag S., 2021. High Throughput Sequencing-aided survey reveals widespread mixed infections of whitefly-transmitted viruses in cucurbits in Georgia, USA. *Viruses* 13: 988. https://doi.org/10.3390/v13060988.

Kumar S., Stecher G., Li M., Knyaz C., Tamura, K., 2018. MEGA X: molecular evolutionary genetics analysis across computing platforms. *Molecular Biology and Evolution* 35: 1547–1549. https://doi.org/10.1093/molbev/msy096

ISTAT, 2024. Stima delle superfici e produzioni delle coltivazioni agrarie, floricole e delle piante intere da vaso. (http://dati.istat.it/index.aspx?queryid=33703#)

La Tourrette K., Holste N.M., Garcia-Ruiz H., 2021. Polerovirus genomic variation. *Virus Evolution* 7, veab102. https://doi.org/10.1093/ve/veab102

Lecoq H., Desbiez C., 2012. Viruses of cucurbit crops in the Mediterranean region: an ever-changing picture. *Advances in Virus Research* 84: 67–126.

López-Martín M., Sifres A., Gómez-Guillamón M. L., Picó B., Pérez-de-Castro A., 2023. Incidence and genetic diversity of cucurbit viruses in the Spanish Mediterranean area. *Plant Pathology* 73: 431–443. https://doi.org/10.1111/ppa.13825

Lu S.H., Chen M., Li J., Shi Y., Gu Q., Yan F., 2019. Changes in *Bemisia tabaci* feeding behaviors caused directly and indirectly by cucurbit chlorotic yellows virus. *Virology Journal* 16: 106. https://doi.org/10.1186/s12985-019-1215-8

Lu S.H., Li J.J., Wang X.L., Song D.Y., Bai R.E., .. Yan F.M., 2017. A semipersistent plant virus differentially manipulates feeding behaviours of different sexes and biotypes of its whitefly vector. *Viruses* 9: 4.

Luigi M., Bertin S., Manglli E., Troiano E., Davino S., Tomassoli L., Parrella G., 2019. First report of tomato leaf curl New Delhi virus causing yellow leaf curl of pepper in Europe. *Plant Disease* 103: 2970.

Maachi A., Donaire L., Hernando Y., Aranda M.A., 2022. Genetic differentiation and migration fluxes of viruses from melon crops and crop edge weeds. *Journal of Virology* 96: e00421–e00422.

Maina S., Donovan N.J., Plett K., Bogema D., Rodoni B.C., 2024. High-throughput sequencing for plant virology diagnostics and its potential in plant health certification. *Frontiers in Horticulture* 3: 1388028. https://doi.org/10.3389/fhort.2024.1388028

Manglli A., Murenu M., Sitzia M., Tomassoli L., 2016. First report of *Cucurbit yellow stunting disorder virus* infecting cucurbits in Italy. *New Disease Report* 34: 23.

Moriones E., Praveen S., Chakraborty S., 2017. Tomato leaf curl New Delhi virus: an emerging virus complex threatening vegetable and fiber crops. *Viruses* 9: 264. https://doi.org/10.3390/v9100264

Muhire B.M., Varsani A., Martin D.P., 2014. SDT: A virus classification tool based on pairwise sequence alignment and identity calculation. *PLoS ONE* 9: e108277. https://doi.org/10.1371/journal.pone.0108277

Nei M., Kumar S., 2000. Molecular evolution and phylogenetics. Oxford University Press,

New York.e.0108277 https://doi.org/10.1093/oso/9780195135848.001.0001

Okuda M., Okazaki S., Yamasaki S., Okuda S., Sugiyama M., 2010. Host range and complete genome sequence of *Cucurbit chlorotic yellows virus*, a new member of the genus *Crinivirus*. *Phytopathology* 100: 560–566.

Orfanidou C.G., Baltzi A., Dimou N.A., Katis N.I., Maliogka V.I., 2017. Cucurbit chlorotic yellows virus: insights into its natural host range, genetic variability, and transmission parameters. *Plant Disease* 101: 2053–2058. https://doi.org/10.1094/PDIS-02-17-0164-RE

Orfanidou C., Katsiani A., Papayiannis L., Katis N.I., Maliogka V.I., 2021. Interplay of cucurbit yellow stunting disorder virus with cucurbit chlorotic yellows virus and transmission dynamics by *Bemisia tabaci* MED. *Plant Disease* 105: 416–424.

Orílio A.F., Navas-Castillo J., 2009. The complete nucleotide sequence of the RNA2 of the crinivirus tomato infectious chlorosis virus: isolates from North America and Europe are essentially identical. *Archives of Virology* 154: 683–687. https://doi.org/10.1007/s00705-009-0354-4

Panno S., Caruso A.G., Troiano E., Luigi M., Manglli A., .. Davino S., 2019. Emergence of tomato leaf curl New Delhi virus in Italy: estimation of incidence and genetic diversity. *Plant Pathology* 68: 601–608.

Parrella G., Scassillo L., Giorgini M., 2012. Evidence for a new genetic variant in the *Bemisia tabaci* species complex and the prevalence of the biotype Q in southern Italy. *Journal of Pest Science* 85: 227–238. https://doi.org/10.1007/s10340-012-0417-2

Parrella G., Nappo A.G., Manco E., Greco B., Giorgini M., 2014. Invasion of the Q2 mitochondrial variant of Mediterranean *Bemisia tabaci* in southern Italy: possible role of bacterial endosymbionts. *Pest Managment Science* 70: 1514–1523. https://doi.org/10.1002/ps.3686

Parrella G., Troiano E., Formisano G., Accotto G.P., Giorgini M., 2018. First report of tomato leaf curl New Delhi virus associated with severe mosaic of pumpkin in Italy. *Plant Disease* 102: 459. https://doi.org/10.1094/PDIS-07-17-0940-PDN

Parrella G., Troiano E., Lee S., Kil E.-J., 2020. Tomato leaf curl New Delhi virus found associated with eggplant yellowing disease in Italy. *Plant Disease* 104: 10.1094.

Parrella G., Troiano E., Desbiez C., 2023. First report of pepo aphid-borne yellows virus on courgette in Italy. *New Disease Report,* 47: e12144. https://doi.org/10.1002/ndr2.12144

Radouane N., Ezrari S., Belabess Z., Tahiri A., Tahzima R., ... Lahlali R., 2021. Viruses of cucurbit crops: current status in the Mediterranean Region. *Phytopathologia Mediterranea* 60: 493–519. https://doi.org/10.36253/phy-to-12340

Rubio L., Abou-Jawdah Y., Lin H.X., Falk BW., 2001. Geographically distant isolates of the crinivirus *Cucurbit yellow stunting disorder virus* show very low genetic diversity in the coat protein gene. *Journal of General Virol*ogy 82: 929–933. https://doi.org/10.1099/0022-1317-82-4-929

Sabanadzovic S., Wintermantel W.M., Valverde R.A., McCreight J.D., Aboughanem-Sabanadzovic N., 2016. Cucumis melo endornavirus: genome organization, host range and co-divergence with the host. *Virus Research* 214: 49–58. https://doi.org/10.1016/j.virusres.2016.01.001

Tomassoli L., Lumia V., Siddu G.F., Barba M, 2003. Yellowing disease of melon in Sardinia (Italy) caused by *Beet pseudoyellows virus*. *Journal of Plant Pathology* 85: 59–61.

Tomassoli L., Meneghini M., 2007. First report of *Cucurbit aphid-borne yellows virus* in Italy. *Plant Pathology* 56: 720.

Troiano E., Parrella G., 2023. First report of tomato leaf curl New Delhi virus in *Lagenaria siceraria* var. *longissima* in Italy. *Phytopathologia Mediterranea* 62: 25–28. https://doi.org/10.36253/phyto-14147

Utili D., 2023. Melone, aree e volumi in calo: le strategie per il futuro del comparto. *Corriere Ortofrutticolo*, 25 ottobre 2023. (http://www.corriereortofrutticolo.it)

Vo T.T.B., Lal A., Ho, P.T., Troiano E., Parrella G., Kil E.-J., Lee S., 2022a. Different infectivity of Mediterranean and Southern Asian tomato leaf curl New Delhi virus isolates in cucurbit crops. *Plants* 11: 704. https://doi.org/10.3390/plants11050704

Vo T.T.B., Troiano E., Lal A., Hoang P.T., Kil E.-J., Lee S., Parrella G., 2022b. ToLCNDV-ES infection in tomato is enhanced by TYLCV: evidence from field survey and agroinoculation. *Frontiers in Microbiology* 13: 954460. https://doi.org/10.3389/fmicb.2022.954460

Vo T.T.B., Tabassum M., Nattanong B., Qureshi M.A., Im H.-J., Parrella G., Kil E—J., Lee S., 2025. The insidious threat: assessing the dangers and spread of tomato leaf curl New Delhi virus. *Plant Pathology Journal* 41: 1–16. https://doi.org/10.5423/PPJ.RW.11.2024.0177

Wintermantel W.M., Cortez A.A., Anchieta A.G., Gulati-Sakhuja A., Hladky L.L., 2008. Co-infection by two criniviruses alters accumulation of each virus in a host-specific manner and influences efficiency of virus transmission. *Phytopathology* 98: 1340–1345. https://doi.org/10.1094/PHYTO-98-12-1340

Phytopathologia Mediterranea
The international journal of the
Mediterranean Phytopathological Union

Firenze University Press
www.fupress.com/pm

Research Papers

Occurrence and identification of a '*Candidatus* Phytoplasma asteris' (subgroup 16SrI-F) strain infecting *Lolium rigidum* in Iran

Seyyed Alireza ESMAEILZADEH-HOSSEINI[1,*], Ghobad BABAEI[2], Assunta BERTACCINI[3]

[1] *Plant Protection Research Department, Yazd Agricultural and Natural Resources Research and Education Centre, AREEO, Yazd, Iran*
[2] *Plant Protection Research Department, Chaharmahal and Bakhtiari Agricultural and Natural Resources Research and Education Centre, AREEO, Shahrekord, Iran*
[3] *Alma Mater Studiorum - University of Bologna, Italy*
*Corresponding author. E-mail: phytoplasma.iran@gmail.com

Summary. From 2016, witches' broom and stunting symptoms were observed in *Lolium rigidum* grown in some fruit tree nurseries in Faragheh (Abarkouh, Yazd province, Iran). Total DNAs were extracted from symptomatic and asymptomatic plants and assessed for phytoplasma presence using direct and nested PCR to detect the 16S ribosomal RNA gene. From all symptomatic *L. rigidum* plant samples, expected length PCR amplicons were obtained. RFLP analysis with informative restriction enzymes showed identical profiles in all the samples resulted positive, that were also consistent with those of one of the subgroups of the aster yellows phytoplasmas (16SrI). The 16S rRNA gene sequence of Faragheh *L. rigidum* bushy stunt strain was 100% identical to some '*Candidatus* Phytoplasma asteris' related strains, and 99.12% similar to the reference '*Ca.* P. asteris' strain. The virtual RFLP pattern was identical (similarity coefficient 1.00) to the pattern of phytoplasmas in subgroup 16SrI-F. This is the first report of occurrence and molecular identification of this phytoplasma strain in *L. rigidum* and indicates a potential phytoplasma reservoir for trees in fruit tree nurseries where insect vectors may be present. This phytoplasma strain has been reported in symptomatic stone fruits in Spain and in potato in Ecuador. Further research on the epidemiology of witches' broom and stunting in *L. rigidum* is required to develop elimination the phytoplasma from areas surrounding agricultural crops and avoid the risks of epidemics.

Keywords. Annual ryegrass, aster yellows, Yazd province, epidemiology.

OPEN ACCESS

Citation: Esmaeilzadeh-Hosseini, S. A., Babaei, G., & Bertaccini, A. (2025). Occurrence and identification of a '*Candidatus* Phytoplasma asteris' (subgroup 16SrI-F) strain infecting *Lolium rigidum* in Iran. *Phytopathologia Mediterranea* 64(3): 597-606. DOI: 10.36253/phyto-16684

Accepted: November 5, 2025

Published: December 11, 2025

Data Availability Statement: All relevant data are within the paper and its Supporting Information files.

Competing Interests: The Author(s) declare(s) no conflict of interest.

Editor: Roberto Buonaurio, University of Perugia, Italy.

ORCID:
SAEH: 0000-0002-0240-7459
GB: 0000-0002-3388-5496
AB: 0000-0002-5650-1512

INTRODUCTION

Lolium rigidum (*Poaceae*) is an annual ryegrass, that is an important weed but is also planted to a limited extent in some local areas in Iran as fodder for livestock feed. This plant species is native to the Mediterranean region and grows naturally in Europe, Africa, Asia and the Indian sub-continent. It is considered invasive in some regions, such as Australia, where it

was introduced as a forage crop in approx. 1880, but it has since become an economically damaging weed. *Lolium rigidum* is mainly grown as a forage crop, but it may be a host for the human and animal pathogens *Clavibacter* spp. and *Claviceps purpurea* (McKay and Riley, 1993; Wegulo and Carlson, 2011).

Phytoplasmas are plant pathogenic bacteria without cell walls, that are associated with many destructive plant diseases, with a variety of symptoms (Bertaccini *et al*., 2014; Bertaccini, 2022). These pathogens are transmitted by phloem feeding insects (mainly leafhoppers and psyllids) and are identified based on 16S rRNA gene sequences due to difficulty growing these organisms in axenic culture (Contaldo *et al*., 2019). Identified phytoplasma strains are grouped in more than 50 '*Candidatus* Phytoplasma' species that are designated based on 16S rRNA gene sequencing (IRPCM, 2004; Bertaccini *et al*., 2022). Moreover, an RFLP-based system distinguishes phytoplasmas into ribosomal groups and subgroups (Lee *et al*., 1998) discriminating strains with high similarities in the 16S rRNA gene.

Presence of phytoplasmas in *Lolium* species in fields has not been previously reported. Symptoms resembling those associated with the phytoplasma presence were observed in plants growing in stone fruit tree nurseries in Faragheh, Abarkouh, Yazd province, Iran. The present study aimed to determine presence and identity of phytoplasmas associated with witches' broom and stunting symptoms in *L. rigidum*, as first step to devise appropriate disease management and maintain nursery plants free from these pathogens.

MATERIALS AND METHODS

Plant sampling and disease incidence

From 2016, witches' broom and stunting symptoms were repeatedly observed in scattered *L. rigidum* plants grown in stone fruit tree nurseries (mainly apricot, plum and peach) in Faragheh, Iran. A survey was carried out from 2016 to 2018 in 10 fruit tree nurseries. These nurseries were of approx. 500 to 1,000 m^2 each. Disease incidence in each nursery was determined by sampling within 1 m^2, and the disease percentage was calculated as the total number of *L. rigidum* plants with symptoms divided by the total number of *L. rigidum* plants growing in each quadrat. Twelve symptomatic and four asymptomatic *L. rigidum* samples were collected and subjected to molecular studies to determine phytoplasma presence and identity.

Molecular detection of phytoplasma presence

Total DNA was extracted from 0.2 g of midrib tissue of fresh leaves from the sampled *L. rigidum* plants showing witches' broom and stunting and from the asymptomatic plants, using the procedure of Healey *et al.* (2014). Total DNA extracted from a witches' broom-symptomatic *Medicago sativa* plant infected by a 16SrII-C phytoplasma strain was used as positive control (Salehi *et al*., 2011). The quality and quantity of extracted total DNA was estimated by spectrophotometer and agarose gel electrophoresis (Green and Sambrook, 2012), and 100 ng of nucleic acids were used for each sample as PCR template. One µL of the P1/P7 PCR product (Deng and Hiruki, 1991; Schneider *et al*., 1995) diluted 1:30 with sterile deionized water, was amplified in nested PCR with R16mF2/R16mR2 and R16F2n/R2 primer pairs (Gundersen and Lee, 1996). The PCR reactions were carried out in 50 µL mixtures, as described by Esmaeilzadeh-Hosseini *et al*. (2020). Five µL of each reaction mixture were electrophoresed in a 1% (w/v) agarose gel in TBE buffer, and were visualized after ethidium bromide staining, using a UV imaging system (Isogene Life Science, Netherlands). The sizes of the PCR products were estimated by comparison with a 100 bp DNA ladder (Biobasic, Canada). The R16F2n/R2 amplified products from *L. rigidum* witches' broom were digested separately with *Mse*I, *Hha*I, *Alu*I, *Hae*III, *Rsa*I, *Hpa*II, *Taq*I and *Kpn*I restriction enzymes, according to the manufacturer's instructions (Thermo Fisher Scientific, USA). These enzymes were selected to compare the main differential profiles reported for aster yellows phytoplasmas (16SrI). The restriction products were separated by 8% polyacrylamide gel electrophoresis, then stained by ethidium bromide and visualized using the UV imaging system (above) for comparison with the reported 16S rDNA pattern profiles of previously described phytoplasma strains (Lee *et al*., 1998).

Sequencing and phylogenetic analyses

Only samples from two of the surveyed nurseries were positive for phytoplasmas for all the 12 symptomatic samples collected. These positive samples showed identical RFLP profiles. The R16mF2/R16mR2 primed PCR products of the nested PCR (1.4 kb) from four randomly selected *L. rigidum* witches' broom and stunting samples were directly sequenced from both ends (Macrogen, South Korea), using the same primers as for the nested amplification. The assembled sequences (DNA BASER assembler program) were compared with sequences deposited in the GenBank database using BLAST analyses at the National Center for Biotechnology Information (NCBI) and were

aligned with the BioEdit 7.2 tool. The comparison with the reference strain of '*Ca*. P. asteris (GenBank accession number M30790) showed 99.12% similarity, identifying the strains as '*Ca*. P. asteris'. A number of other phytoplasma strains showed identity percentages greater than this to the *L. rigidum* witches' broom phytoplasmas and those with 100% similarity were the strains AVUT (GenBank accession number LB388958), AAY (apricot aster yellows operon A, GenBank accession number AB639057), and *Psammotettix* sp. B4 (GenBank accession number MZ458767). The 1,246 bp of 16S rDNA sequences of '*Ca*. Phytoplasma' (Bertaccini *et al.,* 2022) and those of selected '*Ca*. P. asteris' strains, including the *L. rigidum* witches' broom and stunting phytoplasma Faragheh strain of the present study, were aligned using MEGA7 software (Kumar *et al*., 2016). A phylogenetic tree was constructed using the neighbor-joining method (Saitou and Nei, 1987) in MEGA7, with *Acholeplasma laidlawii* as an outgroup to root the tree. Bootstrapping was carried out 1,000 times to estimate stability and support for relationship branches (Felsenstein, 1985). The evolutionary distances were computed using the Maximum Composite Likelihood method (Tamura *et al*., 2004). Virtual RFLP analysis using online program *i*PhyClassifier (Zhao *et al*., 2009) was used on the obtained sequences to determine the ribosomal subgroup affiliations of the strains, digesting them *in silico* with the 17 restriction enzymes available in the program.

RESULTS

Figure 1 shows disease symptoms observed in two of the ten nurseries inspected. All the plants of *L. rigidum* showing witches' broom and stunting symptoms were positive for phytoplasmas, while the asymptomatic samples were negative for phytoplasma.

The overall infection percentage of the disease in the two nursery fields was about 4% and was constant in numbers and locations in both the years of the survey. From all symptomatic *L. rigidum* samples, fragments of about 1.8, 1.4 and 1.2 kb were obtained, while from the symptomless plants no amplifications were obtained.

Restriction fragment length polymorphism (RFLP) analysis of the R16F2n/R2 amplicons using informative selected restriction enzymes produced patterns identical to each other and indistinguishable from those of 16SrI group (aster yellows) (Lee *et al.,* 1998) (Figure 2).

The 1.2 kb DNA fragments of the R16F2n/R2 amplicons sequenced from Faragheh *L. rigidum* witches' broom and stunting phytoplasmas were 100% identi-

Figure 1. *Lolium rigidum* witches' broom and stunting symptoms observed in two of the surveyed stone fruit nurseries in Faragheh (Iran).

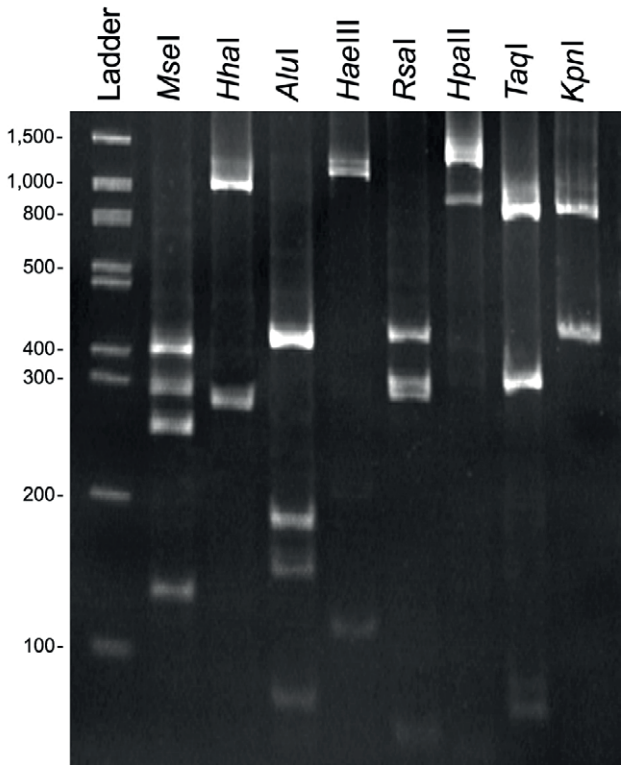

Figure 2. Polyacrylamide gel showing RFLP profiles of 16S rRNA gene fragment a amplified by nested PCR using P1/P7 followed by R16F2n/R2 primer pairs from the *Lolium rigidum* witches' broom and stunting phytoplasma. PCR products were digested by the restriction enzymes listed at the top. Ladder is the 100 bp DNA (Biobasic, Canada).

cal to each other, so one sequence was submitted to the GenBank database under accession number OR365262. The virtual RFLP pattern derived from the R16F2n/R2 fragment of this sequence was identical (similarity coefficient 1.00) to the pattern of the 16SrI-F reference strain in the *i*PhyClassifier (GenBank accession number AY265211) (Figures 3 and 4).

The phylogenetic analysis confirmed that the *L. rigidum* witches' broom and stunting phytoplasma clustered within the '*Ca*. P. asteris' strains enclosed in the subgroup 16SrI-F including phytoplasma strains identified in the putative insect vector *Psammotettix* sp., captured on apricot trees in Turkey (Figure 5).

DISCUSSION

Identification of aster yellows phytoplasmas ('*Ca*. P. asteris', subgroup 16SrI-F) in *L. rigidum* is among the few reports of phytoplasmas in a monocot *Lolium* species. The phytoplasma was detected in nurseries where mainly stone fruit trees are grown. *Lolium rigidum* weeds in apricot seedling nurseries and in general in stone fruit nurseries, cause problems also for weed management. This weed competes with nursery seedlings for water and soil resources, and absorbs many of the fertilizer nutrients required to rapidly produce young fruit tree plants for orchard eastablishment. This competition weakens the fruit tree seedlings and increases their susceptibility to pests and pathogens. Plant pathogens also survive on weeds that act as alternative hosts that are important in disease epidemiology, and can lead to outbreaks of diseases in nurseries and orchards. In the present study cases, *L. rigidum* hosted 16SrI-F phytoplasmas, and could be a source/reservoir for infection by this pathogen.

The only previous reports of phytoplasmas in *Lolium* are in *L. multiflorum* where a phytoplasma 16SrI-L was detected in Lithuania associated with yellowing of leaves and spikes, and general stunting symptoms (Urbanaviciene *et al.,* 2005), and of a 16SrI phytoplasmas in *L. perenne* with similar symptoms in the Russian Federation (Bogoutdinov *et al*., 2021). The symptoms observed in the present study were different from those reported in other agriculturally important monocotledonous plants. These include rice orange leaf and maize leaf reddening (Duduk and Bertaccini, 2006; Jonson *et al*., 2020).

From surveys carried out during the last two decades, the main phytoplasmas identified in Iran were within 16SrI (aster yellows), 16SrII (peanut witches' broom), 16SrIII (X-disease), 16SrVI (clover proliferation), 16SrVII (ash yellows), 16SrIX (pigeon pea witches' broom), 16SrX (apple proliferation), 16SrXI (rice yellow dwarf), 16SrXII ("stolbur"), 16SrXIV (Bermudagrass white leaf), 16SXXIX (*Cassia* witches' broom), and 16SrXXX (salt cedar witches' broom) groups (Esmaeilzadeh Hosseini *et al*., 2023a; 2023b). Aster yellows phytoplasma ('*Ca*. P. asteris', 16SrI) (Lee *et al*., 2004) is the third most widespread phytoplasma identified in Iran, reported from 43 plant species in 19 families. Among the three '*Ca*. Phytoplasma' species described in the 16SrI ribosomal group (*i.e.,* '*Ca*. P. asteris', '*Ca*. P. lycopersici' and '*Ca*. P. tritici') (Bertaccini *et al*., 2022), '*Ca*. P. asteris' and '*Ca*. P. tritici' strains were both detected and identified in this Country. Moreover, for these phytoplasmas four subgroups were reported 16SrI-B, 16SrI-F, 16SrI-R and 16SrI-S (Esmailzadeh Hosseini *et al*., 2023a; 2023b; Salehi *et al*., 2025); however the identified strains are mainly included in subgroup 16SrI-B and have been associated with many diseases including yellowing of *Allium cepa*, phyllody of *Eruca sativa*, little leaf of *Eucalyptus camaldulensis*, phyllody of *Lactuca*

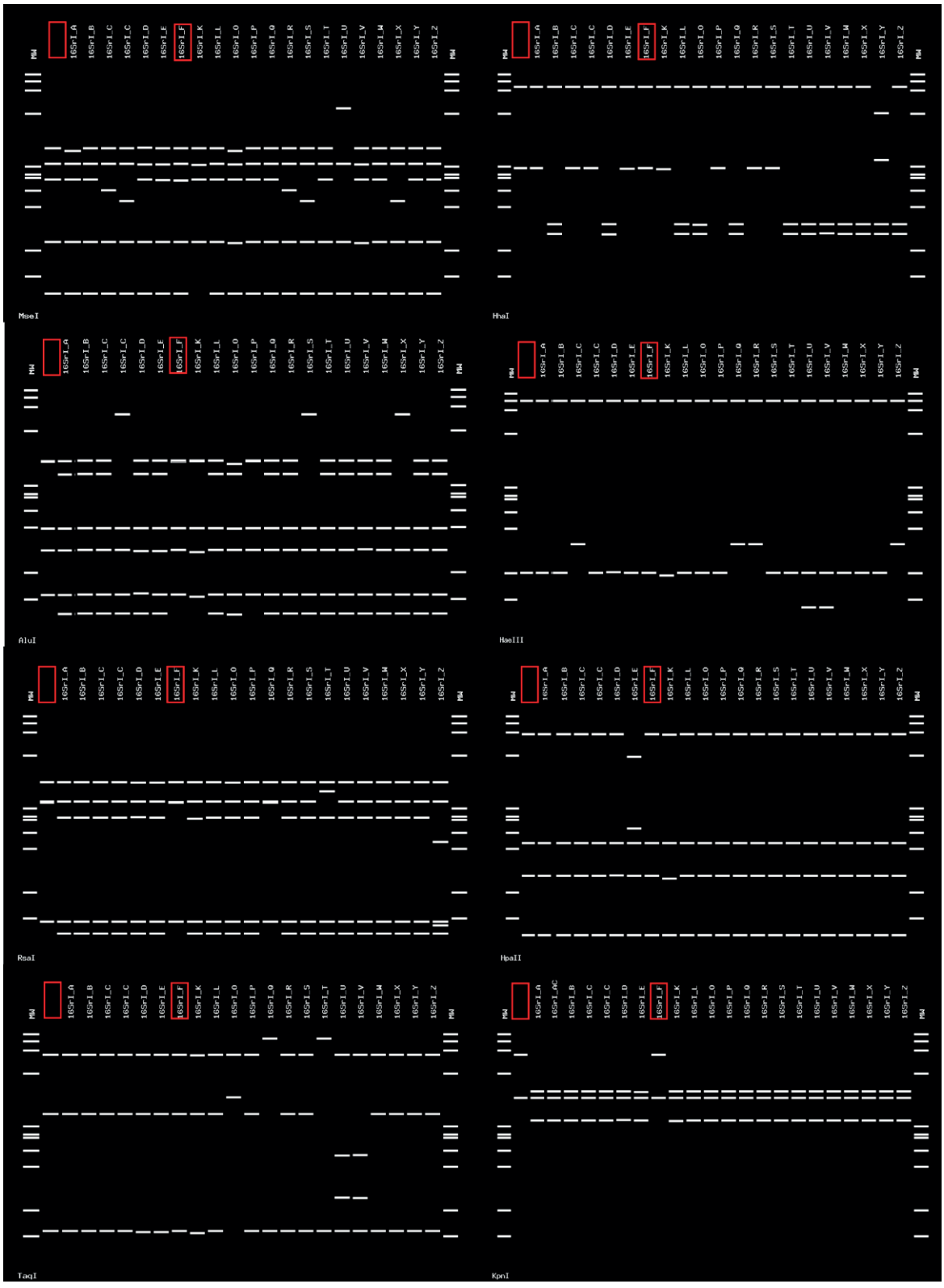

Figure 3. Virtual RFLP patterns generated with the *i*PhyClassifier from *in silico* digestion of the R16F2n/R2 fragment of the *L. rigidum* witches' broom and stunting (GenBank accession number OR365262; lane with no label) with the enzymes used in RFLP on amplicons in Figure 2 confirming that the strain studied is in subgroup 16SrI-F.

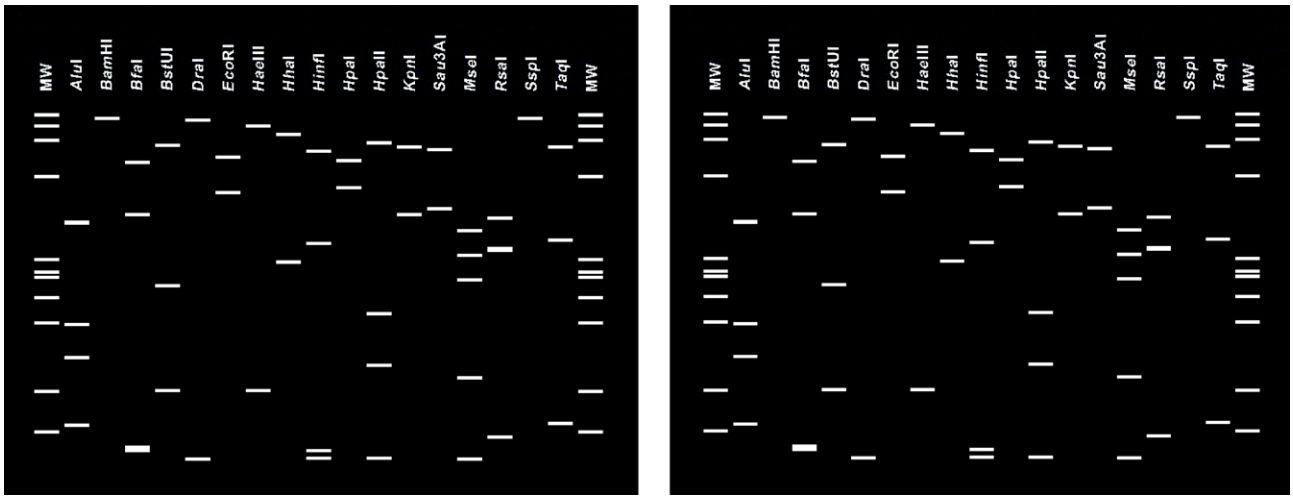

Figure 4. Collective RFLP profile of the Faragheh *L. rigidum* witches' broom and stunting phytoplasma strain on the left (GenBank accession number OR365262) was identical to the pattern for the 16SrI-F reference strain on the right (GenBank accession number AY265211).

sativa, witches' broom of *Morus alba*, *Prunus armeniaca* decline, yellowing of *Rosa canina*, purple top of *Solanum tuberosum*, phyllody of *Sonchus oleraceus*, *Tamarix aphylla* witches' broom, witches' broom of *Tragopogon dubius*, *Vitis vinifera* yellows, and witches' broom and yellowing of *Ziziphus jujuba*. Phytoplasmas in subgroup 16SrI-R was detected and identified in *Aquilegia vulgaris* with phyllody, and subgroup 16SrI-S in *Calendula officinalis* with phyllody (Esmaeilzadeh Hosseini *et al*., 2023a, 2023b). Phytoplasmas belonging to subgroup 16SrI-F were reported in periwinkle plants showing little leaf symptoms in Fars province, Iran (Salehi *et al*., 2025). This phytoplasma has now been identified in *L. rigidum* in Iranian nurseries producing fruit tree propagation materials (apricots). Considering that the same phytoplasma was detected in apricot in Spain, in the putative leafhopper vectors *Psammotettix* sp. in Germany (Bertaccini, 2023) and Turkey (Randa-Zelyut *et al*., 2022), and in *Euscelis incisus* in Serbia (Jakovljevic *et al*., 2020), the present study results have relevance for possible epidemic spread in agricultural situations, since the potential insect vectors are polyphagous. The feeding preferences of these insect vectors and their ability to survive on *L. rigidum* requires further verification. Castillo-Carrillo *et al*. (2018) identified 16SrI-F phytoplasmas in potato plants with purple top symptoms in Ecuador. It is therefore likely that transmission of this phytoplasma from and to nursery trees from herbaceous host species cannot be excluded, although separate surveys in these nurseries have not identified this phytoplasma in trees in Iran. Although stone fruit plants of the investigated nurseries did not have phytoplasma symptoms, there is a risk that this phytoplasma could be transmitted to nurseries.

On the other hand, the presence of the phytoplasma could affect *L. rigidum* when cultivated as forage crop (Oshib Nataj *et al*., 2012), and affect other economically important monocots such as wheat, maize, or barley which are extensively grown in Iran. Since *L. rigidum* is a weed with widespread distribution in this country, its role as phytoplasma reservoir plant should be considered, because a similar role has been demonstrated for phytoplasma-infected alfalfa (Esmailzadeh Hosseini *et al*., 2016) in some areas of Iran. Seeds can be sources of phytoplasma infections in herbaceous hosts including alfalfa, corn, tomato, pea, carrot and eggplant (Calari *et al*., 2011; Zwolinska *et al*., 2012; Satta *et al*., 2020; Mateeti *et al*., 2022, 2023; Gungoosingh Bunwaree *et al*., 2023; Darabakula *et al*., 2024; Bertaccini *et al*., 2025). This makes the detection of 16SrI-F phytoplasmas in *L. rigidum* relevant for management of healthy stone fruit propagation material in Iranian nurseries and in other environments where these crops are grown or where *L. rigidum* is an infesting weed. Large use of herbicides for *L. rigidum* management has resulted in widespread herbicide resistance (Heap, 2019). The majority of *L. rigidum* fields in southern Australian cropping regions are herbicide resistant, based on periodic random surveys (Owen *et al*., 2014), posing threats to elimination of this weed from crops. In some regions environmental temperatures also affect herbicide efficacy. Herbicide resistant *L. rigidum* populations and climate change may provide perennial sources of phytoplasma inoculum, when insect vectors are present. Further research to clarify the epidemiology of diseases associated with 16SrI-F phytoplasmas under Iranian conditions will assist containment of possible disease outbreaks.

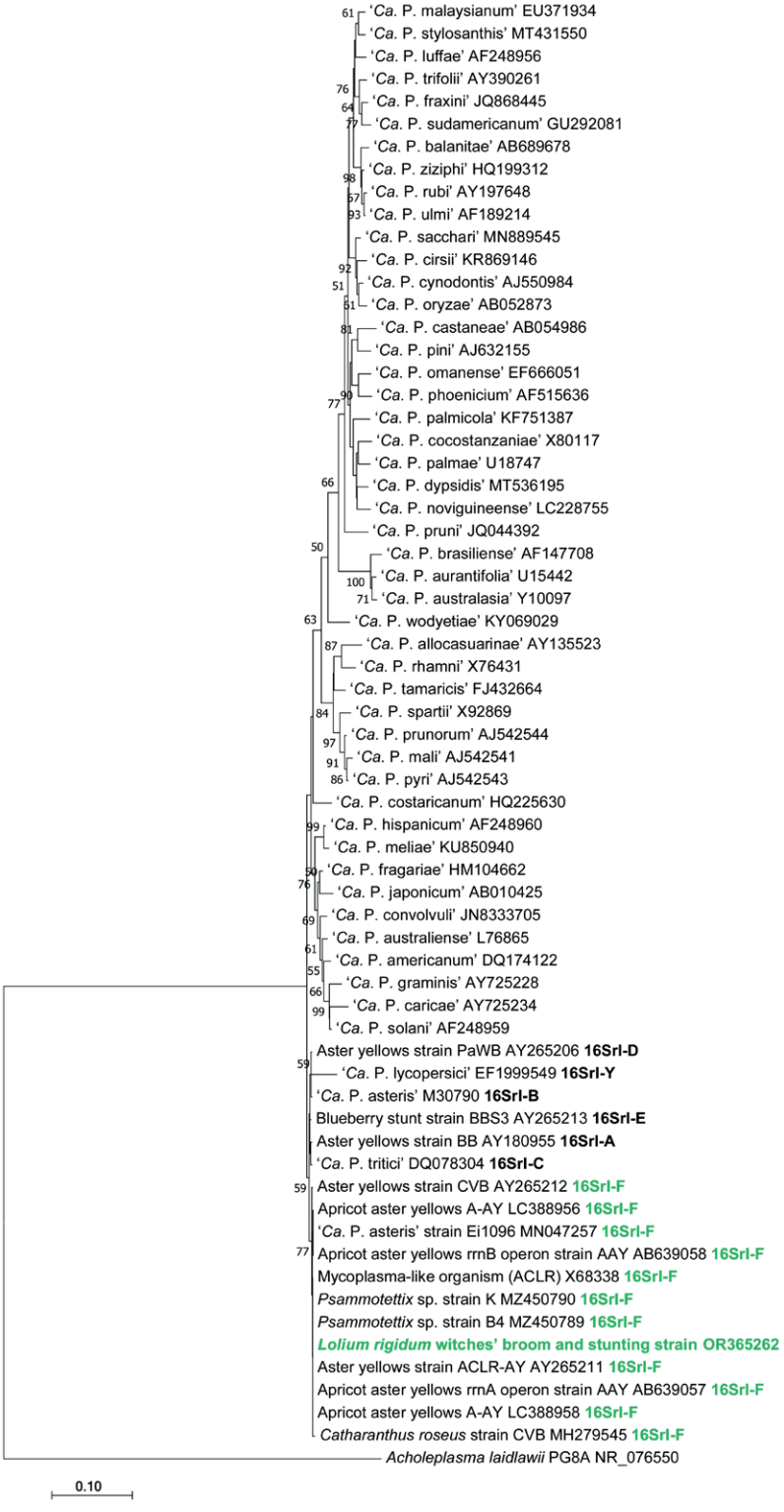

Figure 5. Phylogenetic tree (constructed in MEGA 7) of 16S rRNA gene sequences from 64 phytoplasma strains, and *Acholeplasma laidlawii* as the outgroup. The *Lolium rigidum* witches' broom and stunting phytoplasma and the ribosomal subgroup of related strains, are highlighted in bold green font. Other ribosomal subgroups in group 16SrI are in bold. Proportions (>50%) of replicate trees in which the associated taxa clustered together in the bootstrap test are shown next to relevant branches, the GenBank accession numbers are indicated to the right of phytoplasma names.

ACKNOWLEDGMENTS

This research was a part of results obtained from project no. 24-64-16-067-990413 approved and supported by Agricultural Research, Education and Extension Organization (AREEO), Iran.

LITERATURE CITED

Bertaccini A., 2022. Plants and phytoplasmas: when bacteria modify plants. *Plants* 11: 1425. https://doi.org/10.3390/plants11111425

Bertaccini A., 2023. Phytoplasma collection. https://www.ipwgnet.org/collection

Bertaccini A., Duduk B., Paltrinieri S., Contaldo N., 2014. Phytoplasmas and phytoplasma diseases: a severe threat to agriculture. *American Journal of Plant Sciences* 5: 1763–1788. https://doi.org/10.4236/ajps.2014.512191

Bertaccini A., Arocha-Rosete Y., Contaldo N., Duduk B., Fiore N.,... Zamorano A., 2022. Revision of the '*Candidatus* Phytoplasma' species description guidelines. *International Journal of Systematic & Evolutionary Microbiology* 72: 005353. https://doi.org/10.1099/ijsem.0.005353

Bertaccini A., Gandra R.R., Mateeti S., Pacini F., 2025. Phytoplasma transmission by seeds in alfalfa: a risk for agricultural crops and environment. *Seeds* 4: 39. https://doi.org/10.3390/seeds4030039

Bogoutdinov D., Girsova N., Kastalyeva T., 2021. Danger of phytoplasma diseases for fodder crop cultivation. *Economic and Phytosanitary Rationale for the Introduction of Feed Plants IOP Conference Series: Earth Environment Sciences* 663: 012033. doi 10.1088/1755-1315/663/1/012033

Calari A., Paltrinieri S., Contaldo N., Sakalieva D, Mori N., ... Bertaccini A., 2011. Molecular evidence of phytoplasmas in winter oilseed rape, tomato and corn seedlings. *Bulletin of Insectology* 64(Supplement): S157–S158.

Castillo-Carrillo C., Paltrinieri S., Buitrón Bustamante J., Bertaccini A., 2018. Detection and molecular characterization of a 16SrI-F phytoplasma in potato showing purple top disease in Ecuador. *Australasian Plant Pathology* 47: 311–315. https://doi.org/10.1007/s13313-018-0557-9

Contaldo N., D'Amico G., Paltrinieri S., Diallo H.A., Bertaccini A., Arocha Rosete Y., 2019. Molecular and biological characterization of phytoplasmas from coconut palms affected by the lethal yellowing disease in Africa. *Microbiological Research* 223–225: 51–57. https://doi.org/10.1016/j.micres.2019.03.011

Darabakula M., Mateeti S.T., Pacini F., Bertaccini A. Contaldo N., 2024. Eggplant little leaf-associated phytoplasma detection in seedlings under insect-proof conditions. *International Journal of Plant Biology* 15: 217–229. https://doi.org/10.3390/ijpb15020018

Deng S., Hiruki C., 1991. Amplification of 16S rRNA genes from culturable and non-culturable mollicutes. *Journal of Microbiological Methods* 14: 53–61. https://doi.org/10.1016/0167-7012(91)90007-D

Duduk B., Bertaccini A., 2006. Corn with symptoms of reddening: new host of "stolbur" phytoplasma. *Plant Disease* 90: 1313–1319. https://doi.org/10.1094/PD-90-1313

Esmailzadeh Hosseini S.A., Khodakaramian G., Salehi M., Bertaccini A., 2016. Molecular identification and phylogenetic analysis of phytoplasmas associated with alfalfa witches' broom diseases in the western areas of Iran. *Phytopathogenic Mollicutes* 6: 16–22.

Esmaeilzadeh-Hosseini S.A., Babaei G., Davoodi S., Bertaccini A., 2020. Identification and impact of phytoplasmas associated with greenhouse cucumber phyllody in Iran. *Advances in Horticultural Science* 34(4): 413418. https://doi.org/10.5958/2249-4677.2016.00003.7

Esmailzadeh Hosseini S.A., Azadvar M., Babaei G., Salehi M., Bertaccini A., 2023a. Diversity, distribution and status of phytoplasma diseases in Iran. In: *Phytoplasma Diseases in Asian countries. Diversity, Distribution and Current Status* (Tiwari A.K., Caglayan K., Al-Sadi A., Azadvar M., Abeysinghe S., ed.). Academic Press, pp. 39-83

Esmailzadeh Hosseini S.A., Azadvar M., Babaei G., Salehi M., Bertaccini A., 2023b. Important phytoplasma ribosomal subgroups distributed in Iran. *Phytopathogenic Mollicutes* 13(1): 125–126. https://doi.org/10.5958/2249-4677.2023.00063.4

Felsenstein J., 1985. Confidence limits on phylogenies: an approach using the bootstrap. *Evolution* 39: 783–791. https://doi.org/10.2307/2408678

Green M.R., Sambrook J., 2012. Molecular cloning: a laboratory manual. Fourth edition. Cold Spring Harbor Laboratory Press, Cold Spring Harbor, N.Y, USA.

Gundersen D.E., Lee I-M., 1996. Ultrasensitive detection of phytoplasmas by nested-PCR assays using two universal primer sets. *Phytopathologia Mediterranea* 35: 144–151. https://www.jstor.org/stable/42685262

Gungoosingh Bunwaree A., Contaldo N., Bertaccini A., 2023. Seed transmission of phytoplasmas in tomato and chili varieties commonly grown in Mauritius. *Phytopathogenic Mollicutes* 13: 55–56. doi/10.5958/2249-4677.2023.00028.2

Healey A., Furtado A., Cooper T., Henry R.J., 2014. Protocol: a simple method for extracting next-generation

sequencing quality genomic DNA from recalcitrant plant species. *Plant Methods* 10: 21. https://doi.org/10.1186/1746-4811-10-21

Heap I., 2025. The International Herbicide-Resistant Weed Database. Online. February 5, 2025. Available www.weedscience.org

IRPCM., 2004. '*Candidatus* Phytoplasma', a taxon for the wall-less, non-helical prokaryotes that colonize plant phloem and insects. *International Journal of Systematic & Evolutionary Microbiology* 54: 1243–1255. https://doi.org/10.1099/ijs.0.02854-0

Jakovljević M., Jović J., Krstić O., Mitrović M., Marinković S., Cvrković T., 2020. Diversity of phytoplasmas identified in the polyphagous leafhopper *Euscelis incisus* (Cicadellidae, Deltocephalinae) in Serbia: pathogen inventory, epidemiological significance and vectoring potential. *European Journal of Plant Pathology* 156: 201–221. https://doi.org/10.1007/s10658-019-01878-w

Jonson G.B., Matres J.M., Ong S., Tanaka T., Choi I-R., Chiba S., 2020. Reemerging rice orange leaf phytoplasma with varying symptoms expressions and its transmission by a new leafhopper vector—*Nephotettix virescens* distant. *Pathogens* 9: 990. https://doi.org/10.3390/pathogens9120990

Kumar S., Stecher G., Tamura K., 2016. MEGA7: Molecular evolutionary genetics analysis version 7.0 for bigger datasets. *Molecular Biology and Evolution* 33: 1870-1874. https://doi.org/10.1093/molbev/msw054

Lee I-M., Gundersen-Rindal D.E., Davis R.E., Bartoszyk I., 1998. Revised classification scheme of phytoplasmas based on RFLP analyses of 16S rRNA and ribosomal protein gene sequences. *International Journal of Systematic & Evolutionary Microbiology* 48: 1153–1169. https://doi.org/10.1099/00207713-48-4-1153

Lee I-M., Gundersen-Rindal D.E., Davis R.E., Bottner K.D., Marcone C., Seemüller E. 2004., '*Candidatus* Phytoplasma asteris', a novel phytoplasma taxon associated with aster yellows and related diseases. *International Journal of Systematic & Evolutionary Microbiology* 54: 1037–1048. https://doi.org/10.1099/ijs.0.02843-0

Mateeti S.T., Checchi G., Messina N.A., Feduzi G., Bertaccini A., Contaldo, N., 2022. Presence and seed transmission of phytoplasmas in tomato fields in Italy. *Phytopathogenic Mollicutes* 12: 1–6. doi.org/10.5958/2249-4677.2022.00001.9

Mateeti S.T., Darabakula M., Contaldo N., Pacini F., Bertaccini, A., 2023. Seed transmission of phytoplasmas infecting eggplants in India. *Phytopathogenic Mollicutes* 13: 57–58. doi.org/10.5958/2249-4677.2023.00029.4

McKay A.C., Riley I.T., 1993. Sampling ryegrass to assess the risk of annual ryegrass toxicity. *Australian Veterinary Journal* 70(7): 241–243. https://doi.org/10.1111/j.1751-0813. 1993.tb08038.x

Oshib Nataj M., Shekarchi H., Akbarzadeh M., Keshavarzi M., 2012. An autecological study of *Lolium rigidum* L. in Mazandaran Province. *Journal of Plant Biological Science*, 3(10): 37–46. https://doi.org/20.1001.1.20088264.1390.3.10.5.7

Owen M.J, Martinez N.J., Powles S.B., 2014. Widespread occurrence of multiple herbicide resistance in Western Australian annual ryegrass (*Lolium rigidum*) populations. *Australian Journal of Agricultural Research* 58: 711–718. https://https://doi.org/10.1071/AR06283

Randa-Zelyut F., Inak E., Demire Ozden E., Senal D., Ertunc F., 2022. Determination of potential insect vectors and subgroups of aster yellows phytoplasma in the carrot (*Daucus carota* L.) (Apiaceae) cultivation areas of Ankara and Konya Provinces, Türkiye. *Türkish Entomology Derg* 46(4): 385–398. https://doi.org/https://dx.doi.org/10.16970/entoted.1118787

Saitou N., Nei M., 1987. The neighbor-joining method: a new method for reconstructing phylogenetic trees. *Molecular Biology & Evolution* 4: 406–425. https://doi.org/10.1093/oxfordjournals.molbev.a040454

Salehi M., Izadpanah K., Siampour M., Esmailzadeh Hosseini S.A., 2011. Polyclonal antibodies for the detection and identification of Fars alfalfa witches' broom phytoplasma. *Bulletin of Insectology* 64(Supplement): 59–60.

Salehi M., Esmaeilzadeh-Hosseini S.A., Faghihi M.M., Salehi E., Bertaccini A., 2025. Identification of a '*Candidatus* Phytoplasma asteris' 16SrI-F strain infecting periwinkle in Iran. *Phytopathogenic Mollicutes*, 15(2): 175–180.

Satta E., Carminati G., Bertaccini A., 2020. Phytoplasma presence in carrot seedlings. *Australasian Plant Disease Notes* 15: 11. https://doi.org/10.1007/s13314-020-0377-y

Schneider B., Seemüller E., Smart C.D., Kirkpatrick B.C., 1995. Phylogenetic classification of plant pathogenic mycoplasma-like organisms or phytoplasmas. In: *Molecular and diagnostic procedures in Mycoplasmology* (Razin S. and Tully J.G., ed.). Academic Press. San Diego, CA (USA) pp. 369–380. https://doi.org/10.1016/B978-012583805-4/50040-6

Tamura K., Nei M., Kumar S., 2004. Prospects for inferring very large phylogenies by using the neighbor-joining method. *Proceedings of National Academy of Science (USA)* 101: 11030–11035. https://doi.org/10.1073/pnas.0404206101

Urbanaviciene L., Valiunas D., Jomantiene R., 2005. Molecular detection and identification of subgroup 16SrI-L phytoplasma in ryegrass (*Lolium multiflorum* Lam.). *Phytopathologia Polonica* 35: 121–124.

Wegulo S.N, Carlson M.P., 2011. Ergot of small grain cereals and grasses and its health effects on humans and livestock. University of Nebraska–Lincoln Extension.

Zhao Y., Wei W., Lee I-M., Shao J., Davis R.E., 2009. Construction of an interactive online phytoplasma classification tool, *i*PhyClassifier, and its application in analysis of the peach X-disease phytoplasma group (16SrIII). *International Journal of Systematic & Evolutionary Microbiology* 59: 2582–2593. https://doi.org/10.1099/ijs.0.010249-0

Zwolinska A., Krawczyk K., Pospieszny H., 2012. Molecular characterization of "stolbur" phytoplasma associated with pea plants in Poland. *Journal of Phytopathology* 160: 317–323. https://doi.org/10.1111/j.1439-0434.2012.01903.x

Phytopathologia Mediterranea
The international journal of the
Mediterranean Phytopathological Union

Firenze University Press
www.fupress.com/pm

Research Papers

Prevalence and phylogeny of fig viruses in the South Croatian Adriatic Region

Mate ČARIJA[1], Katarina HANČEVIĆ[1,*], Tomislav RADIĆ[1], Emanuel GAŠI[1], Mira RADUNIĆ[1,2]

[1] *Institute for Adriatic Crops and Karst Reclamation, Put Duilova 11, 21000 Split, Croatia*
[2] *Centre of Excellence for Biodiversity and Molecular Plant Breeding (CoE CroP-BioDiv), Svetošimunska 25,10000 Zagreb, Croatia*
*Corresponding author. E-mail: Katarina.Hancevic@krs.hr

Summary. Fig viruses are major challenges for fig production, and may be widely present in Croatia. A survey was carried out to determine the most economically important viruses of fig trees in the South Croatian Adriatic Region, by analyzing 28 fig genotypes from field sites and a national fig collection. Using RT-PCR and specific primers, five viruses were detected, including: fig badnavirus 1 (FBV-1) in all the assessed samples, fig mosaic virus (FMV) (55% of samples), fig leaf mottle-associated virus 1 (FLMaV-1) (44%), fig fleck-associated virus (FFkaV) (17%), and fig mild mottle-associated virus (FMMaV) (10% of samples). Most of the sampled trees were infected by multiple viruses, and only five harbored only FBV-1. Sequencing and phylogenetic analyses of two representative sequences for each of these viruses confirmed their identities and showed close relationships with Mediterranean isolates, indicating their regional dissemination. This study has provided new information of fig virus presence in the South Croatian Adriatic Region, is the first to report prevalence of FLMaV-1, FMMaV and FFkaV in Croatian fig germplasm, and to determine virus phylogenetic relationships. Virus monitoring in fig plantations and in certified propagation material, and integrated disease management strategies, are required to protect fig production in Croatia.

Keywords. *Ficus carica* L., Fig mosaic disease, Mediterranean region, molecular characterization.

OPEN ACCESS

Citation: Čarija, M., Hančević, K., Radić, T., Gaši, E., & Radunić, M. (2025). Prevalence and phylogeny of fig viruses in the South Croatian Adriatic Region. *Phytopathologia Mediterranea* 64(3): 607-613. DOI: 10.36253/phyto-16611

Accepted: October 21, 2025

Published: December 11, 2025

Data Availability Statement: All relevant data are within the paper and its Supporting Information files.

Competing Interests: The Author(s) declare(s) no conflict of interest.

Editor: Anna Maria D'Onghia, CIHEAM/Mediterranean Agronomic Institute of Bari, Italy.

ORCID:
MČ: 0000-0003-4004-7105
KH: 0000-0001-7993-7450
TR: 0000-0002-1633-6516
EG: 0000-0002-2554-3162
MR: 0000-0003-3929-0239

INTRODUCTION

Fig (*Ficus carica* L.) is an important cultivated perennial fruit species, which originated from the Middle East and Southwest Asia (Kislev *et al*., 2006). This plant is renowned for its rich, nutritional fruit, and became widespread in the Mediterranean basin during the Phoenician, Greek and Roman eras (Bakarić *et al*., 1989; Kislev *et al*., 2006; Zohary *et al*., 2012). Fig is also cultivated in the East Adriatic Coast region, where many unique genotypes have been identified (Radunić *et al*., 2025). In Croatia, figs are mostly grown on the margins of family gardens in combination with other fruit species, olives, grapevines, vegetables, and aromatic plants. Commercial fig orchards

are also present but rare (Radunić *et al*., 2025). The latest available data from 2019 showed that Croatia's annual fig production is approx. 800 tons (FAO stat, 2019).

Fig plants are susceptible to several virus pathogens that can significantly impact growth, fruit quality and yields. The most important virus disease impacting fig trees is fig mosaic disease (FMD), which was first described by Condit and Horne (1933). Symptoms of FMD include vigour reduction of fig trees, the leaves with chlorotic and yellowish spots and mosaic patterns developed on the leaves and fruit (Preising *et al*., 2021). Impacts on tree physiological processes have been little investigated, but recent studies indicate that even in asymptomatic plants, photosynthesis is impaired, along with organic acid biosynthesis (Pedrelli *et al*., 2023).

Several viruses have been identified in trees showing FMD (Preising *et al*., 2021). The main cause of the disease is considered to be fig mosaic virus (FMV, *Emaravirus*; Vončina *et al*., 2015), but other viruses may also be involved in disease etiology. Fig leaf mottle-associated virus 1 (FLMaV-1, *Closterovirus*; Elbeaino *et al*., 2006), fig badnavirus 1 (FBV-1, *Badnavirus*; (Laney *et al*., 2012)), fig mild mottle associated virus (FMMaV, *Closterovirus*; Elbeaino *et al*., 2010), and fig fleck-associated virus (FFkaV, *Maculavirus*; Elbeaino *et al*., 2011) have also been associated with FMD. While a survey of two fig viruses (FMV and FBV-1) contributing to FMD development has been conducted in the northern coastal regions of Croatia (Vončina *et al*., 2015), there are no data on the presence, prevalence and diversity of fig viruses in the South Croatian Adriatic Region, where a large number of unique fig genotypes occur (Radunić *et al*., 2025).

Since the most common mode of virus spread occurs through the main modes of fig propagation (cuttings and grafts), infection rates of fig plants are high. Some viruses (e.g. FMV) are also transmitted by eriophyid mites (e.g., *Aceria ficus*; Caglayan *et al*., 2012). Although uncertainties remain regarding the causal agents of FMD (Elbeaino, 2022), FMV was included in the list of Regulated non-quarantine pests to help prevent spread of this virus through vegetative propagation material (European Commission, 2019). Detecting the presence of major fig viruses and understanding their etiology are essential for developing effective strategies for virus detection, certification of propagation material, and integrated disease management in fig cultivation.

The present study assessed the sanitary (virus) status of 28 fig samples from nine locations in the South Croatian Adriatic Region. From selected positive samples, Sanger sequencing and phylogenetic analyses were carried out to assess their relationships with sequences reported in previous studies.

MATERIALS AND METHODS

Thirteen fig samples were collected from different fig orchards in the South Croatian Adriatic Region, and 15 samples were collected from the fig germplasm collection that is currently being developed at the Institute for Adriatic Crops and Karst Reclamation, in Split. The samples were collected from the nine locations shown in Figure 1.

Total nucleic acid extraction and virus detection

Total nucleic acid (TNA) extractions were each carried out from 150 mg of fresh leaf tissue, using the method of Alsaheli *et al.* (2020). For detection of RNA viruses, each leaf extract was purified from any remaining DNA using TURBO DNA-free™ Kit (Invitrogen), according to the manufacturer's instructions. Reverse transcription was performed on 500 ng of RNA template using M-MLV reverse transcriptase (Invitrogen) with additions of 100 units of RNase inhibitor (Invitrogen) and 5 μM random nonamers (Sigma Aldrich). For the detection of DNA virus (FBV-1), total nucleic acid was used directly as the template without DNase treatment and reverse transcription.

Virus detection was carried out with the primers listed in Table 1, using the following PCR conditions: denaturation at 94°C for 2 min, followed by 35 cycles each at 94°C for 30 sec, primer-specific annealing temperature (Table 1) for 45 sec, and elongation at 72°C for 60 sec, and final elongation at 72°C for 7 min. All PCR products were later analyzed by agarose gel electrophoresis.

Phylogenetic analyses

Two representative isolates of each obtained virus were sequenced by Macrogen Europe Inc. (Amsterdam, Netherlands), and were subsequently deposited in the GenBank under the accession numbers PV942097 to PV942106. Sequences obtained were aligned in Clustal X 2.1 (Larkin *et al*., 2007) and analyzed in Mega 5 (Tamura *et al*., 2011). Phylogenetic trees were constructed using the neighbour-joining method and Tamura–Nei evolutionary model. Bootstrap analysis was based on 1,000 repetitions, and other sequences were obtained using NCBI Blast tool.

RESULTS

Sanitary status

The most prevalent virus detected in all the tested samples was FBV-1, and the least prevalent was FMMaV,

Figure 1. Sampling sites for assessing the virus sanitary status of fig trees in the South Croatian Adriatic Region. The inset (top right) shows the position of the study area within the Mediterranean region.

Table 1. Primers used in RT-PCR and PCR for assessing the sanitary (virus) status of fig trees in the South Croatian Adriatic Region.

Virus	Primer sequence	Protein coding region[a]	Annealing temperature	Reference
Fig badnavirus 1	F: GCTGATCACAAGAGGCATGA R: TCCTTGTTTCCACGTTCCTT	MP	55°C	Tzanetakis *et al.* (2010)
Fig mosaic virus	F: CGGTAGCAAATGGAATGAAA R: AACACTGTTTTTGCGATTGG	RdRp	55°C	Elbeaino *et al.* (2009)
Fig leaf mottle-associated virus 1	F: CGTGGCTGATGCAAAGTTTA R: GTTAACGCATGCTTCCATGA	HSP70h	55°C	Elbeaino *et al.* (2006)
Fig fleck associated virus	F: TCAATCCCAAGGAGGTGAAG R: ACACGGTCAATGAGGGAGTC	RdRp	60°C	Elbeaino *et al.* (2011)
Fig mild mottle associated virus	F: AAGGGGAATCTACAAGGGTCG R: TATTACGCGCTTGAGGATTGC	HSP70h	60°C	Elbeaino *et al.* (2010)

[a]MP = movement protein; RdRp = RNA dependent RNA polymerase; HSP70h = heat shock protein 70 homologue.

identified in 10.35 % of the samples. FMV was detected in 55.17% of the samples while FLMaV-1 and FFkaV were detected in 44.83% and 17.24%, respectively (Table 2.). Most of the samples were infected with multiple viruses and only five samples were singly infected with FBV-1. The most common coinfection occurring was FBV-1 and FMV, either alone or together with other viruses.

Phylogenetic analyses

Sequences obtained from Sanger sequencing were aligned with homologous sequences using the NCBI Blast tool where all sequences available in the NCBI were used to construct the phylogenetic trees. The FMV sequences showed greatest similarity to those reported from Serbia and Bosnia and Herzegovina (Figure 2 a.). They clustered separately from other Croatian sequences of FMV which were obtained in previous research (Vončina *et al*. 2015).

FBV was the most uniform virus, as indicated by the number of clusters formed and sequences obtained that alligned closely to most of the sequences from NCBI BLAST, indicating the low genomic diversity of this virus (Figure 2 b). Sequences of FLMaV obtained in this

Table 2. Distribution of fig viruses in different fig tree varieties and sampling locations.

Sample ID	Fig variety	Location	FMV	FLMaV-1	FFkaV	FMMaV	FBV-1
FCO66	Unknown_Brač	Brač	+				+
FC01	Wild fig	IAC[a]	+				+
FC02	Zamorčica	IAC	+	+	+	+	+
FC03	Zimica	IAC	+	+	+	+	+
FC04	Petrovača bijela	IAC	+	+			+
FC016	Zamorčica	IAC	+	+			+
FC025	Mala Sušioka	IAC	+				+
FCO92	Melanzana nera	IAC		+			+
FCO87	Della Signora	IAC	+				+
FCO88	Dottata bianca	IAC		+			+
FCO93	Melanzana bianca	IAC	+	+			+
FCO91	Verdone	IAC	+				+
FCO90	Turca	IAC					+
FCO27	Modrulja	IAC					+
FCO82	Unknown_IAC82	IAC					+
FCO33	Unknown_IAC33	IAC					+
FCO64	Unknown_64	Kaštela	+	+	+		+
FCO94	Zamorčica	Kaštela	+		+		+
FCO95	Unknown_95	Kaštela	+	+			+
FCO57	Unknown_57	Kaštela		+			+
FCO96	Petrovača bijela	Klis					+
FCO67	Unknown_967	Lastovo	+				+
FCO71	Unknown_Lastovo	Lastovo	+				+
FCO86	Unknown_Mljet	Mljet					+
FCO85	Unknown_Plava	Opuzen		+	+	+	+
FCO59	Unknown_59	Solin	+	+			+
FCO77	Unknown_77	Šipan		+			+
FCO78	Unknown_78	Šipan					+

[a]Fig germplasm collection at the Institute for Adriatic Crops and Karst Reclamation.

study alligned closely to those obtained in studies conducted in Spain, Austria, Bosnia and Herzegovina, and Greece (Figure 2 c). FFkaV sequences showed the closest alignement with sequences from Austria, Italy and Palestine (Figure 2 d).

For FMMaV, the smallest number of reference sequences was available from NCBI BLAST (Figure 2 e). The sequences obtained in the present study clustered together in a separate microgroup, positioned close to Tunisian isolates and one Austrian isolate (Figure 2 e).

DISCUSSION

This study has provided an initial survey of fig viruses in the South Croatian Adriatic Region. In addition to confirming the widespread presence of FBV-1 and FMV, detections of FLMaV-1, FFkaV, and FMMaV in Croatian fig germplasm provide the first records of these viruses in this country. These results expand the known geographic distributions of these viruses, and show that the sanitary status of fig in Croatia is more complex than previously recognized.

Fig mosaic disease (FMD) symptoms were first reported in Croatian fig germplasm by Perišić (1952). However, identification of the infecting viruses was delayed until the application of modern diagnostic techniques to fig tree samples from the Northern Croatian coastal region (Istrian Peninsula) (Vončina *et al*., 2015). In the present study, samples from the South Croatian Adriatic Region were analyzed, and this confirmed presence of FMV and FBV-1 in this region. FMV was detected at lower incidence in the South Croatian Adriatic Region compared to the Istrian Peninsula (55.2% vs. 87%), while FBV-1 was found in all the assessed samples, which is consistent with previous results from Istria) (Vončina *et al*., 2015).

FBV-1 is known to integrate into the fig genome, suggesting a long-term coevolutionary relationship of

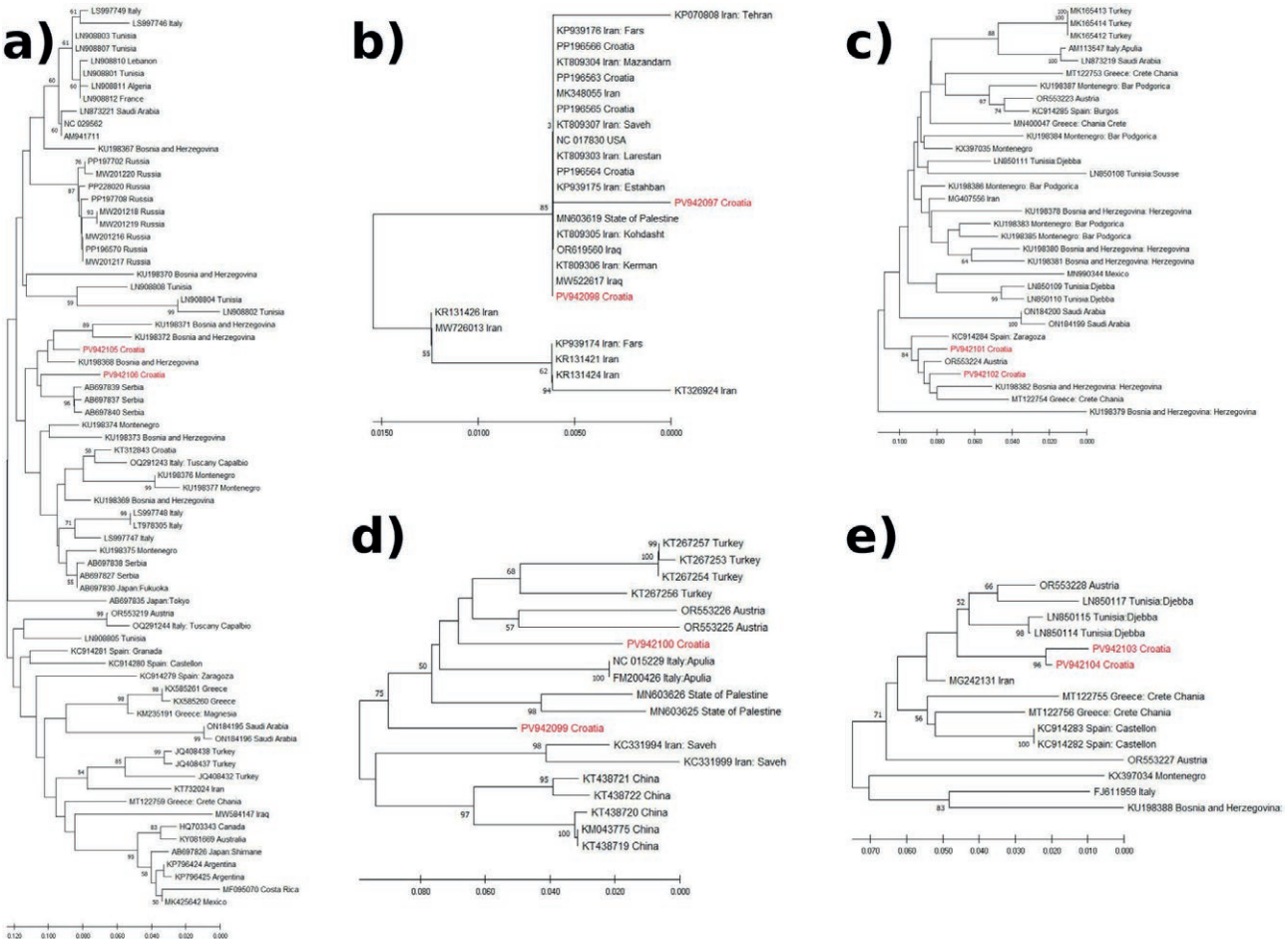

Figure 2. Neighbour-joining trees based on fig mosaic virus (a), fig badnavirus 1 (b), fig leaf mottle-associated virus (c), fig fleck-associated virus (d), and fig mild mottle-associated virus (e). Sequences obtained in the present study (in red font) are presented together with homologous sequences from NCBI BLAST. Bootstrap support values are shown at the branch nodes.

this virus with its host (Tzanetakis *et al*., 2010), and is confirmed to be internationally widespread (Preising *et al*., 2021). Of all viruses known to infect fig trees, FMV is the only one that is clearly associated with FMD development (Elbeaino, 2022) and impacts of this disease on fig tree physiological processes (Pedrelli *et al*., 2023). Spread of FMV may be facilitated by its ability to infect alternative hosts other than fig (Elbeaino *et al*., 2018). FMV has also been reported in neighboring countries, with incidences of 41% in Bosnia and Herzegovina and 26% in Montenegro (Delić *et al*., 2017).

FLMaV-1 was present in 44.8% of the tested samples, which is similar to the results of Delić *et al.* (2017) for Bosnia and Herzegovina and Montenegro. This proportion is different from the more general 22% of figs infected by FLMaV-1 virus proposed by Preising *et al.* (2021), but this indicates the widespread presence of this virus in the Balkan peninsula, probably mediated by the presence of its known vector *Ceroplastes rusci* (Yorganci and Açıkgöz, 2019) which was previously detected in Croatia (Croatian Agency for Agriculture and Food, 2018).

The low detection rates of FMMaV (10.4%) and FFkaV (17.2%) indicate sporadic presence of these viruses, although their pathogenic roles remain poorly understood and merit further study. The detection rate of FMMaV was consistent with similar findings in Syria (12.2%; Elbeaino *et al*., 2012), and slightly greater than reported in neighbouring Bosnia and Herzegovina (8.1%) and Montenegro (5.7%) (Delić *et al*., 2017). The incidence of FFkaV observed in the present study was greater than that reported in neighboring countries (8.2% in Bosnia and Herzegovina and 2.8% in Montenegro; Delić *et al*., 2017), yet it was comparable to the international average of 19% proposed by Preising *et al.* (2021).

Phylogenetic analyses showed that the Croatian virus isolates were genetically close to those reported

in neighboring and Mediterranean countries, indicating potential routes of virus dissemination via trade and historical plant movement. The complexity of dissemination of fig planting material was demonstrated for the Eastern Adriatic Coast by Radunić *et al.* (2025), where no clear patterns of origin at regional level were identified for local varieties, probably due to exchange of plant material which occurred through centuries in the Mediterranean basin. FMV isolates formed a microcluster with sequences of Serbian isolates, and similar clustering patterns were observed for other sequences obtained from Austrian, Palestinean, Greek, and Tunisian fig virus isolates. The FMV isolates obtained in the present study clustered separately from those reported previously (Vončina *et al*., 2015), indicating greater genomic diversity of FMV within Croatian fig germplasm. This highlights the regional nature of fig virus diversity, and emphasizes the need for coordinated phytosanitary regulations and certified propagation material across countries.

The present study has expanded knowledge of fig tree viruses in Croatia, and highlights the importance of comprehensive virus surveillance. Detection of mixed virus infections in the majority of samples underscores the complex nature of FMD, and the challenges it poses for fig cultivation. Overall, this study provides new knowledge of fig virus presence in the South Croatian Adriatic Region, and the first report of incidences of FLMaV-1, FMMaV, and FFkaV in Croatian fig germplasm, and as their phylogenetic relationships. These results provide a foundation for future research in fig, to investigate virus–host interactions, vector dynamics, and integrated disease management strategies. Because only two representative sequences per virus were analyzed, the genomic diversity of Croatian virus isolates from fig should be complemented in future research.

ACKNOWLEDGEMENTS

The author(s) declare financial support by the European Union through the "NextGenerationEU" (project INOMED-2I; 09-207/1-23) and Croatian National Program for Conservation and Sustainable Use of Plant Genetic Resources for Food and Agriculture 2021-2027 (01-181/2-17).

LITERATURE CITED

Alsaheli Z., Contaldo N., Mehle N., Dermastia M., Elbeaino T., Bertaccini A., 2020. First detection of "Candidatus Phytoplasma asteris" - and "Candidatus Phytoplasma solani"-related strains in fig trees. *Journal of Phytopathology* 168: 63–71. https://doi.org/10.1111/jph.12868.

Bakarić P., Brzica K., Omčikus Č., 1989. *Smokva*. Dubrovnik, Stanica za južne kulture.

Caglayan K., Elci E., Serce C.U., Kaya K., Gazel M., Medina V., 2012. Detection of fig mosaic virus in viruliferous eriophyid mite *Aceri ficus*. *Journal of Plant Pathology* 629–634.

Commission E.U., 2019. Commission Implementing Regulation (EU) 2019/2072 of 28 November 2019 establishing uniform conditions for the implementation of Regulation (EU) 2016/2031 of the European Parliament and the Council, as regards protective measures against pests of plants, a. *Official Journal L* 319: 1–278.

Condit I.J., Horne W.T., 1933. A mosaic of the fig in California. *Phytopathology* 23: 887–896.

Croatian Agency for Agriculture and Food, 2018. Regulirani nekarantenski štetni organizmi na sadnom materijalu smokve. *Croatian Agency for Agriculture and Food* 12.

Delić D., Perovlć T., Hrnčić S., Lolić B., Đurić Gord., Elbeaino T., 2017. Detection and phylogenetic analyses of fig-infecting viruses in Bosnia and Herzegovina and Montenegro. *Phytopathologia Mediterranea* 56: 470–478.

Elbeaino T., 2022. Fig Pathogens: viruses, viroids, and phytoplasmas. In: *Advances in Fig Research and Sustainable Production* 279–292. https://doi.org/10.1079/9781789242492.0016

Elbeaino T., Digiaro M., De Stradis A., Martelli G.P., 2006. Partial characterisation of a closterovirus associated with a chlorotic mottling of fig. *Journal of Plant Pathology* 88: 187–192.

Elbeaino T., Digiaro M., Alabdullah A., De Stradis A., Minafra A., … Martelli G.P., 2009. A multipartite single-stranded negative-sense RNA virus is the putative agent of fig mosaic disease. *Journal of General Virology* 90: 1281–1288.

Elbeaino T., Digiaro M., Heinoun K., De Stradis A., Martelli G.P., 2010. Fig mild mottle-associated virus, a novel closterovirus infecting fig. *Journal of Plant Pathology* 95: 165–172.

Elbeaino T., Digiaro M., Martelli G.P., 2011. Complete sequence of Fig fleck-associated virus, a novel member of the family Tymoviridae. *Virus Research* 161: 198–202.

Elbeaino T., Marais A., Faure C., Trioano E., Candresse T., Parrella G., 2018. High-throughput sequencing reveals Cyclamen persicum Mill. as a natural host for Fig mosaic virus. *Viruses* 10: 684.

Food and Agriculture Organization of the United Nations. 2019. FAOSTAT – Food balance (quantity) (QCL). Retrieved June 4, 2025, from https://www.fao.org/faostat/en/#data/QCL

Kislev M.E., Hartmann A., Bar-Yosef O., 2006. Early domesticated fig in the Jordan Valley. *Science* 312: 1372–1374.

Laney A.G., Hassan M., Tzanetakis I.E., 2012. An integrated badnavirus is prevalent in fig Germplasm. *Phytopathology* 102: 1182–1189. https://doi.org/10.1094/PHYTO-12-11-0351.

Larkin M.A., Blackshields G., Brown N.P., Chenna R., McGettigan P.A., ... Lopez R., 2007. Clustal W and Clustal X version 2.0. *Bioinformatics* 23: 2947–2948.

Pedrelli A., Panattoni A., Nali C., Cotrozzi L., 2023. Occurrence of fig mosaic disease in Tuscany, Central Italy: Characterization of new fig mosaic virus isolates, and elucidation of physiochemical responses of infected common fig cv. Dottato. *Scientia Horticulturae* 322: 112440. https://doi.org/10.1016/j.scienta.2023.112440.

Perišić M., 1952. Mozaik smokve. *Zaštita bilja* 9: 62-63.

Preising S., Borges D.F., de Queiroz Ambrósio M.M., da Silva W.L., 2021. A fig deal: A global look at fig mosaic disease and its putative associates. *Plant Disease* 105: 727–738.

Radunić M., Arbeiter A.B., Čarija M., Hančević K., Poljuha D., ... Bandelj D., 2025. Genetic diversity of cultivated figs (Ficus carica L.) from the Eastern Adriatic Coast screened by SSR markers. *Genetic Resources and Crop Evolution* https://doi.org/10.1007/s10722-025-02451-7.

Tamura K., Peterson D., Peterson N., Stecher G., Nei M., Kumar S., 2011. MEGA5: Molecular evolutionary genetics analysis using maximum likelihood, evolutionary distance, and maximum parsimony methods. *Molecular Biology and Evolution* 28: 2731–2739.

Tzanetakis I.E., Laney A.G., Keller K.E., Martin R.R., 2010. New viruses found in fig exhibiting mosaic symptoms. *Julius-Kühn-Archiv* 427: 79–82.

Vončina D., Pilipović P., Škorić D., Krapac M., Prgomet, Milicčvić T., 2015. First report of Fig mosaic virus and Fig badnavirus 1 on common Fig trees in Croatia. *Journal of Plant Pathology* 97: S71. https://doi.org/10.4454/JPP.V97I4SUP.016.

Yorganci S., Açıkgöz S., 2019. Transmission of fig leaf mottle-associated virus 1 by Ceroplastes rusci. *Journal of Plant Pathology* 101: 1199–1201.

Zohary D., Hopf M., Weiss E., 2012. Domestication of Plants in the Old World: The origin and spread of domesticated plants in Southwest Asia, Europe, and the Mediterranean Basin. Oxford University Press, https://doi.org/10.1093/acprof:osobl/9780199549061.001.0001

Phytopathologia Mediterranea
The international journal of the
Mediterranean Phytopathological Union

Firenze University Press
www.fupress.com/pm

Research Papers

Fungicide sensitivity assessment and susceptibility of newly bred olive lines, to improve anthracnose management in South Africa

Lizel MOSTERT[1,*], Kaleigh CARTER[1], Elzane FRONEMAN[1], Jenna B. JOLIFFE[1], Carlo COSTA[2], Minette HAVENGA[2], Antonia CARLUCCI[3], Mariechen VAN BAALEN[1], Marcelle KEET[1], Francois HALLEEN[1]

[1] *Department of Plant Pathology, University of Stellenbosch, Private Bag X1, Matieland, 7602, South Africa*
[2] *Plant Protection Division, Agricultural Research Council, Infruitec-Nietvoorbij, Private Bag X5026, Stellenbosch, 7599, South Africa*
[3] *Department of Agriculture, Food, Natural Resources and Engineering (DAFNE), University of Foggia, 71121 Foggia, Italy*
*Corresponding author. E-mail: lmost@sun.ac.za

Summary. Olive anthracnose is an important disease in South Africa, which can result in high yield losses and reduced oil quality. This study aimed to identify the *Colletotrichum* species associated with olive anthracnose in South Africa, determine the *in vitro* efficacy of four fungicides against the fungi, and evaluate the susceptibility of newly bred olive lines to anthracnose. Olive fruit with typical anthracnose symptoms and twigs showing dieback were collected from olive farms in the Western Cape region. Isolations were made, and causal fungi were identified by amplification and sequencing of the internal transcribed spacers, partial β-tubulin and actin genes as well from their morphological characteristics. All isolates were identified as *Colletotrichum acutatum sensu stricto*. Fungicide sensitivity of mycelium growth and conidium germination were assessed for dodine, thiram and the mixtures of boscalid + pyraclostrobin and cyprodinil + fludioxinil. Mycelium growth and conidium germination of *C. acutatum* were strongly inhibited by boscalid + pyraclostrobin and cyprodinil + fludioxonil. The three most virulent *C. acutatum* isolates were assessed in a wounded fruit droplet inoculation trial on the olive cultivars Manzanilla (susceptible) and Mission (moderately susceptible). These isolates were also used to assess susceptibility of 18 newly bred olive lines and six reference cultivars. Unwounded fruit samples were dip inoculated with a mixture conidium suspension of the three *C. acutatum* isolates, and lesion development was recorded. Four potential oil lines and three green table olive lines showed resistance to the fungi. This study reports the first sequence confirmation of *C. acutatum* s.s. associated with anthracnose of olives in South Africa. Furthermore, the identification of the seven resistant olive lines enabled their selection for further evaluation and development. Fungicide sensitivity, together with newly bred line susceptibility results, will aid in development of integrated disease management for olive anthracnose.

Keywords. *Colletotrichum acutatum*, β-tubulin, actin, host resistance.

OPEN ACCESS

Citation: Mostert, L., Carter, K., Froneman, E., Joliffe, J. B., Costa, C., Havenga, M., Carlucci, A., Van Baalen, M., Keet, M., & Halleen, F. (2025). Fungicide sensitivity assessment and susceptibility of newly bred olive lines, to improve anthracnose management in South Africa. *Phytopathologia Mediterranea* 64(3): 615-629. DOI: 10.36253/phyto-16571

Accepted: November 11, 2025

Published: December 30, 2025

Data Availability Statement: All relevant data are within the paper and its Supporting Information files.

Competing Interests: The Author(s) declare(s) no conflict of interest.

Editor: Epaminondas Paplomatas, Agricultural University of Athens, Greece.

ORCID:
LM: 0000-0001-9063-2447
KC: 0000-0002-1959-748X
EF: 0000-0003-2012-6631
JBJ: 0000-0003-0224-1011
CC: 0009-0001-2041-8960
MH: 0000-0001-5870-3778
AC: 0000-0002-0568-8647
MVB: 0009-0002-2622-7003
MK: 0000-0002-1375-3453
FH: 0000-0002-2348-1201

INTRODUCTION

The South African olive industry is mainly based in the Western Cape region of that country, an area with typical Mediterranean climate which is ideal for growing olives (Costa, 1998). South Africa produces ~2.5 million litres of olive oil and 4000 tonnes of table olives from approx. 4000 ha annually (SA Olive Industry Association, 2024). Local production, although of high quality, is insufficient for local consumption, and a further 2.5 million litres of olive oil and 4000 tonnes of table olives are imported annually (SA Olive Industry Association, 2024). Most orchards are spaced conventionally and irrigated, while some super-intensive orchards have been recently established (C. Costa pers. comm.). The widely adapted *Olea europaea* subsp. *cuspidata* grows throughout Southern Africa and was initially used as a rootstock. Since the 1960s, commercial orchards consist of own-rooted trees of the cultivated European olive, *O. europaea* subspecies *europaea* (Mukadam, 2014). The cultivars grown commercially, in order of importance, include Frantoio, Mission, Coratina, Favalosa, Kalamata, Arbequina, Manzanilla, Picual, Koroneiki, Nocellara del Belice, Barouni and Leccino (C. Costa pers. comm.).

Anthracnose of olives is a severe disease which occurs in many olive-growing countries, including Argentina, Australia, Greece, Italy, Morocco, Portugal, South Africa, Spain, and Uruguay (Talhinhas *et al*., 2011; Cacciola *et al*., 2012; Msairi *et al*., 2017; Kolainis *et al*., 2020; Moreira *et al*., 2021). The most typical symptoms of this disease are observed on olive fruits after cuticle penetration by pathogens has occurred (Talhinhas *et al*., 2011; Cacciola *et al*., 2012). In moist conditions, the infected fruits show a growing brown rot lesions which ooze orange gelatinous matrices containing pathogen conidia, and in dry conditions, the affected fruit becomes mummified due to dehydration (Cacciola *et al*., 2012). Symptoms of leaf necrosis and branch dieback of infected olive trees have also been reported (Gorter, 1956; Talhinhas *et al*., 2011; Cacciola *et al*., 2012). Fruit yields for the table olive industry and oil quality for the olive oil industry are affected by this disease. Oil produced from infected fruit has a reddish colour, is off-flavour, of increased acidity, and has reduced contents of β-sitosterol, polyphenols, and α-tocopherol (Cacciola *et al*., 2012).

Yield losses due to anthracnose can be severe, as for Italy's Puglia olive oil sector, which incurred losses of $71 million due to the disease in 2011 (Butler, 2012). In Spain, overall industry income losses due to this disease were estimated to be $93 million per annum (Cacciola *et al*., 2012). In South Africa, anthracnose was reported on olives by Verwoerd (1929). Isolates from olives with anthracnose were later characterised morphologically as *Gleosporium fructigenum* f. sp. *chromogenum* by Gorter (1962). Baxter *et al*., (1983) identified isolates from anthracnose-affected olive fruit, based on cultural and morphological features, as *Colletotrichum acutatum*.

Anthracnose of olives can be caused by 14 *Colletotrichum* species, and these belong to three *Colletotrichum* complexes: *C. acutatum sensu lato* (*s.l.*), *C. boninense s.l*., and *C. gloeosporioides s.l.* (Moral *et al*., 2021). Inside the *C. acutatum s.l.* species complex *C. acutatum sensu stricto s.s*, *C. godetiae* and *C. nymphaeae* have been the most frequently reported, with *C. fiorinae*, *C. lupini*, *C. rhombiforme* and *C. simmondsii* reported less frequently (Moral *et al*., 2014; Materatski *et al*., 2018; Msairi *et al*., 2020). Species within the *C. gloeosporioides s.l.* species complex occur less than those of *C. acutatum s.l.* and include *C. aenigma*, *C. gloeosporioides* s.s., *C. kahawe* subp. *ciggaro*, *C. quenslandium, C. siamense* and *C. theobromicola* (Schena *et al*., 2014; Moral *et al*., 2014). Within the *C. boninense s.l.* species complex, only *C. karsti* has been associated with olive anthracnose in Italy (Schena *et al*., 2014). *Colletotrichum acutatum s.s.* has been reported in Australia, Brazil, Greece, Italy, Morocco, Portugal, South Africa, Tunisia and Uruguay (Gorter, 1956; Talhinhas *et al*., 2005; Sergeeva *et al*., 2008; Duarte *et al*., 2010; Chattaoui *et al*., 2016; Iliadi *et al*., 2018; Moreira *et al*., 2021; Msairi *et al*., 2020; Licciardello *et al*., 2022).

Damm *et al*., (2012) studied 331 isolates previously identified as *C. acutatum* or related species and identified 31 species using a sixgene phylogenetic approach. The 5.8S nuclear ribosomal gene with the two flanking internal transcribed spacers (ITS), partial sequences of the genes for glycelalderhyde-3-phosphate dehydrogenase (*gapdh*), chitin synthase 1 (*chs-1*), histone3 (*his3*), actin (*ACT*) and β-tubulin (*TUB2*) genes were used (Damm *et al*., 2012). With ITS, only 11 species could be identified (Damm *et al*., 2012). ITS and *TUB2* were enough to infer *Colletotrichum* species within the *C. acutatum* complex (Moral *et al*., 2021). No sequence analyses have been reported for *Colletotrichum* isolates from olive fruit in South Africa.

Olive anthracnose is known as a latent disease, as the symptoms are often only seen once fruit begins to ripen (Cacciola *et al*., 2012). Mature olive fruit is more susceptible to anthracnose due to changing pH and sugar content, as well as the changing structure and content of olive fruit cuticles (Da Silva, 2016). However, susceptible cultivars can show symptoms of disease on immature fruit drupes (Gomes *et al*., 2009). During unfavourable and non-fruiting seasons, *C. acutatum*

can be found on the surfaces of leaves and branches without appearance of any disease symptoms (Wharton and Diéguez-Uribeondo, 2004). Therefore, leaves and branches are where the pathogen overwinters, and are essential for inoculum survival (Crump, 2009). The latent nature of anthracnose and presence of overwintering structures make management of the disease difficult, as symptoms appear late in fruit maturity and can cause large yield losses.

Since unripe olives are more resistant to anthracnose than mature fruit, early harvesting to avoid the pathogen is effective and environmentally friendly (Moral *et al*., 2017). However, this method of disease management has disadvantages, since fully ripe fruit is required for natural black table olives, and immature fruit has low oil content (Moral *et al*., 2017). Therefore, use of resistant cultivars, if available, would be an effective control measure, and could be integrated with other control methods such as chemical and/or biological controls (Moral *et al*., 2017).

In South Africa, olive breeders select lines with anthracnose resistance to include in future breeding programmes. These selections usually occur in the field, and are dependent on a season that favours anthracnose development. Laboratory screening of olives from new olive tree lines for their resistance or tolerance towards anthracnose will aid breeders in future.

Chemical control of olive anthracnose in South Africa includes spraying of copper oxychloride, copper hydroxide, cuprous oxide and mancozeb (Croplife South Africa, 2024). While *Colletotrichum* spp. are sensitive to copper-containing fungicides, the pathogens are not effectively controlled under high disease pressure (Butler, 2012). To control anthracnose with copper fungicides, high numbers of spray treatments are required in rainy environmental conditions, as copper residues are easily washed away (Cacciola *et al*., 2012). This can create problems as copper ions in high concentrations can have adverse effects on soils and water near treated areas (Cacciola *et al*., 2012). Since the withdrawal of fungicides that include carcinogenic, mutagenic and reprotoxic (CMR) substances, according to the globally harmonised system of classification of chemicals, mancozeb is not be available for use on olives in South Africa from May 2025. In practice, copper fungicides are used on olives in South Africa to control anthracnose, including two sprays, one in spring and one in autumn. Therefore, other effective fungicides must be available for inclusion in efficient spray programmes.

The present study aimed to identify the *Colletotrichum* species associated with anthracnose of olives in South Africa and to improve current management of olive anthracnose, through identification of resistance in newly bred olive lines and possible effective fungicides. The objectives included: i) identifying the *Colletotrichum* species associated with symptomatic olives; ii) assessing the virulence of obtained *Colletotrichum* isolates on olive fruit; iii) assessing newly bred olive tree lines for anthracnose susceptibility and iv) determining the sensitivity of *Colletotrichum* isolates to four fungicide products that could be used for the control of olive anthracnose.

MATERIAL AND METHODS

Isolate collection and storage

Olive fruit with typical anthracnose symptoms and twigs with dieback were collected from olive orchards in the Western Cape region, South Africa, from April to August during 2014 to 2016. Collection locations are listed in Table 1 (Agter Paarl -33.589126 S, 18.860141 E; Paarl -33.709709 S, 19.031734 E; Durbanville -33.82950 S, 18.59325 E; Stellenbosch -33.916735 S, 18.919443 E). Lesioned fruit was placed in moist chambers, and incubated to allow conidiomata to sporulate. Shoots with dieback were surface sterilised (30 s in 70% ethanol, 2 min in 1 % NaOCl, 30 s in 70 % ethanol), and small sections of tissue between the dead and live parts of each shoot were removed and placed onto potato dextrose agar (PDA, Biolab) (39 g/L) amended with streptomycin (0.04 g/L). The PDA plates were incubated at 25°C, and inspected for *Colletotrichum* mycelial growth. From the incubated fruit, single conidium cultures were made from developed conidia plated onto PDA amended with streptomycin. Resulting pure cultures were stored in double-sterilised distilled water (dH_2O) in 14 mL capacity McCartney bottles, in the culture collection of the Department of Plant Pathology, Stellenbosch University (STEU).

Colletotrichum *species identification*

Molecular identification

Twenty *Colletotrichum* isolates were plated onto PDA Petri dishes and incubated at 25°C for approx. 2 weeks. DNA was extracted from mycelia of each isolate using a Wizard® Genomic DNA Purification Kit (Promega), with some amendments. Mycelia of each isolate were scraped into a 2 mL Eppendorf tube with 0.5 mg glass beads and 400 µL lysis buffer. The tubes were shaken for 5 min at 30 Hz in a Retsch Mixer Mill MM301 (Retsch). The Promega protocol was further followed, and DNA was eluted with 40 µL of nuclease-free water.

Table 1. Isolation details for *Colletotrichum acutatum* isolates identified in this study and reference isolates used in the phylogenetic analyses.

STEU isolate	Collector	Location	Cultivar	Date of collection	GenBank accession numbers		
					ITS	*TUB2*	*ACT*
8047	L. Mostert, A. Carlucci	Agter Paarl	Haas	May 2014	N/A	PV061016	PV061030
8048	L. Mostert, A. Carlucci	Agter Paarl	Picual	May 2014	PV035882	PV040775	PV040778
8049	L. Mostert, A. Carlucci	Agter Paarl	Picual	May 2014	PV035883	PV040776	PV040779
8050	L. Mostert, A. Carlucci	Agter Paarl	Picual	May 2014	PV035884	PV040777	PV040780
8061	C. Spies	Durbanville	Mission[a]	March 2015	PV055838	PV061017	PV061031
8064	C. Costa	Paarl	Mission	June 2016	PV055835	PV061010	PV061013
8065	C. Costa	Paarl	Mission	June 2016	PV055836	PV061011	PV061014
8067	C. Costa	Paarl	Mission	June 2016	PV055837	PV061012	PV061015
8068	C. Costa	Agter Paarl	Vdl sl A, tree seedling	June 2016	PV055839	PV061018	PV061032
8069	C. Costa	Agter Paarl	Vdl sl A, tree seedling	June 2016	PV055840	PV061019	PV061033
8070	C. Costa	Agter Paarl	Vdl sl A, tree seedling	June 2016	PV055841	PV061020	PV061034
8071	C. Costa	Agter Paarl	Vdl sl A, tree seedling	June 2016	PV055842	PV061021	PV061035
8072	C. Costa	Agter Paarl	Vdl sl A, tree seedling	June 2016	PV055843	PV061022	PV061036
8220	J. Scrimegeour	Paarl	Mission	August 2016	PV055844	PV061023	PV061037
8221	J. Scrimegeour	Paarl	Mission	August 2016	PV055845	PV061024	PV061038
8222	J. Scrimegeour	Paarl	Mission	August 2016	PV055846	PV061025	PV061039
8223	J. Scrimegeour	Paarl	Mission	August 2016	PV055847	PV061026	PV061040
8226	J. Scrimegeour	Paarl	Mission	August 2016	PV055848	PV061027	PV061041
8227	J. Scrimegeour	Paarl	Mission	August 2016	PV055849	PV061028	PV061042
8229	F. Halleen	Stellenbosch	Unknown	August 2016	PV055850	PV061029	PV061043

[a] Isolate was obtained from twig dieback symptom. All other isolates were from symptomatic olive fruit.

For the identification of the *Colletotrichum* isolates, three gene regions were amplified and sequenced. The internal transcribed spacer (ITS) gene region was amplified with the ITS4 and ITS5 primer pair (White *et al*., 1990), the partial beta-tubulin gene region (*TUB2*) using T1 (O'Donnell and Cigelnik 1997) and Bt2b (Glass and Donaldson 1995) primer pair and the partial actin (*ACT*) gene using the ACT-512F and ACT-783R primer pair (Carbone and Kohn 1999). Each 20 µL reaction comprised 2 µL of DNA, 10 µL Amplicon Taq DNA Polymerase Master Mix RED (ThermoFisher), 7 µL of ddH_2O and 0.50 µL (10 mM) of each primer.

The PCR conditions for ITS consisted of an initial denaturation of 5 min at 94°C, followed by 35 cycles each of 30 s at 94°C, 30 s at 55°C, 30 s at 72°C and a final extension of 72°C for 6 min. The reaction conditions for *TUB2* consisted of initial denaturation at 94°C for 5 min, followed by 36 cycles each of 94°C for 45 s, 58°C for 30 s for the annealing, 72°C for 90 s and a final extension of 72°C for 6 min. For the *ACT* gene region, reaction conditions consisted of initial denaturation of 94°C for 5 min, followed by 40 cycles each of 94°C for 30 s, 52°C for 30 s, and 72°C for 30 s, and a final extension at 72°C for 7 min.

The PCR products were separated and visualised with electrophoresis on a 1% (w/v) agarose gel which was stained with SYBR Safe DNA gel stain (Thermo Fisher Scientific) in TAE running buffer (0.4 M Tris, 0.05 M NaAc, and 0.01 M EDTA, pH 7.5). PCR products were sequenced in both directions at the Central Analytical Facilities (CAF), Stellenbosch University, South Africa.

Consensus sequences were generated from the forward and reverse sequences in Geneious 11.1.5 (Biomatters Ltd.). To determine the *Colletotrichum* species complex, preliminary identification was based on Basic Local Alignment Search Tool for nucleotides (BLASTn) searches against the National Center for Biotechnology Information (NCBI, https://www.ncbi.nlm.nih.gov/) nucleotide database. Reference sequences of the *C. acutatum* species complex (Table S1), based on Damm *et al*., (2012) and Vieira *et al*., (2020), were obtained from GenBank (http://www.ncbi.nlm.nih.gov/genbank). Consensus sequences from each gene region were aligned with reference sequences using MAFFT v.1.3.6 with the L-INS-I method (Katoh and Standley, 2013) in Geneious. Concatenated sequences were generated. A maximum likelihood (ML) phylogeny was constructed for the 20 *Colletotrichum* isolates using the ITS, *TUB2* and *ACT* gene regions using PhyML v2.2.3 (Guindon *et al*., 2010) under the general time reversible (GTR) model. The gamma distribution and proportion of non-variable sites

were estimated. Bootstrap support values were calculated with 1000 replicates and clades with bootstrap support of 70% or more were considered significant and supported (Hills and Bull, 1993).

Morphological and cultural characterisation of isolates

Eight *Colletotrichum* isolates were plated onto water agar containing sterile dried carnation leaves and were incubated at 25°C in the dark until sporulation. Microscope preparations of the conidial masses were made in 70% lactic acid and observed at 1000× magnification using a Nikon Eclipse E600 compound microscope with a Nikon DS-Ri2 digital camera attachment. Lengths and widths of 30 conidia per isolate were measured. The eight *Colletotrichum* isolates were plated onto PDA and incubated at 25°C for 14 d in the dark and resulting colony colours were determined using Rayner's colour chart (Rayner, 1970).

Virulence assessment of isolates

The virulence of twenty isolates was assessed on cultivars Manzanilla (anthracnose susceptible) and Mission (moderately susceptible). The isolates were each plated onto water agar (WA) (12 g/L) containing sterile carnation leaves, to induce conidium formation, and were incubated at 25°C for 5 days in the dark. A conidium suspension of each isolate was prepared by vigorously mixing a carnation leaf covered with acervuli in 2 mL of sterile water using a vortex mixer. The suspension was then filtered using sterile cheesecloth and conidium concentration was adjusted to 1×10^6 conidia mL^{-1} using sterile water. Olive fruit was collected in March 2018. The fruits were surface sterilised for 30 s in 70% ethanol, 30 s in 1% NaOCl and 30 s in 70% ethanol, and then allowed to dry in a laminar flow cabinet. One wound per fruit was made using a sterile needle, after which each fruit was inoculated by pipetting 10 mL of conidium suspension directly onto the wound. Six fruits were inoculated with each isolate treatment, and the trial was repeated once. Plastic containers were sprayed with 70% ethanol and left to dry in a laminar flow cabinet. Sterile tissue paper was placed in each container and moistened with 50 mL of sterile water. In each container, three fruits per treatment and three treatments were incubated (nine fruits per container), in a randomised arrangement. Twelve control fruit were inoculated with sterile water. The containers were then incubated at 25°C under a 12 h light 12 h dark regime for 8 d, and the the fruits were assessed for lesions every 24 h. The numbers of fruit infected at each assessment interval was recorded and lesions size was measured after 8 d. Analyses of Variance (ANOVA) were used to compare each cultivar for experiments and isolates, using the GLM procedure and using the LSD t-test (at $P = 0.05$). The three most virulent isolates were selected based on their cultivar reactions and consistency among fruit replicates.

Susceptibility of different olive lines

Olive fruit of 18 newly bred lines and six cultivars with known anthracnose resistance (Moral *et al*., 2017) were provided by Carlo Costa in March and April 2019 (ARC Infruitec-Nietvoorbij), from unsprayed trees. The cultivars were: Haas (highly susceptible to anthracnose); Kalamata (susceptible); Mission (moderately susceptible); Nandi (resistant); Coratina (resistant) and Frantoio (highly resistant). Three trials were carried out where black table olive, green table, and oil olive lines were assessed.

Fruit was collected at three time during 2019 from which three trials were carried out. For the first trial, fruit were collected on 12 March 2019, and included the newly bred olive lines: B03.30 (3/4 ripe); B07.12 (1/2 ripe); B07.26 (1/2 ripe); B12.12 (1/2 ripe); and B5.22 (1/2 ripe) which were tested with the reference cultivars: Coratina (green); Frantoio (3/4 ripe); Haas (green); Haas (1/2 ripe); Kalamata (ripe); Mission (green) and Mission (1/2 ripe). For the second trial, fruit were collected on 27 March 2019, and included the newly bred lines: A29.32 (green); B12.42 (1/4 ripe); B43.16 (1/4 ripe); C31.26 (green); C36.02 (1/4 ripe); and VC14.40 (1/4 ripe) which were tested with the reference cultivars: Coratina (green); Frantoio (green); Haas (green); Nandi (green); Kalamata (ripe) and Mission (green). For the third trial, fruit were collected on 16 April 2019, and included the newly bred lines: A15.36 (green); A16.42 (green); A23. CD (green); B04.22 (1/4 ripe); B11.34 (1/4 ripe); B22.02 (ripe); and B34.40 (ripe). The fruit of these lines were tested with fruit from the following reference cultivars: Coratina (green); Frantoio (green); Kalamata (ripe); Mission (green); and Mission (ripe).

The three most virulent isolates (STEU 8049, STEU 8220, and STEU 8226) were each cultured on WA with sterile carnation leaves for 5 d. A conidium suspension was prepared from each isolate, as described (above), and was adjusted to 1×10^6 conidia mL^{-1}. Fruit (unwounded) were surface sterilised as described (above), were left to air dry in laminar flow cabinet, and were then each submerged in conidium suspension for 1 min. For the negative controls, ten fruit per cultivar were treated with sterile water instead of the conidium suspension. The fruit were then incubated at 25°C with a

12-h photo period in sterile moisture chamber (ten fruit per chamber). Each treatment was inoculated onto ten olive fruits, and was repeated three times.

The fruits were visually assessed for lesions every 24 h from 5 d to 8 d post-inoculation. To determine resistance levels of the fruit, the number of infected fruits at each assessment interval was recorded using a visual disease severity index for lesions on fruits (Moral *et al*., 2008). If no lesion was present on an olive, fruit severitywas recorded as 0, and lesions covering the entire fruit were recorded as 5. First sign of lesion development was scored as 1, lesions covering a quarter of the fruit as 2, covering half of the fruit as 3, and covering three quarters of the fruit were recorded 4.

Mean disease severity indices for each cultivar and line tested were used to calculate the McKinney's Index (MKI; McKinney, 1923). In the McKinney's Index the disease severity per cultivar was converted into a percentage of the maximum severity level, using the following equation: McKinney's Index = $[S(n_i\text{-}i) / 5 \times N] \times 100$, where i represents the infection severity (0-5), n_i is the number of fruit with severity and N is the total number of fruit for that replicate.

ANOVA was carried out to compare trials and olive cultivars, using the GLM procedure, and means were compared using LSD t test (at $P = 0.05$).

Fungicide sensitivity of Colletotrichum *isolates*

Fungicide inhibition of mycelium growth of the 20 *Colletotrichum* isolates was determined for the fungicides boscalid + pyraclostrobin (BASF), dodine (Campbell Chemicals), cyprodinil + fludioxinil (Syngenta) and thiram (Villa Crop). The concentration range for each fungicide is indicated in Table S2. For mycelium growth inhibition, each concentration was added to molten PDA at 55°C. PDA containing no fungicide was used as negative controls. Two replicates per trial were conducted, and the trials were repeated. Petri plates containing the media were incubated at 25°C for 8 d in the dark. Colony diameters were measured, and growth of each isolate at different fungicide concentrations was determined by calculating the mean diameters of the two colonies of each isolate.

Conidium germination of five *Colletotrichum* isolates was assessed as affected by the four fungicides, using an adjusted method of Gramaje *et al*., (2009). A conidium suspension was prepared by placing a carnation leaf with sporulating *Colletorichum* acervuli in 5 mL of half-strength potato dextrose broth (12 g/L) (Biolab). The conidium suspension concentration was determined with a haemocytometer, and was adjusted to 1×10^5 conidia mL^{-1}. One millilitre of conidium suspension each was dispersed into 2 mL Eppendorf tubes, and 1 mL of fungicide was added to each tube to obtain the correct fungicide concentration. Six concentrations per fungicide were tested (Table 2), and the negative control contained only broth. A total volume of 36 µL (containing 3600 conidia) was pipetted per microscope slide, a coverslip was placed on, and the slides were incubated in a moist chamber at 25°C in the dark. Conidium germination was assessed after 24 h by evaluating the germination of 100 conidia per slide. Conidia were considered germinated when the germ tubes had exceeded one-half of the length of the conidia. Two repeats of each isolate and fungicide concentration, were made and the trial was repeated once.

The percentage conidium inhibition per isolate per fungicide concentration was calculated as a proportion of the experimental controls. Percentage inhibition was fitted against fungicide concentration using the Mitsherlich function for boscalid + pyraclostrobin and thiram [PInhibition = 100(1-exp(-rate × concentration] and Gompertz for cyprodinil + fludioxonil and dodine [PInhibition = a*exp(-exp(-b*(LConc-c)))] (Koya and Goshu, 2013). Concentrations at which 50% of the mycelium growth or conidium germination was inhibited (EC_{50}) were calculated using Mitsherlich parameters [EC_{50} = log(1-50/100)/(-rate)] or Gompertz [LEC_{50}=((log(-log(50/a)))/-b)+c]. Regression parameters obtained were subjected to ANOVA for each fungicide, where trials were considered as block replicates for isolates. Standard residuals were tested using the Shapiro-Wilk test (Shapiro and Wilk, 1965), to determine deviations from normality. Isolate means were compared by calculating Fisher's least significance at $P = 0.05$ (Ott, 1998), and that probability level was considered significant for all tests.

RESULTS

In the field, mostly anthracnose affected olive fruits and occasionally twig dieback were observed (Figure 1). Twenty *Colletotrichum* isolates were obtained, of which 19 were from diseased fruit, and one was from twig dieback (Table 1).

Colletotrichum *species identification*

All 20 *Colletotrichum* isolates formed a monophyletic clade with the *C. acutatum s.s.* type isolate (CBS 112996), with 100% bootstrap support (Figure 2). Isolate growth in culture was typical of *C. acutatum*, with buff to salmon pink mycelium. For one isolate (STEU 8061), the colonies were pale grey with white aerial mycelium (Figure 3 a and b). Acervuli contained orange masses of conidia

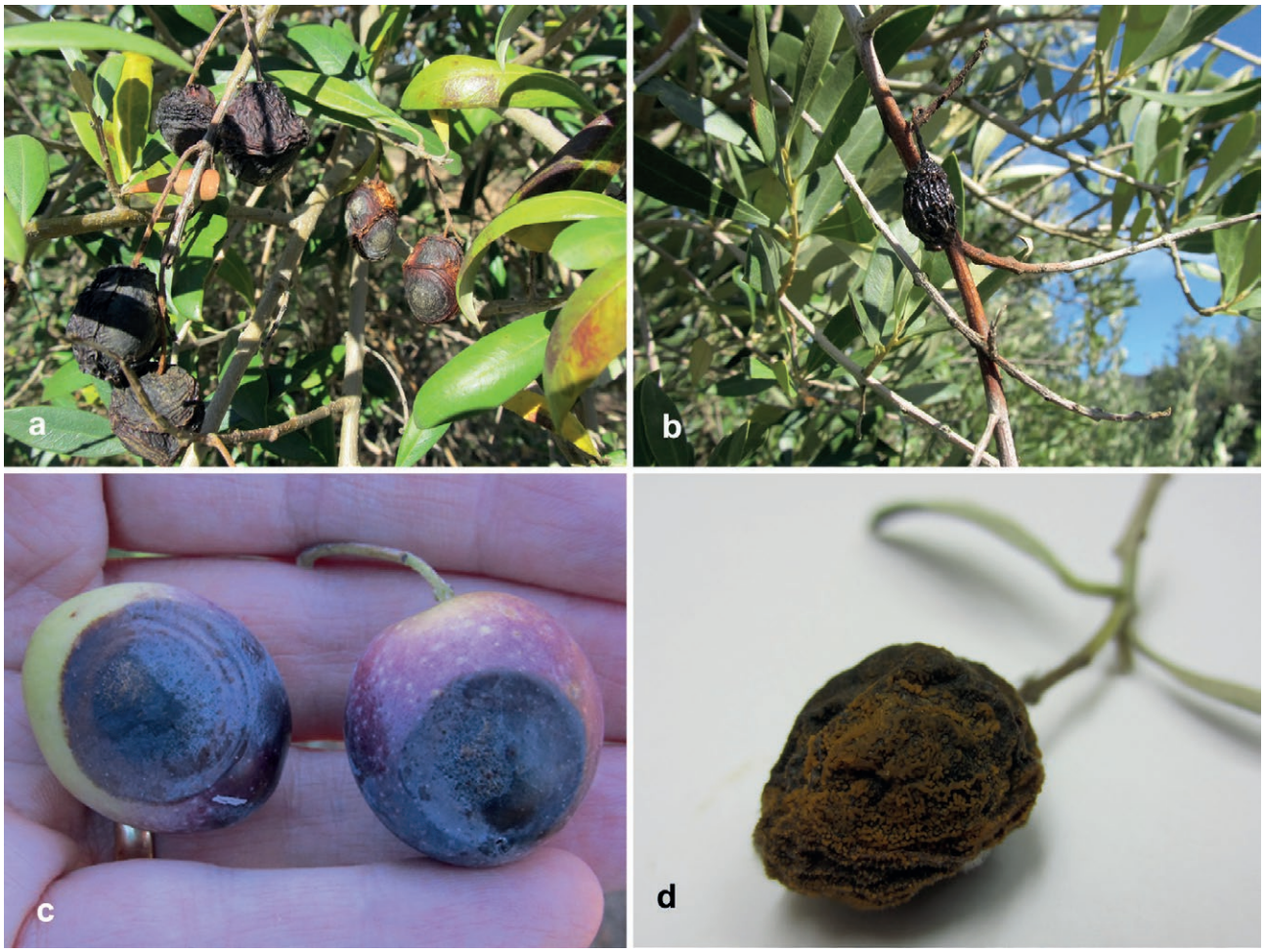

Figure 1. Symptoms associated with *Colletotrichum acutatum* infections. Fruit in an orchard with anthracnose symptoms (a) and infected olive drupe with twig showing dieback (b). Typical olive fruit symptoms with concentric rings (c) and orange masses associated with acervuli present on infected fruit (d).

on the carnation leaves (Figure 3 c and d). Conidia were hyaline, aseptate and fusiform, and measured (12-)14-16(-18) × 4-5 mm, averaged for the eight isolates (Figure 3 e and f) (Table S3).

Virulence assessments of isolates

Mean lesion lengths varied from 3.4 to 12.9 mm on Mission and 3.4 to 12.8 mm on Manzanilla (Figure 4). Isolates STEU 8049, STEU 8220 and STEU 8226 with respective average lesion lengths of 12.8, 10.1 and 11.2 mm on Manzanilla and 12.9, 11.1 and 11.3 mm on Mission, were identified as the most virulent *C. acutatum* isolates (Table S2). Two isolates (STEU 8048 and STEU 8223) produced small lesions on both cultivars, which were not significantly different from those from the water experimental control (Table S4). Isolate STEU 8061, which was from a dieback twig, was pathogenic on both fruit types and formed lesions of mean length 8.8 mm on Manzanilla and 9.8 mm on fruit of Mission.

Susceptibility of newly bred olive lines

Mean infection severity for the repeat of each trial was not significantly different ($P = 0.1921$ for trial 1, 0.6298 for trial 2, and 0.4600 for trial 3, so results of the experimental repeats were combined. There were significant cultivar and time after inoculation interactions ($P < 0.0001$), so the results are provided in this format in Table 2. For the reference cultivars, Kalamata (ripe) was the most susceptible

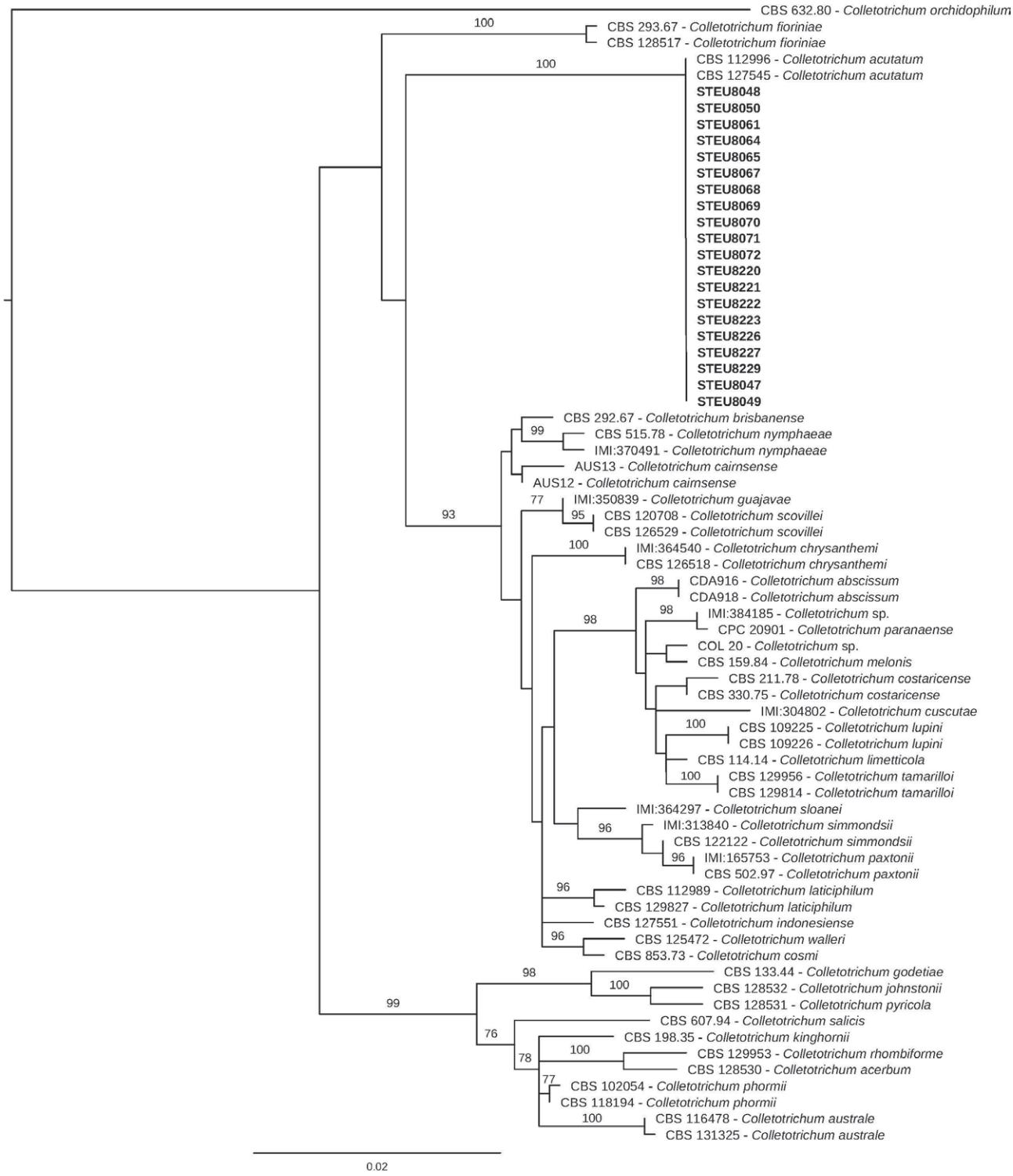

Figure 2. Maximum likelihood (ML) phylogenetic tree for *Colletotrichum acutatum* species complex based on *ACT*, *TUB2* and *ITS* gene regions. Bootstrap values of 70% and greater are shown. *Colletotrichum orchidophilum* (CBS 128530) was used as the outgroup and sequences generated in the present study are in bold font.

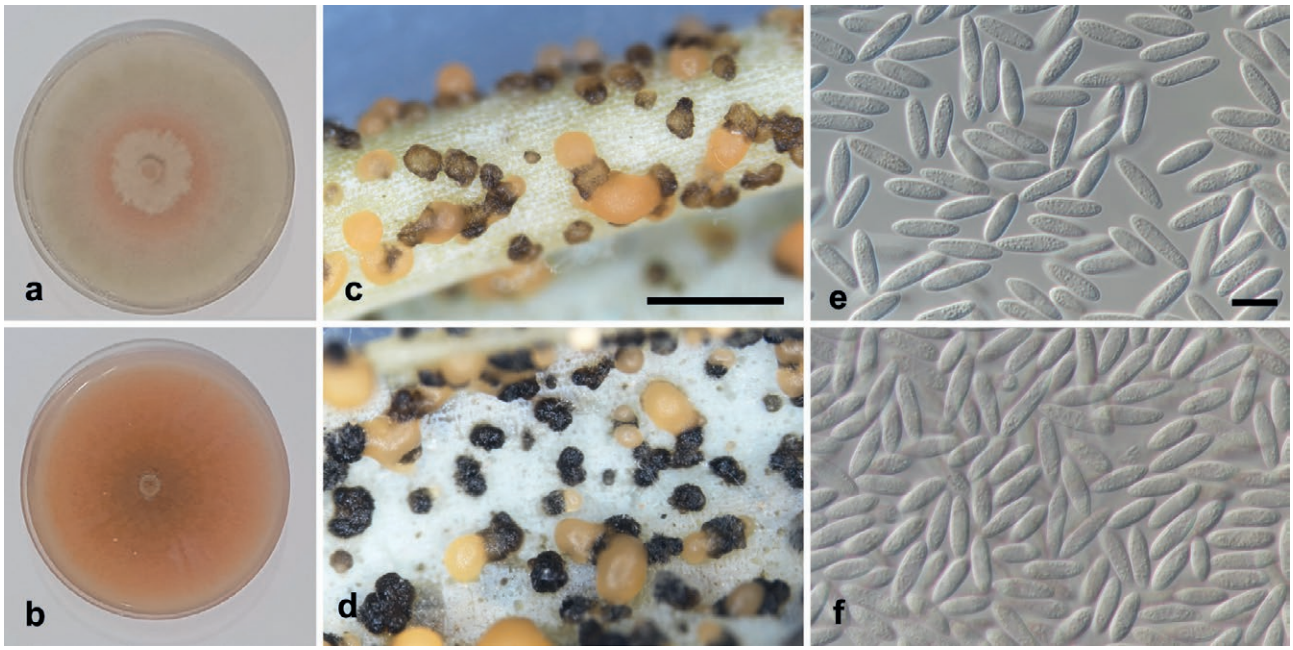

Figure 3. Cultural growth of *Colletotrichum acutatum* on PDA after two weeks (a and b), acervuli formed on carnation leaves (c and d) and conidia (e and f). Scale bar in c = 1000 μm (applies to d); e = 10 μm (applies to f). STEU8061 is shown in a, c and e; STEU8229 is shown in b, d and f.

Figure 4. Olive fruits after inoculations with different STEU isolates of *Colletotrichum acutatum*, assessed for virulence on olive fruits of Manzanilla and Mission. Control fruit (left and right ends of each row) were inoculated with sterile water as inoculation controls.

(in all three trials). Four potential oil olive lines showed resistance of which A29.32 (green) and C31.26 (green) were identified as highly resistant, and A16.42 (green) and C36.02 (1/4 ripe) were identified as resistant. Of the green table olive lines, B11.34 (1/4 ripe) and B12.42 (1/4 ripe) as highly resistant, B04.22 (1/4 ripe) as resistant, and B07.26 (1/2 ripe) was identified as moderately susceptible. Only one potential black table olive B34.40 (ripe) was identified as moderately susceptible (Table 2).

Fungicide sensitivity of Colletotrichum *isolates*

For the mycelium growth inhibition experiments, there were no significant differences between experiments [boscalid + pyraclostrobin ($P = 0.232$), dodine ($P = 0.924$), cyprodinil + fludioxonil ($P = 0.690$), thiram ($P = 0.593$)], so the results for the three experiments were combined. Sensitivity of the isolates was significantly different ($P < 0.0001$) for each fungicide, and-

Table 2. Mean infection severity calculated using the McKinney's Index, for the most virulent isolates of *Colletotrichum acutatum* tested on 18 newly bred olive lines and six olive reference cultivars.

Cultivar	Ripeness	Olive type of new lines	Mean infection severity[a]			
			At 120 h	At 144 h	At 168 h	At 192 h
Trial 1 (fruit collected 12 March 2019)						
Kalamata	ripe		74.67h[b]	99.33a	100.00a	100.00a
Haas	green		58.33j	89.00ed	97.67ab	100.00a
Haas	1/2 ripe		81.00g	98.67a	100.00a	100.00a
B12.12	1/2 ripe	oil	34.00mn	67.00i	83.67fg	96.33ab
Mission	1/2 ripe		29.00o	57.67j	82.33fg	94.00bc
B5.22	1/2 ripe	oil	28.67o	57.67j	85.67ef	91.67cd
Mission	green		21.33p	40.00l	57.67j	83.33fg
B03.30	3/4 ripe	oil	0.00u	2.33tu	30.33on	47.67k
B07.12	1/2 ripe	oil	1.67tu	12.00rq	22.42p	38.33ml
B07.26	1/2 ripe	oil	0.33u	3.67stu	14.33q	28.67o
Frantoio	3/4 ripe		1.00tu	2.33tu	5.00st	7.67rs
Coratina	green		0.00u	0.00u	0.00u	0.00u
Trial 2 (fruit collected 27 March 2019)						
Kalamata	ripe		59.33e	73.33c	87.00b	98.67a
B43.16	1/4 ripe	green table	18.00j	32.67h	53.67f	65.00d
Haas	green		11.00k	24.00i	41.67g	64.00d
Mission	green		11.67k	20.00j	32.33h	60.33e
VC14.40	1/4 ripe	green table	0.67on	1.67on	7.00l	17.67j
C36.02	1/4 ripe	green table	0.67on	3.33mn	7.33l	13.67k
Nandi	green		0.33on	0.67on	2.00on	5.33ml
B12.42	1/4 ripe	oil	0.00o	0.00o	0.33on	3.00mno
A29.32	green	green table	1.67on	1.67on	1.67on	2.00on
C31.26	green	green table	0.00o	0.00o	0.00o	0.33on
Coratina	green		0.00o	0.00o	0.00o	0.00o
Frantoio	green		0.00o	0.00o	0.00o	0.00o
Trial 3 (fruit collected 16 April 2019)						
Kalamata	ripe		34.33j	66.67e	82.00c	100.00a
Mission	ripe		14.33op	56.33g	72.00d	90.33b
B22.02	ripe	green table	18.00n	44.00i	63.33f	79.67c
A15.36	green	green table	19.67mn	29.33k	41.67i	51.67h
Mission	green		1.33uv	11.00q	16.67no	34.33j
A23.CD	green	oil	4.33surt	11.00q	14.67op	23.00l
B34.40	ripe	black table	2.67suvt	4.67srt	12.33qp	22.00ml
B04.22	1/4 ripe	oil	0.00v	2.67suvt	6.00r	11.00q
A16.42	green	green table	1.00v	1.67uvt	1.67uvt	5.67sr
B11.34	1/4 ripe	green table	0.00v	0.00v	0.00v	0.00v
Coratina	green		0.00v	0.00v	0.00v	0.00v
Frantoio	green		0.00v	0.00v	0.00v	0.00v

[a] Olive fruit was dip inoculated with *C. acutatum* conidium suspensions and incubated for 8 d. Lesion development was recorded from day 5 to day 8. For each olive line ten olive fruit were inoculated and this was repeated twice, the mean severity index was calculated from 30 observations.

[b] Means accompanied by the same letter in each column and row do not differ significantly ($P < 0.0001$) for separate trials.

mean EC_{50} values for the isolates are presented in Table 3. Ranges in mean EC_{50} values were: boscalid + pyraclostrobin, 0.20 to 0.51 µg mL^{-1}; dodine, 93.36 to 897.21 µg mL^{-1}, cyprodinil + fludioxonil, 0.03 to 0.06 and thiram, 19.32 to 104.20 µg mL^{-1} (Table 3). The isolates of *C. acutatum* were least sensitive to dodine and thiram,

Table 3. Mean colony diameter growth inhibition EC_{50} values (μg mL^{-1}) determined for 20 *Colletotrichum acutatum* isolates exposed to four different commercial fungicides.

STEU isolate	Boscalid + pyraclostrobin	Dodine	Cyprodinil + fludioxinil	Thiram
8047	0.46	499.49	0.03	60.72
8048	0.33	502.36	0.04	97.47
8049	0.40	277.62	0.04	54.82
8050	0.45	657.01	0.03	41.30
8061	0.30	473.19	0.04	75.81
8064	0.33	587.83	0.04	27.09
8065	0.41	365.33	0.04	37.08
8067	0.36	652.65	0.04	87.53
8068	0.30	820.82	0.04	75.26
8069	0.30	799.19	0.04	52.60
8070	0.35	755.78	0.04	104.20
8071	0.20	770.43	0.06	98.81
8072	0.26	897.21	0.03	42.18
8220	0.37	359.68	0.03	53.49
8221	0.50	800.09	0.03	41.51
8222	0.51	741.57	0.03	79.52
8223	0.49	635.75	0.04	57.67
8226	0.42	561.27	0.04	29.14
8227	0.38	93.36	0.04	69.35
8229	0.36	841.20	0.04	19.32

[a] Colony diameters for each isolate were measured twice (perpendicularly and horizontally) at different concentrations of fungicides, and were each determined by calculating the mean diameter of two colonies.

Table 4. Mean EC_{50} values (μg mL^{-1}) calculated from conidium germination inhibition determined for five *Colletotrichum acutatum* isolates.

STEU isolate	Boscalid + pyraclostrobin	Dodine	Cyprodinil + fludioxinil	Thiram
8047	1.53	6.67	0.16	0.04
8049	0.02	10.50	0.55	0.03
8220	0.89	8.00	0.41	0.06
8221	1.48	6.11	0.30	0.09
8226	1.02	5.07	0.37	0.07

[a] One-hundred conidia were counted for two replicates per fungicide concentration per isolate and the trial was repeated twice.

but were most sensitive to boscalid + pyraclostrobin and cyprodinil + fludioxinil.

For conidium germination, mean proportions for the experiments were not significantly different from each other [boscalid + pyraclostrobin, $P = 0.497$; dodine, $P = 0.310$; cyprodinil + fludioxonil, $P = 0.697$ for dodine, $P = 0.517$ for thiram], so results from the experiments were combined. There were significant isolate differences for all the fungicides ($P < 0.03$) (Table 4). The conidium germination results showed that *C. acutatum* was least sensitive to dodine (EC_{50} range 5.05 to 10.50 μg mL^{-1}). The EC_{50} ranges from the other fungicides treatments were 0.02 to 1.53 μg mL^{-1} for boscalid + pyraclostrobin, 0.16 to 0.55 μg mL^{-1} for cyprodinil + fludioxinil and 0.03 to 0.09 μg mL^{-1} for thiram.

DISCUSSION

Only *C. acutatum s.s.* was identified as the cause of olive anthracnose plant samples collected from in the Western Cape of South Africa. In Tunisia and Uruguay, *C. acutatum s.s.* was also the major species associated with olive anthracnose (Chattaoui *et al.*, 2016; Moreira *et al.*, 2021), and in Pakistan, only *C. acutatum* has been associated with olive anthracnose (Nawaz *et al.*, 2023). However, other major olive-producing countries have more than one *Colletotrichum* species associated with olive anthracnose. In Portugal, the major species is *C. nymphaeae* and to a lesser extent *C. godetiae*, in Spain, it is *C. godetiae* followed by *C. nymphaeae*, *C. acutatum* and *C. fructicola* and in Italy, the three major species are *C. godetiae* followed by *C. nymphaeae* and *C. acutatum* (Moral *et al.*, 2021). In Australia, eight species of *Colletotrichum* were identified from olives (Moral *et al.*, 2021).

In the present study, a polyphasic approach for species identification was followed, which included colony characters and conidium dimensions. The phylogenetic analyses that included three gene regions, ITS, *ACT* and *TUB2* determined all the isolates were *C. acutatum s.s.* Of the two most diagnostic genes for *C. acutatum* s.l., *TUB2* was slightly better than *gapdh* for resolving species (Damm *et al.*, 2012). Even though multiple gene regions have been employed to distinguish *Colletotrichum* species, it has been shown that ITS combined with *TUB2* is generally sufficient for species identification within the *C. acutatum* s.l. complex (Moral *et al.*, 2021).

In the present study, unwounded detached fruit from 18 newly bred olive lines, as well as five reference cultivars, were used to evaluate cultivar susceptibility to *C. acutatum* infections. Four oil olive lines and three green table lines were identified as resistant to this fungus. Severity of infection differed between the cultivars, and and cultivar differences have also been noted in previous studies (Moral *et al.*, 2008; Moral and Trapero, 2009; Talhinhas *et al.*, 2011; Cacciola *et al.*, 2012; Moral *et al.*, 2014). Moral *et al.*, (2017) evaluated 308 cultivars for anthracnose susceptibility, and categorised the cultivars as highly resistant, resistant, moderately susceptible,

susceptible, or highly susceptible. Of these, 32 cultivars were highly resistant, and 61 were resistant to *C. acutatum* infections.

Different cultivar reactions to *C. acutatum* infection could be a result of several genes interacting between the olive host and this pathogen (Wharton and Dieguez-Uribeondo, 2004). This type of resistance is known as dynamic incompatibility, where pathogen avirulence gene products cause host resistance genes to inhibit pathogen's growth under specific physiological conditions, such as fruit maturity (Wharton and Dieguez-Uribeondo, 2004). The different reactions of cultivars to *C. acutatum* infections could also be due to varying cuticle thicknesses and chemical compounds on fruit surfaces of different cultivars (Gomes *et al*., 2012). These characteristics have been shown to differ among the different cultivars (Gomes *et al*., 2012; Da Silva, 2016). Cuticles of olive fruit have a large amounts of lipids, which act as barriers for conidia adhesion, which slows *C. acutatum* infection processes (Da Silva, 2016).

Physical disease management strategies which are being used to control anthracnose of olives includes early harvesting of very susceptible cultivars to prevent secondary infections occurring, pruning trees to improve air circulation and reduce humidity because high levels are favourable for the pathogen, and removal of infected twigs and mummified fruit to reduce the amounts of inoculum (Cacciola *et al*., 2012). In the present study, one *C. acutatum* isolate, obtained from a twig with dieback, also induced symptoms on Manzanilla and Mission. This illustrates the importance of the removal of infected twigs from orchards to reduce pathogen inoculum.

The four fungicides tested in the present study inhibited the mycelium growth and conidium germination of *C. acutatum* isolates. For mycelium growth inhibition, boscalid + pyraclostrobin and cyprodinil + fludioxinil gave lower EC_{50} values than thiram or dodine. However, thiram gave lowest EC_{50} values for conidium germination inhibition, followed by cyprodinil + fludioxonil and boscalid + pyraclostrobin. Boscalid + pyraclostrobin is registered in South Africa for the control of *Colletotrichum* spp. on chillies, peppers, strawberries and tree nuts. The active ingredient pyraclostrobin has been shown to completely inhibit growth of *C. gloeosporioides* and *C. truncatum* which causes anthracnose on avocadoes, mangoes, papayas and peppers (Rampersad and Teelucksingh, 2012). Pyraclostrobin is a quinone outside inhibitor fungicide, and boscalid is a succinate dehydrogenase inhibitor (SDHI), with both fungicides inhibiting mitochondrial respiration in fungi (FRAC, 2025). In the present study, no mycelium growth was observed for nine of the isolates at the greatest tested concentration of boscalid + pyraclostrobin. Pyraclostrobin strongly inhibits conidium germination, whereas boscalid inhibits mycelium growth more (Piccirillo *et al*., 2018; Yang *et al*., 2021; Usman *et al*., 2022). EC_{50} values for four of the five *C. acutatum* isolates' (1.02 to 1.53 mg/mL) for conidial germination were greater than those for mycelium growth inhibition (EC_{50} = 0.20 to 0.51 mg mL^{-1}). Everett and Timudo-Torrevilla (2007) also assessed boscalid + pyraclostrobin *in vitro* on PDA for effects on *C. acutatum* isolates from avocados, and reported greater EC_{50} values for conidium germination (7 mg mL^{-1}) than mycelium growth (0.2 mg mL^{-1}).

Dodine (in the guanidine fungicide group) is used to control diseases such as leaf spot, brown rot, blossom rot, Fusarium wilt, and downy mildew on different tree fruit crops (Pesticide Property Database, 2019). The mode of action of dodine is unknown, but is proposed to be cell membrane disruption in some pathogens, and has been shown to inhibit conidium germination in *Venturia oleagineum,* which causes olive leaf spot (Rongai *et al*., 2012; Almadi *et al*., 2024). This fungicide was the least effective of those assessed in the present study, giving the greatest EC_{50} values for inhibition of *C. acutatum* mycelium growth and conidium germination. Dodine was tested and found ineffective for inhibiting mycelium growth of *C. acutatum* from Uruguay, and is not recommended for anthracnose control on olives (Moreira *et al*., 2024).

Cyprodinil + fludioxonil is a translaminar systemic and contact fungicide, including anilinopyrimidine (cyprodinil) and phenylpyrrole (fludioxinil) active ingredients. Cyprodinil inhibits amino acid biosynthesis in fungi, and fludioxonil is a contact fungicide that inhibits conidium germination, and the tube and mycelium growth. This fungicide mixture has been registered in South Africa for the control of *Colletotrichum* spp. of berries, strawberries, and tropical fruit including avocado. The two fungicide mixtures were tested in the present study, rather than the single actives, to aid decision-making for product registration trials, and to ultimately provide options for disease management for olive growers. Both of these mixtures have been registered for *Colletotrichum*/anthracnose on other crops in South Africa.

Thiram is a contact fungicide, and is registered in South Africa for the control of scab of apples and pears, blossom blight of stone fruit trees, leaf curl of peaches, and for apple seed decay and seedling rot. Three thiram products have been assessed for effects on *C. acutatum* isolates from strawberries, and were found to be moderately effective for inhibition of mycelium growth, but very effective for inhibiting conidium germination (Es-Soufi *et al*., 2018).

In conclusion, *C. acutatum s.s.* is the only species to be associated with olive anthracnose in South Africa. Seven newly bred olive lines were identified as resistant to *C. acutatum* infection. These potential olive lines can be used by breeders to produce commercial olive cultivars that have increased tolerance to this pathogen. Potential fungicides for the chemical control of olive anthracnose were tested for their ability to inhibit mycelial growth and conidial germination. Boscalid + pyraclostrobin, cyprodinil + fludioxonil, and thiram have potential, and require further assessments in olive orchards. Effects of application of the fungicides on olive fruit and oil residues have yet to be determined.

ACKNOWLEDGEMENTS

The authors thank the Alternative Crops Fund of the Western Cape Government of South Africa, and the South African olive industry for funding this research.

LITERATURE CITED

Almadi L., Frioni T., Farinelli D., Paoletti A., Cinosi N., Rosati A., Moretti C., Buonaurio R., Famiani F., 2024. Dodine an effective alternative to copper for controlling *Venturia oleaginea*, the causal agent of Pea-Cock Eye Disease, in highly infected olive trees. *Frontiers Plant Science* 15: 1369048. https://doi.org/10.3389/fpls.2024.1369048

Baxter A.P, van der Westhuizen G.C.A., Eicker A., 1983. Morphology and taxonomy of South African isolates of *Colletotrichum*. *South African Journal of Botany* 2: 259–289. https://doi.org/10.1016/S0022-4618(16)30090-0

Butler J., 2012. *The cost of anthracnose*. Olive Oil Times. Available at https://www.oliveoiltimes.com/olive-oil-making-and-milling/anthracnose/25145. Accessed September 23, 2019.

Cacciola S., Faedda R., Sinatra F., Agosteo G., Schena L., Frisullo S., Magnano di San Lio G., 2012. Olive anthracnose. *Journal of Plant Pathology* 94: 29–44.

Carbone I., Kohn L.M., 1999. A method for designing primer sets for speciation studies in filamentous ascomycetes. *Mycologia* 91: 553–556.

Chattaoui M., Raya M.C., Bouri M., Moral J., Perez-Rodriguez M., Trapero A., … Rhouma A., 2016. Characterization of a *Colletotrichum* population causing anthracnose disease on olive in northern Tunisia. *Journal of Applied Microbiology* 120: 1368–1381. https://doi.org/10.1111/jam.13096

Costa C., 1998. *Olive production in South Africa: A Handbook for Olive Growers*. ARC-Infruitec, Stellenbosch.

Croplife South Africa, 2024. Available at https://croplife.co.za/. Accessed November 24, 2024.

Crump A., 2009. Anthracnose management guidelines-UC IPM. Available at http://ipm.ucanr.edu/PMG/PESTNOTES/pn7420.html. Accessed March 20, 2018.

Da Silva V.C.F., 2016. *Olive anthracnose: passive defense of tolerant and susceptible Portuguese* Olea europaea *L. cultivars and its effect on olive oil quality*. MSc thesis, Polytechnic Institute of Bragança Portugal.

Damm U., Cannon P., Woudenberg J., Crous P., 2012. The *Colletotrichum acutatum* species complex. *Studies in Mycology* 73: 37–113.

Duarte H.S.S., Cabral P.G.C., Pereira O.L., Zambolim L., Gonçalves E.D. … Sergeeva V., 2010. First report of anthracnose and fruit mummification of olive fruit (*Olea europaea*) caused by *Colletotrichum acutatum* in Brazil. *Plant Pathology* 59: 1170.

Es-Soufi R., L'bachir El Kbiach M., Errabii T., Saidi R., Badoc A. … A. Lamarti, 2018. *In vitro* evaluation of the resistance of seven isolates of *Colletotrichum acutatum* to thiram and copper. *Journal of Microbiology Research* 8: 60–68.

Everett K.R., Timudo-Torrevilla O.E., 2007. *In vitro* fungicide testing for control of avocado fruit rots. *New Zealand Plant Protection* 60: 99–103.

FRAC (Fungicide Resistance Action Committee), 2025. FRAC recommendations. Online. Available at https://www.frac.info/fungicide-resistance-management. Accessed October 15, 2025.

Glass N.L., Donaldson G., 1995. Development of primer sets designed for use with PCR to amplify conserved genes from filamentous ascomycetes. *Applied and Environmental Microbiology* 61: 1323–1330.

Gomes S., Bacelar E., Martins-Lopes P., Carvalho T., Guedes-Pinto H., 2012. Infection process of olive fruits by *Colletotrichum acutatum* and the protective role of the cuticle and epidermis. *Journal of Agricultural Science* 4: 101–110.

Gomes S., Prieto P., Martins-Lopes P., Carvalho T., Martin A. and Guedes-Pinto H., 2009. Development of *Colletotrichum acutatum* on tolerant and susceptible *Olea europaea* L. cultivars: A Microscopic Analysis. *Mycopathologia* 168: 203-211.

Gorter G.J.M.A., 1956. Anthracnose fungi of olives. *Nature* 178: 1129-1130.

Gorter G.J.M.A., 1962. The identity of the fungus causing anthracnose of olives in South Africa. *Bothalia* 7: 769–778.

Gramaje D., Aroca Á., Raposo R., García-Jiménez J., Armengol J., 2009. Evaluation of fungicides to con-

trol Petri disease pathogens in the grapevine propagation process. *Crop Protection* 28: 1091-1097. https://doi.org/10.1016/j.cropro.2009.05.010

Guindon S., Dufayard J.F., Lefort V., Anisimova M., Hordijk W., Gascuel O., 2010. New algorithms and methods to estimate maximum-likelihood phylogenies: assessing the performance of PhyML 3.0. *Systems Biology* 59: 307–321. https://doi.org/10.1093/sysbio/syq010.

Hillis D.M., Bull J.J., 1993. An empirical test of bootstrapping as a method for assessing confidence in phylogenetic analysis. *Systematic Biology* 42: 182–192.

Iliadi M.K., Tjamos E., Antoniou P., Tsitsigiannis D.I., 2018. First report of *Colletotrichum acutatum* causing anthracnose on olives in Greece. *Plant Disease* 102: 820. https://doi.org/10.1094/PDIS-09-17-1451-PDN

Katoh K., Standley D.M., 2013. MAFFT multiple sequence alignment software version 7: improvements in performance and usability. *Molecular Biology Evolution* 30: 772–780. https://doi.org/10.1093/molbev/mst010

Kolainis S., Koletti A., Lykogianni M., Karamanou D., Gkizi D., ... Aliferis K.A., 2020. An integrated approach to improve plant protection against olive anthracnose caused by the *Colletotrichum acutatum* species complex. *PLoS One* 15(5): p.e0233916.

Koya P.R., Goshu A.T. 2013. Generalized Mathematical Model for Biological Growths. *Open Journal of Modelling and Simulation* 1(4): 42–53. https://doi.org/10.4236/ojmsi.2013.14008

Licciardello G., Moral J., Strano M.C., Caruso P., Sciara M., ...Di Silvestro S., 2022. Characterization of *Colletotrichum* strains associated with olive anthracnose in Sicily. *Phytopathologia Mediterranea* 61, 139–151.

Materatski P., Varanda C., Carvalho T., Dias A.B., Campos M.D., ...Félix M.R., 2018. Diversity of *Colletotrichum* species associated with olive anthracnose and new perspectives on controlling the disease in Portugal. *Agronomy* 8: 301. https://doi.org/10.3390/agronomy8120301

McKinney H.H., 1923. Influence of soil temperature and moisture on infection of wheat seedlings by *Helmintosporium sativum*. *Journal of Agricultural Research* 26: 195–218.

Moral J., Trapero A., 2009. Assessing the susceptibility of olive cultivars to anthracnose caused by *Colletotrichum acutatum*. *Plant Disease* 93: 1028–1036.

Moral J., Bouhmidi K., Trapero A., 2008. Influence of fruit maturity, cultivar susceptibility, and inoculation method on infection of olive fruit by *Colletotrichum acutatum*. *Plant Disease* 92: 1421–1426.

Moral J., Xaviér C., Roca L.F., Romero J., Moreda W., Trapero A., 2014. Olive anthracnose and its effect on oil quality. *Grasas Aceites* 65: e028. https://doi.org/10.3989/gya.110913

Moral J., Xaviér C., Viruega J., Roca L., Caballero J., Trapero A., 2017. Variability in susceptibility to anthracnose in the world collection of olive cultivars of Cordoba (Spain). *Frontiers in Plant Science* 8: 1-11.

Moral J., Agusti-Brisach C., Raya M.C., Jurado-Bello J., Lopez-Moral A., ... Trapero A., 2021. Diversity of *Colletotrichum* species associated with olive anthracnose worldwide. *Journal of Fungi* 7: 741. https://doi.org/10.3390/jof7090741

Moreira V., Mondino P., Alaniz S., 2021. Olive anthracnose caused by *Colletotrichum* in Uruguay: Field symptoms, species diversity and flowers and fruits pathogenicity. *European Journal of Plant Pathology* 160: 663–681. https://doi.org/10.1007/s10658-021-02274-z

Moreira V., Carbone M.J., Ferronato B., González-Barrios P., Alaniz S., Mondino P., 2024. Role of fungicides to control blossom blight and fruit rot the main symptoms of olive anthracnose in Uruguay. *International Journal of Pest Management* 71: 29–41. https://doi.org/10.1080/09670874.2024.2388158

Msairi S., Chliyeh M., Rhimini Y., Selmaoui K., Mouria A., ... Douira A., 2017. First report on *Colletotrichum acutatum* of olives in Morocco. *Annual Research and Review in Biology* 16: 1–8. https://doi.org/10.9734/arrb/2017/35341

Msairi S., Chliyeh M., Touhami A.O., El Alaoui A., Selmaoui K., ... A. Douira 2020. First report on *Colletotrichum lupini* causing anthracnose disease in olive fruits in Morocco. *Plant Cell Biotechnology and Molecular Biology* 21: 1–11.

Mukadam S. 2014. *SA steps up to the plate in olive oil industry*. The M&G Online. Available at https://mg.co.za/article/2014-10-16-source-your-olive-oil-in-sa. Accessed April 6, 2019.

Nawaz H.H., Manzoor A., Iqbal M.Z., Ansar M.R., Ali M., ... M. Weiguo, 2023. *Colletotrichum acutatum*: causal agent of olive anthracnose isolation, characterization, and fungicide susceptibility screening in Punjab, Pakistan. *Plant Disease* 107: 1329–1342. https://doi.org/10.1094/PDIS-09-22-2260-RE

O'Donnell K., Cigelnik E., 1997. Two divergent intragenomic rDNA ITS2 types within a monophyletic lineage of the fungus *Fusarium* are nonorthologous. *Molecular Phylogenetics and Evolution* 7: 103–116.

Ott R.L., 1998. *An Introduction to Statistical Methods and Data Analysis*, Duxbury Press, Belmont, California.

Pesticide Property Database (PPDB), 2019. *Dodine*. Available at https://sitem.herts.ac.uk/aeru/ppdb/en/Reports/263.htm. Accessed September 28, 2019.

Piccirillo G., Carrieri R., Polizzi G., Azzaro A., Lahoz E., … Vitale A., 2018. *In vitro* and *in vivo* activity of QoI fungicides against *Colletotrichum gloeosporioides* causing fruit anthracnose in *Citrus sinensis*. *Scientia Horticulturae* 236: 90–95. https://doi.org/10.1016/j.scienta.2018.03.044

Rampersad S.N., T.L.D., 2012. Differential responses of *Colletotrichum gloeosporioides* and *C. truncatum* isolates from different hosts to multiple fungicides based on two assays. *Plant Disease* 96: 1526–1536.

Rayner R.W., 1970. *A Mycological Colour Chart*. Commonwealth Mycological Institute & British Mycological Society, Kew, London.

Rongai D., Basti C., Di Marco C., 2012. A natural product for the control of olive leaf spot caused by *Fusicladium oleagineum*. *Phytopathologica Mediterranea* 51: 276–282.

SA Olive, 2024. *Olive Growing*. SA Olive. Available at https://www.saolive.co.za/olive-growing/. Accessed August 6, 2024.

Schena L., Mosca S., Cacciola S.O., Faedda R., Sanzani S.M., … Magnano di San Lio G., 2014. Species of the C*olletotrichum gloeosporioides* and *C. boninense* complexes associated with olive anthracnose. *Plant Pathology* 63: 437–446.

Sergeeva V., Spooner-Hart R., Nair N.G., 2008. First report of *Colletotrichum acutatum* and *C. gloeosporioides* causing leaf spots of olives (*Olea europaea*) in Australia. *Australasian Plant Disease Notes* 3: 143–144.

Shapiro S., Wilk M., 1965. An Analysis of Variance Test for Normality (Complete Samples). *Biometrika* 52: 591.

Talhinhas P., Sreenivasaprasad S., Neves-Martins J., Oliveira H., 2005. Molecular and phenotypic analyses reveal the association of diverse *Colletotrichum acutatum* groups and a low level of *C. gloeosporioides* with olive anthracnose. *Applied Environmental Microbiology* 71: 2987–2998.

Talhinhas P., Mota-Capitão C., Martins S., Ramos A., Neves-Martins J., … H. Oliveira, 2011. Epidemiology, histopathology and aetiology of olive anthracnose caused by *Colletotrichum acutatum* and *C. gloeosporioides* in Portugal. *Plant Pathology* 60: 483–495.

Usman H.M., Tan Q., Fan F., Karim M.M., Yin W.X., … Luo, C.X., 2022. Sensitivity of *Colletotrichum nymphaeae* to six fungicides and characterization of fludioxonil-resistant isolates in China. *Plant Disease* 106(1): 165–173. https://doi.org/10.1094/PDIS-05-21-0993-RE

Verwoerd L., 1929. A preliminary check list of diseases of cultivated plants in the winter rainfall area of the Cape Province. *Science Bulletin Department of Agriculture* 88: 237–239.

Vieira W., Bezerra P.A., Silva A.C.D., Veloso J.S., Camara M.P.S., Doyle V.P., 2020. Optimal markers for the identification of *Colletotrichum* species. *Molecular Phylogenetics and Evolution* 143: 106694. https://doi.org/ 10.1016/j.ympev.2019.106694

Wharton P., Dieguez-Uribeondo J., 2004. The biology of *Colletotrichum acutatum*. *Anales del Jardin Botanico de Madrid* 61: 3–22.

White T. J., Bruns T., Lee S., Taylor J., 1990. Amplification and direct sequencing of fungal ribosomal RNA genes for phylogenetics. *PCR protocols: a guide to methods and applications* 18(1): 315–322.

Yang X., Gu C.Y., Sun J.Z., Bai Y., Zang H.Y., Chen Y., 2021. Biological activity of pyraclostrobin against *Coniella granati* causing pomegranate crown rot. *Plant Disease* 105(11): 3538–3544. https://doi.org/10.1094/PDIS-01-21-0144-RE

Phytopathologia Mediterranea
The international journal of the
Mediterranean Phytopathological Union

Firenze University Press
www.fupress.com/pm

Research Notes

The most informative loci to identify trunk disease pathogens associated with grapevine and perennial fruit and nut crops

David GRAMAJE[1,*], Lizel MOSTERT[2], Florent P. TROUILLAS[3], José Ramón ÚRBEZ-TORRES[4], Artur ALVES[5]

[1] *Instituto de Ciencias de la Vid y del Vino (ICVV), Consejo Superior de Investigaciones Científicas - Universidad de la Rioja - Gobierno de La Rioja, Ctra. LO-20 Salida 13, Finca La Grajera, 26071 Logroño, Spain*
[2] *Department of Pant Pathology, Stellenbosch University, Private Bag X1, Matieland, 7602, South Africa*
[3] *Department of Plant Pathology, University of California, Davis and Kearney Agricultural Research and Extension Center, Parlier, CA, 93648, United States of America*
[4] *Summerland Research and Development Centre, Agriculture and Agri-Food Canada, 4200 Highway 97, Box 5000. Summerland, BC V0H 1Z0, Canada*
[5] *Departamento de Biologia, CESAM, Universidade de Aveiro, 3810-193 Aveiro, Portugal*
*Corresponding author. E-mail: david.gramaje@icvv.es

Summary. Trunk disease (TD) fungi are taxonomically diverse, and accurate species delimitation relies on multilocus phylogenetic analyses. However, the loci commonly employed vary among fungal groups, leading to inconsistencies in species recognition. This paper provides a comparative overview of the most informative genetic loci for species identification within the main families associated with TDs, including *Botryosphaeriaceae*, *Cytosporaceae*, *Diaporthaceae*, *Diatrypaceae*, *Phaeomoniellaceae*, *Togniniaceae*, *Nectriaceae* (*Ascomycota*), and *Hymenochaetales* (*Basidiomycota*). The internal transcribed spacer region (*ITS*) remains the universal primary barcode, but its discriminatory power is often limited. The most informative loci [translation elongation factor 1-α (*tef1*), β-tubulin (*tub2*), actin (*act1*), calmodulin (*cal*), histone (*his3*), and the RNA polymerase II second largest subunit (*rpb2*)] are identified, and optimal locus combinations for each fungal group are identified. This synthesis will aid selection of the most appropriate loci for robust phylogenetic inference and accurate pathogen identification, thereby improving epidemiological and management studies of TDs.

Keywords. Fungal taxonomy, multi-locus phylogeny, molecular identification, pathogen diagnosis.

OPEN ACCESS

Citation: Gramaje, D., Mostert, L., Trouillas, F. P., Úrbez-Torres, J. R., & Alves, A. (2025). The most informative loci to identify trunk disease pathogens associated with grapevine and perennial fruit and nut crops. *Phytopathologia Mediterranea* 64(3): 631-636. DOI: 10.36253/phyto-16857

Accepted: December 7, 2025

Published: December 30, 2025

Data Availability Statement: All relevant data are within the paper and its Supporting Information files.

Competing Interests: The Author(s) declare(s) no conflict of interest.

Editor: Michael J Wingfield, University of Pretoria, South Africa.

ORCID:
DG: 0000-0003-1755-3413
LM: 0000-0001-9063-2447
FPT: 0000-0002-9884-058X
JRÚ-T: 0000-0002-0753-9928
AA: 0000-0003-0117-2958

Trunk diseases (TDs) are among the most economically destructive disorders of woody plants, affecting forest trees and perennial fruit crops across temperate and tropical regions (Slippers and Wingfield, 2007; Gramaje *et al*., 2018; Guarnaccia *et al*., 2022; Martino *et al*., 2025). The pathogens involved are a highly diverse assemblage of *Ascomycota* and *Basidiomycota*, including members of the *Botryosphaeriaceae*, *Cytosporaceae*, *Diaporthaceae*, *Dia-*

trypaceae, *Nectriaceae*, *Phaeomoniellaceae*, *Togniniaceae*, and the *Hymenochaetales*. These fungi colonize woody tissues of their hosts primarily via wounds and/or natural openings, and cause vascular dysfunction, dieback, progressive yield decline, and eventual plant death. Accurate species-level identification is essential to underpin epidemiological studies, and to develop evidence-based, durable management strategies. The present paper specifically relates to fungal trunk pathogens associated with grapevine and perennial fruit and nut crops. Forest pathogens (e.g. *Cryphonectriaceae*), although relevant to canker diseases in woody plants, fall outside the scope of this review.

Identification of TD pathogens has relied heavily on morphological and cultural characteristics, which are often insufficient due to phenotypic plasticity and overlapping traits (Figure 1). The advent of molecular phylogenetics has revolutionized the taxonomy of these fungi, allowing for the use of multiple gene regions to resolve species boundaries. However, the loci selected for phylogenetic analyses have not been standardized, leading to discrepancies among studies. To address this, the present paper reviews current knowledge to determine which loci or locus combinations provide the best resolution for each TD-related fungus group.

The most complete taxonomic and phylogenetic studies describing TD-associated fungi were reviewed. These sources included revisions and monographs for each family, including Phillips *et al*. (2013) for *Botryosphaeriaceae*, Santos *et al*. (2017) and Manawasin-

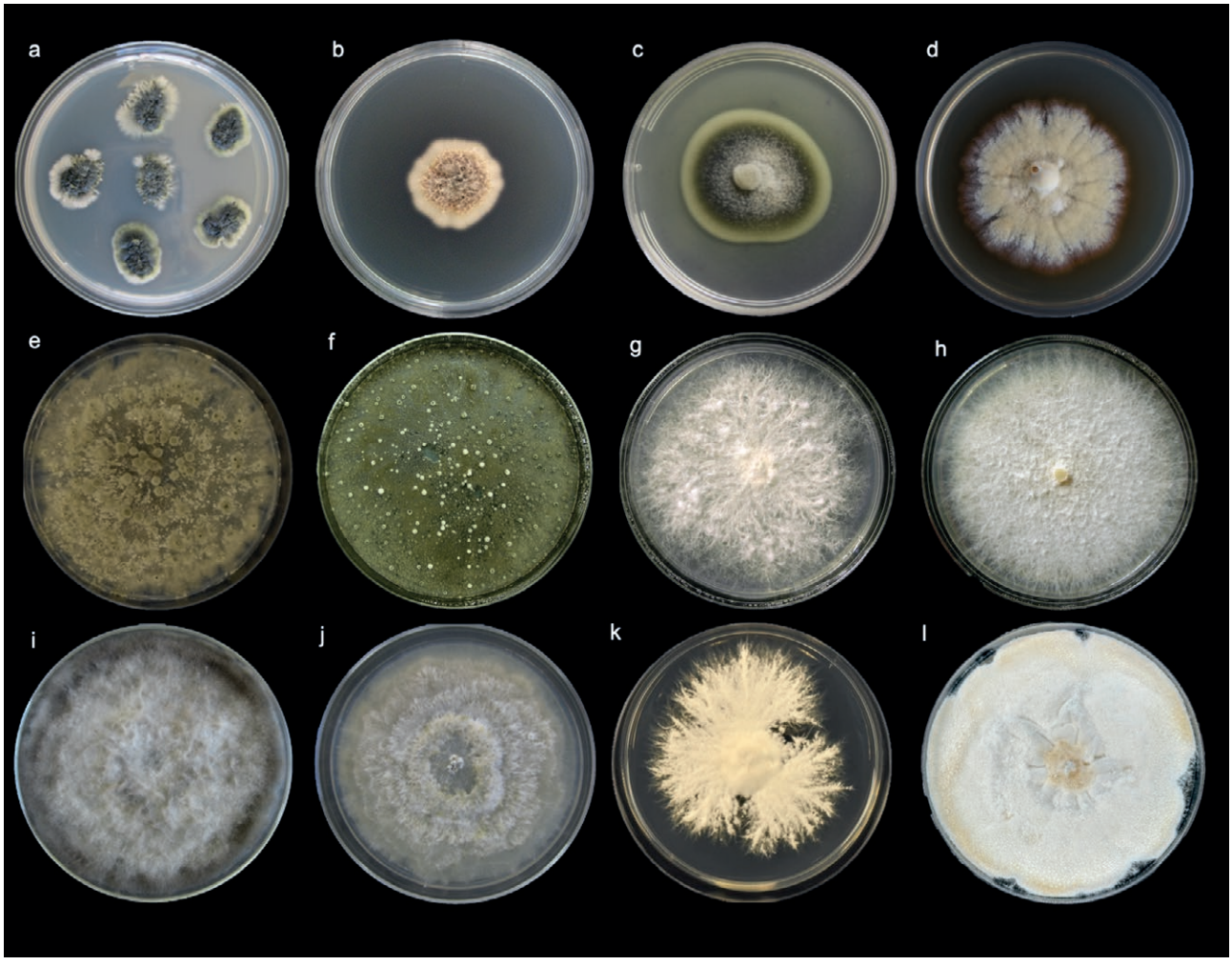

Figure 1. Colony morphologies of wood-inhabiting fungi grown on potato dextrose agar at 25°C: (a) *Phaeomoniella chlamydospora*, (b) *Phaeoacremonium parasiticum*, (c) *Cadophora luteo-olivacea*, (d) *Dactylonectria torresensis*, (e) *Cytospora pistaciae*, (f) *Cytospora sorbicola*, (g) *Diatrype stigma*, (h) *Eutypa leptoplaca*, (i) *Neofusicoccum parvum*, (j) *Diaporthe ampelina,* (k) *Schizophyllum commune*, and (l) *Ganoderma adspersum*.

ghe *et al*. (2019) for *Diaporthe*, Trouillas *et al*. (2010) for *Diatrypaceae*, Tegli *et al*. (2000) and Chen *et al*. (2022) for *Phaeomoniellaceae*, Cabral *et al*. (2012) for *Cylindrocarpon*-like species, Mostert *et al*. (2006) and Marin-Felix *et al*. (2019) for *Togniniaceae*, Travadon *et al*. (2015) and Chen *et al*. (2022) for *Cadophora* spp., Lin *et al*. (2024) for *Cytospora* spp., and Amalfi *et al*. (2012) for *Hymenochaetales*.

Each gene region reported in these studies was evaluated for its phylogenetic informativeness and resolution power. The analysis focused on loci commonly used in fungal taxonomy, including the internal transcribed spacer (*ITS*), translation elongation factor 1-α (*tef1*), β-tubulin (*tub2*), actin (*act1*), calmodulin (*cal*), histone (*his3*), and the RNA polymerase II second largest subunit (*rpb2*). Table 1 lists the respective primer pairs and amplification conditions for these gene regions. The loci were chosen based on their abilities to resolve closely related species, their reproducibility, and their representation in publicly available databases.

The comparative analysis revealed substantial variation in the informativeness of loci among fungal families associated with TDs. While ITS remains a universal barcode, it often lacks discriminatory power for closely related taxa. Figure 2 provides an overview of the optimal loci combinations for each group, with the most informative markers highlighted. Loci shown in green represent the most phylogenetically informative gene for each family, while loci in orange indicate additional markers necessary to resolve species complexes or describe new taxa. Table 1 presents the recommended primer pairs for each locus.

Table 1. Loci and respective primer pairs used to identify trunk disease fungi.

Loci	Primers	Sequence 5′-3′	References	Target Fungi
act1	ACT-512F	ATGTGCAAGGCCGGTTTCGC	Carbone and Kohn (1999)	ACT-512F & ACT-728R: *Cytosporaceae*
	ACT-783R	TACGAGTCCTTCTGGCCCAT	Carbone and Kohn (1999)	ACT-512F & ACT-783R: *Diaporthaceae* and *Togniniaceae*
	ACT-728R	TGGAGGGAGAAGAGCTACGA	Carbone and Kohn (1999)	
cal	CAL-228F	GAGTTCAAGGAGGCCTTCTCCC	Carbone and Kohn (1999)	CAL-228F & CAL-737R: *Diaporthaceae*
	CAL-737R	CATCTTCTGGCCATCATGG	Carbone and Kohn (1999)	
his3	CYLH3F	AGGTCCACTGGTGGCAAG	Crous *et al.* (2004)	CYLH3F & CYLH3R: *Nectriaceae*
	CYLH3R	AGCTGGATGTCCTTGGACTG	Crous *et al.* (2004)	CYLH3F & H3-1b: *Diaporthaceae*
	H3-1b	GCGGGCGAGCTGGATGTCCTT	Glass and Donaldson (1995)	
ITS	ITS1	TCCGTAGGTGAACCTGCGG	White *et al.* (1990)	ITS1-F & ITS4: *Botryosphaeriaceae*, *Nectriaceae*, and *Hymenochaetales*
	ITS1-F	CTTGGTCATTTAGAGGAAGTAA	Gardes and Bruns (1993)	ITS4 & ITS5: *Cytosporaceae*
	ITS4	TCCTCCGCTTATTGATATGC	White *et al.* (1990)	ITS1 & ITS4: *Diaporthaceae*, *Diatrypaceae*, and the genus *Cadophora*
	ITS5	GGAAGTAAAAGTCGTAACAAGG	White *et al.* (1990)	PCH1 & PCH2: *Phaemoniellaceae*
	PCH1	CTCCAACCCTTTGTTTATC	Tegli *et al.* (2000)	
	PCH2	TGAAAGTTGATATGGACCC	Tegli *et al.* (2000)	
rpb2	RPB2-5F	GAYGAYMGWGATCAYTTYGG	Liu *et al.* (1999)	RPB2-5F & RPB2-7cR: *Cytosporaceae*
	RPB2-7cR	CCCATRGCTTGYTTRCCCAT	Liu *et al.* (1999)	
tef1	EF1-728F	CATCGAGAAGTTCGAGAAGG	Carbone and Kohn (1999)	EF1-688F & EF1-986R: *Botryosphaeriaceae*
	EF1-986R	TACTTGAAGGAACCCTTACC	Carbone and Kohn (1999)	EF1F & EF2R: *Cytosporaceae*
	EF1-688F	CGGTCACTTGATTTGTTGG	Alves *et al.* (2008)	EF1-728F & EF1-986R: *Diaporthaceae*
	EF1-1251R	CCTCGAACTCACCAGTACGA	Alves *et al.* (2008)	CylEF-1 & CylEF-R2: *Nectriaceae*
	EFIF	ATGGGTAAGGARGACAAGAC	O'Donnell and Cigelnik (1997)	EF1-688F & EF1-1251R: genus *Cadophora*
	EF2R	GGARGTACCAGTSATCATGTT	O'Donnell and Cigelnik (1997)	
	CylEF-1	ATGGGTAAGGAVGAVAAGAC	J.Z. Groenewald, unpublished	
	CylEF-R2	GCCATCCTTGGAGATACCAGC	Crous *et al.* (2004)	
tub2	BT2a	GGTAACCAAATCGGTGCTGCTTTC	Glass and Donaldson (1995)	BT2a & Bt2b: *Botryosphaeriaceae*, *Cytosporaceae*, and *Diaporthaceae*
	Bt2b	ACCCTCAGTGTAGTGACCCTTGGC	Glass and Donaldson (1995)	T1 & Bt2b: *Nectriaceae*, *Togniniaceae*, and *Diatrypaceae*
	T1	AACATGCGTGAGATTGTAAGT	O'Donnell and Cigelnik (1997)	
	BTCadF	MATGCGTGAAATYGTAAGT	Travadon *et al.* (2015)	BTCadF & BTCadR: genus *Cadophora*
	BTCadR	TCAGCACCCTCAGTGTAATG	Travadon *et al.* (2015)	

Taxonomic group	ITS	*TEF1*	*TUB2*	*ACT1*	*RPB2*	*HIS3*	*CAL*	DNA lyase
Ascomycota								
Botryosphaeriaceae	X	X	X	X	X		X	
Cytosporaceae	X	X	X	X	X			
Diaporthaceae	X	X	X	X		X	X	X
Diatrypaceae	X		X		X			
Nectriaceae	X	X	X	X	X	X	X	
Phaeomoniellaceae	X	X		X				
Togniniaceae	X	X	X	X				
Cadophora	X	X	X					
Basidiomycota								
Hymenochaetales	X	X			X			

Excluding SSU and LSU.
The most informative locus to identify and analyse species in each group is highlighted in green. Sequencing additional loci, highlighted in orange in each group, is required for species separation for new species descriptions.

Figure 2. Genes for phylogenetic analyses and species identifications of fungi causing trunk diseases.

For the *Botryosphaeriaceae*, *tef1* and *tub2* consistently provide the greatest resolution for species delimitation, with *ITS* alone being insufficient. Additional markers such as *act1*, *rpb2*, and *cal* may further improve phylogenetic robustness (Inderbitzin *et al*., 2010; Phillips *et al*., 2013). Within *Diaporthaceae*, species delimitation requires a multilocus dataset combining *ITS*, *tef1*, *tub2*, *cal*, and *his3*, with *tef1* offering the best resolution (Santos *et al*., 2017; Manawasinghe *et al*., 2019). For *Diatrypaceae*, *ITS* and *tub2* consistently provide the highest resolution for species delimitation, with *ITS* being the most informative (Trouillas *et al*., 2010). Members of the *Phaeomoniellaceae*, including *Phaeomoniella*, are best resolved using *ITS* (Tegli *et al*., 2000; Chen *et al*., 2022). *Togniniaceae*, encompassing *Phaeoacremonium* spp., benefit from the combined use of *tub2* and *act1*. For *Nectriaceae*, encompassing '*Cylindrocarpon*'-like fungi, *his3* is the most informative locus, complemented by *ITS*, *tef1*, and *tub2* (Cabral *et al*., 2012; Lawrence *et al*., 2019). In *Cadophora* species, *ITS*, *tef1*, and *tub2* are typically used, with *tub2* being the most informative locus (Travadon *et al*., 2015). Within *Cytospora*, species delimitation requires a multilocus dataset combining *ITS*, *tef1*, *tub2*, *act1*, and *rpb2*, with *TEF1* offering the best resolution (Lawrence *et al*., 2018; Chen *et al*., 2022; Lin *et al*. 2024). Finally, within the Basidiomycota (*Hymenochaetales*), *ITS*, *tef1*, and *rpb2* suffice for accurate identification, with *ITS* being the most informative locus (Amalfi *et al*., 2012).

Advances in molecular taxonomy have considerably improved understanding of TD fungi. Despite significant progress, however, several challenges remain. A major obstacle is the heterogeneity of loci that have been used across studies, which complicates cross-comparison and meta-analyses of phylogenetic data. While *ITS* remains the official fungal barcode, it is often inadequate for species-level resolution among TD pathogens, due to low interspecific variability. Therefore, multi-locus sequencing analyses (MLSA) using *tef1*, *tub2*, and *his3*, as applicable to each fungal group (Figure 2), and these analyses have become the standard for accurate species delimitation, although this approach requires more laboratory resources and expertise than for single locus analyses.

The continuing discovery of cryptic and newly described species highlights the need for a unified molecular framework. Integration of genomic approaches, such as whole-genome sequencing (WGS) and MLSA, offers unprecedented opportunities. Genomic data provide increased resolution for population-level analyses, which enables increased understanding of evolutionary relationships, host adaptation, and pathogenicity. Nevertheless, these approaches are costly and require robust bioinformatic resources and capability.

To standardize taxonomy of TD pathogens, a community-based reference database should be established, including curated multi-locus datasets and metadata. This would facilitate consistent identification across laboratories, promote reproducibility, and reduce misidentifications that can hinder epidemiological interpretations. Furthermore, advances in high-throughput sequencing (Nilsson *et al*., 2019; Lofgren and Stajich, 2021), field-

deployable (portable) DNA barcoding using nanopore devices (Srivathsan *et al*., 2021), and machine-learning-based taxonomic classifiers (Wang and Cole, 2024), are likely to play important roles in the near future.

This summary highlights that there is no universal multilocus scheme suitable for all TD pathogens. Instead, optimal locus selection must be tailored to each fungus family to achieve accurate and reproducible results. The comparative framework presented here will support harmonization among laboratories, improve species delimitation, and facilitate further research into the biology and management of TD pathogens.

ACKNOWLEDGEMENTS

Artur Alves acknowledges financial support to CESAM by national funds through Fundação para a Ciência e a Tecnologia (FCT) I.P., under the project/grant UID/50006 + LA/P/0094/2020 (https://doi.org/10.54499/LA/P/0094/2020).

LITERATURE CITED

Alves A., Crous P.W., Correia A., Phillips A.J.L., 2008. Morphological and molecular data reveal cryptic speciation in *Lasiodiplodia theobromae*. *Fungal Diversity* 28: 1–13. https://www.fungaldiversity.org/fdp/sfdp/28-1.pdf

Amalfi M., Raymundo T., Valenzuela R., Decock C., 2012. *Fomitiporia cupressicola* sp. nov., a parasite on *Cupressus arizonica*, and additional unnamed clades in the southern USA and northern Mexico, determined by multilocus phylogenetic analyses. *Mycologia* 104(4): 880–893. https://doi.org/10.3852/11-196

Chen Q., Bakhshi M., Balci Y., Broders K.D., Cheewangkoon R., … Crous P.W., 2022. Genera of phytopathogenic fungi: GOPHY 4. *Studies in Mycology* 101: 417–564. https://doi.org/10.3114/sim.2022.101.06

Cabral A., Rego C., Nascimento T., Oliveira H., Groenewald J.Z., Crous P.W., 2012. Multi-gene analysis and morphology reveal novel *Ilyonectria* species associated with black foot disease of grapevines. *Fungal Biology* 116: 62–80. https://doi.org/10.1016/j.funbio.2011.09.010

Carbone I., Kohn L.M., 1999. A method for designing primer sets for speciation studies in filamentous ascomycetes. *Mycologia* 91: 553–556. https://doi.org/10.1080/00275514.1999.12061051

Crous P.W., Groenewald J.Z., Risede J.M., Hywel-Jones N.L., 2004. *Calonectria* species and their *Cylindrocladium* anamorphs: species with sphaeropedunculate vesicles. *Studies in Mycology* 50: 415–429.

Gardes M., Bruns T.D., 1993. ITS primers with enhanced specificity for basidiomycetes – application to the identification of mycorrhizae and rusts. *Molecular Ecology* 2: 113–118. https://doi.org/10.1111/j.1365-294x.1993.tb00005.x

Glass N.L., Donaldson G.C., 1995. Development of primer sets designed for use with the PCR to amplify conserved genes from filamentous ascomycetes. *Applied and Environmental Microbiology* 61: 1323–1330. https://doi.org/10.1128/aem.61.4.1323-1330.1995

Gramaje D., Úrbez-Torres J.R., Sosnowski M.R., 2018. Managing grapevine trunk diseases with respect to etiology and epidemiology: current strategies and future prospects. *Plant Disease* 102: 12–39. https://doi.org/10.1094/PDIS-04-17-0512-FE

Guarnaccia V., Kraus C., Markakis E., Alves A., Armengol J., Eichmeier A., Compant S., Gramaje D., 2022. Fungal trunk diseases of fruit trees in Europe: pathogens, spread and future directions. *Phytopathologia Mediterranea* 61: 563–599. https://doi.org/10.36253/phyto-14167

Inderbitzin P., Bostock R.M., Trouillas F.P., Michailides T.J., 2010. A six locus phylogeny reveals high species diversity in Botryosphaeriaceae from California almond. *Mycologia* 102: 1350–1368. https://doi.org/10.3852/10-006

Lawrence D.P., Holland L.A., Nouri M.T., Travadon R., Abramians A., … Trouillas F.P., 2018. Molecular phylogeny of *Cytospora* species associated with canker diseases of fruit and nut crops in California, with the descriptions of ten new species and one new combination. *IMA Fungus* 9: 333–369. https://doi.org/10.5598/imafungus.2018.09.02.07

Lawrence D.P., Nouri M.T., Trouillas F.P., 2019. Taxonomy and multi-locus phylogeny of cylindrocarpon-like species associated with diseased roots of grapevine and other fruit and nut crops in California. *Fungal Systematics and Evolution* 4: 59–75. https://doi.org/10.3114/fuse.2019.04.06

Lin L., Fan X.L., Groenewald J.Z., Jami F., Wingfield M.J., … Crous P.W., 2024. *Cytospora*: an important genus of canker pathogens. *Studies in Mycology* 109: 323–340. https://doi.org/10.3114/sim.2024.109.05

Liu Y.J., Whelen S., Hall B.D., 1999. Phylogenetic relationships among ascomycetes: evidence from an RNA polymerase II subunit. *Molecular Biology and Evolution* 16: 1799–1808. https://doi.org/10.1093/oxfordjournals.molbev.a026092

Lofgren L.A., Stajich J.E., 2021. Fungal biodiversity and conservation mycology in light of new technology,

big data, and changing attitudes. *Current Biology* 31: 1312–1325. https://doi.org/10.1016/j.cub.2021.06.083

Manawasinghe I.S., Dissanayake A.J, Li X., Liu M., Wanasinghe D.N., ..., Yan J., 2019. High genetic diversity and species complexity of *Diaporthe* associated with grapevine dieback in China. *Frontiers in Microbiology* 10: 1936. https://doi.org/10.3389/fmicb.2019.01936

Marin-Felix Y., Hernández-Retrepo M., Wingfield M.J., Akulov A., Carnegie A.J., ... Crous P.W., 2019. Genera of phytopathogenic fungi: GOPHY 2. *Studies in Mycology* 92: 47–133. https://doi.org/10.1016/j.simyco.2018.04.002.

Martino I., Spadaro D., Guarnaccia V., 2025. Fungal trunk pathogens of fruit and nut tree crops: identification, characterization, detection, and perspectives for a critical global issue. *Plant Disease* 109: 1192–1210. https://doi.org/10.1094/PDIS-10-24-2069-FE

Mostert L., Groenewald J.Z., Summerbell R.C., Gams W., Crous P.W., 2006. Taxonomy and pathology of *Togninia* (Diaporthales) and its *Phaeoacremonium* anamorphs. *Studies in Mycology* 54: 1–113. https://doi.org/10.3114/sim.54.1.1

Nilsson R.H., Anslan S., Bahram M., Wurzbacher C., Baldrian P., Tedersoo L., 2019. Mycobiome diversity: high-throughput sequencing and identification of fungi. *Nature Reviews Microbiology* 17: 95–109. https://doi.org/10.1038/s41579-018-0116-y

O'Donnell K., Cigelnik E., 1997. Two divergent intragenomic rDNA ITS2 types within a monophyletic lineage of the fungus *Fusarium* are nonorthologous. *Molecular Phylogenetics and Evolution* 7: 103–116. https://doi.org/ 10.1006/mpev.1996.0376

Phillips A.J.L., Alves A., Abdollahzadeh J., Slippers B., Wingfield M.J., ... Crous P.W., 2013. The *Botryosphaeriaceae*: genera and species known from culture. *Studies in Mycology* 76: 51–167. https://doi.org/10.3114/sim0021

Santos L., Alves A., Alves R., 2017. Evaluating multi-locus phylogenies for species boundaries determination in the genus *Diaporthe*. *PeerJ* 5: e3120. https://doi.org/10.7717/peerj.3120

Slippers B., Wingfield M.J., 2007. Botryosphaeriaceae as endophytes and latent pathogens of woody plants: diversity, ecology and impact. *Fungal Biology Reviews* 21: 90–106. https://doi.org/10.1016/j.fbr.2007.06.002

Srivathsan A., Lee L., Katoh K., Hartop E., Kutty S.N., ... Meier R., 2021. ONTbarcoder and MinION barcodes aid biodiversity discovery and identification by everyone, for everyone. *BMC Biology* 19: 217. https://doi.org/10.1186/s12915-021-01141-x

Tegli S., Bertelli E., Surico G., 2000. Sequence analysis of ITS ribosomal DNA in five *Phaeoacremonium* species and development of a PCR-based assay for the detection of *P. chlamydosporum* and *P. aleophilum* in grapevine tissue. *Phytopathologia Mediterranea* 39: 134–149. https://doi.org/10.14601/Phytopathol_Mediterr-1555

Travadon R., Lawrence DP., Rooney-Latham S., Gubler W.D, Wilcox W.F., ... Baumgartner K., 2015. *Cadophora* species associated with wood-decay of grapevine in North America. *Fungal Biology* 119: 53–66. htpps://doi.org/10.1016/j.funbio.2014.11.002

Trouillas F.P., Urbez-Torres J.R., Gubler W.D., 2010. Diversity of diatrypaceous fungi associated with grapevine canker diseases in California. *Mycologia* 102: 319–336. https://doi.org/10.3852/08-185

Wang Q., Cole J.R., 2024. Updated RDP taxonomy and RDP Classifier for more accurate taxonomic classification. *Microbiology Resource Announcements* 13: e01063-23. https://doi.org/10.1128/mra.01063-23

White T.J., Bruns T., Lee S., Taylor J., 1990. Amplification and direct sequencing of fungal ribosomal RNA genes for phylogenetics. In: *PCR Protocols: A Guide to Methods and Applications* (Eds. M.A. Innis, D.H. Gelfand, J.J. Sninsky, T.J. White), Academic Press, San Diego, CA, USA: 315–322. https://doi.org/10.1016/B978-0-12-372180-8.50042-1

Phytopathologia Mediterranea
The international journal of the
Mediterranean Phytopathological Union

Firenze University Press
www.fupress.com/pm

Research Papers

Optimization of DNA extraction and application of qPCR and ddPCR assays for detection of toxigenic *Aspergillus flavus* in hazelnut kernels

Alessia CASU[1], Giorgio CHIUSA[1], Paola BATTILANI[1,*], Hillary L. MEHL[2]

[1] *Department of Sustainable Crop Production, Università Cattolica del Sacro Cuore, Via Emilia Parmense 84, Piacenza, 29122, Italy*
[2] *United States Department of Agriculture, Agricultural Research Service, Tucson, AZ, United States of America*
*Corresponding author. E-mail: paola.battilani@unicatt.it

Summary. Aflatoxin contamination in hazelnuts, primarily caused by *Aspergillus flavus*, poses significant risks to food safety and public health, requiring highly sensitive and robust toxin detection strategies. While conventional culturing techniques remain relevant, they are time-consuming and prone to misidentifications. A molecular workflow for early detection of aflatoxigenic *A. flavus* in hazelnuts was developed and validated, combining an optimized DNA extraction protocol with quantitative PCR (qPCR) and droplet digital PCR (ddPCR) assays. Four DNA extraction methods were compared for their DNA yields and purity. DNA extraction protocol was optimized introducing a Tween-80 separation step, and was tested on hazelnuts artificially inoculated with aflatoxigenic *A. flavus* conidia. The optimized protocol was then validated for naturally contaminated hazelnut samples to assess its practical applicability, and to benchmark the performance of qPCR and ddPCR on real samples. The optimized protocol gave yield, purity and amplifiability, and appeared more appropriate for detecting aflatoxigenic *A. flavus* DNA in complex food matrices such as hazelnuts. The qPCR and ddPCR protocols detected target DNA, with ddPCR offering enhanced sensitivity and superior analytical performance. The developed protocol showed an increased sensitivity and quantification precision compared with previously developed methods. This research provides a validated molecular workflow for the early and sensitive detection of *A. flavus* in hazelnuts, offering a tool for preventive food safety monitoring and supporting aflatoxin risk assessment strategies for the hazelnut value chain.

Keywords. Aflatoxins, food safety, molecular diagnostics, digital PCR, fungal contamination.

OPEN ACCESS

Citation: Casu, A., Chiusa, G., Battilani, P., & Mehl, H. L. (2025). Optimization of DNA extraction and application of qPCR and ddPCR assays for detection of toxigenic *Aspergillus flavus* in hazelnut kernels. *Phytopathologia Mediterranea* 64(3): 637-648. DOI: 10.36253/phyto-16897

Accepted: December 10, 2025

Published: December 30, 2025

Data Availability Statement: All relevant data are within the paper and its Supporting Information files.

Competing Interests: The Author(s) declare(s) no conflict of interest.

Editor: Mario Masiello, National Research Council, (CNR), Bari, Italy.

ORCID:
AC: 0009-0000-5044-4329
PB: 0000-0003-1287-1711
HLM: 0000-0001-8570-3562

INTRODUCTION

Hazelnut (*Corylus avellana L.*) is an economically important tree nut, widely used in chocolate and confectionery industries. It has high nutritional

and lipidic content, but it is susceptible to fungal contamination during growth, harvest, processing and storage (Kabak, 2016; Şen *et al.,* 2025). *Aspergillus flavus* is a significant threat to the safety of human and animal food due to its capacity to synthetize aflatoxins (AFs), which are toxic and carcinogenic secondary metabolites. Among these, aflatoxin B_1 (AFB_1) is recognized as a Group 1 human carcinogen by the International Agency for Research on Cancer (IARC, 1993; Rushing *et al*., 2019).

The presence of AFs poses serious health concerns and has major economic implications. The European Union has set strict limits (5 μg kg^{-1} for AFB_1; 10 μg kg^{-1} for total AFs, in nuts for direct consumption; European Commission (EC), 2023), and products exceeding these thresholds are routinely rejected, leading to trade losses. Notifications from the Rapid Alert System for Food and Feed (RASFF) indicate recurrent AFs contamination in hazelnuts, particularly from Turkey, Georgia, and Azerbaijan (RASFF, 2025). With climate change extending AFs risk into temperate areas, the challenge of ensuring hazelnut safety is increasing (Şen *et al.,* 2025).

Identifying *Aspergillus* species in food has relied on plate counts and culturing methods that focus on macro- and micro-morphological characteristics. These techniques are time-consuming and require skilled personnel for fungus identifications. Molecular methods mitigate the chances of incorrect identification, and efforts have been made to design techniques that are highly specific and sensitive for detecting and quantifying aflatoxigenic *Aspergillus* species. Several methods have been developed for detection of these fungi, using polymerase chain reaction (PCR) and quantitative PCR (qPCR) assays (Shapira *et al.,* 1996; Chen *et al.,* 2002; Scherm *et al.,* 2005; Latha *et al*., 2008; Degola *et al.,* 2009; Luo *et al*., 2009; Passone *et al.,* 2010; Sardiñas *et al.,* 2011; Rodríguez *et al*., 2012; Shweta *et al.,* 2013; Ahmad *et al*., 2014; Mahmoud, 2015; Mitema *et al.,* 2019; Ortega *et al.,* 2020; Garcia-Lopez *et al.,* 2021; Leharanger *et al.,* 2024), or loop-mediated isothermal amplification (LAMP) assays (Luo *et al.,* 2012; Liu *et al.,* 2014; Luo *et al.,* 2014; Niessen *et al*., 2018; Douksouna *et al.,* 2020; Ortega *et al*., 2020). However, applications for hazelnuts remain limited (Gallo *et al.,* 2010; Hamed *et al*., 2016; Ortega *et al.,* 2020; Habibi, 2021; Lombardi *et al.,* 2022; Nooralden *et al*., 2022; Hassan *et al*., 2023; Aghayev *et al.,* 2025).

Droplet digital PCR (ddPCR) has gained prominence as a sensitive and accurate method for the detection and quantification of microbial populations, and some assays for *A. flavus* are already available (Hua *et al.,* 2018; Schamann *et al.,* 2022; Wang *et al.,* 2022; Palumbo *et al.,* 2023). Unlike qPCR, ddPCR enables absolute quantification of target DNA, by partitioning PCR reactions into thousands of nanoliter-sized droplets. In addition, ddPCR offers high sensitivity, making it suitable for identifying low concentrations of fungal DNA, which are often encountered in the initial phases of contamination or within food matrices with minimal fungal presence. Resilience of ddPCR where PCR inhibitors (polyphenols, fats, polysaccharides) are present, which commonly occurs in complex food matrices such as hazelnuts, further enhances ddPCR effectiveness.

The objectives of the present study were: to (i) compare different DNA extraction protocols for hazelnut matrices and evaluate their DNA purity and yields; (ii) assess the sensitivity and reliability of qPCR and ddPCR assays for *A. flavus* detection, including determination of their analytical detection limits of detection; (iii) optimize the extraction procedure with additional pretreatment steps to reduce inhibition and improve *A. flavus* recovery; and (iv) validate the optimized workflow for naturally *A. flavus* contaminated hazelnut samples, benchmarking molecular assays against conventional measures.

MATERIALS AND METHODS

Fungus strains and conidium suspension preparation

Aflatoxigenic *A. flavus* isolate AF13, from the USDA-ARS Aflatoxin Reduction in Crops Laboratory (Tucson, Arizona), was used for artificial inoculations of hazelnut samples (Cotty *et al*., 1993). DNA from the non-aflatoxigenic isolate AF36 of *A. flavus*, and a strain of *Fusarium verticillioides* from the same laboratory collection, were included as negative controls in qPCR and ddPCR assays.

To produce conidium suspensions, isolate AF13 was cultured on 5/2 agar supplemented with salt (5% V8 vegetable juice, 2% agar, 2% NaCl, pH 5.2). After 7 d incubation at 31°C, conidia were harvested using sterile cotton swabs, and were suspended in 10 mL water solution containing 0.01% Tween-80. Subsequently, 1 mL of this suspension was transferred to a tube containing 5 mL of sterilized water and 6 mL of pure ethanol (Sigma-Aldrich). Turbidity of the conidium suspension was measured using a TB300IR turbidimeter (Tintometer GmbH), and conidium concentration was calculated based on a nephelometric turbidity unit (NTU) and a colony forming units (CFUs) per mL standard curve, where CFU mL^{-1} = NTU (5.0×10^4) (Mehl *et al.,* 2010). The conidium suspension was diluted with sterile water to final concentrations of 1.2×10^6, 1.2×10^5, or 1.2×10^4 conidia mL^{-1}. These suspensions were used to artificially infest non-contaminated hazelnut samples in subsequent experiments.

Hazelnut samples

Two categories of hazelnut kernels were used in this study. Commercially available raw hazelnuts, purchased from the U.S. market, were supplied as pre-packed, deshelled kernels. These were ground into flour and considered as non-contaminated material, and the flour was subsequently used for artificial inoculations with AF13 conidia to optimize DNA extraction protocols and evaluate the limits of detection (LOD) of molecular assays.

In parallel, a total of ten hazelnut samples originating from local commercial markets in Azerbaijan, were collected from the 2023/2024 cropping season from the Khachmaz and Zaqatala regions. The samples, delivered in-shell after approx. 6 months of storage at room temperature (18–22°C), were each manually deshelled, ground into flour, and analyzed as naturally contaminated material with unknown levels of *A. flavus*. These samples were included to evaluate the initial DNA extraction performance and to validate the final optimized protocol.

All hazelnuts were ground into fine flour using the Grindomix GM200 knife mill (Retsch GmbH). Samples from Azerbaijan were analyzed by culture-based and molecular methods.

Culture-based assessments of fungal contamination

To estimate the initial fungal load in naturally contaminated hazelnuts, 1 g of hazelnut flour from each Azerbaijani sample was suspended in a final volume of 10 mL of sterile water, and was then homogenized using a Vortex ZX3 (Genelab Srl). Serial dilutions (10^{-1}, 10^{-2}, 10^{-3}) were prepared, and 500 µL from each dilution was plated onto each of three Petri plates containing Dichloran Rose Bengal Chloramphenicol (DRBC) agar (DRBC Agar Base; Biolife Italiana S.r.l), supplemented with 0.05 g L^{-1} chloramphenicol. The plates were then incubated at 31°C in the dark for 4 d, and *A. flavus* colonies were enumerated based on morphology. LOD was calculated on the most concentrated aliquot plated. One gram of sample was diluted 1:10 (0.1 g mL^{-1}), and 0.5 mL of this suspension was plated onto each of five replicate plates (volume of 2.5 mL, corresponding to 0.25 g of each sample). Assuming 1 CFU as the minimum detectable number, each LOD was calculated as 1 CFU per 0.25 g = 4 CFU g^{-1}.

DNA extraction tests

Four different DNA extraction methods were evaluated for their performance on naturally contaminated hazelnut samples. The methods were: the DNeasy Plant Pro Kit (Qiagen), the FastDNA Spin Kit (MP Biomedicals), the protocol described by Callicott *et al.* (2015), and a method based on InstaGene Matrix (Bio-Rad Laboratories).

The four DNA extraction methods were selected based on their documented use in mycological and food-related applications, particularly those involving *A. flavus*, and on their diversity of chemical–physical extraction principles. The DNeasy Plant Pro Kit was chosen because it is widely employed for genomic DNA extraction from filamentous fungi, and has demonstrated high performance and consistency across multiple fungal taxa (Conlon *et al.,* 2022). The DNeasy Plant Pro system has also been successfully applied for *A. flavus* detection in pure cultures, contaminated plant tissues, and food matrices (González-Salgado *et al.,* 2011). The FastDNA Spin Kit was included due to its extensive use in *A. flavus* research, showing high lysis efficiency and tolerance to inhibitory matrices. It has been successfully used to extract DNA from mycelia, conidia, soil, and nut-based matrices, such as pistachio kernels and hulls (Luo *et al.,* 2009; Mehl *et al.,* 2010; Grubisha *et al.,* 2015; Garcia-Lopez *et al.,* 2021). The Callicott *et al.* (2015) protocol was incorporated as a reference method, as it was specifically developed for *A. flavus* and is routinely employed in aflatoxin ecology and toxigenicity studies. The InstaGene Matrix (Bio-Rad) was included as a rapid, resin-based extraction method that is commonly used for preparing PCR-ready DNA from filamentous fungi, including *Aspergillus spp.*, in clinical and food-related contexts (Ciardo *et al.,* 2007; Soliman *et al.,* 2015).

For the ten hazelnut samples from Azerbaijan, and for each of the four extraction methods, a subsample of hazelnut flour was taken, giving ten biological replicates analyzed using each of the four methods.

For the DNeasy Plant Pro Kit, 0.2 g of hazelnut flour was homogenized in 500 µL of lysis buffer (Solution CD1), using a TissueLyser II (Qiagen) set at 24 Hz for 2 × 2 min cycles. After centrifugation (12,000 × g for 2 min), the supernatant was purified through binding and washing steps following the manufacturer's guidelines. DNA was then eluted in 75 µL of Buffer EB, and was stored at -20°C until further analysis.

For the FastDNA Spin Kit, 0.2 g of hazelnut flour were added to Lysing Matrix A tubes with lysis and precipitation solutions (800 µL CLS-VF and 200 µL PPS), and was homogenized using a TissueLyser II (24 Hz, 2 × 2 min). After centrifugation to pellet debris, the supernatant was mixed with Binding Matrix and applied to SPIN Filters for sequential binding and washing steps.

DNA was eluted in 100 µL of DES after incubation at 55°C, and was stored at -20°C until further use.

For the Callicott *et al.* (2015) DNA extraction protocol, 0.2 g of each sample was combined with 450 µL of lysis buffer (30 mM Tris, 10 mM EDTA, 1% SDS, pH 8·0). The samples were then incubated in Thermomixer 5436 (Eppendorf Inc.) for 1 h at 60°C and 800 rpm. Following the removal of plant fragments using centrifugation, the supernatant was transferred to a new tube and DNA was precipitated with 4M ammonium acetate and 100% cold ethanol. The pellet was then air dried, and DNA was resuspended in 25 µL of sterile water.

For the InstaGene DNA extraction protocol, 0.10 mg of hazelnut flour was mixed with 40 µL of InstaGene Matrix (Bio-Rad Laboratories) in 0.2 mL capacity PCR strip tubes. DNA was then extracted by incubating the samples at 95°C for 10 min in an All In One Cycler PCR Thermocycler (Bioneer), followed by centrifugation at 3800 rpm for 3 min to remove plant particles. The supernatant was then transferred to a new strip tube with a final maximum volume of 20 µL (based on extraction efficiency).

DNA concentrations were measured with a Qubit 4 fluorometer, using the Qubit 1X dsDNA Broad Range (BR) Assay kit (Thermo Fisher Scientific). Quality of the DNA was assessed with a NanoDrop One Spectrophotometer (Thermo Fisher Scientific).

All values obtained from Qubit and Nanodrop measurements (expressed in ng DNA μL^{-1}) were multiplied by the total volume (µL) of each extract to obtain the total ng of DNA per sample.

qPCR and ddPCR assays

The qPCR assay was carried out using primers Fw-nomutB (5′-CTTGGTCTACCATTGTTTGG-3′) and RV-nomut267 (5′-GGTAGGCGTCGTGTCTAG-3′), targeting the aflC gene, which encodes a key enzyme in the aflatoxin biosynthesis pathway. This primer pair specifically amplifies a 284-bp fragment in *A. flavus* isolates that lack the AF36 SNP, allowing selective detection of aflatoxigenic strains (Garcia-Lopez *et al.,* 2021). PCR amplifications were each carried out with two technical replicates per sample in a CFX96 Touch Instrument (Bio-Rad). Reactions (each 20 µL) included 10 µL iTaq SYBR Green Supermix (Bio-Rad), 0.6 µL of each 10 µM primer, 2 µL of undiluted DNA template, and 6.8 µL of sterile water. To evaluate possible PCR inhibition, each sample was also tested in an inoculated version, where 2 µL of water was replaced with 2 µL of AF13 DNA (0.1 ng μL^{-1}, 0.2 ng per reaction, for a total of 5×10^3 copies per reaction). Cycling was proceeded using the following conditions: 95°C for 5 min, 40 cycles each of 95°C for 5 s and 64°C for 30 s, followed by melting curve analysis. Standard curves were constructed using serial dilutions of AF13 DNA (5.0×10^4 to 0.5 copies per reaction) performed in triplicate.

The ddPCR assay followed the outline by Schamann *et al.* (2022), using a Bio-Rad custom assay (ID: dMDS741862930), targeting a single nucleotide polymorphism (SNP) in the *pksA* gene that distinguishes between the functional gene in aflatoxigenic *A. flavus* (labelled with a HEX probe) versus the mutation that confers non-aflatoxigenicity in the *A. flavus* biocontrol strain AF36 (labelled with a FAM probe). Since the goal of the present study was detection of aflatoxigenic *A. flavus*, only HEX fluorescence was considered for quantifications. Each reaction mix contained 10 µL 2× ddPCR Supermix (no dUTP), 1 µL primer/probe mix, 1 µL enzyme mix (0.5 µL HaeIII, 0.1 µL Cutsmart buffer, 0.4 µL water), 6 µL water, and 2 µL of template DNA, for a total volume of 20 µL. Droplets were generated and amplified (95°C for 10 min; 40 cycles each of 94°C for 30 s, 53°C for 60 s; 98°C for 10 min), then read on a QX200 Droplet Reader. Data were analyzed using QuantaSoft software with default amplitude thresholds and manual confirmation of positive droplet separation.

Each qPCR and ddPCR assay included non-template controls (NTCs) and *F. verticillioides* DNA as negative controls. Additionally, ddPCR included AF13 and AF36 DNA as positive controls. All control DNAs were originally at 1 ng μL^{-1} and were each diluted 1:10 in sterile water to a working concentration of 0.1 ng μL^{-1} prior to use.

All raw data obtained from qPCR and ddPCR were converted to copies per g. For qPCR results, copies of DNA/µL = [Avogadro's constant × DNA conc. (ng μL^{-1})]/[genome size (bp) × 10^9 ng/g × average weight of bp]. Copies per µL were multiplied by µL of extract to obtain total copies, and this was then divided per g of extract to obtain copies g^{-1}. For ddPCR, copies per reaction value were multiplied by the reaction volume to obtain copies per reaction. This was then divided by µL of DNA extract per reaction to get copies per reaction extract. These were then multiplied by total volume (µL) of extract to obtain total copies, that were divided by the hazelnut quantity used for extraction to obtain copies per g of hazelnut.

Optimization of DNA extraction

Initial quantification results indicated that concentrations of *A. flavus* in DNA extracts were below detectable levels. To determine the limit of *A. flavus* propagule

quantification and potentially increase the concentration of *A. flavus* in DNA extracts, non-infested hazelnuts were artificially inoculated with AF13 conidium suspensions at initial concentrations of approx. 1.2×10^6, 1.2×10^5, or 1.2×10^4 conidia mL^{-1}. For inoculation, 200 µL of each suspension were thoroughly mixed with 2 g of ground hazelnut, resulting in final concentrations of approx. 1.2×10^5, 1.2×10^4, and 1.2×10^3 conidia g^{-1}. A control sample to which 200 µL of sterile water was added. DNA extractions were carried out immediately after inoculations. The 2 g of inoculated hazelnut flour were then added to 20 mL of 0.01% Tween-80 and mixed for 20 min at 175 rpm on a horizontal shaker (IKA Werke GmbH & Co.). Following mixing, the solid (kernel) and liquid (Tween-80 suspension) fractions were manually separated by carefully pouring the liquid fraction into a new 50 mL tube while leaving the fatty deposit in the original tube. The liquid fraction was first centrifuged at 7,000 × g for 10 min, and the resulting pellet was transferred into 2 mL a microcentrifuge tube. In parallel, the kernel fraction was directly transferred into a 2 mL tube without prior centrifugation. Both fractions were then subjected to a second centrifugation at 8,000 × g for 10 min. After this step, resulting pellets from the liquid and the kernel fractions (approx. 500 to 600 µL) were collected and used for DNA extraction.

DNA was extracted using DNeasy Plant Pro and FastDNA Spin kits, with modifications: tough microorganism lysing tubes (Revvity) substituted standard disruption tubes, and each tube was loaded with two 6 mm ceramic beads (MP Biomedicals) to improve cell disruption. For the DNeasy protocol, the CD1 buffer volume was increased to 600 µL. Mechanical lysis was carried out using a Tissuelyser (Qiagen) at 25 Hz for 2 min. The experiment was carried out in triplicate, and DNA quantities and quality were assessed following the procedures outlined above. Performance of the two DNA extraction protocols was evaluated using qPCR and ddPCR with the methods outlined above.

Validation of optimized protocol on naturally contaminated hazelnut samples

The DNeasy Plant Pro Kit optimized DNA extraction protocol (with modifications) was applied to the ten Azerbaijani hazelnut samples. From each sample, 2 g of hazelnut flour were suspended in 20 mL of 0.01% Tween-80, was then homogenized, and the liquid fraction was retained. Following sequential centrifugation (7,000 rcf for 10 min; 8,000 rcf for 10 min), approx. 500 to 600 µL of fungal pellet were collected and subjected to DNA extraction. The experiment was conducted in duplicate, and qPCR and ddPCR were both employed for DNA detections and quantification (as described above).

Statistical analyses

An initial statistical assessment compared the four DNA extraction methods, using quantitative and qualitative data from Nanodrop and Qubit measurements. These results underwent a univariate analysis of variance (UNIANOVA). Tukey's test was used to evaluate means and detect statistically significant differences. A subsequent analysis was conducted following the optimization of DNA extraction, incorporating quantitative and qualitative data from Nanodrop and Qubit alongside qPCR and ddPCR results. Considered factors included the extraction method (DNeasy or FastDNA), the spore inoculum concentration (1.2×10^5, 1.2×10^4, or 1.2×10^3 conidia g^{-1}), and the hazelnut fraction used for DNA extraction (liquid or kernel). UNIANOVA and Tukey's test were applied to assess means and reveal statistically significant differences.

The relationship between molecular detection results (qPCR and ddPCR copy numbers) and culture-based contamination levels (expected copies g^{-1} derived from CFU counts) was evaluated using correlation analyses. Pearson's rank correlation coefficient was calculated to assess linear associations amongst the data, and Spearman's rank correlation coefficient to assess monotonic associations. Prior to these analyses, data were $\log_{10}$-transformed to normalize distributions and stabilize variances. Correlations were computed using IBM SPSS Statistics software, version 29.0.1.0 (IBM Corp.), and statistical significance was determined at $P < 0.05$.

RESULTS

Fungal contamination in naturally infected hazelnut samples

Colonies were identified as *A. flavus* based on macroscopic and microscopic morphological characteristics, including colony colour and texture on DRBC agar, presence of radiate conidial heads, rough conidiophores, and globose vesicles, following standard taxonomic keys (Pitt *et al.,* 2009).

Fungus contamination among the ten naturally contaminated hazelnut samples ranged from non-detectable levels to a maximum of 1.5×10^3 CFU g^{-1}, with a mean value of approx. 3.9×10^2 CFU g^{-1}. In some cases, no colony growth was observed, indicating the presence of non-viable propagules, or absent fungal colonization (Table 1).

Table 1. Number of *Aspergillus flavus* colony-forming units per gram (CFU g-1) in hazelnut flour from ten naturally contaminated nut samples.

Sample	*A. flavus* (CFUs g^{-1})
1	3.17×10^2
2	1.24×10^2
3	< LOD[b]
4	5.20×10^2
5	5.00×10^1
6	2.00×10^1
7	< LOD
8	< LOD
9	1.53×10^3
10	< LOD

[a] CFUs were determined by serial dilution and plating on DRBC agar. Values represent the average CFU g^{-1} obtained from two replicate plates and three dilutions (10^{-1}, 10^{-2} and 10^{-3}).
[b] Limit of detection = 4 CFU g^{-1}.

Quantities and quality of DNA extracted from naturally infested hazelnut samples

To identify the most suitable DNA extraction protocol for detecting *A. flavus* in naturally contaminated hazelnut samples, four methods were evaluated, focusing on their DNA yield, purity, and compatibility with downstream molecular assays. While all protocols yielded measurable DNA from the samples, the protocols differed for consistency, purity, and PCR inhibition (Table 2; Supplementary Table S1).

Overall, total DNA yields measured by Nanodrop varied considerably among the extraction methods. The InstaGene Matrix protocol produced greater DNA quantities than the other three methods ($P < 0.01$), whereas the Callicott *et al.* (2015), FastDNA, and DNeasy kits yielded similar total DNA amounts to each other.

However, these elevated Nanodrop results were not consistent with Qubit quantification. Qubit measurements gave increased DNA recovery for the FastDNA and DNeasy kits compared with the Callicott and Cotty (2015) method (Table 2). No Qubit data were obtained for the InstaGene Matrix protocol, due to lack of sufficient DNA material.

For DNA purity, the A260/A280 ratios showed differences among the extraction methods ($P < 0.01$; Table 2). The DNeasy Plant Pro Kit gave the greatest purity values, while the InstaGene Matrix gave the least, indicating substantial protein contamination in the assessed samples. The A260/A230 ratios also differed ($P < 0.01$) across methods. The DNeasy Plant Pro Kit gave the greatest values, whereas the FastDNA Spin Kit gave low values. However, all four methods produced values below the optimal A260/ A230 level, indicating persistent carryover of organic residues or salts.

Analytical validation of qPCR and ddPCR assays

In qPCR, amplification was observed across five of the concentrations in the six-point ten-fold dilution series of AF13 DNA, from 5×10^4 copies down to 0.5 copies per reaction. The assay reliably detected DNA down to 50 copies per reaction, with amplification observed in all experimental replicates. At five copies per reaction, amplification became inconsistent, and no amplification was observed at 0.5 copies, establishing, under the tested condition, 50 copies per reaction as the limit of quantification (LOQ), and five copies per reaction as the limit of detection (LOD).

Non-template controls gave no amplifications, confirming absence of contamination or background signals. For *F. verticillioides*, two replicates showed no amplification, while one gave a non-specific melting peak, indicating that the assay discriminated positive signals from background or non-target amplifications.

ddPCR confirmed the specificity of probe-based detection. AF13 DNA generated a clear signal in channel 2 (HEX, targeting the aflatoxigenic strain), while AF36

Table 2. Mean DNA purity parameters (± standard deviations) from four assessed extraction methods. tested.

Method	Nanodrop[a] (total ng)	A260/A280	A260/A230	Qubit (total ng)
	**	**	**	**
Callicott *et al.* (2015)	$7.5 \times 10^3 \pm 1.9 \times 10^3$ b	1.53 ± 0.10 b	0.44 ± 0.05 b	$6.8 \times 10^2 \pm 3.5 \times 10^2$ b
DNeasy Plant Pro Kit (Qiagen)	$7.0 \times 10^2 \pm 2.0 \times 10^2$ b	2.07 ± 0.36 a	0.75 ± 0.39 a	$10.0 \times 10^2 \pm 2.9 \times 10^2$ b
FastDNA Spin Kit (MP Biomedicals)	$3.6 \times 10^3 \pm 4.6 \times 10^2$ b	1.65 ± 0.12 b	0.03 ± 0.01 c	$1.8 \times 10^3 \pm 2.8 \times 10^2$ a
InstaGene Matrix (Bio-Rad)	$5.0 \times 10^4 \pm 1.3 \times 10^4$ a	1.25 ± 0.12 c	0.31 ± 0.02 b	*n.a*

[a] Nanodrop and Qubit values are expressed as total ng per sample. n.a indicates data not measured/calculated.
** $P < 0.01$; Different letters accompanying means indicate statistically significant differences, according to Tukey's tests.

was detected exclusively in channel 1 (FAM, targeting the non-aflatoxigenic strain). No droplets were observed in either channel when using *F. verticillioides* DNA or sterile water.

Compatibility of extracted DNA with qPCR and ddPCR assays

The four DNA extraction methods were assessed for their compatibility with qPCR and ddPCR amplifications. For amplification efficiency, *A. flavus* DNA was detected by qPCR only where the fungus was added to samples, while naturally contaminated samples remained below the detection threshold for all four extraction methods. Among *A. flavus* inoculated samples, both the DNeasy and FastDNA kits yielded detectable amplification signals, while no amplification occurred with the Callicott *et al.* (2015) and InstaGene methods (Supplementary Table S1).

Quantitatively, DNeasy consistently yielded greater copy numbers per reaction, corresponding to approx. 40 to 60% of the expected added concentration, whereas FastDNA averaged 30 to 40% of the expected values. This difference reflects a lower degree of PCR inhibition in the DNeasy extracts than for the FastDNA extracts, likely due to increased DNA purity from the FastDNA system.

In contrast, ddPCR assays yielded no detectable *A. flavus* DNA in any of the naturally contaminated hazelnut samples. Inoculated controls were not included for ddPCR, as the method is largely unaffected by PCR inhibitors. Therefore, absences of amplification were probably true negatives rather than inhibition artifacts.

Optimization of DNA extraction using artificially infested hazelnuts

To refine the DNA extraction process and improve assay performance, hazelnuts were artificially infested with 1.2×10^5, 1.2×10^4, or 1.2×10^3 conidia g^{-1} of *A. flavus* AF13. Each sample was pre-treated with a Tween-80 solution to facilitate fungus recovery. After mixing on the horizontal shaker, the mixture divided into two fractions, one that was whitish liquid and the other a brown sedimented kernel fraction. The two fractions were manually separated by carefully pouring the liquid into a new 50 mL capacity tube, while leaving the plant residues in the original tube. The liquid fraction after being re-centrifuged, gave a whitish sediment corresponding to fat residues from the hazelnuts. The solid kernel fraction consisted of plant residues occupying only the tip of the tube. Both pellets (white sediment from liquid fraction, brown plant residue sediment from kernel fraction) were taken (~500 to 600 µL) and were analyzed independently (Supplementary Table S2).

According to UNIANOVA (Table 3, Supplementary Table S3), both the extraction method and the sample fraction data affected DNA yield and quality parameters, whereas inoculum concentration influenced only the quantification results obtained by qPCR and ddPCR.

DNA yield estimated by Nanodrop was similar ($P > 0.05$) among the methods. In contrast, Qubit measurements and purity ratios (A260/A280 and A260/A230) revealed distinctions between the extraction methods. The DNeasy kit produced DNA of greatest purity, with A260/A280 and A260/A230 ratios close to optimum values, whereas the FastDNA kit gave consistently lower purity values, indicating presence of protein and salt contaminants.

Fraction type also gave a statistically significant effect. Samples derived from the liquid fractions consistently provided greater DNA quantities and better amplification results than those obtained from the kernel fractions, confirming that the Tween-80 washing step improved recovery of fungal material. The method × fraction interaction was significant ($P < 0.05$) for some parameters, indicating that while both kits performed comparably in terms of yield, the DNeasy method was more effective in extracting clean, amplifiable DNA from the liquid fraction, and the FastDNA method tended to produce lower purity extracts, particularly from the kernel fraction (Figure 1).

Table 3. Summary of significant main effects identified by UNIANOVA across DNA yield, purity parameters, and molecular detection assays.

Factors	Nanodrop	A260/A280	A260/A230	Qubit	qPCR	ddPCR
Method (M)	*n.s*	*n.s*	$P < 0.01$	$P < 0.05$	$P < 0.01$	*n.s*
Concentration (C)	*n.s*	*n.s*	*n.s*	*n.s*	$P < 0.01$	$P < 0.01$
Fraction (F)	*n.s*	$P < 0.05$	*n.s*	$P < 0.01$	$P < 0.01$	$P < 0.05$

n.s. = non-significant ($P > 0.05$); * $P < 0.05$; ** $P < 0.01$.
Full numerical results, factor levels, and interaction terms (M × C, M × F, C × F, M × C × F) are reported in Supplementary Table S3.

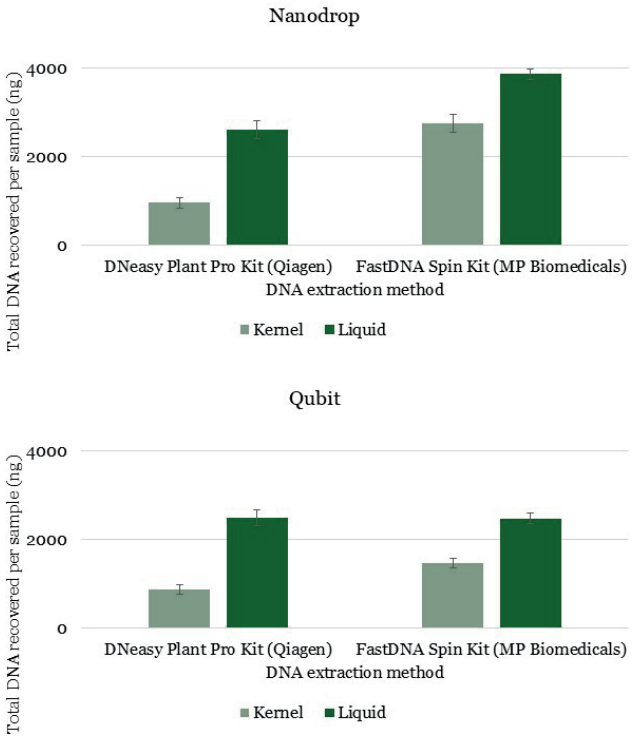

Figure 1. Mean total amounts of DNA per sample from Nanodrop and Qubit quantification for two DNA extraction methods (DNeasy Plant Pro Kit, FastDNA Spin Kit), for two hazelnut fractions (kernel or liquid). Bars indicate standard errors of means.

The qPCR and ddPCR data further confirmed these trends. Both assays detected *A. flavus* DNA in all conidium concentrations, but signal strength and consistency declined with decreasing inoculum. qPCR amplification was generally more robust than ddPCR for DNA extracted with the DNeasy kit and from the liquid fractions, reflecting greater recovery efficiency and lower inhibition. ddPCR results showed a similar pattern, detecting target DNA even at the lowest contamination level, confirming greater analytical sensitivity of ddPCR than for qPCR.

When comparing the measured and expected values (Supplementary Table S2), both qPCR and ddPCR results showed recovery ratios below 1 across all treatments, indicating that only a small fraction of the expected target DNA was recovered after extraction. Nevertheless, the DNeasy kit consistently produced greater measured/expected ratios than the FastDNA kit, particularly for the liquid fraction, suggesting a more effective recovery of amplifiable DNA and reduced inhibition for the DNeasy than the FastDNA kit.

The FastDNA kit, in contrast, yielded lower and more variable ratios than the DNeasy kit. Although total DNA quantities measured fluorometrically were comparable between the two kits, these values may reflect plant-derived DNA. The lower measured/expected ratios obtained with FastDNA therefore indicate less efficient extraction of *A. flavus* DNA rather than reduced availability of amplifiable templates.

For both extraction methods, the absolute amount of target DNA detected decreased with decreasing conidium concentration, as was expected. However, recovery efficiency (measured/expected ratios) remained stable across concentrations. Notably, the DNeasy kit maintained detectable amplification even at the lowest inoculum level, whereas FastDNA frequently approached the detection limit.

Validation of the optimized protocol on naturally contaminated hazelnut samples

To validate the optimized extraction protocol, the ten naturally contaminated hazelnut samples were reanalyzed using the DNeasy Plant Pro Kit, following sample pre-treatment with Tween-80 and selective recovery of the liquid fractions. Overall, the results confirmed that the optimized protocol efficiently extracted amplifiable DNA from naturally contaminated material, yielding consistent quantities of satisfactory purity suitable for downstream molecular analyses (Supplementary Table S4). Both Nanodrop and Qubit measurements showed reproducible DNA recovery across samples, while A260/A280 ratios remained close to the ideal value for pure DNA, indicating minimal protein contamination. The A260/A230 ratios were more variable among samples, reflecting the heterogeneous composition and matrix complexity of naturally contaminated nuts.

qPCR detection confirmed the presence of *A. flavus* DNA in most samples, although copy numbers were generally low, consistent with the low fungal counts in naturally contaminated material (Table 4). Both qPCR and ddPCR results correlated positively with culture-based CFU-derived estimates. The correlation was stronger for qPCR (Spearman's $\rho = 0.77$, $P = 0.07$) than for ddPCR ($\rho = 0.66$, $P = 0.16$), indicating an overall positive relationship between molecular and culture-based detections, although these were not statistically significant due to the limited number of naturally contaminated samples. Some samples that yielded no detectable colonies on agar plates gave qPCR and ddPCR signals, suggesting that the molecular assays detected non-culturable or residual fungal DNA that remained undetected by culture-based methods.

ddPCR analyses supported these results, providing absolute quantification of *A. flavus* DNA with slightly

Table 4. Quantification and quality assessment of DNA extracted from ten naturally contaminated hazelnut samples using the optimized DNeasy Plant Pro Kit protocol.

Sample	qPCR (copies g^{-1})[a]	ddPCR (copies g^{-1})[a]	Expected copies per g[b]
1	$1.8 \times 10^2 \pm 1.6 \times 10^2$	$1.5 \times 10^2 \pm 1.1 \times 10^2$	3.2×10^2
2	$6.4 \times 10^1 \pm 1.3 \times 10^2$	$2.9 \times 10^1 \pm 5.8 \times 10^1$	1.2×10^2
3	$3.1 \times 10^2 \pm 2.7 \times 10^2$	$1.5 \times 10^2 \pm 8.0 \times 10^1$	*n.d*
4	$1.3 \times 10^2 \pm 2.5 \times 10^2$	$5.2 \times 10^1 \pm 3.8 \times 10^1$	5.2×10^2
5	$6.3 \times 10^1 \pm 8.8 \times 10^1$	$2.7 \times 10^1 \pm 3.3 \times 10^1$	5.0×10^1
6	$2.3 \times 10^2 \pm 1.3 \times 10^2$	$9.2 \times 10^1 \pm 5.2 \times 10^1$	2.0×10^1
7	$2.4 \times 10^1 \pm 4.8 \times 10^1$	$2.0 \times 10^1 \pm 2.3 \times 10^1$	*n.d*
8	$1.5 \times 10^2 \pm 3.0 \times 10^2$	$1.1 \times 10^1 \pm 2.3 \times 10^1$	*n.d*
9	$1.2 \times 10^3 \pm 1.8 \times 10^3$	$1.2 \times 10^2 \pm 1.3 \times 10^1$	1.5×10^3
10	*n.d*	$2.1 \times 10^1 \pm 4.1 \times 10^1$	*n.d*

[a] qPCR and ddPCR were carried out on each sample.
[b] Expected copies are expressed in CFU g^{-1}, and were derived from plate counting analysis.
All values are means ± standard deviations from two independent replicates. N.d indicates where *A. flavus* was not detected through plate counting or that its DNA was not measured using qPCR.

greater detection consistency compared to qPCR. ddPCR confirmed low but measurable levels of target DNA across most samples, even when qPCR amplification was weak or absent, highlighting the superior sensitivity of droplet-based quantification.

When comparing molecular quantification with culture-derived estimates (CFU g^{-1}), the measured/expected ratios were generally below 1.0, indicating that the amount of amplifiable DNA was less than predicted based on counts of viable conidia. In a few samples, ratios could not be calculated (*n.a.*), corresponding to cases with zero CFU counts but detectable DNA.

DISCUSSION

Presence of aflatoxigenic *A. flavus* in hazelnuts is a persistent challenge for food safety, particularly due to the complex nature of the nut matrix and the typically low levels of fungal contamination encountered in commercial products (Gallo *et al.,* 2010).

Results from the present study demonstrate that optimization of DNA extraction is important for overcoming matrix-related limitations for toxigen detection. By systematically comparing four extraction protocols and introducing a Tween-80 washing step to separate the liquid and kernel fractions, it was possible to improve DNA yield and purity. Liquid fractions, in particular, concentrated most of the fungus spores while minimizing co-extraction of inhibitory compounds such as lipids and polysaccharides. These results highlight how simple pre-processing adjustments can enhance nucleic acid recovery and PCR detection performance.

When compared to previous research, this study represents a significant methodological advancement. Most previous studies investigating *A. flavus* in hazelnuts have relied on artificially inoculated hazelnut kernels or pre-cultured fungal biomass, rather than on direct analysis of the nut matrices. Gallo *et al.* (2010) examined fungal metabolism using hazelnut-based culture media, while Ortega *et al.* (2020) tested qPCR assays mostly on artificially inoculated kernels. Similarly, Hamed *et al.* (2016) and Hassan *et al.* (2023) extracted DNA from cultured mycelia, and Lombardi *et al.* (2022) characterized fungal communities of ready-to-eat hazelnuts using a polyphasic, culture-dependent approach that combined morphological and molecular identification of isolated colonies. In contrast, the results from the present study indicate that fungus cultivation is not required, but that direct targeting *A. flavus* DNA within hazelnut matrices can provide sensitive (low contamination) detection of aflatoxigenic strains.

Among the evaluated protocols, the DNeasy Plant Pro Kit provided the best compromise between yield, purity, and PCR compatibility. Column-based methods minimized contamination from proteins and organic residues, as indicated by stable A260/A280 ratios and reduced PCR inhibition. This extraction protocol was also effective in artificially contaminated hazelnuts and naturally infected samples, demonstrating robustness across contamination levels and matrix conditions.

Both qPCR and ddPCR assays successfully detected *A. flavus* DNA in inoculated samples, though ddPCR had superior analytical sensitivity and quantification accuracy, particularly at low inoculum levels. Unlike qPCR, ddPCR does not rely on calibration curves, and is less affected by PCR inhibitors, allowing for absolute quantification even in inhibitor-rich matrices such as hazelnuts. These results align with previous results in rice- and wheat-derived food matrices (Wang *et al.,* 2022), where ddPCR consistently outperformed qPCR in detecting low contamination levels of toxigenic fungi. Nevertheless, qPCR remains a highly practical tool for large-scale screening, providing rapid and cost-effective results suitable for industrial quality control *(*Shang *et al.*, 2025). Both techniques are complementary: qPCR for high-throughput surveillance and ddPCR for confirmatory trace-level quantification.

The validation of the optimized extraction method on naturally contaminated hazelnuts confirmed its applicability under real conditions. Both qPCR and ddPCR

detected *A. flavus* DNA in multiple samples, often correlating with CFU estimates. In several cases, molecular detection was achieved even when CFUs were not detected, indicating that the method can identify non-culturable or residual fungal DNA that remains undetectable by classical microbiological assays. The number of naturally contaminated samples (n = 10) was limited, as the primary aim of this study was methodological rather than epidemiological. Samples were selected to represent commercial material, originating from different production batches and showing variable contamination levels. The sample set was therefore considered sufficient to evaluate robustness, sensitivity, and practical applicability of optimized DNA extraction and molecular detection. Nevertheless, larger surveys than for the present study, covering additional origins, seasons, and storage conditions, will be necessary to further consolidate quantitative performance of PCR detection under diverse conditions.

An important limitation of DNA-based detection is that presence of aflatoxigenic *A. flavus* does not directly imply active AFs production or presence of AFs in analyzed samples. AFs biosynthesis depends on multiple environmental and physiological factors, and DNA detection alone cannot distinguish between toxigenic potential and actual toxin accumulation. Consequently, molecular detection should be used as an early warning and risk-indication tool that complements chemical aflatoxin analysis (Northolt *et al.,* 1977; Caceres *et al.,* 2020).

In conclusion, this study has provided a validated and matrix-adapted molecular workflow for sensitive detection of aflatoxigenic *A. flavus* in hazelnut kernels. By integrating optimized DNA extraction with complementary qPCR and ddPCR assays, the proposed approach offers a practical tool for preventive monitoring and risk assessment in hazelnut supply chains. Beyond its analytical performance, the workflow has clear operational relevance. Its sensitivity can enable early detection of aflatoxigenic *A. flavus* in incoming batches, supporting risk-based acceptance decisions and strengthening HACCP monitoring at critical control points. Future studies may extend this framework to other mycotoxigenic species and food matrices, strengthening the role of molecular diagnostics in integrated food safety management systems.

FUNDING

This research was partly funded by the United States Department of Agriculture (Project number, 2020-42000-022-00D).

AUTHOR CONTRIBUTIONS

A. Casu: Conceptualization (equal), Data Curation (lead), Formal Analysis (equal), Investigation (lead), Validation (lead), Visualization (lead), Writing – Original Draft Preparation (lead); G. Chiusa: Methodology (supporting), Writing – Review & Editing (equal); P. Battilani: Conceptualization (equal), Methodology (supporting), Project Administration (equal), Supervision (equal), Writing - Review & Editing (equal); H. L. Mehl: Conceptualization (equal), Formal Analysis (equal), Funding Acquisition (lead), Methodology (lead), Project Administration (equal), Resources (lead), Supervision (equal), Validation (supporting), Writing – Review & Editing (equal).

ACKNOWLEDGEMENTS

Alessia Casu is part of the PhD school in Agro-Food System (Agrisystem) of the Università Cattolica del Sacro Cuore (Italy). This study was therefore supported by the PhD in Agro-Food System and by Portus project funded by Romeo and Enrica Invernizzi Foundation. The authors acknowledge Soremartec Italia s.r.l. for supporting the research project, and the USDA-ARS Aflatoxin Reduction in Crops Laboratory for providing materials and technical support, and hosting Alessia Casu during her research stay. Mention of trade names or commercial products in this publication is to providing specific information, but does not imply recommendation or endorsement by the U.S. Department of Agriculture. The US Department of Agriculture is an equal-opportunity employer and provider.

LITERATURE CITED

Aghayev F., Bandyopadhyay R., Battilani P., Ortega-Beltran A., 2025. Mycotoxin contamination of hazelnut grown in Azerbaijan and *Aspergillus* communities associated with the crop. *Plant Disease* https://doi.org/10.1094/pdis-12-24-2623-SC

Ahmad M.M., Ahmad M., Ali A., Hamid R., Javed S., Abdin M.Z., 2014. Detection of *Aspergillus flavus* and *Aspergillus parasiticus* from aflatoxin-contaminated peanuts and their differentiation using PCR-RFLP. *Annals of Microbiology* 64(4): 1597–1605. https://doi.org/10.1007/S13213-014-0803-5

Caceres I., Khoury A. Al, El Khoury R., Lorber S., Bailly J.D., 2020. Aflatoxin biosynthesis and genetic regulation: a review. *Toxins* 12(3): 150. https://doi.org/10.3390/toxins12030150

Callicott K.A., Cotty P.J., 2015. Method for monitoring deletions in the aflatoxin biosynthesis gene cluster of *Aspergillus flavus* with multiplex PCR. *Letters in Applied Microbiology* 60(1): 60–65. https://doi.org/10.1111/lam.12337

Chen R.S., Tsay J.G., Huang Y.F., Chiou R.Y.Y., 2002. Polymerase chain reaction–mediated characterization of molds belonging to the *Aspergillus flavus* group and detection of *Aspergillus parasiticus* in peanut kernels by a multiplex polymerase chain reaction. *Journal of Food Protection* 65(5): 840–844. https://doi.org/10.4315/0362-028X-65.5.840

Ciardo D.E., Schär G., Altwegg M., Böttger E.C., Bosshard P.P., 2007. Identification of moulds in the diagnostic laboratory: an algorithm implementing molecular and phenotypic methods. *Diagnostic Microbiology and Infectious Disease* 59(1): 49–60. https://doi.org/10.1016/j.diagmicrobio.2007.04.020

Conlon B.H., Schmidt S., Poulsen M., Shik J.Z., 2022. Orthogonal protocols for DNA extraction from filamentous fungi. *STAR Protocols* 3(1): 101126. https://doi.org/10.1016/j.xpro.2022.101126

Cotty P.J., Bayman P., 1993. Competitive exclusion of a toxigenic strain of *Aspergillus flavus* by an atoxigenic strain. *Phytopathology* 83: 1283–1287. https://doi.org/10.1094/Phyto-83-1283

Degola F., Berni E., Spotti E., Ferrero I., Restivo F.M., 2009. Facing the problem of "false positives": reassessment and improvement of a multiplex RT-PCR procedure for the diagnosis of *A. flavus* mycotoxin producers. *International Journal of Food Microbiology* 129(3): 300–305. https://doi.org/10.1016/j.ijfoodmicro.2008.12.016

Douksouna Y., Kwallah A.O., Nyerere A., Runo S., Ambang Z., 2020. Application and evaluation of the loop-mediated isothermal amplification assay for the detection of aflatoxigenic fungi contaminants of rice grains in Kenya. *Plant Pathology & Microbiology* 11: 491.

European Commission (EC), 2023. Commission Regulation (EU) 2023/915 of 25 April 2023 on maximum levels for certain contaminants in food and repealing Regulation (EC) No 1881/2006. *Official Journal of the European Union* L119: 103–127.

Gallo A., Epifani F., Bonsegna S., Pascale M., Santino A., Perrone G., 2010. Analysis of genes early expressed during *Aspergillus flavus* colonisation of hazelnut. *International Journal of Food Microbiology* 137(1): 111–115. https://doi.org/10.1016/j.ijfoodmicro.2009.11.010

Garcia-Lopez M.T., Luo Y., Ortega-Beltran A., Jaime R., Moral J., Michailides T.J., 2021. Quantification of the aflatoxin biocontrol strain *Aspergillus flavus* AF36 in soil and in nuts and leaves of pistachio by real-time PCR. *Plant Disease* 105(6): 1765–1772. https://doi.org/10.1094/pdis-05-20-1097-RE

González-Salgado A., González-Jaén T., Vázquez C., Patiño B., 2011. Highly sensitive PCR-based detection specific to *Aspergillus flavus*. *Methods in Molecular Biology* 739: 211–216. https://doi.org/10.1007/978-1-61779-102-4_19

Habibi A., 2021. *Aspergillus* species in retail samples of pistachio, walnut, and hazelnut in Kerman, Iran. *Mycologia Iranica* 8(2): 77–94. https://doi.org/10.22092/mi.2022.359369.1223

Hamed N.A.S., Murad A.F., Abdul-Rahim E.A.W., 2016. Molecular diagnosis of aflatoxigenic *Aspergillus flavus* isolated from nuts. *Research Journal of Environmental Toxicology* 10(1): 39–45.

Hassan K.I., Hama Sharef P., 2023. Identification of fungi associated with hazelnuts and determination of their mycotoxin. *IOP Conference Series: Earth and Environmental Science* 1213(1): 012074. https://doi.org/10.1088/1755-1315/1213/1/012074

Hua S.S.T., Palumbo J.D., Parfitt D.E., Sarreal S.B.L., O'Keeffe T.L., 2018. Development of a droplet digital PCR assay for population analysis of aflatoxigenic and atoxigenic *Aspergillus flavus* mixtures in soil. *Mycotoxin Research* 34(3): 187–194. https://doi.org/10.1007/S12550-018-0313-6

IARC, 1993. *Monographs on the Evaluation of Carcinogenic Risks to Humans*. Vol. 56. International Agency for Research on Cancer, Lyon, France.

Kabak B., 2016. Aflatoxins in hazelnuts and dried figs: occurrence and exposure assessment. *Food Chemistry* 211: 8–16. https://doi.org/10.1016/j.foodchem.2016.04.141

Latha R., Manonmani H.K., Rati E.R., 2008. Multiplex PCR assay for the detection of aflatoxigenic and non-aflatoxigenic *Aspergilli*. *Research Journal of Microbiology* 3(3): 136–142. https://doi.org/10.3923/jm.2008.136.142

Leharanger A., Paumier D., Orlando B., Bailly S., Valade R., 2024. Two new qPCR assays for detecting and quantifying the *Aspergillus flavus* and *Aspergillus parasiticus* clades in maize kernels. *Plant Pathology* 73(9): 2372–2381. https://doi.org/10.1111/ppa.13982

Liu P., Li B., Yin R., Weng Q., Chen Q., 2014. Development and evaluation of ITS- and aflP-based LAMP assays for rapid detection of *Aspergillus flavus* in food samples. *Canadian Journal of Microbiology* 60(9): 579–584. https://doi.org/10.1139/cjm-2014-0202

Lombardi S.J., Pannella G., Tremonte P., Mercurio I., Vergalito F., Coppola R., 2022. Fungi occurrence in ready-to-eat hazelnuts (*Corylus avellana*) from

different boreal hemisphere areas. *Frontiers in Microbiology* 13: 900876. https://doi.org/10.3389/fmicb.2022.900876

Luo Y., Gao W., Doster M., Michailides T.J., 2009. Quantification of conidial density of *Aspergillus flavus* and *A. parasiticus* in soil from almond orchards using real-time PCR. *Journal of Applied Microbiology* 106(5): 1649–1660. https://doi.org/10.1111/j.1365-2672.2008.04132.x

Luo J., Vogel R.F., Niessen L., 2012. Development and application of a loop-mediated isothermal amplification assay for rapid identification of aflatoxigenic molds and their detection in food samples. *International Journal of Food Microbiology* 159(3): 214–224. https://doi.org/10.1016/j.ijfoodmicro.2012.08.018

Luo J., Taniwaki M.H., Iamanaka B.T., Vogel R.F., Niessen L., 2014. Application of loop-mediated isothermal amplification assays for direct identification of pure cultures of *Aspergillus flavus*, *A. nomius* and *A. caelatus* and for their rapid detection in shelled Brazil nuts. *International Journal of Food Microbiology* 172: 5–12. https://doi.org/10.1016/j.ijfoodmicro.2013.12.001

Mahmoud M.A., 2015. Detection of *Aspergillus flavus* in stored peanuts using real-time PCR and expression of aflatoxin genes in toxigenic and atoxigenic isolates. *Foodborne Pathogens and Disease* 12(4): 289–296. https://doi.org/10.1089/fpd.2014.1854

Mitema A., Okoth S., Rafudeen S.M., 2019. The development of a qPCR assay to measure *Aspergillus flavus* biomass in maize and the use of a biocontrol strategy to limit aflatoxin production. *Toxins* 11(3): 179. https://doi.org/10.3390/toxins11030179

Niessen L., Bechtner J., Fodil S., Taniwaki M.H., Vogel R.F., 2018. LAMP-based group-specific detection of aflatoxin producers within *Aspergillus* section *Flavi* in food raw materials, spices and dried fruit using neutral red for visible-light signal detection. *International Journal of Food Microbiology* 266: 241–250. https://doi.org/10.1016/j.ijfoodmicro.2017.12.013

Northolt M.D., Van Egmond H.P., Paulsch W.E., 1977. Differences between *Aspergillus flavus* strains in growth and aflatoxin B1 production in relation to water activity and temperature. *Journal of Food Protection* 40(11): 778–781. https://doi.org/10.4315/0362-028X-40.11.778

Nooralden Z.N., Mohammed H.A., 2022. Isolation and identification of fungi associated with walnuts, almonds, hazelnuts, cashews, pistachios and peanuts using molecular diagnostics (PCR) in local markets of Kirkuk Governorate, Iraq. *Journal of Pharmaceutical Negative Results* 13: 1–8.

Ortega S.F., Siciliano I., Prencipe S., Gullino M.L., Spadaro D., 2020. Development of PCR, LAMP and qPCR assays for the detection of aflatoxigenic strains of *Aspergillus flavus* and *A. parasiticus* in hazelnut. *Toxins* 12(12): 757. https://doi.org/10.3390/toxins12120757

Passone M.A., Rosso L.C., Ciancio A., Etcheverry M., 2010. Detection and quantification of *Aspergillus* section *Flavi* spp. in stored peanuts by real-time PCR of the *nor-1* gene and effects of storage conditions on aflatoxin production. *International Journal of Food Microbiology* 138(3): 276–281. https://doi.org/10.1016/j.ijfoodmicro.2010.01.003

Pitt J.I., Hocking A.D., 1997. *Fungi and food spoilage*. Blackie Academic & Professional, London, UK. https://doi.org/10.1007/978-1-4615-6391-4

RASFF, 2025. Rapid Alert System for Food and Feed. Available at: https://webgate.ec.europa.eu/rasff-window/screen/search (accessed 27 October 2025).

Rodríguez A., Rodríguez M., Luque M.I., Martín A., Córdoba J.J., 2012. Real-time PCR assays for detection and quantification of aflatoxin-producing molds in foods. *Food Microbiology* 31(1): 89–99. https://doi.org/10.1016/j.fm.2012.02.009

Rushing B.R., Selim M.I., 2019. Aflatoxin B1: a review on metabolism, toxicity, occurrence in food, occupational exposure and detoxification methods. *Food and Chemical Toxicology* 124: 81–100. https://doi.org/10.1016/j.fct.2018.11.047

Sardiñas N., Vázquez C., Gil-Serna J., González-Jaén M.T., Patiño B., 2011. Specific detection and quantification of *Aspergillus flavus* and *Aspergillus parasiticus* in wheat flour by SYBR® Green quantitative PCR. *International Journal of Food Microbiology* 145(1): 121–125. https://doi.org/10.1016/j.ijfoodmicro.2010.11.041

Scherm B., Palomba M., Serra D., Marcello A., Migheli Q., 2005. Detection of transcripts of the aflatoxin genes *aflD*, *aflO* and *aflP* by reverse transcription–polymerase chain reaction allows differentiation of aflatoxin-producing and non-producing isolates of *Aspergillus flavus* and *Aspergillus parasiticus*. *International Journal of Food Microbiology* 98(2): 201–210. https://doi.org/10.1016/j.ijfoodmicro.2004.06.004

Shapira R., Paster N., Eyal O., Menasherov M., Mett A., Salomon R., 1996. Detection of aflatoxigenic molds in grains by PCR. *Applied and Environmental Microbiology* 62(9): 3270–3273. https://doi.org/10.1128/AEM.62.9.3270-3273.1996

Shweta S., Madhavan S., Paranidharan V., Velazhahan R., 2013. Detection of *Aspergillus flavus* in maize kernels by conventional and real-time PCR assays. *International Food Research Journal* 20(6): 3329–3335.

We warmly thank for their kind cooperation the following referees who have reviewed papers during this year in order to publish this Volume (Phytopathologia Mediterranea 64, 2025):

Agustí-Brisach Carlos, Córdoba, Spain
Al-Sadi Abdullah, Al-Khod, Oman
Alaniz Sandra, Montevideo, Uruguay
Aliferis Konstantinos, Athens, Greece
Altomare Claudio, Bari, Italy
Anelli Pamela, Bari, Italy
Atanasova Vessela, Villenave d'Ornon, France
Babaei Ghobad, Shahrekord, Iran
Barrès Benoit, Maisons-Alfort, France
Beluzán Francisco, Santiago de Chile, Chile
Berraf-Tebbal Akila, Algiers, Algeria
Buonaurio Roberto, Perugia, Italy
Burbank Lindsey, Washington, D.C., Usa
Buzkan Nihal, Kahramanmaraş, Turkey
Caballol Maria, Solsona, Catalonia, Spain
Caffi Tito, Piacenza, Italy
Calzarano Francesco, Teramo, Italy
Candresse Thierry, Bordeaux, France
Castillo Pablo, Córdoba, Spain
Chammem Hamza, Elvas, Portugal
Choueiri Elia, Tel Amara, Lebanon
Cobos Rebeca, León, Spain
Collina Marina, Bologna, Italy
Cook Glynnis, Mpumalanga, South Africa
Daami Mejda, Chott Mariem, Tunisia
Del Frari Giovanni, Udine, Italy
Dlugos Daniel, Clemson, SC, USA
El Shafey Naglaa Fathi, Arish, Egypt
Elbeaino Toufic, Bari, Italy
Ermacora Paolo, Udine,Italy
Felici Linda, Viterbo, Italy
Fia Giovanna, Firenze, Italy
Fontdevila Pareta Nuria, Nyon, Suisse
Franova Jana, Ceske Budejovice, Czech Republic
Gargouri Samia, Tunis, Tunisia
Ghelardini Luisa, Firenze, Italy
Gialluisi Katia, Bari, Italy
Gkizi Danai, Athens, Greece
Gomes Ines, Lisboa, Portugal
Guarnaccia Vladimiro, Torino, Italy
Gutiérrez Gutiérrez Carlos, Évora, Portugal
Hanana Mohsen, Hammam-lif, Tunisia
Havenga Minette, Stellenbosch, South Africa
Henriquez Jose Luis, Santiago, Cile
Hu Mengjun, Maryland,Usa,
Isakeit Thomas, College Station, Texas, Usa
Kaluzna Monika, Skierniewice, Poland
Karanfil Ali, Çanakkale, Türkiye
Kil Eui-Joon, Andong, South Korea
Kumari Safaa, Beirut, Lebanon
Leonardi Giuseppa Rosaria, Catania, Italy
Livieratos Ioannis, Chania, Crete, Greece
Maclot Francois, Gembloux, Belgium
Margaria Paolo, Braunschweig, Germany
Markakis Emmanouil, Irákleion, Greece
Masuya Hayato, Tsukuba, Ibaraki, Japan
Montarry Josselin, Le Rheu, France
Murillo Jesus, Pamplona, Spain
Nancarrow Narelle, Melbourne, Australia
Nigro Franco, Bari, Italy
Önelge Nukht, Adana, Turkey
Parrado Guevara Luisa, East Lansing, Michigan, USA
Paudel Dinesh Babu, Saskatoon, Canada
Peneva Vlada, Sofia, Bulgaria
Platel Rémi, Lambersart, France
Quaglino Fabio, Milano, Italy
Ramos Madalena, Bologna, Italy
Roberts Pamela, North Immokalee, FL, USA
Rossi Vittorio, Milano, Italy
Salem Nida, Amman, Jordan
Savoie Jean-Michel, Villenave d'Ornon, France
Scali Edoardo, Berkeley, CA, USA
Serna-Escolano Vicente, Elche, Alicante, Spain
Serrano Maria, Elche, Alicante, Spain
Shiskoff Nina, Fort Detrick, MD, Usa
Skoric Dijana, Zagreb, Croatia
Solis Myriam, Pretoria, South Africa
Somma Stefania, Bari, Italy
Stazione Leonel, Firenze, Italy
Testempasis Stefanos, Thessaloníki, Greece
Tienda Sandra, Malaga, Spain
Topalidou Eleni, Thessaloníki, Greece
Tzima Aliki, Athens, Greece
Urbez-Torres Jose, Summerland, British Columbia, Canada
Valdez Adrian, Talca, Chile
Valentini Franco, Bari, Italy
Van Der Waals Jacquie, Pretoria, South Africa
Vettraino Anna Maria, Viterbo, Italy
Voncina Darko, Zagreb, Croatia
Walker Anne-Sophie, Thiverval-Grignon, France
Wingfield Michael, Pretoria, South Africa
Ziebell Heiko, Quedlinburg, Germany

Mediterranean Phytopathological Union

Founded by Antonio Ciccarone

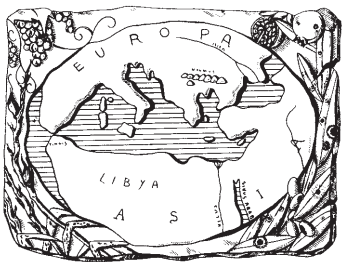

The Mediterranean Phytopathological Union (MPU) is a non-profit society open to organizations and individuals involved in plant pathology with a specific interest in the aspects related to the Mediterranean area considered as an ecological region.
The MPU was created with the aim of stimulating contacts among plant pathologists and facilitating the spread of information, news and scientific material on plant diseases occurring in the area. MPU also intends to facilitate and promote studies and research on diseases of Mediterranean crops and their control.
The MPU is affiliated to the International Society for Plant Pathology.

2026 Information for authors of the Open Access journal *Phytopathologia Mediterranea*

Only MPU members are eligible to publish according to MPU membership categories (see https://oajournals.fupress.net/index.php/pm/about):

– All authors belonging to an MPU National Society Member (see list above) or to an MPU Affiliated Member (international organizations or networks), that signed a Memorandum of Understanding with MPU, are entitled to publish with a contribution to publication cost (https://oajournals.fupress.net/index.php/pm/about)
– All Individual Members (not in the above categories), including members of profit or non-profit entities, and physical person.

To become an Individual Member see www.mpunion.org or contact secretariat@mpunion.org

To receive the paper version of the journal please contact phymed@unifi.it

For information visit the MPU web site:
www.mpunion.org
or contact us at: Phone +39 39 055 2755861/862 – E-mail: phymed@unifi.it

Phytopathologia Mediterranea
Volume 64, December, 2025

Contents

Direttore responsabile: Giuseppe Surico • Autorizzazione del Tribunale di Firenze n. 4923 del 5-1-2000 • *Printed by* Logo S.r.l. - Padova, January 2026